



**UNIVERSITY *of the*
WESTERN CAPE**

**Identification, separation and quantification of persistent organic
pollutants using capillary electrophoresis**

By

Emmanuel Oluseyi Omoniyi

BTech Chemistry –Lautech, Ogbomoso

MTech Chemistry – Cape Peninsula University of Technology

**A thesis submitted in fulfilment of the requirements for the degree of Doctor of
Philosophy in Chemistry, Faculty of Natural Sciences, University of the Western Cape.**

Supervisor: Prof. Leslie F. Petrik

December, 2021

ABSTRACT

Water quality deterioration and scarcity can be attributed to natural causes and anthropogenic activities which include climate change and an incessant industrialisation, yet with lack of functional and reliable wastewater treatment facilities. As a consequence of these activities, many chemicals have found their way into water bodies and subsequently compromise the quality of water systems. Among these chemicals are persistent organic pollutants (POPs), including pharmaceuticals, endocrine disrupting compounds (EDCs), etc. In order to separate, identify and quantify persistent and emerging contaminants in the water samples, this study considered the pre-concentration and separation steps followed by quantification using capillary electrophoresis. The persistent organic pollutants investigated in this study were pharmaceuticals including: acetaminophen, aspirin, diclofenac, ibuprofen, salicylic acid, sulphamethoxazole; and steroid hormones including: androstenedione, testosterone, progesterone and 17-beta estradiol. Low nanogram per litre levels of organic pollutants (pharmaceuticals and steroid hormone compounds) in environmental samples could be determined after cleaning the water matrix and enriching the analytes (organic pollutants) by solid-phase extraction (SPE).

In the analysis carried out with HPLC-MS, different water samples including effluent wastewater from the wastewater treatment plant, cold tap water, hot tap water and milli-Q water samples were investigated for the pharmaceuticals under study, including 17-beta estradiol. Only diclofenac (3.306 ng/mL) and sulphamethoxazole (1.18 ng/mL) were detected from the effluent sample; while other compounds were below the level of quantification in remaining water samples.

Capillary electrophoresis (CE) with its high separation efficiency is a worthy alternative to chromatographic techniques in the determination of persistent organic pollutants. Optimisation of capillary electrophoresis was carried out to investigate the factors affecting the performance of the CE instrument. Different parameters studied were the voltage that affects the field strength, the pH of the electrolyte solution that affects the separation and dissociation of the analytes according to their pKa values, and the injection type used that affects the detectability. Capillary zone electrophoresis (CZE) with UV detection (CZE-UV) was employed in the identification and quantification of pharmaceuticals including: acetaminophen, aspirin, diclofenac, ibuprofen, salicylic acid, and sulphamethoxazole in the

environmental water samples. For influent A sample, aspirin was quantified to be 13.52 ng/L, diclofenac as 14.15 ng/L, salicylic acid as 6.514 ng/L and sulphamethoxazole as 11.79 ng/L respectively. The influent B water sample contained 4.23 ng/L of aspirin, 8.235 ng/L of diclofenac, 1.199 ng/L of salicylic acid, 1.095 ng/L of ibuprofen and 13.170 ng/L of sulphamethoxazole respectively. And in the effluent water samples of sewage water treatment plants the measurable pharmaceuticals quantities include 0.836 ng/L of aspirin, 0.802 ng/L of diclofenac, 1.343 ng/L of salicylic acid, 0.842 ng/L of ibuprofen and 10.241 ng/L of sulphamethoxazole. Partial-filling micellar electrokinetic capillary chromatography (PF-MEKC) method was adopted for the identification and quantification of the steroid hormones. In the influent A water sample, androstenedione was quantified to be 2.224 ng/L, testosterone was quantified to be 3.474 ng/L, 17- β -estradiol was quantified to be 0.96 ng/L and progesterone was 1.503 ng/L. The influent B water sample contained 2.224 ng/L of androstenedione, 3.142 ng/L of testosterone, 0.954 ng/L of 17- β -estradiol and 0.691 ng/L of progesterone respectively. While in the purified effluent water samples of sewage water treatment plants, the measurable steroid hormones quantities include 1.205 ng/L of androstenedione, 3.037 ng/L of testosterone, 0.550 ng/L of 17- β -estradiol and 0.440 ng/L of progesterone respectively. The steroid compounds content of the tap water (hot and cold) was also measured. For androstenedione, 0.031 ng/L and 0.025 ng/L were quantified for hot tap water and cold tap water respectively; testosterone accounted for 0.016 ng/L and 0.013 ng/L of hot tap water and cold tap water respectively; 17- β -estradiol accounted for 0.11 ng/L and 0.09 ng/L of hot tap water and cold tap water respectively; while progesterone gave 0.049 ng/L and 0.031 ng/L of hot tap water and cold tap water respectively. For inorganic ions, the capillary zone electrophoresis (CZE) with an indirect UV detection was employed in the quantification of the anions and cations in the water samples. The optimized capillary electrophoresis method for the inorganic ions investigation of the environmental water samples, the anions were separated in a buffer solution containing 2.25 mM pyromellitic acid, 6.50 mM NaOH, 0.75 mM hexamethonium hydroxide and 1.60 mM triethanolamine (pH 7.7 \pm 0.2, Fluka). On the contrary, the optimized capillary electrophoresis for the cations was performed in 9 mM pyridine-12 mM glycolic acid-5 mM 18-crown-6 ether at pH 3.6, adjusted with 0.1 M HCl. The cations studied include sodium, potassium, calcium and magnesium ions, the sulphate ions had the highest concentrations across all the 10 water samples, followed by chloride, and then nitrates were found in the least amount across the respective water samples. The highest concentrations of chlorides was found in the river

water samples (RW), followed by tap water samples, the drilled well water (DW), and the milli-Q water (MQW) samples respectively.

Similarly, Surface enhanced Raman Spectroscopy (SERS) was evaluated for the detection of pollutant analytes (acetaminophen and 4-aminothiophenol, 4-ATP). In this study, a silver-coated track-etched polyethylene terephthalate (PET) membrane was developed as a platform for the detection of acetaminophen and 4-aminothiophenol (4-ATP). The silver-coated track-etched polyethylene terephthalate (PET) membrane was fabricated by the modification of the PET membrane surface with diethylenetriamine (DETA) through solid-liquid interface reaction called aminolysis. Fourier transform infrared (FTIR) and X-ray photoelectron spectroscopy (XPS) techniques were employed to confirm the surface modification of the track-etched PET membrane and immobilisation of silver nanoparticles was carried out on the amine-modified surface of track-etched PET membrane. The silver nanoparticles immobilised were of different sizes with an average size of 64 nm, mostly spherical in shape. This silver nanoparticles immobilised on the modified track-etched PET membrane was then characterised by scanning electron microscopy (SEM), ultraviolet-visible (UV-Vis) spectroscopy, and X-ray photoelectron spectroscopy (XPS). The silver-coated track-etched polyethylene terephthalate membrane was then employed as platform for the detection of the analytes (acetaminophen and 4-aminothiophenol, 4-ATP) by surface enhanced Raman spectroscopy (SERS). The analytes concentration solutions of acetaminophen (1 mg/L, 0.1 mg/L and 0.01 mg/L) and 4-aminothiophenol (10^{-4} M, and 10^{-6} M) were prepared; and Raman spectroscopy was used for the detection of both acetaminophen and 4-aminothiophenol (4-ATP) on the surface of the silver-coated track-etched polyethylene terephthalate membrane. The analyte samples (acetaminophen and 4-aminothiophenol, 4-ATP) were identified when dropped and dried on the surface of silver-coated track-etched polyethylene terephthalate membrane. This is confirmatory of the fact that the detection of acetaminophen and 4-aminothiophenol (4-ATP) by Raman spectroscopy was due to Raman signal enhancement by silver nanoparticles immobilised on the surface of the amine-modified track-etched polyethylene terephthalate membrane.

The study carried out by the capillary electrophoresis instrument revealed the versatility and sensitivity of the CE instruments in the identification, separation and quantification of organic pollutants. In this study, CE showed a better sensitivity than HPLC, and this is evident in the lower LOD values for all analytes in CE compared to the LOD values for

analytes in HPLC. Furthermore, CE methods were successfully applied in the detection of pharmaceuticals and other POPs, and the study confirmed the presence persistent organic pollutants in the both drinking and environmental water samples.



UNIVERSITY *of the*
WESTERN CAPE

KEYWORDS

Bioaccumulation

Capillary electrophoresis

Diethylenetriamine

Endocrine disrupting compounds

Immobilisation

Modification

Organic pollutants

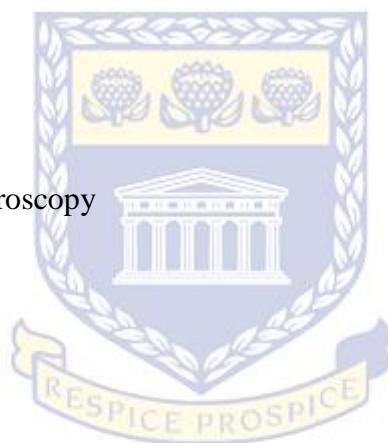
Persistent organic pollutants

Pollutants

Polyethene terephthalate

Surface-enhanced Raman spectroscopy

Silver nanoparticles



UNIVERSITY *of the*
WESTERN CAPE

DECLARATION

I declare that '**Identification, separation and quantification of persistent organic pollutants using capillary electrophoresis**' is my own work, that it has not been submitted for any degree or examination in any other university, and that all the resources I have used or quoted have been indicated and acknowledged by means of complete references.

Emmanuel Oluseyi Omoniyi

December, 2021

Signed.....



UNIVERSITY *of the*
WESTERN CAPE

ACKNOWLEDGEMENTS

I express my utmost gratitude to the Almighty for making this project a reality. I am particularly grateful for his abundant grace and mercy throughout the course of this study.

I also express my honest appreciation to my supervisor, Prof. Leslie Petrik for her mentorship and excellent guidance all through this academic journey. I am grateful for your guidance, tireless commitment to my growth, unwavering support and nourishment given to me throughout the period of this research project. You have instilled in me, the courage to face research challenges and equipped me with the needed expertise to excel in academic research and human capacity development; as a matter of fact, you are second to none. I am eternally grateful. I also appreciate the guidance and mentorship of Dr O. Fatoba and Dr Paul Eze, thank you so much for your wonderful contributions.

I owe a debt of gratitude to Prof Heli Siren of the University of Helsinki, Finland, whose knowledge impartation and immense contributions have made this study a reality; and for availing me the opportunity to tap from her wealth of knowledge. My appreciation also goes to Dr Alexander Nikolaivich Necheav, Dr Olga Artoshina and Arnoux Rossouw for their technical assistance and material support during my research visit to the Joint Institute for Nuclear Research (JINR) in Dubna, Russia.

My gratitude also goes to the entire administrative and technical staff of Environmental and Nano Sciences Research Group (ENS), at the University of the Western Cape; Ilse Wells, Vanessa Kellerman, for their assistance throughout the course of this study. I would also like to thank my colleagues at the Environmental and Nano Sciences Research (ENS) group; Dr Emmanuel Ameh, Dr Chris Bode-Aluko, Jean-Luc Mukhaba, Dr Kassim Badmus, Dr Omoniyi Perea, Dr Cosmas Uche, Dr Emile Massima, Dr Cecilia Ojemaye, just to mention a few.

To the first member and rock of my family, Dr Gifty Omoniyi, I want to thank you so much for being a stakeholder in this journey, and for having my back in whatsoever situation. To my only brother, Hon. Gbenga Omoniyi, thank you for your understanding and assistance all through.

This acknowledgement is incomplete without the recognition of the love, care, prayers, and support of my other sisters, Bukola Adeyemo, Fisayo Olagunju, and Omotayo Ikiwon. You are all precious to me, and without you, this would not be possible.

To my particular friends, Akintunde Awe, Dr Chris Samakinde, Dotun Ibiroonke for standing by me and offering me material and moral support. To Dr Wasiu Afolabi, Dr Jimoh Tijani for their willingness to help at all times. To Rumbidzai Chitongo, for being there always when I needed help. Special thanks to Dr Emmanuel Alechine Ameh for his willingness to assist every now and then.

Finally, I would like to appreciate my mother, Faramade Adunni Omoni, for the uncommon affection, love and support throughout this study.



UNIVERSITY *of the*
WESTERN CAPE

DEDICATION

This thesis is dedicated to:

My mother

Faramade Adunni Omoniyi

And

To her turmoil of motherhood.



UNIVERSITY *of the*
WESTERN CAPE

TABLE OF CONTENTS

ABSTRACT.....	i
KEYWORDS.....	v
DECLARATION.....	vi
ACKNOWLEDGEMENTS.....	vii
DEDICATION.....	ix
TABLE OF CONTENTS.....	x
LIST OF FIGURES.....	xvii
LIST OF TABLES.....	xxiii
LIST OF ABBREVIATIONS.....	xxvii
CHAPTER ONE.....	1
1 Introduction.....	1
1.1 Background to the problem.....	1
1.2 Rationale and Motivation.....	3
1.3 Problem Statement.....	5
1.4 Aim and objectives.....	6
1.4.1 Research objectives.....	6
1.5 Research questions.....	7
1.6 Research approach.....	7
1.7 Research hypothesis.....	8
1.8 Scope and delimitation.....	9
1.9 Thesis outline.....	9
CHAPTER TWO.....	12
LITERATURE REVIEW.....	12
2 Introduction.....	12
2.1 Conceptualization of Emerging Contaminants (ECs).....	13
2.1.1 Characteristics and Classification of Emerging Contaminants (ECs).....	14
2.1.2 Means of Entry into Water Environment.....	19
2.1.3 Pollutants concentrations in water.....	22
2.1.4 Bioavailability and Uptake of Ionisable PPCPs.....	28
2.1.5 Characterization of Effects.....	29
2.1.6 Antibiotic resistance.....	30

2.1.7	Health and Environmental Risks	31
2.1.8	The Means to Improvement	35
2.2	Capillary Electrophoresis (CE)	38
2.2.1	Fundamentals and basic principles of Capillary Electrophoresis	38
2.2.2	Capillary electrophoresis applications	41
2.2.3	Electrophoresis in a Capillary	41
2.2.4	Capillary advantages	42
2.2.5	Electroosmosis (EOF)	42
2.2.6	Electrophoretic Mobility	46
2.2.7	Separation buffers	46
2.2.8	The significance of pH	47
2.2.9	The benefits of CE over conventional techniques	48
2.2.10	Separation Modes in capillary electrophoresis	49
2.2.11	Capillary zone electrophoresis (CZE)	49
2.2.12	Capillary Gel Electrophoresis (CGE)	51
2.2.13	Capillary Isoelectric Focusing (cIEF)	53
2.2.14	Capillary Isotachopheresis (cITP)	54
2.2.15	Micellar Electrophoresis (MEKC)	54
2.2.16	Nonaqueous Electrophoresis	55
2.2.17	Chiral Electrophoresis	55
2.2.18	Conclusion	57
2.3	Recovery and Detection of Pharmaceuticals	58
2.4	Surface-enhanced Raman spectroscopy	59
2.4.1	Raman spectroscopy	59
2.4.2	The Inception of Surface-enhanced Raman spectroscopy (SERS)	60
2.4.3	The active materials for surface-enhanced Raman spectroscopy	62
2.4.4	Silver nanoparticles	64
2.5	The applications of surface-enhanced Raman spectroscopy	67
2.5.1	Polymeric membranes	68
2.5.2	Track-etched polymeric membrane	69
2.5.3	Separation and filtration process in membrane technology	70
2.5.4	Polymer membrane surface modification	70
2.5.5	The Physicochemical techniques for polymer membrane modification	71

2.5.6	Chemical modification methods for polymer membrane surface.....	71
2.5.7	Chemical linkers for polymeric surfaces	73
2.5.8	Metal nanoparticles immobilisation.....	75
2.5.9	Characterisation methods.....	76
2.5.9.1	Scanning electron microscopy (SEM).....	77
2.5.9.2	Transmission electron microscopy (TEM).....	77
2.5.9.3	Ultraviolet - visible spectroscopy (UV-Vis)	77
2.5.9.4	Fourier-transform infrared spectroscopy (FT-IR).....	78
2.5.9.5	Thermogravimetric analysis (TGA).....	78
2.5.9.6	Contact angle measurement	79
2.5.9.7	Raman spectroscopy.....	79
2.5.9.8	X-ray photoelectron spectroscopy (XPS).....	80
2.5.9.9	Zeta potential.....	80
2.6	Chapter summary	80
CHAPTER THREE		83
MATERIALS AND METHODOLOGY.....		83
3	Introduction	83
3.1	Chemicals.....	83
3.2	Instrument and methods (CE)	84
3.2.1	Electrolyte solutions for CE optimisation.....	85
3.2.2	Ionic strengths.....	86
3.2.3	Conditioning of the Capillary	88
3.2.4	Method development:	88
3.2.4.1	Analyses with BGE1 electrolyte (pH 8.5; I = 10 mM)	88
3.2.4.2	Analyses with BGE2 electrolyte (pH 7.5; I = 10 mM)	89
3.2.5	CE analysis methods for steroids, pharmaceuticals and inorganic ions	89
3.2.5.1	Electrolytes for steroids, pharmaceuticals and inorganic ions analyses.....	90
3.2.6	Sampling	90
3.2.7	Sample preparation with solid phase extraction (SPE).....	91
3.3	Preparation of Standard Solutions for CE optimisation	92
3.3.1	Preparation of calibration standards for quantification of aspirin	93
3.3.2	Preparation of the Disprin Sample	94
3.4	Preparation of Standard Solutions and calibration standards for pharmaceuticals analysis using CZE-UV method.....	95

3.5	Concentration calibration for steroids (PF-MEKC-UV).....	95
3.6	Preparation of Standard Solutions and calibration standards for the inorganic ions (CZE-indirect-UV).....	95
3.7	Sample analysis with HPLC.....	95
3.7.1	Sampling	95
3.7.2	Preparation of standard solutions.....	96
3.7.3	Instrumentation and methods.....	96
3.7.3.1	Mass spectrometry (MS)	96
3.7.4	Determination of accuracy, linearity, precision and selectivity.....	97
3.7.5	LOD and LOQ determination	98
3.8	Analysis using SERS.....	98
3.8.1	Materials used for SERS study	99
3.8.1.1	Aminolysis of the polyethene terephthalate (PET) membrane	101
3.8.1.2	Silver nanoparticles synthesis	101
3.8.1.3	Immobilisation of Silver nanoparticles	102
3.8.2	Detection using silver-coated track-etched polyethene terephthalate (PET) membrane by SERS.....	103
3.9	Characterisation.....	104
3.9.1	Contact angle measurements.....	105
3.9.2	Fourier transform infrared spectroscopy (FTIR)	105
3.9.3	Raman spectroscopy	105
3.9.4	Scanning electron microscopy (SEM)	106
3.9.5	Thermogravimetric analysis (TGA).....	106
3.9.6	Ultraviolet-visible spectroscopy (UV-Vis).....	107
3.9.7	X-ray photoelectron spectroscopy (XPS)	107
3.9.8	Zeta (ζ) potential	107
3.10	Chapter summary	108
CHAPTER FOUR.....		109
EFFLUENT WASTEWATER ANALYSIS USING LIQUID CHROMATOGRAPHY-MASS SPECTROSCOPY (LCMS)		109
4	Introduction	109
4.1	Background	109
4.2	Results and discussion.....	111

4.2.1	Optimization of High Performance Liquid Chromatographic (HPLC) Method	111
4.2.2	Chromatograms of standard analyte samples	112
4.3	Recovery studies for standard analytes using Solid Phase Extraction (SPE)	116
4.4	Pharmaceutical analytes present in the water samples.....	117
4.5	Conclusion.....	119
CHAPTER FIVE		120
IDENTIFICATION, SEPARATION AND QUANTIFICATION OF PERSISTENT ORGANIC POLLUTANTS USING CAPILLARY ZONE ELECTROPHORESIS (CZE) AND PARTIAL-FILLING MICELLAR ELECTROKINETIC CAPILLARY CHROMATOGRAPHY (PF-MEKC)		120
5	Introduction	120
5.1	Background	120
5.2	Factors affecting capillary electrophoresis (CE).....	121
5.2.1	BGE1 analysis.....	123
5.2.2	BGE2 analysis.....	123
5.2.3	Repeatability Study results in BGE1 repetition series.....	124
5.2.4	Electrophoretic mobilities in the voltage series for analytes	125
5.2.5	Comparison of background buffer electrolyte (BGE1 and BGE2).....	125
5.2.6	Degree of dissociation of analytes	126
5.2.7	Effect of injection time	128
5.2.8	Effect of injection time in constant pressure injection BGE2.....	129
5.2.9	Effect of voltage in CE	130
5.3	Absorptivity constant (ϵ).....	133
5.3.1	Effect of field strength on electrophoretic mobility.....	134
5.3.2	Effect of constant pressure injection against electrokinetic injection in BGE2	135
5.3.3	Effect of wavelength	138
5.4	Disprin sample quantification	139
5.5	Identification and quantification of pharmaceuticals contents in water: determination with capillary zone electrophoresis (CZE) and UV detection.....	146
5.5.1	Calibration and optimisation.....	146
5.5.1.1	Final optimisation.....	155
5.5.2	Results for repeatability in CAPS 4 replication series for individual standard analyte	159

5.5.3	Concentration linearity and sensitivity for the six standard analytes	163
5.5.4	Recovery studies for standard analytes using Solid Phase Extraction (SPE)..	165
5.5.5	Determination of the pharmaceutical analytes in water.....	166
5.5.6	SPE extractions of hot tap water (HTW), cold tap water (CTW) and milli-Q water (MQW) in CZE analysis	178
5.6	Steroid content in waters of wastewater purification plants: determination with partial-filling micellar electrokinetic capillary chromatography (PF-MEKC) and UV detection	181
5.6.1	Separation parameters optimisation	182
5.6.2	Repeatability in PF-MEKC repetition series for individual steroid standard analytes	185
5.6.3	Concentration linearity and sensitivity	188
5.6.4	Recovery studies for steroid standard analytes using Solid Phase Extraction (SPE).	192
5.6.5	Determination of steroid hormones in water	192
5.7	Inorganic anions and cations quantification in the household water and environmental water samples: Measurement with capillary electrophoresis and indirect-UV detection	204
5.7.1	The background electrolyte solutions and optimization of the separation parameters.....	204
5.7.2	Determination of the inorganic ions with CZE-UV.....	205
5.8	Chapter summary	213
CHAPTER SIX.....		216
APPLICATION OF SILVER NANOPARTICLES-COATED POLYMER MEMBRANE IN THE DETECTION OF ORGANIC POLLUTANTS USING SURFACE-ENHANCED RAMAN SPECTROSCOPY		216
6	Introduction	216
6.1	Track-etched polyethylene terephthalate membrane chemical modification.....	217
6.2	Aminolysis of the track-etched polyethylene terephthalate (PET) membrane.....	219
6.2.1	Analysis using the FTIR	219
6.2.1.1	Study of the reaction times for surface modification	219
6.2.1.2	Modification concentration studies	222
6.2.2	X-ray photoelectron spectroscopy analysis	223
6.3	Silver nanoparticles synthesis and immobilisation on polyethylene terephthalate (PET) membrane.....	227
6.3.1	Silver nanoparticles synthesis and characterisation.....	228

6.3.1.1	Ultraviolet-visible spectroscopy of silver nanoparticles	228
6.3.1.2	Effect of temperature on silver nanoparticles synthesis.....	229
6.3.1.3	Effect of volume of trisodium citrate on silver nanoparticles synthesis	230
6.3.1.4	Effect of reaction time on silver nanoparticles synthesis.....	231
6.3.2	Zeta potential analysis of silver nanoparticles	232
6.3.3	Silver nanoparticles immobilisation and characterisation of track-etched polyethene terephthalate (PET) membrane	234
6.3.3.1	Ultraviolet-visible spectroscopy (UV-Vis)	235
6.3.3.2	X-ray photoelectron spectroscopy of silver-coated modified track-etched polyethene terephthalate (PET) membrane.....	237
6.3.3.3	Scanning electron microscopy (SEM).....	238
6.3.3.4	Thermogravimetric analysis (TGA).....	241
6.3.3.5	Contact angle measurements analysis	243
6.4	Applications of the silver nanoparticles-immobilised PET membrane for the detection of organic pollutants	244
6.4.1	Platform preparation for Surface-enhanced Raman Spectroscopy	245
6.4.2	Acetaminophen detection using silver-coated track-etched polyethene terephthalate (PET) membrane.....	247
6.4.3	Study of concentration for acetaminophen detection.....	248
6.4.4	Study of concentration for 4-ATP detection.....	251
6.4.5	Aminothiophenol (4-ATP) detection using silver-coated track-etched polyethene terephthalate (PET) membrane	252
6.5	Chapter summary	254
CONCLUSION AND RECOMMENDATIONS		256
7	Introduction	256
7.1	Overview	256
7.2	Significant findings of the study	261
7.2.1	Analysis with capillary electrophoresis (CE) and HPLC	261
7.2.2	Analysis with SERS	264
7.3	Recommendations	267
REFERENCES		268
APPENDIX.....		306

LIST OF FIGURES

Figure 2.1: The routes by which pharmaceuticals enter the environment (Boxall, <i>et al.</i> , 2003).	20
Figure 2.2: Simple electrophoresis.	39
Figure 2.3: Principle of Capillary Electrophoresis.	40
Figure 2.4: Separations by capillary electrophoresis.	42
Figure 2.5: EOF as a function of pH.	43
Figure 2.6: Flow profiles in CE (Whatley, 2001).	44
Figure 2.7: Separation with EOF (Whatley, 2001).	45
Figure 2.8: Energy level diagram showing the states involved in Raman spectrum and the elastic and inelastic Raman scatterings (Raleigh, Stokes and Anti-Stokes).	60
Figure 2.9: Monomer structure of polyethylene terephthalate polymer.	69
Figure 2.10: The aminolysis reaction (Drobota <i>et al.</i> , 2013).	73
Figure 3.1: The structures of Tricine (pKa-value 8.15) in pH 7.5 and 8.5 solutions BGE2 and BGE1 respectively. NH can also protonate and form NH ₃ ⁺	86
Figure 3.2: Structure of the compounds used as standards.	93
Figure 3.3: Schematic experimental procedure for surface modification of PET membrane.	100
Figure 4.1: Chromatogram for Acetaminophen.	112
Figure 4.2: Chromatogram for Diclofenac.	112
Figure 4.3: Chromatogram for Sulphamethoxazole.	113
Figure 4.4: Chromatogram for Aspirin.	113
Figure 4.5: Chromatogram for Ibuprofen.	114
Figure 4.6: Chromatogram for 17-β-estradiol.	114
Figure 4.7: Pharmaceutical analyte concentration amounts in the water samples.	118
Figure 5.1: The analyte structures in pH 7.5 and pH 8.5.	128
Figure 5.2: Injection time vs. injection volume for benzylamine (25 kV, 35 mbar).	129
Figure 5.3: Effect of injection time for benzylamine in constant pressure injection in BGE2 (25 kV, 35 mbar).	130
Figure 5.4: Correlation of migration time against voltage (35 mbar).	131
Figure 5.5: Migration times (MT) against voltage plot in BGE1 for the standard analyte mixture (35 mbar).	132
Figure 5.6: Plot of voltage against current in BGE1 for benzylamine (35 mbar, 13 mins). ...	133

Figure 5.7: Electrophoretic mobility against field strength of benzylamine in BGE1 (25 kV, 35 mbar).....	135
Figure 5.8: Plot of peak areas against voltage in BGE2 in electrokinetic injections (35 mbar, 5 secs).....	136
Figure 5.9: Wavelength overlay showing 214 nm as the best for all the analytes.....	138
Figure 5.10: An overlay of the peak heights obtained from different detector wavelengths.	139
Figure 5.11: Degradation of aspirin or acetylsalicylic acid (ASA).	140
Figure 5.12: Calibration curve for acetylsalicylic acid (25 kV, 35 mbar).	141
Figure 5.13: Calibration curve for salicylic acid (25 kV, 35 mbar).....	141
Figure 5.14: Electropherogram of Acetaminophen.	146
Figure 5.15: Electropherogram of Diclofenac.	147
Figure 5.16: Electropherogram of Aspirin and the degradation product Salicylic acid.	148
Figure 5.17: Electropherogram of Ibuprofen.	148
Figure 5.18: Electropherogram of Sulphamethoxazole.....	149
Figure 5.19: Electropherogram of the SAI mixture.	150
Figure 5.20: Electropherogram of the AID mixture.	151
Figure 5.21: Electropherogram of the ASID mixture.	152
Figure 5.22: Electropherogram of the ASIDAS mixture.....	153
Figure 5.23: Peakmaster software showing the migration order for the six MIX analytes. ..	154
Figure 5.24: Electropherogram showing acetaminophen as the first peak and the rest of the analytes co-eluted within the last two peaks.....	155
Figure 5.25: Electropherogram without integration of peaks showing the six standard analytes in their respective order as predicted by the peakmaster.	156
Figure 5.26: Electropherogram with integration of peaks showing the six standard analytes in their respective order as predicted by the peakmaster.	156
Figure 5.27: The overlay of electropherograms from the 8 ppm standard mixture of analytes with different solvent dilution ratios.....	157
Figure 5.28: Electropherogram for influent A sample showing the peaks for the identified analytes including diclofenac, aspirin (ASA), salicylic acid (SA), and sulphamethoxazole.	169
Figure 5.29: Electropherogram for influent B sample showing the peaks for the identified peaks: Diclofenac, aspirin, salicylic acid, ibuprofen and sulphamethoxazole.....	170
Figure 5.30: Electropherogram for effluent sample showing the peaks for the identified peaks including diclofenac, aspirin, salicylic acid, ibuprofen and sulphamethoxazole.....	174

Figure 5.31: Electropherogram profile showing the standards mixture profile (blue) overlay with the influent B sample profile (red).....	175
Figure 5.32: Electropherogram profile showing the standards mixture profile overlay with 2 µg/mL sulphamethoxazole-spiked effluent water sample profile.....	176
Figure 5.33: Electropherogram profile showing the standards mixture profile overlay with 2 µg/mL diclofenac-spiked influent A water sample profile.	177
Figure 5.34: Sulphamethoxazole electropherogram profile overlay of both spiked (blue) and unspiked (red) influent B water sample profiles.....	177
Figure 5.35: Electropherogram profile for Milli-Q water (MQW).....	179
Figure 5.36: Electropherogram profile for cold tap water (CTW).....	179
Figure 5.37: Electropherogram profile for hot tap water (HTW).	180
Figure 5.38: Electropherogram for the steroid standards at 5 ppm concentration. (70 cm capillary length, 25 °C cassette temperature, 25 kV voltage, 30 mM ammonium acetate buffer concentration at pH 9.68, 50 mbar pressure, 10 seconds injection time).	183
Figure 5.39: Electropherogram for the steroid standards at 6ppm concentration.....	184
Figure 5.40: Calibration curve for Androstenedione standard.....	190
Figure 5.41: Calibration curve for Testosterone standard.	190
Figure 5.42: Calibration curve for 17-β-estradiol standard.	191
Figure 5.43: Calibration curve for Progesterone standard.	191
Figure 5.44: Electropherogram for influent A sample showing the peaks for the identified peaks including androstenedione (1), testosterone (2), 17-β-estradiol (3) and progesterone (4).	195
Figure 5.45: Electropherogram for influent B sample showing the peaks for the identified peaks including androstenedione (1), testosterone (2), 17-β-estradiol (3) and progesterone (4).	196
Figure 5.46: Electropherogram for effluent sample showing the peaks for the identified peaks including androstenedione (1), testosterone (2), 17-β-estradiol (3) and progesterone (4).....	199
Figure 5.47: Electropherogram profile showing the steroids standards mixture profile overlay with the influent A sample profile.	200
Figure 5.48: Electropherogram profile showing the steroids standards mixture profile overlay with the influent B sample profile.	200
Figure 5.49: Electropherogram profile showing the steroids standards mixture profile overlay with the effluent sample profile.	201

Figure 5.50: Electropherogram profile showing the androstenedione and testosterone-spiked and unspiked effluent profile	202
Figure 5.51: Steroid hormones concentration amounts in the influent A, influent B and effluent water samples.	203
Figure 5.52: Steroid hormones concentration amounts in the hot tap water (HTW) and cold tap water (CTW) samples.	203
Figure 5.53: Electropherogram showing 2 ppm concentration of the anions' standard	205
Figure 5.54: Electropherogram showing 10 ppm concentration of the anions standard.	206
Figure 5.55: Electropherogram showing the anions profile for river water 2 (RW 2) sample.	207
Figure 5.56: Electropherogram showing the profile for kitchen hot tap water (KHTW)	207
Figure 5.57: Electropherogram showing 15 ppm concentration of the cations standard.....	209
Figure 5.58: Electropherogram showing the cations profile for river water 2 (RW 2) sample.	209
Figure 5.59: Cations in the drinking and environmental water samples.....	211
Figure 5.60: Anions in the drinking and environmental water samples.	211
Figure 6.1: Aminolysis reaction equation.....	217
Figure 6.2: Modification mechanism of PET membrane with DETA and immobilisation of silver nanoparticles on the modified surface.	218
Figure 6.3: FTIR spectra for the unmodified track-etched PET membrane (Con-PET) and the modified track-etched PET membrane at 100% concentration of DETA and varied reaction times 10 hours (10-APET), 15 hours (15-APET), and 20 hours (20-APET).	220
Figure 6.4: The FTIR spectra of unmodified track-etched PET membrane (Con-PET) and modified track-etched PET membranes at 24 hours reaction time and variable concentration of DETA of 100% (100A-PET), 80% (80A-PET), and 60% (60A-PET).	222
Figure 6.5: X-ray photoelectron spectroscopy general survey graphs of unmodified track-etched PET (Con-PET) and modified track-etched PET (100A-PET) showing elements within the detection limits.....	225
Figure 6.6: X-ray photoelectron spectroscopy spectra of N1s peaks of amine-modified track-etched PET (A) and C1s peaks for both unmodified (dotted black) and amine-modified (red) PET membrane (B).	226
Figure 6.7: Ultraviolet-visible spectra of silver nanoparticles synthesised for 20 minutes using 2 mL of 1% trisodium citrate at varied temperatures of 100 °C (100C-AgNP), 90 °C (90C-AgNP) or 80 °C (80C-AgNP).	229

Figure 6.8: Ultraviolet-visible spectra of silver nanoparticles synthesised for 20 minutes at temperature of 100 °C at varied volumes of 1% trisodium citrate of 2 mL (2mL-TriNa), 3 mL (3mL-TriNa) and 4 mL (4mL-TriNa).	230
Figure 6.9: Ultraviolet-visible spectra of silver nanoparticles synthesised at temperature of 100 °C and 2 mL volume of 1% trisodium citrate at varied times of 10 minutes (10-AgNP), 20 minutes (20-AgNP) and 30 minutes (30- AgNP).	231
Figure 6.10: Graphical presentation showing the relationship between zeta potential (mV) of silver nanoparticles and time of synthesis.	233
Figure 6.11: Ultraviolet-visible spectra of track-etched polyethene terephthalate (PET) membranes coated at 100 °C and with 2 mL volume of 1% trisodium citrate for different immobilisation times of 10 minutes (10-AgPET), 15 minutes (15-AgPET), 20 minutes (20-AgPET).	235
Figure 6.12: Graphical correlation of absorbance peak height to time of silver nanoparticle immobilisation.	236
Figure 6.13: SEM images of silver-coated track-etched polyethene terephthalate (PET) membrane prepared at 100 °C and with 2 mL volume of 1% trisodium citrate for samples of A - 10-AgPET (10 minutes), B - 15-AgPET (15 minutes) and C - 20-AgPET (20 minutes).	239
Figure 6.14: SEM images of silver-coated track-etched polyethene terephthalate (PET) membrane prepared at 100 °C and with 2 mL volume of 1% trisodium citrate for samples of D - 25-AgPET (25 minutes) and E - 30-AgPET (30 minutes).	240
Figure 6.15: Thermogravimetric analysis (TGA) graph showing the thermal profile of unmodified track-etched PET (Con-PET), amine-modified track-etched PET (100A-PET) and silver-coated amine-modified track-etched PET (30-AgPET) membranes.	242
Figure 6.16: Chemical structure of acetaminophen.	245
Figure 6.17: Raman spectra of silver-coated track-etched PET membranes at reaction times 10 minutes (10-AgPET), 20 minutes (20-AgPET), 30 minutes (30-AgPET) prepared at 100 °C using 2 mL of 1% trisodium citrate and unmodified PET membrane (Con-PET) as control.	246
Figure 6.18: Raman spectra of 0.1 mg/L of acetaminophen on the surface of Con-PET (unmodified track-etched PET) membrane, Quartz (Non-porous) and 30-AgPET (silver-coated track-etched PET membrane).	248

Figure 6.19: Raman spectra showing variations in peak intensity of different concentrations of acetaminophen in aqueous media 1 mg/L (Acet-001), (b) 0.1 mg/L (Acet-002) and 0.01 mg/L (Acet-003).249

Figure 6.20: The graphical relationship between concentration of acetaminophen and trends in Raman peak height intensity at specific bond vibrations C-O (861), C-O (1170), C-N (1328) and C=C (1608).250

Figure 6.21: Raman spectra showing variations in intensity of different concentrations of 4-ATP in aqueous media 10^{-4} M or 0.0125 mg/L (4-ATP 1) and 10^{-6} M or 0.000125 mg/L (4-ATP 2).252

Figure 6.22: Structure of 4-ATP.253

Figure 6.23: Raman spectrum of 10^{-4} M of 4-aminothiophenol (4-ATP) on the surface of 30-AgPET (silver nanoparticles-coated track-etched PET membrane).253



UNIVERSITY of the
WESTERN CAPE

LIST OF TABLES

Table 2.1: Pharmaceuticals and endocrine disrupting hormones.....	16
Table 2.2: The detected pharmaceuticals in surface water monitoring studies	23
Table 2.3:Reported subtle effects of pharmaceutical compounds on aquatic and terrestrial organisms	25
Table 3.1:Preparation of calibration standard solutions	94
Table 3.2: Gradient elution method	97
Table 3.3: HPLC instrumentation and analytical conditions summary	97
Table 3.4: Track-etched polymer membrane	99
Table 3.5: Quartz:- Silver- coated glass.....	99
Table 3.6: Experimental parameters for modification of polyethene terephthalate (PET) membrane with sample codes, immobilisation of silver nanoparticles and the application of surface-enhanced Raman spectroscopy (SERS)	104
Table 4.1: Structures of acetaminophen, diclofenac, aspirin, salicylic acid, ibuprofen, sulphamethoxazole and 17-beta-estradiol. Theoretical and experimentally measured exact molar masses with retention times	115
Table 4.2: Calibration data for standard analytes	116
Table 4.3: Mean recovery percentages for standard analytes by SPE method	117
Table 4.4: Identification of pharmaceuticals in the Effluent water sample. Determination made with HPLC. Effluent water sample purified with C18 (Strata-X) non-polar sorbent ..	117
Table 5.1: The migration order of the standard analytes	122
Table 5.2: Comparison of electrophoretic mobilities in BGE1 and BGE2.....	126
Table 5.3: The degrees of dissociation for the standard compounds in BGE 1 and BGE 2 ..	127
Table 5.4: Effect of injection time to injection volume	129
Table 5.5: Migration time (MT) against voltage	132
Table 5.6: The intensities and absorptivity constant, ϵ , values for the standard analytes. BGE1 (25 kV, 35 mbar).....	134
Table 5.7: Comparison of constant pressure injection with varying injection times for Benzylamine (pKa = 9.4) using BGE 2 (25 kV, 35 mbar)	137
Table 5.8: Comparison of constant pressure injection with varying injection times for Imidazole (pKa = 7.0) using BGE 2 (25 kV, 35 mbar).....	137
Table 5.9: Comparison of migration times and peak areas in Disprin, Aspirin standard and standard mixture (STD MIX).....	140

Table 5.10: Result of Disprin samples	142
Table 5.11: Average calibration concentration for acetylsalicylic acid and salicylic acid	142
Table 5.12: Calculation of the Acetylsalicylic acid (ASA) concentration in the Disprin™ tablet sample	144
Table 5.13: Electrophoretic mobilities of ASA and SA	145
Table 5.14: Calibration data for Aspirin and Salicylic acid in Disprin.....	145
Table 5.15: Analytes divided into portions.....	149
Table 5.16: Electrophoretic mobility of analytes in different electrolyte methods	158
Table 5.17: Electrophoretic mobility of analytes in CAPS 4 buffer method.....	158
Table 5.18: The migration order of the standard analytes	159
Table 5.19: Results of the replication calculations for Electroosmosis using CAPS 4	160
Table 5.20: Results of the replication calculations for Acetaminophen using CAPS 4	160
Table 5.21: Results of the replication calculations for Diclofenac using CAPS 4	161
Table 5.22: Results of the replication calculations for Acetylsalicylic acid using CAPS4 ...	161
Table 5.23: Results of the replication calculations for Salicylic acid using CAPS 4	162
Table 5.24: Results of the replication calculations for Ibuprofen using CAPS 4	162
Table 5.25: Results of the replication calculations for Sulphamethoxazole using CAPS4 ...	163
Table 5.26: Linear regression calibration data of standard analytes.....	164
Table 5.27: Mean recovery percentages for standard analytes by SPE method	165
Table 5.28: Structures of acetaminophen, diclofenac, aspirin, salicylic acid, ibuprofen and sulphamethoxazole. Theoretical and experimentally measured exact molar masses with migration times in CE.....	168
Table 5.29: Correlation between the electrophoretic mobilities of the standards analytes with influent and effluents water samples.....	170
Table 5.30: Identification of pharmaceuticals in the Influent A sample. Determination made with CZE. Influent A water sample purified with C18 (Strata-X) nonpolar sorbent	171
Table 5.31: Identification of pharmaceuticals in the Influent B sample. Determination made with CZE. Influent B water sample purified with C18 (Strata-X) nonpolar sorbent.....	172
Table 5.32: Identification of pharmaceuticals in the Effluent water sample. Determination made with CZE. Effluent water sample purified with C18 (Strata-X) nonpolar sorbent	173
Table 5.33: Electrophoretic mobilities of the peaks in hot, cold and milli-Q water samples	178
Table 5.34: Electrophoretic mobility of steroid analytes in PF-MEKC-UV	184
Table 5.35: The migration order of the steroid standard analyte.....	185

Table 5.36: Results of the repeatability calculations for electroosmosis using PF-MEKC. (70 cm capillary length, 25 °C cassette temperature, 25 kV voltage, 30 mM ammonium acetate buffer concentration at pH 9.68, 50 mbar pressure, 10 seconds injection time).....	186
Table 5.37: Results of the repeatability calculations for androstenedione using PF-MEKC. (70 cm capillary length, 25 °C cassette temperature, 25 kV voltage, 30 mM ammonium acetate buffer concentration at pH 9.68, 50 mbar pressure, 10 seconds injection time)	186
Table 5.38: Results of the repeatability calculations for testosterone using PF-MEKC. (70 cm capillary length, 25 °C cassette temperature, 25 kV voltage, 30 mM ammonium acetate buffer concentration at pH 9.68, 50 mbar pressure, 10 seconds injection time)	187
Table 5.39: Results of the repeatability calculations for 17-β-estradiol using PF-MEKC. (70 cm capillary length, 25 °C cassette temperature, 25 kV voltage, 30 mM ammonium acetate buffer concentration at pH 9.68, 50 mbar pressure, 10 seconds injection time).....	187
Table 5.40: Results of the repeatability calculations for progesterone using PF-MEKC. (70 cm capillary length, 25 °C cassette temperature, 25 kV voltage, 30 mM ammonium acetate buffer concentration at pH 9.68, 50 mbar pressure, 10 seconds injection time).....	188
Table 5.41: Linear regression calibration data of standard analytes.....	189
Table 5.42: Mean recovery percentages for steroid standard analytes by SPE method	192
Table 5.43: Structures of androstenedione, testosterone, 17-β-estradiol and progesterone. Theoretical and experimentally-measured exact masses with migration times in CE.....	194
Table 5.44: Correlation between the electrophoretic mobilities of the steroid standards analytes with influent and effluents water samples	195
Table 5.45: Identification of steroid hormones in the Influent A sample. Determination with PF-MEKC. Influent water sample purified with C18 (Strata-X) nonpolar sorbent.....	197
Table 5.46: Identification of steroid hormones in the Influent B sample. Determination with PF-MEKC. Influent sample purified with C18 (Strata-X) nonpolar sorbent.....	197
Table 5.47: Identification of steroid hormones in the Effluent water sample. Determination made with PF-MEKC. Effluent sample purified with C18 (Strata-X) nonpolar sorbent	198
Table 5.48: Calibration data of inorganic cations (metals) and anions measured with CZE-indirect-UV methods.....	210
Table 6.1: Sample codes for Fourier transform infrared and X-ray photoelectron spectroscopy with fixed and variable parameters (time of reaction and concentration of diethylenetriamine)	219

Table 6.2: Elemental percentages from X-ray photoelectron spectroscopy for the surface of unmodified (CO-APET) and modified (75A-PET) track-etched PET membranes224

Table 6.3: The changes in peak heights of carbon chemical states227

Table 6.4: Zeta potential of the colloidal silver nanoparticles synthesised at 100 °C and with 2 mL volume of 1% trisodium citrate at 10 minutes (10-ANP), 20 minutes (20-AgNP) and 30 minutes (30-AgNP).....233

Table 6.5: X-ray photoelectron spectroscopy results depicting the percentage of silver relative to immobilisation times on PET membrane surface at 10 minutes (10-AgPET), 20 minutes (20-AgPET), 30 minutes (30-AgPET).....237

Table 6.6: Contact angles measurements of Con-PET, 100A-PET and 30-AgPET samples 243

Table 6.7: Peaks in Raman spectrum of acetaminophen245



UNIVERSITY *of the*
WESTERN CAPE

LIST OF ABBREVIATIONS

AA	Ammonium acetate
AID	Acetaminophen, Ibuprofen, Diclofenac
APTMS	Aminopropyltrimethoxysilane
AS	Artificial sweeteners
ASA	Acetylsalicylic acid
ASID	Acetaminophen, Sulphamethoxazole, Ibuprofen, Diclofenac
4-ATP	4-Aminothiophenol
BDL	Below detection limit
BGE	Background buffer electrolyte
BOD	Biochemical oxygen demand
CD	Cyclodextrin
CE	Capillary electrophoresis
CE-UV	Capillary electrophoresis with UV detection
CEC	Chemicals of emerging concern
CGE	Capillary gel electrophoresis
CiEF	Capillary isoelectric focussing
CITP	Capillary isotachopheresis
CL1TW	Cold laboratory 1 tap water
CL2TW	Cold laboratory 2 tap water
CMC	Critical micellar concentration
COD	Chemical oxygen demand
CTW	Cold tap water
CZE	Capillary zone electrophoresis
CZE-UV	Capillary zone electrophoresis with UV detection
DAD	Diode array detector
DETA	Diethylene triamine
DBPs	Disinfection by-products
DNA	Deoxyribonucleic acid
DW	Drilled well water
DWA	Department of Water Affairs
ECs	Emerging contaminants
EDCs	Endocrine disrupting compounds

EOF	Electroosmotic flow/Electroendoosmotic flow
EPA	Environmental Protection Agency
ESI	Electrospray Ionisation
FTIR	Fourier transform infrared spectroscopy
GC	Gas chromatography
GCMS	Gas chromatography mass spectrometry
GC-MS/MS	Gas chromatography tandem mass spectrometry
HAA	Haloacetic acid
HL1TW	Hot laboratory 1 tap water
HPCE	High performance capillary electrophoresis
HPLC	High-pressure liquid chromatography
HPLC/MS	High-pressure liquid chromatography mass spectrometry
HTW	Hot tap water
KCTW	Kitchen cold tap water
KHTW	Kitchen hot tap water
LC	Liquid chromatography
LC/MS	Liquid chromatography mass spectrometry
LC-MS/MS	Liquid chromatography tandem mass spectrometry
LOD	Limit of detection
LOQ	Limit of quantification
MBR	Membrane bioreactor
MEKC	Micellar electrokinetic capillary chromatography
MQW	Milli-Q water
MS	Mass spectrometry
MS/MS	Tandem mass spectrometry
MT	Migration time
MTBE	Methyltertiarybutyl ether
NHS	N-hydroxysulfosuccinimide
NDMA	Nitrosodimethylamine
NERs	Non-extractable residues
NMs	Nanomaterials
OTC	Over-the-counter
OECD	Organisation for Economic Cooperation and Development
PAHs	Polyaromatic hydrocarbons

PC	Polycarbonate
PCPs	Personal care products
PEG	Polyethylene glycol
PET	Polyethene terephthalate
PF-MEKC	Partial filling micellar electrokinetic capillary chromatography
PF-MEKC-UV with UV detection	Partial filling micellar electrokinetic capillary chromatography
PFCs	Perfluorinated compounds
PFOA	Perfluorooctanoic acid
PFOS	Perfluorooctane sulfonate
PI	Polyimide
POPs	Persistent organic pollutants
PPCP	Pharmaceutical and personal care products
PTFE	Polytetrafluoro ethylene
PVA	Polyvinyl alcohol
ROS	Reactive oxygen species
RW 1	River water 1
RW 2	River water 2
SA	Salicylic acid
SAI	Salicylic acid, Acetylsalicylic acid, Ibuprofen
SDS	Sodium dodecyl sulphate
SDS-CGE	Sodium dodecyl sulphate-capillary gel electrophoresis
SEM	Scanning electron microscopy
SERS	Surface-enhanced Raman spectroscopy
SPE	Solid phase extraction
SPR	Surface Plasmon Resonance
TDS	Total dissolved solid
TEA	Triethylamine
TEM	Transmission electron microscopy
THMs	Trihalomethanes
TGA	Thermogravimetric analysis
TOC	Total organic content
TTAB	Tetradecyltrimethyl ammonium bromide

UHPLC/MS/MS spectrometry	Ultra high-pressure liquid chromatography tandem mass spectrometry
UNEP	United Nations Environment Programme
USEPA	United States Environmental Protection Agency
UV-Vis	Ultraviolet-visible spectroscopy
WHO	World health organization
WWTP	Wastewater treatment plant
XPS	X-ray photoelectron spectroscopy



UNIVERSITY *of the*
WESTERN CAPE

CHAPTER ONE

1 Introduction

This chapter offers a brief background on the scarcity and importance of clean water globally; and the bottlenecks which limit the abundance and availability of potable water are presented.

The chapter also discusses the presence of persistent organic pollutants in water. The background, problem statement, motivations, aims and objectives, research approach, research hypothesis encompassing the scope, delimitations and thesis outline are also detailed.

1.1 Background to the problem

The contamination of water is a major global issue contingent upon the rapid increase in human development, increased urbanisation and industrialisation. This has resulted in unsustainable use of environmental resources and the indiscriminate disposal of contaminated wastewater and solid waste into different environmental matrices. Among the wastes are many emerging contaminants, organic contaminants, nutrients, heavy metals, and others pollutants. The emerging contaminants include phenolic compounds, pharmaceuticals and personal care products (PPCP), veterinary medicines, endocrine disrupting compounds (EDCs), phthalates, flame retardants, perfluorinated and brominated substances, pesticides and herbicides, nanomaterials, amongst others (Houtman, 2010; Fawell & Ong, 2012). The non-availability of clean and fresh water is now a concern globally, attracting scientists' attention all over the world. The unavailability of sufficient and sustainable sources of drinkable water could be linked to factors such as climate change, rapid industrialisation, overpopulation, agricultural practices and lack of functional water treatment plants. It is important to know that in spite of the efforts put in place by various organisations globally, United Nations Environment Programme (UNEP) and World Health Organization (WHO) reported in 2013 that approximately 1.1 billion people cannot access reliable drinking water. It is expected that by 2025, over two-third of the world population will not be able to access drinkable water (Belgiorno *et al.*, 2007; Fawell & Ong, 2012).

In the republic of South Africa, approximately 5.7 million people do not have access to drinkable water, while 17–18 million people lack access to sufficient sanitary services

(DWA, 2012). Amidst the serious concerns of persistent water shortages, the limited available potable water is not usually completely suitable as a result of the presence of low concentration of persistent and emerging contaminants which are potentially harmful to humans and other living organisms (Boithias *et al.*, 2014; Petrie *et al.*, 2015; Steffen *et al.*, 2011). As a result of anthropogenic activities, many chemicals have infiltrated into water bodies. Despite the growing awareness and stringent environmental regulations, environmental pollution still remains endemic; therefore it is imperative to seek urgent interventions. However, the direct discharge of domestic and untreated industrial wastewater containing high pH, high chemical oxygen demand (COD), biochemical oxygen demand (BOD), unpleasant odour, strong colour, total organic carbon (TOC) and certain soluble substances into water bodies continues to impact water quality negatively (Hussaini *et al.*, 2013).

As some harmful chemicals are being phased out, certain new chemicals are being produced to meet human needs. These groups of chemicals are of serious public health concern and are referred to collectively as chemicals of emerging concern (CEC) (Richardson and Ternes, 2011; Kolle *et al.*, 2013). A report by the US Geological survey, (2014), stated that CEC are new chemicals having no regulatory status which modulate the hormonal growth in the endocrine system and disrupt the physiological activities of the endogenous hormones. The advancement of analytical instrumentation and detection techniques has led to the identification and quantification of a sizeable number of CEC at low concentrations in different aqueous matrices as well as drinking water by different scientists (Magureanu *et al.*, 2008; Trapido *et al.*, 2014). Subsequently, the exposure to these chemicals through drinking water, or perhaps, the consumption of food materials irrigated with reclaimed water having these substances has been reported to disrupt hormonal body functions and lead to birth defects, cancerous tumours, early puberty, heart disease, obesity and other abnormalities especially in aquatic species (Kolle *et al.*, 2013; Tijani *et al.*, 2013). In the conceptualisation of emerging contaminants (ECs), chemicals that are legally synthesised are monitored by local and international standards for environmental protection.

The formulation of chemical products is for human, animals and plants' benefit. Meanwhile, once some of these chemicals are released into the environment, they may resist decomposition and undergo bioaccumulation, bioconcentration and persistence in the aquatic environment (Clarke & Cummins, 2015). The health implications of these persistent organic pollutants on humans have been a basis of discussion which demands further investigations.

These persistent organic pollutants have been responsible for many human health deficiencies and health defects, including reduced fertility, low sperm count, reproductive malfunctions and other defects. Consequently, the identification, quantification of these chemicals in their lowest concentrations in the environment is necessary, so that appropriate awareness can be created as to the danger of exposure to humans. Therefore, the environmental wastewaters, industrial wastewater including the effluent being discharged by the wastewater treatment plants (WWTP), containing diverse micropollutants including the endocrine disrupting compounds, must be thoroughly treated before being discharged into the environment.

1.2 Rationale and Motivation

In South Africa, several chemicals of emerging concern have been identified in water and wastewater sources due to industrial processes and disposal of untreated wastewater. Patterton, (2013), conducted a scoping study on emerging contaminants in drinking water in certain cities in South Africa, and discovered over 32 compounds, comprising predominantly pharmaceuticals and pesticides. The presence of these contaminants in water has become life-threatening for humans and the ecosystems. For instance, the veterinary use of diclofenac, known to be a human pharmaceutical and used as an anti-inflammatory treatment, was documented as being responsible for the massive decline in the population of vulture species in some areas of Asia (Oaks *et al.*, 2004). Ethinylestradiol, steroidal estrogen and a derivative of estradiol, one of the active ingredients in the contraceptive pill, is associated with the endocrine disruption in fish (Lange *et al.*, 2001). Ivermectin, a veterinary drug used in the treatment of parasitic infections in livestock, has been revealed to affect the growth of aquatic invertebrates at concentrations lower than those expected to occur in the aquatic environment (Garric *et al.*, 2007). Raghav *et al.*, (2013) classified the emerging contaminants (ECs) with respect to suspected health effects. There is also a growing concern that long-term exposure to antibiotic pharmaceuticals used in human and veterinary medicine may be promoting the selection of resistant bacteria in our environment, and may have significant implications on human health (Boxall *et al.*, 2003). Therefore, there is a need for proper monitoring and quantification of these compounds in our waters to fully understand their chemical properties, degrade, and reduce their impact on human health and ecosystems. It is however a difficult task to monitor organic pollutants in water, as a result of the complexity of most of the organic pollutants. For instance, out of thousands of organic pollutants that may have endocrine disrupting effects, only a few compounds have methods in place to detect and

extract them. With the advancement in detection techniques and analytical instrumentation, a significant number of chemicals of emerging concern (CEC) have been identified successfully and their quantities measured at low concentrations in different water sources including drinking water (Magureanu *et al.*, 2008; Trapido *et al.*, 2014). Exposure to these chemicals through drinking water, or perhaps consumption of food materials irrigated with recycled water containing chemicals of emerging concern have been reported to disrupt hormonal body functions, leading to birth defects, cancerous tumours, early puberty, obesity, heart disease and other abnormalities, especially in aquatic species (Kolle *et al.*, 2013). Regulations have been put in place for industries to recycle and reuse water to minimise the intake of fresh water from rivers by the water utility companies and eliminate the continuous decantation of polluted water into the environment and local river systems (Bell *et al.*, 2011). Wastewater reuse is a possible exposure pathway to a significant number of emerging contaminants and their metabolites. It is important to monitor persistent organic pollutants so as to determine the water's fitness for use. Efforts have been made to detect some of the emerging micropollutants in the water systems in South Africa, but only a few cities in the country have been monitored for some compounds. No studies have been conducted in most other cities relating to micropollutants monitoring, thereby, limiting the information available on all the categories of emerging micropollutants present in South African waters that need to be detected, removed or degraded. When emerging contaminants (ECs) are present in the environment, they are more acidic, or alkaline or polar than natural chemicals. They are designed to be stable and active at small concentrations. They accumulate in lipid-rich tissues owing to their hydrophobic nature therefore, they move up through the food chain (Bao *et al.*, 2015). As a result of their low concentrations, their detection and removal from the environment becomes difficult (Snyder *et al.*, 2004). ECs have been generally quantified by GC/MS and/or GC/MS/MS after solid phase extraction. Therefore, there is a need to develop suitable analytical methods for the identification of these contaminants. The most widely used conventional method of identification and quantification of organic pollutants has been the use of high pressure liquid chromatography (HPLC) and gas chromatography (GC). They are the mostly used methods for the analysis of organic pollutants and proven through the time; however, another method which avoids the limitations of these conventional techniques is the capillary electrophoresis method; which will be explored to carry out the analysis alongside other less well-known methods including Surface-enhanced Raman Spectroscopy (SERS). Capillary Electrophoresis (CE), the modern approach to instrumental electrophoresis, is arguably the most rapidly expanding analytical technique in recent years. It

is a concept that uses electrical field to separate the components of a mixture. Electrophoresis in a capillary differs from other forms of electrophoresis because it is carried out within a narrow tube. Capillary electrophoresis application started in the fields of traditional electrophoresis, and has been extensively applied in the analysis and separation of components such as peptides, proteins, nucleotides and DNA. In recent times, its applications have now spread over as many other areas, invading those typical of chromatography, which include the analysis of drugs and pharmaceuticals (Altria, 1999), and clinical and forensic pharmacology and toxicology (Thorman, *et al.*, 1994). In reality, CE has been successfully applied in the separation of ionic, hydrophilic and lipophilic compounds, including organic and inorganic ions, amino acids, biological amines, biopolymers, drugs and nucleic acids (Tagliaro *et al.*, 1995). However, CE analysis of compounds still requires method development for accurate identification and quantification of chemical compounds (EDCs, POPs, pharmaceuticals, etc.).

1.3 Problem Statement

The significant increase in the production and use of chemically manufactured products, due to the rapid growth in population, industrialisation and extensive agricultural activities has led to the accumulation and presence of different recalcitrant organic pollutants in the environment. In many water and wastewater treatment plants, a variety of organic pollutants have been found and both conventional and novel treatment methods are related directly to the type of compounds found in such effluents. When effluents are passed through different stages of treatment processes, certain contaminants are present in the treated effluents at low concentration which could be harmful to ecosystems and humans. This is attributed to lack of adequate treatment technologies. To adopt suitable treatment techniques, contaminants of priority should be identified first in the effluents. Meanwhile, very few studies have developed methods to rapidly identify various classes of contaminants in water and wastewater treatment plants before and after treatment processes; unlike SERS which have a narrow spectra band for the detection of pollutants in a complex mixture. In some cases where detection methods have been developed, the developed identification methods only target one or two classes of organic pollutants while several other compounds that may have endocrine disrupting and other health effects are yet to be identified. It is necessary therefore, to develop detection and monitoring methods that can be commonly applied to identify and quantify several classes of emerging micropollutants. This will enhance a good understanding

of the effluent composition before and after treatment, as this is beneficial to the development of treatment methods. Moreover, identification of the range of various persistent organic pollutants before treatment or remaining after treatment is significant for method development. A new analytical method using capillary electrophoresis coupled to UV-detector or mass spectrometer to identify various classes of persistent and organic contaminants will be developed in this study. This method will be compared to existing analytical methods to determine the advantage of the new method over the existing ones.

1.4 Aim and objectives

The aim of this research is to separate, identify, and quantify selected persistent organic micropollutants in environment wastewater. This study will also investigate and compare detection/monitoring methods for the selected emerging and persistent contaminants. It will also identify and quantify inorganic ions present in the environmental water samples with the use of capillary zone electrophoresis method with an indirect UV detection (CZE-UV).

1.4.1 Research objectives

The overall objectives will include the investigation of the following aspects:

- To develop a method in CE to identify selected persistent organic pollutants in environmental wastewater before and after treatment.
- To develop clear, concise and suitable effluent sampling procedures.
- To develop suitable extraction procedures for the detection of a variety of emerging micropollutants.
- To compare the separation, identification and quantification of emerging micropollutants using capillary electrophoresis with UV detection, with high pressure liquid chromatography (HPLC) and Surface Enhanced Raman Spectroscopy (SERS).
- To facilitate the separation of different organic pollutants from the aqueous matrix using the capillary electrophoresis system.
- To determine and quantify the inorganic ions (anions and cations) present in the environmental water samples using CE
- To compare the benefits of the new analytical method with existing techniques so as to determine the advantage of the new method over the conventional methods.

1.5 Research questions

This study aims at providing answers to the following questions:

- Which extraction procedure is most suitable for the detection of a variety of emerging micropollutants in wastewater?
- How effective is the capillary electrophoresis system in the separation of organic pollutants?
- What effect would pollutants concentration have on the capillary electrophoresis sensitivity?
- What class of organic pollutants can be separated by capillary electrophoresis (with regards to functionality, hydrophilicity, hydrophobicity, polarity, etc.)?
- Is CE-UV detection mechanism suitable in the capillary electrophoretic system?
- How does the quantification done by HPLC compare to that of capillary electrophoretic system?
- Are the nanoparticles deposited on the modified track-etched polyethylene terephthalate (PET) membrane physically stable?
- Can the modified and nanoparticles-immobilised track-etched PET membrane able to enhance the Raman signal in order to detect trace level analytes in water samples using SERS?
- Can the SERS technique be able to identify and quantify the targeted organic pollutants (pharmaceuticals) from the aqueous matrices?

1.6 Research approach

The following measures were taken to achieve the set aim and objectives of the study:

➤ Sampling and sample preparation

Surface water samples from different points were collected to assess levels of organic pollutants. The water samples were collected into clean 2 L amber coloured glass containers filled to the bottle neck. Each bottle was labelled corresponding to the site where it was collected and rinsed with the site water prior to collection. The samples were filtered on arrival in the laboratory using qualitative Whatman (150 mm) filter paper through vacuum filtration and kept in clean amber coloured bottles in a refrigerator (< 4 °C) until extraction. However, sample preparation and analysis was done within 48 hours of sample collection.

The in-situ physicochemical properties measurement involved the measurement of the conductivity, pH, dissolved oxygen (i.e. to determine whether anoxic or hypoxic), TDS, turbidity and temperature of the water samples using a pH meter.

Solid phase extraction (SPE) was applied for the pre-concentration of the water samples. It was also applied for recovery studies that were conducted in order to assess the efficiency of the method and the SPE cartridges used. Recovery studies were also carried out.

➤ **Optimisation of the instrument and method development**

An efficient and selective method used to detect and quantify the organic pollutants of interest in this research was developed on capillary electrophoresis coupled to UV-detector. Validation tests for the credibility of the method were performed and the calibration curves for the analytes were plotted. Analytical parameters explored included injection temperature, column temperature, pump pressure and the applied voltage that were optimised for the best resolution and detection of specific analytes.

➤ **Separation of contaminants using PET track-etch membrane**

Contaminants or persistent pollutants were pre-concentrated from the aqueous matrix through nanosized pores in the PET track-etch membrane.

➤ **Quantification of organic pollutants after separation**

Capillary electrophoresis coupled to UV-detector or mass spectrometer was employed in the quantification of the organic pollutants. Suitable methods were developed and optimised to achieve the best possible result.

1.7 Research hypothesis

The research questions would be answered by the following hypotheses, based on the literature review carried out:

- Track-etched PET membrane can be used to pre-concentrate analytes (organic pollutants) of low concentration by retaining them on the modified PET surface.
- Capillary electrophoretic system is capable of carrying out the separation of organic pollutants from their aqueous matrices.
- Capillary electrophoretic system coupled to UV-detector or mass spectrometer is capable of quantifying the various organic pollutants.

- Capillary electrophoresis with an indirect UV detection can be used to determine and quantify the inorganic ions in environmental waters.
- SERS is capable of detecting a single molecule, which makes it possible to detect the organic pollutants adsorbed on the SERS substrate.

1.8 Scope and delimitation

This study focused on addressing the limitations of conventional analytical techniques in the detection of organic pollutants present in water in trace amounts before and after treatment. Capillary electrophoretic system was used to carry out the separation of organic pollutants from their aqueous matrices, while the subsequent detection was achieved through the UV-Vis, a diode array detector (DAD), in the capillary electrophoretic system. The track-etched PET membrane was also used to pre-concentrate analytes (organic pollutants) of low concentration by retaining them on the modified PET surface.

This research study only considered the use of capillary electrophoresis methods, which include the capillary zone electrophoresis (CZE) with a direct and an indirect UV detection mechanisms, for the identification and separation of persistent organic pollutants and determination of inorganic ions respectively; partial-filling electrokinetic capillary chromatography (PF-MEKC) for the identification and separation of steroid hormones; high pressure liquid chromatography (HPLC) for organic pollutants; and the use of Surface-enhanced Raman Spectrometer (SERS). The performances of these procedures would be juxtaposed.

1.9 Thesis outline

This thesis is made up of seven chapters which are outlined below:

Chapter 1: Introduction

This chapter gives an insight into the introduction and an overview of the study, including the motivation and objectives of the study, the problem statement, research approach, research hypothesis, scope and delimitations of the study alongside the thesis framework.

Chapter 2: Literature review

This chapter unveils the review of the literature which is relevant to the research study. It is a general overview of the persistent organic micropollutants in their types, including

pharmaceuticals, endocrine disrupting compounds (EDCs), personal care products (PCPs), disinfection by-products (DBPs), flame retardants, perfluorinated surfactants, pesticides, herbicides, nanomaterials (NMs), etc; including their sources, effects and environmental fate is given. An insightful appraisal of selected pharmaceuticals and steroid hormones compounds is covered, including different separation methods such as the capillary electrophoresis, high pressure liquid chromatography (HPLC), Surface-enhanced Raman Spectroscopy (SERS); and literature gaps will also be pointed out in this chapter. The method development relevant to each analytical technique, cutting across the capillary electrophoresis, the conventional analytical methods (HPLC/GC), and the surface-enhanced Raman spectroscopy (SERS), the factors affecting their optimal performances, and their respective methods for the identification, detection and quantification of analytes are given in the literature review.

Chapter 3: Materials and Experimental procedures

This chapter provides the experimental procedures undertaken in the generation of data needed to accomplish the outlined aims and objectives of the study in details. The materials and sampling procedures that were employed, as well as the description of the analytical characterization tools used in the study will also be included.

Chapter 4: Identification, separation and quantification of persistent organic pollutants using the HPLC

This chapter will give the detailed results and discussion of the identification and separation of persistent organic pollutants carried out by high pressure liquid chromatography (HPLC). The pharmaceuticals include acetaminophen, diclofenac, aspirin, salicylic acid, ibuprofen, sulphamethoxazole, and 17-beta estradiol, a steroid hormone. The discussion will detail the procedures including standard preparation, solid phase extraction (SPE), solvent composition effective for the separation of individual analytes, the retention times of the analytes, limits of detection (LODs) of analytes, limits of quantification (LOQs), and the information regarding the method development will be highlighted.

Chapter 5: Identification, separation and quantification of persistent organic pollutants using capillary zone electrophoresis (CZE) and partial-filling micellar electrokinetic capillary chromatography (PF-MEKC); and determination of inorganic ions in water samples

This chapter will outline the optimisation of the capillary electrophoresis (CE) instrument, including the factors affecting the CE instrument; the results and discussion of the identification, separation and quantification of pharmaceutical compounds (acetaminophen,

diclofenac, aspirin, salicylic acid, ibuprofen and sulphamethoxazole), using the capillary zone electrophoresis (CZE) method, and the results of the identification, separation and the quantification of steroid hormones (androstenedione, testosterone, 17- β -estradiol and progesterone), using the partial-filling micellar electrokinetic capillary chromatography (PF-MEKC). In addition, the results of the determination and quantification of inorganic ions in the environmental water samples details are discussed.

Chapter 6: Identification of persistent organic pollutants using SERS

In this chapter, the synthesis and optimisation of silver nanoparticles will be extensively discussed. Also, the detailed discussion of the surface activation of the polyethylene terephthalate (PET) membrane to enhance the sensitivity under Raman spectrometry, and the subsequent immobilisation of silver nanoparticles on the already-activated surface of the PET membrane. Analytes will be preconcentrated on the surface of the silver nanoparticles-immobilised activated PET membrane and detection will be made with Raman spectrometry. These and other relevant procedures will be discussed and detailed in this chapter.

Chapter 7: Conclusion and Recommendations

This chapter highlights the overall findings of the study and the recommendations for further studies on the basis of the outcome of the research investigations are provided.



CHAPTER TWO

LITERATURE REVIEW

2 Introduction

The contamination of water is a major global issue contingent upon the rapid increase in human development, increased urbanization and industrialization. This has resulted in unsustainable use of environmental resources and the indiscriminate disposal of contaminated wastewater and solid waste into different environmental compartments. Among the waste are many emerging contaminants, organic contaminants, nutrients, heavy metals, and many others. These emerging contaminants include phenolic compounds, pharmaceuticals and personal care products (PPCP), veterinary medicines, endocrine disrupting compounds (EDCs), phthalates, flame retardants, perfluorinated and brominated substances, pesticides and herbicides, nanomaterials amongst others (Houtman, 2010; Fawell & Ong, 2012). Sourcing water from unconventional sources has caused health challenges in humans and some biological species.

The non-availability of clean and fresh water is now a concern globally, attracting scientists' attention all over the world. The unavailability of sufficient and sustainable sources of drinkable water could be linked to factors such as climate change, rapid industrialization, overpopulation, agricultural practices and lack of functional water treatment plants. It is important to know that in spite of the efforts put in place by various organizations globally, United Nations Environment Programme (UNEP) and World Health Organization (WHO) reported in 2013 that approximately 1.1 billion people do not have access to reliable drinking water. It is expected that by 2025, more than two-thirds of the world population will be without access to drinkable water (Belgiorno *et al.*, 2007; Fawell & Ong, 2012). In South Africa, approximately 5.7 million people do not have access to drinkable water, while 17–18 million people lack access to sufficient sanitary services (DWA, 2012). Amidst the serious concern of persistent water shortages, the limited available potable water is not usually completely suitable due to the presence of low quantities of persistent and emerging contaminants which are potentially harmful to humans and other living organisms (Boithias *et al.*, 2014; Petrie *et al.*, 2015; Steffen *et al.*, 2011). Despite the growing awareness and stringent environmental regulations, environmental pollution still remains endemic, therefore it is imperative to seek urgent interventions. However, the direct discharge of domestic and

untreated industrial wastewater containing high chemical oxygen demand (COD), biochemical oxygen demand (BOD), unpleasant odour, strong colour, total organic carbon (TOC) and certain soluble substances into the water bodies continues to degrade water quality (Hussaini *et al.*, 2013). As a result of anthropogenic activities, many chemicals have infiltrated into the water bodies. As some harmful chemicals are being phased out, certain new chemicals are being produced to meet human needs. These groups of chemicals are of serious public health concern and are referred to collectively as emerging contaminants (ECs) or chemicals of emerging concern (CEC) (Richardson and Ternes, 2011; Kolle *et al.*, 2013). A report by the US Geological survey, (2014), stated that CEC are new chemicals having no regulatory status which modulate the hormonal growth in the endocrine system and disrupt the physiological activities of the endogenous hormones.

The advancement of analytical instrumentation and detection techniques has led to the identification and quantification of a sizeable number of low concentrations of CECs in different aqueous matrices as well as in drinking water (Magureanu *et al.*, 2008; Trapido *et al.*, 2014). Subsequently, the exposure to some of these chemicals through drinking water, or perhaps, the consumption of food materials irrigated with reclaimed water contaminated with these substances have been reported to disrupt hormonal body functions and lead to birth defects, cancerous tumours, early puberty, heart disease, obesity and other abnormalities especially in aquatic species (Kolle *et al.*, 2013; Tijani *et al.*, 2013).

2.1 Conceptualization of Emerging Contaminants (ECs)

Chemicals that are legally synthesized should comply to local and international standards for environmental protection. The formulation of chemical products is for human, animal and plant use. Meanwhile, once these chemicals are released into the environment, they tend to bioaccumulate/bioconcentrate due to their persistence in the environment (Clarke & Cummins, 2015). Emerging contaminants or chemicals of emerging concern cannot be specifically defined and have no comprehensive list. These terms have been interchangeably used among researchers due to misconception. In the opinion of Houtman, (2010), emerging contaminants do not only mean compounds that are newly developed or detected in the environment; he rather classified them into three categories. The first category is made up of compounds released into the environment recently. The second category consists of compounds already existing in the environment for a longer period of time but have recently

detected as a result of development in analytical techniques. The third category points to compounds in which their negative health effects are just manifesting.

2.1.1 Characteristics and Classification of Emerging Contaminants (ECs)

When emerging contaminants are present in the environment, they may be more acidic, or alkaline and polar than natural chemicals making them fatal at low concentrations. They accumulate in lipid-rich tissues owing to their hydrophobic nature therefore; they are being dynamic through the food chain (Bao *et al.*, 2015). Due to their low concentrations, detection and removal from the environment becomes difficult (Snyder *et al.*, 2004). ECs have been generally quantified by GC/MS and/or GC/MS/MS after solid phase extraction. Raghav *et al.*, 2013 classified the Emerging Contaminants (ECs) with respect to suspected health effects. Numerous substances are used for different purposes in modern life. They include cleaning products of various types, wide range of medicines, cosmetics and personal care products, over-the-counter remedies and prescribed pharmaceuticals that are extensively being used around the world. Other contaminants of emerging concern being included in recent lists are nanoparticles, artificial sweeteners, flame retardants, perfluorinated compounds, and other well-known contaminants such as the fuel additive methyl tertiary butyl ether (MTBE) (Fawell & Ong, 2012). Also, some natural substances excreted by humans such as hormones, are very active biologically. Certain substances in this category possess endocrine activity, and have subsequently raised concerns as a result of the changes observed in fish, in waters containing treated wastewater effluent (Fawell & Ong, 2012). Several types of persistent organic pollutants or emerging contaminants, grouped generally by their initial use, and at times, by structure or mechanism of action include the following:

i. Pharmaceuticals

Pharmaceuticals are a broad range of chemicals which include diagnostic agents, prescribed drugs, veterinary drugs and vitamins which could either be synthetic or natural medicines. They are administered or used for the alteration of physiological and biochemical processes in animals and humans, for the purpose of diagnosis, treatment and prevention of diseases. The occurrence of these pharmaceuticals in aquatic areas, freshwater, groundwater and wastewaters is a clear indication of contamination through excretion of incompletely metabolized drugs or direct disposal of expired and unwanted medicines in household wastes, landfills and toilets. They induce antibiotic resistance to disease-causing organisms and increase the rate of cancer and organ damage (Bound & Voulvoulis, 2005). Their occurrence

in water must be checked on a country-by-country basis. This is because there is a wide variation in what is being used in different countries, and also the means by which they enter the water sources (WHO, 2011a). In some developing countries in Asia, the discharge of pharmaceutical waste into lakes and rivers is reported to be as high as over 30 mg/L in places close to the factory outlets. The concern is that the water may be used in households and also for agriculture (Lubick, 2009).

ii. Endocrine Disrupting Compounds (EDCs)

According to WHO, endocrine disruptors “are exogenous substances or mixtures that alters function(s) of the endocrine system and consequently causes adverse health effects in an intact organism, or its progeny” (WHO, 2002). The endocrine disrupting compounds (EDCs) are diverse group of substances which includes human hormones and a range of industrial chemicals. These chemicals impact and affect the hormonal control, sexual and reproductive behaviour (Bradley & Journey, 2014). EDCs were the first of the emerging contaminants that drew the media attention, owing to the observed feminization of male fish downstream of wastewater discharges. They all have in common the ability to act as hormones or mimic hormones or even to interfere with the endocrine system at different concentrations (Watts *et al.*, 2002). Much less is known about the effects of the EDCs in the environment apart from oestrogenicity. Human oestrogens naturally excreted in the urine as well as artificial oestrogens used in oral contraceptives are the most potent EDCs. Also, there are some other problematic industrial substances such as organotins, detergent building blocks, including the alkyphenols and bisphenol A (Lam *et al.*, 2011).

iii. Personal Care Products (PCPs)

These are often grouped with the pharmaceuticals in “pharmaceuticals and personal care products” (PPCPs). However, they are comprised of a wide range of substances used in domestic cleaning, air-freshening products, make-up, toiletries and other purposes such as insect repellent. The UV/Sunscreen filters in the personal care products act by absorbing, reflecting and scattering UV light. Examples of PCPs include benzophenone-3, octyldimethyl-p-aminobenzoic acid, siloxanes and disinfection products like triclosan. These are used in body sprays, cosmetics, lipsticks and a wide range of home products. The compounds used for the purpose of disinfection, such as chlorophene and triclosan are often used on a larger scale compared to pharmaceuticals. For example, triclosan has been in use for several years in several consumer products, ranging from body creams, deodorants,

perfumes, toothpaste, soap, etc. They get into the aquatic environment through bathing, domestic wastes, swimming, washing, thereby presenting the risk of exposure that leads to endocrine disruption, carcinogenicity, cytotoxicity and genotoxicity (Fawell & Ong, 2012). When some organisms are exposed, there may be an accumulation of these compounds in them; an example of triclosan and chlorophene in bile from bream in the Dutch River Dommel was reported (Houtman *et al.*, 2004).

Table 2.1 shows the details of some pharmaceuticals and endocrine disrupting hormones with their respective quantities reported in different countries.

Table 2.1: Pharmaceuticals and endocrine disrupting hormones

Class	Drug/hormones	Amount reported (µg/L)/ Country
Antimalaria	Artemether Lumefantrine	No immediate report yet.
Analgelsics for pain relief	Acetaminophen Ibuprofen	0.211 (USA), 10.19 (Spain), 10 (USA), 516 (USA), 0.174 (China), 2.5 (Poland), 6.0 (Spain), 70.35 (USA)
Antipyretics for fever reduction	Aspirin Naproxen	0.22 (Germany), 13 (Greek, Spain) <0.1 (USA), 0.958 (EU), 0.108 (Spain), 0.7 (Poland)
Estrogen, Endocrine disrupting hormones	Estradiol Estriol	0.017 (USA), 0.0014–0.002 (Netherlands), 0–0.670 (Ecuador), 0.0002 (USA) 0.0004 (USA), 0.0049–0.0121 (France), 0.005 (USA)
Hormone replacement	Estrone Progesterone	0.0004 (USA), 0.0001–0.00157 (France), 0–0.67 (Ecuador), 0.0001–0.017 (USA) 1.0 (USA), 3.1 (USA), 0.005 (USA)
β-blocker for abnormal heart rhythm	Atenolol	0.4 (Spain), 0.036 (USA), 0.86 (USA), 1.872 (Spain), 0.026 (USA)
Antibiotic for bacterial infection	Metronidazole Tetracycline Amoxicillin	0.176 (Spain), 0.9 (Switzerland) 0.10 (USA), 0.4 (Serbia), 0.69 (Spain), 0.023 (Spain) 0.12 (Spain), 2.69–31.71 (Tanzania)

(Miraji *et al.*, 2016)

iv. Artificial Sweeteners (ASs)

Artificial sweeteners are added into drinks, hygienic products, drugs and foods in order to induce sweetness with low content of calorie. Examples of these artificial sweeteners include aspartame, saccharin, sucralose, cyclamate and stevia. Generally, these substances are used for dental care, diabetes mellitus control, weight loss, reactive hypoglycaemia and cost effectiveness. When they are present in the environment, it serves as an indication for the contamination of wastewater that flows into surface and groundwater (Tran *et al.*, 2014). However, adverse effects associated with artificial sweeteners contamination include cancer risks, glucose intolerance in human health, dysbiosis and weight gain in children (Weihsrauch & Diehl, 2004; Suez *et al.*, 2014; Brown *et al.*, 2010). Tran *et al.*, (2014), reported the occurrence of artificial sweeteners in the range of 47–1640 ng/L in Singapore, 610–3200 ng/L in Germany and 2800–6800 ng/L in Switzerland.

v. Disinfection By-Products (DBPs)

Disinfection agents are oxidizing agents used in the course of water treatment, for example, chlorine and chloramine. Their mode of operation involves the destruction of pathogenic microorganisms and oxidation of taste and odour-forming compounds (Miraji *et al.*, 2016). This forms a disinfectant residue which prevents the further growth or contamination by microbes along the line. However, the reaction between the disinfecting chemicals with natural fluvic acid, amino acids, humic acid, iodide and bromide ions gives rise to DBPs like haloacetic acids, HAAs (chloroacetic acid, bromoacetic acid, dibromoacetic acid, dichloroacetic acid and trichloroacetic acid), trihalomethanes, THMs (bromoform, bromodichloromethane, chloroform and dibromochloromethane), bromates and chlorates (USEPA, 2013). Other DBPs include bromonitromethanes and nitrosodimethylamine (NDMA). However, brominated disinfectants are more harmful than the chlorinated ones, therefore, the use of chlorinated disinfectants is favoured, particularly chloramines (Battaglin *et al.*, 2007). Dermal absorption, direct ingestion and showering are the means through which DBPs get into humans. A continuous exposure for a long time has been associated with genotoxicity and carcinogenic effects (Miraji *et al.*, 2016).

vi. Perfluorinated Surfactants

Perfluorooctane sulfonate (PFOS) and perfluorooctanoic acid (PFOA) are perfluorinated substances that have been used widely as building blocks in non-stick coatings such as grease-repellent coatings, sprays for leather and textiles and dirt-repellent coatings, while

polytetrafluoroethylene (PTFE) is used in fire-fighting foams and non-stick cookware (Fawell & Ong, 2012). These substances are persistent in the environment and are found often in groundwater where they can accumulate. They are unusual owing to the fact that they are water-soluble, but yet extremely resistant to environmental degradation (Fawell & Ong, 2012). There is a growing concern about perfluorinated compounds owing to their persistence, potential for accumulation in organisms and their toxic properties, which include developmental toxicity and possibly carcinogenicity (Skutlarek *et al.*, 2006; McLachlan *et al.*, 2007). Cases of perfluorinated compounds have been reported in surface waters across Europe (Ahrens *et al.*, 2009; Loos *et al.*, 2010; Kwadijk *et al.*, 2010) and they pose a serious problem for groundwater, where they are capable of remaining for a very long time, even when the source is stopped.

vii. Benzotriazoles and Naphthenic Acids

The anti-corrosive agents used industrially and at household scales are benzotriazole and tolyltriazole. Their occurrence in surface water and sewage is due to their high water solubility, resistance to biodegradation and photosensitivity (Miraji *et al.*, 2016). Naphthenic acid is made up of several cyclohexyl and cyclopentyl carboxylic acids which are naturally found in bitumen, crude oils, oil sands and petroleum. Their major uses include paint additive and wood preservation. The primary medium of discharge into the environment is mostly through discharges (Miraji *et al.*, 2016). Weak degradation, corrosion properties, and tailing concentrations are the causes of environmental persistence of naphthenic acid (Jones *et al.*, 2001; Headley & Mcmartin, 2004).

viii. Algal Toxins Produced by Blue-Green Algae

The blue-green algae are also known as cyanobacteria. They occur naturally as photosynthetic simple plants in non-turbulent surface waters. Their ability to fix nitrogen and vertical migration in the water column makes them prevalent in aquatic ecosystems (Miraji *et al.*, 2016). The discharge of nutrient-rich waste into the aquatic environment causes algal blooms. The toxins produced by the blue-green algae include anatoxin, microcystin and saxitoxins. These toxins target the brain, liver and the nervous system, which means that at very low concentrations, adults and toddlers are vulnerable and they were also suspected to cause paralytic shellfish poisoning (Miraji *et al.*, 2016). In the USA, it was reported that approximately 50–75 μg microcystin/L intoxicated aquatic organisms, and may kill fish if

exposed for 24 hours (Rodgers, 2008; Illinois EPA, 2012). The Australian government has set 1.3 $\mu\text{g/L}$ of microcystin as the limit in drinking water (Richardson, 2006).

ix. Perchlorate

Perchlorates occur environmentally both naturally and synthetically. They find their applications in energetic boosters such as explosive, fertilizers, fireworks, rocket fuel, flame and missiles. The available reports about perchlorates show their abundance in aquifers, sewages and natural waters as a contaminant. Perchlorates in the environment are very soluble in water, not volatile and very stable (Miraji *et al.*, 2016). Short time exposure to perchlorates causes eye, respiratory tract and skin irritation, coughing, diarrhoea, nausea and vomiting (EPA, 2014). Perchlorate contamination also disrupts the thyroid ability to produce hormones. Urbansky and Schock, (1999), reported that EPA has set perchlorate risk level of 5 ng/L, which was considered to be below the ion chromatography detection limit. Therefore, owing to the EPA standards, just less than 2.5 ng/L of perchlorate is allowed in the water supply. An average of perchlorate concentration of about 2 $\mu\text{g/L}$ was reported in New York (Parker, 2009).

x. Nanomaterials (NMs)

Nanomaterials have been classified by the US Environmental Protection Agency (EPA) as emerging contaminants. As a result of their unique properties, they are used in a wide range of industrial, scientific and medical applications. Their occurrence as nanoparticles in the environment even though, has no data yet, but there is a major concern about the lack of environmental health and safety data for nanomaterials. Currently, there are not sufficient scientific data to determine if nanomaterials under pragmatic exposure conditions may pose adverse health effects on humans, because there are currently no specific standards or guidelines that regulate nanomaterials. Some major nanomaterials sources having potential impacts to both surface and groundwater result from industrial production, which include carbon black and fullerenes, silica, titanium and zinc oxide (Borm *et al.*, 2006). Certain nanomaterials may also generate reactive oxygen species (ROS) that can lead to cell or membrane damage (Li *et al.*, 2010).

2.1.2 Means of Entry into Water Environment

The persistent organic pollutants may find their way into the environment in a variety of ways, these include agricultural, industrial and urban routes. The discharge into surface waters is one of the primary portals whereby treated wastewater effluent gets into the

environment. Also, some organic pollutants may reach the groundwater through sewers that are leaking and poorly maintained or from poorly designed landfills. An important source of these contaminants found in both surface and groundwater may also be industrial wastewater and sewage. The application of veterinary medicines in animal husbandry is potentially a source of some animal drugs, which could be found in animal manures and slurries; also in other circumstances, it is ultimately a more direct route into surface waters when such substances are used in fish farming in fresh water systems (Fawell & Ong, 2012). The routes by which the the organic pollutants enter the environment is shown in Figure 2.1.

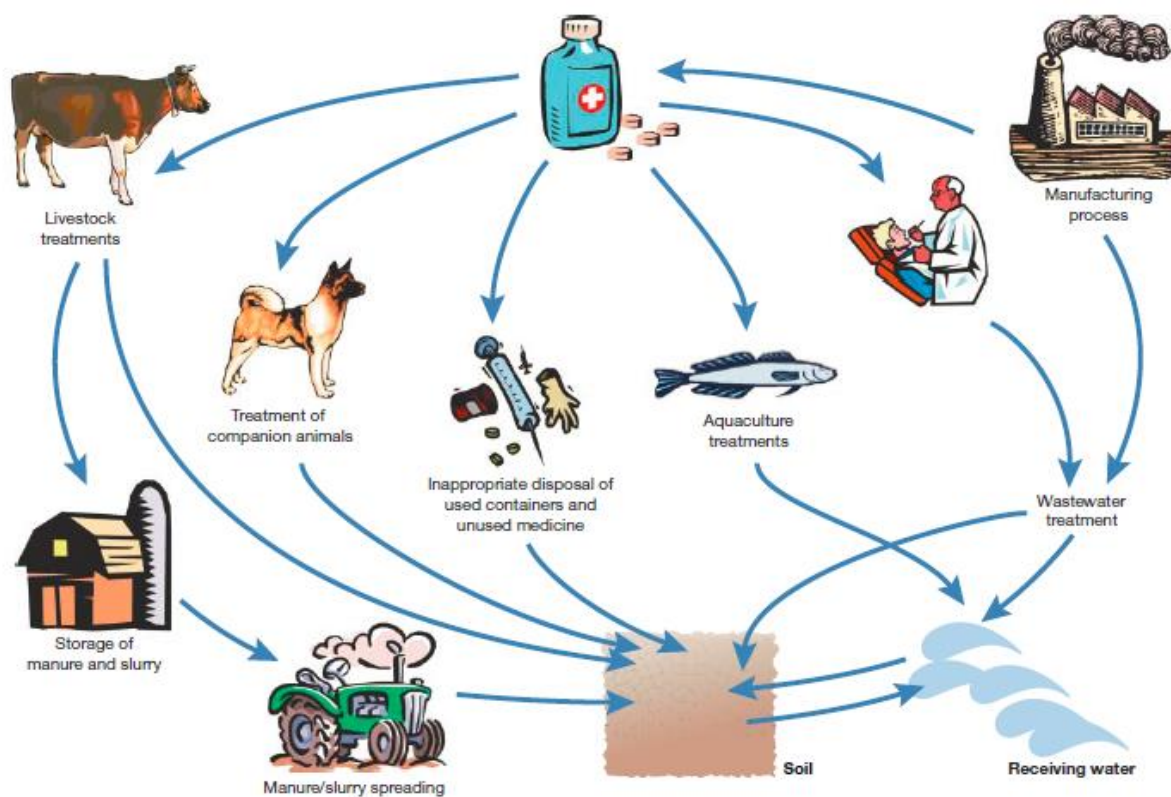


Figure 2.1: The routes by which pharmaceuticals enter the environment (Boxall, *et al.*, 2003).

Furthermore, these persistent organic pollutants enter the sewer system mostly from domestic or industrial portals and there is a possibility for degradation or removal in wastewater treatment. Ingested substances like pharmaceuticals will usually be excreted as the parent compound or as metabolites; the other ones get into the environment through wastewater in the process of washing or showering. However, others usually come from their use in a range of domestic activities which include cleaning and the washing of clothes. Many of these

pollutants will be degraded by biological processes during the wastewater treatment; meanwhile, some of these substances will be broken down only partially or may not even breakdown at all, and therefore will get to the surface water in the treated wastewater discharge. Certain substances like hormones which are excreted as glucuronides or sulphates in order to make them water-soluble, will metabolize into the original compound in wastewater treatment and this reduces the solubility significantly. Furthermore, wastewater treatment efficiency does vary significantly and it is dependent on the kind of technology employed. This applies also to biological systems efficiency by virtue of temperature and storm water dilution (Fawell & Ong, 2012). Low water soluble substances having a high octanol/water partition coefficient tend to adsorb to the solid phase during treatment process, and there will be a continuation of these adsorption and biodegradation processes in surface water systems so the amelioration of concentrations will continue in the environment. Very high concentrations of the active compounds will be present potentially where the treatment is minimal, while glucuronides and sulphates will enable the hormones to stay in solution for a longer period (Fawell & Ong, 2012). Additionally, evidence has been given about some Asian countries where there is an industry for the formulation and manufacture of generic pharmaceuticals having limited controls on discharges, thus these pharmaceutical concentrations may much higher than usual concentrations and certain specific substances may be present in high concentrations. There is a significant variation in the potentials of different water treatment technologies or combinations of treatments for the removal of emerging contaminants in the treatment of water for drinking purposes. Some drinkable water treatment methods may not be efficient enough to completely eliminate some of these contaminants, especially some pharmaceutical compounds. This is as a result of the fact that trace levels of some contaminants have been found in drinking water (Benotti *et al.*, 2009; Kolpin *et al.*, 2002; Kuster *et al.*, 2008; Cooney, 2009).

As a result of the use of pharmaceuticals and other emerging contaminants all over the world, the higher population density is proportional to the potential for these contaminants being present in treated wastewater. In Europe alone, the estimated pharmaceuticals registered for use in human and veterinary medicines are more than 4,000 (Hayward, 2011), but it is uncertain to give an estimation of how many of these are likely to reach the aquatic environment. The expansion of cities and megacities evolution can be a vital yardstick in the assessment of whether these contaminants are present in surface waters. Also, the strain or pressure on water resources from the increasing population and expansion of cities show a

significant increase in the reliance on surface water for drinking. In certain other areas, there is also an effort to plan wastewater re-use for the purpose of water supply, but because the dilution will be less, due consideration should be made of the contaminants which may be present. The WHO already made a proposal and promoted the use of water safety plans as a means of drinking water safety assurance and one of the major steps is to identify the hazards present and the subsequent risks they pose to health (WHO, 2011b).

Some other contaminants classified as emerging contaminants may also follow the same route, an example is human hormones that we excrete, including synthetic hormones used as contraceptive (ethinyl oestradiol). Other forms of contaminants like alkyl phenols may also get into wastewater from industrial wastewater discharged to sewers or by direct discharges. Fluorinated substances such as PFOS and PFOA are examples of a group of contaminants that find their way into groundwater as a result of their use in the environment as detergent building blocks (Fawell & Ong, 2012). One of the sources of this class of contaminants is their use in fire-fighting foams at airports. This has accounted for a measurable build-up of these substances in the groundwater underneath certain airports and aerodromes (Fawell & Ong, 2012).

2.1.3 Pollutants concentrations in water

There are increasing number of reports concerning the presence of pharmaceuticals and other emerging contaminants in drinking water and source water. These reports usually are from ad hoc surveys or some targeted research projects. But till date, no systematic investigations have provided a thorough overview of the occurrence and concentrations of different contaminants in different part of the water cycle over time. Also, routine monitoring studies to measure pharmaceuticals and other emerging contaminants in drinking water is difficult and expensive, and most regulatory agencies do not require them. This makes it difficult to give an account concerning the presence of certain specific substances and their concentrations. These concentrations are very low and vary depending on the dilution in the receiving waters and the extent of use, except in some specific situations. The WHO group of working experts on pharmaceuticals in drinking water gave the conclusion that “available studies have reported that concentrations of pharmaceuticals in surface waters, groundwater and partially treated water are typically less than 0.1 µg/L and concentrations in treated drinking water are generally below 0.05 µg/L” (WHO, 2011a). Furthermore, these are the highest levels of concentrations seen so far, and most of the contaminants present are only at

much lower concentrations. At times, not all the drinking water and source waters contain emerging contaminants; occasions where contaminants are present, they vary in significant concentration and number relative to location and circumstances (Bull *et al.*, 2011; Focazio *et al.*, 2008; Ternes, 2001; Mons *et al.*, 2003). Table 2.2 highlights the pharmaceuticals detected in surface water monitoring studies alongside their maximum concentrations.

Table 2.2: The detected pharmaceuticals in surface water monitoring studies

Class of Drug	Detected Substances	Maximum Concentration ng/L
Antacid	Cimetidine	580
	Ranitidine	10
Antibiotics	Chloramphenicol	355
	Chlortetracycline	690
	Ciprofloxacin	30
	Lincomycin	730
	Norfloxacin	120
	Oxytetracycline	340
	Roxithromycin	180
	Sulphadimethoxine	60
	Sulphamethazine	220
	Sulphamethizole	130
	Sulphamethoxazole	1,900
	Tetracycline	110
	Trimethoprim	710
	Tylosin	280
Analgesic	Codeine	1,000
	Acetylsalicylic acid	340
	Carbamazepine	1,100
	Diclofenac	1,200
	Aminopyrine	340
	Indomethacine	200
	Ketoprofen	120
	Naproxen	390

	Phenazone	950
Antianginal	Dehydronifedipine	30
Antidepressant	Fluoxetine	12
Antidiabetic	Metformin	150
Antihyperlipidemic	Gemfibrozil	790
Antihypertensive	Diltiazem	49
Anti-inflammatory	Ibuprofen	3,400
Antipyretic	Acetaminophen	10,000
Antiseptic	Triclosan	150
Beta blockers	Betaxolol	28
	Bisoprolol	2,900
	Carazolol	110
	Metoprolol	2,200
	Propranolol	590
	Timolol	10
Bronchodilator	Clenbuterol	50
	Fenoterol	61
	Salbutamol	35
Contraceptive	17a-Ethinylestradiol	4.3
Ectoparasiticides	Cypermethrin	85,100
	Diazinon	580,000
	Emamectin benzoate	1,060
Lipid regulator	Bezafibrate	3,100
	Clofibrate	40
	Gemfibrozil	510
Stimulant	Caffeine	6,000
X-ray contrast media	Diatrizoate	100,000

Daughton & Ternes, 1999; Kolpin *et al*, 2002; Boxall *et al*, 2004a.

The incessant large-scale expansion of animal feeding services to solve the problem associated with population increase is responsible for the increase in environmental contaminations brought about by veterinary medicines in the water bodies. In the United States, different classes of antimicrobial compounds could be detected at concentrations

greater than 100 µg/L (Boxall *et al.*, 2003). Their detection in surface water and groundwater samples was more significant, with samples collected near swine and poultry farms at concentrations 1 µg/L in the swine and trace levels in the poultry farms.

Table 2.3: Reported subtle effects of pharmaceutical compounds on aquatic and terrestrial organisms

Substance(s)	Drug class	Reported effect	Reference
Amlodipine	Calcium channel blocker	Inhibition in the ability of dissected polyps from the cnidarian <i>Hydra Vulgaris</i> to regenerate a hypostome, tentacles and a foot	Pascoe <i>et al.</i> , 2003
Avermectins	Parasiticide	Adults insects: loss of water balance, disruption of feeding and reduced fat accumulation, delayed ovarian development, decreased fecundity and impaired mating Juvenile insects: delayed development, reduced growth rates, development of physical abnormalities, impairment of pupariation or emergence and a loss of developmental symmetry	Floate <i>et al.</i> , 2005
Carbamazepine	Analgesic	Inhibition of basal EROD activity in cultures of rainbow trout hepatocytes Inhibition of emergence of <i>Chironomus riparius</i>	Laville <i>et al.</i> , 2004; Nentwig <i>et al.</i> , 2004
Clofibrate	Lipid regulator	Inhibition of basal EROD activity in cultures of rainbow trout hepatocytes	Laville <i>et al.</i> , 2004
Cypermethrin	Ectoparasiticide	Impact on dung decomposition	Sommer & Bibby, 2002
Diazepam	Antianxiety drug	Inhibition in the ability of dissected polyps from the cnidarian <i>Hydra Vulgaris</i> to regenerate a hypostome, tentacles and a foot	Pascoe <i>et al.</i> , 2003
Diclofenac	Analgesic	Inhibition of basal EROD activity in cultures of rainbow trout hepatocytes	Laville <i>et al.</i> , 2004
Digoxin	Cardiac glycoside	Inhibition in the ability of dissected polyps from the cnidarian <i>Hydra Vulgaris</i> to regenerate a hypostome, tentacles and a foot	Pascoe <i>et al.</i> , 2003
17a-Ethinylestradiol	Synthetic steroid	Endocrine-disrupting effects on fish, reptiles and invertebrates	Young <i>et al.</i> , 2002

Erythromycin	Antibacterial	Inhibition of growth of cyanobacteria and aquatic plants	Pomati <i>et al</i> , 2004
Fenbendazole	Parasiticide	Impact on dung decomposition	Sommer & Bibby, 2002
Fenfluramine	Anorexic	Enhances release of serotonin (5-HT) in crayfish which in turn triggers the release of ovary-simulating hormone resulting in larger oocytes with enhances amounts of vitellin In fiddler crabs, stimulates the production of gonad-stimulating hormone accelerating testicular maturation	Daughton & Ternes, 1999
Fenofibrate	Lipid regulator	Inhibition of basal EROD activity in cultures of rainbow trout hepatocytes	Laville <i>et al</i> , 2004
Methyltestosterone	Synthetic steroid	Impersex, reduced fecundity, oogenesis, spermatogenesis in snails	Schulte-Oehlmann <i>et al</i> , 2004
Propranolol	Beta blocker	Weak EROD inducer in cultures of rainbow trout hepatocytes	Laville <i>et al</i> , 2004
Sulphamethazole	Antibacterial	Inhibition of basal EROD activity in cultures of rainbow trout hepatocytes	Laville <i>et al</i> , 2004
Tetracyclines, macrolides and streptomycin	Antibacterials	Antibacterial resistance measured in soil bacteria obtained from sites treated with pig slurry	Sengelov <i>et al</i> , 2003
Tylosin	Antibacterial	Impacts on the structure of soil microbial communities	Westergaard <i>et al</i> , 2001

Table 2.3 shows a wide range of subtle impacts of pharmaceutical compounds on aquatic and terrestrial organisms which research has reported so far, including effects on oocytes and testicular maturation, effects on dung decomposition, impacts on insect physiology and behaviour, inhibition or stimulation of growth in aquatic and algae species and antibacterial resistance development in soil microbes. Also, the steroids coming from contraceptives are suspected to affect the development and fertility of fish, reptiles and aquatic invertebrates. In the same vein, the antibiotics coming from humans and veterinary use have an effect on soil algae and microbes. The account of the effects of other classes of pharmaceuticals is given in the table.

The natural and synthetic hormones are other emerging contaminants found at concentrations in the nanogram-per-litre range. Moreover, the majority of these substances are hydrophobic and have the tendency to adsorb upon particulate matter and sediments. As a result, there may be a reduction in the bioavailability to pelagic organisms, but perhaps can be bioavailable to the sediment-dwelling organisms (Ojemaye & Petrik., 2021).

The breakdown products of alkylphenol ethoxylates used in detergents, which are substances like alkylphenols, nonylphenol and octylphenol, can be found in microgram-per-litre concentrations inside the wastewater effluents and effluents coming from industrial facilities that make use of these materials, also, they will be constantly associated with particles and sediments. It is possible some other substances are found in surface waters proximal to discharges at microgram-per-litre concentrations which frequently reduce upon breakdown, dilution and interaction with sediments. In most developed countries, the groundwater concentrations are much less generally, owing to the fact that many groundwaters are protected or the reduction potential is significant in the soil and the rock in which the water must filter through to reach the groundwater. Also, there would be regions of direct routes to the groundwater as a result of splitting and fracturing, or perhaps where the groundwater is shallow and prone to contamination (Fawell & Ong, 2012). Groundwater becomes vulnerable to contamination if it is constantly affected by surface rainfall.

The concentrations of persistent organic pollutants in drinking water have not been given utmost attention compared to the attention given to the effluents and surface waters. Moreover, some data from Europe and the US show that the levels of persistent organic pollutants detected are well below the concentrations that could be of serious health concern (Bull *et al.*, 2011; Watts & Crane Associates, 2007; WHO, 2011a).

Extensive studies have been done on perfluorinated organic compounds (PFCs) in some Asian countries over the last decade, in contrast to pharmaceuticals. Perfluorooctanic acid (PFOA) happened to be the most dominant compound among the various PFCs found in surface water and aquatic animals which can be detected (Kunacheva *et al.*, 2011; Nguyen *et al.*, 2011). In the majority of the findings, it could be suggested that human and industrial activities revealed proximal correlations to the concentrations found in waters. The detected concentrations were often in the range of 1 – 100 ng/L in lake, reservoir and river water (Nguyen *et al.*, 2011; Zhang *et al.*, 2011), these concentrations were higher generally in dry

weather, compared to season of storm water flow (Nguyen *et al.*, 2011). According to Ericson *et al.*, (2009), perfluorooctane sulphonate (PFOS) was also detected in Asian water bodies and surface water in Europe. PFOA and PFOS estimated concentrations in drinking water in various cities in China ranged from 0.12 to 0.92 ng/L, and the estimated daily intake of PFOA and PFOS through drinking water ranged from 0.006 to 0.15 ng per kg body weight per day (Sun *et al.*, 2011). In the authors' conclusion, it was found that drinking water was a minor source of PFC exposure among the adults in the cities studied. Also, the result of 62 samples of potable water sampled from 34 locations throughout Australia proved a similar conclusion; that the combined PFCs in drinking water was low generally and below 2-5 ng per kg body weight (Thompson *et al.*, 2011). In the surveys where pharmaceuticals have been studied, there are just a few individual substances which have been found in drinking water. Some other substances which have been identified in Europe and the US are of quantities below the lowest clinical dose (Loos *et al.*, 2010; Reddersen, 2002).

2.1.4 Bioavailability and Uptake of Ionisable PPCPs

Bioavailability aims at the prediction of the uptake of ionisable pharmaceutical and personal care products (PPCPs) into aquatic and terrestrial organisms and via the food chains. A substantial amount of PPCPs are ionisable substances. Although there are methods available for the estimation of ionisable compounds uptake into fish and invertebrates (Fu *et al.*, 2009; Meredith-Williams *et al.*, 2012), however, the understanding of the factors and processes affecting the uptake of PPCPs from various environmental matrices into organisms is far less developed than for non-ionisable chemicals (Brooks *et al.*, 2009). Changes in environmental conditions such as the pH, soil and sediment characteristics are also factors which the uptake of ionisable PPCPs is very sensitive to. It is therefore important to focus future work on understanding the uptake routes for PPCPs from a range of matrices into unit organisms and food web that cover different traits; for example, life cycle characteristics, respiration methods, size. These studies should enhance the upgraded models that would enable the estimation of the uptake of ionisable PPCPs into organisms and via food chains.

It is also necessary to probe the bioavailability of non-extractable residues of PPCPs as many of these chemicals spread rapidly in animal manure, biological treatment processes, sediments and soils. The data obtained from degradation studies with radio-labelled PPCPs reveal that, in some instances, the dissipation observed can as a result of the formation of non-extractable residues (NERs) (Kreuzig and Höltege, 2005). These NERs are species of a

chemical which cannot be extracted from a given matrix (soil, sediment, etc.) by methods which do not significantly alter the chemical nature of the residues. Generally speaking, the chemical identities of these NERs are unknown. It is however of serious concern, that in the nearest future, NERs may become bioavailable as a result of the breakdown of biosolid materials added to soils and manures, or perhaps, as a result of alterations in the agricultural practices or the environment (e.g. changes in the ionic strength and pH of a system (Barraclough *et al.*, 2005; Gevao *et al.*, 2000). Efforts are needed to show whether NERs for PPCPs are bioavailable or perhaps are likely to become bioavailable. It is not just for PPCPs risk assessment challenge, but also for other classes of chemicals which include the pesticides (Calderbank, 1989; ECETOC, 2010).

2.1.5 Characterization of Effects

Characterization of effects involves the effort to harness the pharmaceutical preclinical and clinical information to assess the potential for adverse pharmaceuticals environmental impacts. There is a lot of available information from mammalian studies and clinical trials on the behaviour and effects of active pharmaceutical ingredients. Significant resources are devoted by the pharmaceutical industry to gather new and emerging data which forms part of their post-authorization pharmacovigilance programs, also, many epidemiological studies have been done to research the long-term health effects on workers in the pharmaceutical industry (Heron and Pickering, 2003). Contrarily, detailed information on the fate and effects in the environment is available publicly for just a few pharmaceuticals, with a few exceptions, according to the U.K. Veterinary Medicines Directorate Suspected Adverse Effects Reporting Scheme, environmental effects are not examined by the pharmacovigilance programs. Furthermore, if the wealth of data obtained from the clinical trials, mammalian studies and by upgrading the advanced methods for predicting the long-term, low-level effects arising from occupational exposure, it may possibly be established if low levels of pharmaceuticals in the environment pose a threat to the environmental and human health (Ankley *et al.*, 2007; Berninger and Brooks, 2010; Huggett *et al.*, 2003; Seiler, 2002).

Subsequently, it is also necessary to consider how ecotoxicity test methods that reflect the different modes of action of active PPCPs can be developed and harnessed in customized risk assessment strategies. In Europe and North America, the existing risk assessment approaches for PPCPs employ standard Organisation for Economic Co-operation and Development (OECD) test methods for examining effects on organisms (CDER 1998; CHMP 2006; CVMP

2000, 2004). When a certain risk cannot be ruled out by standard tests, certain authorities demand non-standardized studies. Meanwhile, there have been concerns over whether standard methods would identify ecologically important effects of specifically acting PPCPs (Brooks *et al.*, 2009; ECETOC 2008). In the case of the impact of non-steroidal, anti-inflammatory compound diclofenac on vulture populations (Oaks *et al.*, 2004), it is an example of an end point which could not have been predicted from standard studies. Future research work is needed to fully understand the PPCPs effects with different modes of action on both aquatic and terrestrial organisms. As a result of the outcome of research effort, it might be necessary to develop a new set of procedures on the selection of ecotoxicological test methods (species and end points) in the risk assessment process. Moreover, it would be myopic to reserve testing strategies only to methods which reflect specific modes of action because unexpected effects in organisms can take place, as shown by the high potency of fluoxetine, a selective serotonin reuptake inhibitor in algae (Oakes *et al.*, 2010).

2.1.6 Antibiotic resistance

The environmental exposure to PPCP residues may result in the selection of antimicrobial-resistant microorganisms, and maybe vital in terms of human health outcomes. The emergence of antimicrobial resistance as one of the serious concerns of health policies in the future was identified by WHO (1998). The potential for selection of resistant microbial species is one of the major concerns relating to the occurrence of antibiotic compounds in the environment. The antibiotics in the environment may enable the formation of single, cross-, and multiple-resistance in bacteria (Byrne-Bailey *et al.*, 2009; Gaze *et al.* 2011; Knapp *et al.* 2010; Kristiansson *et al.* 2011). Meanwhile, the role of environmental residues of antibiotics in the selection of antibiotic resistance is still unclear, but only available for just a few antibiotics (fluoroquinolones, sulphonamides, etc.). It is important to understand how antibiotic residues in the environment are involved in selecting for antibiotic resistance, and the potential for the acquired resistance to transfer to human and animal pathogens and therefore affect human health. The assessment should be interpreted against the backdrop of antibiotic resistance which are found naturally in the environment or caused by inappropriate clinical use of antibiotics or other environmental contaminants. The human health risks that arise from antibiotic resistance selection by PPCPs in the natural environment can be assessed, but the current regulatory prototypes do not consider the potential for antibiotic resistance selection in soils and surface waters. It is necessary to develop approaches for the consideration of resistance selection in the natural environment serving as an endpoint in the assessment of

safety for new antibiotic compounds, provided the occurrence of antibiotics in the natural environment is portrayed to be an important conveyor for resistance selection.

2.1.7 Health and Environmental Risks

Insight can be gained into how to identify the regions where PPCPs pose the highest risk to environmental and human health, perhaps now and in the nearest future. The risks of PPCPs vary in the environment in various geographical regions as a result of differences in the presence or absence of the level of PPCPs used, manufacturing sites, demographics, cultural practices, climatic and environmental practices, the dilution potential of the receiving environments and the infrastructure related to drinking water and wastewater treatment. Potential risks might change in the long term as a result of factors such as increased urbanization and effluent-dominated in-stream flows (Brooks *et al.* 2006), population increase, increased disease pressure, technological developments (e.g., advancement from small molecules to biologics, drug delivery improvements, nanomedicines improvement) demographic change and climate change. Through the understanding of the drivers for PPCPs exposure in various regions, it is possible to identify those areas which are at the highest risk, which means, control options can be focussed on areas where they would be most effective. Through the effective understanding of how risks would change in the longer term, it is possible to expect and mitigate pre-emptively against unacceptable changes of risks (Boxall *et al.*, 2003).

Considering the importance of PPCPs is needed; relative to some other chemicals and non-chemical stressors in terms of biological impacts in the natural environment. PPCPs are discharged into the environment alongside other chemicals (for example, industrial chemicals, metals, natural hormones, nutrients, industrial chemicals, pesticides). Subsequently, the natural environment is also exposed to non-chemical stressors like the changes in temperature and water flow. The PPCPs effect could be low compared with many other chemicals and non-chemical stressors which are present in the natural environment. It is also important to comprehend the relative impact of PPCPs in comparison to other pressures in a certain situation.

It would also be interesting to probe if the PPCPs pose a threat to wildlife such as amphibians, birds, mammals and reptiles. Majority of the studies have mainly focussed on the effects of PPCPs on fish and invertebrates, but the knowledge of the threats to other wildlife

species, like the birds and small mammals, is less developed. Many studies have stressed the necessity of understanding the effects on birds and mammals (Boxall *et al.*, 2003). For example, the use of diclofenac inappropriately, and the cultural practices concerning the disposal of animal carcasses, in combination with the hypersensitivity of vultures to diclofenac, were responsible for the decline in population of three vulture species in Asia (Oaks *et al.*, 2004), which resulted in cultural, ecological, socioeconomic and human health impacts (Markandya *et al.*, 2008). There are also concerns that antiparasitic veterinary medicines might be involved indirectly, by affecting the population of insect-eating bats and birds by affecting the amount of food available (McCracken, 1993). In order to better understand the exposure of amphibians, birds and mammals to PPCPs, and other potential toxicological effects of the PPCPs on these species, more research work is needed.

When the risks to public health and aquatic populations are being considered, it is important that the first step is to assess the dose and the exposure extent, particularly for mixtures with different types of contaminants (Fawell & Ong, 2012). On the basis of data currently available, the levels of emerging contaminants detected are typically of low concentrations (nanograms to micrograms per litre). For most of these compounds, acute toxicity can only be observed at relatively high doses; however, they are not expected at low environmental concentrations and to assess the risks will be highly technical and demanding as a result of the need for data on long-term exposure (Schriks *et al.*, 2009). Generally, low concentration mixtures are not likely to show any specific impact but rather give additive effects and often when the contaminants have the same toxicity or mechanisms of physiological action.

The risk for adverse effects is much greater for aquatic life owing to the fact that the total dose can be potentially much greater in the organisms that are exposed through the medium they live every time and all through their life cycle. Additionally, substances adsorbed to the sediments may be absorbed by the sediment-dwelling organisms and this has the potential of being magnified through the food chain if the substance is not metabolized. It is clearly evident for the impact of endocrine disrupting compounds on the feminization development in male fish or amphibians, additional evidence is necessary to clarify if this has had a significant impact on their populations. However, on the basis of the mixtures, the studies done on fish exposed to the endocrine disrupting compounds from effluent wastewater do show an additive effect from the same mechanism of action (Fick *et al.*, 2010; Barber *et al.*, 2011). Furthermore, for aquatic organisms, it is supposed that the proximity of organisms to

the source of wastewater effluent will enhance the exposure to the concentration in the diluted flow; whereas, there is the opportunity for further physical, chemical and biological attenuation in surface water and drinking water treatment, this will also lessen the concentration that might get into drinking water. It is certainly evident that some pharmaceutical concentrations found in surface water may be close to concentrations which would be toxic to some aquatic organisms. Therefore, the possible risks to aquatic life prove uncertain but remain possible in certain parts of some receiving waters. Meanwhile, the general impact on the aquatic ecosystem may either be difficult to detect or even negligible, unless the species that are affected remain important to the well-being of that ecosystem and are not readily replaced, perhaps by upstream or downstream recruitment or by a different species which could fill the gap (Fawell & Ong, 2012). Oestrogens are among the most intensely studied group of substances as well as their mimics and effects on fish populations in surface waters. But where there is minimal treatment of sewage or the treatment is bypassed regularly, there is a risk of the concentration being much greater, and therefore, aquatic populations stand the risks of increased adverse effects.

The potential risk posed by drinking water differs between compounds and it is dependent on the concentrations relative to those compounds in the other matrices, relative to exposure volumes and relative to the uptake efficiency after exposure. At this point, effects resulting from human exposure to trace levels of emerging contaminants in drinking water cannot be denied but the effects would be difficult to detect against the natural disease background in human population. A comparative study on an exposure to oestrogenic activity and trace contaminants in US municipal drinking water, beverage, food and air showed that consumption of water accounts only for a small fraction of endocrine disrupting compounds, pharmaceuticals and personal care products (Stanford *et al.*, 2010). It was further buttressed by the same study that there was no visible evidence of adverse effects on human health on the basis of the concentration present in the US drinking waters and the pattern of consumption. The US and European studies support these conclusions (Watts & Crane Associates, 2007; Mons *et al.*, 2003; Bull *et al.*, 2011). Also, the evidence suggests, with regards to endocrine disrupting compounds, that the concentrations in drinking water are too low normally even if detectable at all (Wenzel *et al.*, 2003; Fawell & Chipman, 2000). It is however unclear what the extent of exposure is where there is only minimal sewage or water treatment.

It is however important to mention that the risk assessment for emerging contaminants is capital-intensive and highly technically demanding because their presence is often at extremely low concentrations and very near the detection limits. The invention of new methods to screen the chemicals in water would lead to the discovery of more emerging contaminants in water. Though these compounds are present in water, their presence does not necessarily mean they would facilitate a health risk; it is proposed that they have to be present in an appreciable concentration and over an adequate length of time at that concentration to cause any effects (Fawell & Ong, 2012). If monitoring is going to be prioritized, especially investigative monitoring for emerging contaminants, it is valuable to develop innovative and new methods to enhance early detection of biological activity. The measurement of biological effects of both detected and undetected compounds in water can be enabled by biomonitoring methods. Through this method, the presence of compounds with a wide range of particular effects such as cytotoxicity, genotoxicity, or hormonal activity can be detected before the analysis, using chemical techniques. These methods give a means of attention to the possible effect of compounds with the same mechanism of action, and in certain cases may give an integration of response with time (Fawell & Ong, 2012).

The interest in biomonitoring systems has increased over the past decade as a route to integrating exposure (Petrovic *et al.*, 2002). The purpose of this is to try and improve the detection of unknown or uncharacterized contaminants by their combined biological action and to enable the trust in water quality (Lam *et al.*, 2008). Contrary to the conventional chemical analysis, animal model use may reflect the toxicological effects of contaminants better and permit deduction on human health impact, in theory at least. Systems like these have been successfully tested as acute warning systems for serious pollutant levels that threaten public supplies. Even though, constant and long-term exposure of fish particularly can be effective in checking if anything has been missed, it however requires thorough and detailed biochemical and pathological enquiry which is a bit difficult in small fish (Fawell & Ong, 2012). This can provide an additional means of public reassurance as it is monitoring an integrated vertebrae physiology and histology; however, an extrapolation from fish to humans is probably not simple (Sukardi *et al.*, 2011). Up until now, zebra fish have been used as a model to conduct numerous studies for emerging contaminants and the general results have shown well biomonitoring augmented with chemical assays gives a more explicitly robust system for risk assessment than chemical concentration. It is very important to point out that the majority of these studies were carried out with high ranges of exposure often in

micromolar concentrations. Furthermore, for better risk assessment of low-level chronic exposure with pragmatic concentrations, more systematic investigations are needed urgently. Also, certain substances that affect fish may not be significant for mammals, and vice versa. However, monitoring does not solve these challenges; it can only give vital information about the status of a problem (Fawell & Ong, 2012).

2.1.8 The Means to Improvement

The advancement in analytical capability to identify and quantify nanogram-per-litre concentrations of wide spectrum chemical types has steadily increased the range of substances identified as emerging contaminants (Fawell & Ong, 2012). It is generally costly and equally energy-intensive to employ technologies that are adequate enough to remove or treat persistent trace contaminants in drinking water. As a matter of fact, most available technologies presently are unable to remove many of the emerging contaminants below detection limits of sophisticated analytical instruments. On the contrary, too much emphasis on routine monitoring and perpetual upgrade is not sustainable, even as the emerging contaminants list will continue to evolve (Boxall *et al.*, 2003).

However, it is important to take a careful and systematic evaluation of the potential risk of emerging contaminants in water; as the likelihood of new emerging contaminants will be identified in the future, therefore, dealing with these issues on a case-by-case basis would not offer the best possible long-term or cost-effective solution (Fawell & Ong, 2012). The guidelines by WHO for drinking water quality offer the blueprint for ensuring safe drinking water and this is needed in the development of water safety plans, representing an approach that is proactive and preventive to risk management. These water safety plans are based on comprehensive risk assessment and management from the source to the tap; the first shield to contamination and hazards would be the prevention of source contamination (WHO, 2011b). Therefore, source contamination prevention is considered appropriate as the first and the most detailed means of dealing with the problem in the long term. Both drinking water and the aquatic ecosystem are addressed by this proactive approach.

The three sources of contamination which are regarded as primary sources include wastewater discharges from the industry, wastewater from villages, towns and cities and sewage additions from agriculture, human dwellings and industry; however, there is a requirement for different approach in treating different waste streams (Fawell & Ong, 2012).

A comprehensive method of prevention is to reduce or prohibit the use and release of persistent organic pollutants which can result in extensive contamination and which have biological effects potential. Certain steps are already in place for dealing with some groups of emerging contaminants, for example, alkylphenols and perfluorinated compounds like PFOS to minimize or abolish their use. Sewage is the most important source of emerging contaminants in terms of number and quantity of substances, and sewage collection is a vital step in ensuring hygienic waste disposal. This was one of the key steps employed to improve health around the cities in the 19th century, which allows the sewage disposal and concept for drinking water to be separated. In taking steps to improve the health of city inhabitants, the introduction of sewage treatment (wastewater treatment) and drinking water treatment is key.

It is also important to recognize that methods currently adopted in wastewater treatment are not sufficient enough to guarantee total removal of such contaminants or perhaps reasonable levels of reduction in ensuring aquatic life or human health is not threatened. This shows development of newer and less energy-intensive treatment is necessary so as to deliver a measure of assurance that problems in the nearest future are properly managed. Reasonable coordinated effort in research and the readiness to try new ideas will be required to achieve this aim; although, such concept might take time but the general assessment for health denotes that there is time to follow this route.

In the meantime, there are certain important actions that will be of help generally, for sources which are not centralized like agriculture and industrial discharges, and for wastewater collection and wastewater treatment that are centralized. The establishment of wastewater treatment in places where there is none and to always ensure that these facilities are properly managed and optimized from time to time in order to achieve the required result, are vital factors and there are cost-efficient means of actualising them. Also, education is also a vital part of this exercise. It was a common practice in some parts of Europe in the past to allow chlorinated solvents disposal into pits in order to allow evaporation. But nowadays, we understand that these solvents did not evaporate but rather entered the groundwater; this is no longer acceptable. Having already discussed the control of the persistent organic pollutant use, it is necessary to minimize a range of compounds which are emerging contaminants. The disposal of certain pharmaceuticals that are unwanted into the sewer system is undesirable; and it would be more effective if these drugs were not released at all. Another point of control is to mitigate the amount used which can be achieved by the refusal to embark on over-

prescription of drugs and not administering them in an inappropriate manner which is mostly the case in many veterinary applications. Education regarding responsible drug prescription is also important and it is required that some thought should be considered by health care professionals and consumers in handling pharmaceutical products. By so doing, guidance from the central sources would be an important step in mitigating the quantity and doses of drugs prescribed. Clark *et al.*, (2010) gave an illustration of “green” chemistry, which is another long-term approach in the manufacture and development of chemicals and pharmaceuticals. This would mean that chemicals and pharmaceuticals that are responsive to treatment are designed that they do not persist in the environment. It is more important as suggested that the way forward should be the introduction of regulations for the emerging contaminants. Certain few individual substances may possibly be regulated, it is however unlikely that a substantial range of emerging contaminants can be handled in this fashion.

New discoveries about emerging contaminants in water sources and drinking water at very low levels of concentrations still raise concerns as regards the impact of range and mixtures of contaminants on human health and aquatic life. With the invention of new analytical tools, these emerging contaminants have become mostly recognisable and therefore termed “contaminants of emerging concern” (Fawell & Ong, 2012). Mostly, these compounds are present at concentration levels that seemingly pose no threat to human health, but there are still uncertainties in assessing the risks involved. In some local situations however, the concentrations on individual compounds or certain mixtures might be of immediate concern. But the big question remains concerning the potential impact of multiple components upon aquatic life, though; there is currently increasing evidence of toxic risks on aquatic populations.

The major source of these emerging contaminants is the sewage from human dwellings and industries, although there are other sources. The sources of water prone to contamination are majorly the surface waters contaminated by sewage effluent and diffuse agricultural inputs. Pharmaceuticals and personal care products also attract considerable attention. They reach the sewage primarily through human excretions by humans taking pharmaceuticals or through the drainage of personal care products in effluent waste from domestic and industrial premises. Many of these compounds are broken down, partially at least, in the sewage treatment, while some are resistant. Some of these contaminants are also removed in drinking water treatment depending on the stage of treatment.

Moreover, there is a probability to further identify unrecognized contaminants in the nearest future with an approach different from the existing ones, in order to address trace contaminants such as the residues of pharmaceuticals in drinking water and water sources.

Most importantly, it is imperative to do more in the prevention of contamination in the first place. With the afore-mentioned steps, the establishment and enforcement of environmental protection legislation is needed as well as the installation and operation of wastewater treatment plants at the best possible standard, and mitigating the unnecessary use of substances that are potential emerging contaminants. It is also important for the sake of future, to ensure the improvement of wastewater treatment plants to effectively remove more of the trace organic matter available; however, this should be established on environmentally sound and sustainable systems which are not energy-intensive.

Furthermore, as this study focuses on improving analytical protocols for chemicals of emerging concerns, it is also important to discuss about the identification, separation and quantification of persistent organic pollutants relative to the instruments employed and the analytical methods, including capillary electrophoresis methods, other conventional methods and the Surface-enhanced Raman spectroscopy (SERS).

2.2 Capillary Electrophoresis (CE)

2.2.1 Fundamentals and basic principles of Capillary Electrophoresis

Capillary Electrophoresis (CE) (or high-performance CE, HPCE), the modern approach to instrumental electrophoresis, is arguably the most rapidly expanding analytical technique in recent years (Tagliaro *et al.*, 1995). CE has proved to have great potential, since its introduction, not only in biopolymer analysis, where electrophoresis has long since been applied, but also in areas (e.g. inorganic ion and drug analysis) where electrophoretic techniques have never been used before, for example, inorganic ion and drug analysis (Tagliaro *et al.*, 1998). It is a concept that uses an electrical field to separate the components of a mixture. Electrophoresis in a capillary differs from other forms of electrophoresis because it is carried out within a narrow tube.

In CE, a conductive fluid at a certain pH is fed into a capillary. This fluid represents the buffer solution in which the sample will be separated. However, a sample is introduced into the capillary either by electrokinetic injection or by pressure injection, and a high voltage is then generated over the capillary. Due to this electric field, the sample components migrate through the capillary at different speed. Molecules can be either positively or negatively charged. When the numbers of positively or negative charges are the same, the charges nullify, thereby creating a neutral molecule. When the molecules are given freedom to move, the charged particles seek regions, such as an electrode with an opposite charge that attract the charged particles. For example, Figure 2.2 explains when a mixture of ionic substances is dissolved in a suitable solvent such as water; the motion of these ions is essentially random in the absence of an electric field. But when an electric field is applied, the charged species begin to move. As a result, a crude separation occurs, this results in a less random distribution of charged particles. Cations move toward the cathode and anions move toward the anode. Another aspect of electrophoresis in solution is also illustrated in Figure 2, the significance of the mass charge ratio (m/z). In this figure, four types of charged particles can be identified: large and small positively charged and large and small negatively charged. When the capillary is viewed at a certain place with a detector, the fast components pass first, and later on the slower components.

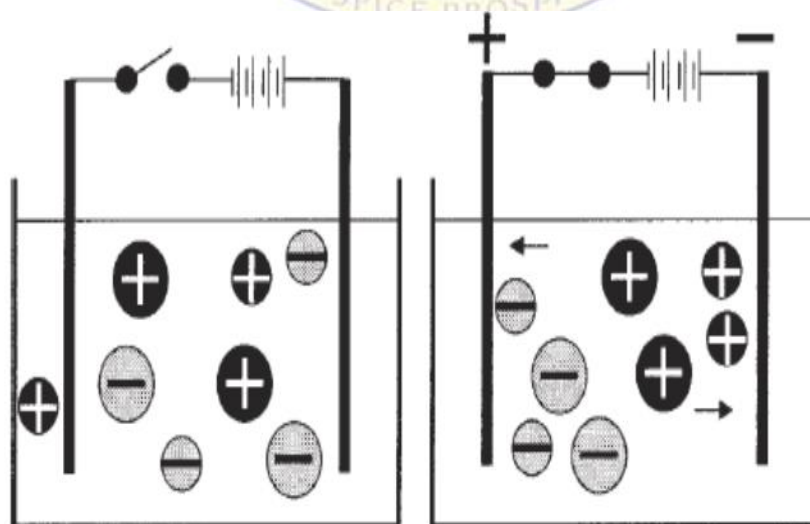


Figure 2.2: Simple electrophoresis.

When each particle possesses a single charge, the absolute value of the electrophoretic force on each particle will be same. The acceleration created by this force is calculated by the

relationship $\text{Force} = \text{mass} \times \text{acceleration}$ ($F = ma$) (Whatley, 2001). The separation medium viscosity opposes the acceleration resulting in a steady velocity being achieved under constant conditions.

This shows that the system cannot only separate particles having opposite charges, but can also separate particles of the same charge provided there are other differences between them. Electrophoresis science is based on creating systems that exploit the differences between molecules. However, the analyst may wish to develop a system which creates differences between molecules alternatively. An example is by varying the pH of the separation method (Whatley, 2001). At the pH of 10.0, glycine and acetic acid will have the same charge (-1). At pH = 7.0, glycine will have a very small net charge whereas acetic acid will still have a charge of -1. Separating these two molecules would thereafter be different at pH = 7.0 and at pH = 10.0.

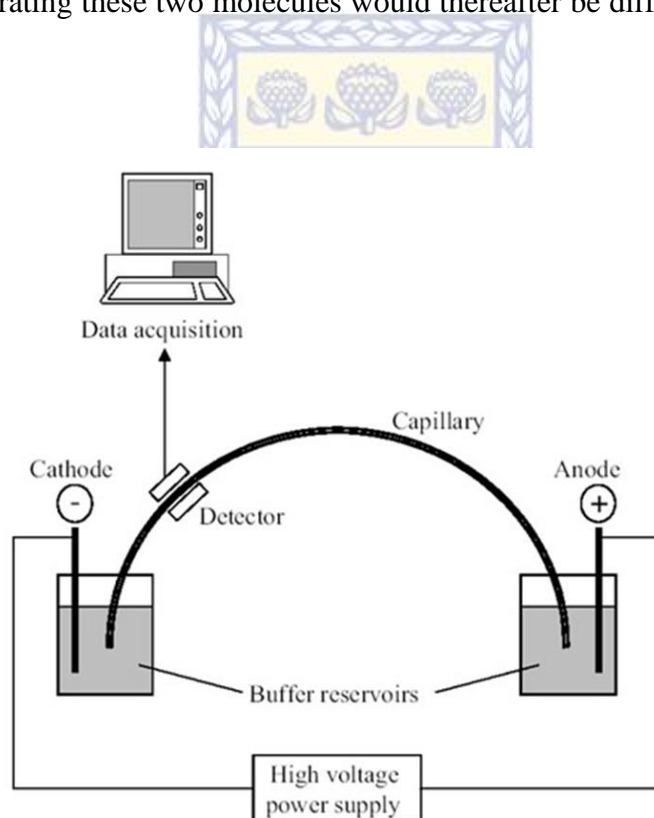


Figure 2.3: Principle of Capillary Electrophoresis.

Figure 2.3 illustrates the principle of Capillary Electrophoresis. The mobility of any component is dependent on the size and charge of such species. This size is a combination of the sample component and the shield of water bound to such component. Generally, the bigger the component, the slower it migrates through the buffer. Another important factor is the charge of ions which strongly depends on the pH value. This is why a buffer at a certain

pH value is used to carry out separations. By altering the pH of a buffer system, the mobilities of the different components can be altered to achieve the best separation. Meanwhile, the best pH for any separation is between the pK values of the components.

2.2.2 Capillary electrophoresis applications

CE application started in the fields of traditional electrophoresis, and has been extensively applied in the analysis and separation of components such as peptides, proteins, nucleotides and DNA. In recent times, its applications have now spread over many other areas, invading those typical of chromatography, which include the analysis of drugs and pharmaceuticals (Altria, 1999), and clinical and forensic pharmacology, and toxicology (Thorman, *et al.*, 1994). In reality, CE has been successfully applied in the separation of ionic, hydrophilic and lipophilic compounds, including organic and inorganic ions, amino acids, biological amines, biopolymers, drugs and nucleic acids (Tagliaro *et al.*, 1995).

Other numerous factors besides pH influence electrophoretic separations, and these include hydrodynamic radius of the molecules, the temperature and the viscosity of the separation medium. Meanwhile, there are other forces in real systems, in addition to the electrical field, acting on the charged molecules, for example, the fluid mass may entirely be moving relative to the vessel in which it is contained. Electrophoresis can be affected by some of these factors in a complex manner; for instance, the temperature of a liquid can be raised by the passage of current through it. The electrical resistance (and hence the current), the velocity and the viscosity of the molecules moving in the field can be influenced by this change in temperature.

2.2.3 Electrophoresis in a Capillary

In addition to the already described features of the capillary electrophoretic process, the small diameter of the capillary and its large aspect ratio (length/width) contribute additional factors. Capillaries formed from fused silica and having an inner diameter (i.d.) of 100 μm or less would also be discussed in this section. Usually, the inner diameter range is from 20-100 μm . The capillaries used in CE are typically circular in cross-section; however, capillaries with square cross-sections have also been produced. These may give additional advantages in terms of thermal regulation and detection sensitivity (Cifuentes & Poppe, 1994), but have not been widely used to date. Figure 2.4 shows the migration profile of two different compounds in the capillary relative to the time of migration.

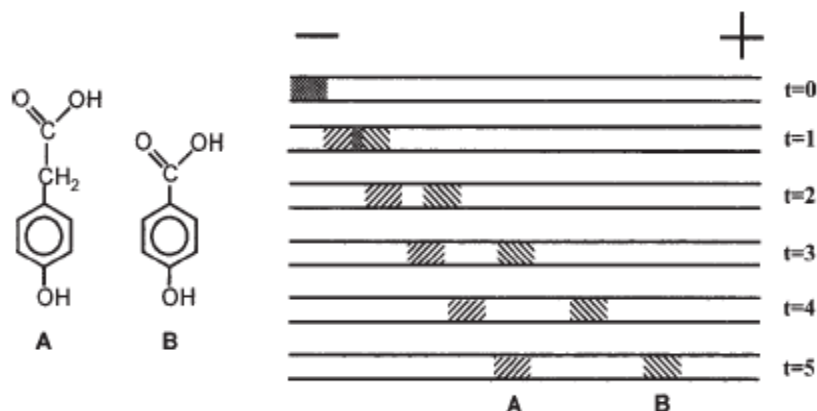


Figure 2.4: Separations by capillary electrophoresis.

2.2.4 Capillary advantages

Capillaries were introduced into electrophoresis as an anti-convective and heat controlling innovation. With the wide tubes, thermal gradients cause band mixing and loss of resolution. Use of glass capillaries of 200–500- μm i.d. was reported by Virtanen & Kivalo, (1969). The introduction of 75 μm capillary tubes was the start of modern “high-performance” CE (Jorgensen & Lukacs, 1981). In Figure 4, the separation of a mixture of two components (both negatively charged) in a capillary is shown. A little amount of sample is introduced and when an electrical field is applied, the components start to move in the field as described earlier. The narrow capillary reduces lateral diffusion and ensures that the differences in temperature between the centre of the capillary and the wall are really small. As a result of the fact that the two components in this example move at different velocities, their separation can be achieved. The geometry of the capillary electrophoretic separation and other properties also lead to a condition known as the “plug flow”. With an ideal plug flow condition, the singular factor leading to sample dispersion is diffusion. And this contributes to the high efficiency of CE separations.

2.2.5 Electroosmosis (EOF)

This is a phenomenon whereby the small diameter of the capillary contributes to the separation process. It is called electroosmosis, electroosmotic flow, or EOF. Electroosmosis exists in any electrophoretic system. It occurs when the liquid near a charged surface is placed in an electric field, which results in the bulk movement of fluid near the surface. Owing to the high surface to volume ratio inside the capillary, EOF becomes a

significant factor in CE (internet ref). The EOF velocity through a capillary is given by the Smoluchowski equation (Smoluchowski, 1905).

$$V_{\text{eof}} = \frac{\varepsilon}{4\pi\eta} \zeta E \quad (2.1)$$

Where ε is the dielectric constant of the electrolyte,

ζ is the zeta potential (Volts),

η is the viscosity (Poise), and

E is the potential applied (Volts/cm).

In CE, the zeta potential (ζ) is a measure of the charge on the wall of the capillary. The charge arises from the nature of the material which composes the capillary as well as the composition of the electrolyte (buffer). Mostly, the commonly used capillary material is fused silica. The fused silica capillary surface can be hydrolysed to give a negatively charged surface. The cations which are hydrated from the electrolyte solution are attracted to the negatively charged wall, thereby creating an electrical double layer. These migrate toward the cathode in an electric field, creating a pumping action by pulling water along. The zeta potential is directly proportional to the density of the charge on the surface. In the case of fused silica and some other materials, charge density will vary with the pH (Lukacs & Jorgensen, 1985). Bare fused silica with a pKa of 6.25 behaves much like a weak acid.

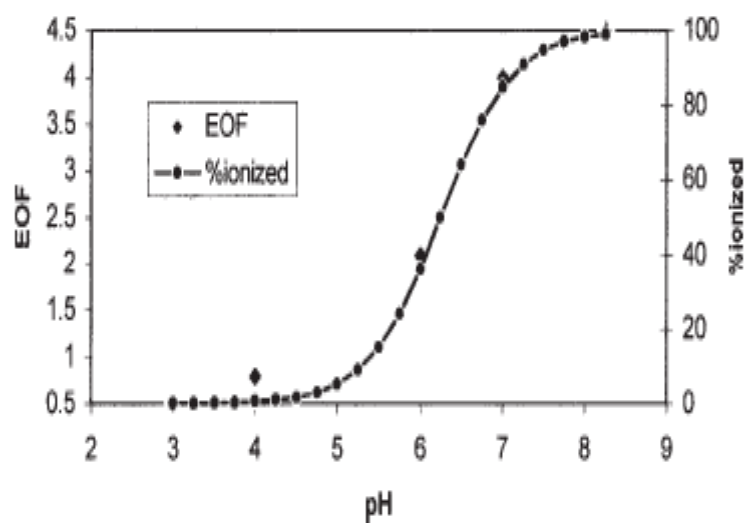


Figure 2.5: EOF as a function of pH.

Figure 2.5 shows the relationship between EOF and pH. EOF decreases with the square root of the concentration of the electrolyte, i.e., when the buffer concentration increases, the velocity of the EOF decreases. The previous discussion has focussed on bare fused silica capillaries, but some other types of surfaces can be chemically created from fused silica, and the new surface may be positive, negative or neutral. Therefore, the direction of the EOF will depend on the sign of the charge on the wall of the capillary. However, the flow is generally toward the electrode having the same charge as the capillary wall. This suggests in theory that an uncharged wall has no EOF, which is difficult to accomplish in reality (Whatley, 2001). An illustration of the comparison of laminar flow and plug flow is shown in Figure 2.6.

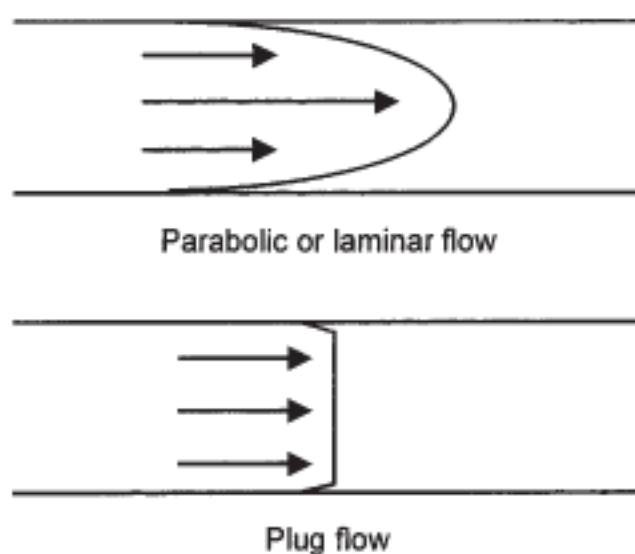


Figure 2.6: Flow profiles in CE (Whatley, 2001).

Within the narrow confines of the capillary, the liquid velocity is almost uniform across the internal diameter of the capillary which results in what has been termed the “plug flow” (Jorgensen & Lukacs, 1981). Whereas, this is contrasting to the laminar flow exhibited by pumped systems that creates a velocity profile across the diameter of the tube. The plug flow, on the other hand, greatly reduces the band broadening seen in systems such as high-performance liquid chromatography (HPLC) that are pumped by a pressure differential.

In practice, it is difficult to eliminate the EOF completely, even though, it can be reduced to a near zero level. But in many separations, it is a significant factor and it may affect the net movement of the analyte molecules more than the electrophoretic force does. These vector

movements that are principally due to the electrophoretic and electroosmotic forces, may as well be in opposite directions (Whatley, 2001).

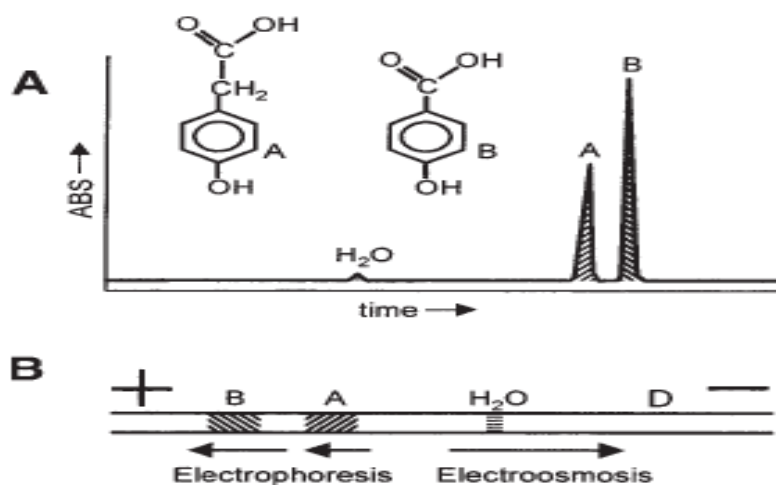


Figure 2.7: Separation with EOF (Whatley, 2001).

The illustration in Figure 2.7A shows the separation of two negatively charged species in a fused silica capillary at pH 8.3, and both analytes have a charge of -1 under these conditions. In this case, the EOF is toward the cathode while the analytes move toward the anode electrophoretically. The contribution of the EOF is larger than the electrophoretic movement, therefore the net movement is toward the cathode. The tiny peak labelled H₂O represents the water used in dissolving the sample. The water plug does not possess any electrophoretic mobility and the movement of this plug is ultimately due to the electroosmotic flow (EOF), and also the first peak to reach the detector. The following peak A to emerge has the higher mass/charge ratio of the two analytes. However, this is in contrast to the situation where there is no EOF (Figure 2.1), the first peak to emerge in such scenario would have a lower mass/charge ratio. It can also be noted that the polarity of the electrodes have been reversed compared to the situation in Figure 2.1. In Figure 2.7B, a snapshot of the inside of the capillary during separation is shown before any peak reached the detector (D). Owing to the fact that Figures 2.7A and 2.7B are influenced by both EOF and electrophoretic force; their resultant movement is the sum of the electroosmotic and the electrophoretic vectors (Whatley, 2001).

2.2.6 Electrophoretic Mobility

In capillary electrophoresis, the theory basically is that when the electric field is applied to a solution of charged molecules, the movement starts. However, the factors governing the mobility of the ion are its charge-to-size-ratio (size is dependent on the molecular weight), the degree of solvation and the three-dimensional structure (Whatley, 2001). The electrophoretic mobility forms a balance between the electromotive and frictional forces and can be given as:

$$\mu_{ep} = \frac{q}{6\pi\eta r} \quad (2.2)$$

Where q = net charge,

η = viscosity,

r = ionic radius.

Based on their electric charge and the differences in the electrophoretic mobilities, smaller ions move faster than the larger ions and oppositely-charged ions move in opposite directions. The efficiency of separation can be expressed as the number of theoretical plates (N), and therefore related to the applied voltage (V), the mobility (μ) and the diffusion coefficient (D) by the equation:

$$N = \mu V / 2D \quad (2.3)$$

In Equation 2.3, it can be deduced that when high voltages are applied, efficient separation can be achieved. Therefore, it is adopted for the separation of large and small molecules (Malik & Faubel, 2001).

2.2.7 Separation buffers

The significance of the capillary wall in controlling the process of CE separation cannot be overstated, and the separation takes place in the separation buffer. The conditions in the buffer are such that the differences in mobility can exist. The quality of the buffer employed in CE is independent of the instrument system used. The buffer can either be made or purchased. As such, the best instrument system however cannot perform effectively with a poorly prepared buffer.

Buffers are compounds generally employed to control the pH of a solution. They are either weak acids or weak bases which can accept or donate protons. They reduce the change in pH that is caused by the introduction of additional acid or base. CE buffers are selected on the basis of the range of pH to be maintained in addition to other factors (Whatley, 2001).

CE systems use a wide range of buffers, with the most commonly used including acetate, borate, citrate, phosphate and Tris (trishydroxymethylamino methane). Meanwhile, zwitterionic buffers possess the advantage of carrying less current compared to mono-functional buffer molecules. The selection of a buffer for CE systems should however be based on certain factors which include: desired pH value; operating temperature; buffer charge relative to the analytes and the capillary wall; and the effects on detection.

When the composition of the buffer has been selected, it is necessary to prepare the buffer properly. In order to make the buffer consistent, it is necessary to make the buffer the same way everytime (Whatley, 2001).

The concentration of a buffer is directly proportional to the buffering capacity of the system, which makes it unlikely to alter the pH with any addition of acid or base. Additionally, some other factors in CE can be affected by the concentration of the buffer (VanOrman *et al.*, 1991; Ferguson *et al.*, 1980). They can be critical factors when trying to achieve an optimum resolution and reproducibility (Whatley, 2001).

When the composition of the sample plug is different from the composition of the buffer in a capillary, stacking phenomenon may occur (Vinther & Soeberg, 1991A; Vinther & Soeberg, 1991B). When stacking is properly exploited, it can result in sharper peaks and greater sensitivity. To achieve stacking, the conductivity of the sample should be kept lower than the conductivity of the running buffer by reducing the concentration of the sample buffer relative to the run buffer.

2.2.8 The significance of pH

In CE, the proper control of pH is important as it affects the analyte charge, electroosmotic flow, also, by affecting current and heat production. Therefore, slight changes in pH tend to have much greater impact in CE than comparable pH variations in HPLC. Figure 2.5 displays the titration curve for a silica surface that behaves like a typical weak acid (e.g., acetic acid). At the ionization of acetic acid with pKa of 4.76, the analyte will be 50% charged.

Meanwhile, it does not mean each molecule carries one-half of a charge, but instead, at any point in time one-half of the molecules are charged and the other half are uncharged (Whatley, 2001). The titration curve shown in Figure 2.5 depicts the probability that any given molecule will be charged at a given pH. A molecule is said to be under the influence of the electroosmotic flow, but not the electrical field, when the molecule is uncharged. But when the molecule is charged, it responds to both forces. As the time fraction in which the molecule spends in each state varies with pH, the net migration velocity changes (Whatley, 2001).

2.2.9 The benefits of CE over conventional techniques

In terms of development when compared to other conventional methods of analysis, CE can be broadly defined to be in a refining stage; with routine implementation in certain areas. These areas include chiral analysis DNA analysis, metal ion/inorganic anion analysis and clinical applications, CE can always be proved to be an obvious improvement over rival techniques, in terms of cost, efficiency, reliability and routine methods have also been established (Altria, 1999). Among a number of merits CE possesses over other traditional analytical methods include: analysis of solutes with limited UV chromophores, reduced operating costs, a reduced method development time, low solvent consumption and higher separation efficiencies (Altria, 1999). Capillary electrophoresis is also superior to other separation techniques in many regards; CE is more effective compared to common liquid and gas techniques as a result of its maximum theoretical plate number. The limit of detection of CE is one-thousandth that of GC or HPLC, the capillaries can also be conditioned easily with buffer before the analysis starts. With CE, nearly one-thousandth of the solvent is used compared with HPLC and the detection limit as low as 10 yoctomolar (10×10^{-24} M) levels (six molecules) may be attained using laser-induced fluorescence detection devices. Also, a wide range of analytes can be easily analysed with CE.

The major drawback of capillary electrophoresis is that it is affected by the mode of its detection system. This is because the CE laser-induced fluorescence and photothermal systems produce sensitive detection at the trace levels, but other detection systems are incapable of adequate detection limits (Malik & Faubel, 2001)

2.2.10 Separation Modes in capillary electrophoresis

While using the same CE hardware, several modes of separation can be carried out, based on different physico-chemical principles by changing the buffer and/or the capillary. Basically, capillary zone electrophoresis (CZE), including separations based on inclusion complex formation, capillary electrochromatography (CEC), micellar electrokinetic chromatography (MEKC or MECC), capillary gel electrophoresis (CGE), capillary isoelectric focusing (CIEF) and capillary isotachopheresis (CITP) can all be accomplished with a capillary electropherograph (Tagliaro *et al.*, 1998).

2.2.11 Capillary zone electrophoresis (CZE)

Capillary zone electrophoresis (CZE) is essentially high voltage electrophoresis in free solution. In this method, the capillary is filled with the running buffer solution, so that the ionic analytes can be separated under high electric fields (hundreds of volts per centimetre) based on their electrophoretic mobilities. The outstanding heat dissipation, as a result of the favourable surface-to-volume ratio, and the fundamental anticonvective characteristics of the capillary allows the attainment of high efficiency separation (usually, hundreds of thousands of theoretical plates) without using gels as anticonvective media (Tagliaro *et al.*, 1998). It can also be said to be characterised by the use of open capillaries with relatively low viscosity buffer systems. Analyte molecules migrate from one end of the capillary to the other relative to the vector sum of electrophoresis and electroosmotic mobility (Whatley, 2001). The electrophoretic migration velocity (v) of a charged particle is dependent on its electrophoretic mobility (μ_e) and the applied electric field (E):

$$v = \mu_e E \quad (2.4)$$

For weak acids and weak bases, the effective charge on the molecule and also its effective mobility is dependent on the degree of dissociation of the different ionisable groups, as given in the equation:

$$v_{\text{eff}} = \alpha \mu_e \quad (2.5)$$

where α is the degree of dissociation, and is dependent on the pK_a of the groups and on the pH of the buffer (Whatley, 2001).

Apart from electrophoretic migration, a basic factor in CZE is the electroosmosis (or electroendoosmosis), which emanates at the capillary wall, thereby giving rise to the EOF. Though ultimately variable in dependence of experimental conditions, EOF is mostly in the order of fractions of $\mu\text{L}/\text{min}$, therefore can be measured empirically by injecting a neutral marker. A distinct characteristic feature of the EOF is that its flow profile is nearly flat and not parabolic like the laminar flow which is generated by pressure. This is a characteristic feature which is greatly of benefit in limiting band broadening during electrophoretic migration and also in assuring high efficiency (Whatley, 2001).

The capillary electropherograph set-up is usually with injection at the anodic end and detection close to the cathodic end of the capillary. While taking into cognizance that EOF is ultimately directed towards the cathode and its mobility is greater than that of most analytes, it then follows in the order of cations, neutral species then anions, in this manner, passing through the detector in the same run. Apparently, the migration velocities of cations and anions are dependent on their electrophoretic mobilities, on that of EOF, the applied voltage and the capillary length. The entire neutral species migrate at the same velocity as the EOF, in a single band (Whatley, 2001). The following equation shows the migration velocity of the analytes in the presence of the EOF:

$$v = \frac{(\mu_{eo} + \mu_e)V}{L} \quad (2.6)$$

Where μ_{eo} = mobility of the EOF; μ_e = mobility of the analyte; V = applied voltage (potential); L = capillary length.

It is possible to control the EOF effectively by changing several experimental conditions, including: buffer pH (influencing the dissociation of the wall silanols), buffer additives (methyl cellulose, polyacrylamide, quaternary amines, surfactants, etc.), ionic strength (influencing the zeta ζ potential) and organic solvents which act on buffer viscosity and zeta ζ potential. The coatings of the capillary wall [for example, cellulose, polyacrylamide, polyethylene glycol (PEG), polyvinyl alcohol (PVA), C_8 , C_{18}], either chemically bound or physically adsorbed, also actively suppress or modulate the EOF (Tagliaro *et al*, 1998). Generally, for separation optimization, it can be categorically stated that efficiency and resolution are higher at higher voltages, in compatibility with Joule heat generation and

dissipation. With the use of narrow bore capillaries, efficient capillary thermostating and low conductivity buffers, Joule heating can be controlled. The ionic conductivity mismatch between the sample and the running buffer may result in peak defocussing and peak distortion as a result of local changes in the electric field, and at the same time, in the migration velocity of ions.

High buffer concentrations have generally been shown to reduce the adsorption of analytes to the capillary walls and as a result of a better buffering capacity, buffers with high molarity are often the first choice in CZE, being compatible with the resulting currents, especially for the analysis of biological samples. Mostly, borate, citrate, phosphate and phosphate–borate buffers are used, but sometimes, zwitterionic buffers (for example, Tris, 3-[(cholamidopropyl)dimethylamino]-1-propanesulfonate etc.) are important in order to work at high buffer concentrations so as to avoid excessive Joule heat generation (Tagliaro et al, 1998). However, in the electrophoretic separation process, buffer additives may be beneficial through the introduction of additional interactions. Additives of importance in CE include: anionic [for example, sodium dodecyl sulfate (SDS)], cationic (for example, cetyltrimethylammonium bromide), organic solvents (methanol, acetonitrile etc.), to increase the solubility of the sample components in the running buffer; or neutral (e.g. Brij) surfactants [below their critical micellar concentration (CMC)], in order to increase solubility or to act as ion pairing agents; metal ions, to reduce wall adsorption; organic amines [triethylamine (TEA), triethanolamine], to change wall charges; urea, as denaturing agent; and linear polymers (PEG, polyacrylamide, methyl cellulose), to increase viscosity, mask wall charges and, at sufficient concentrations, introduce a sieving selectivity into the system. The separation may be affected by complexing agents by the introduction of highly selective interactions like stereoselectivity (Tagliaro *et al.*, 1998). CZE finds its application as the most widespread mode of CE. CZE has been used for analytes such as drugs, sodium ions and protein molecules.

2.2.12 Capillary Gel Electrophoresis (CGE)

Gel electrophoresis is the most traditional separation technique in biochemistry and biomedicine for the separation and characterization of proteins (DNA sequencing (polyacrylamide gels), SDS-polyacrylamide gel electrophoresis and DNA fragment mapping (agarose gels)). In actual fact, the separation mechanism operating in CGE looks like the traditional agarose and polyacrylamide gel electrophoresis, the only substantial difference is

the technology. Capillary gel electrophoresis (CGE) is a type of CE separation based on viscous drag. In this CE technique, the capillary is filled with a gel or a viscous solution. Often, the EOF is suppressed so that the sole migration of the analytes is done by electrophoresis. This viscous separation causes the retardation of larger molecules compared to the smaller molecules, so that the separation is effectively achieved on the basis of molecular size (Tagliaro *et al.*, 1998).

Serious problems are encountered in reality, when resembling slab gels CE capillaries are filled with crosslinked gels. Sometimes, the EOF is adequately strong to release the gel from the capillary, in a situation where the gel is bound to the wall covalently. The formation of gas bubbles inside the capillary and at the capillary ends is another problem, where there could be a possible exposure to air, leading to unstable currents. Another problem is that gel-filled capillaries are prone to clogging by the particulate materials contained in the sample, and this can only be removed by cutting the clogged part of the capillary. Meanwhile, if this is handled carefully, it is possible to attain excellent separations with gel capillaries, typically of 1% relative standard deviation in migration times and outstandingly high efficiencies, even up to millions of theoretical plates (Tagliaro *et al.*, 1998).

Non-crosslinked polymers are a good alternative to crosslinked polymer gels, in which case when above a given concentration, called the entanglement threshold, they apply a sieving separation mechanism identical to the traditional gels. It is possible to replace noncrosslinked polymer solutions in the capillary several times by simply applying pressure, and therefore subdue the majority of the problems typical of traditional gel-filled capillaries. Currently, linear polymers, such as hydroxyalkyl celluloses and linear polyacrylamide have become the most popular sieving matrices in CGE for DNA fragment and protein separation (Tagliaro *et al.*, 1998).

CGE is a method employed for molecules that differ in size but not in mass/charge ratio. The molecules of the DNA can vary greatly in length but the charge per unit length is constant. For a pure CZE separation, the molecules move at almost the same velocity but no separation occurs. However, in a viscous gel, the longer molecules are retarded compared to shorter molecules. As a result, the shorter pieces of DNA pass the detector sooner than the larger pieces of DNA. Molecules of protein are made up of more complex subunits than DNA

molecules, whereas, proteins vary widely in their size, and the wide range of charge states possible in a protein sequence makes size separation complicated.

2.2.13 Capillary Isoelectric Focusing (cIEF)

Capillary isoelectric focussing (cIEF) is a well-known and extensively embraced separation mode in the analysis of protein. In isoelectric focussing, substances are separated through the application of an electric field in a complex buffer system which forms a pH gradient between the two electrodes; making the analytes focus where the local pH is equal to their individual isoelectric point (Tagliaro *et al.*, 1998). The mechanism here involves the process whereby the molecules carrying both negative charges collect at a specific pH. This specific pH is known as the isoelectric pH or pI. At this pH, the charged molecule behaves as though it were neutral as a result of the positive and negative charges cancelling out each other (Whatley, 2001). Therefore, the molecule has no tendency to migrate in an electric field. In this mechanism (cIEF), special reagents known as ampholytes are employed to create a pH gradient within the capillary. Ampholytes are a mixture of buffers with a range of pKa values. When ampholytes are in an electric field, they will arrange themselves in order of pKa and this gradient is trapped between a strong acid and a strong base. The analytes introduced into this particular gradient will migrate to a certain point where the gradient pH equals their pI. However, the analyte at this point, having no net charge ceases to migrate. It remains at position as long as the pH gradient is stable or constant as long as voltage is applied (Tagliaro *et al.*, 1998).

The capillary isoelectric focussing (cIEF) finds application for the separation of closely related protein species (Whatley, 2001). This technique can be used to separate haemoglobin into several bands, whereas, the separation by SDS-CGE often results in a single form being identified. cIEF is also widely applied for the examination of distribution of carbohydrate isoforms of glycoproteins. In another technique such as SDS-CGE (pseudostationary capillary gel electrophoresis) or CZE, these proteins tend to migrate as diffuse bands and to generate broad peaks. Meanwhile, cIEF usually can resolve these bands into peaks that differ by as little as one charged sugar group (Tagliaro *et al.*, 1998).

2.2.14 Capillary Isotachophoresis (cITP)

Capillary isotachophoresis mostly resembles classical isotachophoresis (Everaerts *et al.*, 1976). The mechanism of this technique involves the introduction of a sample plug between two different buffers. One of the buffers which is the leading electrolyte possesses the highest mobility in the separation process. The trailing electrolyte has a lower mobility compared to any other. The sign of the charge on both the analytes and the buffers must be identical. The ions in the sample form discrete zones that are not separated into peaks when the voltage is applied, and one zone is adjacent to the next one. Analyte concentration within a zone is constant within that zone, also the length of the zone is directly proportional to the concentration within that zone. Isotachophoretic methods are compatible with conductance detectors as a result of uniform voltage drop within a zone (Whatley, 2001). Peptides and proteins have been detected using Capillary isotachophoresis (cITP) coupled to MS detection (Smith *et al.*, 1990). Because this separation technique offers zones of uniform concentration to the MS, it may offer to be an ideal separation mechanism for this detection technique (Whatley, 2001).

2.2.15 Micellar Electrophoresis (MEKC)

When analytes are not charged, electrophoresis remains impossible and to analyse such analytes, it is important to employ certain agents in the separation buffer to aid the transportation of the analytes through the capillary. The most commonly used electrophoretic technique for these analytes is MEKC. In this mode of separation, a suitable charged detergent, like 'pseudostationary' phase (SDS), is added to the separation buffer in a sufficiently high concentration to enable the formation of micelles (Whatley, 2001). Micelles are defined as the arrangements of detergent molecules with hydrophobic inner core and a hydrophilic outer surface to the separation buffer in a sufficiently high concentration to enable the formation of micelles. They are dynamic and constantly form and break apart. There is a probability for any given analyte that its molecules will associate within the micelles at any given time. This probability refers to the partition coefficient in classical chromatography. When this is associated with the micelle, then the analyte molecule migrates at the velocity of the micelle. But when the analyte molecules are not associated with the micelle, the analyte molecule will migrate with the EOF (if any). Although, the time differences that analytes spend in the micellar phase determines the separation.

MEKC has found application for a wide range of small molecules for example, drugs, pesticides and food additives which are not charged and are hydrophobic enough to associate with the micelle. Cationic detergents such as tetradecyltrimethylammonium bromide (TTAB) can also be used, but SDS is the widely used detergent for this purpose. There is no way non-ionic detergents can provide mobility to uncharged analytes, but when in combination with charged detergents, they will modify the separation (Whatley, 2001).

2.2.16 Nonaqueous Electrophoresis

The general idea of electrophoresis is usually considered to only occur in aqueous solutions, however, capillary electrophoresis (CE) can also be performed using non-aqueous systems based on solvents such as acetonitrile, formamide, methanol and dimethylformamide and small amounts of anhydrous acid or buffer salts are added to the solvent used. Because the EOF is low under these conditions, the separation is carried out by simple electrophoresis (Whatley, 2001).

Sometimes, two analytes share the same charge to mass ratio and cannot be easily separated. In other cases, the same analyte pair can be separated in a non-aqueous environment in which case they may have different pK_a values than that expressed in water. In this case, the degree of solvation and the radius of solvated species may differ between aqueous and non-aqueous environments. Therefore, an alternative non-aqueous CE is provided for analytes that are difficult to separate under aqueous conditions. Also, certain analytes are difficult to solubilise in aqueous systems but they readily dissolve in organic solvents, therefore, non-aqueous CE offers an alternative to MEKC for such analytes. Non-aqueous CE separations have been reported for drugs, dyes, inorganic ions, preservatives and surfactants (Whatley, 2001).

2.2.17 Chiral Electrophoresis

Molecules that can exist in two stereo-specific forms are referred to as chiral molecules. CE plays a major role in separating chiral compounds, as given by some particular reviews (Terabe *et al.*, 1994; Novotny *et al.*, 1994; Ward, 1994; Fanali, 1996), and began to recently also penetrate the forensic drug analysis field (Lurie, 1992; Lurie *et al.*, 1994; Scarcela *et al.*, 1997). Chirally-active selectors that are used in CE include complexes like: antibiotics (vancomycin), bile salts, cyclodextrins (CDs), crown ethers, proteins (bovine serum albumin, a -acid glycoprotein etc.), Cu(II)-aspartame, Cu(II)-L-histidine, modified CDs, etc, (Tagliaro *et al.*, 1998). Chiral forms or enantiomers are identical in molecular weight and chemical

formula but they are different in their arrangement of the atoms in space. Through different mechanisms that are dependent on individual chiral selectors, the chiral resolution arises from stereospecific interactions of the selector molecules which display different affinities for the two enantiomers of the compounds that give rise to a difference in the respective migration velocities under the applied electric field. Cyclodextrins (CDs) and cyclic oligosaccharides have an external hydrophilic surface and a hydrophobic cavity, where they can contain other compounds through hydrophobic interaction. This mechanism of inclusion is sterically selective because analytes must fit the cavity size, the diameter of which is dependent on the number of the glucose units in the cyclodextrin (CD) structure (6, 7, 8, for α -, β - and γ -CDs, respectively) (Tagliaro *et al.*, 1998). As a result of the chirality of the hydroxyls in the glucose molecules that form the rim of the cyclodextrin (CD) cavity, and the inclusion complex, formation will be chirally selective. Separation of these chiral or enantiomeric forms is dependent on the tendency to associate differentially with other chiral molecules called the chiral selectors. When a chiral selector is incorporated into the CE buffer, it often becomes possible to separate enantiomers of a chiral molecule. The native CDs are hydrophilic and neutral and subsequently migrate at the velocity of the electroosmotic flow (EOF). This migration velocity of the complexed form is different from that of the free molecule, as a result of the bigger size of the complex having the same charge as the free form. However, the higher the affinity for the CD, the lower the overall electrophoretic mobility of the analyte. Chiral electrophoresis is similar in some ways to MEKC. The analyte-selector complex migrates at a different rate than the analyte alone will. When one of the two enantiomers associates more strongly with the selector than the other form, a separation can be achieved (Tagliaro *et al.*, 1998).

In capillary electrophoresis, the commonly employed chiral selector is cyclodextrin, a ring shaped carbohydrate consisting of 6, 7, or 8 D-glucose sub-units. Chemical modifications can be done to cyclodextrin to alter their hydrophobicity or charge. When cyclodextrins are not charged, they become unsuitable for the analysis of uncharged analytes because the complex will move with the EOF. Furthermore, when cyclodextrins are modified to carry a charge by the addition of sulphate groups, they can serve as both chiral selectors and as carrier molecules, this is similar to the detergent in MEKC. Some other molecules have also been employed as chiral selectors, an example is vancomycin (an antibiotic) (Whatley, 2001). Chiral capillary electrophoresis can also be used to separate the enantiomeric forms of

pharmaceuticals as well as natural substances like amino acids. This method is sensitive that impurities as small as 0.1% can be easily detected.

2.2.18 Conclusion

Capillary electrophoresis has been already established as a versatile analytical technique, reliable and utterly independent, and, in terms of reagent and sample consumption, with overall running costs ultimately lower than chromatography. Meanwhile, the hindrance for its adoption in most analytical laboratories, which include forensic laboratories, is as a result of the lack of electrophoretic background of most analysts working in the analytical chemistry field and by the reason of instrumental analysis unfamiliarity of molecular biologists (Tagliaro *et al.*, 1998).

Therefore, at the tip of the two consolidated disciplines of chromatography and electrophoresis, CE may find more vital difficulties in acceptance, arising mostly from the problems of comprehension by the potential users rather than from the inherent limitations of its analytical performances. At the same time, this situation offers CE an extensively wide field of application, which includes the majority of the analytical problems typical of forensic sciences, such as drug analysis in confiscated materials and biological samples, having a great potential in chiral separations, ink analysis, explosive and gunshots residue analysis, protein and DNA fragment analysis.

Based on these facts, it is generally believed that in the next few years, CE will become one of the current analytical techniques in forensic science and forensic toxicology laboratories complementing gas and liquid chromatography and slab gel electrophoresis. By developing an efficient coupling of CE with MS at cost-effective rates would enhance its introduction in the forensic analysis laboratories. It is important to note that in this study, CZE and MEKC electrophoretic methods were employed in the analysis of persistent organic pollutant analytes of interest in the relevant samples. CZE was employed due to its suitability for the analysis of polar or ionic compounds. Also, since CZE separations are not suited for neutral analytes or substances, then MEKC was applied in the separation of non-polar compound.

2.3 Recovery and Detection of Pharmaceuticals

Persistent organic pollutants have been disposed into the environment for a long time now. Available analytical instrumentations at the time could not achieve the lower detection limits of as low as parts per billion (ppb) levels until recent modern analytical instruments became available (Nebot *et al.*, 2007). Various wastewater treatment practices are employed globally to get rid of these compounds. However, the presence of these pollutants has often been reported in wastewater treatment plant (WWTP) effluents at nanogram per litre (ng/L) concentrations. Many studies conducted in the WWTPs have reported that the wastewater treatment plants have the capability of eliminating about 60% of antibiotics (Batt *et al.*, 2006). In the case of these persistent organic pollutants, there is hardly any environmental survey data, and they are not regulated in the environment. One of the reasons for this is the lack of analytical methods for proper risk assessment and for monitoring of waste, surface and drinking water quality (Simon & John, 2005). However, analysing these typically polar contaminants in environmental matrices (water, wastewater, soils, and sediments) is challenging in particular, because low detection limits are required, the samples are complex in nature and separating these compounds from interferences is extremely difficult. (Nikolaou *et al.*, 2007).

The analysis of high molecular weight compounds (>900 amu) and polar compounds are now being achieved by the use of liquid chromatographic methods, with the advent and developments of analytical techniques; where different types of liquid chromatography (LC) methods have been suggested for the analysis of human pharmaceuticals in both natural and wastewaters (Nebot *et al.*, 2007).

The needed sensitivity and specificity for accuracy in measurement are provided by new extraction and clean-up methods, in addition to instrumental technologies improvements. In environmental samples, selective and quantitative extraction is important to achieve accurate and sensitive detection (Vieno *et al.*, 2007). In usual practice, the common approach for antibiotics analysis of aquatic environment includes pre-concentration with the aid of solid phase extraction (SPE) procedure and a liquid chromatography method of separation. The SPE method is employed for the purpose of enrichment and clean-up of aqueous samples and their extraction from aqueous matrices. By the application of such methods, the separation and detection (qualitative and quantitative) of antibiotics, or other pharmaceuticals having

low detection limits can be achieved (Lin *et al.*, 2009). Identifying pharmaceutical residues in the environment is of paramount interest, owing to the fact that the knowledge of those compounds is required so as to devise measures that will regulate and lessen their impacts in the environment. The question of a chemical or other contaminants being an emerging contaminant is dependent on whether there is an analytical technique available for its detection or not (Homem & Santos, 2011). Due to the required low detection limits, sample's complex nature, and difficult separation of compounds to avoid interferences, the analysis of typically polar contaminants in water, wastewater, soils and sediments becomes particularly challenging (Nebot *et al.*, 2007; Homem & Santos, 2011).

2.4 Surface-enhanced Raman spectroscopy

The surface-enhanced Raman spectroscopy (SERS) is a combination of vibrational spectroscopy and surface chemistry techniques. In this technique, the Raman scattering signal enhancement is provided by the localised surface plasmon resonance in metallic nanostructures (Le Ru & Etchegoin, 2008). Surface-enhanced Raman spectroscopy (SERS), is therefore an extension of Raman spectroscopy (Lamsal *et al.*, 2012). SERS can be applied where an ordinary Raman spectroscopy is short of an identifiable signal from a particular analyte. Though the SERS application has been studied in the life sciences sector extensively, it is also being employed more recently in the chemical and materials sciences (Schlücker, 2014).

2.4.1 Raman spectroscopy

Raman spectroscopy is an analytical technique based on the interactions between molecules and photons that result in scattering of radiation (McMahon, 2008). This type of spectroscopy is based on the detection of vibrations coming from the changes in polarizability of bonds in an excited molecule as a result of the Raman effect. The phenomenon which takes place when the inelastic monochromatic light is scattered by molecules at a different wavelength to that of the incident light is called the Raman effect (Lombardi & Birke, 2009). The Raman effect happens when a molecule is struck by the electromagnetic radiation, which results in a shift of the wavelength of the inelastically scattered radiation. When the Raman is shifted towards the longer wavelength, it is called Stokes scattering, and when shifted towards the shorter wavelength, it is called Anti-stokes scattering (Meyers, 2000). Raleigh scattering takes place when the overall Raman shift is zero i.e. there is no energy increase or decrease

related to vibrational energy levels in the ground electronic state of the molecule (Meheretu, *et al.*, 2014). This Raman shift occurrence can be explained in the energy diagram in Figure 2.8 Raman scattering occurs when a laser in the visible or near infrared strikes a molecule and interacts with the electron cloud of the molecule.

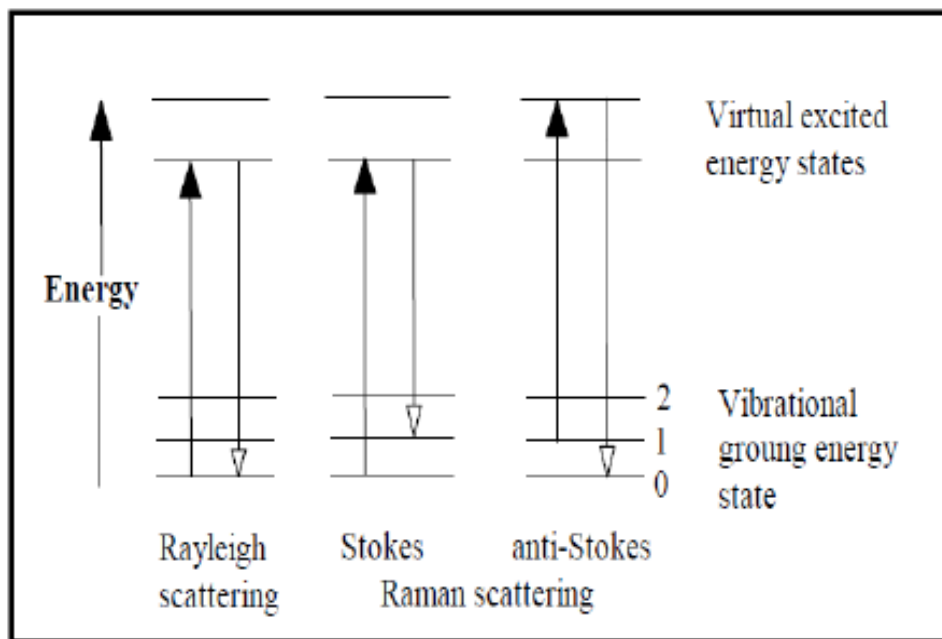


Figure 2.8: Energy level diagram showing the states involved in Raman spectrum and the elastic and inelastic Raman scatterings (Rayleigh, Stokes and Anti-Stokes).

Raman scattering is also dependent on the polarizability of molecules to yield scattered light with diminished energy (Reichenbacher & Popp, 2012). The signals of Raman are weak relatively when compared to infrared signals, and they are shadowed easily by fluorescence (Boujday *et al.*, 2015). Raman has got an advantage over the infrared, in that, it can be used in an aqueous environment as water causes a negligible Raman effect (McMahon, 2008; Matousek *et al.*, 2006). As a result of the weak signals of Raman spectroscopy, it has therefore not been used extensively. Due to this, much attention has been centred around surface-enhanced Raman scattering through which the Raman signal is enhanced by metal nanostructures (Le Ru & Etchegoin, 2008).

2.4.2 The Inception of Surface-enhanced Raman spectroscopy (SERS)

The surface-enhanced Raman spectroscopy (SERS) is dependent on electromagnetic and chemical interactions acting on an analyte which is adsorbed on the surface of a material that is SERS-active, and has been irradiated by a laser light (McNay *et al.*, 2011). In surface-enhanced Raman spectroscopy (SERS), the Raman scattering signal is amplified through the

excitation of localised surface plasmons on a roughened metal which generates an amplified electromagnetic fields (Sharma *et al.*, 2013), and charge transfer which occurs in the analyte-metal complex (Halvorson & Vikesland, 2010). In SERS, Raman scattering enables vibrational absorbance of analytes adsorbed on or rather, in close proximity (Lamsal *et al.*, 2012) to metal nanoparticles or roughened surfaces (Boujday *et al.*, 2015; Craig *et al.*, 2013). The signal intensities of Raman scattering is increased by the plasmonic metallic nanostructures, and this enables detection of single molecules (Guhlke *et al.*, 2016).

The origin of surface-enhanced Raman spectroscopy dates back to 1974 (Boujday *et al.*, 2015), when it was observed during the study of pyridine on a roughened silver electrode but, however, was not recognised as a phenomenon of an enhanced surface Raman scattering, before it was eventually reported in 1977 (Sharma *et al.*, 2013). Some other authors later claimed to have detected a single molecule of the analytes of interest (Kleinman *et al.*, 2013). As the years passed by, the narrative about the occurrence of the SERS signal enhancement has been discussed and debated, and eventually, the resolution is given to be caused by the contributions from the electromagnetic effect, a chemical mechanism, and molecular resonance enhancement (Muehlethaler *et al.*, 2015). The electromagnetic effect arises from the interaction of the excitation laser with an oscillating electron wave on the metal surface ((Halvorson & Vikesland, 2010). Of the three contributions, the electromagnetic enhancement is the most prominent (Péron *et al.*, 2009), as it neither requires the molecules of an analyte under study to be attached to SERS active materials, nor the absorption wavelength of the analyte to be equal or near that of exciting laser (Boujday *et al.*, 2015). When the excitation radiation wavelength is resonant with the analyte-metal complex's charge transfer electronic states, then the chemical mechanism enhancement occurs (McNay *et al.*, 2011). Thus, the molecular resonance enhancement exists when an absorption wavelength of the analyte occurs near the exciting laser wavelength (Muehlethaler *et al.*, 2015; Pieczonka *et al.*, 2008). Therefore, the molecular resonance enhancement is scarcely cited by earlier authors (Lombardi and Birke, 2009).

The surface plasmon resonance (SPR) is the assembly movement of surface electrons of the random or ordered metal nanostructures (Banholzer *et al.*, 2008). The excitation of the metal in the charge transfer complex by the incident laser, results in the creation of an electron-hole through which energy is transferred to the analyte and Raman scattering occurs (McNay *et al.*, 2011). The energy from the surface plasmon is then absorbed by an analyte nearby or

adsorbed on the metallic SERS-active material, which then transfers the energy back to the SERS-active material less the amount it transferred to its nucleus (McNay *et al.*, 2011). The magnitude of the enhancement mechanism depends on the morphology of the metal nanoparticles, the localisation of a molecule, the excitation wavelength and light polarisation (Craig *et al.*, 2013; Lombardi & Birke, 2009). The effect of domination of spectral enhancement characteristic of the analyte caused by the surface roughness are the surface plasmon resonance of the metallic surfaces and their corresponding variations (Craig *et al.*, 2013; Pieczonka *et al.*, 2008). The collective excitation of surface plasmon resonance (surface electrons) is affected by the distance between metal nanoparticles, the shape of nanoparticles and their dielectric functions (Rodrigues *et al.*, 2013). The plasmonic metal nanostructures cause resonance Raman scattering that results in enhancement of both incident light and the inelastic light scattered by the adsorbed analyte (Craig *et al.*, 2013).

2.4.3 The active materials for surface-enhanced Raman spectroscopy

The most active materials for surface-enhanced Raman spectroscopy (SERS) are metallic nanostructures with localised surface plasmons, which upon excitation enhance the Raman scattering signals of proximate or adsorbed analyte molecules (Wang *et al.*, 2015).

Gold, silver and copper, which are noble metal nanoparticles, provide good SERS-active materials in comparison to other transition metals (Sharma *et al.*, 2013; Wang *et al.*, 2015). It is easier to obtain the surface plasmon resonance of these noble metals within the visible and near infrared region, compared to other metals whose plasmonic effects lie outside the visible region (Alvarez-Puebla, 2012). The sensitivity of SERS to dilute solutions is improved by metallic nanostructures which increase the signal intensity of the Raman scattering through many factors (Guhlke *et al.*, 2016). The effectiveness of the active materials in terms of sensitivity and reproducibility are enhanced by a number of optimisation factors. The factors which can be controlled are the morphology of the metal nanostructures (Kruszewski *et al.*, 2011; Muehlethaler *et al.*, 2015). In addition to the morphology of the nanostructures and their orientation, the close spacing of the nanostructures on the surface of an anchor material of benefit to the production of strong localized field enhancement (Schlücker, 2014). The classification of active materials is in groups, and this is based on how they are fabricated and used such as colloidal suspension, immobilisation on solid supports and template synthesis or lithography. In any attempt to synthesise SERS-active materials, the shape and size of nanoparticles are determined by the intended application and environments of use (Culha *et*

et al., 2012). For instance, colloidal suspensions are mostly used in liquid environments (*Fan et al.*, 2011). The advantage of using plasmonic nanostructures as SERS active materials is that they come with the provision of a large surface area, which forms one of the fundamental basis of nanotechnology. Colloidal metallic nanoparticles are produced through simple and efficient bottom-up methods, by the addition of reducing agents to aqueous solutions of noble metal salts (*Cialla et al.*, 2012). There are other efficient methods for the preparation of SERS surfaces such as vapour deposition and ion beam sputtering. The challenge is the requirement for sophisticated equipment which makes it expensive (*Ma et al.*, 2013). SERS-active colloidal materials which are self-assembled on planar supports through heteroatom molecules, such as thiols and amines (*Carol et al.*, 2008), that can serve as anchors on which the arrangement is made in large arrays for SERS application (*Cialla et al.*, 2012). SERS-active materials' immobilisation on stable supports like modified membranes serves to improve the reproducibility of active materials and also the flexibility of their application in various fields (*Taurozzi & Tarabara*, 2007).

Noble metal nanoparticles are known to enhance the Raman signal when molecules of the analytes are attached to them or are in close proximity (*Schmidt et al.*, 2004). Those analytes having thiol and amine functional groups possess an intrinsic affinity towards the SERS-active materials that are made of gold (Au), silver (Ag) and copper (Cu), and where localised surface plasmon resonances are created (*Du et al.*, 2011). The effective adsorption of analytes on the active materials are critical only when working with low concentrations of the analytes (*Lamsal et al.*, 2012; *Smith*, 2008), and this could be achieved by creating an environment that encourages high affinity of the analyte towards SERS-active materials (*Bantz et al.*, 2009). *Guhlke et al.*, (2016), noted that less water-soluble organic compounds like non-polar carotenoids have a poor affinity for silver nanoparticle surfaces. Therefore, in an attempt to improve enhanced SERS spectra of organic compounds with a low affinity towards silver nanoparticles, the nanoparticles were functionalised with an organic layer that provided a hydrophobic environment (*Guhlke.*, 2016). This kind of hydrophobic environment could be prepared by the chemisorption of thiol or amine-terminated organic molecules on silver or gold nanoparticles. Amine-terminated organic compounds and thiols form covalent bonds between silver, gold and nitrogen (or sulphur) atoms. Some straight chain alkanethiols such as pentanethiol and hexanethiol (*Li et al.*, 2014a), have been employed previously to create hydrophobic environments which allow the interactions of the hydrophobic analytes with the functionalised nanoparticles (*Bantz et al.*, 2009). *Costa et al.*, (2006), detected polycyclic

aromatic hydrocarbons (PAHs) using SERS, via the successful functionalisation of alkanethiol on gold nanoparticles used as SERS-active materials, and showed improved selectivity of hydrophobic polycyclic aromatic hydrocarbons (PAHs) and enhanced concentration of PAHs close to SERS-active materials. It was reported by Luo *et al.*, (2014), that the alkanethiol-coated gold-active materials immobilised on quartz, offered strong Raman signals (high sensitivity), and were reproducible. However, it should be noted that the selectivity of analytes on SERS active materials could be intensified by intermolecular attractions such as electrostatic forces, van der Waals forces, hydrogen bonding between the analyte and metal nanostructure SERS-active material (Schlücker, 2014). The stability of SERS active materials can be enhanced by functionalising the SERS-active material with analyte specific molecules such as thiol-terminated molecules which form self-assembled monolayers on metal nanoparticles. In addition, such functionalised molecules interact selectively with the molecules of the analyte of interest, as a result, attracting the analyte to the surface of the SERS-active material (Schlücker, 2014). Furthermore, silver nanoparticles have the highest surface plasmon resonance in an easily accessible spectral region that is visible or near infra-red region (Muehlethaler *et al.*, 2015). In this research study, silver nanoparticles will serve as the SERS-active materials and will be immobilised on the surface of amine-modified track-etched PET membrane through a chemical bond with nitrogen.

2.4.4 Silver nanoparticles

Nanoparticles can be defined as the cluster of atoms which have formed nanoscale structures in the size ranging from 1 to 100 nanometres (Sharma *et al.*, 2009). The nanostructured materials exhibit biological, chemical, electrical and physical properties, which differ substantially from bulk materials (Abou-el-Nour *et al.*, 2010; Khodashenas *et al.*, 2015). The properties which the nanoparticles exhibit are dependent on size, shape and distribution. Nanoparticles have been of special interest in the areas of biotechnology, sensing, optics and surface-enhanced Raman spectroscopy (Khan *et al.*, 2011; Patil *et al.*, 2012), catalysis and photography (Abou-El-Nour *et al.*, 2010; Sharma *et al.*, 2009; Smyth *et al.*, 2013). They exhibit enhanced properties compared to bulk properties as a result of their high surface-to-volume ratio (Abou-El-Nour *et al.*, 2010).

There are diverse applications of novel metal nanoparticles as a result of their versatile nature, for example, silver nanoparticles have anti-bacterial activity and therefore exhibit narrowly localised surface plasmon resonance within the visible and near infrared region

(Meng *et al.*, 2010). Due to the good conductivity, chemical stability, antibacterial activity, unique electrical and optical qualities of silver nanoparticles, researchers' attention has been attracted towards them (Khodashenas *et al.*, 2015). And as a result of the surface plasmon resonance qualities, silver nanoparticles have been studied as SERS-active materials in the fields of biomedical, biotechnology, sensing and environmental monitoring (Natsuki *et al.*, 2015; Reddy, 2015).

There are two approaches for the synthesis of silver nanoparticles. These include the chemical approach, which is the use of silver salts as precursors (bottom-up), and the physical approach, which is top-down, for example, lithography (Biswas *et al.*, 2012). With the exception of the physical route, other routes to silver nanoparticles synthesis involves the reduction of silver salts with chemical reducing agents, or laser irradiation, micro-organisms, ultrasonic radiation, ultraviolet visible light, etc. (Ramírez-Meneses *et al.*, 2015). The synthesis of silver nanoparticles by the physical approaches are carried out by processes such as evaporation-condensation and mechanical processes that require designated equipment for the control of fabrication parameters such as temperature and pressure (Abou-El-Nour *et al.*, 2010; Tolaymat *et al.*, 2010). A great deal of energy is required in order to synthesise stable nanoparticles using the physical approach, since it is based on external parameters (Biswas *et al.*, 2012). The advantage of the physical approach over the wet chemical method is possible large-scale production of silver nanoparticles with very narrow size distribution. Meanwhile, this physical approach makes use of external physical energy which requires capital-intensive equipment that renders the whole process very expensive (Tran *et al.*, 2013). The synthetic methods that fall under the approach of chemical reduction are biological routes, electrochemical, photochemical, radiation, sonochemical and wet chemistry (Tan *et al.*, 2013). The choice of the method of synthesis is related to the particular field of the application which in turn is based on cost, stability, shape and size of nanoparticles and the applicable properties (Natsuki *et al.*, 2015; Niu *et al.*, 2016; Reddy, 2015). And as a result of its cost-effectiveness among the existing synthesis routes, the wet chemistry reduction method has been widely adopted owing to its cost-effectiveness (Khan *et al.*, 2011).

The cost-effectiveness and stability of colloidal silver nanoparticles compared to gold nanoparticles and copper nanoparticles respectively, have offered preference for their use as SERS-active materials (Natsuki *et al.*, 2015). The parameters that influence the synthesis of silver nanoparticles' size, shape and dispersion are: controlled pH of solution; molar ratio of

stabilising agents to that of silver salt precursors; temperature (Khodashenas *et al.*, 2015); time of reaction or exposure; and power of photo-irradiation (Kshirsagar *et al.*, 2011). By the careful control of the reaction parameters such as pH, temperature, concentrations of the silver salts and reducing agents systematic nucleation and subsequent growth of initial silver nuclei can be achieved (Tran *et al.*, 2013). Silver nitrate is the most commonly used silver salt precursor and water is the most common solvent. The reducing agents used in most studies regarding the synthesis of silver nanoparticles have been sodium borohydride and sodium citrate (Tolaymat *et al.*, 2010). In a research study carried out by Patil *et al.*, (2012), it was discovered that by varying the concentration of the silver salt precursor (silver chloride) or the stabilising agent (polyvinyl alcohol) or time of reaction, the size of silver nanoparticles synthesised at fixed alkaline pH could be controlled. Also, in the study carried out by Khan *et al.*, (2011), it was noted that changing the concentration of the reducing agent (aniline) had a significant effect on the size, shape and size distribution of synthesised silver nanoparticles. It was observed following a study to synthesise silver nanoparticles by photo-reduction of silver nitrate by Kshirsagar *et al.*, (2011), that the rate of synthesis of silver nanoparticles varied with the power of the source for photoirradiation. It was observed that the silver nanoparticles were synthesised at a faster rate when high-powered sources of photo irradiation were used compared to low powered sources (Kshirsagar *et al.*, 2011). Strong reducing agents such as sodium borohydride, reacted with silver salt precursors, resulted in smaller spherical nanoparticles due to the spontaneous reaction which induces rapid nucleation which is controlled by using dilute solutions (Qin *et al.*, 2010). Whereas, at elevated temperatures, weak reducing agents such as ascorbic acid become more effective, but their effectiveness could be enhanced by the use of a catalyst (Singha *et al.*, 2014). It was noted in a review by Tan *et al.*, (2013), that the size and shape of the synthesised silver nanoparticles depended on the pH of the reaction solution. For example, the medium alkaline pH values (between 9 and 11) resulted in smaller sized nanoparticles compared to weakly alkaline and slightly acidic reagents (Qin *et al.*, 2010). In a research study carried out by Xu *et al.*, (2008), it was reported that increasing the molar ratio in favour of the reducing and stabilising agent resulted in a faster rate of silver nanoparticle formation at the same UV irradiation time and alkaline pH. This was attributed to the generation of more photoelectrons by a higher concentration of reducing and stabilising agent, resulting in a subsequent reduction of silver salts to metallic nanoparticles. As a result of the ever-increasing environmental concerns, green chemistry principles have attracted the interest of researchers globally, and this has led

to the synthesis of silver nanoparticles using approaches that alleviate environmental degradation (Sharma *et al.*, 2009).

In green chemistry, the vital and necessary principles to put into consideration in the synthesis of silver nanoparticles are the use of environmentally-friendly solvents, environmental friendly reducing and stabilising agents, and non-toxic silver salt precursors (Raveendran *et al.*, 2003). Most reducing and stabilising agents which are environmentally-friendly such as citrate ions, possess a weak binding interaction with metal nanoparticles (Schlücker, 2014), and are therefore easily displaced by strong binding ligands such as thiols or amines during ligand exchange reactions (Caragheorgheopol *et al.*, 2008; Raveendran *et al.*, 2003).

In this research study, the citrate ions coming from the reducing agent trisodium citrate, that were used to stabilise silver nanoparticles, would be displaced by amines or thiols during the ligand exchange reactions (Sperling and Parak, 2010). Ligand exchange takes place during the immobilisation of silver nanoparticles on amine-modified track-etched polyethylene terephthalate membrane. These citrate ions are chemisorbed to the noble metal nanoparticles through the carboxylate groups, which have weak binding energy compared to thiols and amines (Schlücker, 2014).

2.5 The applications of surface-enhanced Raman spectroscopy

Surface-enhanced Raman spectroscopy (SERS) is an analytical technique which has found diverse applications in the fields of biotechnology (Boujday *et al.*, 2015), drug abuse (Craig *et al.*, 2013) and environmental applications (Halvorson and Vikesland 2010), electrochemistry, food industry, warfare anti-terrorism (Craig *et al.*, 2013), surface and material science (Hering *et al.*, 2008). This technique has drawn the attention of researchers in the environmental pollutant analysis, with the particular objective on the identification, detection and quantification of very low concentrations of pollutants found either in air or water sources (Le Ru and Etchegion, 2008). The trace level analysis capability of the SERS technique and cost-effectiveness has basically been the driving force behind its research and development (Lucotti *et al.*, 2007). This technique also offers effective practical utility (Li *et al.*, 2014a). The SERS technique possesses numerous analytical merits ahead of other methods, including ultra-sensitivity selectivity and inherent molecular specificity (Boujday *et*

al., 2015; Huh *et al.*, 2009). SERS requires little or no sample preparation for chemical analysis (Zhang *et al.*, 2015), it is easy and cost-effective for development of miniaturised equipment (Ma *et al.*, 2015; Lucotti *et al.*, 2007), it possesses an edge over infrared spectroscopy, as it can be directly applied in the aquatic environment with negligible background noise due to low polarizability index of water (Li *et al.*, 2014a). Even though, other identical techniques such as fluorescence are already well entrenched, the emerging SERS has interesting properties such that it can be used both in the near-infrared and the visible spectral region and does not require labelling the analyte of interest as is practised in the fluorescence technique (Cialla *et al.*, 2012). SERS performance is based on its sensitivity, which also depends on the surface property of the SERS-active materials (Botti *et al.*, 2014) that can be tailored to suit the intended application (Péron *et al.*, 2009; Costa *et al.*, 2006). SERS is also envisaged to be used for simultaneous identification of multiple pollutants in a sample, in a rapid, reliable way and at lower cost (Halvorson and Vikesland, 2010). The Surface-enhanced Raman spectroscopy (SERS) is flexible, as it can be applied in sequence with other separation techniques, such as nano filtration polymer membrane technology and chromatography (Muehlethaler *et al.*, 2015) scanning probe microscopy and microfluidics (Cialla *et al.*, 2012).

2.5.1 Polymeric membranes

Polymeric membranes are organic membranes which are synthesised from chemically reactive monomers, and having desirable gaseous and liquid separation capabilities. They are thin physical interfaces which regulate the movement of certain species, and this depends on the physicochemical properties and interaction of the membrane surface and the species (Lee *et al.*, 2016). The polymeric membrane materials have several applications in fields such as biotechnology, coating, filtration, microelectronics, thin-film technology, etc, that depend on their bulk properties and surface chemistry (Nady *et al.*, 2011). Polymeric membranes are employed in filtration technologies due to their flexibility, stability and the ease of processing compared to inorganic membranes (Ahmad *et al.*, 2013).

High-performance polymer membranes include polymers such as polycarbonate (PC), polyethylene terephthalate (PET), polyimide (PI), etc. Amongst all these, polyethylene terephthalate (PET) has good mechanical strength as well as thermal and chemical resistance (Korolkov *et al.*, 2015; Muthuvijayan *et al.*, 2009). Polyethylene terephthalate (PET) is a linear

aromatic polyester type of organic polymer; its monomer is shown in Figure 2.9 (Marchand-Brynaert *et al.*, 1995).

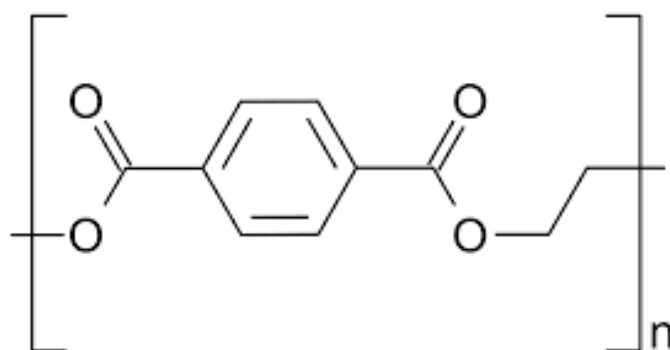


Figure 2.9: Monomer structure of polyethylene terephthalate polymer.

Polymeric membranes which have passed through bulk modification such as track-etching could be employed as permeable supports for the surface-enhanced Raman spectroscopy SERS-active materials (Taurozzi and Tarabara, 2007).

2.5.2 Track-etched polymeric membrane

The track-etched polymeric membranes are porous polymer membranes or films, which have been bombarded with inert energetic ions (e.g. Argon), or reactive gases (e.g. Nitrogen), followed by the physicochemical treatment with an alkali solution (Fatiyants *et al.*, 2013). Microporous track-etched membranes are often generally used in microfiltration to separate solutes based on the size of particulate matter and the size of pores of the membrane (Lee *et al.*, 2016). The most commonly used track-etched polymer membranes in the polymer industry are polycarbonate and polyethylene terephthalate (Apel, 2001), owing to their mechanical properties and stability when exposed to acids and organic solvents (Lalia *et al.*, 2013).

The pore sizes and shapes of track-etched membranes are determined through a process known as chemical etching; where etchants such as sodium hydroxide are used to control or increase the sizes of pores (Lalia *et al.*, 2013). Track-etched membranes have an edge over nonporous membranes as their pore structures can be controlled in terms of size, shape and density of pores to suit the intended application such as ultra filtration (Apel, 2001). The track-etched membranes are prepared by bombarding polymer membranes with swift heavy ions that lead to the formation of latent tracks in the membrane. The membrane is then

exposed to chemical etchants such as sodium hydroxide to reveal randomly distributed but uniform pores of a specific diameter, in a process called chemical etching (Apel *et al.*, 2015). The density of heavy ions, the concentration and type of etching reagents used to create tracks in the membrane are the determining factors in the pore density on the surface of the track-etched membrane and the size of pores respectively (Dauginet *et al.*, 2001).

2.5.3 Separation and filtration process in membrane technology

In water quality assurance, membrane technology has been in extensive use as a result of its good flexibility and performance (Lee *et al.*, 2016). Membrane separation processes in the aquatic environment have been applied largely due to their advantages, which include the production of high water quality with ease of maintenance, inertness, flexibility and excellent separation efficiency (Fatiyants *et al.*, 2013; Lee *et al.*, 2016; Velleman *et al.*, 2012). Though the microporous membranes have pores with sizes much larger than the molecular sizes of organic micropollutants, surface modification of the polymer has been used to enhance adsorption via hydrophobic interaction (Luo *et al.*, 2014), and the hydrophobic polymer membrane surfaces were used to retain hydrophobic pharmaceuticals such as estradiol due to higher octanol-water (K_{ow}) partitioning coefficient (Luo *et al.*, 2014). This sort of separation chemistry could be employed to retain hydrophobic organic molecules of pharmaceuticals on track-etched PET membrane that has been subjected to an appropriate modification.

2.5.4 Polymer membrane surface modification

There have been various techniques reported in the literature for polymer membrane surface modification which include chemical, physical and bulk modification (Goddard and Hotchkiss, 2007). These techniques include: chemical treatment e.g. cross linking and functionalising with reactive species; surface coating e.g. sputtering; and annealing with heat treatment for bulk modification (Zhao *et al.*, 2013). In the surface modification process, a certain number of factors are considered including reproducibility, stability, uniformity, process control and cost effectiveness (Nady *et al.*, 2011). Degradation to the surface of the polymer membrane can be limited through the control of reaction conditions. It is a result of the wet chemical modification that results in chain scission of the polymer which activates reactive moieties e.g. carboxyl and hydroxyl on the polyethylene terephthalate (PET) membrane surface (Noel *et al.*, 2013). In principle, polymer membrane surfaces are modified by two methods: the chemical methods which involve treatment with reagents, and the

physicochemical methods that use external factors to induce chemical transformations (Fatiyants *et al.*, 2013) and are further described in the following subsections.

2.5.5 The Physicochemical techniques for polymer membrane modification

The procedures that modify polymer membrane surface properties have captured the interest of scientists in polymer science with the purpose of functionalising and immobilising compounds of interest on the surfaces for various applications (Talbert *et al.*, 2012). Polymeric membranes are inert and as a result, lack reactive functional groups on which biomolecules, chemical linkers and metal nanoparticles could be attached sustainably (Goddard and Hotchkiss, 2007). The inert nature of most polymer surfaces limits their use in applications, therefore, surface modification is required to achieve the desired properties while maintaining the bulk polymer properties (Reznickova *et al.*, 2014).

In the physicochemical surface modification processes, the most widely used techniques are corona discharge, plasma treatment, surface graft polymerisation and ultraviolet (UV) irradiation (Dauginet *et al.*, 2001; Marchand-Brynaert *et al.*, 1995). The physicochemical modification methods such as plasma treatment result in the ablation of polymer surface layers, chemical bonds cleavage, conjugation of double bonds and the creation of free radicals (Švorčík *et al.*, 2011). Plasma treatment is also used to impart reactive species such as amines if nitrogen gas is used as plasma treatment medium or to introduce hydroxyl moieties when water is used in the treatment, and inert gases are applied in plasma treatment if no specific functional groups are to be introduced apart from the radicals resulting from chain scission of the polymer membrane (Drobota *et al.*, 2013). The plasma process is mostly preferred among the physicochemical modification methods because it results in the introduction of specific reactive species needed for the intended application (Long *et al.*, 2006).

2.5.6 Chemical modification methods for polymer membrane surface

The methods of chemical modifications are cost-effective and enable the control of the functionalisation of molecules and immobilisation of nanoparticles actually easy (Xue *et al.*, 2013). Generally, it is considered that the physicochemical techniques are precursors to chemical modification. For example, it is considered that plasma activation could be followed by aminolysis or silanisation (Goddard and Hotchkiss, 2007). Yet, the most reliable and effective way of modifying the surface of a polymeric membrane is the use of wet chemical

treatment when other parameters have been duly optimised to offer the best result (Ozcam *et al.*, 2009). Several methods used to modify the surfaces of polyethylene terephthalate membranes, these include: aminolysis, carboxylation, glycolysis, reduction and wet chemical treatment by hydrolysis (Muthuvijayan *et al.*, 2009; Ozcam *et al.*, 2009). The method of polymer surface modification is dependent on the intended application that demands modification of the surface of the polymer membrane (Fávaro *et al.*, 2007). Polymer surface modifications have definitive purposes, and this is based on the functional groups of molecules (Velleman *et al.*, 2012), and nanoparticles to be immobilised for that intended application (Deldime *et al.*, 1995). A smart choice of conditions for the modification of surface should be made to limit degradation of the desirable mechanical and chemical properties of the bulk polymer (Fatiyants *et al.*, 2013). The parameters for the wet chemistry including temperature and time of treatment as well as solvent type and concentration must be accurately controlled to maintain consistent surface modification (Drobota *et al.*, 2013; Xue *et al.*, 2013). A PET surface modification study observed that aminolysis depended on the choice of amine and the varied treatment parameters which were temperature, time and amine solution concentration (Irena *et al.*, 2009). The number of reactive amine functionalities on PET surface increased with an increase in amine concentration until it reached an optimum point but decreased with a further increase in the amine concentration (Irena *et al.*, 2009). During the aminolysis reaction, amine nitrogen attacks an electron deficient carbonyl carbon of the ester link of PET through its lone pair to form an amide bond (Drobota *et al.*, 2013) as shown in Figure 2.10.

UNIVERSITY of the
WESTERN CAPE

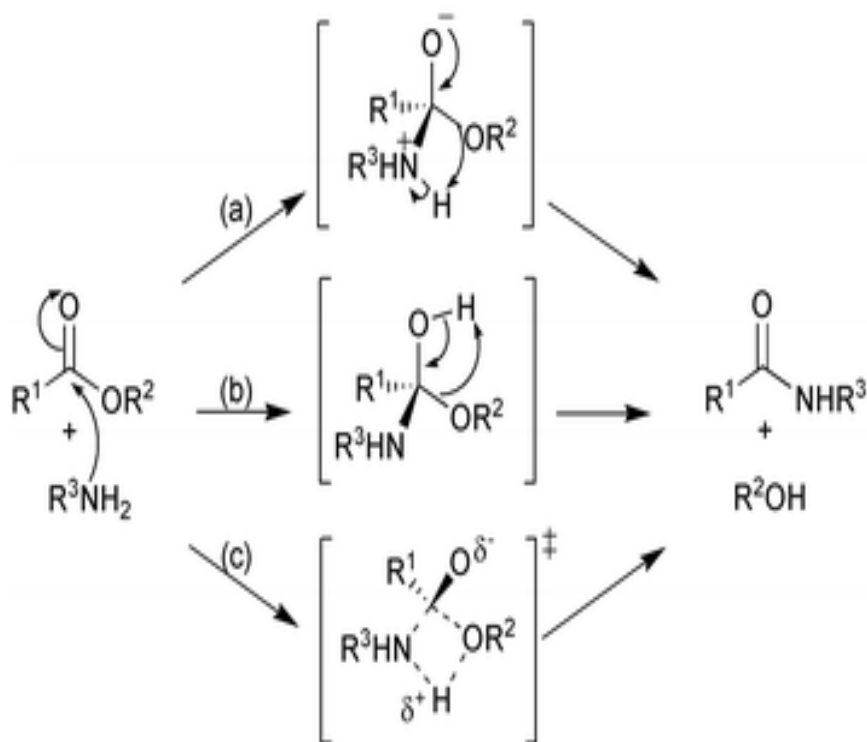


Figure 2.10: The aminolysis reaction (Drobota *et al.*, 2013)

It is important to note that covalent bond immobilisations provide the most stable bond between the functionalised polymer surface and the adsorbed compounds (biomolecules or nanoparticles) (Goddard & Hotchkiss, 2007). Xue *et al.*, (2013), made a comparison of suitable solvents for amine reagents and it was observed that amines in ethanol and dimethylsulphoxide introduced more reactive amine functionalities on PET surface than when water was used as a solvent.

2.5.7 Chemical linkers for polymeric surfaces

According to Sperling & Parak, (2010), the chemical linker choice is dependent on the chemical properties of the compound to be immobilised. For example, thiols and amines have a high affinity for noble metal nanoparticles (Braun *et al.*, 2009). In addition, the molecules of the linker functionalised on the modified membrane surface serve to modify the chemical properties of the surface; e.g. the aliphatic and aromatic linkers provide a hydrophobic environment (Kubackova *et al.*, 2014). Usually, the functionalised molecules are bifunctional in such a way that one terminal group is chemisorbed to the metal nanoparticle or biomolecule and the other functional group is coupled to the modified polymer surface (Goddard & Hotchkiss, 2007). The number of immobilised metal nanoparticles or biomolecules on the functionalised membrane surface is dependent on the available affinity functional groups such as thiols and amines (Caragheorghopol *et al.*, 2008). As a result, the

noble metal nanoparticles chemisorb on thiols and amino terminal groups and form covalent bonds (Sperling & Parak, 2010). Similarly, other molecules having polyfunctional groups have been coupled to modified polymer surfaces in order to increase the reactive sites on the polymer surface for immobilisation of metal nanoparticles and biomolecules (Goddard & Hotchkiss, 2007). In the research study by Taurozzi & Tarabara, (2007), successful functionalisation of aminopropyltrimethoxysilane (APTMS) was achieved via amide bond formation on the surface of a polycarbonate membrane and the immobilisation of colloidal silver nanoparticles via an amine-silver bond. During the experiment, the immobilised silver nanoparticles sustained hydraulic conditions applied, although, the nanoparticles were scratched off under mechanical stress (Taurozzi & Tarabara, 2007). Hence, this is the benefit of a covalently bonded nanoparticle to polymer surface as there is no leaching into the environment. The immobilisation of silver nanoparticles was achieved on the surface of modified glass via APTMS, which was coupled via siloxy linkages and the materials were used to detect congo red dyes by SERS (Andrade *et al.*, 2010). Modified glass surfaces used by Andrade *et al.*, (2010), on which the siloxy linkages were functionalised, were unstable when exposed to some solvent conditions. These siloxane linkages undergo hydrolysis upon exposure to alkaline and high-temperature environments (Goddard & Hotchkiss, 2007). The immobilisation of gold nanoparticles on modified track-etched PET membranes through biphenyl-4, 4'-dithiol was reported by Švorčík *et al.*, (2011). Therefore, the availability of the phenyl moiety eliminates any possibility of having both thiol terminals functionalised to the polymer surface.

The introduction of cross-linking agents offers a complete reaction which improves the number of tethered amines to the carboxyl reactive moieties on the surface of the membrane. Mauter *et al.*, (2011), showed that when the coupling agent, 1-(3-dimethylaminopropyl)-3-ethyl carbodiimide hydrochloride (EDC), was used to facilitate the formation of amide bonds between carboxyl and amine moieties, a higher concentration of immobilised silver nanoparticles is obtained. The EDC reacts with carboxyl functionalities to form an amine-reactive intermediate, O-acylisourea, which then reacts with an amine to form an amide bond (Vashist, 2012). The intermediate O-acylisourea hydrolyses easily, which makes it unstable in an aqueous environment. N-hydroxysulfosuccinimide (NHS) is employed to react with the amine-reactive intermediate in order to increase the efficiency of EDC-mediated coupling reactions, as a result, it hinders the susceptibility of O-acylisourea to hydrolysis (Liu *et al.*, 2013). The combination of EDC and NHS results in the conversion of the carboxyl group to

succinimide ester, an amine-reactive intermediate, therefore making it susceptible to nucleophilic attack from a lone pair of electrons on the nitrogen of amine to form an amide bond (Chow *et al.*, 2005). On the other hand, the EDC/NHS chemistry could be used to functionalise chemical linkers at room temperature rather than at elevated temperatures and under aqueous conditions, as this would limit the exposure of the polymer membrane to heat and strong organic reagents/solvents. EDC/NHS chemistry has not been extensively used in coupling amine terminated molecules to reactive carboxyl moieties on track-etched PET membranes (Mauter *et al.*, 2011). To achieve the amide bond formation, the EDC-mediated coupling reaction involves many reaction steps, therefore, not specific and challenging in its synthesis.

2.5.8 Metal nanoparticles immobilisation

The integrity and performance of surface-enhanced Raman spectroscopy (SERS) active materials' stability over time has been maintained with the improvements of the adhesion properties of metal nanoparticles on solid supports (Park *et al.*, 2013). The immobilisation of metal nanoparticles through electrostatic interactions is unstable in aqueous environments due to weak binding forces (Caro *et al.*, 2008). In order to reduce the risk of releasing a high load of nanoparticles into the aquatic environment, the use of silver-coated membranes in an aqueous environment needs a stable nanoparticles immobilisation (Yin *et al.*, 2013). During filtration, the unstable, immobilised metal nanoparticles on modified track-etched membranes could easily leach through the membrane leading to the deterioration and loss of application (Park *et al.*, 2013). Reznickova *et al.*, (2014), reported that silver nanoparticles were immobilised on plasma treated polyethylene terephthalate (PET) membrane through a biphenyl-4,4'-dithiol. A thiol terminal end was used to form the silver-sulphur bond and the other terminal thiol formed a bond with reactive species on the modified track-etched PET membrane surface. However, the report by Yin *et al.*, (2013), illustrated the successful immobilisation of silver nanoparticles on polyamide thin film composite membranes through cysteamine as a chemical linker, where the amine was coupled to carboxyl and thiol was covalently bonded to the silver nanoparticle.

In the literature, it has been observed that most of the polymer membrane modifications are applied in biotechnology, where proteins (amino acids), such as deoxyribonucleic acid (DNA) are anchored to the polymer surface through bi-functional molecules (Li *et al.*, 2014a). In the same vein, in certain other literature, the hydrophobic interactions existing

between the polymer surface and organic compounds are the reason for polymer fouling during water filtration (Kochkodan & Hilal, 2015). This mechanism of fouling could be made applicable in the creation of a hydrophobic environment on the surfaces of the SERS-active materials in order to improve hydrophobic attraction between lipophilic organic micro pollutants (for example trace level pharmaceuticals) and the modified polymer surface (Nghiem *et al.*, 2005).

In this research study, the aminolysis of the PET membrane surface would be carried out using a mild reactant known as diethylenetriamine. This would not lead to the degradation of the track-etched PET membrane surface, so as to preserve the bulk properties, like the mechanical strength. To be put into consideration are other factors which would be the use of functionalising chemicals/reagents whose reaction times are shorter than long chains and high molecular weight chemical linkers, so as to functionalise the surface of track-etched PET membrane.

In addition, this part of the research study also includes the direct immobilisation of silver nanoparticles on the surface of aminolysed track-etched PET membrane during reduction of silver salt precursor (silver nitrate) by a reducing and stabilising agent (trisodium citrate). The method of direct immobilisation is conservative of energy and time, as the other immobilisation methods require long hours of immobilisation under fragile conditions. The fabricated platform of silver-coated track-etched PET membrane would act as surface-enhanced Raman spectroscopy platform for detection of the persistent organic pollutants.

2.5.9 Characterisation methods

There are various characterisation methods involved in the investigation of processes which involve functionalisation of chemical linkers and immobilisation of silver nanoparticles on the modified polymer membrane, as well as the synthesis of silver nanoparticles. In addition to the characterisation of the materials, Raman spectroscopy is also used in the detection of persistent organic pollutants which would be dropped and dried on the silver-coated track-etched polyethylene terephthalate (PET) membrane. The techniques which are usually employed for characterisation and which are going to be used in this study include: contact angle measurements, Fourier transform infrared spectroscopy (FTIR), Raman spectroscopy, scanning electron microscopy (SEM), thermogravimetric analysis (TGA), transmission electron microscopy (TEM), X-ray photoelectron spectroscopy (XPS) and zeta (ζ) potential. In this section, a brief description of each characterisation technique which would be

employed for the analysis of silver nanoparticles, modified and unmodified track-etched membranes.

2.5.9.1 Scanning electron microscopy (SEM)

SEM is an analytical technique used in membrane technology to characterise the surface morphology (size, shape and arrangement of particles), porosity, pore size and topography (surface features and texture) of sample materials (Lin *et al.*, 2016). The electron scanning microscope generates an image of a sample's topography, morphology and also gives the chemical composition and relative ratios of elements and compounds constituting a sample when coupled with electron dispersive spectroscopy (McMahon, 2008). When a sample is scanned with a focused beam of electrons, it leads to the production of various signals which are as a result of electrons interaction with the atoms in the sample. The images creation comes from the detected secondary electrons which have been reflected from the sample's surface as a result of excitation by the primary electron beam (McMahon, 2008).

SEM is used in this study for the characterisation and confirmation of the modification made, and also, to confirm the functionalisation of diethylenetriamine as a chemical linker on the track-etched PET membrane surfaces. It is also used to characterise the immobilisation of silver nanoparticles on the chemical linker attached to the modified membrane.

2.5.9.2 Transmission electron microscopy (TEM)

TEM is another electron microscopy technique, in which a beam of electrons passes through the sample as opposed to reflected electrons used in the scanning electron microscopy technique. When the beam of electrons passes through the sample, it interacts with atoms in the sample and the electron beam is attenuated and finally collected from below the sample through a camera or phosphorescent screen (McMahon, 2008). TEM has been employed in the environmental studies in the identification and quantification of colloidal nanoparticles in samples (Khan *et al.*, 2011). TEM is useful in the characterisation of the synthesised silver nanoparticles in order to qualitatively determine structural information (shape, size) and particle size distribution (whether mono- or poly-dispersed).

2.5.9.3 Ultraviolet - visible spectroscopy (UV-Vis)

The UV light with a 190 – 350 nm range and visible (Vis) light with a 350 – 800 nm range radiations are absorbed by many molecules, upon excitation of the outer electrons in the molecule (McMahon, 2008). When radiation with a specific intensity is passed through a

liquid sample, it loses some of its energy resulting in a reduction in intensity, as a result of reflection off the sample holder (cuvette), scattering and absorption by the sample itself (McMahon, 2008). To obtain the intensity attenuation due to absorption only, a control is used as a reference solution with no analyte. The absorbance of radiation by the sample is shown by the absorption spectrum which is normally continuous and is a plot of absorbance versus wavelength in nanometres (McMahon, 2008). The technique is employed to ascertain the formation of silver nanoparticles and information regarding size and shape of colloidal nanoparticles in the sample (Khan *et al.*, 2011, Xu *et al.*, 2008). Therefore, ultraviolet-visible spectroscopy (UV-Vis) would be used to characterise how successfully the silver nanoparticles have been synthesised in terms of size and shape).

2.5.9.4 Fourier-transform infrared spectroscopy (FT-IR)

FT-IR is a non-destructive technique, whose absorption bands expressed in wavenumbers (cm^{-1}), are used to investigate deformations, bending and ring vibrations in a molecule (Schmitt *et al.*, 1998). It is a technique mostly used to study the chemical nature of polymer membranes, focusing on the chemical functionalities on the surface (Lin *et al.*, 2016). It gives fingerprint information that is specific to frequencies of vibrations of the bonds present in a sample material. This offers an easy way to determine composition of a polymer through analysis of absorption bands and peaks of functional groups in polymer membranes (Lin *et al.*, 2016; McMahon, 2008).

2.5.9.5 Thermogravimetric analysis (TGA)

TGA is a characterisation technique used in the determination of the thermal profile of a material for comparison purposes when such material has been subjected to applied temperature. It is used in the measurement of the mass of a material as a function of time over temperature in order to determine the degradation, glass transition point of polymers and the melting point (McMahon, 2008). The technique would be used to investigate the thermal profile of the unmodified, modified and silver-coated track-etched polyethylene terephthalate (PET) membranes in terms of their mass loss as a function of temperature. This is for the purpose of monitoring if the thermal properties of the PET membrane change with exposure to the modification conditions.

2.5.9.6 Contact angle measurement

Contact angle measurement is also a widely used method for the determination of hydrophobic and hydrophilic behaviour of polymer membranes (Korolkov *et al.*, 2015). The attraction between two interfaces is indicated by the contact angle, and if the contact angle is more than 90°, then there is less attraction, indicating hydrophobicity.

There are three options for the measurement of contact angle: (1) the static contact angle which is measured between a liquid and solid without a change from outside during the measurement, (2) the dynamic contact angle (advancing angle) that is measured in the course of wetting of the solid interface and is not affected by time and (3) receding angle which is also a dynamic contact angle, but is measured during the de-wetting process and is usually smaller than the advancing angle. The static contact angle option is used to typically determine the contact angles.

This technique enables the confirmation of surface changes in terms of hydrophobicity and hydrophilicity between unmodified track-etched polyethylene terephthalate (PET), amine-modified track-etched PET and silver-coated track-etched PET surface. The presence of amines on the PET surface would result in increased hydrophilic behaviour (Korolkov *et al.*, 2015).

2.5.9.7 Raman spectroscopy

Raman spectroscopy is a technique of characterisation based on the spectroscopic concept of light scattering by the sample rather than light absorption (McMahon, 2008; Meyers, 2000). According to O'Connor *et al.*, (2013), Raman spectroscopy is dependent on the Raman effect which offers structural information in terms of functional groups in a molecule, based on the energy vibrational bands. The Raman spectroscopy finds its application in testing laboratories as it gives data with chemical specificity (Matousek *et al.*, 2006).

In this research study, Raman spectroscopy was employed in two modes: (i) applied as a characterisation technique, (ii) used as an analytical technique for the detection of molecules on the surface of the silver nanoparticles-coated track-etched polyethylene terephthalate (PET) membrane. It is used in complementing other surface chemistry analytical methods such as

the X-ray photoelectron spectroscopy (XPS), and the technique is also employed as a method for the detection of pollutants in the concept of surface-enhanced Raman spectroscopy.

2.5.9.8 X-ray photoelectron spectroscopy (XPS)

XPS is an analytical method widely used to characterise surface chemistry of thin films such as polymer membranes (Duwez, 2004). Therefore X-ray photoelectron spectroscopy (XPS) is used to characterise elemental composition by electron spectroscopic means on the surface of the polymer membranes (Finklea et al., 2000; Meyers, 2000). The spectra data of the XPS gives the binding energies of the atoms on the surface and their chemical environments and complements the Fourier-transform infrared (FT-IR) spectra. According to O'Connor et al., (2013), the binding energy of electrons emitted from an atom is characteristically-specific to that atom, and therefore, offers a fingerprint information. The XPS is used in this study to investigate the composition of the unmodified and modified track-etched polyethylene terephthalate (PET) membrane, so as to track the surface changes emanating from the solid-liquid interface reactions between the amine and PET membrane. The XPS technique is further used to investigate the immobilisation of silver nanoparticles on the surface of modified track-etched PET membrane via nitrogen atoms.

2.5.9.9 Zeta potential

The zeta (ζ) potential is a method used to determine the stability of the colloidal nanoparticles. The electric charges on the nanoparticles are a factor in their stability; the electric charge on a nanoparticle hinders agglomeration of the nanoparticles by charge repulsion. The criteria are on the basis of like charges of nanoparticles which would repel one another in order to debar the formation of clusters by nanoparticles. The zeta potential values in either positive or negative direction of more than 20 mV are considered good for stability. For this study, zeta potential is employed for the determination of the colloidal silver nanoparticles synthesised by the reduction of silver nitrate by trisodium citrate in the aqueous media.

2.6 Chapter summary

In this chapter, the persistent organic pollutants in their types and means of entry into the environment have been extensively detailed. These organic pollutants become a major threat to human health, and aquatic organisms. Due to the often minute concentrations and the

complex nature of the matrices that the target compounds are found in the aquatic environments, it becomes a challenging task to analyse those pharmaceuticals present in the environment. The presence of these compounds at trace levels in complex water matrices makes it difficult to carry out an effective analysis; as a result, an analytical method which is sensitive and suitable to monitor these analytes at low levels must be developed.

There are various conventional methods available such as high-performance liquid chromatography (HPLC), gas chromatography coupled with mass spectroscopy (GC/MS), and liquid chromatography coupled with mass spectrometry (LC/MS), and electrochemical and spectrophotometry methods; and these are all established techniques for the analysis of water pollutants (Li *et al.*, 2013a). These conventional techniques demand complex sample preparation processes for different persistent organic pollutants. However, quantification of low concentrations of persistent organic pollutants has also been a challenge, as some studies have recently shown that most of the persistent organic pollutants could not be quantified, even though they were detected in treated drinking water (Luo *et al.*, 2014). According to the study on antiretroviral drugs' occurrence in surface water across South Africa by Wood *et al.*, (2015), an average detection limit of 90 ng/L was reported by the use of ultra high-pressure liquid chromatography tandem mass spectrometry (UHPLC/MS/MS).

These challenges, therefore, trigger the efforts to develop methods that are novel and are able to rapidly detect micro-pollutants to a single molecule limit. The 2012 report of World Health Organization on pharmaceuticals in drinking water indicated that "monitoring programs for pharmaceuticals in water face practical difficulties due to lack of standardised analytical protocols, high costs and limited availability of analytical instruments". The conventional analytical techniques currently employed for the detection and quantification of organic pollutants such as GC/MS and HPLC/MS are expensive to operate, restricted to non-mobile operations and time-consuming, which makes them less attractive during emergencies and out of laboratory analysis (Li *et al.*, 2013b). It was noted in a study conducted by Yuan *et al.*, (2013), that though LC/MS/MS is a selective and versatile technique, it is susceptible to matrix interferences that suppress the analyte signals, and thereby generate inaccurate results. Also, the validation process of the results is also time-consuming; thereby making the recovery prone to inaccuracy.

As a result of these limitations, the need exists to explore the novel detection technologies such as biosensors, fluorescence probes, surface-enhanced Raman spectroscopy (SERS), and

so on, with the object of trace micro pollutants detection (Comerton *et al.*, 2009; Pavlović *et al.*, 2013). SERS has gained a lot of attention among other emerging techniques in the detection of trace level analytes in chemical analysis, (Smith, 2008) and biotechnology (Botti *et al.*, 2014). As a result, portable SERS equipment could be employed as a technique for on-site detection, contrary to chromatography and mass spectrometry which are laboratory-based technique. It has also been reported that SERS has a finger-printing capability, an ultra-high sensitivity and a rapid detection (Botti *et al.*, 2014). In cases of an emergency, where it is necessary to identify pollutants in remote areas, there is a need to develop a simple analytical technique or method for identification and quantification without the recovery protocol needs (Li *et al.*, (2014a).

With the inability of the conventional chromatography techniques like the HPLC to detect and quantify low levels persistent organic pollutants due to low sensitivity, as a result of complex method development, resulting in the low limit of detection (LOD), making it difficult to be sensitive to very low nanogram per litre range; it is important for adequate methods to be developed for accurate identification and quantification by capillary electrophoresis in the analysis of selected pharmaceuticals and other organic pollutants in aqueous solutions. The high efficiency and analysis speed, low sample consumption coupled with fast method development of capillary electrophoresis has put it in a position of advantage over HPLC. CE is also found to be less selective compared to HPLC; rather, it offers improved resolution, sensitivity at low level, speed, good analyte separation in short period of time (Swartz *et al.*, 2018b).

Therefore, capillary electrophoresis methods as discussed earlier in the chapter will be employed to exploit the limitations of the conventional methods for the analysis of the selected persistent organic pollutants under investigation in this research study.

CHAPTER THREE

MATERIALS AND METHODOLOGY

3 Introduction

In this chapter, the materials and chemicals used in this study are highlighted. This chapter also details the experimental step-by-step procedure employed in the actualisation of the research aims and objectives. The analytical techniques employed in the sample analysis, material synthesis and characterisation are also described.

3.1 Chemicals

Acetylsalicylic acid ($C_9H_8O_4$), benzoic acid ($C_7H_6O_2$, 99.5%) from Sigma-Aldrich, Benzylamine (C_7H_9N , 99%) from Sigma Aldrich, imidazole ($C_3H_4N_2$, 99%) from Sigma-Aldrich, salicylic acid ($C_7H_6O_3$), 2,3-dichlorophenol ($C_6H_4Cl_2O$, 98%) from Sigma Aldrich, and 2,4-dinitrophenol ($C_6H_4N_2O_5$, 98%) from Sigma-Aldrich; were used in the CE optimisation analysis. The pharmaceutical reagents used in the CZE-UV methods and analysis of the water samples include: acetaminophen ($C_8H_9NO_2$, 98%) and sulphamethoxazole ($C_{10}H_{11}N_3O_3S$, 98%) which were purchased from Alfa Aesar, Germany, ibuprofen ($C_{13}H_{18}O_2$, 98%), diclofenac ($C_{14}H_{11}Cl_2NNaO_2$, 98.5%), aspirin ($C_9H_8O_4$, 99.0%) and salicylic acid ($C_7H_6O_3$, 99.0%) were purchased from Sigma-Aldrich. The steroid reagents employed in the PF-MEKC methods and water samples analysis include: androstenedione ($C_{19}H_{26}O_2$, assay $\geq 98\%$) which was purchased from Sigma-Aldrich (Germany), whereas, testosterone ($C_{19}H_{28}O_2$, assay $\geq 98\%$), progesterone ($C_{21}H_{30}O_2$, assay $\geq 98\%$), and 17 β -estradiol ($C_{18}H_{24}O_2$, assay $\geq 98\%$) from Sigma-Aldrich. The steroids were stored in a dark and cold room (+4 °C).

The remaining reagents include ammonia (min. purity 25%) purchased from VWR International S.A.S. (France), ammonium acetate (98%) purchased from Sigma-Aldrich, and diethyl ether (GC assay, min 99.5%) purchased from Merck. Methanol (HPLC grade) was purchased from Fisher Scientific (UK) and ethyl acetate (GC assay N 99.5 percentage) purchased from Sigma-Aldrich. The sodium salt of taurocholic acid monohydrate (BioXtra, $\geq 95\%$ and sodium dodecyl sulphate (99%) were purchased from Sigma-Aldrich. Hydrochloric acid (1.0 M, analysis result 0.9995 mol/L, ± 0.0021 mol/L) and sodium

hydroxide (1 M, analysis result 1.0003 mol/L, ± 0.0021 mol/L) were purchased from Oy FFChemicals (Finland). Methanol was employed as the solvent in standards and as electroosmosis marker. Pyridine (N99.8%), glycolic acid (N99%), and 18-crown-6 (1,4,7,10,13,16-hexaoxacyclooctadecane, N99%) were from Sigma-Aldrich Finland Oy (Helsinki, Finland). Ultrapure water used in the analyses was purified with a Direct-Q UV Millipore water purification system (Millipore S.A., France). Diethylenetriamine (DETA) (98%) from Alfa Aesar, (Germany), 4-aminothiophenol [4-ATP 10^{-3} M (Merck 99%)], absolute ethanol (99.9%) from Sigma-Aldrich, (Germany). Silver nitrate (99+ %) from Alfa Aesar (Germany), trisodium citrate ($\text{Na}_3\text{C}_6\text{H}_5\text{O}_7$, 98%) from Alfa Aesar, (Germany).

3.2 Instrument and methods (CE)

The separation principle of CE is due to different ionic mobilities of the analytes and partitioning to different phases via hydrophobic interactions; and the analytes migrate through the electrolyte solutions in the capillaries in electric fields, (Voeten *et al.*, 2018). In this study, capillary zone electrophoresis (CZE) and partial filling micellar electrokinetic chromatography (PF-MEKC) were used. Electroosmotic flow (EOF) is the motion of the ions in the capillary liquids. The flow is induced by the electric potential in the capillary. The capillary can also contain some membrane, channels or porous material, for example. The electroosmotic flow gives the ions in the solution the kinetic energy to move forward under the electric field influence.

A commercial capillary electrophoresis instrument (Agilent Technologies, Germany) having a diode array detector and air cooler system was employed for the determination. The CE instrument was applied with ChemStation programmes (Agilent) for instrument running and data handling. PeakMaster software was used to predict the migration order of the analytes. Bare fused silica capillaries (inner diameter 50 μm , outer diameter 375 μm , total length 70 cm, length to detector 61.5 cm) were used. Prior to use, the capillaries were conditioned by sequentially flushing with 0.1 M NaOH, Milli-Q water, and the electrolyte solution, for 20 minutes each at 13.634 psi (940 mbar). Prior to each analysis, the capillary was flushed with 0.1 M NaOH and the electrolyte solution for 2 to 5 minutes depending on the method.

3.2.1 Electrolyte solutions for CE optimisation

Tricine buffer (Tricine $\geq 99\%$ (titration), pKa 8.15, Sigma) was prepared from the 400 mM stock solution. Two electrolyte solutions were prepared from the stock solution. Their pHs were adjusted with 1.0 M NaOH and 0.1 M NaOH. The exact volume of each buffer was recorded. The freshly prepared buffered electrolyte solutions had nearly the same ionic strengths, but different concentrations and pH-values: **I=10 Mm**; background buffer electrolyte 1 & 2 (**BGE1**) (14 mM, **pH 8.5**) and **BGE2** (50 mM, **pH 7.5**). The final volumes of the buffers were 50 mL made up with Milli-Q water. The final dilution to the mark of the volumetric flask was made after the pH adjustment. An inoLab pH 7110 WTW pH-meter was used for the measurements. VWR Chemicals AVS TITRINORM Buffer solutions with pH 4.00, 7.00 and 10.00 were used for the calibration of the pH meter. MilliQ-water was used to dilute the solutions to 50 mL measuring bottles. Neutral and low basic buffers are good for the analysis because they increase the electroosmotic flow and help the anions to move faster. If the pH is too low, the anions travel very slowly.

First the “BGE1” buffer solution of tricine concentration 14 mM with pH 8.5 was prepared. The calculation done with equation 3.1 for the volume of tricine is presented below.

$$C_1V_1 = C_2V_2 \quad (3.1)$$
$$V_{1, \text{tricine, BGE1}} = \frac{C_2V_2}{C_1} = \frac{14 \text{ mM} \times 50 \text{ mL}}{400 \text{ mM}} = 1.75 \text{ mL}$$

The tricine and some MilliQ-water was added to the 50 mL measuring bottle. 1650 μL of 0.1 M NaOH and 300 μL of 1.0 M NaOH were added to get pH 8.5. According to equation 2 the molar amount of NaOH added was:

$$n_{\text{NaOH, BGE1}} = cV \quad (3.2)$$
$$= 0.1 \text{ M} \times 1650 \times 10^{-6} \text{ L} + 1.0 \text{ M} \times 300 \times 10^{-6} \text{ L}$$
$$= 4.65 \times 10^{-4} \text{ mol.}$$

Then the bottle was filled to 50 mL with MilliQ-water and the NaOH concentration was:

$$C_{\text{NaOH, BGE1}} = \frac{n}{V} = \frac{4.65 \times 10^{-4} \text{ mol}}{50 \times 10^{-3} \text{ L}} = 9.3 \text{ mM}$$

The “BGE2” buffer solution of tricine concentration 50 mM with pH 7.5 was done the same way as BGE1. The volume of tricine solution used was:

$$V_{1, \text{tricine}, \text{BGE2}} = \frac{C_2 V_2}{C_1} = \frac{50 \text{ mM} \times 50 \text{ mL}}{400 \text{ mM}} = 6.25 \text{ mL}$$

200 μL of 1.0 M NaOH and 2200 μL of 0.1 M NaOH were added to get pH 7.5. The molar amount of NaOH was:

$$\begin{aligned} n_{\text{NaOH}, \text{BGE2}} &= cV \\ &= 0.1 \text{ M} \times 2200 \times 10^{-6} \text{ L} + 1.0 \text{ M} \times 200 \times 10^{-6} \text{ L} \\ &= 4.2 \times 10^{-4} \text{ mol.} \end{aligned}$$

The concentration of NaOH after filling to 50 mL was:

$$C_{\text{NaOH}, \text{BGE2}} = \frac{n}{V} = \frac{4.2 \times 10^{-4} \text{ mol}}{50 \times 10^{-3} \text{ L}} = 8.4 \text{ mM}$$

Both tricine buffers solutions were transferred to CE vials (800 μL) used in the CE instrument carousels. Three vials each of both buffer solutions were taken.

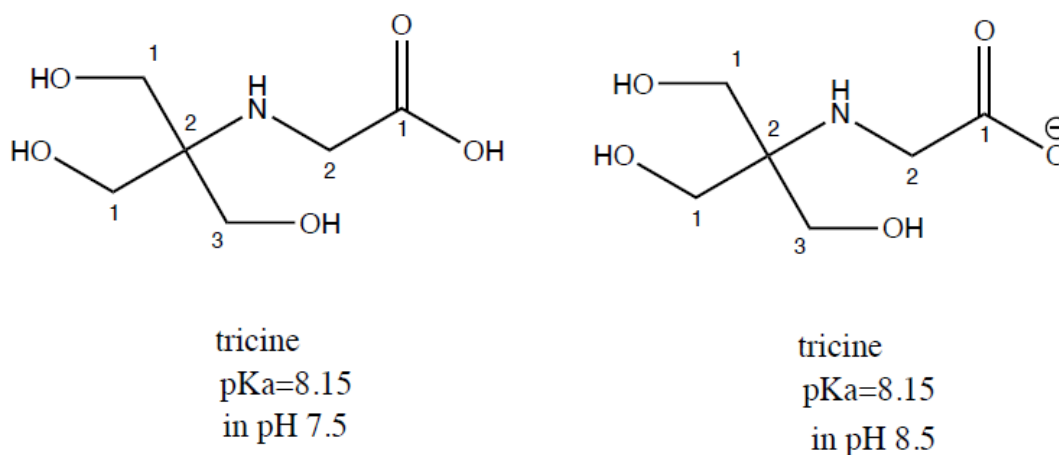


Figure 3.1: The structures of Tricine (pKa-value 8.15) in pH 7.5 and 8.5 solutions BGE2 and BGE1 respectively. NH can also protonate and form NH₃⁺.

3.2.2 Ionic strengths

The concentration of tricine in BGE1 is 14 mM and in BGE2 50 mM. The concentration of NaOH in BGE1 is 9.3 mM and in BGE2 8.4 mM. The ionic strengths of the buffer solutions were calculated with the equation for molar ionic strength. The degree of dissociation for

tricine is 18.29% in pH 7.5 and 69.12% in pH 8.5. An example of the calculation is below for pH 7.5.

$$\alpha = \frac{1}{1 + 10^{pK_a - pH}} \quad (3.3)$$

$$= \frac{1}{1 + 10^{8.15 - 7.5}} = 0.1829$$

In BGE1 pH 8.5 69.12 % of tricine concentration is in ionic form. Thus, the ionic strength for BGE1 is:

$$I_{BGE1} = \frac{1}{2} \times \sum CZ^2 \quad (3.4)$$

$$= \frac{1}{2} \times (c_{NaOH, BGE1} \times nr(Na^+) \times 1^2 + c_{NaOH, BGE1} \times nr(OH^-) \times (-1)^2 + 0.6912 \times (c_{tricine}) \times 1^2)$$

$$= \frac{1}{2} \times (9.3 + 9.3 + 14 \times 0.6912) mM = 14.14 mM$$

The same way the ionic strength for BGE2 pH 7.5 where 18.29 % of the tricine is in ionic form is:

$$= \frac{1}{2} \times (8.4 + 8.4 + 50 \times 0.1829) mM = 12.97 mM$$

The electrophoretic mobility for cations can be calculated with equation 3.5a, where μ_{ep} is the electrophoretic mobility, μ_{eo} is the mobility of the electroosmotic flow and μ_{tot} is the total mobility of the compound.

$$\mu_{tot} = \mu_{ep} + \mu_{eo} \quad (3.5a)$$

For anions the electrophoretic mobility is calculated as presented in equation 3.5 b:

$$\mu_{tot} = \mu_{ep} - \mu_{eo} \quad (3.5b)$$

$$\mu_{ep} = \frac{L_{cap} \times L_{det} (m^2)}{Voltage (V) \times Time (s)} [m^2 / Vs] \quad (3.5c)$$

Where L_{cap} = Length of the capillary (m);

Ldet = Length to the detector (m);

V = Voltage applied (V);

T = Migration time (s).

3.2.3 Conditioning of the Capillary

Before any analysis, the capillary was conditioned by flushing it with 0.1 M NaOH for 5 minutes, followed by Milli-Q water for 10 minutes, then finally with the BGE1 electrolyte for 10 minutes respectively. Subsequently, when the BGE2 electrolyte was used, the capillary was rinsed with BGE2 electrolyte for 5 minutes before any analysis. In total, 20 vials were used altogether (NaOH, Milli-Q water, 4BGE1 (for 6 standard MIX), 3BGE1 (for Disprin), 4BGE2 (for 6 standard MIX), standard MIX (containing all the 6 analytes), the pre-treated Disprin sample, 6 standard MIX solutions (concentrations from 5 to 25 µg/mL) for quantification of acetylsalicylic acid, and a waste vial).

3.2.4 Method development:

The methods were prepared offline while conditioning the capillary; the vials were placed into the sample carousel, the needed methods were programmed and combined into a sequence. The temperature of the capillary cassette was 25 °C, and the detection wavelength was 214 nm in all methods. (However, to measure the differences in intensities, 4 other wavelengths were chosen). Current was detected in each analysis; and between the runs, the capillary was flushed for 2 minutes with the BGE used (BGE1 or BGE2; depending on the analysis).

3.2.4.1 Analyses with BGE1 electrolyte (pH 8.5; I = 10 mM)

The constant pressure injection was 35 mbar, and the injection time was 10 seconds. The following analyses were carried out with the BGE1:

a. Control analysis for electroosmosis

A mixture of methanol and MilliQ-water (50:50, v/v) was injected as a control sample (blank) for the measurement of the EOF mobility. Analysis voltage was 25 kV and analysis time ranged from 5 to 13 minutes.

b. Voltage series

Analyses of the standard sample with different voltages (10, 15, 20 and 25 kV). One run per voltage was made, and the analysis time ranged about 5-13 minutes.

c. Repeatability and identification

Six repetitions of the standard solution (mixture of all the analytes) were carried out, with the voltage set at 25 kV. Analysis time was 5 minutes.

The peakmaster 5.1-software was used to predict the migration order of the analytes.

3.2.4.2 Analyses with BGE2 electrolyte (pH 7.5; I = 10 mM)

Six analyses were carried out. The constant pressure injection was 35 mbar, and the injection (or separation) voltage was 25 kV.

a. Control analysis for electroosmosis

Analysis of the Milli-Q water with 25 kV (a control sample, blank) for measuring the mobility of the EOF.

b. Constant pressure injection

The standard sample (analyte mixture) was injected with constant pressure of 35 mbar with different injection times (5, 10, 15, 20, and 30 seconds). Analysis voltage was 25 kV.

c. Electrokinetic injection

The standard sample (analyte mixture) is injected with different voltages of 5, 10, 20 and 25 kV. Injection time was 5 seconds.

3.2.5 CE analysis methods for steroids, pharmaceuticals and inorganic ions

Four methods of analysis types were used: a partial filling micellar electrokinetic chromatography (PF-MEKC), capillary zone electrophoresis with direct UV detection (CZE-UV) and two capillary zone electrophoresis methods with indirect UV detection (CZE with indirect-UV). The temperature for the analyses was +25 °C. Positive polarity and voltage of 25 kV was set for the steroids analysis, and 20 kV set as the constant value for pharmaceuticals and inorganic cation analyses, respectively. Negative polarity of voltage -20 kV was used for inorganic anion analyses. In the PF-MEKC, the electrolyte solution was prepared to give a current of 17 μ A, while in the cation and anion analyses the current was between 30 and 40 μ A. The analysis times were 20 minutes, 10 minutes, 10 minutes, and 10 minutes for steroids, pharmaceuticals, cations, and anions, respectively. To quantify steroids, pharmaceuticals, cations and anions, the samples were injected with 0.50 psi (35 mbar) for 6 s, 0.7 psi (50 mbar) for 10 s and with 0.73 psi (50 mbar) pressure for 10 s and 5 s, respectively. In PF-MEKC analysis, the steroids were detected at 214, 220, and 247 nm. Cations and anions studies were carried out with indirect-UV detection at 200 nm, 214 nm, 220 nm, and 254 nm with the reference wavelength of 420 nm.

3.2.5.1 Electrolytes for steroids, pharmaceuticals and inorganic ions analyses

The electrolyte solutions in the analyses of steroids, pharmaceuticals, and inorganic ions are different, and based on the method and composition of the relevant samples. For steroid analysis, the electrolyte solution in the partially-filled micelle composition was 30 mM ammonium acetate, with pH adjusted to pH 9.68 with 25% ammonia. The eventual micelle composition was prepared by adding 1000 μL of 30 mM ammonium acetate (AA), 440 μL of 100 mM sodium dodecyl sulphate (SDS) to 30 mM ammonium acetate solution followed by addition of 50 μL of 100 mM sodium taurocholate solution, specifically in that order. The micelle and the electrolyte solutions were sequentially introduced into the 70 cm long capillary. The micelle plug was placed between the electrolyte solution and the sample solutions.

For the electrolyte solution in the CZE-UV method for the pharmaceuticals analysis, 30 mM ammonium acetate adjusted to the pH 9.68 was the main buffer electrolyte and tagged CAPS 4 method. The parameters for CAPS 4 method include: a buffer concentration of 30 mM ammonium acetate, pH 9.68, 50 mbar pressure, 10 seconds injection time, 70 cm capillary length, 25 $^{\circ}\text{C}$ cassette temperature, and 20 kV voltage. Subsequently, in the inorganic ions analysis, the cations were separated in the buffer solution containing 9 mM pyridine-12 mM glycol acid-5 mM 18-crown-6 ether in milli-Q water (pH adjustment done with 0.1 M HCl). Also, in the optimised CE method, the anions separation was carried out in a buffer solution containing 2.25 mM pyromellitic acid, 6.50 mM NaOH, 0.75 mM hexamethonium hydroxide and 1.60 mM triethanolamine (pH 7.7 ± 0.2). The pyromellitic acid electrolyte (BGE) pH 7.7 for HPCE anions separation was from Fluka Chemie AG (Switzerland). The pH of the electrolyte for anions was 7.7. The pH values were adjusted and checked using InoLab pH 7110 (WTW) instrument. The electrodes calibration was done with commercial buffer solutions at pH 4.00, 7.00 and 10.00 (Fisher Scientific, UK).

3.2.6 Sampling

Real water samples were also studied which include: 2 L blank Milli-Q water, 2 L hot tap water, 2 L cold tap water and 2 L distilled water spiked with the 5 standard analytes. The analysis was in three parts: Solid phase concentration of clean water sample, the mixture of the respective standard analyte samples and the influent and effluent water samples.

Cold tap water (2 L) and hot water (2 L) samples were taken within the University campus. The sample was collected into clean plastic bottles (2 L). These bottles were prewashed with ultra-pure water; for the cold water sampling, the tap water was let to flow (3 x 2 L volume) before the final sampling and the bottle was filled completely. For hot water sampling, the water was allowed to run for at least 10 minutes at its maximum flow to ensure the water temperature stability before the sample was taken. The bottles were tightly capped and taken to the laboratory where they were kept in a dark place at 4 °C until the water was used, and the extraction procedure was performed before 3 days after sampling. Subsequently, sampling was also done at the wastewater treatment plant (WWTP) of the University of Helsinki, Finland. Two different influent water samples were taken on different dates (Influents A & B), and an effluent sample was also taken, with the bottles tightly capped and taken to the laboratory where they were kept in a dark place at 4 °C until preconcentration was carried out. Subsequently, another effluent sampling was carried out at the wastewater treatment plant (WWTP) in Bellville, Cape Town, South Africa. The effluent sample was taken after the membrane bioreactor (MBR) stage treatment. The inorganic ions sampling was also carried out, the water samples represented include RW 1 (river water 1), RW 2 (river water 2), DW (drilled well water), MQW (milli-Q water), KHTW (kitchen hot tap water), KCTW (kitchen cold tap water), HL1W (hot laboratory 1 tap water), CL1W (cold laboratory 1 tap water), HL2W (hot laboratory 2 tap water), and CL2W (cold laboratory 2 tap water) respectively.

3.2.7 Sample preparation with solid phase extraction (SPE)

The SPE device VacMaster (Biotage® VacMaster™ 20 Sample Processing Station) was employed for sample concentration (solid phase extraction of the water samples). The water samples were preconcentrated with Strata-X 33µm polymeric C₁₈ reverse phase columns (500 mg/6 mL) which were obtained from Phenomenex (Denmark). The Reacti-Vap Evaporation unit (Thermo Scientific, Finland) was used for evaporation of the extracts under N₂ gas. All waters used were purified with a Direct-Q UV Millipore water purification system (Millipore S.A., France).

2 L each of hot tap water, cold tap water, and Milli-Q were preconcentrated by running each sample through SPE cartridge (2 cartridges for each 2 L of samples). Prior to the extraction process, the SPE cartridges (C₁₈ columns) were preconditioned with 6 mL absolute methanol (HPLC grade) and 6 mL Milli-Q water was also used to flush the cartridges. The respective

water samples were run through the cartridges at a slow rate, thereafter, the sorbent materials (SPE cartridges) were left to dry for 12 hours. Extraction from the sorbent materials was then carried out by running 6 mL methanol slowly through each one. The eluates were collected in test tubes and separately evaporated under nitrogen with mild heating (40 °C) to dryness, followed by dissolution with 2 mL methanol with agitation. The sample volumes from the C₁₈ columns were 2 mL in each case. The final sample volume of 250 µL was separated from the pre-concentrated analytical sample for the analysis and the study was performed with four replicates and with eight sequential analyses. Recovery studies were carried out using the SPE method. Analytes were recovered from solution of 5 mg/L cocktail analyte standards in Milli-Q water. For the inorganic ions analysis, the 10 water samples were filtrated with both glass fibre and membrane filters to trap the unwanted particles in the water sample, thereafter, the sample for analysis was taken.

3.3 Preparation of Standard Solutions for CE optimisation

Working solutions (standard solution, abbreviated as the MIX) of the six analytes (benzoic acid, 2,3-dichlorophenol, acetylic salicylic acid benzylamine, and imidazole) were prepared as a mixture for the qualitative studies. Their pK_a-values, which inform their ionization in the electrolytes, are listed accordingly:

- Benzoic acid (pK_a = 4.2)
- 2,3-dichlorophenol (pK_a = 7.5)
- 2,4-dinitrophenol (pK_a = 4.0)
- Acetylsalicylic acid (Aspirin) (pK_a = 3.5)
- Benzylamine (pK_a = 9.4)
- Imidazole (pK_a = 7.0)
- Salicylic acid (pK_a = 2.98)

The working solution was made from 1000 µg/mL solutions (individual solutions for each standard in methanol; solutions are ready to use) by first preparing a mixture of 100 µg/mL from the stock solutions in methanol. The starting concentrations of all analyte solutions were 1000 µg/mL, except benzylamine that was 1600 µg/mL. At first, all of the standard solutions were diluted to 100 µg/mL concentrations in methanol to 10 mL volume. 1000 µL of the five standard solutions and 625 µL of benzylamine solution were measured into 10 mL volumetric

flask to get the 100 µg/mL. Thereafter, the MIX solution was prepared by taking 1300 µL of all the 100 µg/mL solutions into a 10 mL vial and filling it to the mark with Milli-Q water-methanol (50:50). The concentration of the MIX standard solution was 13 µg/mL for all of the six analytes. (A fresh stock was made each time for acetylsalicylic acid, to avoid easy degradation to salicylic acid). A methanol – Milli-Q water (50:50, v/v) sample was needed for detecting the mobility of electroosmosis.

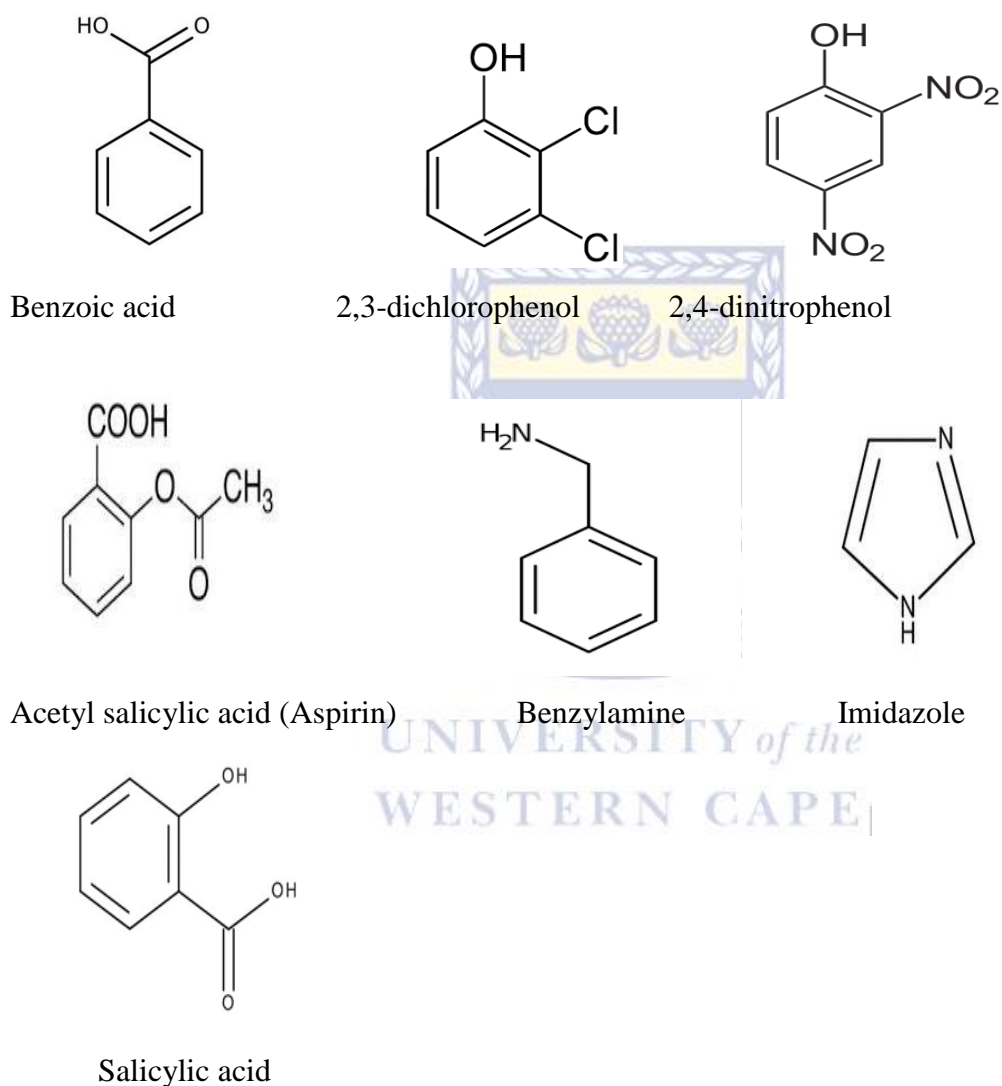


Figure 3.2: Structure of the compounds used as standards.

3.3.1 Preparation of calibration standards for quantification of aspirin

Acetylsalicylic acid (ASA) or aspirin reference samples for quantification were prepared to determine the concentration of aspirin in Disprin™ tablets. To measure the amount of acetylsalicylic acid (aspirin) and the degradation product, salicylic acid, a concentration

calibration curve with 2, 5, 10, 15, 20, and 25 µg/mL standard mixtures were prepared (only the two compounds in the mixture; preparation from 100 µg/mL solutions). Concentrations 2, 5, 10, 15, 20 and 25 µg/mL were prepared in 5 mL vials. The solutions were diluted with Milli-Q - water-methanol (50:50); and subsequently analysed using BGE1 buffer solution at 25kV. In Table 4.1 are the volumes of the 100 µg/mL acetylsalicylic acid and salicylic acid solutions and water:methanol that were used in the dilutions.

Table 3.1: Preparation of calibration standard solutions

Concentration (µg/mL)	2	5	10	15	20	25
Acetylsalicylic acid (mL)	0.1	0.25	0.5	0.75	1	1.25
Salicylic acid (mL)	0.1	0.25	0.5	0.75	1	1.25
Water : Methanol (mL)	4.8	4.5	4	3.5	3	2.5

3.3.2 Preparation of the Disprin Sample

A sample was prepared from the pharmaceutical Disprin™ 500 mg (Orion Pharma). The pill contains acetylsalicylic acid 63% (w/w). The whole Disprin tablet was crushed in a mortar and 10.1 mg was taken for the analysis. It was dissolved in Milli-Q water by the way of ultrasonication for 5 minutes. The Disprin concentration of the 10 mL was 1010 µg/mL. After sonication, the sample was syringe-filtered and diluted to three subsamples of volume 5 mL with the concentration of 25 µg/mL that were determined with CE. Equation 1 was used to calculate the volume of 1010 µg/mL Disprin solution needed for the three 5 mL subsamples.

$$V_1 = \frac{C_2 V_2}{C_1} = \frac{25 \mu\text{g/mL} \times 5\text{mL}}{1010 \mu\text{g/mL}} = 0.12376 \text{ mL} \approx 124 \mu\text{L}$$

3.4 Preparation of Standard Solutions and calibration standards for pharmaceuticals analysis using CZE-UV method

The working solution of the six standard analyte samples (acetaminophen, sulphamethoxazole, ibuprofen, diclofenac, dspirin, and salicylic acid) was made from 1000 µg/mL solutions (individual solutions for each standard analyte in methanol) by first preparing a mixture of 100 µg/mL from the stock solutions in methanol. 1000 µL of the six standard solutions were measured into a 10 mL volumetric flask to get the 100 µg/mL. A solvent dilution ratio of 30:70 (MeOH/H₂O) mixture was used to prepare the concentration calibration range of 0.5 µg/mL, 1 µg/mL, 2 µg/mL, 4 µg/mL, 6 µg/mL and 8 µg/mL respectively, for the six analyte mixtures.

3.5 Concentration calibration for steroids (PF-MEKC-UV)

The working solution of the six steroid standard analyte samples (androstenedione, testosterone, 17-beta-estradiol, and progesterone) was also made from 1000 µg/mL solutions (individual solutions for each standard analyte in methanol), and the steroid concentrations in concentration calibration were 0.5, 1, 2, 3, 5, 6 µg/mL for androstenedione, testosterone, 17-beta-estradiol, and progesterone.

3.6 Preparation of Standard Solutions and calibration standards for the inorganic ions (CZE-indirect-UV)

The standard analytes for the anion and cation analyses include potassium chloride (KCl), magnesium sulphate (MgSO₄), sodium nitrate (NaNO₃), and calcium chloride (CaCl₂). 1000 µg/mL of the analytes was prepared, and 50 µL aliquot was taken into 800 µL vial and diluted with 750 µL of Milli-Q water making 800 µL volume. The concentration calibration range for the cations were 2, 5, 10, 15, 20 µg/mL. For the anions analysis, the standard calibration range were 1, 2, 5, 10, 15 µg/mL.

3.7 Sample analysis with HPLC

3.7.1 Sampling

Effluent water samples were taken from the wastewater treatment plant located in Bellville, Cape Town, South Africa. The sampling was carried out after the membrane bioreactor (MBR) stage treatment. 2 L of the effluent wastewater was taken into 2.5 L amber coloured

glass bottles. The water sample collected was kept in an ice chest during transportation to the laboratory for analysis (Nikolaou et al., 2007). The bottle was tightly capped and taken to the laboratory where it was kept in a dark place at 4 °C until the water was used, and the extraction procedure was performed before 3 days after sampling. Tap water (cold and hot) samples were sampled and stored in the same manner. The sample preparation with solid phase extraction (SPE) procedure is extensively detailed in section 3.2.7 of Chapter 3.

3.7.2 Preparation of standard solutions

The stock solutions of the standards were prepared in methanol at 1000 µg/mL for individual analytes, and stored at 4 °C in glass vessels until used. The preparation of the working solutions from the stocks was achieved by diluting a specific concentration into Milli-Q water. The stock solutions were allowed to equilibrate to room temperature and thoroughly mixed before use. The working solutions of the analyte standards were made as 500, 100, 20, 4, 0.8, 0.16 and 0.032 ng/mL. Working standard solutions were used for the calibration curves preparation and for spiking samples in the validation study.

3.7.3 Instrumentation and methods

A Shimadzu LC 20AD HPLC system coupled to a Xevo TQ-MS mass spectrometer (MS/MS) (Waters, USA) was used for high-resolution LC-MS/MS analysis. Separation of the analytes of interest was achieved using a Poroshell 20 EC C₁₈ column (3 x 100 mm; 2.7 µm particle size) at the temperature of 40 °C and a flow rate of 0.4 mL/min. The mobile phase was a mixture of 0.02 M formic acid (solvent A) in water, and methanol (solvent B). Linear gradient elution of 0.4 mL/min with a mixture of 70 % solvent A and 30 % solvent B was used for 4 minutes, after which the methanol percentage was increased linearly from 30 % to 90 % until 6.5 minutes. And at 7.5 minute, 70 % of solvent A and 30 % of solvent B was achieved and maintained until the run was 10 minutes. 5 µL of each sample was injected into the LC/MS system.

3.7.3.1 Mass spectrometry (MS)

The HPLC system was coupled to a triple quadrupole mass spectrometer (Shimadzu LCMS-8040), with an electrospray ionisation (ESI) source. Source cone voltage, temperature, cone gas flows, capillary voltage and desolvation temperatures were used to obtain the maximum sensitivity. It was achieved by direct injection of 10 µg/mL concentration of the stock solutions. The capillary voltage of 3.5 kV, drying gas flow of 15 L/min, nebulizing gas 3

L/min, source heat block temperature of 400 °C and desolvation temperature of 250 °C were applied.

Table 3.2: Gradient elution method

Time (min)	Flow (mL/min)	%A	%B
0.5	0.400	70	30
4.0	0.400	10	90
6.5	0.400	10	90
7.5	0.400	70	30
10.0	0.400	70	30

Table 3.3: HPLC instrumentation and analytical conditions summary

HPLC conditions	
LC System	Shimadzu LC 20AD HPLC
LC Column	Poroshell 20 EC C18, 3 x 100, 2.7µm
Column temperature	40 °C
Eluent	(A) 0.02 FA v/v; 2mM Ammonium formate in Milli-Q water (B) 0.02 FA v/v; 2mM Ammonium formate in methanol
Run time	10.00 min
MS conditions	
MS System	Shimadzu LCMS-8040
Ion Mode	ESI+
Desolvation Temperature	250 °C
Nebulizing gas (L/min)	3
Drying gas (L/min)	15
Capillary Voltage (KV)	3.5

3.7.4 Determination of accuracy, linearity, precision and selectivity

Accuracy was expressed as a function of recovery percentage, and determined by comparing the concentrations found in the spiked samples with the added concentration. Assessment of

linearity was done by using calibration curves at the concentrations range and peak area was plotted against the concentration of each analyte. Determination of precision was achieved by the replicate standards injection. Selectivity evaluation was carried out by qualitatively comparing the retention time of the peaks obtained with the ones obtained from standard solution, and the analytes identification was simultaneously confirmed by comparing the peaks spectra in the chromatograms of the sample and those of standard solutions.

3.7.5 LOD and LOQ determination

The determination of the limits of detection (LOD) and quantification (LOQ) was calculated on the basis of the standard deviation of blank-sample responses and the calibration curve slope for each analyte. For each compound, the instrumental LOD and LOQ were calculated. The LODs and LOQs were determined using the following formula: $LOD = 3.3 \alpha/S$ and $LOQ = 10 \alpha/S$, where α is the standard deviation of the response and S is the average slope of the calibration curves, with the same curves. The validation of the method was against a set of quality control parameters which include laboratory and field blanks, matrix spikes and triplicate samples. Precautionary measures were observed to avoid contamination from personnel, organic solvents, equipment and glasswares, as contamination of the blank is the most common problem noticed in the determination of emerging contaminants. Along with the samples and laboratory spikes in monitoring the likely laboratory contamination of the compounds under investigation, blank samples of Milli-Q water were extracted and analysed. In order to monitor instrumental contamination and carryover, methanol blanks were also run between samples. Chromatographic peak area, height and signal noise were used in the characterization of the analytes of interest; peak area was used to measure the optimal signal intensities for quantification.

3.8 Analysis using SERS

Detailed information on methodology as well as parameters investigated in the modification process of track-etched polyethylene terephthalate (PET) membrane and synthesis of nanoparticles is discussed here. The characterisation techniques and their sample preparation procedures used to investigate the PET membrane and silver nanoparticles are also described. This section details four experimental steps which are (i) materials; (ii) surface modification of the PET membrane; (iii) synthesis of silver nanoparticles; and (iv) characterisation techniques used in the SERS study.

In this SERS study, the methods applied were the direct immobilisation of silver nanoparticles on amine-treated, track-etched polyethylene terephthalate membrane. The track-etched PET membrane was modified through wet chemistry methods which have been applied in biotechnology studies where proteins or enzymes are immobilised on the modified membranes (Irena et al., 2009; Ozcam et al., 2009). The amine modifications conducted for the membranes were carried out at ambient conditions.

3.8.1 Materials used for SERS study

The track-etched polyethylene terephthalate (PET) membrane used in the study was prepared by bombarding the PET membrane with 147 MeV krypton ions. The latent track PET membrane was then radiated with ultraviolet (UV) light of wavelength 310 nm in order to enhance the shape of latent tracks caused by krypton ions. The PET membrane was then etched using 6 M of sodium hydroxide in a thermo-bath between 70 °C and 90 °C. Whilst the track-etched membrane was still wet with etching agent (sodium hydroxide), it underwent neutralisation in diluted acetic acid. Thereafter the track-etched membrane was washed with distilled water and dried in hot air using hot air vents.

Table 3.4: Track-etched polymer membrane

Name	Polyethylene terephthalate (PET)
Supplier	JINR, Dubna, Russia
Thickness	23 µm
Pore density	$1 \times 10^9 \text{ cm}^{-2}$
Pore size	0.100 µm

Table 3.5: Quartz:- Silver- coated glass

Name	Silver-coated glass (Quartz)
Supplier	JINR, Dubna, Russia

The surface of the quartz was prepared by the modification of silicon oxide solid substrate with silver nanoparticles through thermo vacuum and reactive magnetron sputtering. The sputtered silver nanoparticles were of size 30 nm. The silver-coated quartz is given the code name “Quartz” throughout. The Polyethylene terephthalate (PET) membrane was thoroughly

cleaned in a mixture of absolute ethanol and distilled water (1:1 v/v), dried in air under ambient conditions and used without further treatment. Figure 3.3 shows the schematic experimental procedure for the surface modification and immobilisation of silver nanoparticles on track-etched PET membrane.

3.8.2 Polyethylene terephthalate (PET) membrane surface modification

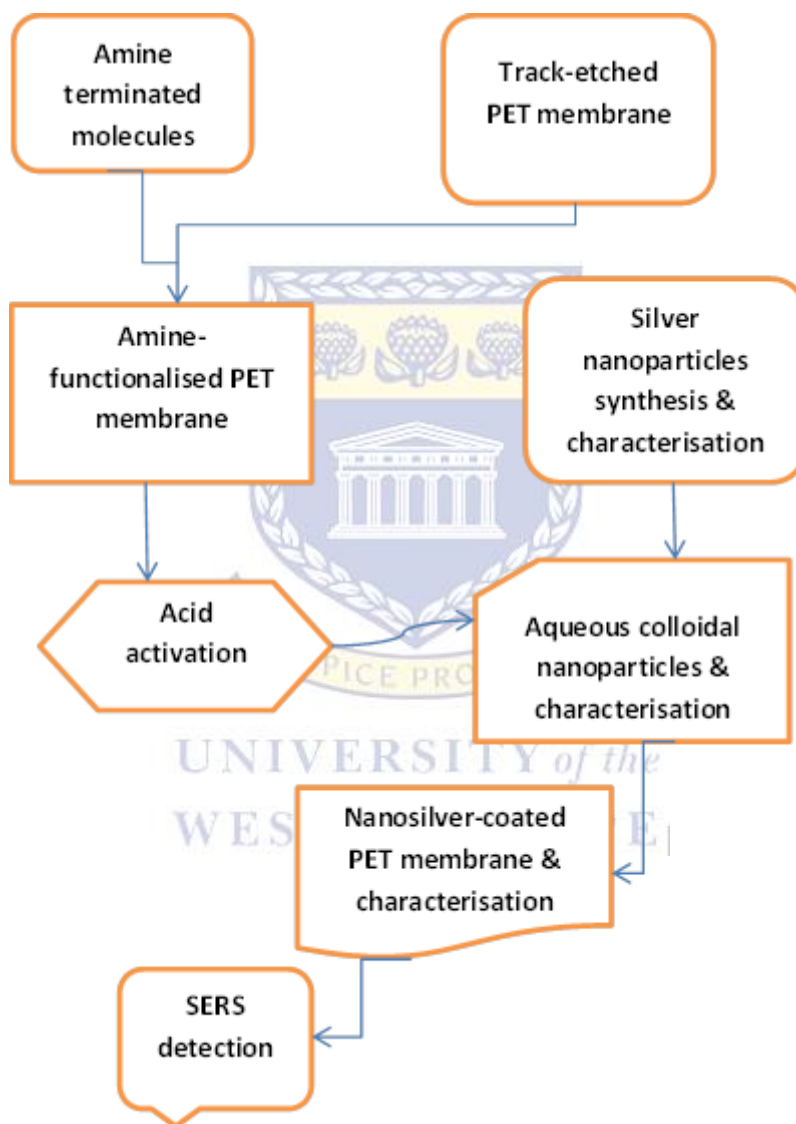


Figure 3.3: Schematic experimental procedure for surface modification of PET membrane.

The experimental steps involved in the surface modification of polyethylene terephthalate track-etched membranes include: (i) functionalisation (aminolysis) of the PET membrane surface with diethylenetriamine (DETA) via an amide bond; (ii) and immobilisation of silver nanoparticles on the surface via the silver-nitrogen bond.

3.8.1.1 Aminolysis of the polyethene terephthalate (PET) membrane

The polyethene terephthalate (PET) membrane surface modification was achieved by immersing a 3 x 3 cm piece of track-etched PET membrane in a 50 mL aqueous solution of diethylenetriamine (DETA). Aqueous DETA concentrations of 60%, 80%, and 100% (v/v) were used for samples 60A-PET, 80A-PET and 100A-PET respectively. These sample codes are described in Table 3.6. One 3 x 3 cm piece of polyethene terephthalate (PET) membrane was immersed in each of the concentrations of the aqueous DETA solution. The size of the PET membrane pieces was kept constant, to ensure that any changes to the surface were solely due to external effect and not due to the size and area of the membrane. The period of exposure of PET membranes to the amine solution was carried out at an ambient temperature (approximately 25 °C) for 10 hours, 15 hours or 20 hours. The codes for the samples are given in Table 3.6.

The aminolysis reaction occurred at the solid-liquid interface and was left to run under agitation for given times of 10 hours, 15 hours or 20 hours for samples 10-APET, 15-APET or 20-APET respectively. After the aminolysis of the PET membranes with the aqueous DETA concentrations of 60%, 80%, and 100% respectively, the membranes were double-washed with distilled water and absolute ethanol (1:1 v/v) to remove physically adhered DETA from the surface of PET membranes. Thereafter, the modified track-etched PET membranes were activated in 1 mM hydrochloric acid for 1 hour under agitation at ambient conditions. The rinsed PET membranes were air-dried at room temperature for 24 hours. Both the modified and unmodified track-etched PET membranes were characterised by Fourier transform infrared (FTIR), X-ray photoelectron spectroscopy (XPS) to confirm the formation of the amide bond and the presence of amine groups on the surface.

3.8.1.2 Silver nanoparticles synthesis

The synthesis of silver nanoparticles in this study was carried out using a modified wet chemical method by Lee and Meisel (1982). Silver nitrate was used as a silver salt precursor and trisodium citrate served both as a reducing and stabilising agent. The silver nanoparticles synthesis was achieved by taking 100 mL volume of 1 mM of aqueous silver nitrate (AgNO_3) to 100 °C, 90 °C, and 80 °C; and the samples were coded 100C-AgNP, 90C-AgNP, and 80C-AgNP respectively. Aliquots of 2 mL, 3 mL and 4 mL solution of trisodium citrate (1 g/100 mL) representing samples 2mL-TriNa 3mL-TriNa and 4mL-TriNa respectively were slowly

added dropwise to the solution of silver nitrate upon reaching the determined temperature. The mixture was then left to react for 10 minutes, 20 minutes or 30 minutes, after which the samples were coded as 10-AgNP, 20-AgNP, and 30-AgNP respectively

Table 3.6 describes the codes given to the samples, and details the optimisation studies as well. Subsequently, the solution was cooled an ambient temperature (25 °C). The optimisation of the three parameters (temperature, time and volume) in the synthesis of silver nanoparticles were separately carried out for the best conditions which were applied during direct immobilisation of silver nanoparticles on the PET membrane as described in Section 3.8.3.3. The results of the optimisation study are presented in Section 6.3.1 of Chapter 6.

The silver nanoparticles synthesis was confirmed by ultraviolet-visible (UV-Vis) spectroscopy of the silver nanoparticles solution after the reduction of silver nitrate (AgNO_3), and the results are presented in Section 6.3.1.1 of chapter 6.

3.8.1.3 Immobilisation of Silver nanoparticles

Silver nanoparticles were immobilised on the amine-modified surface of the track-etched PET membrane. This was achieved by immersing the amine-modified membranes in the preheated silver nitrate solution to which trisodium citrate had been added. Silver nanoparticles immobilisation on the surface was simultaneously carried out as the synthesis of silver nanoparticles occurred via reduction of silver nitrate by trisodium citrate. A volume of 100 mL solution of silver nitrate (1 mM) was heated to a temperature of 100 °C. Subsequently, a volume of 2 mL of an aqueous solution of trisodium citrate (1 g/100 mL) was added to the preheated silver nitrate solution followed by immersion of the amine-modified track-etched PET membrane. Silver nitrate reduction was carried out for 10 minutes, 15 minutes, 20 minutes, 25 minutes, and 30 minutes for samples 10-AgPET, 15-AgPET, 20-AgPET, 25-AgPET, and 30-AgPET respectively. Thereafter, the silver nanoparticle-coated track-etched PET membranes were rinsed twice with distilled water to remove physically adsorbed nanoparticles on the surface membrane, and were air-dried at room temperature for 24 hours. The sample code descriptions and experimental parameters are presented in Table 3.6.

Characterisation of the surface morphology of silver-coated track-etched PET membrane was done by scanning electron microscopy (SEM) and the chemisorption of silver nanoparticles

on the modified track-etched PET membrane was characterised by X-ray photoelectron spectroscopy (XPS). XPS gives the percentage of silver nanoparticles immobilised on the modified surface of modified track-etched PET membrane. The XPS results are presented in Section 6.3.3.2, while the SEM results are presented in Section 6.3.3.3 of Chapter 6 respectively.

3.8.2 Detection using silver-coated track-etched polyethene terephthalate (PET) membrane by SERS

Surface-enhanced Raman spectroscopy (SERS) technique was used to detect the presence of the persistent organic pollutants (analytes) on the surface of unmodified and silver nanoparticles-coated track-etched polyethene terephthalate (PET) membranes. Two particular analytes, acetaminophen and 4-aminothiophenol (4-ATP), were used to carry out the detection by Raman spectroscopy. However, it is presumed that the silver nanoparticles on the surface would enhance the Raman signal, and therefore generate a more visible and readable spectrum of the persistent organic pollutants (analytes). In the case of concentration studies, three different concentrations with their given sample codes in brackets, of 1 mg/L (Acet-001), 0.1 mg/L (Acet-002) and 0.01 mg/L (Acet-003) for acetaminophen; 10^{-6} M (4-ATP 1) and 10^{-4} M (4-ATP 2) for 4-aminothiophenol (4-ATP), were all prepared in 20 μ L aliquots. A 1 x 1 cm piece of the membrane was cut from the 3 x 3 cm piece which was prepared as described in Section 3.8.2.1; and 20 μ L of the analyte was dropped on the surface. This was left to dry under ambient conditions for 24 hours, since detection was impossible without drying. After the analyte solution on the membrane had dried up, it was subsequently placed on the Raman spectrometer for detection. The codes for the samples are described in Table 3.6. The results are presented in Sections 6.2, 6.3 and 6.4 respectively.

Table 3.6: Experimental parameters for modification of polyethene terephthalate (PET) membrane with sample codes, immobilisation of silver nanoparticles and the application of surface-enhanced Raman spectroscopy (SERS)

Aminolysis of polyethene terephthalate (PET) membrane				
Parameters	Time	Concentration%		Sample code
Time of reaction	10 hours	DETA 100%		10-APET
	15 hours	DETA 100%		15-APET
	20 hours	DETA 100%		20-APET
Concentration of DETA	20 hours	DETA 100%		100A-PET
	20 hours	DETA 80%		80A-PET
	20 hours	DETA 60%		60A-PET
	0 hour	DETA 0%		Con-PET
Silver nanoparticles synthesis and optimisation				
Parameters	Volume	Time	Temperature	Sample Code
Volume of trisodium citrate	2 mL	20 min	100 °C	2mL-TriNa
	3 mL	20 min	100 °C	3mL-TriNa
	4 mL	20 min	100 °C	4mL-TriNa
Time of reduction reaction	2 mL	10 min	100 °C	10-AgNP
	2 mL	20 min	100 °C	20-AgNP
	2 mL	30 min	100 °C	30-AgNP
Temperature of reduction reaction	2 mL	20 min	100 °C	100C-AgNP
	2 mL	20 min	90 °C	90C-AgNP
	2 mL	20 min	80 °C	80C-AgNP
Silver nanoparticles immobilisation on modified track-etched PET membrane				
Parameters	Volume	Time	Temperature	Sample Code
Time of immobilisation	2 mL	10 min	100 °C	10-AgPET
	2 mL	15 min	100 °C	15-AgPET
	2 mL	20 min	100 °C	20-AgPET
	2 mL	25 min	100 °C	25-AgPET
	2 mL	30 min	100 °C	30-AgPET
				Control
Analyte detection using 30-AgPET sample (concentration)				
Parameters	Volume	Time	Concentration	Sample Code
Concentration of analyte	20 µL	24 Hrs	1 mg/L	Aceta-001
	20 µL	24 Hrs	0.1 mg/L	Aceta-002
	20 µL	24 Hrs	0.01mg/L	Aceta-003
	20 µL	24 Hrs	10 ⁻⁴ M	4-ATP 1
	20 µL	24 Hrs	10 ⁻⁶ M	4-ATP 2

3.9 Characterisation

In this section, the main conditions and steps employed to analyse the polymer samples and silver nanoparticles prepared with variable parameters are described. The characterisation techniques employed in the achievement of the SERS goals include: Contact angle

measurement, Fourier transform infrared (FTIR), Raman spectroscopy, Scanning electron microscopy (SEM), thermogravimetric analysis (TGA), UV-Vis spectroscopy, X-ray photoelectron spectroscopy (XPS), and zeta (ζ) potential. The procedures for sample preparation for specific characterisation techniques are also outlined in this section.

3.9.1 Contact angle measurements

The contact angle measurement was carried out using the Kruss DSA 100, which is a drop shape analyser. Milli-Q water was used for the measurement at ambient conditions. The purpose of the contact angle measurements was to characterise the variations in the hydrophobicity and hydrophilicity of the polymer (track-etched membrane), before and after modification.

3.9.2 Fourier transform infrared spectroscopy (FTIR)

Fourier transform infrared spectroscopy (FTIR) is an analytical technique based on the transmission of infrared energy through the sample, which gives out the spectra of vibrations of bonds or a collection of bonds. The technique was conducted to determine changes in functional groups on the polyethylene terephthalate (PET) membrane surface. These spectra are however analysed to investigate the existing bonds and their associated functional groups. FTIR was used to characterise the modified and unmodified track-etched PET membranes, in order to ascertain the formation of an amide bond and presence of amine moieties following the scission of the ester bond on the surface of the track-etched PET membrane. Perkin Elmer model Spectrum TwoTM spectrometer was used to obtain the FTIR spectra of the modified and unmodified track-etched PET membrane samples. These spectra were obtained within the wavenumber range of 4000 to 400 cm^{-1} at a resolution of 4 cm^{-1} and the scan rate was set at 20 scans per second. No further sample preparation was carried out after the samples were characterised as obtained after modification.

3.9.3 Raman spectroscopy

The Raman spectrometer that was used to carry out the Raman spectroscopy of the surface chemistry of the unmodified and modified track-etched polyethylene terephthalate (PET) membrane samples was a portable version of Enspectr R532 Raman spectrometer. This Raman spectrometer was also employed for the surface-enhance Raman spectroscopy (SERS) application to detect analytes on the surface of unmodified and modified track-etched PET membranes besides the surface chemistry of silver-coated track-etched PET membrane.

The Raman spectrometer has an internal laser with an excitation wavelength 532 nm. The spectrometer is also equipped with the objective lens, Olympus CX22 LED of magnification x10 and x40. The output power 20 mW was used, and the exposure time was set at 600 ms with 20 frames. Also, a manual locator was used to find the spot where to place the sample on the sample holder; and manual adjustments were properly made to get the right focus in order to get a focused spectrum. The sample preparation was achieved by drop and dry method for the SERS application; the analyte solution was dropped on the surface of the PET membrane and left to dry at room temperature prior to characterisation with the Raman spectrometer.

3.9.4 Scanning electron microscopy (SEM)

The changes to the surface morphology of track-etched polyethylene terephthalate (PET) polymer membrane samples after the exposure to silver nanoparticle solutions, was studied by scanning electron microscopy (SEM). The morphological characteristics were investigated at different magnifications to study the effects of experimental parameters on every sample. The surface morphology characterisation was done using the Hitachi SU8020 scanning electron microscope. The samples were mounted on carbon coated aluminium stubs and were coated by sputtering with carbon using Quorum T150T for 5 minutes before characterisation. The non-conductive surface of the PET polymer membrane was made conductive by the sputter coating procedure.

3.9.5 Thermogravimetric analysis (TGA)

Thermal analysis examination for the unmodified, modified and silver-coated track-etched polyethylene terephthalate (PET) membranes with respect to weight loss as a result of degradation as a function of temperature was characterised by thermogravimetric analysis (TGA). The thermal profile resulting from the continuous degradation of the polymers through weight loss with increasing temperature was used to compare the PET membrane samples (unmodified track-etched PET, Amine-modified track-etched PET and silver-coated amine PET). Perkin Elmer TGA 4000 was used to carry out the thermogravimetric analysis (TGA). The PET membrane polymer sample of at least 1.2 g was put in a platinum heating pan (which was cleaned by exposing the pan to the hottest part of the Bunsen burner flame for 5 minutes). The applied heating rate during the thermal analysis was 10 °C/min beginning from an initial temperature setting of 30 °C to a maximum of 600 °C in a nitrogen inert

atmosphere. The nitrogen gas flow was maintained at 20 mL per minute and at a pressure of 3.8 bars.

3.9.6 Ultraviolet-visible spectroscopy (UV-Vis)

Thermo Fisher Evolution 200 spectrometer was employed to perform the ultraviolet-visible (UV-Vis) spectroscopy. It was used to determine plasmonic peaks for the confirmation of synthesis of silver nanoparticles. Approximately 1.5 mL of the colloidal silver nanoparticles solution was placed in a 1 cm path length cuvette. Milli-Q water was used as a blank to give the baseline spectrum, and the spectral characterisation was performed in a 200 - 600 nm range at room temperature.

3.9.7 X-ray photoelectron spectroscopy (XPS)

The XPS measurement was carried out using a Thermo Scientific K-Alpha X-ray photoelectron spectrometer. The X-ray source type was a monochromated, micro-focused Al K-Alpha. The X-ray photoelectron spectroscopy (XPS) was used to characterise the surface chemistry of the polyethene terephthalate (PET) membranes for elemental analysis and binding energies. The technique used to confirm the presence of silver on the surface of the modified track-etched PET membrane after immobilising silver nanoparticles; and it complements the Fourier transform infrared (FTIR) and Raman spectroscopy results regarding the introduction of amine and amide functional group on the surface of the PET membrane.

3.9.8 Zeta (ζ) potential

The surface zeta potentials were measured using the zeta analyser, a Malvern Zetasizer Nano Z model. The measurements of zeta potential were carried out in order to study the stability of the colloidal silver nanoparticles. 5 mL colloidal silver nanoparticles solution samples were diluted with 10 mL Milli-Q water, and the pH was adjusted to the required value of pH 6.5, then shaken for 10 minutes. Thereafter, the zeta potential of the metallic particles was measured, and the sample was placed in a folded capillary cell with a minimum volume of 1.5 mL. The zeta potential values were read from the computer screen connected to the sizer, and the characterisation was done at ambient conditions.

3.10 Chapter summary

The descriptions of chemicals, materials, experimental layout and protocols, involving characterisation techniques have been detailed in this chapter. The chapter description centres specifically on how the experiments were carried out in the laboratory; and how various samples were prepared for every characterisation technique.

The next chapter details the results and discussions concerning the effluent wastewater analysis using the HPLC.



UNIVERSITY *of the*
WESTERN CAPE

CHAPTER FOUR

EFFLUENT WASTEWATER ANALYSIS USING LIQUID CHROMATOGRAPHY- MASS SPECTROSCOPY (LCMS)

4 Introduction

In this chapter, the purpose of the study was to investigate certain persistent organic pollutants in the effluent wastewater sample from a wastewater treatment plant (WWTP) in Bellville, Cape Town, tap water (hot and cold) and Milli-Q water respectively; using the Liquid Chromatography-Mass Spectroscopy (LC-MS) methods. The analysis of pharmaceutical compounds included acetaminophen, aspirin (ASA), diclofenac, ibuprofen, sulphamethoxazole; and 17- β -estradiol, which is a steroid hormone. As discussed in Chapter one, this chapter gives the detailed results and discussion of the identification and separation of persistent organic pollutants carried out by LC-MS, with the aim of establishing the sensitivity of the technique. The discussion here details the procedures which include: the methods, the retention times of the analytes, recovery studies, the chromatograms of the respective analytes, limits of detection (LODs) of analytes, and the limits of quantification (LOQs); solid phase extraction (SPE) details are given in section 3.2.7 of Chapter 3, while the information regarding the method development and solvent composition effective for the separation of individual analytes are highlighted in section 3.7 of Chapter 3.

4.1 Background

The presence of persistent organic pollutants such as endocrine disrupting chemicals (EDCs), flame retardants pharmaceuticals and personal care products (PPCPs), pesticides, perfluorinated compounds (PFCs) etc, in the environment is of environmental and public concern (Daughton and Ternes 1999; Jin and Peldszus 2012). These pollutants get into the environment continuously via sewage effluents, wastewater discharge, agricultural runoff, inappropriate cleaning and run-off from yards, lawns and roadways through local wastewater and municipal landfill leachates raising concerns for regulatory agencies worldwide (Gaw *et al.* 2014; Luo *et al.* 2014). The increase over the years of persistent organic pollutants in the environment is attributed to the increase in the human population, inadequate wastewater treatment plants, poor refuse disposal, urbanisation, poor agricultural practices and so on (Badmus *et al.*, 2018).

Literature reports that the Stockholm Convention targets only a group of POPs (26 with additional) (Stockholm Convention Secretariat, 2001) whereas there are over 100 000 chemicals in use with over 30 000 commercially used (Howard and Muir, 2010). This is a concerning scenario as all these POPs need to be monitored, regulated and their fate known. Therefore, there is a need for proper identification and quantification of these compounds, monitoring their presence in our waters to fully understand their chemical properties, and their effect on human health and ecosystems. With the advancement in detection techniques and analytical instrumentation, a significant number of chemicals of emerging concern (CEC) have been identified successfully and quantified at low concentrations in different water sources including drinking water by scientists (Magureanu *et al.*, 2008; Trapido *et al.*, 2014). Exposure to these chemicals is possible through drinking water, or perhaps via consumption of crops irrigated with recycled water containing chemicals of emerging concern. These compounds have been reported to disrupt hormonal body functions, leading to birth defects, feminization, cancerous tumours, early puberty, obesity, heart disease and other abnormalities, especially in aquatic species (Kolle *et al.*, 2013).

Regulations have been put in place for industries to recycle and reuse water to minimise the fresh water intake from rivers by the water utility companies and stop the continuous discharge of polluted water into the environment and local river systems (Bell *et al.*, 2011). Wastewater reuse is a possible exposure pathway to a significant number of emerging contaminants and their metabolites. It is therefore important to identify and monitor emerging micro pollutants in the recovered water so as to determine its fitness for use. Efforts have been made to detect some of the emerging micropollutants in the water systems in South Africa, but only a few emerging micro pollutants have been identified and monitored (Swartz *et al.*, 2018a). One of the challenges in identifying some of these micro pollutants is the suppression of low concentrations of one kind by the higher concentration of other compounds during the analysis due to the presence of several thousands of them in water. As result of this, there is a great need to develop a rapid separation technique whereby the micro pollutants will be separated for easy identification and quantification. The LC-MS is well known for its sensitivity, specificity and selectivity in the analysis of trace compounds. (Fatta *et al.*, 2007; Dams *et al.*, 2003). LC-MS is suitable for analysis of large molecular weights and thermally liable polar compounds not suitable for GC-MS. A lot of scientists have performed extensive work on these POPs and hence have validated LC-MS as the analytical tool for pharmaceutical analysis. However, Swartz *et al.*, (2018a) pointed out that in recent

years, there have been significant changes in the analytical techniques employed in the analysis of persistent organic compounds (POPs). Also, the identification, quantification of these compounds is dependent on the availability of these instruments. The types of liquid chromatography techniques include: high performance liquid chromatography (HPLC), high performance liquid chromatography coupled with mass spectrometry (HPLC-MS), liquid chromatography mass spectrometry (LC-MS), and liquid chromatography mass spectrometry coupled with mass spectrometry (LC-MS/MS). Whereas, the application of LC-MS/MS for environmental analysis enables the determination of a wide range of compounds. In most the sampling campaigns carried out by Swartz *et al.*, (2018a), acetaminophen was detected in all the influent (inlet) samples in the range 0.0046 – 0.359 ng/L; but not detected in most of the effluent sampling campaigns. Ojemaye & Petrik, (2021) also reported the presence of persistent organic compounds in several environmental samples in which diclofenac was dominantly detected with higher concentration than other pharmaceuticals.

4.2 Results and discussion

The methodology used for the assessment of the levels of the selected persistent organic pollutants (POPs) under study in wastewater sample (effluent), tap water sample (hot and cold) and milli-Q water sample using solid phase extraction are described in section 3.2.7 of Chapter 3 of this thesis, followed by the LC-MS analysis. The results of the analysis are presented in this chapter, while the calibration curves of the respective analytes are given in Appendix 2.

4.2.1 Optimization of High Performance Liquid Chromatographic (HPLC) Method

A method for the quantitation of acetaminophen, diclofenac, aspirin, ibuprofen and sulphamethoxazole was developed based on a High Pressure Liquid Chromatograph (HPLC) coupled to a triple quadrupole mass spectrometer (Shimadzu LCMS-8040), with an electrospray ionisation (ESI) source mass spectrometer (MS/MS). These include triplicate runs of 5-set calibration standards for each analyte, plotting of calibration curves, determination of the equations for the linear regression lines, LOD and LOQ determination for each analyte, evaluation of the repeatability and reproducibility of method selectivity and sensitivity for each analyte.

4.2.2 Chromatograms of standard analyte samples

The optimised method for the identification and quantification of the analytes was adopted for subsequent analyses. The respective retention times can be seen in the chromatograms as given in Figures 4.1 – 4.5.

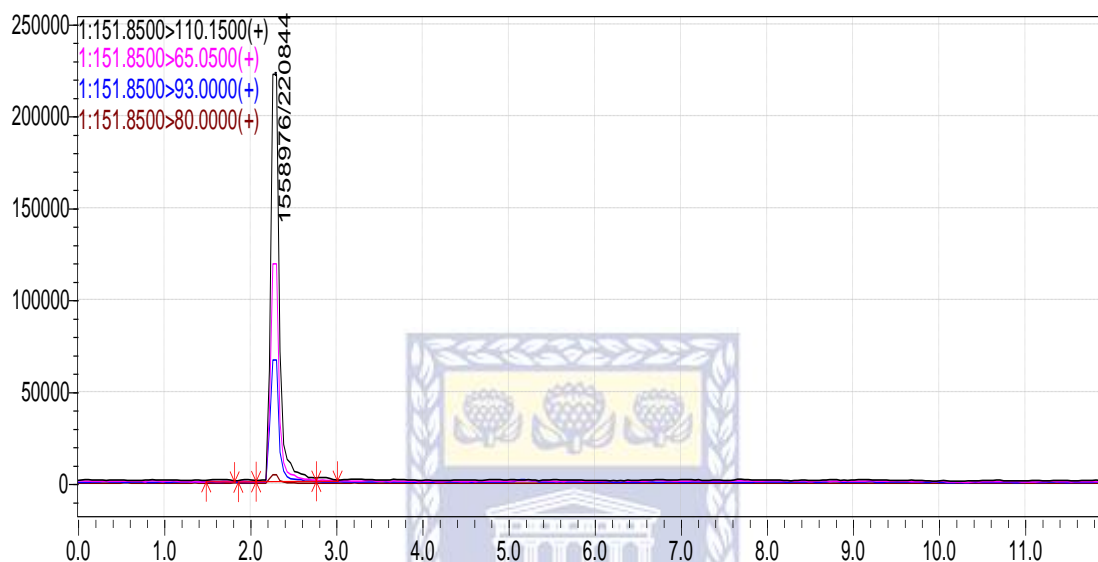


Figure 4.1: Chromatogram for Acetaminophen.

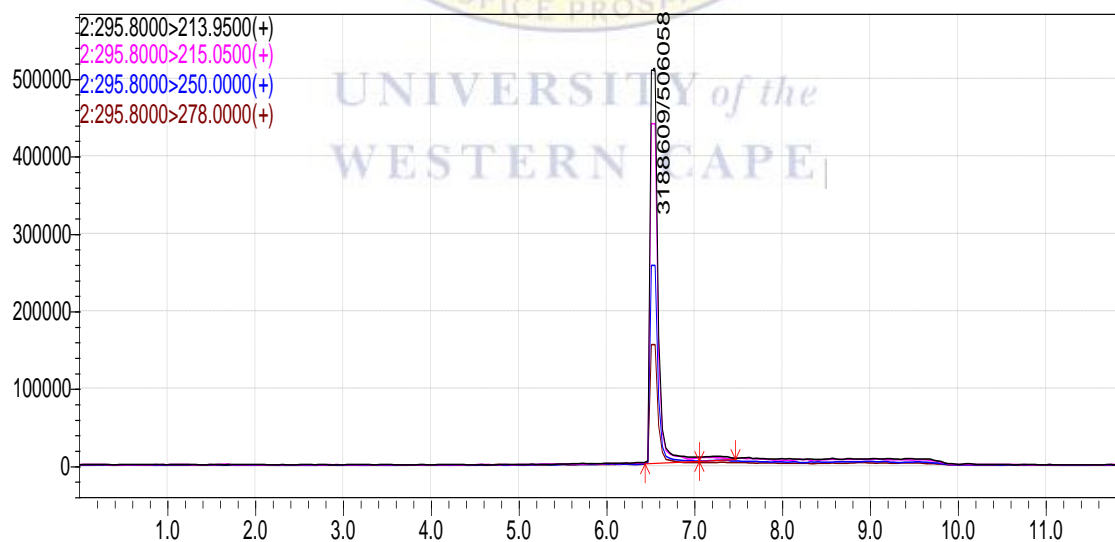


Figure 4.2: Chromatogram for Diclofenac.

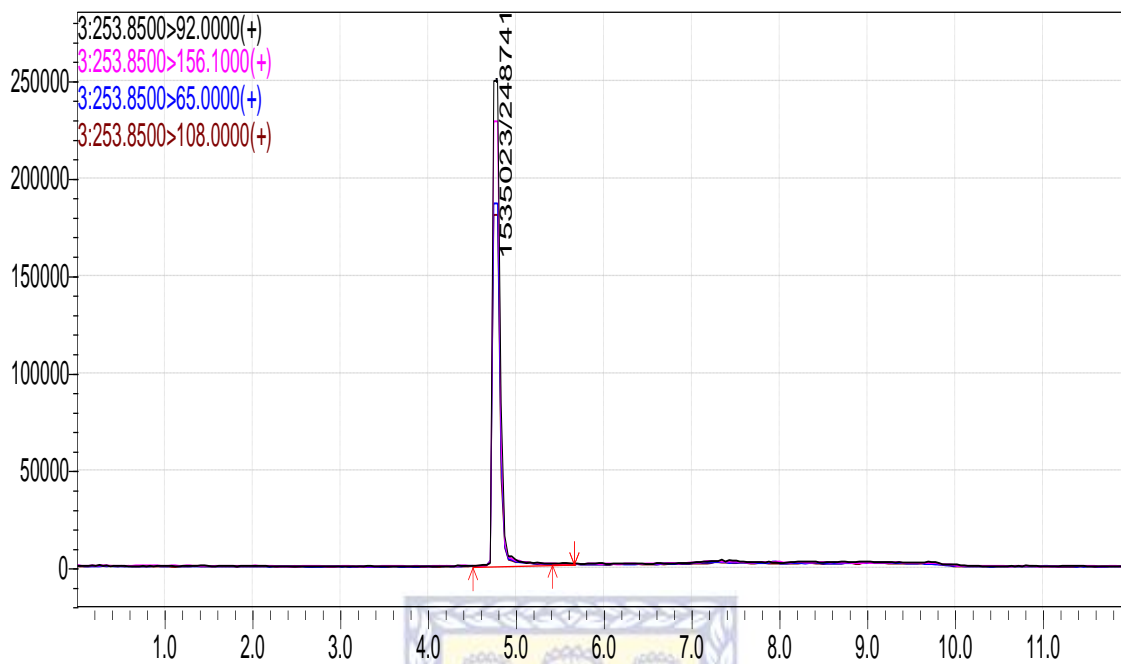


Figure 4.3: Chromatogram for Sulphamethoxazole.

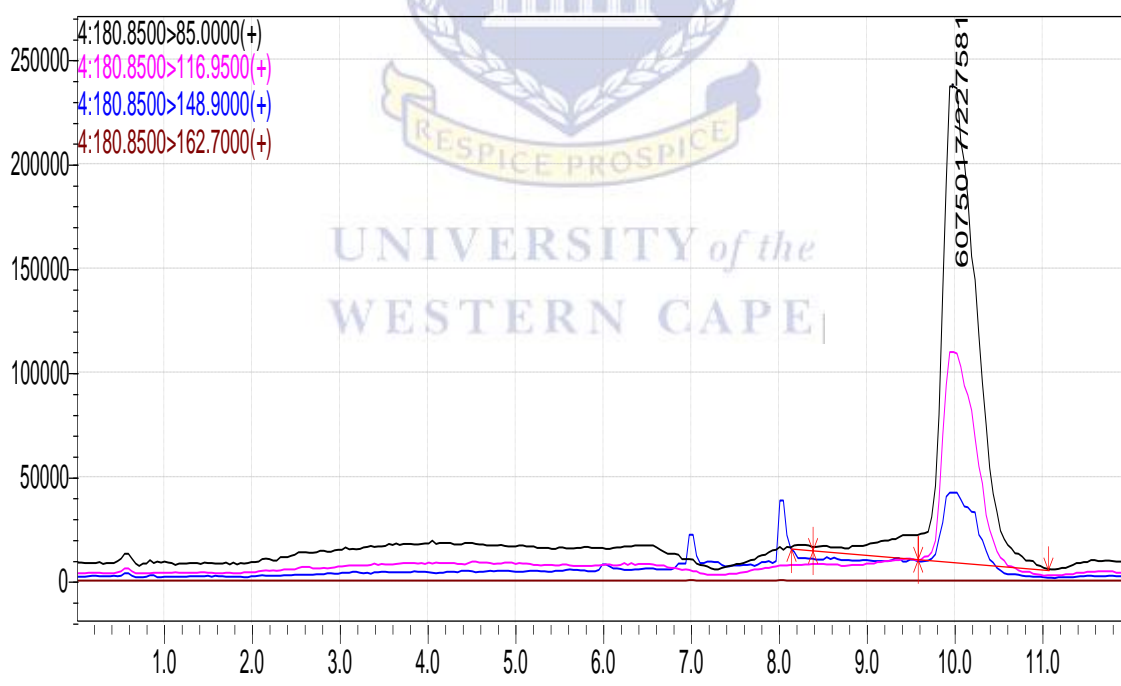


Figure 4.4: Chromatogram for Aspirin.

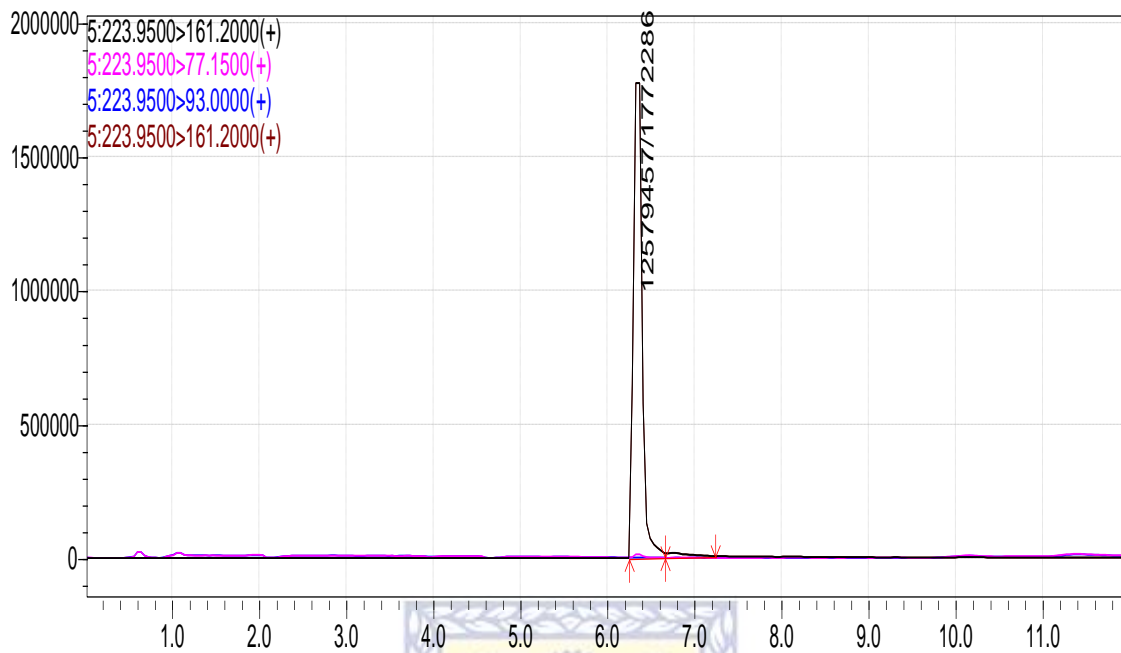


Figure 4.5: Chromatogram for Ibuprofen.

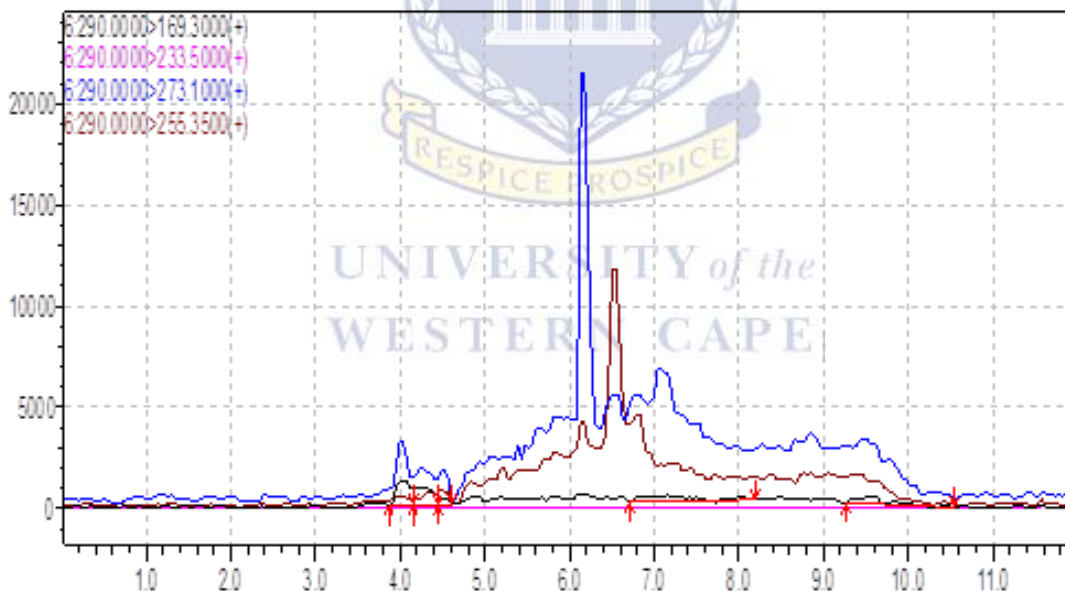
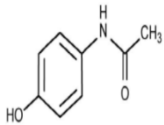
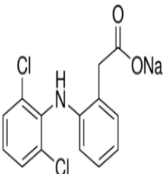
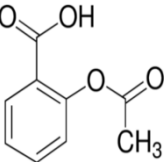
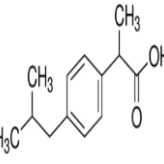
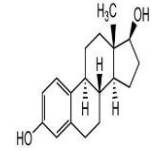
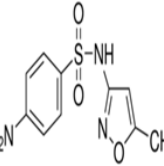


Figure 4.6: Chromatogram for 17-β-estradiol.

The respective chromatograms show the retention times for the different analytes. The response of the instrument to the detection of each of the analytes gave linear sensitivity as the concentrations increased with the R^2 values of all the analytes.

Table 4.1 shows the structures of acetaminophen, diclofenac, aspirin, salicylic acid, ibuprofen, sulphamethoxazole and 17-beta-estradiol; with their theoretical and experimentally measured molar masses with retention times.

Table 4.1: Structures of acetaminophen, diclofenac, aspirin, salicylic acid, ibuprofen, sulphamethoxazole and 17-beta-estradiol. Theoretical and experimentally measured exact molar masses with retention times

Compound	Structure	Molar mass [g/mol]	Experimental molar mass [M + H]	Retention time [min]
Acetaminophen $C_8H_9O_2$		151.17	152.071	2.370
Diclofenac $C_{14}H_{10}Cl_2NNaO_2$		318.10	319.024	6.640
Aspirin $C_9H_8O_4$		180.16	181.05	10.110
Ibuprofen $C_{13}H_{18}O_2$		206.29	207.138	6.406
17-β-estradiol		272.38	273.185	6.006
Sulphamethoxazole $C_{10}H_{11}N_3O_3S$		253.28	254.059	4.810

The method's LOD and LOQ values for each analyte were statistically calculated and presented in Table 4.2. The instrument's response to the detection of the analytes showed linearity to the increasing concentrations. The coefficient of linear regression R^2 values ranged between 0.9389 (17-beta estradiol) and 0.9981 (diclofenac), as shown in Table 4.2. The calibration curves for the respective standard analytes are given in Appendix A59, A62, A65, A68, A70 and A71 respectively. The R^2 values the calibration curves were above 0.990, except for ibuprofen and 17-beta-estradiol. This could be as a result of the method or instrument's sensitivity to the compounds.

Table 4.2: Calibration data for standard analytes

Standards	Calibration Range[ng/mL]	Linear equation	R^2	λ_{\max} nm	LOD ng/mL	LOQ ng/mL
<i>Acetaminophen</i>	0.032 - 500	$y = 5.28x + 438$	0.9902	210	0.286	0.857
<i>Aspirin</i>	0.032 - 500	$y = 3.96x + 124$	0.9920	210	0.195	0.584
<i>Sulphamethoxazole</i>	0.032 - 500	$y = 2.86x + 584$	0.9949	210	0.224	0.673
<i>Diclofenac</i>	0.032 - 500	$y = 1.28x + 248$	0.9981	210	0.412	1.236
<i>Ibuprofen</i>	0.032 - 500	$y = 582x + 884$	0.9707	210	0.291	0.873
<i>17-beta estradiol</i>	0.032 - 500	$y = 1.32x + 221$	0.9389	254	0.331	0.993

4.3 Recovery studies for standard analytes using Solid Phase Extraction (SPE)

The efficiencies of the quantitative recovery of the standard analytes (acetaminophen, aspirin, sulphamethoxazole, diclofenac, ibuprofen and 17-beta estradiol) using the SPE method were evaluated using the data from recovery experiments, as described in section 3.2.7 of Chapter 3. The analytes were recovered from solution of 5 mg/L cocktail analyte standards in Milli-Q water. The relative percentage recovery of the analytes is given in Table 4.3. The details of recovery are provided in Table 4.3; where the average recovery of the analytes was above 95 percent, except for ibuprofen and 17-beta estradiol where average recoveries were 93.4 and 93.8 percent respectively.

Table 4.3: Mean recovery percentages for standard analytes by SPE method

Standards Analytes	Expected concentration (mg/L)	Measured concentration (mg/L)	Average recovery (%)
<i>Acetaminophen</i>	5	4.81	96.2
<i>Aspirin</i>	5	4.96	99.2
<i>Sulphamethoxazole</i>	5	4.88	97.6
<i>Diclofenac</i>	5	4.76	95.2
<i>Ibuprofen</i>	5	4.67	93.4
<i>17-beta estradiol</i>	5	4.69	93.8

4.4 Pharmaceutical analytes present in the water samples

Four water samples studied in this work included an effluent sample from the Bellville wastewater treatment plant, tap water (cold and hot), and Milli-Q water. The results from the analysis are presented in Table 4.4.

Table 4.4: Identification of pharmaceuticals in the Effluent water sample. Determination made with HPLC. Effluent water sample purified with C18 (Strata-X) non-polar sorbent

Analytes	Effluent [ng/mL]	Hot tap water [ng/mL]	Cold tap water [ng/mL]	Milli-Q water [ng/mL]
<i>Acetaminophen</i>	BDL	BDL	BDL	BDL
<i>Aspirin</i>	BDL	BDL	BDL	BDL
<i>Sulphamethoxazole</i>	1.18	BDL	BDL	BDL
<i>Diclofenac</i>	3.306	BDL	BDL	BDL
<i>Ibuprofen</i>	BDL	BDL	BDL	BDL
<i>17-beta estradiol</i>	BDL	BDL	BDL	BDL

In the effluent sample, 3.306 ng/mL of diclofenac and 1.18 ng/mL of sulphamethoxazole were quantified to be present as shown in Figure 4.7. Other pharmaceuticals under study were below detection limit (BDL). Furthermore, in the other water samples, none of the analytes

under investigation was detected. It is important to emphasize the low sensitivity of the technique, which might be the reason these analytes were not detectable.

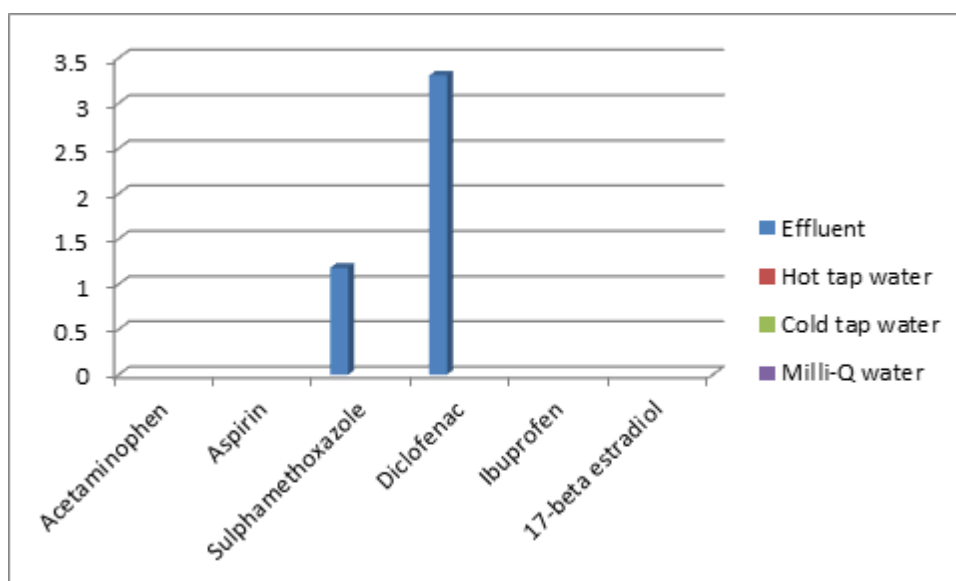


Figure 4.7: Pharmaceutical analyte concentration amounts in the water samples.

In a study by Swartz *et al.*, (2018a), priority list persistent organic compounds which include acetaminophen, diclofenac, sulphamethoxazole, and other pharmaceuticals were detectable in some sampling campaigns, while they were not detectable in other sampling campaigns. For instance, Swartz *et al.*, (2018b) detected acetaminophen in the influent (inlet) sampling campaigns, but acetaminophen was not detectable in the effluent of most of the sampling campaigns. On the balance of probabilities, this could either be as a result of degradation of acetaminophen into other metabolites, thereby making it not detectable, or the purification system of the WWTP was able to remove the compound. However, if the technique was sensitive enough, it should have been able to detect one of the remaining analytes under investigation in the nanogram per litre range.

It is important to make comparison of the concentrations of diclofenac and sulphamethoxazole found in this study with certain studies in the literature. Ojemaye & Petrik, (2021) reported diclofenac to be dominant across all the environmental matrices in their study. This discovery could be attributed to the prescription rate of diclofenac, considering the fact it is an anti-inflammatory drug which is even sold as one of the over-the-counter (OTC) drugs. Swartz *et al.*, (2018b) also reported levels of several of the pharmaceuticals in the final effluent disposed into the environment from many wastewater

treatment plants in Cape Town. Therefore, continuous discharge of these pharmaceuticals and other persistent organic pollutants into the environment and water bodies account for bioaccumulation of contaminants in the environment and aquatic species, thereby making these compounds persistent in organisms, as they are perpetually exposed to them (Li *et al.*, 2012).

4.5 Conclusion

This study investigated various water samples including effluent wastewater from the wastewater treatment plant in Bellville, Cape Town, cold tap water, hot tap water and milli-Q water samples. The purpose is to investigate the presence of some pharmaceuticals including acetaminophen, aspirin, diclofenac, ibuprofen, sulphamethoxazole, and 17-beta estradiol, a steroid hormone compound; all of which are present in sewage according to Swartz *et al.*, (2018a). The study shows that the method employed is not fully capable of detecting low nanogram per litre (ng/L) concentrations in the wastewater (effluent) sample. The application of this method indicated that persistent organic pollutants (POPs) are present in wastewaters (effluent samples). It also shows that these chemical concentrations can be linked to anthropogenic activities, which include the sewage discharge, contributing to these chemicals getting their route back into the environment. Solid phase extraction (SPE) method was employed to concentrate the analyte and LC-MS was used for the analysis. However, only diclofenac (3.306 ng/mL) and sulphamethoxazole (1.18 ng/mL) were detected from the effluent sample; while no compound was detectable in the other water samples, this emphasizes the need for more sensitive methods.

CHAPTER FIVE

IDENTIFICATION, SEPARATION AND QUANTIFICATION OF PERSISTENT ORGANIC POLLUTANTS USING CAPILLARY ZONE ELECTROPHORESIS (CZE) AND PARTIAL-FILLING MICELLAR ELECTROKINETIC CAPILLARY CHROMATOGRAPHY (PF-MEKC)

5 Introduction

This chapter focuses on the instrumental and chemical parameters affecting the capillary electrophoresis instrument; and the identification, separation and quantification of persistent organic pollutants, as well as the determination of inorganic ions (cations and anions) in water samples. The analysis of pharmaceutical compounds which include acetaminophen, aspirin (ASA), diclofenac, ibuprofen, salicylic acid and sulphamethoxazole, using the capillary zone electrophoresis method; and the analysis of steroid hormone compounds (androstenedione, testosterone, 17- β -estradiol and progesterone) using the partial-filling micellar electrokinetic capillary chromatography method are presented and discussed in this chapter.

5.1 Background

The unavailability of fresh and clean water has become a global concern that attracts scientific attention. The non-availability of clean water and deterioration of water quality globally can be attributed to natural and anthropogenic activities such as population growth, climate change and rapid industrialization in conjunction with lack of functional wastewater treatment facilities. Through these processes, many chemicals have found their ways into water bodies thereby compromising the quality of our water systems (Patterton, 2013).

Monitoring of organic pollutants in waters is a difficult task due to the complexity of most of the persistent organic pollutants. For instance, out of thousands of organic pollutants that may have endocrine disrupting effects, methods of extracting and detecting only a few compounds have been developed. In order to be able to detect and monitor the persistent and emerging micropollutants with ease, there is a need to develop suitable analytical methods of identifying these contaminants. A few studies have developed methods to identify various classes of contaminants in water and wastewater treatment plants before and after treatment

processes. However, in most cases where detection methods have been developed, the developed identification methods only target one or two classes of organic pollutants while many other compounds that may have endocrine disrupting and other health effects are yet to be identified. This is probably due to the complexity of their chemical properties, as well as low concentrations in the environment, the complex matrices in which these compounds occur (Petrovic *et al.*, 2002), their high polarity and their thermal stability (Yang *et al.*, 2017). Some analytical techniques, including high performance liquid chromatography and gas chromatography coupled with mass spectrometry, which have been used worldwide, could only detect a limited number of organic contaminants in water and wastewater. For accurate monitoring of persistent and emerging contaminants in aqueous environmental samples (ground, surface, drinking and waste water), there is a need for development and validation of precise and highly sensitive analytical techniques that can effectively identify and quantify contaminants at very low level (ng/L range). This will enable researchers to have a good understanding of the effluent composition before and after treatment. Having a good knowledge of the nature of contaminants in the effluents before and after treatment is beneficial in the development of treatment methods.

Recently, capillary electrophoresis (CE) is gaining more attention in the analysis of environmental xenobiotic contaminants due to its high separation efficiency, short analysis time and minimal reagent consumption. Literature has not fully exploited CE for the analysis of environmental pollutants with the most attention given to other conventional analytical methods (HPLC & GC). However, both separation and analysis clearly demonstrated the high potential of CE in this field (Megson *et al.*, 2016).

5.2 Factors affecting capillary electrophoresis (CE)

The aim of this study is to explore the parameters influencing capillary electrophoresis (CE) and which may affect the performance of the equipment. Different parameters studied were the voltage that affects the field strength, the pH of the electrolyte solution that affects the separation and dissociation of the analytes according to their pKa values, and the injection type used that affects the detectability. The acetylsalicylic acid (aspirin) concentration was also investigated from the analysis of a Disprin tablet. The instrument, experimental procedure and methods for the CE study are detailed in section 3.2 to section 3.2.4.2 of Chapter 3.

The peakmaster 5.1-software was employed to predict the migration order of the individual analytes, and the parameters that ensure correct prediction are shown in the peakmaster table shown in Appendix A1. The peak order from left to right is presented in Table 5.1. The migration orders of analytes were the same in both pH 7.5 and pH 8.5 as shown in Appendix A2 – Appendix A5. Instead of 2,3-dichlorophenol, 2,4-dichlorophenol was used in the estimation of the compound migration time because 2,3-dichlorophenol was not in the database. Appendix A6 shows a display of the method sequence in capillary electrophoresis, using the background electrolytes 1 & 2 (BGE1 and BGE2 electrolytes). Different analyses with different methods can be carried out simultaneously. Therefore, all the analyses described in section 3.2 to section 3.2.4.2 of Chapter 3 were performed simultaneously, and to ensure also that the commands were correct (injection times, method names, sample names, and vial number). Disprin samples were analysed using separate CE equipment simultaneously.

Table 5.1: The migration order of the standard analytes

Order	Compound
1	benzylamine
2	imidazole
3	acetylsalicylic acid
4	2,3-dichlorophenol
5	2,4-dinitrophenol
6	benzoic acid
7	salicylic acid

After the necessary information were entered into the menu boxes of the peakmaster software shown in Appendix A1, then the migration order was calculated and predicted in the results shown in Appendix A2 – Appendix A5. Appendix A2 and A3 show the migration of the analytes in two different pH values of 7.5 and 8.5 respectively, as described in section 3.2.1. of Chapter 3. The analytes include: benzylamine (1), imidazole (2), acetylsalicylic acid (3), 2,3-dichlorophenol (4), 2,4-dinitrophenol (5), benzoic acid (6) and salicylic acid (7).

5.2.1 BGE1 analysis

All the analyses performed with BGE1 are detailed in section 3.2.4.1 of chapter 3. The injection was a constant pressure injection of 35 mbar and the injection time used was 10 seconds. Methanol and Milli-Q water mixture (50:50) was used as a control sample to measure the mobility of the electroosmotic flow. The analysis voltage was 25 kV and the time was 5 minutes. In addition to the blank, a voltage series of the standard sample MIX (discussed in section 3.3 of Chapter 3) was measured with voltages 10, 15, 20 and 25 kV. The analysis time was 13 minutes. Then six repetitions with the standard solution (MIX) were done in 25 kV with analysis time 5 minutes. The electropherograms for the BGE1 analyses for the migration order of the standard compounds as predicted by the PeakMaster 5.1 are shown in Appendix A7 – A11. Thereafter, once the prediction and the experiments were carried out using both buffered electrolytes BGE1 and BGE2 (the experimental protocols for the electrolyte solutions are detailed in section 3.2.1 of Chapter 3), the electropherograms of the result showed the individual analytes were obtained in their correctly predicted order, as shown in Appendix A2 and Appendix A3.

5.2.2 BGE2 analysis

Milli-Q water was analyzed as a blank at 25 kV for 15 minutes; the electropherogram is shown in Appendix A12. Then the standard sample mixture was analyzed with injection times of 5, 10, 15, 20 and 30 seconds respectively, at the analysis of voltage 25 kV; the electropherograms are displayed in Appendix A13 – Appendix A17. Then electrokinetic injections with voltages 5, 10, 20 and 25 kV were carried out for the standard solution with 5 seconds injection time, the electropherograms are shown in Appendix A18 – Appendix A21. It can be observed in Appendix A7 – A11, that there are visible changes in the electropherograms of BGE1 and BGE2 respectively. The slight differences in instrumental and chemical parameters are a proof of these differences. The BGE1 buffer (pH 8.5; I = 10mM) electropherogram shares the same ionic strength with the BGE2 buffer (Appendix A7 – A11), but the differences in the pH and degree of dissociation, can be the cause of their slight differences in separation efficiency and peak intensities of individual analytes.

In the electropherograms obtained from the analyses, the analytes appeared in the correct order of prediction. The order is benzylamine, imidazole, aspirin, 2,3-dichlorophenol, 2,4-dinitrophenol, benzoic acid and salicylic acid. The analyte peak appearing before the electroosmosis have their electrophoretic mobilities μ_{ep} added to electroosmotic mobility μ_{eo} , this is

expressed in Equation 5.1, the equation is for cations, but electroosmosis is subtracted from the electrophoretic mobility when the compound migrates after electroosmosis, which means that the anions have negative electroosmosis values.

$$\mu_{tot} = \mu_{ep} + \mu_{eo} \quad (5.1)$$

In the equation 5.1, μ_{tot} is the total mobility of a compound. μ_{eo} is the mobility of the electro-osmosis (EOF).

5.2.3 Repeatability Study results in BGE1 repetition series

The results of the repeatability study carried out with the six analytes in order to validate the instrument's performance and reliability are presented in Appendix A22 – A29; presenting the electrophoretic data for the repetition runs to calculate the repeatability. Repeatability calculations were made from the six repetitions of the standard mix solution with BGE1 (analysis time 5 minutes, voltage 25 kV). It was noticed that the standard deviations remain relatively low and the repeatability seems good as shown in Appendix A22 – A29.

The electrophoretic mobilities were calculated with equation 5.2. For example, the electrophoretic calculation for the first runs of benzylamine is given as follows:

$$\begin{aligned} \mu_{ep} &= \frac{L_{tot}L_{det}}{Ut} \quad (5.2) \\ &= \frac{0.485m \times 0.4m}{25000 V \times 79.4 s} = 9.77 \times 10^{-8} \frac{m^2}{Vs} \approx 9.7719 \times 10^{-8} \frac{m^2}{Vs} \end{aligned}$$

The total electrophoretic mobilities were calculated by adding the electroosmosis to the electrophoretic mobility of the compounds that migrated before the electroosmosis and subtracting the electroosmosis from the compounds that migrated after it.

In the repeatability study for benzylamine in Appendix A22, it can be observed that the migration times are very close to one another; this is evident in the closeness in values of the respective electrophoretic mobility readings. The RSD value of 0.463 for the electrophoretic mobility shows the repeatability of the analysis. In the same vein, the rest of the analytes gave similar results of good repeatability, with their standard deviation and relative standard

deviation values as shown in Appendix A23 –A29. The RSD values of 0.544, 0.544, 0.544, 0.524, 0.515, and 0.476; belonging to imidazole, acetylsalicylic acid, 2,3-dichlorophenol, 2,4-dichlorophenol, benzoic acid and salicylic acid respectively.

5.2.4 Electrophoretic mobilities in the voltage series for analytes

The results presented in this section are from the procedure detailed in section 3.2.4.1 of Chapter 3. In the voltage series analysis, the results are also compiled in tabular format to portray the changes that take place when the voltage is varied during capillary electrophoresis analysis.

The voltage series analysis was also conducted for each of the analytes using the BGE1 buffer. For comparison of the effects of different voltages, the standard mix was analyzed in BGE1 at 10, 15, 20 and 25 kV. The migration times, areas, and electrophoretic mobilities of the voltage series are represented in Appendix A30 – Appendix A37. It can be seen from the results in Appendix A30 – A37 that the electrophoretic mobility value increases with the increase in voltage for each of the analytes. Averages for the migration times and areas were used from the replicate analyses for the calculation of electrophoretic mobilities, 10-20 kV had 2 replicates and 25 kV 6 replicates. The distance (s) used for velocity (v) was 0.40 m which is the length to the detector and the time (t) used was the migration time. The distance used in the electric field calculation was the whole length of the capillary, 0.485 m. The electrophoretic mobilities were calculated with Equation 5c in section 3.2 of chapter 3. The electrophoretic mobilities of the compounds could be calculated by dividing the linear velocity with the electric field (v/E). For the compounds migrating before the electroosmosis, the total electrophoretic mobility was calculated by adding the electroosmotic mobility to the electrophoretic mobility. For the compound migrating after the electroosmosis, the electroosmotic mobility was subtracted from the electrophoretic mobility. The compounds migrating after the electroosmosis are anions and they have negative electrophoretic mobilities.

5.2.5 Comparison of background buffer electrolyte (BGE1 and BGE2)

From the analyses carried out with BGE1 and BGE2 as described in sections 3.2.4.1 and 3.2.4.2 of Chapter 3, it is important to make a comparison to explain the instrument relative to the two different electrolytes. This is displayed in Table 5.2.

Table 5.2: Comparison of electrophoretic mobilities in BGE1 and BGE2

Compound	(E=10 ⁴)			
	BGE1 μ (m ² /V*s)	BGE2 μ (m ² /V*s)	BGE1 μ_{ep} (m ² /V*s)	BGE2 μ_{ep} (m ² /V*s)
Benzylamine	1.690E-07	1.344E-07	9.783E-08	8.239E-08
Imidazole	1.443E-07	1.184E-07	7.316E-08	6.640E-08
Electroosmosis peak	7.116E-08	5.201E-08	-	-
Acetylsalicylic acid	-2.266E-08	-8.252E-09	4.850E-08	4.376E-08
2,3-dichlorophenol	-2.455E-08	-2.527E-08	4.660E-08	2.674E-08
2,4-dinitrophenol	-2.883E-08	-3.005E-08	4.233E-08	2.195E-08
Benzoic acid	-2.992E-08	-3.101E-08	4.124E-08	2.100E-08
Salicylic acid	-3.193E-08	-3.325E-08	3.923E-08	1.876E-08

By the comparison of BGE1 and BGE2 mobilities in Table 5.2, it can be seen that the electroosmotic flow is slightly faster in BGE1 (with pH 8.5) than in BGE2 (with a pH 7.5). The electrophoretic mobilities of both the cations and anions are also a little faster in BGE1 than in BGE2. The comparison values are represented in Table 5.2; where it can be seen that the values in BGE1 are greater than that in BGE2, and this confirms that the effect of pH is significant in capillary electrophoresis. Also, a big difference in separation happens for imidazole; in BGE1 imidazole migrates very close to the electroosmosis peak, but in BGE2 imidazole separates better. In general, the separation of the test compound peaks is better in BGE2. When comparing the 25 kV runs, (this can be observed in Appendix A11 and Appendix A21) in BGE2 the migration times are longer in general. In BGE2 the benzylamine and imidazole peaks are somewhat higher. However, BGE1 is more suitable for separation efficiency owing to the faster electroosmotic flow and electrophoretic mobilities of the cations and anions.

5.2.6 Degree of dissociation of analytes

In this section, the various degrees of dissociation for the analytes were calculated as described in section 3.2.2 of Chapter 3.

The values for the degree of dissociation for the analytes that are weak acids were calculated with Equation 3, in section 3.2.2 of Chapter 3. For example, for benzoic acid (pKa=4.2) in BGE 1 (pH=8.5) the degree of dissociation is:

$$\alpha_{benzoic\ acid} = \frac{1}{1 + 10^{pK_a - pH}} = \frac{1}{1 + 10^{4.2 - 8.5}} = 0.999$$

The percentage for the degree of dissociation for the charged forms of acids is the percentage of that value for degree of dissociation (α). The charged percentage of cationic acids on the other hand is 1- α , because cationic acids form neutral molecules when they transfer their proton. Benzylamine and imidazole are cationic acids and they migrate before electroosmosis. Table 5.3 presents the values of the degrees of dissociation for the standard compounds in BGE 1 and BGE 2.

Table 5.3: The degrees of dissociation for the standard compounds in BGE 1 and BGE 2

Compound	pKa	α_{BGE1} (pH 8.5)	α_{BGE2} (pH 7.5)	α_{BGE1} (%)	α_{BGE2} (%) charged
Benzylamine	9.40	0.11	0.01	88.82 %	98.76 %
Imidazole	7.00	0.97	0.76	3.07 %	24.03 %
Acetylsalicylic acid	3.50	0.99	0.99	100.00%	99.99 %
2,3-dichlorophenol	7.50	0.91	0.50	90.91 %	50.00 %
2,4-dinitrophenol	4.00	0.99	0.99	100.00%	99.97 %
Benzoic acid	4.20	0.99	0.99	99.99 %	99.95 %
Salicylic acid	3.00	0.99	0.99	100.00%	100.00%

Acids (HA) are more in their charged deprotonated form (A^-) when the pH is higher than their pKa. When pH = pKa, 50 % of the acid is in charged form (A^-) and 50 % in neutral form (HA) as seen of 2,3-dichlorophenol in pH 7.5. Regarding cationic acids (HA^+), the ionic form is more abundant when the pH is lower than the pKa of the acid because then the acid is not really deprotonated and still in the cationic form (HA^+). The acid will donate the proton and

be more in the neutral acid form (A) when the pH is higher than the pKa of the acid. This can be seen, for example, with imidazole when the pH is 8.5 (that is 1.5 units higher than the pKa), the imidazole is mostly deprotonated to A⁻. Imidazole being mostly in A⁻ form means that the α (%) of charged acid form is small (Table 4.3). The analyte structures in BGE1 (pH 8.5) and BGE2 (pH 7.5) respectively, are shown in Figure 5.1.

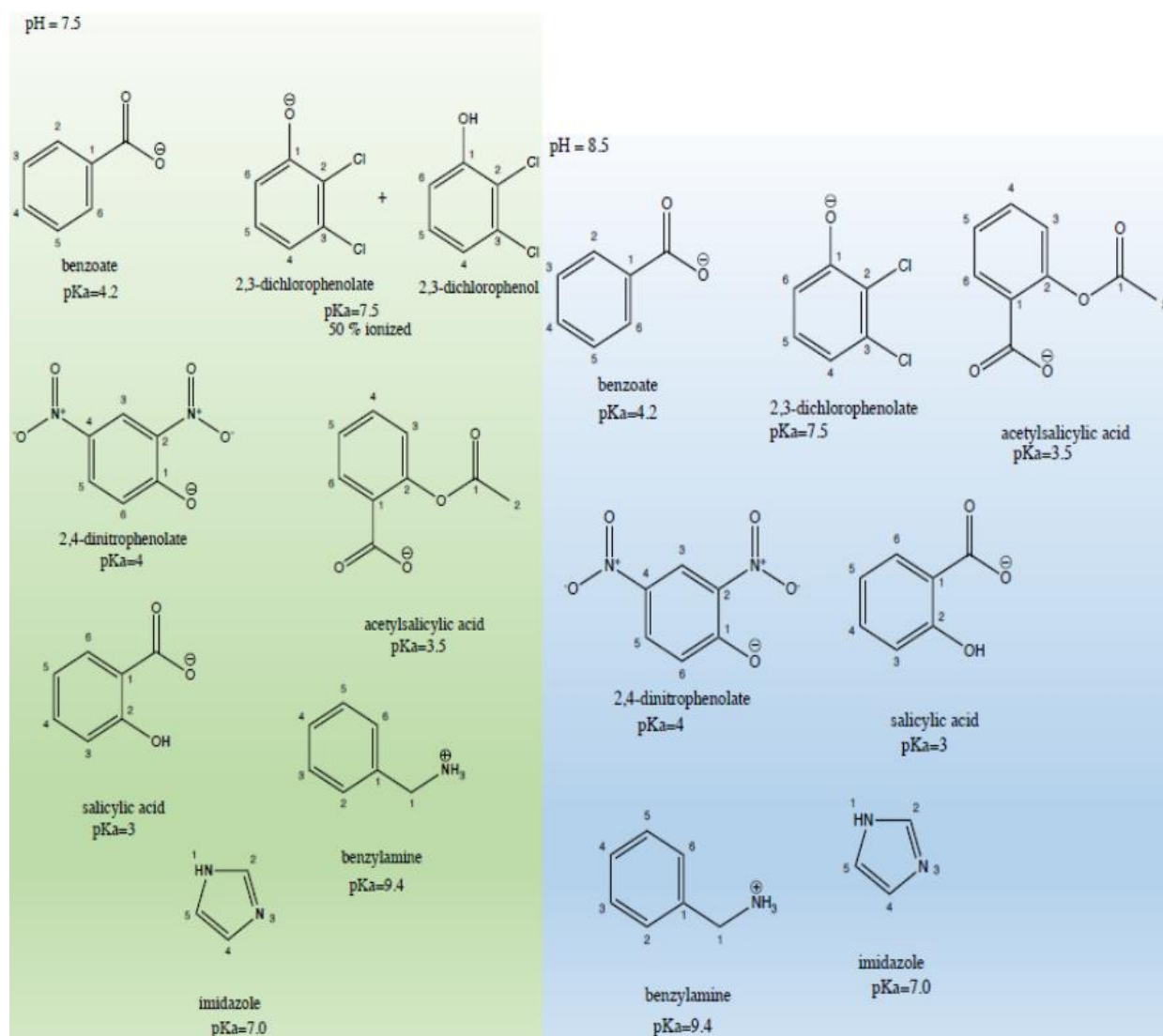


Figure 5.1: The analyte structures in pH 7.5 and pH 8.5.

5.2.7 Effect of injection time

As part of the investigation of the factors affecting capillary electrophoresis as a chromatographic method, the effect of injection time was studied against the volume of injection automatically carried out by the instrument. The experimental procedures are detailed in section 3.2.4 of Chapter 3. Table 5.4 shows the time and volume of injection for

benzylamine, and the result of the plot is given in Figure 5.3. In Table 5.4 and Figure 5.2, it can be seen that by increasing the injection time the injection volume also increases linearly.

Table 5.4: Effect of injection time to injection volume

Injection time (s)	Injection volume (nL)
5	6.12
10	12.24
15	18.37
20	24.49
30	36.73

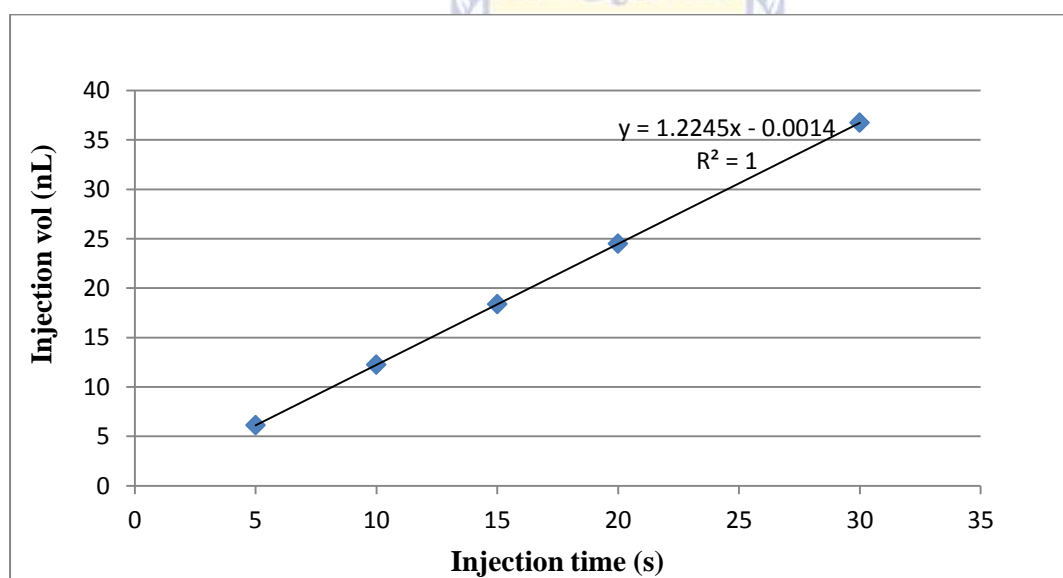


Figure 5.2: Injection time vs. injection volume for benzylamine (25 kV, 35 mbar).

The next section presents the result of the effect of injection time in constant pressure injection in BGE2.

5.2.8 Effect of injection time in constant pressure injection BGE2

As part of the analyses carried out with BGE2 electrolyte as detailed in section 3.2.4 of Chapter 3, the effect of injection time in constant pressure was also studied for benzylamine, with 25 kV and 35 mbar as the fixed parameters.

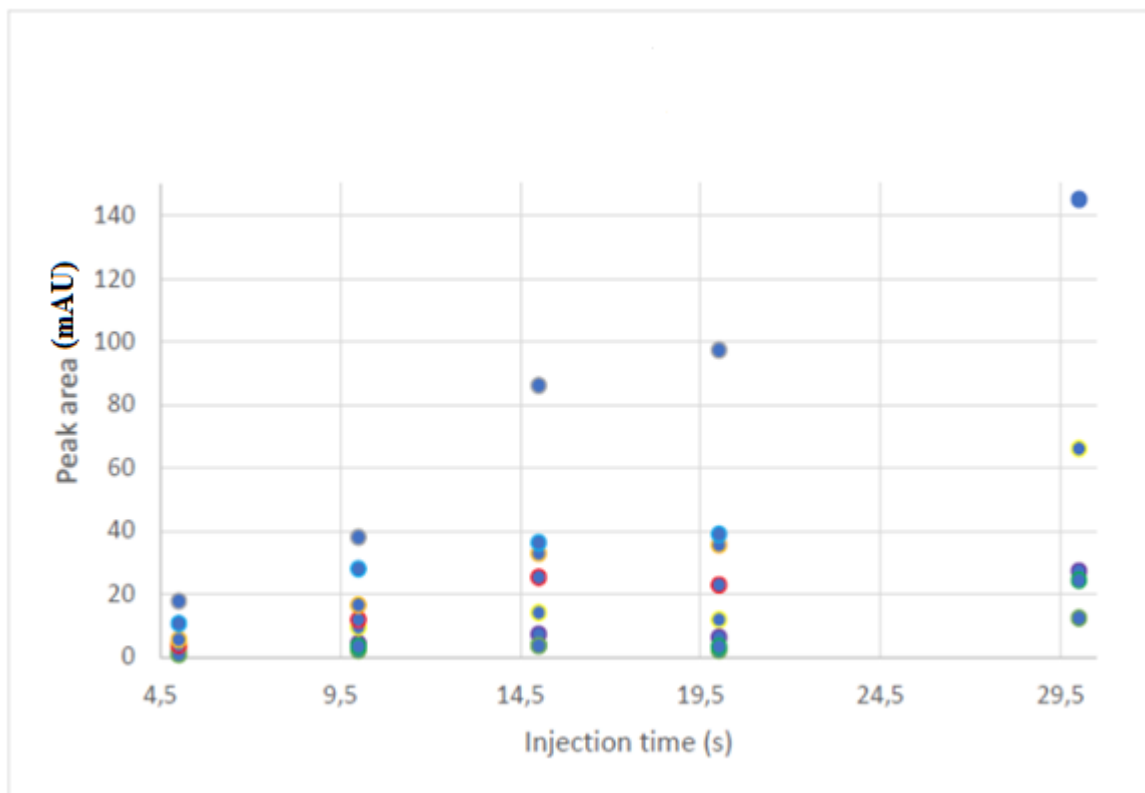


Figure 5.3: Effect of injection time for benzylamine in constant pressure injection in BGE2 (25 kV, 35 mbar).

The linear relationship between injection time and injection volume was observed in the constant pressure injection where only the injection time was increased. Figure 5.3 shows that higher injection time of the analytes caused higher peak areas as a result of the high concentration of the compounds. The correlation of the peak area against the injection time is presented in Figure 5.3.

5.2.9 Effect of voltage in CE

The experimental details for the effect of voltage in capillary electrophoresis are given in section 3.2.4.1 of Chapter 3. In the voltage series experiments, the plot of migration time against the voltage for benzylamine shows an inverse proportionality. Figure 5.4 shows the plot of migration time against voltage.

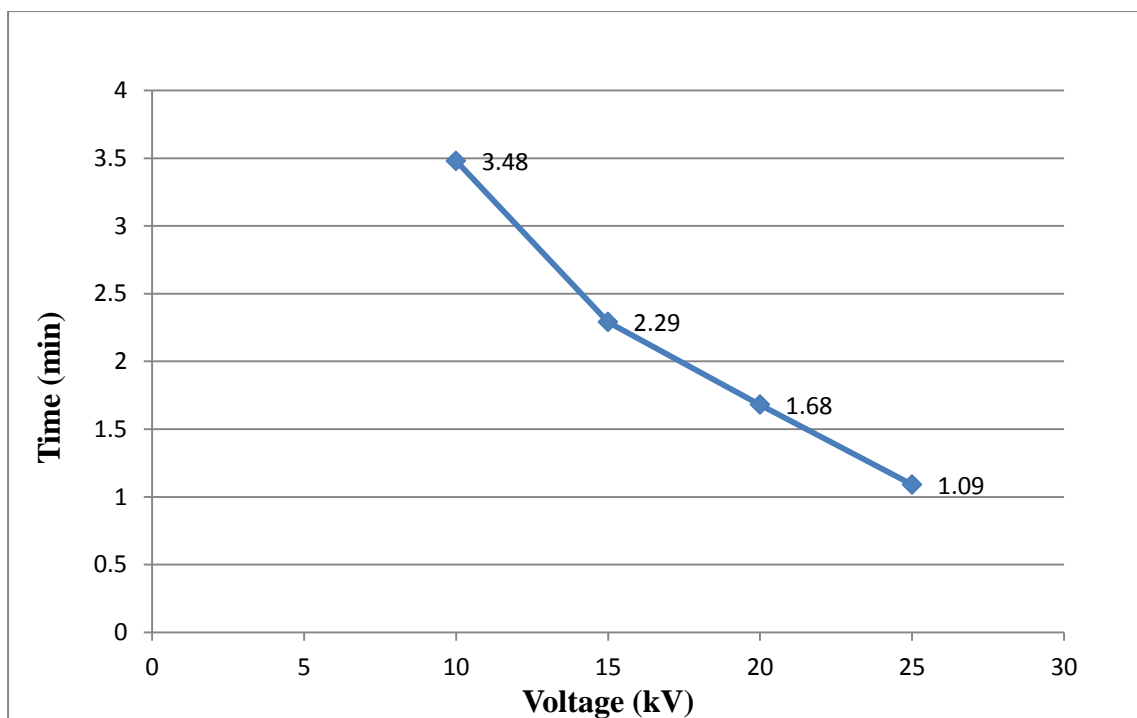


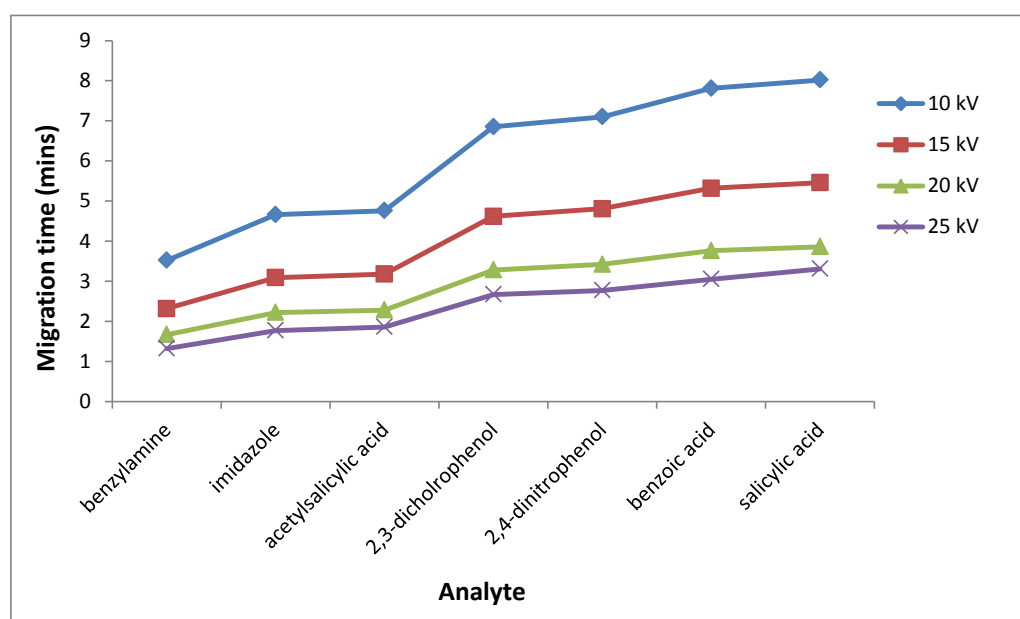
Figure 5.4: Correlation of migration time against voltage (35 mbar).

In the comparison of the migration time with varying voltage, it can be observed in Figure 5.4 that the migration time of benzylamine decreased as the voltage increased; this trend applies to other parameters including the electrophoretic mobility, which also decreased with increasing voltage.

To complement the observation in Figure 5.4, the migration times of all the seven analytes including: benzylamine, imidazole, acetylsalicylic acid (ASA), 2,3-dichlorophenol, 2,4-dinitrophenol, benzoic acid and salicylic acid were plotted against voltage as described in section 3.2.4.1 of Chapter 3. Table 5.5 and Figure 5.5 show the migration time of the seven standard analytes against voltage respectively. The migration time (MT) of each analyte is represented as MT 1 = benzylamine; MT 2 = imidazole; MT 3 = acetylsalicylic acid; MT 4 = 2,3-dichlorophenol; MT 5 = 2,4-dinitrophenol; MT 6 = benzoic acid; MT 7 = salicylic acid.

Table 5.5: Migration time (MT) against voltage

	MT 1 (min)	MT 2 (min)	MT 3 (min)	MT 4 (min)	MT 5 (min)	MT 6 (min)	MT 7 (min)
10 kV	3.52	4.66	4.76	6.85	7.10	7.81	8.02
15 kV	2.32	3.09	3.18	4.62	4.81	5.32	5.46
20 kV	1.67	2.22	2.28	3.28	3.42	3.76	3.86
25 kV	1.32	1.77	1.86	2.67	2.77	3.05	3.31

**Figure 5.5: Migration times (MT) against voltage plot in BGE1 for the standard analyte mixture (35 mbar).**

In Figure 5.5, it can be observed that the higher the voltage applied the shorter the migration times of the analytes. The reason is that the cathode attracts cations more effectively and the electroosmotic flow is increased. Anionic analytes are not as much affected by the increase in voltage. As the migration times get shorter it is also observed that the analytes migrate closer to each other which can affect the separation efficiency. That is why the voltage and other parameters should be optimized to obtain the best separation efficiency with the shortest possible optimal migration time. Similarly, the plot of voltage (kV) against current (mA) from the voltage series experiment described in section 3.2.4.1 of Chapter 3 is presented in Figure 5.6. The current increase should be linear to the voltage increase according to Ohm's law where $I = V/R$, and $I =$ current, where $V =$ voltage and $R =$ Resistance. The idea is that

the higher the voltage applied the higher the current in the capillary, and this is confirmed in Figure 5.6.

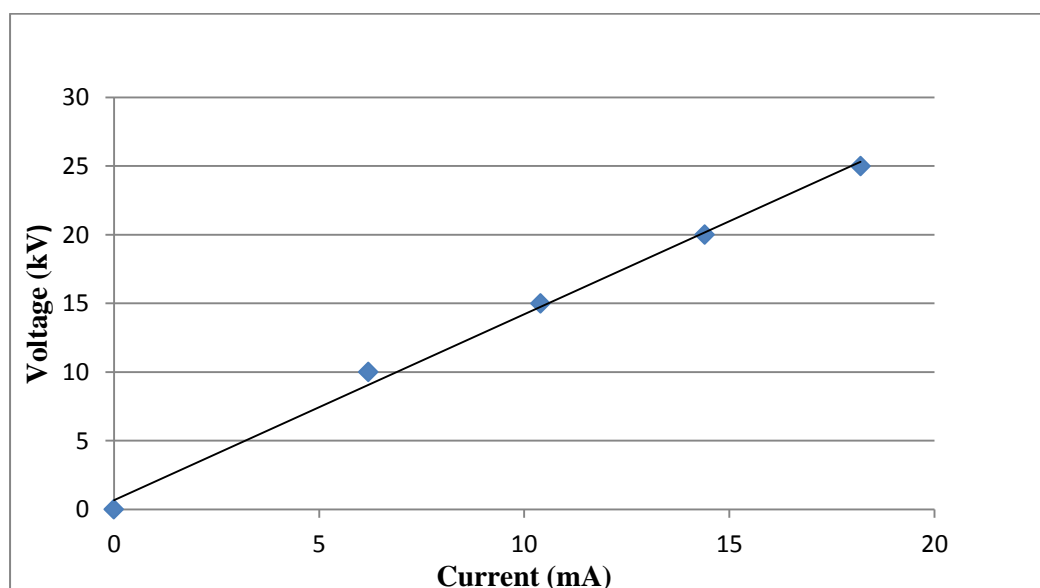


Figure 5.6: Plot of voltage against current in BGE1 for benzylamine (35 mbar, 13 mins).

The next section presents the absorptivity constant and the intensity of the analytes peak heights.

5.3 Absorptivity constant (ϵ)

The intensities of the standard analyte samples in the form of peak heights were determined, alongside the absorptivity constant. According to Beer-Lambert law, the absorptivity constant, ϵ , was calculated from equation:

$$A = \epsilon lc \quad (6)$$

Where A = Absorbance (peak height),

l = Path length from analyte to detector = 50 μm and

c = Concentration of the compound.

The concentration for all the analytes was 13 $\mu\text{g/mL}$ in the standard MIX solution. For example, for benzylamine the absorptivity constant, ϵ , was:

$$\epsilon = A/(lc) = 7.82/(50 * 10^{-6} \text{ m} * 13 * 10^{-3} \text{ g/L})$$

$$= 1.202 * 10^7 \text{ (M}^{-1}\text{cm}^{-1}\text{)}.$$

The intensities and absorptivity constant (ϵ) values for the analytes are presented in Table 5.6. The intensities differ from compound to compound because the acids are more or less concentrated depending on their cationic qualities and quantities in cationic form.

Table 5.6: The intensities and absorptivity constant, ϵ , values for the standard analytes. BGE1 (25 kV, 35 mbar)

Compound	Absorptivity constant, ϵ , ($\text{M}^{-1}\text{cm}^{-1}$) ($E=10^{\wedge}$)	Intensities (peak height)
Benzylamine	1.203E+05	7.817
Imidazole	3.933E+04	2.556
Acetylsalicylic Acid	1.674E+05	10.879
2,3-Dichlorophenol	1.472E+05	9.570
2,4-Dinitrophenol	6.861E+04	4.460
Benzoic Acid	2.338E+05	15.195
Salicylic Acid	3.849E+05	25.017

5.3.1 Effect of field strength on electrophoretic mobility

By comparing the effect of field strength to electrophoretic mobility it could be seen that the increase in field strength has an increasing effect on the mobility for cationic acids that are going toward the cathode. For anions, the effect is opposite because they are moving in the opposite direction.

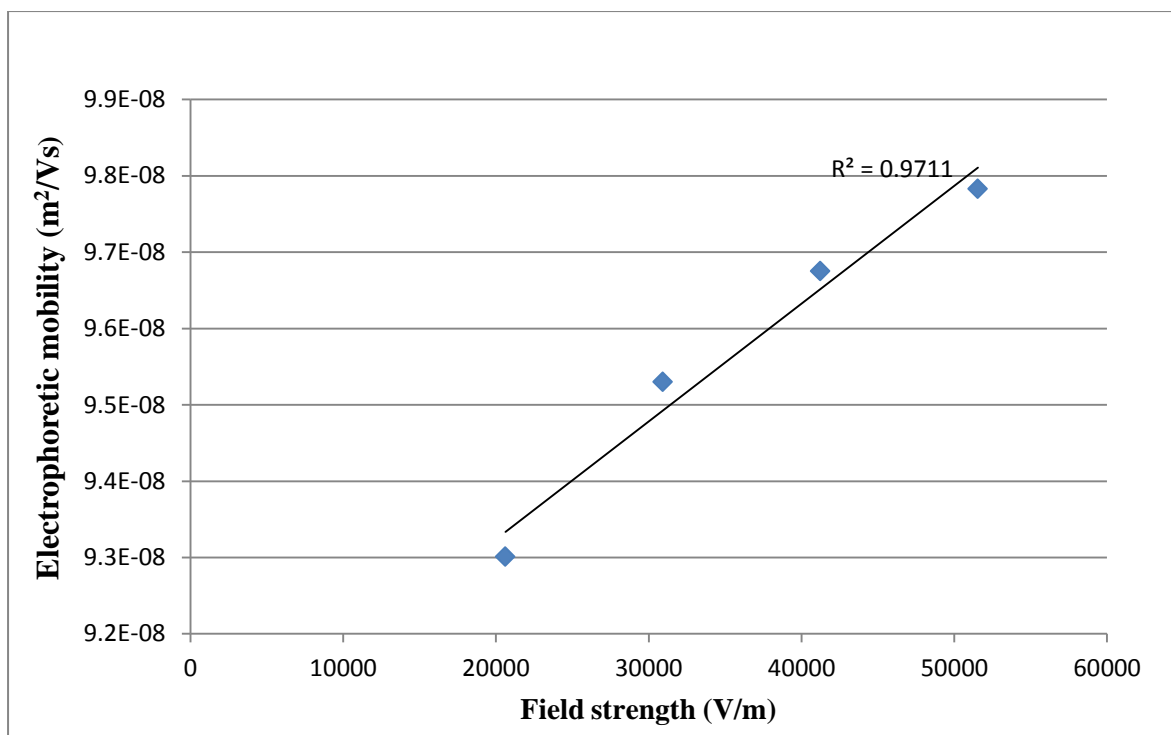


Figure 5.7: Electrophoretic mobility against field strength of benzylamine in BGE1 (25 kV, 35 mbar).

Figure 5.7 shows the direct proportionality between the electrophoretic mobility and the field strength in capillary electrophoresis, it can be seen that as the field strength increased, electrophoretic mobility also increased.

5.3.2 Effect of constant pressure injection against electrokinetic injection in BGE2

The experimental details for the constant pressure injection and electrokinetic injection in BGE2 are given in section 3.2.4.2 of Chapter 3.

With the electrokinetic injections, the voltages used were 5, 10, 20 and 25 kV. It was noticed that with lower voltages only one or two of the compound peaks were visible, as shown in Figure 5.8.

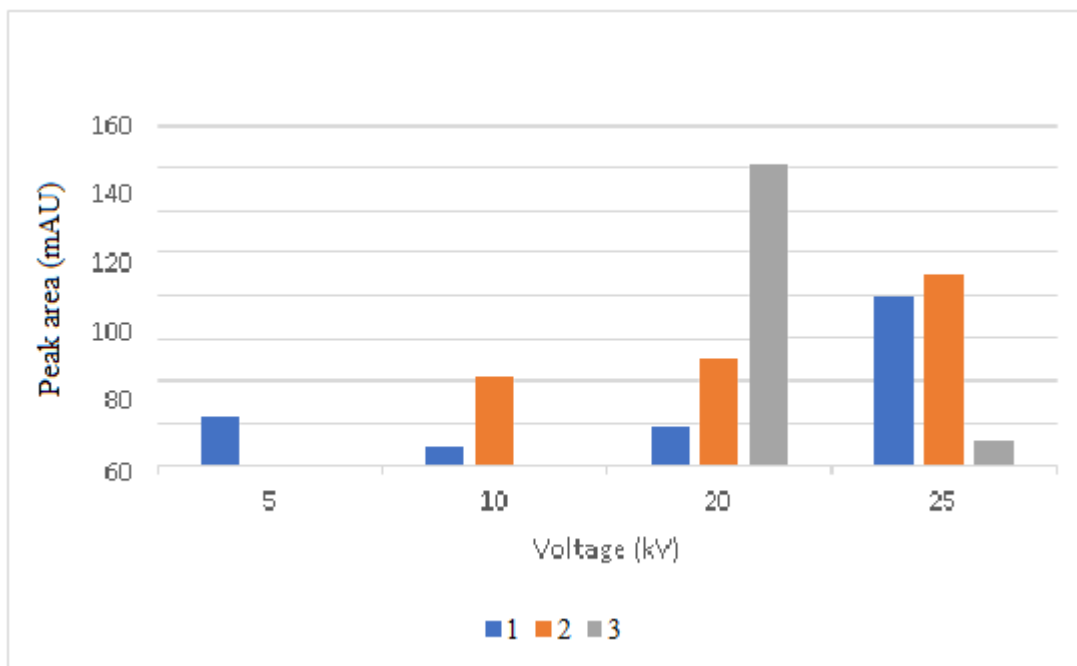


Figure 5.8: Plot of peak areas against voltage in BGE2 in electrokinetic injections (35 mbar, 5 secs).

Therefore by decreasing the voltages, the electrophoretic migration decreases, and the last compounds do not migrate in the time of 15 minutes. Voltage is the factor that gives rise to the cations' movement. When electrokinetic injections are made, there is an increase in the concentration of cationic acids leading to higher peak areas.

Tables 5.7 and 5.8 show the calculation results for the comparison of the constant pressure injection with varying injection times for benzylamine and imidazole in BGE2 buffer/electrolyte.

Table 5.7: Comparison of constant pressure injection with varying injection times for Benzylamine (pKa = 9.4) using BGE 2 (25 kV, 35 mbar)

	5s	10s	15s	20s	30s
Migration time [min]	1.53	1.57	1.65	1.90	2.39
Area	1.134	2.407	4.127	6.329	27.495
Velocity [m/s]	5.283×10^{-3}	5.149×10^{-3}	4.899×10^{-3}	4.254×10^{-3}	3.382×10^{-3}
$\mu \left[\frac{m^2}{Vs} \right]$	5.072×10^{-8}	5.194×10^{-8}	4.994×10^{-8}	4.293×10^{-8}	2.980×10^{-8}
$\mu_{ep} \left[\frac{m^2}{Vs} \right]$	1.353×10^{-7}	1.343×10^{-7}	1.283×10^{-7}	1.110×10^{-7}	8.391×10^{-8}

Table 5.8: Comparison of constant pressure injection with varying injection times for Imidazole (pKa = 7.0) using BGE 2 (25 kV, 35 mbar)

	5s	10s	15s	20s	30s
Migration time [min]	1.94	1.95	2.02	2.31	3.07
Area	2.854	4.456	7.516	12.009	12.478
Velocity [m/s]	4.167×10^{-3}	4.145×10^{-3}	4.002×10^{-3}	3.499×10^{-3}	2.633×10^{-3}
$\mu \left[\frac{m^2}{Vs} \right]$	5.072×10^{-8}	5.194×10^{-8}	4.994×10^{-8}	4.293×10^{-8}	2.980×10^{-8}
$\mu_{ep} \left[\frac{m^2}{Vs} \right]$	1.174×10^{-7}	1.183×10^{-7}	1.140×10^{-7}	9.892×10^{-8}	7.193×10^{-8}

Comparison of the constant pressure injection with varying injection time, showed that the migration time increases with an increase in the injection time, and the peak areas. The electrophoretic mobility however decreases as the injection time increases.

5.3.3 Effect of wavelength

The effect of wavelength is an important key in the detection of analytes in capillary electrophoresis. The experimental procedures in section 3.2.4 of Chapter 3 were executed applying a range of wavelengths to determine the best wavelength suitable for effective detection of the analyte samples. Different wavelengths were employed in the analysis to optimise/validate the best wavelength for the best sensitivity. These wavelengths included: 200 nm, 214 nm, 220 nm, 254 nm, 320 nm.

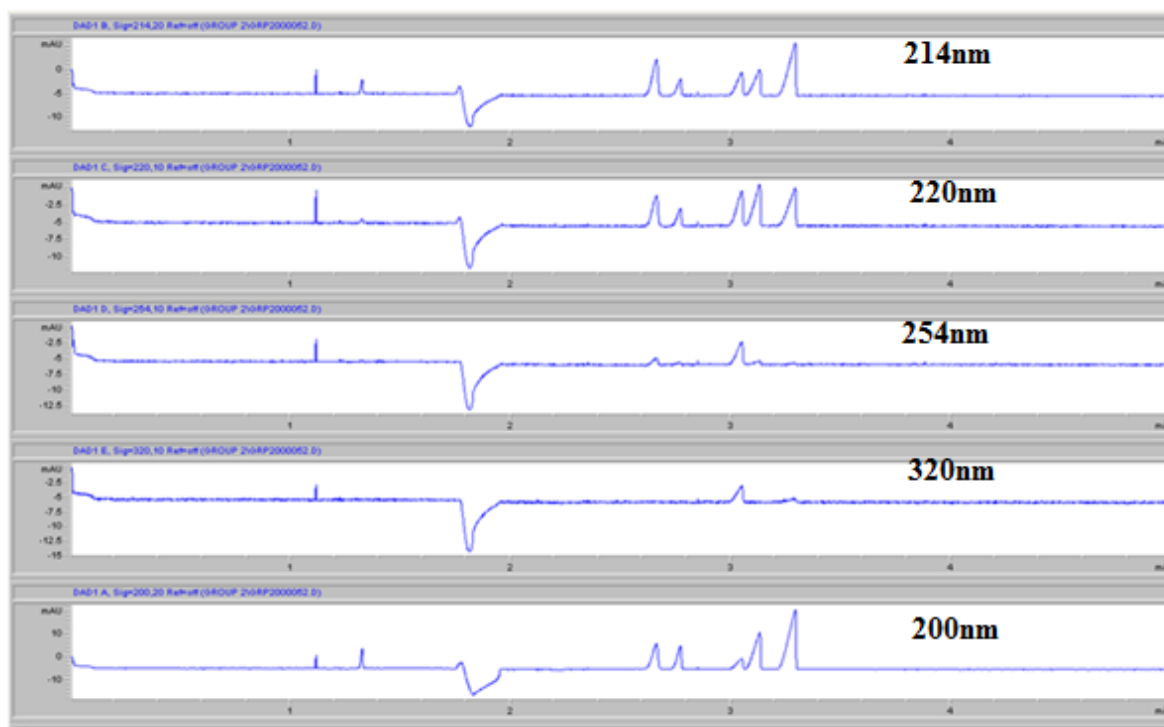


Figure 5.9: Wavelength overlay showing 214 nm as the best for all the analytes.

In Figure 5.9, an overlay of electropherograms of the standard analytes carried out at different wavelengths is presented. The electropherogram obtained at 214 nm gave the best detection for the seven standard analytes. Therefore, wavelength of 214 nm was chosen for the Capillary Zone Electrophoresis detection, because this is the wavelength where the sensitivity was highest for all the selected analytes. Figure 5.10 shows the overlay of the different wavelength values to reveal the best wavelength value. This is shown by the sensitivity and peak intensity of each analyte in the electropherogram.

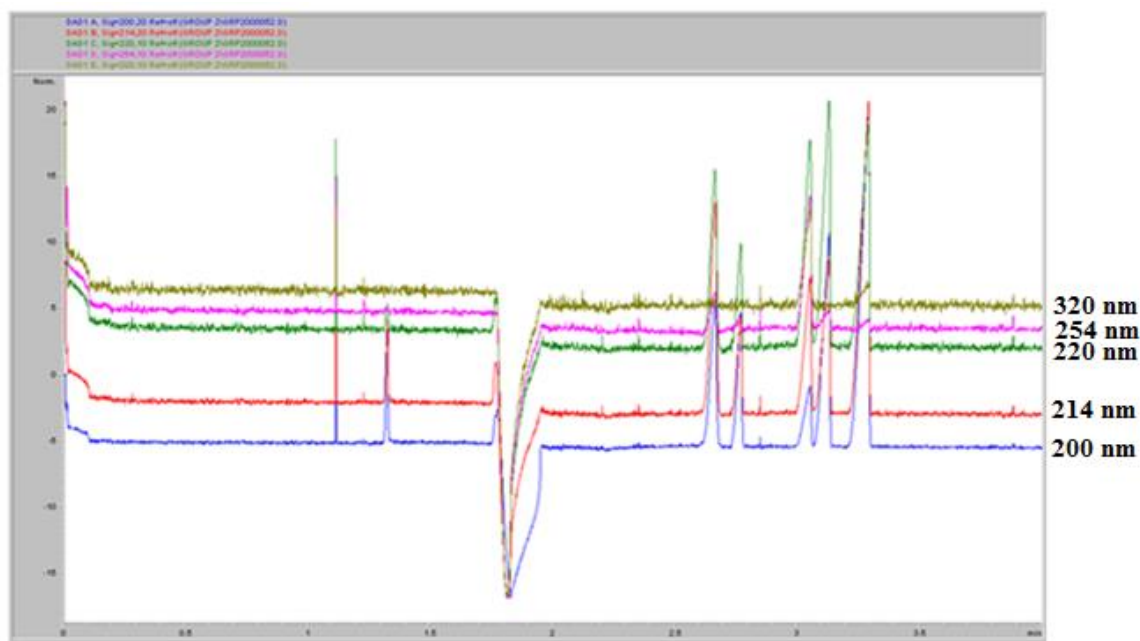


Figure 5.10: An overlay of the peak heights obtained from different detector wavelengths.

The overlay of the different detector wavelengths also shows clearly that the peak height belonging to 214 nm gives the best signal intensity for all the analytes, thereby justifying the 214 nm wavelength used for the CE optimisation.

5.4 Disprin sample quantification

This analysis was carried out as a quality control measure for the CE instrument, and to calculate the concentration of aspirin or acetylsalicylic acid (ASA) in DisprinTM tablets, alongside salicylic acid (SA) which is the degradation product.

The experimental details for the analysis of aspirin in DisprinTM tablets are given in section 3.3.2 section of Chapter 3. The Disprin samples were analyzed using BGE1 buffer solution at 25 kV. All three Disprin samples were analyzed 4 times. In Appendix 40 is the electropherogram of one Disprin sample. The calibration standards of acetylsalicylic acid and salicylic acid with concentrations 2, 5, 10, 15, 20 and 25 ppm were analyzed at pH 8.5, 35 mbar and 25 kV with BGE1. All of the concentrations were analyzed six times. The electropherograms are displayed in Appendix A38 – A43.

Acetylsalicylic acid (ASA) gives salicylic acid (SA) as the degradation product. The hydrolysis of the drug can be attributed to its instability in solutions. Therefore, when aspirin

(acetylsalicylic acid) undergoes hydrolysis, the degradation products are salicylic acid and acetic acid as shown in Figure 5.11.

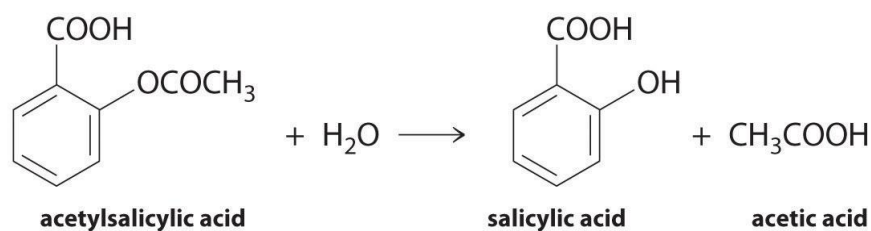


Figure 5.11: Degradation of aspirin or acetylsalicylic acid (ASA).

Table 5.9: Comparison of migration times and peak areas in Disprin, Aspirin standard and standard mixture (STD MIX)

	EOF (t/min)	EOF (area)	SA (t/min)	SA (area)	ASA (t/min)	ASA (area)
Disprin sample	1.82	30.50	2.69	4.40	3.09	7.00
Aspirin STD	1.85	16.80	2.80	5.10	3.26	14.40
STD MIX	1.82	9.80	2.67	14.40	3.29	25.20

EOF = electroosmotic flow; SA = salicylic acid; ASA = acetylsalicylic acid.

The migration times between the aspirin in the DisprinTM tablet sample, aspirin standard sample and ASA in the standard mixture were not profound as seen in Table 5.9. The voltage was 25 kV and the solution used was BGE1 (pH 8.5) as stated in section 3.3.2 of Chapter 3; so the applied conditions were similar. The areas of the analytes (aspirin and salicylic acid) are smaller in Aspirin (ASA) standard than in standard mixture mostly because of the differences in concentrations. The ASA standards were diluted with MeOH-water mixture, but Disprin sample only in water, which could be one reason for the difference in the electroosmosis (EOF) peak area.

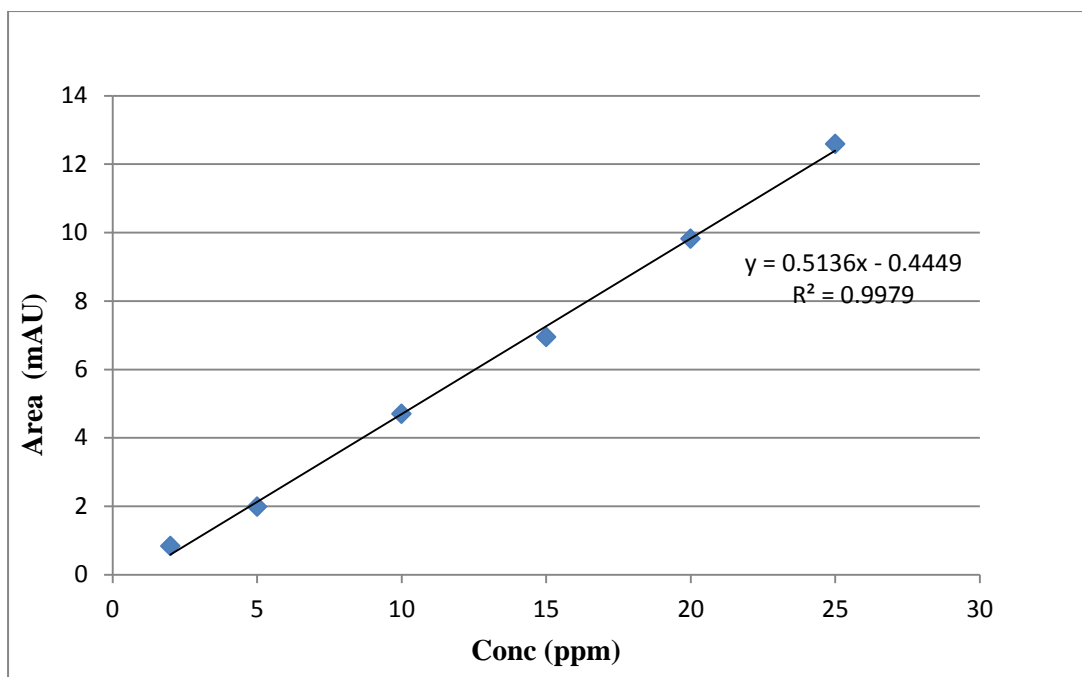


Figure 5.12: Calibration curve for acetylsalicylic acid (25 kV, 35 mbar).

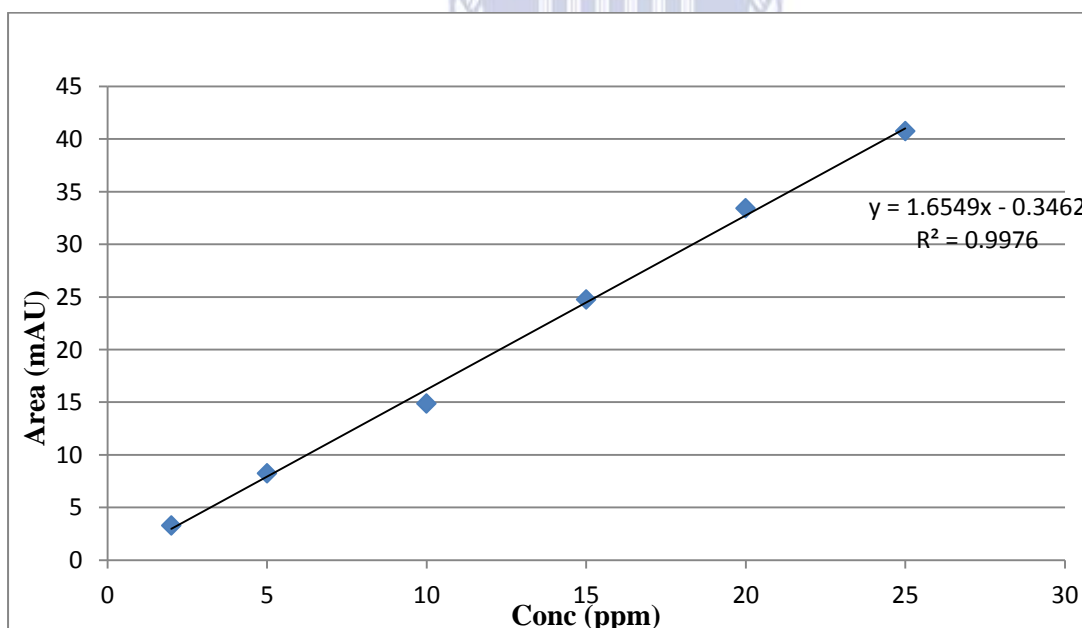


Figure 5.13: Calibration curve for salicylic acid (25 kV, 35 mbar).

Figures 5.12 – 5.13 are the calibration curves for the acetylsalicylic acid (ASA) and salicylic acid that were calculated from the averages of the six replicates of the calibration standard measurements in BGE1 electrolyte and at 25 kV. The concentrations of the calibration standard samples were 2, 5, 10, 15, 20 and 25 $\mu\text{g/mL}$.

The average areas for acetylsalicylic and salicylic acid and the standard deviations in Disprin samples 1-3 are presented in Table 5.10.

Table 5.10: Result of Disprin samples

	Disprin 1 avg	STD 1	Disprin 2 avg	STD2	Disprin 3 avg	STD3
Acetylsalicylic Acid (ASA)	5.360	0.334	4.338	0.727	4.215	0.169
Salicylic Acid (SA)	4.209	0.940	5.328	0.187	7.143	0.667

Using the calibration curve equations, the concentrations of ASA and SA could be calculated in the samples 1-3 (Table 5.11).

Table 5.11 gives the details of the average calibration concentration for acetylsalicylic acid and salicylic acid.

Table 5.11: Average calibration concentration for acetylsalicylic acid and salicylic acid

Calibration concentration (ppm = µg/mL)	
Acetyl salicylic acid 1	11.302
Acetyl salicylic acid 2	9.313
Acetyl salicylic acid 3	9.072
ASA Average	9.896
Salicylic acid 1	2.753
Salicylic acid 2	3.429
Salicylic acid 3	4.525
SA Average	3.569
SA + ASA Average	14.551

The total concentration of ASA is calculated by the addition of the average ASA concentration (9.896 µg/mL), and the concentration of ASA derived from salicylic acid (SA) by multiplying the SA concentration with the relation of the molar masses of ASA and SA.

$$3.56894168 \mu\text{g/mL} \times (180.16 \text{ g/mol}/138.12 \text{ g/mol}) = 4.655 \mu\text{g/mL}.$$

Thus, the total concentration for ASA is $4.6552 \mu\text{g/mL} + 9.896 \mu\text{g/mL} = 14.551 \mu\text{g/mL}$. The calculated concentration of ASA in the sample is presented in Table 5.12. The mass of acetylsalicylic acid (ASA) in one pill was 438.546 mg that was 57.62 % by mass. The mass of ASA determined was 91.46 %, and this is the mass % compared to the advertised content in the Disprin tablet.



UNIVERSITY *of the*
WESTERN CAPE

Table 5.12: Calculation of the Acetylsalicylic acid (ASA) concentration in the Disprin™ tablet sample

Pipetted volume (V_1)	0.125 mL
Volume of sample (V_2)	5 mL
Total ASA conc. (C_2)	14.55 $\mu\text{g/mL}$
$C_1=(C_2 V_2)/V_1$	582 $\mu\text{g/mL}$
mass (ASA, in 10.1 g sample)	582 $\mu\text{g/ml}$ *10 mL =5820 μg =5.82 mg
mass-% (ASA) in the pill	= 5.82 mg /10.1mg *100 % = 57.62 %
mass(pill)	761.1 mg
mass(ASA)= mass-% (ASA)*mass(pill)	438.546 mg
(Theoretical ASA mass) (63 % of the pill)	479.493 mg
mass(ASA)/m(theoretical) * 100 %	
Mass compared to the theoretical value	= 91.46 %

The electrophoretic mobility of aspirin and salicylic acid in Disprin tablet is shown in Table 5.13. Acetylsalicylic acid (Aspirin) has a greater electrophoretic mobility value than the degradation product (salicylic acid), resulting in the faster migration time for acetylsalicylic acid as predicted in the peakmaster software.

Table 5.13: Electrophoretic mobilities of ASA and SA

Electrophoretic Mobility (μ_{ep}) [m^2/Vs]

Method	Aspirin	Salicylic acid
BGE1	-2.485×10^{-8}	-3.188×10^{-8}

Table 5.14 shows the instrument's response to the detection of each of the analytes, and linear sensitivity to increasing concentrations with R^2 values > 0.99 for both acetylsalicylic acid and salicylic acid. The method's LOD and LOQ values for each analyte were statistically calculated.

Table 5.14: Calibration data for Aspirin and Salicylic acid in Disprin

Standards	Calibration					
	range $\mu g/mL$	Linear equation	R^2	λ_{max}	LOD $\mu g/mL$	LOQ $\mu g/mL$
<i>Aspirin</i>	2 – 25	$y = 0.5136x - 0.4449$	0.9979	214 nm	0.004	0.012
<i>Salicylic acid</i>	2 – 25	$y = 1.6549x - 0.3462$	0.9976	214 nm	0.003	0.009

In conclusion, the mass determined for the acetylsalicylic acid (ASA) was quite close to the specified value by the manufacturer. In this capillary electrophoresis optimisation analysis, the different parameters affecting electrophoretic analysis have been detailed and demonstrated.

5.5 Identification and quantification of pharmaceuticals contents in water: determination with capillary zone electrophoresis (CZE) and UV detection

This section details the results and discussion of the identification and quantification of pharmaceuticals in various water samples (influent, effluent and tap water). The sampling procedures are described in section 3.2.6 of Chapter 3; the sample preparation with solid phase extraction (SPE) is described in section 3.2.7; while the method designed for the analysis is described in section 3.2.5 of Chapter 3.

5.5.1 Calibration and optimisation

The six MIX standard analytes which include: acetaminophen, diclofenac, aspirin, salicylic acid, ibuprofen and sulphamethoxazole; were subjected to analysis using the capillary electrophoresis instrument. Different methods were employed alongside the changes made to the capillary length of the instrument to achieve an effective separation of compounds.

At first, individual analytes were each run as a single separate analysis to ascertain the compound's elution time (migration time) and detection sensitivity. The conditions applied include: 48.5 cm capillary length, 10.6 pH, 20 kV voltage, 50 mbar pressure, 5 seconds injection time, 25 °C cassette temperature, 50:50 MeOH/H₂O ratio, and 20 mM ammonium acetate buffer concentration.

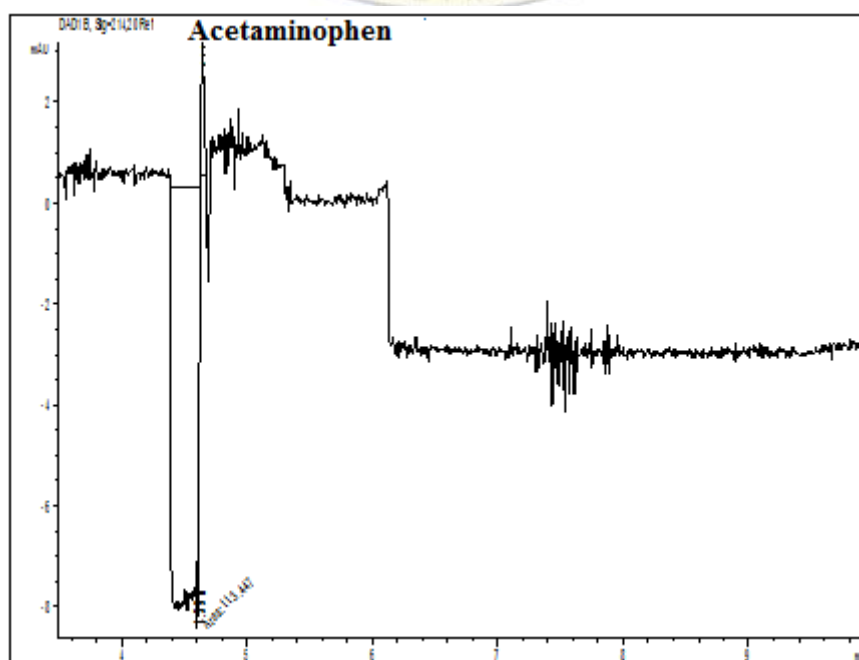


Figure 5.14: Electropherogram of Acetaminophen.

In the single analysis of acetaminophen in Figure 5.14, it can be observed that acetaminophen peaked almost immediately after the electroosmosis, with an elution time of 4.6 minutes, in a seemingly tiny peak. This electropherogram result suggests that an optimisation of different chemical and instrumental parameters are needed to ensure that acetaminophen comes out in a better peak, this is important, especially when the six different analytes are combined in a mixture in order to guarantee an effective separation.

In Figure 5.16, the electropherogram of aspirin (acetylsalicylic acid) with the degradation product salicylic acid is shown; with elution times 5.0 and 6.2 minutes respectively.

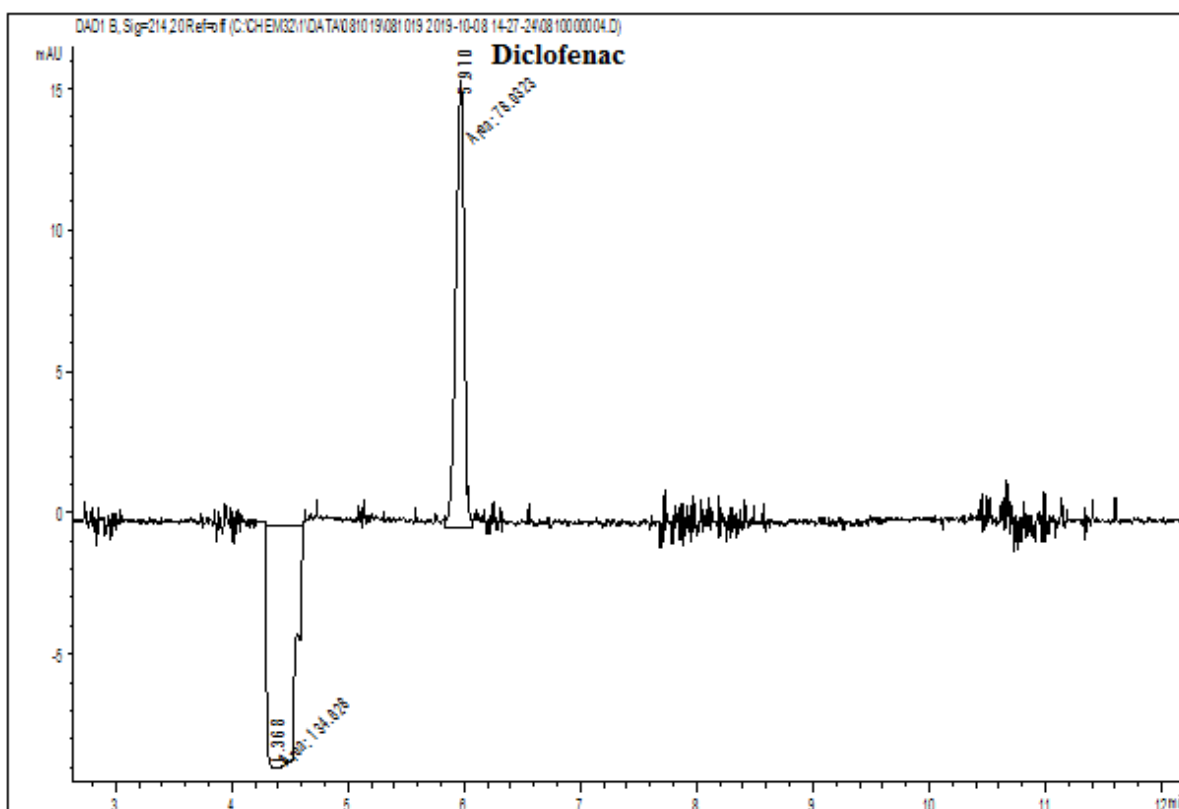


Figure 5.15: Electropherogram of Diclofenac.

Figure 5.15 shows the electropherogram of diclofenac having an elution time of 5.9 minutes in a distinct peak.

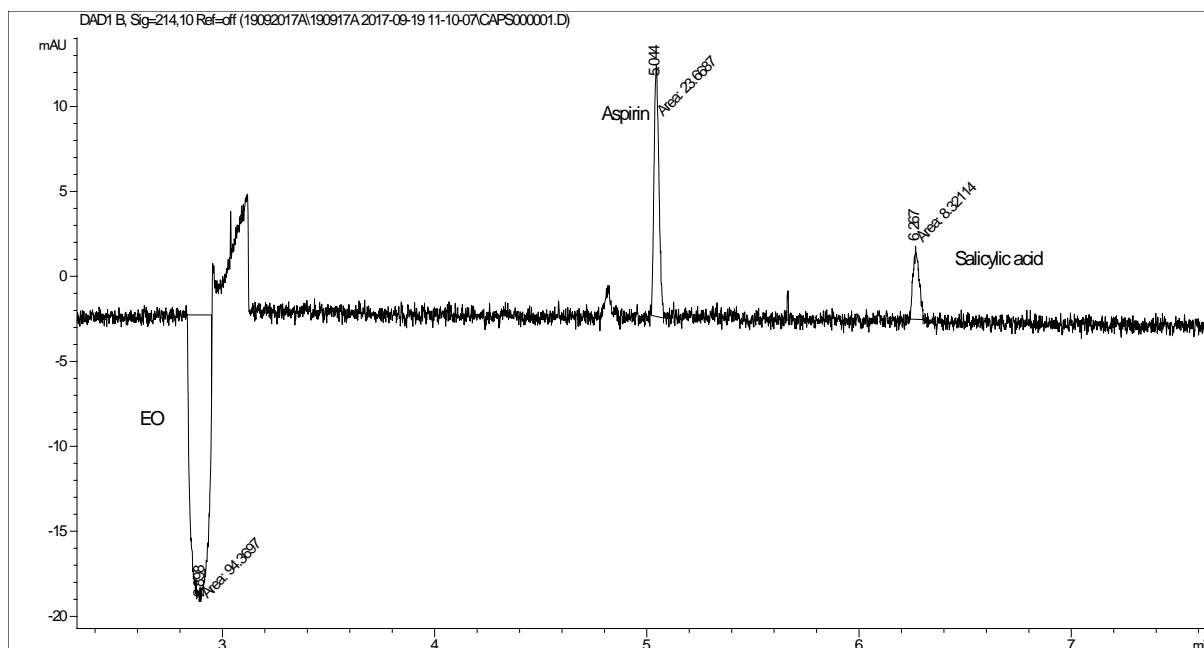


Figure 5.16: Electropherogram of Aspirin and the degradation product Salicylic acid.

Figure 5.17 shows the electropherogram of Ibuprofen with the elution time of 5.6 minutes and Figure 5.18 shows the electropherogram of sulphamethoxazole with the elution time of 6.5 minutes. In the first batch of analysis, 48.5 cm length of capillary was used for the separation of analytes, but the results were not satisfactory.

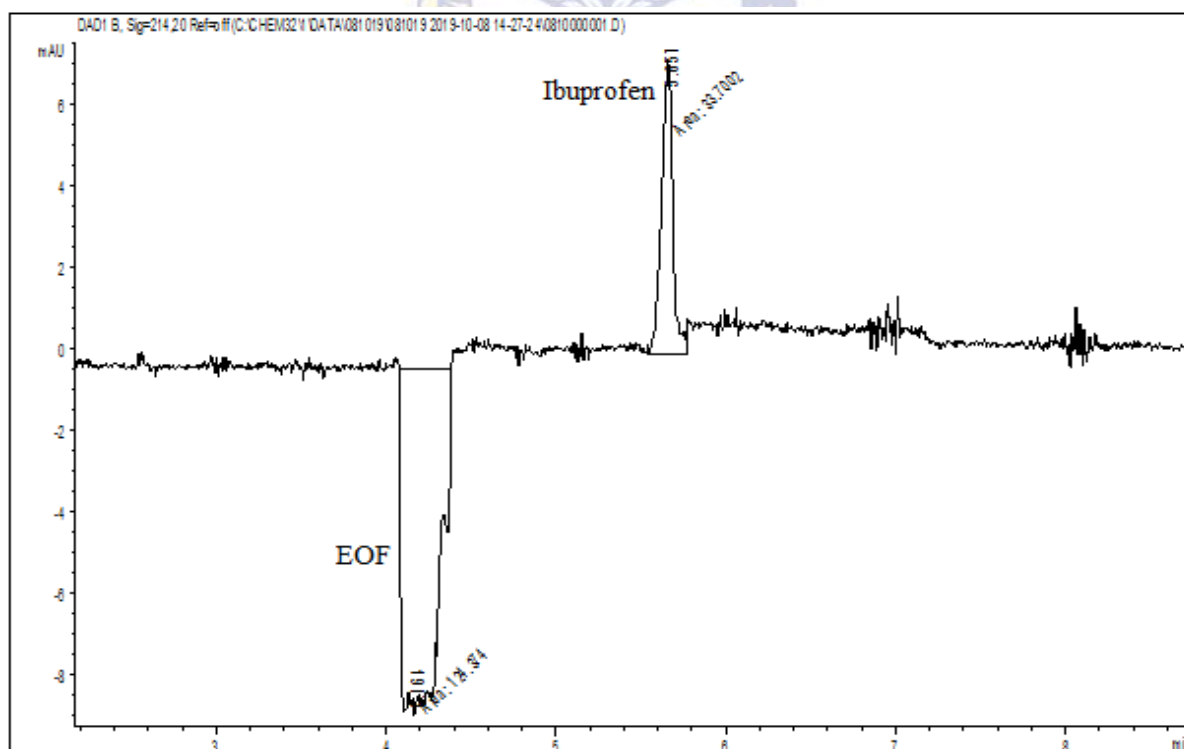


Figure 5.17: Electropherogram of Ibuprofen.

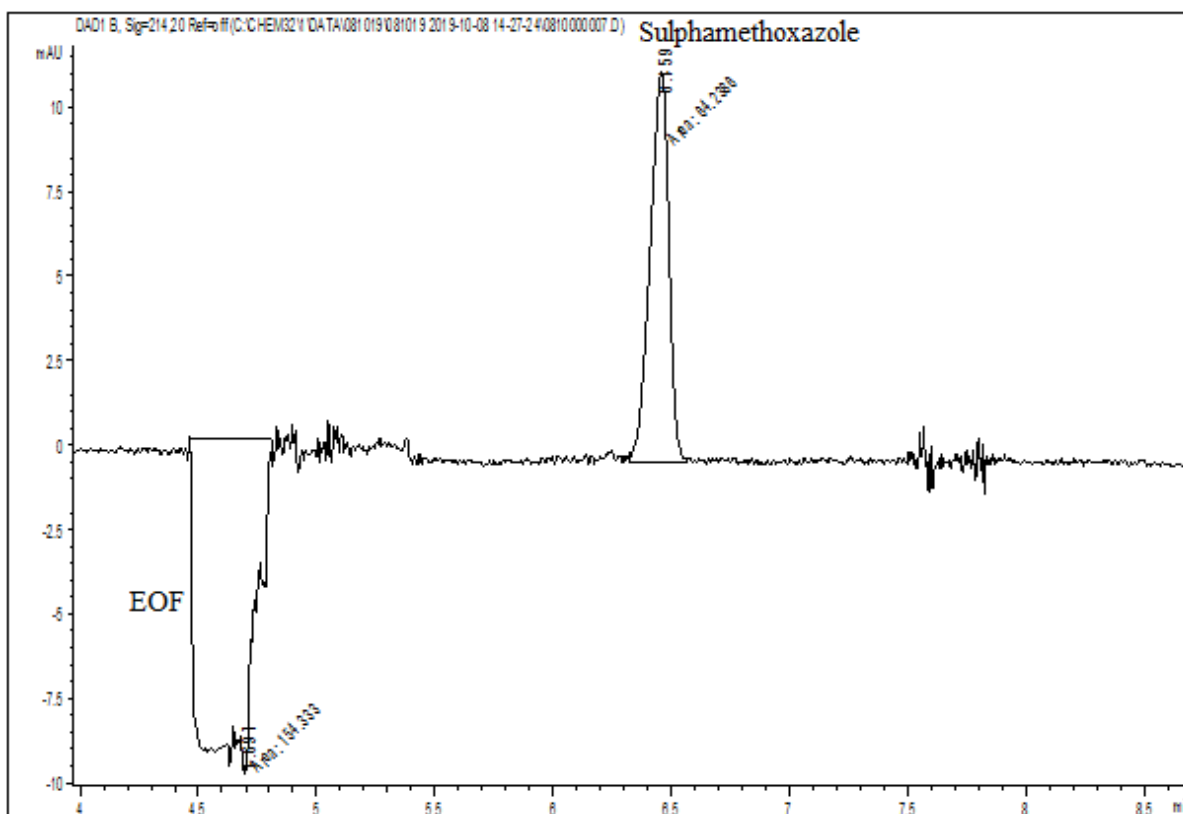


Figure 5.18: Electropherogram of Sulphamethoxazole.

However, the capillary length was changed to 60 cm in order to achieve better efficiency of separation, and used to carry out analysis of mixtures. The remaining applied parameters include: 9.678 pH, 20 kV voltage, 50 mbar pressure, 5 seconds injection time, 25 °C cassette temperature, 50:50 MeOH/H₂O ratio, and 20 mM ammonium acetate buffer concentration. The mixtures were divided into portions as shown in the Table 5.15.

Table 5.15: Analytes divided into portions

SAI	Salicylic acid, Acetylsalicylic acid, Ibuprofen,
AID	Acetaminophen, Ibuprofen, Diclofenac
ASID	Acetaminophen, Sulphamethoxazole, Ibuprofen, Diclofenac
ASIDAS	Acetaminophen, Sulphamethoxazole, Ibuprofen, Diclofenac, Aspirin, salicylic acid

In Table 5.15, these combinations of analytes were made to investigate the separation efficiency of the different combinations compared to the final MIX which contains all the six analytes.

Figure 5.19 shows the electropherogram of the SAI mixture; with aspirin, salicylic acid and ibuprofen well separated using 50:50 H₂O/MeOH mixture. This electropherogram for the SAI mixture is suitable result for the combination of the solvent mixture ratio.

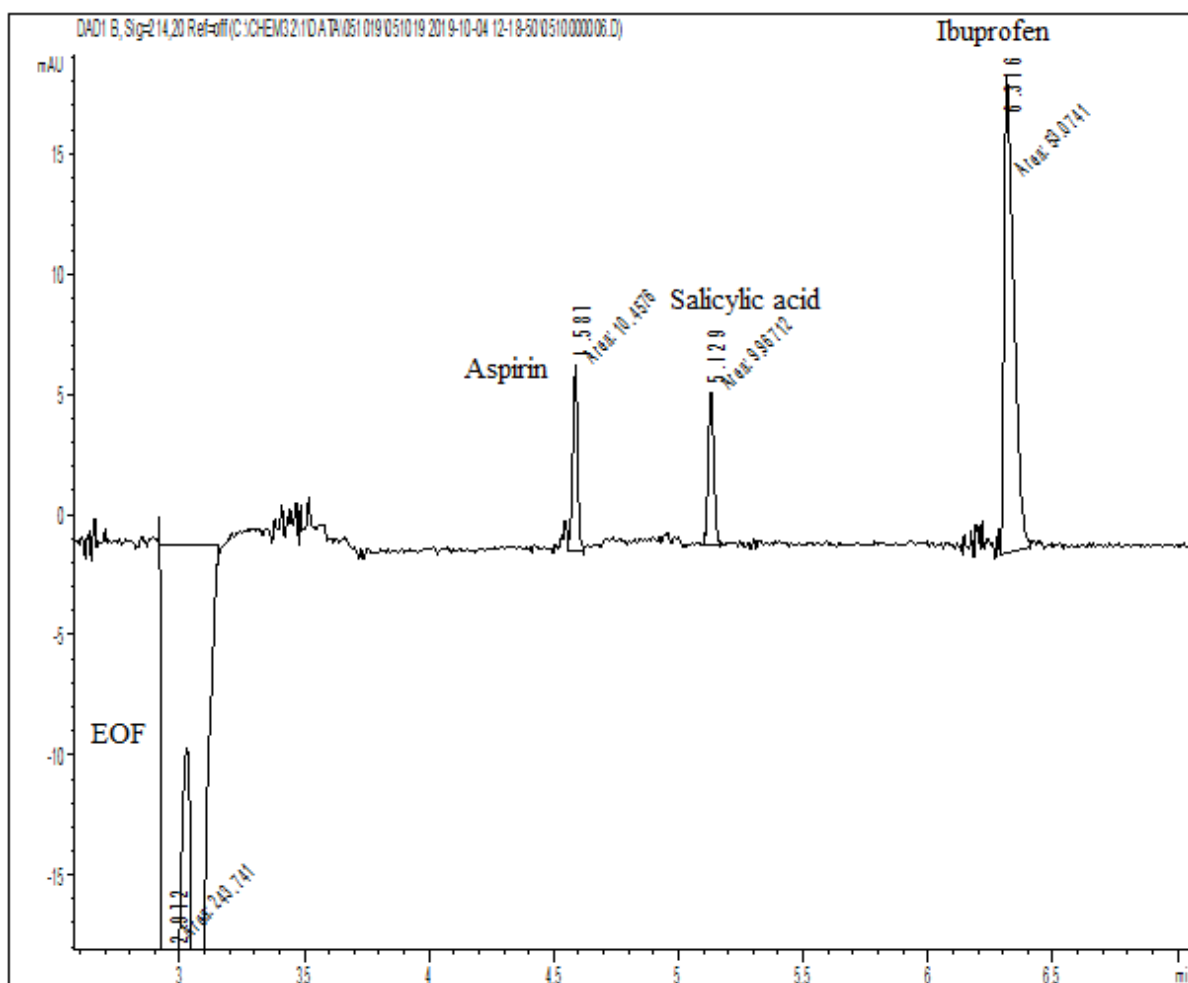


Figure 5.19: Electropherogram of the SAI mixture.

The applied parameters for the AID mixture include: 60 cm capillary length, 9.678 pH, 20 kV voltage, 50 mbar pressure, 5 seconds injection time, 25 °C cassette temperature, 50:50 MeOH/H₂O ratio, and 20 mM ammonium acetate buffer concentration. The electropherogram in Figure 5.20 shows there is not an efficient separation in the three components of the AID mixture, as it is difficult to identify each component since there is a co-elution in the electropherogram.

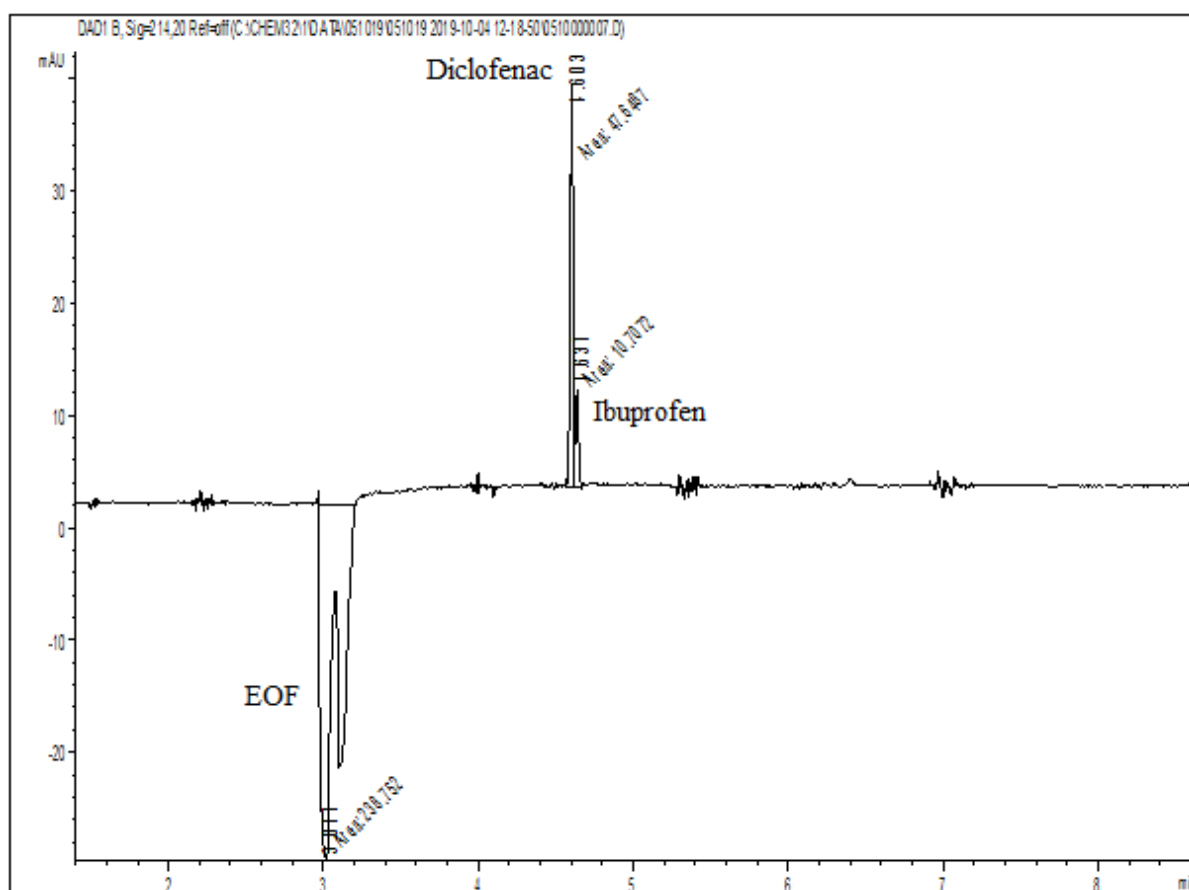


Figure 5.20: Electropherogram of the AID mixture.

This implies that in the eventual mixture containing all the analyte components, there would be a difficulty in the effective separation of these three analytes.

In the ASID mixture, the applied parameters include: 60 cm capillary length, 9.678 pH, 20 kV voltage, 50 mbar pressure, 5 seconds injection time, 25 °C cassette temperature, 50:50 MeOH/H₂O ratio, and 20 mM ammonium acetate buffer concentration. Figure 5.21 shows the separation on the electropherogram. The first peak being diclofenac, followed by ibuprofen, then sulphamethoxazole. While acetaminophen is missing on the electropherogram, it suggests that both chemical and instrumental parameters should be optimised for the effective separation of the combined analytes in the mixture.

Chemical parameters in terms of the solvent dilution ratio, and pH should be optimised to ensure that acetaminophen is among the peaks on the electropherogram.

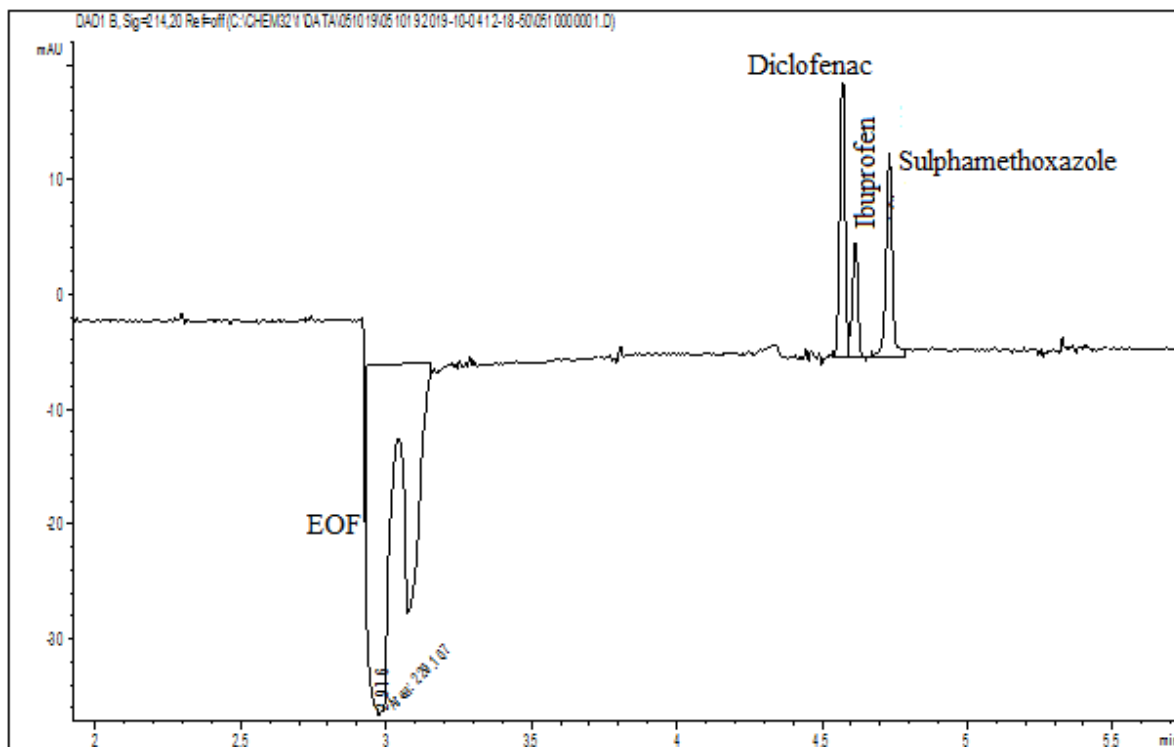


Figure 5.21: Electropherogram of the ASID mixture.

In the electropherogram of the ASIDAS mixture, 20 ppm Standard MIX analysis of the six analytes was carried out, new buffer ammonium acetate (pH 9.68 and 20 mM concentration) was prepared to enhance better analyte separation efficiency, injection time was changed to 10 seconds and pressure was changed to 35 mbar. Other applied parameters remained as 20 kV voltage, 25 °C cassette temperature, and 50:50 MeOH/H₂O ratio. The electropherogram of this analysis is displayed in Figure 5.22.

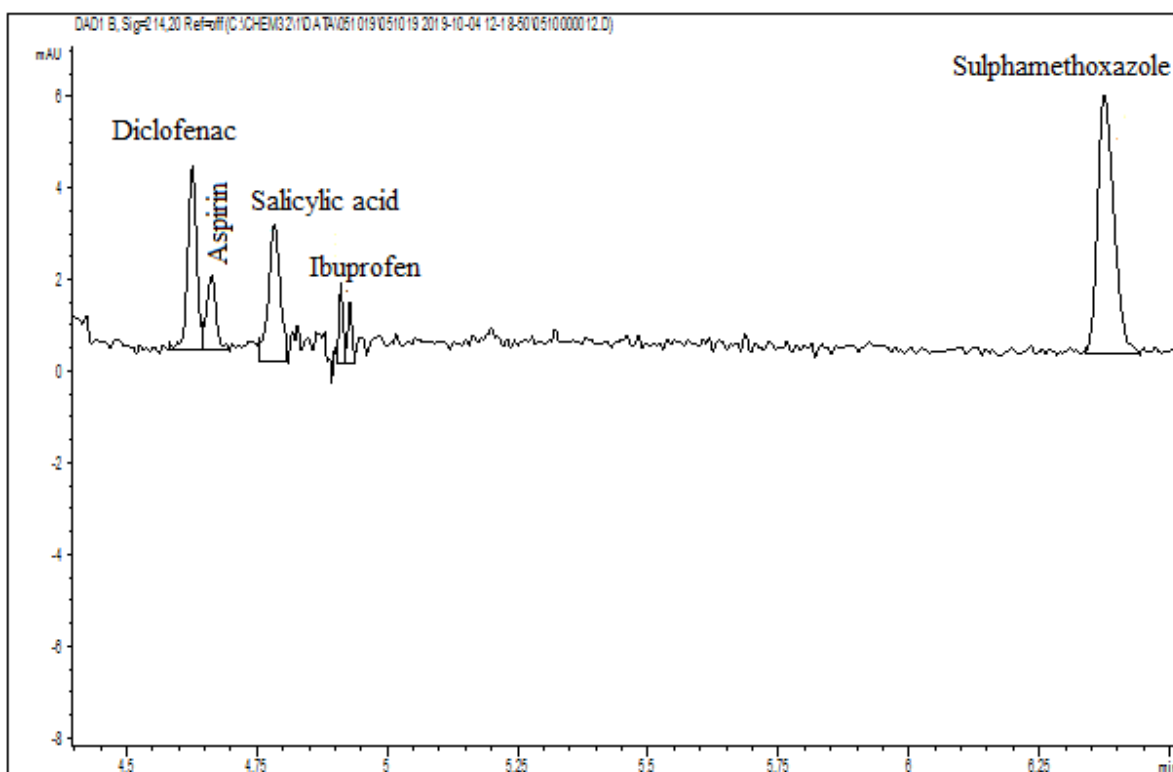


Figure 5.22: Electropherogram of the ASIDAS mixture.

In this electropherogram, it can be observed that five peaks are visible, with the exclusion of acetaminophen. This electropherogram is supposed to give six distinct peaks, and the efficiency of separation is not well-defined. Therefore, it is important to further optimise the conditions that would give an effective separation and the emergence of the complete peaks on the electropherogram.

In order to improve the sensitivity and separation efficiency of the six analytes, the instrumental operating parameters and chemical parameters were optimised to achieve better results. In this case, a buffer concentration of 30 mM ammonium acetate, pH 7.5, 50 mbar pressure, 10 seconds injection time, 60 cm capillary length, 20 kV voltage and a solvent dilution ratio of 50:50 (MeOH/H₂O) mixture were applied.

In the peakmaster software, not all the analytes of interest could be found on the list of compounds, however, the compounds nearest the chemicals of interest in terms of molecular weight and characteristics were used to mimic the behaviour of the compound of interest. In this case, p-chlorophenol was used in place of acetaminophen, diphenylacetic acid was used in place of diclofenac, propionic acid was used in place of ibuprofen and sulphamic acid was used in place of sulphamethoxazole. Therefore, it is expected that the migration order in the electropherogram would be: acetaminophen, diclofenac, aspirin, salicylic acid, ibuprofen and sulphamethoxazole respectively, as shown in Figure 5.23 peakmaster software.

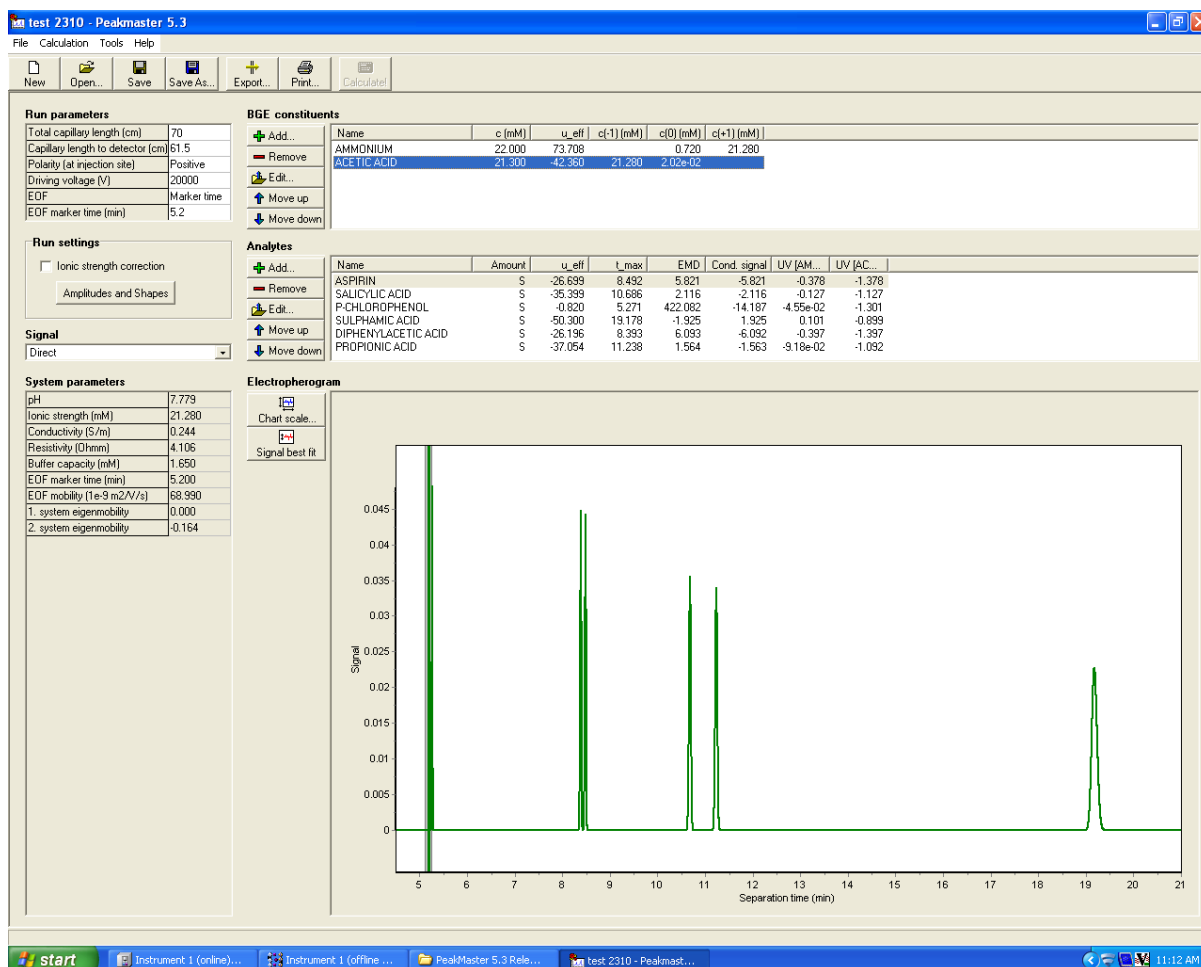


Figure 5.23: Peakmaster software showing the migration order for the six MIX analytes.

Figure 5.24 shows that the electropherogram obtained from this optimised method gave the peak for acetaminophen but the rest of the five analytes were co-eluted within the last two peaks.

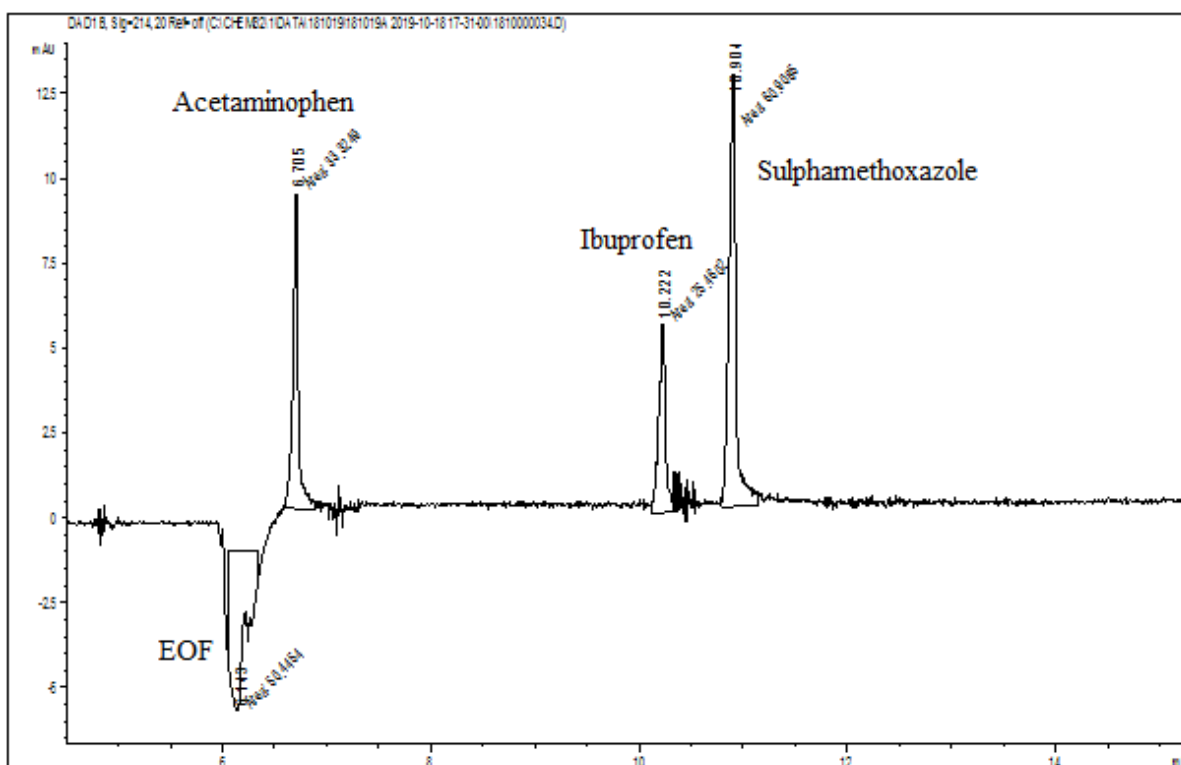


Figure 5.24: Electropherogram showing acetaminophen as the first peak and the rest of the analytes co-eluted within the last two peaks.

From the result in the electropherogram in Figure 5.24, it is apparent that there is a need to further optimise the method to get a good separation and sensitivity of each compound on the electropherogram. As a result, a further step was taken to actualise the objective of getting a good separation and better sensitivity by optimising both the instrumental and chemical parameters.

5.5.1.1 Final optimisation

A solvent dilution ratio of 30:70 (MeOH/H₂O) mixture was used to prepare the concentration calibration range of 0.5 ppm, 1 ppm, 2 ppm, 4 ppm, 6 ppm and 8 ppm respectively, for the six analyte mixture. A buffer concentration of 30 mM ammonium acetate, pH 9.68, 50 mbar pressure, 10 seconds injection time, 70 cm capillary length, 25 °C cassette temperature, and 20 kV voltage. The result of this optimisation is shown in Figures 5.25 & 5.26 respectively. The electropherogram of the 8 ppm MIX analysis with the individual analytes well separated and with good sensitivity from the capillary electrophoresis instrument. The separation of individual analytes followed the exact prediction as shown in the peakmaster software in Figure 5.23.

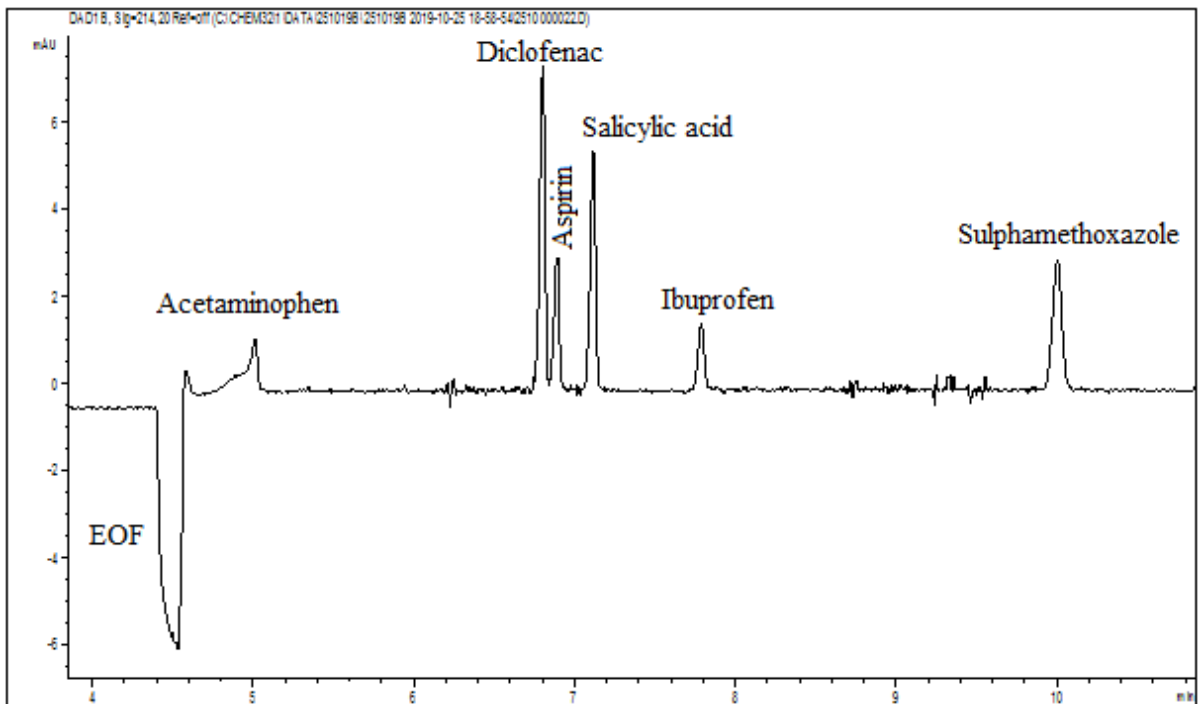


Figure 5.25: Electropherogram without integration of peaks showing the six standard analytes in their respective order as predicted by the peakmaster.

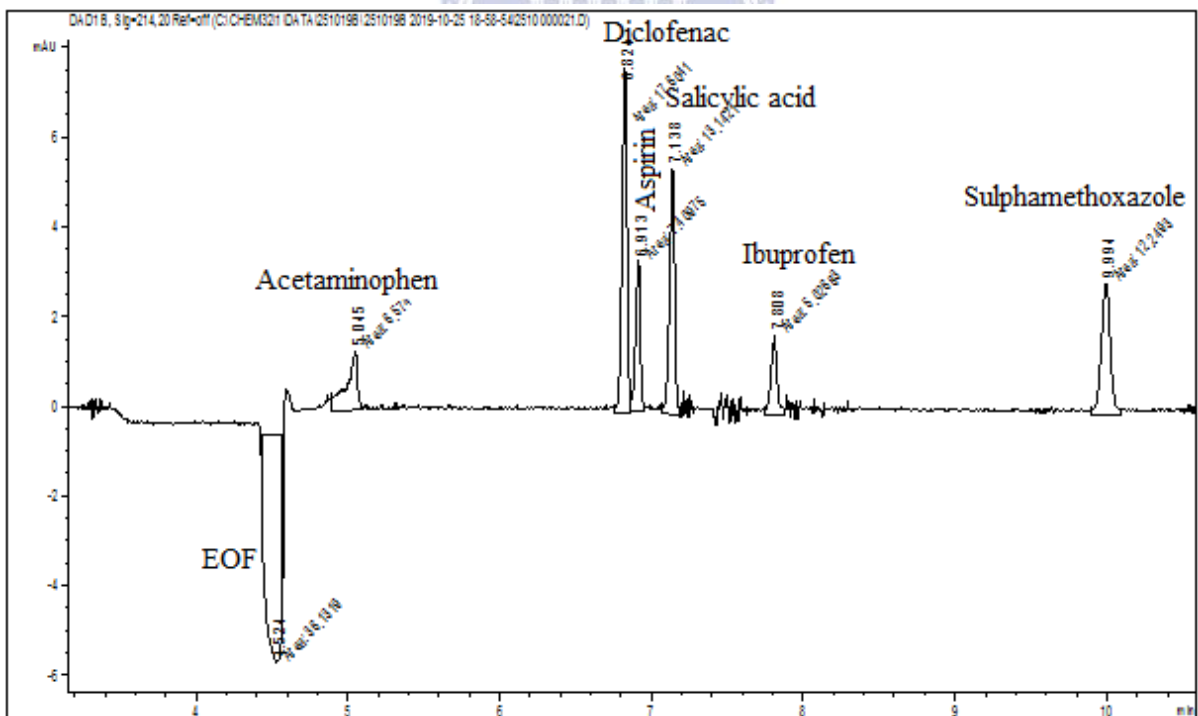


Figure 5.26: Electropherogram with integration of peaks showing the six standard analytes in their respective order as predicted by the peakmaster.

Figure 5.27 shows the overlaid electropherograms of two solvent dilution ratios, the two electropherograms are of 8 ppm mixture of six standard analytes. However, the one above was of 70:30 (H₂O:MeOH) solvent dilution, while the other below was of 50:50 (H₂O:MeOH) solvent dilution. This explicitly explains the importance of the dilution ratio of solvent in the separation of analytes. The solvent dilution ratio of 70:30 (H₂O/MeOH) gave the best separation of analytes, as all the analytes peaks were present in the correct order as predicted by the peakmaster software.

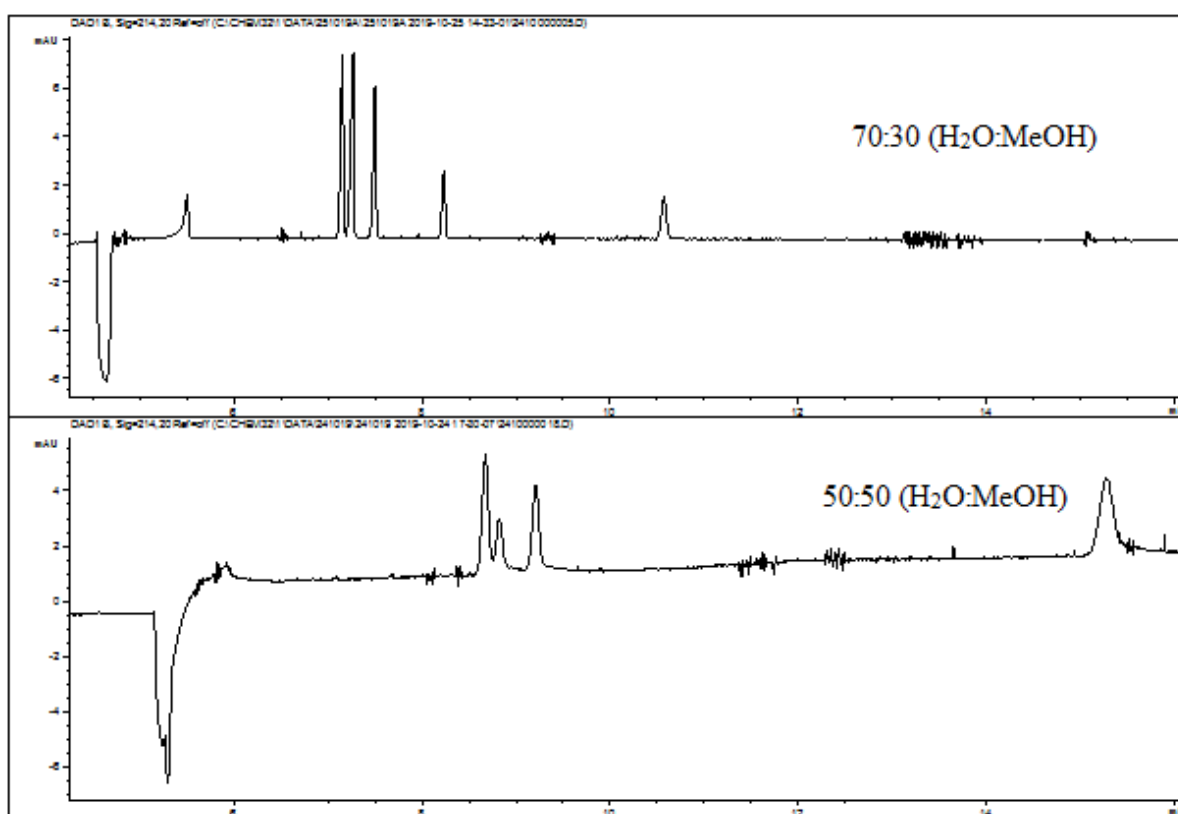


Figure 5.27: The overlay of electropherograms from the 8 ppm standard mixture of analytes with different solvent dilution ratios.

In Table 5.16, the electrophoretic mobilities of analytes for different methods are displayed. BGE 1 and BGE 2 parameters are given in section 3.2.4 of Chapter 3, while the applied parameters for CAPS 4 method include: a buffer concentration of 30 mM ammonium acetate, pH 9.68, 50 mbar pressure, 10 seconds injection time, 70 cm capillary length, 25 °C cassette temperature, and 20 kV voltage.

Table 5.16: Electrophoretic mobility of analytes in different electrolyte methods

Method	Acetaminophen	Aspirin	Sulphamethoxazole	Salicylic Acid
<i>BGE 1</i>	-1.87×10^{-9}	-2.61×10^{-8}	-2.2×10^{-8}	-3.32×10^{-8}
<i>BGE 2</i>	-2.35×10^{-9}	-2.53×10^{-8}	-2.19×10^{-8}	-3.21×10^{-8}
CAPS 4	-9.70×10^{-9}	-2.90×10^{-8}	-4.32×10^{-8}	-3.33×10^{-8}

In Table 5.17, the respective electrophoretic mobilities for analytes in CAPS4 method are given. Different methods including BGE 1, BGE 2, and CAPS 4 methods were all employed in the analysis of the standard mixture to determine the best method suitable for the separation of various individual analytes, having been carefully optimised.

Table 5.17: Electrophoretic mobility of analytes in CAPS 4 buffer method

ANALYTE	(μ_{ep}) [m ² /Vs]
Acetaminophen	-9.70×10^{-9}
Diclofenac	-2.66×10^{-8}
Aspirin	-2.90×10^{-8}
Salicylic acid	-3.33×10^{-8}
Ibuprofen	-2.73×10^{-8}
Sulphamethoxazole	-4.32×10^{-8}

The CAPS 4 method was therefore adopted for the analysis of the standard mixtures, and consequently for the analysis of the environmental matrix samples, being the most suitable method to effectively separate the different analytes simultaneously; and with the best electrophoretic mobility values. The next section presents the repeatability results using the CAPS 4 method for individual analytes.

5.5.2 Results for repeatability in CAPS 4 replication series for individual standard analyte

The order for the migration of the individual analytes as predicted by the peakmaster software is shown in Table 5.18. After this order was ascertained by the optimised method CAPS 4, the electrophoretic data for the replication runs to calculate the repeatability were calculated.

Table 5.18: The migration order of the standard analytes

Order	Compound
1	Acetaminophen
2	Diclofenac
3	Acetylsalicylic acid (Aspirin)
4	Salicylic acid
5	Ibuprofen
6	Sulphamethoxazole

Repeatability calculations were made from the four replications of the standard MIX solution with CAPS 4 (30 mM ammonium acetate, pH 9.68, 50 mbar pressure, 10 seconds injection time, 70 cm capillary length, 25 °C cassette temperature, and 20 kV voltage)..

The electrophoretic mobilities were calculated with equation 5.3.

$$\mu_{ep} = \frac{L_{tot}L_{det}}{Ut} = \frac{0.615m \times 0.7m}{20000 V \times 301.94 s} = 7.129 \times 10^{-8} \frac{m^2}{Vs} \quad (5.3)$$

The various electrophoretic mobilities of the individual analytes were calculated, and the total electrophoretic mobilities were calculated by subtracting the electroosmosis from the compounds that migrated after it. Here, all the analytes migrated after electroosmosis. Tables 5.19 – 5.25 give the results for the replication analysis and calculations for electrophoretic mobility and migration times for various individual standard analytes.

Table 5.19: Results of the replication calculations for Electroosmosis using CAPS 4

Electroosmosis (E=10 [^])				
Repetition Number	Migration [min]	Migration [s]	Area	$\mu_{eo}[\frac{m^2}{Vs}]$
1	4.361	261.650	34.579	8.226E-08
2	4.402	264.088	35.632	8.149E-08
3	4.349	260.982	36.205	8.248E-08
4	4.340	260.424	37.510	8.266E-08
AVG	4.363	261.786	35.982	8.222E-08
STD DEV	0.027	1.614	1.221	0.052
RSD	0.628	0.617	3.395	0.626

Table 5.20: Results of the replication calculations for Acetaminophen using CAPS 4

Acetaminophen (E=10 [^])				
Repetition Number	Migration [s]	Area	$\mu [\frac{m^2}{Vs}]$	$\mu_{ep}[\frac{m^2}{Vs}]$
1	301.938	1.281	-1.097E-08	7.129E-08
2	305.370	1.668	-1.099E-08	7.050E-08
3	298.788	1.563	-1.044E-08	7.204E-08
4	298.500	1.965	-1.056E-08	7.210E-08
AVG	301.149	1.620	-1.074E-08	7.148E-08
STD DEV	3.216	0.282	0.028	0.075
RSD	1.068	17.442	2.621	1.051

Table 5.21: Results of the replication calculations for Diclofenac using CAPS 4

Diclofenac (E=10 [^])				
Repetition Number	Migration [s]	Area	$\mu \left[\frac{m^2}{V_s}\right]$	$\mu_{ep}\left[\frac{m^2}{V_s}\right]$
1	389.469	3.582	-2.696E-08	5.530E-08
2	399.870	3.509	-2.766E-08	5.383E-08
3	387.014	3.655	-2.686E-08	5.562E-08
4	387.480	3.393	-2.711E-08	5.555E-08
AVG	390.958	3.535	-2.715E-08	5.508E-08
STD DEV	6.036	0.112	0.036	0.084
RSD	1.544	3.159	1.314	1.528

Table 5.22: Results of the replication calculations for Acetylsalicylic acid using CAPS4

Acetylsalicylic acid (E=10 [^])				
Repetition Number	Migration [s]	Area	$\mu \left[\frac{m^2}{V_s}\right]$	$\mu_{ep}\left[\frac{m^2}{V_s}\right]$
1	394.116	1.609	-2.765E-08	5.461E-08
2	404.518	1.638	-2.829E-08	5.320E-08
3	391.630	1.678	-2.752E-08	5.496E-08
4	391.959	1.702	-2.775E-08	5.491E-08
AVG	395.556	1.657	-2.775E-08	5.442
STD DEV	6.076	0.041	0.034	0.083
RSD	1.536	2.490	1.217	1.521

Table 5.23: Results of the replication calculations for Salicylic acid using CAPS 4

Salicylic acid				
(E=10[^])				
Repetition Number	Migration [s]	Area	μ [$\frac{m^2}{Vs}$]	μ_{ep} [$\frac{m^2}{Vs}$]
1	406.380	2.537	-2.923E-08	5.297E-08
2	405.200	2.923	-2.829E-08	5.149E-08
3	403.800	2.677	-2.752E-08	5.330E-08
4	403.920	3.012	-2.937E-08	5.329E-08
AVG	404.825	2.787	-2.860E-08	5.276E-08
STD DEV	1.215	0.219	0.087	0.086
RSD	0.300	7.854	3.029	1.634

Table 5.24: Results of the replication calculations for Ibuprofen using CAPS 4

Ibuprofen				
(E=10[^])				
Repetition Number	Migration [s]	Area	μ [$\frac{m^2}{Vs}$]	μ_{ep} [$\frac{m^2}{Vs}$]
1	442.440	1.431	-3.356E-08	4.870E-08
2	456.900	1.483	-3.439E-08	4.710E-08
3	439.440	1.445	-3.350E-08	4.898E-08
4	439.980	1.441	-3.374E-08	4.892E-08
AVG	444.690	1.450	-3.380E-08	4.843E-08
STD DEV	8.244	0.023	0.041	0.089
RSD	1.854	1.583	1.207	1.841

Table 5.25: Results of the replication calculations for Sulphamethoxazole using CAPS4

Sulphamethoxazole				
(E=10 [^])				
Repetition Number	Migration [s]	Area	μ [$\frac{m^2}{Vs}$]	μ_{ep} [$\frac{m^2}{Vs}$]
1	555.282	2.087	-4.350E-08	3.876E-08
2	579.020	2.076	-4.429E-08	3.720E-08
3	551.430	2.024	-4.345E-08	3.903E-08
4	552.462	2.099	-4.370E-08	3.896E-08
AVG	559.549	2.071	-4.374E-08	3.850E-08
STD DEV	13.083	0.033	0.039	0.087
RSD	2.338	1.584	0.881	2.250

It is noticed that the standard deviations remain relatively low and the repeatability seems good for all the analytes. The calculated electrophoretic mobility values for individual standard analytes will be compared to the electrophoretic mobility of the analytes in the samples, to ascertain the presence of the particular compounds in the samples under investigation.

5.5.3 Concentration linearity and sensitivity for the six standard analytes

A quadruple set of runs of the six calibration standards were done for each analyte. Then plots of calibration curves in Figures 5.28 – 5.33 were constructed for the determination of equations for the linear regression lines. The LOD and LOQ for each analyte, reproducibility evaluation, as well as method selectivity and sensitivity of each analyte was evaluated. The linearity of the method was measured at a concentration range of 0.5–8 $\mu\text{g/mL}$ using the standard analyte mixture. Table 5.26 reveals that equations correlate linearly with the detector response (area) obtained for the standard analyte mixtures. The capillary zone electrophoresis with UV detection (CZE-UV) gave limits of detection (LOD) and quantification (LOQ) from 0.073 to 0.230 $\mu\text{g/mL}$ and from 0.219 to 0.690 $\mu\text{g/mL}$ respectively. The instrument response to the detection of each of the standard analytes (pharmaceuticals) showed linear sensitivity to increasing concentrations with R^2 values > 0.99 for all the six analytes (Table 5.26). The

LOD value correlating the signal-to-noise ratio of 3 was measured from the concentrations of the analytes as a mixture. The LOQ value for each analyte was then calculated with signal-to-noise ratio of $3 \times \text{LOD}$ ($9 \times S/N$). Appendix A76, A77, A78, A79, A80 and A81 show the plots of calibration curves, determining the equations for the linear regression lines from the calibration curves for each of the six standard analytes, with their respective linear regression equations and R^2 values.

Table 5.26: Linear regression calibration data of standard analytes

Standards	Calibration					
	range [$\mu\text{g/mL}$]	Linear equation	R^2	λ_{max} [nm]	LOD $\mu\text{g/mL}$	LOQ $\mu\text{g/mL}$
Acetaminophen	0.5 - 8	$y = 0.8929x + 0.178$	0.9939	214	0.230	0.690
Diclofenac	0.5 - 8	$y = 2.2196x - 0.6422$	0.9938	214	0.073	0.219
Acetylsalicylic acid (Aspirin)	0.5 - 8	$y = 1.2749x + 0.0188$	0.9951	214	0.137	0.411
Salicylic acid	0.5 - 8	$y = 0.5711x + 0.1691$	0.9975	214	0.209	0.627
Ibuprofen	0.5 - 8	$y = 0.9844x - 0.2302$	0.9937	214	0.085	0.255
Sulphamethoxazole	0.5 - 8	$y = 1.2806x - 0.3020$	0.9952	214	0.186	0.557

The result gave a linear correlation between the concentration and the peak area of each analyte. Also, the calibration curves revealed linear regression values > 0.99 . The next section presents the recovery studies for standard analytes.

5.5.4 Recovery studies for standard analytes using Solid Phase Extraction (SPE).

The efficiencies of the quantitative recovery of the standard analytes (Acetaminophen, Diclofenac, Acetylsalicylic acid (ASA), Salicylic acid, Ibuprofen and Sulphamethoxazole) using the SPE method were evaluated using the data from recovery experiments. The analytes were recovered from a solution of 5 mg/L cocktail of each analyte standard mixed in 70:30 (MeOH/H₂O) mixture. The relative percentage recoveries of the analytes are given in the Table 5.27.

Table 5.27: Mean recovery percentages for standard analytes by SPE method

Standard Analytes	Expected concentration (mg/L)	Measured concentration (mg/L)	Average recovery (%)
Acetaminophen	5	4.81	96.20
Diclofenac	5	4.79	95.80
Acetylsalicylic acid (Aspirin)	5	4.96	99.20
Salicylic acid	5	4.76	95.20
Ibuprofen	5	4.83	96.60
Sulphamethoxazole	5	4.88	97.60

The results show that the affinity efficiency of the C₁₈ (Strata-X) non-polar sorbent cartridges to concentrate the six tested pharmaceuticals (standard analytes) was effective. This suggests that the use of C₁₈ (Strata-X) nonpolar sorbent cartridges in SPE procedure is effective and satisfactory for the concentration and recoveries of the selected pharmaceutical analytes from aqueous matrices.

5.5.5 Determination of the pharmaceutical analytes in water

This section study focuses on quantitatively measuring the selected pharmaceutical compounds in wastewater. Since the concentrations are perceived to be low, the pharmaceuticals in the water sample must be enriched using an SPE cartridge and extracted from the major matrix. However, in the present study, the sampled water volume was made to be 2 L so as to enrich the pharmaceutical concentrations for optimum UV detection in the CZE analyses and to validate the system capability for long-term pharmaceuticals monitoring. In the cleaning process and enrichment with SPE, the pharmaceuticals were eluted 20 times more concentrated than the original plant effluent sample. Pharmaceutical compounds such as acetaminophen, diclofenac, aspirin, ibuprofen, sulphamethoxazole, etc, are present in environmental water (Swartz *et al.*, 2018a). The water samples studied include: two different influent water samples (influent A & influent B) and an effluent water sample from sewage water treatment plants of the University of Helsinki, Finland; hot tap water, cold tap water, and Milli-Q water. In the two influent water samples influent A and influent B, the pharmaceutical found in the highest quantities include aspirin, diclofenac and sulphamethoxazole respectively. In the influent A water sample, aspirin was quantified to be 13.52 ng/L, diclofenac as 14.15 ng/L, salicylic acid as 6.514 ng/L and sulphamethoxazole as 11.79 ng/L respectively. Acetaminophen and ibuprofen were not detected in influent A water sample. In the same vein, influent B water sample contained 4.23 ng/L of aspirin, 8.235 ng/L of diclofenac, 1.199 ng/L of salicylic acid, 1.095 ng/L of ibuprofen and 13.170 ng/L of sulphamethoxazole respectively. In the purified effluent water samples of sewage water treatment plants, the measurable pharmaceuticals quantities include 0.836 ng/L of aspirin, 0.802 ng/L of diclofenac, 1.343 ng/L of salicylic acid, 0.842 ng/L of ibuprofen and 10.241 ng/L of sulphamethoxazole.

Acetaminophen was not found in either influent or effluent water samples. While ibuprofen was also not found in the influent A water sample, only acetaminophen was not detected in the influent B water sample. It is not surprising that both the influent and effluent water samples for the sewage treatment plant contained some of these pharmaceuticals under study. The measured quantities of these pharmaceuticals determined from the electropherograms of the influent and effluent water samples are ascertained by comparing the respective electrophoretic mobilities of the individual analytes in the standards calibration to the electrophoretic mobilities of the individual analytes in the influent and effluent water samples.

As expected, the effluent quantities were lower than the quantities in the influents. When the analyte in a sample concentrate was clearly identified on the basis of absolute migration time, specific wavelengths, relative migration time and electrophoretic mobility in the electropherogram, the sample was spiked with a 2 $\mu\text{g}/\text{mL}$ standard and the quantification was carried out using the standard addition method. As a result, it was possible to confirm the respective peaks belonging to the analytes under investigation.

Table 5.28 shows the pharmaceutical analytes with their structures, theoretical and experimentally measured exact molar masses with migration times and electrophoretic mobilities.

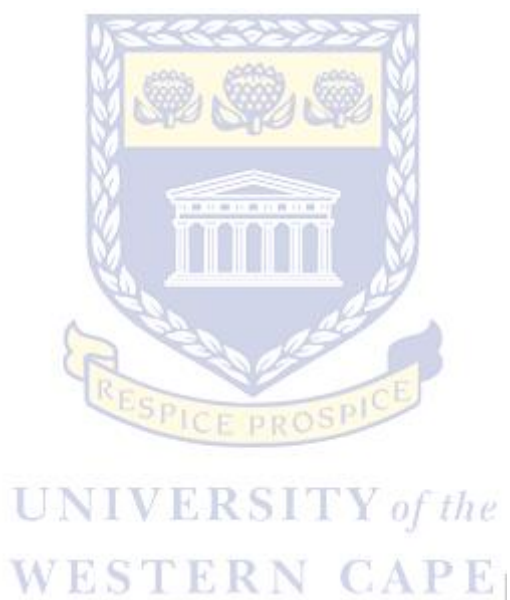


Table 5.28: Structures of acetaminophen, diclofenac, aspirin, salicylic acid, ibuprofen and sulphamethoxazole. Theoretical and experimentally measured exact molar masses with migration times in CE

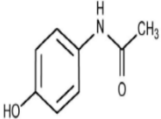
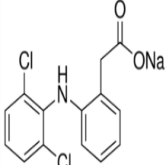
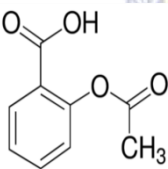
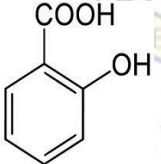
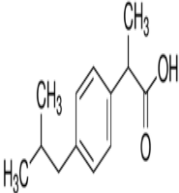
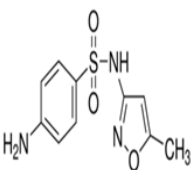
Compound	Structure	Molar mass [g/mol]	Experimental molar mass [M + H]	CZE-UV Migration time [min]	(μ_{ep}) [m^2/Vs]
Acetaminophen $C_8H_9O_2$		151.17	152.071	4.980	-9.70×10^{-9}
Diclofenac $C_{14}H_{10}Cl_2NNaO_2$		318.1	319.024	6.510	-2.66×10^{-8}
Aspirin $C_9H_8O_4$		180.16	181.05	6.598	-2.73×10^{-8}
Salicylic acid $C_7H_6O_3$		138.12	139.039	6.803	-2.89×10^{-8}
Ibuprofen $C_{13}H_{18}O_2$		206.29	207.138	7.406	-3.33×10^{-8}
Sulphamethoxazole $C_{10}H_{11}N_3O_3S$		253.28	254.059	9.320	-4.32×10^{-8}

Figure 5.28, shows the electropherogram for influent A sample which unveils the presence of four of the analytes under investigation, including diclofenac, aspirin, salicylic acid and sulphamethoxazole; acetaminophen and ibuprofen were not detected in this influent sample. The respective analyte peaks were identified based on the calculation of their individual electrophoretic mobilities, in comparison or correlation to their respective mobilities in the standard analytes electrophoretic mobility calculations.

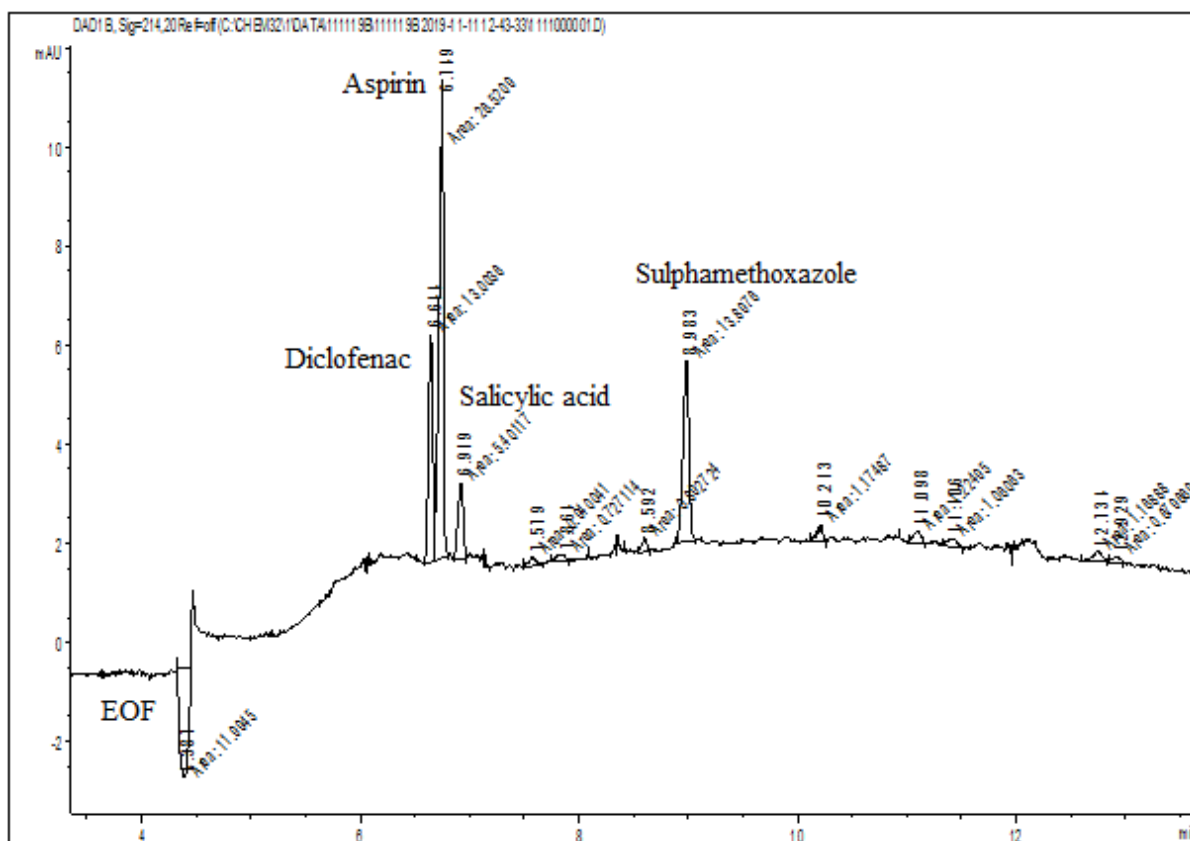


Figure 5.28: Electropherogram for influent A sample showing the peaks for the identified analytes including diclofenac, aspirin (ASA), salicylic acid (SA), and sulphamethoxazole.

These individual analytes peaks are ascertained by the nearness in value to their respective peaks in the standard analytes electrophoretic mobility calculations by ± 0.2 . This is showcased in Table 5.29, where the electrophoretic mobilities calculations for the standard analytes, influent A, influent B and effluent water samples are displayed.

Table 5.29: Correlation between the electrophoretic mobilities of the standards analytes with influent and effluents water samples

Compounds	Standards (μ_{ep}) [m ² /Vs]	Influent A (μ_{ep}) [m ² /Vs]	Influent B (μ_{ep}) [m ² /Vs]	Effluent (μ_{ep}) [m ² /Vs]
Acetaminophen	-9.70 x 10 ⁻⁹	ND	ND	ND
Diclofenac	-2.66 x 10 ⁻⁸	-2.78 x 10 ⁻⁸	-2.55 x 10 ⁻⁸	-2.59 x 10 ⁻⁸
Aspirin (ASA)	-2.73 x 10 ⁻⁸	-2.84 x 10 ⁻⁸	-2.71 x 10 ⁻⁸	-2.79 x 10 ⁻⁸
Salicylic acid (SA)	-2.89 x 10 ⁻⁸	-2.99 x 10 ⁻⁸	-2.78 x 10 ⁻⁸	-2.92 x 10 ⁻⁸
Ibuprofen	-3.33 x 10 ⁻⁸	ND	-2.93 x 10 ⁻⁸	-3.51 x 10 ⁻⁸
Sulphamethoxazole	-4.32 x 10 ⁻⁸	-4.19 x 10 ⁻⁸	-4.10 x 10 ⁻⁸	-4.14 x 10 ⁻⁸

Figure 5.29 shows the electropherogram for the influent B water sample and it contains five of the pharmaceutical analytes under investigation, including diclofenac, aspirin, salicylic acid, ibuprofen and sulphamethoxazole respectively.

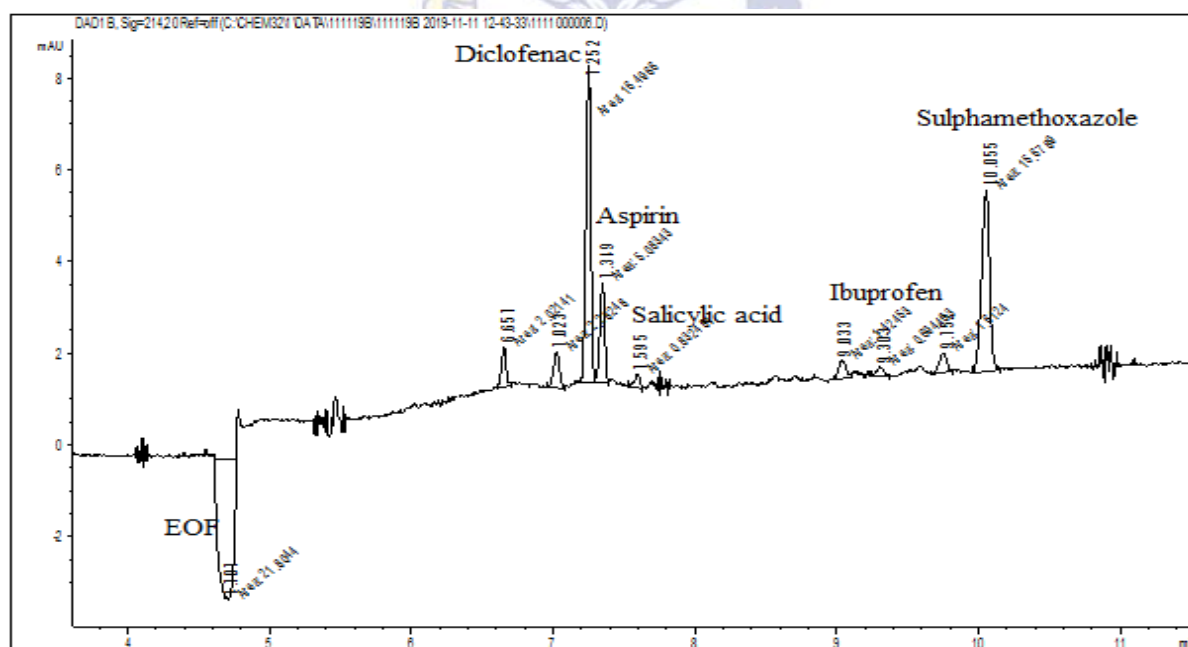


Figure 5.29: Electropherogram for influent B sample showing the peaks for the identified peaks: Diclofenac, aspirin, salicylic acid, ibuprofen and sulphamethoxazole.

In Tables 5.30 – 5.32, the results of the analytes concentration in the influent A, influent B and effluent are respectively presented.

Table 5.30: Identification of pharmaceuticals in the Influent A sample. Determination made with CZE. Influent A water sample purified with C18 (Strata-X) nonpolar sorbent

Compound	Migration time [min]	Peaks area [min × mAU]	Peak height [mAU]	Amount [ng/L]
Acetaminophen				
Mean	Not Found	Not Found	Not Found	Not Found
SD				
RSD%				
Diclofenac				
Mean	7.042	32.052	11.250	
SD	0.275	16.852	5.496	14.150
RSD%	3.906	52.576	48.856	
Aspirin				
Mean	7.142	17.258	6.412	13.520
SD	0.271	6.648	2.463	
RSD%	3.790	38.522	38.418	
Salicylic acid				
Mean	7.346	3.889	1.123	
SD	0.300	1.621	0.351	6.514
RSD%	4.088	41.694	31.297	
Ibuprofen				
Mean	Not Found	Not Found	Not Found	Not Found
SD				
RSD%				
Sulphamethoxazole				
Mean	9.741	14.710	3.513	
SD	0.532	1.133	0.212	11.790
RSD%	5.463	7.703	6.022	

Table 5.31: Identification of pharmaceuticals in the Influent B sample. Determination made with CZE. Influent B water sample purified with C18 (Strata-X) nonpolar sorbent.

Compound	Migration time [min]	Peaks area [min × mAU]	Peak height [mAU]	Amount [ng/L]
Acetaminophen				
Mean	Not found	Not found	Not found	Not found
SD				
RSD%				
Diclofenac				
Mean	7.238	17.635	6.964	
SD	0.036	1.084	0.153	8.235
RSD%	0.492	6.146	2.195	
Aspirin				
Mean	7.334	5.407	2.165	4.226
SD	0.035	0.557	0.066	
RSD%	0.476	10.293	3.051	
Salicylic acid				
Mean	7.544	0.854	0.271	
SD	0.098	0.104	0.028	1.199
RSD%	1.296	16.331	10.404	
Ibuprofen				
Mean	8.528	0.848	0.221	1.095
SD	0.058	0.139	0.013	
RSD%	0.675	16.331	5.979	
Sulphamethoxazole				
Mean	10.057	16.564	3.940	13.170
SD	0.055	0.904	0.037	
RSD%	0.545	5.459	0.932	

Table 5.32: Identification of pharmaceuticals in the Effluent water sample. Determination made with CZE. Effluent water sample purified with C18 (Strata-X) nonpolar sorbent

Compound	Migration time [min]	Peaks area [min × mAU]	Peak height [mAU]	Amount [ng/L]
Acetaminophen	Not found	Not found	Not found	Not found
Mean				
SD				
RSD%				
Diclofenac	7.052	1.137	0.268	0.802
Mean	0.038	0.267	0.054	
SD	0.538	23.511	20.063	
RSD%				
Aspirin	7.607	1.084	0.304	0.836
Mean	0.048	0.059	0.014	
SD	0.627	5.420	4.716	
RSD%				
Salicylic acid	8.627	0.598	0.157	1.343
Mean	0.036	0.184	0.008	
SD	0.411	30.767	4.947	
RSD%				
Ibuprofen	8.627	0.599	0.157	0.842
Mean	0.036	0.184	0.008	
SD	0.411	30.767	4.947	
RSD%				
Sulphamethoxazole	10.251	12.813	3.061	10.241
Mean	0.089	1.998	0.064	
SD	0.873	15.591	2.074	
RSD%				

Tables 5.30, 5.31 and 5.32 give the detailed analysis account of the influent A, influent B and effluent water samples respectively, including the measured quantities of the analytes, the

mean, standard deviation and relative standard deviation of the parameters such as the migration time, peak area and peak height respectively.

Figure 5.30 shows the electropherogram for effluent sample where the peaks for analytes including diclofenac, aspirin, salicylic acid, ibuprofen and sulphamethoxazole were identified by virtue of their electrophoretic mobility values compared to those of the standards.

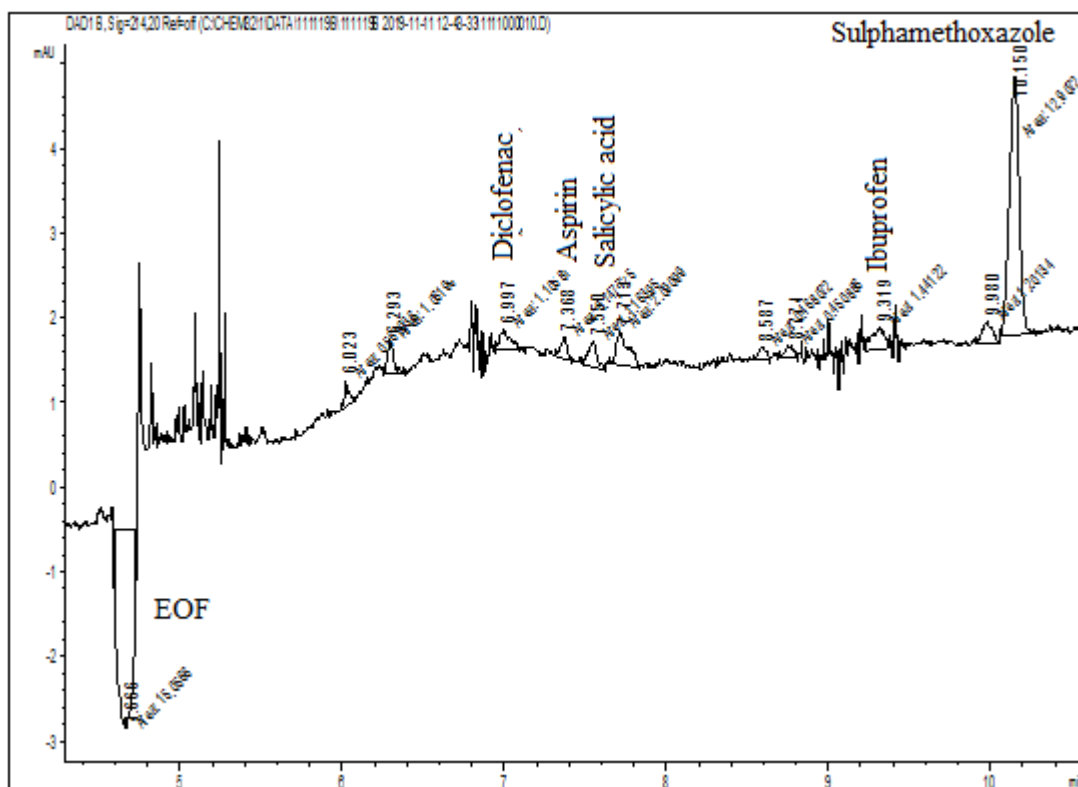


Figure 5.30: Electropherogram for effluent sample showing the peaks for the identified peaks including diclofenac, aspirin, salicylic acid, ibuprofen and sulphamethoxazole.

The electropherogram for the effluent water sample and it contains five of the pharmaceutical analytes under investigation, which includes diclofenac, aspirin, salicylic acid, ibuprofen and sulphamethoxazole respectively. There are many other peaks in the electropherogram of the effluent water sample, which were not among the analytes being investigated in this study. The electropherogram profile shows the water sample contains several other components, indicating the presence of other pharmaceutical compounds in the effluent water sample, which were not investigated.

The electropherogram in Figure 5.31 shows the overlay of the standard mixture profile with the influent B water sample profile. It can be observed in the electropherogram that the influent B water sample profile correlates with the standard sample profile in terms of the observable peaks belonging to the studied analytes in the two profiles, except for the shift in the position of one profile relative to the other due to the effect of the matrix. In both profiles, the peaks belonging to diclofenac, aspirin, salicylic acid, ibuprofen and sulphamethoxazole can be observed, in spite of the shift due to the matrix effect.

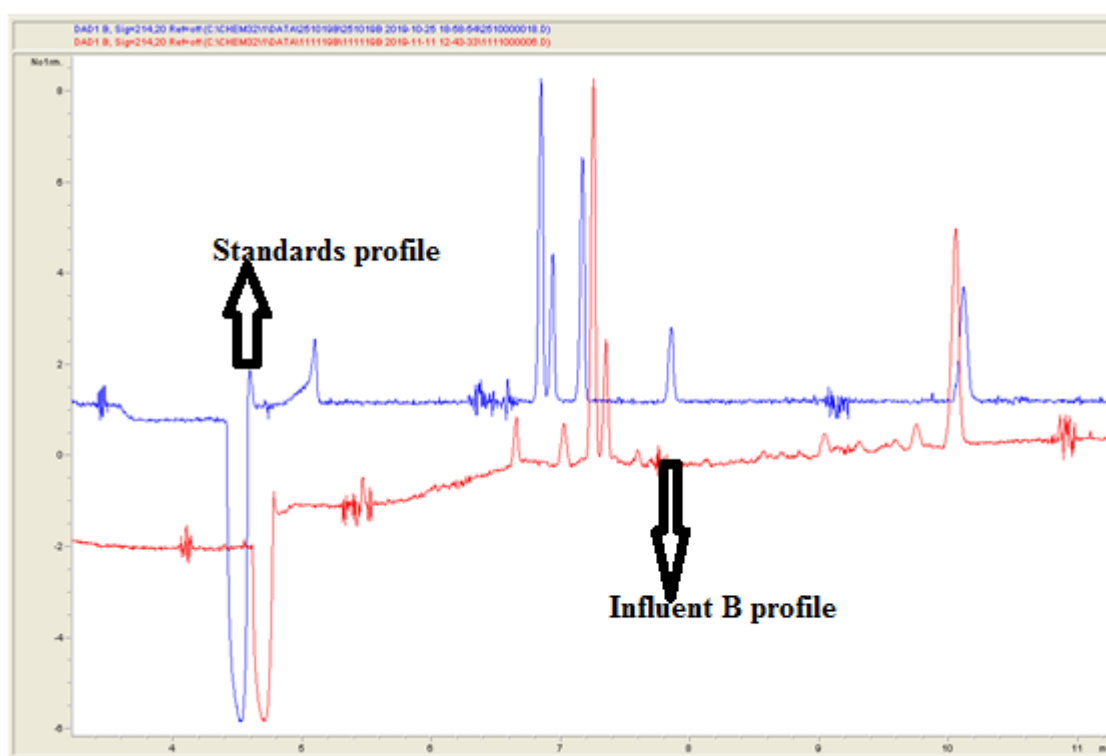


Figure 5.31: Electropherogram profile showing the standards mixture profile (blue) overlay with the influent B sample profile (red).

However, to ascertain the authenticity of the analytes peaks, 2 $\mu\text{g/mL}$ of the standard of the specified analyte was spiked into the influent and the effluent water samples to double-check if the peaks actually were of the analyte or not. Figures 5.32 presents the spiking of the effluent water sample with 2 $\mu\text{g/mL}$ sulphamethoxazole in an overlay with the standard analytes mixture profile, and showed that the peak really belongs to sulphamethoxazole. The spiked profile can be seen in colour red.

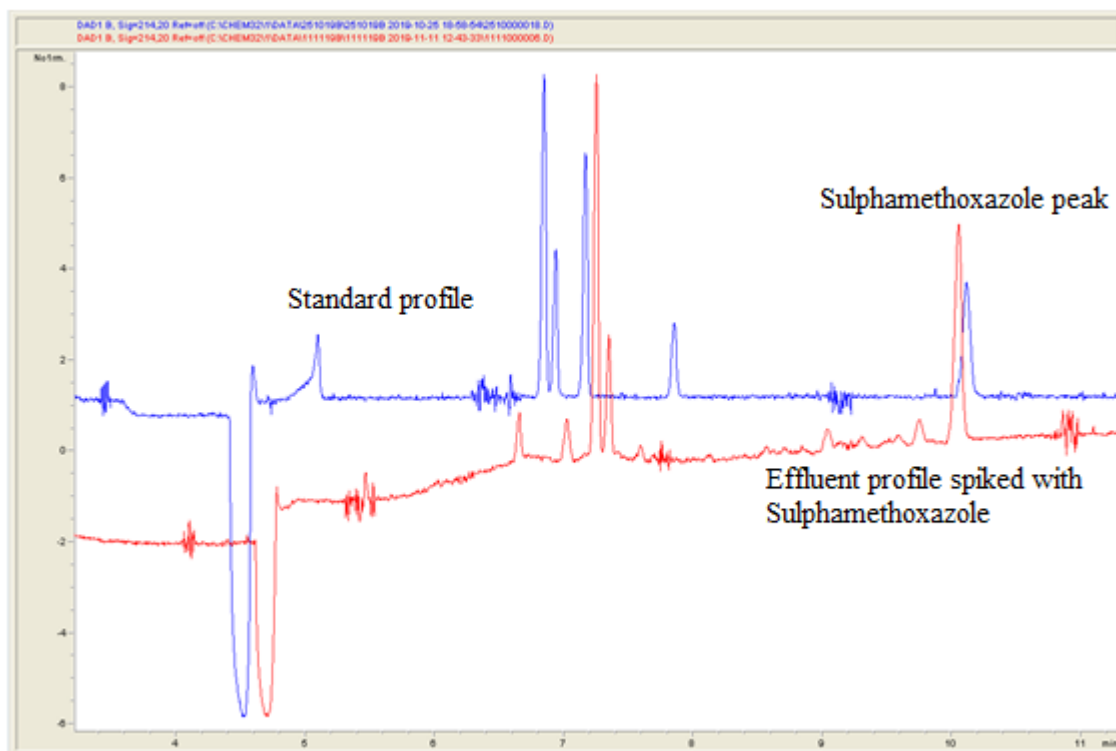


Figure 5.32: Electropherogram profile showing the standards mixture profile overlay with 2 µg/mL sulphamethoxazole-spiked effluent water sample profile.

In Figure 5.33, the influent A water sample was spiked with 2 µg/mL diclofenac standard and the electropherogram profile compared to that of the standard analyte mixture. The shift in the positioning of the peaks can be attributed to the matrix effect in the influent water sample, but the profile explicitly depicts how the analytes peaks are positioned in the profile.

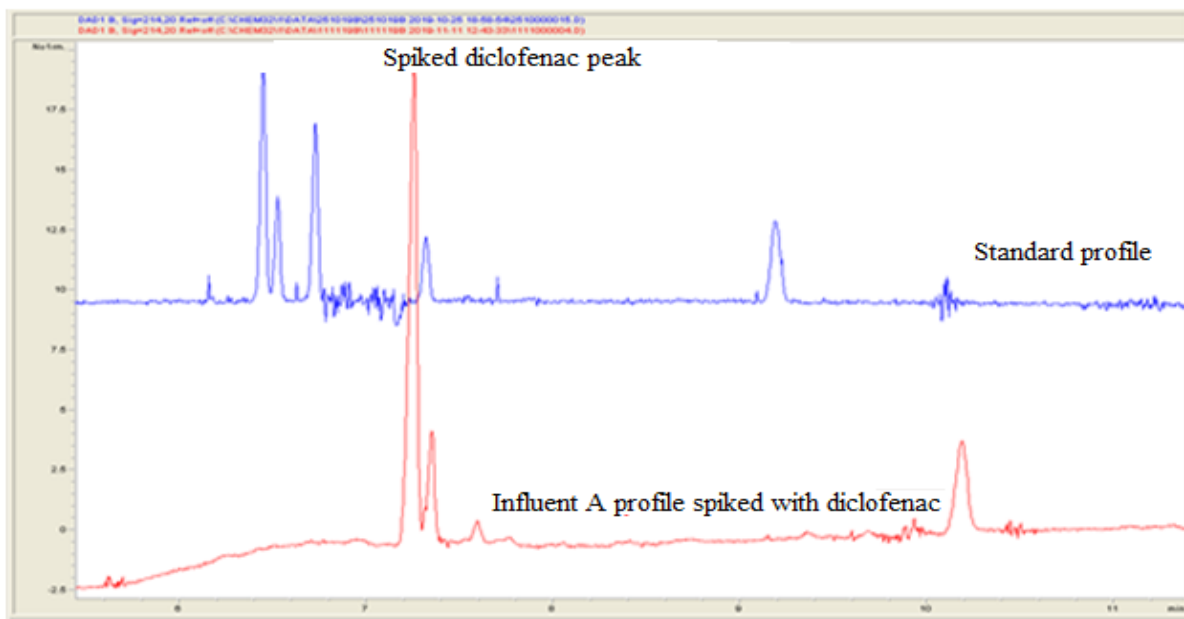


Figure 5.33: Electropherogram profile showing the standards mixture profile overlay with 2 µg/mL diclofenac-spiked influent A water sample profile.

Figure 5.34 shows the electropherogram profiles of influent B profiles. The electropherogram in blue colour represents the spiked profile with 2 µg/mL of sulphamethoxazole, and the profile in red represents the unspiked. By spiking the sample, it becomes easier to ascertain the correct peaks of particular analytes.

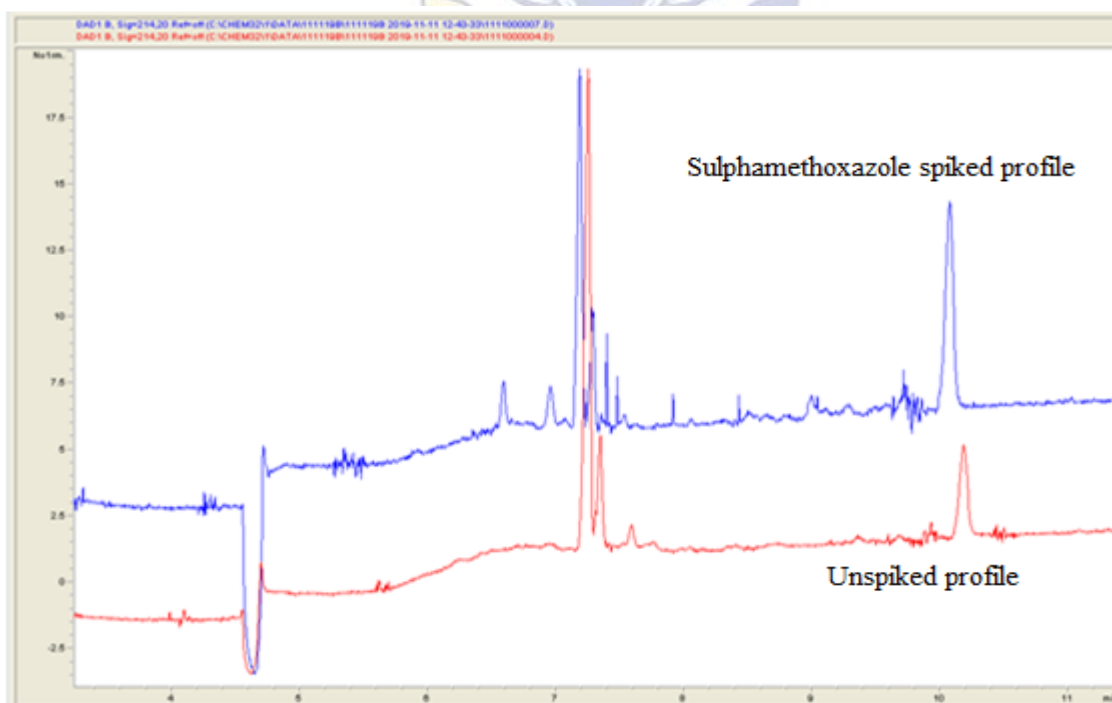


Figure 5.34: Sulphamethoxazole electropherogram profile overlay of both spiked (blue) and unspiked (red) influent B water sample profiles.

5.5.6 SPE extractions of hot tap water (HTW), cold tap water (CTW) and milli-Q water (MQW) in CZE analysis

The sampling procedure for this analysis is as given in section 3.2.6 of Chapter 3, and the sample preparation with solid phase extraction procedure is described in section 3.2.7 of Chapter 3 respectively. Tap water (hot and cold) and milli-Q water samples were also investigated for the presence of the pharmaceuticals.

The SPE extraction was carried out for hot tap water, cold tap water and milli-Q water respectively. The electrophoretic mobilities of the observable peaks are presented in Table 5.33.

Table 5.33: Electrophoretic mobilities of the peaks in hot, cold and milli-Q water samples

Compounds	Standards (μ_{ep}) [m ² /Vs]	Cold water (μ_{ep}) [m ² /Vs]	Hot water (μ_{ep}) [m ² /Vs]	Milli-Q water (μ_{ep}) [m ² /Vs]
Unknown	-	-1.87 x 10 ⁻⁸	-1.74 x 10 ⁻⁸	-1.98 x 10 ⁻⁸
Sulphamethoxazole	-4.32 x 10 ⁻⁸	-4.17 x 10 ⁻⁸	-4.17 x 10 ⁻⁸	-4.16 x 10 ⁻⁸

Figures 5.35, 5.36 and 5.37 show the electropherogram profiles of the three samples (hot tap water, cold tap water and milli-Q water). One of the two peaks had an electrophoretic mobility value and peak profile exactly the same as that of sulphamethoxazole; and the other peak does not share any similar profile with the analytes under investigation. This shows that even in the purified water for household consumption in Finland and milli-Q water for laboratory analysis, there exists some minute quantities of persistent organic pollutants.

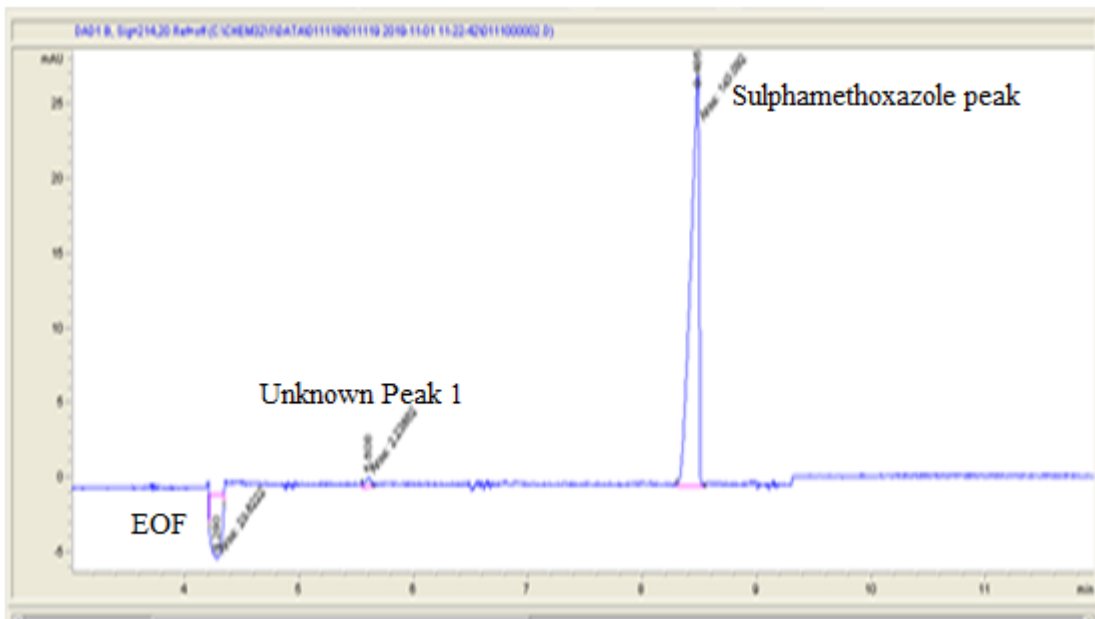


Figure 5.35: Electropherogram profile for Milli-Q water (MQW).

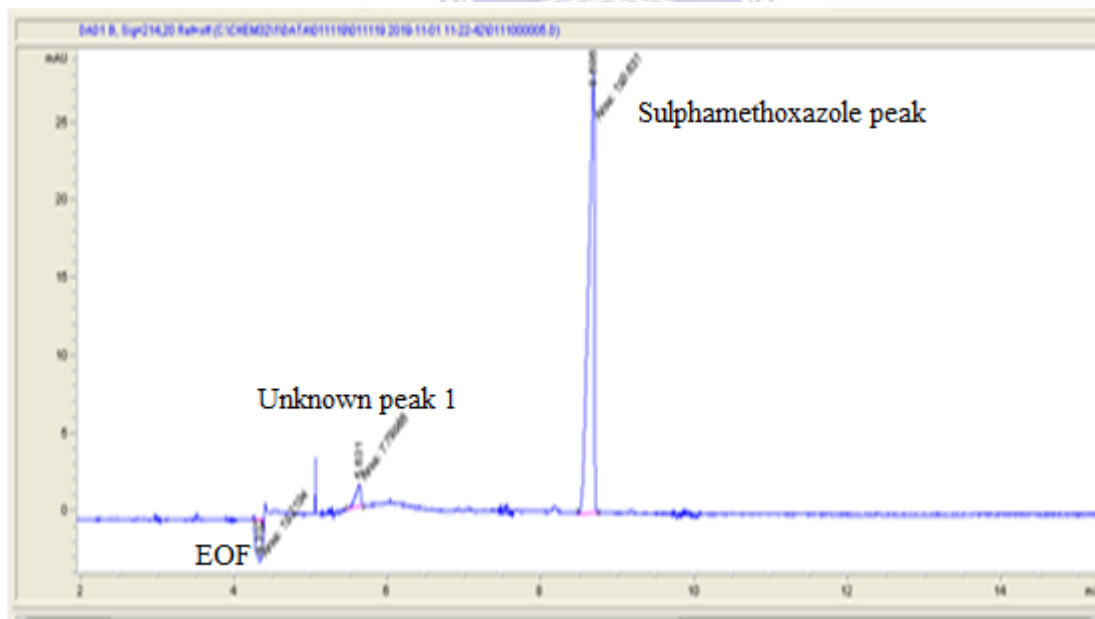


Figure 5.36: Electropherogram profile for cold tap water (CTW).

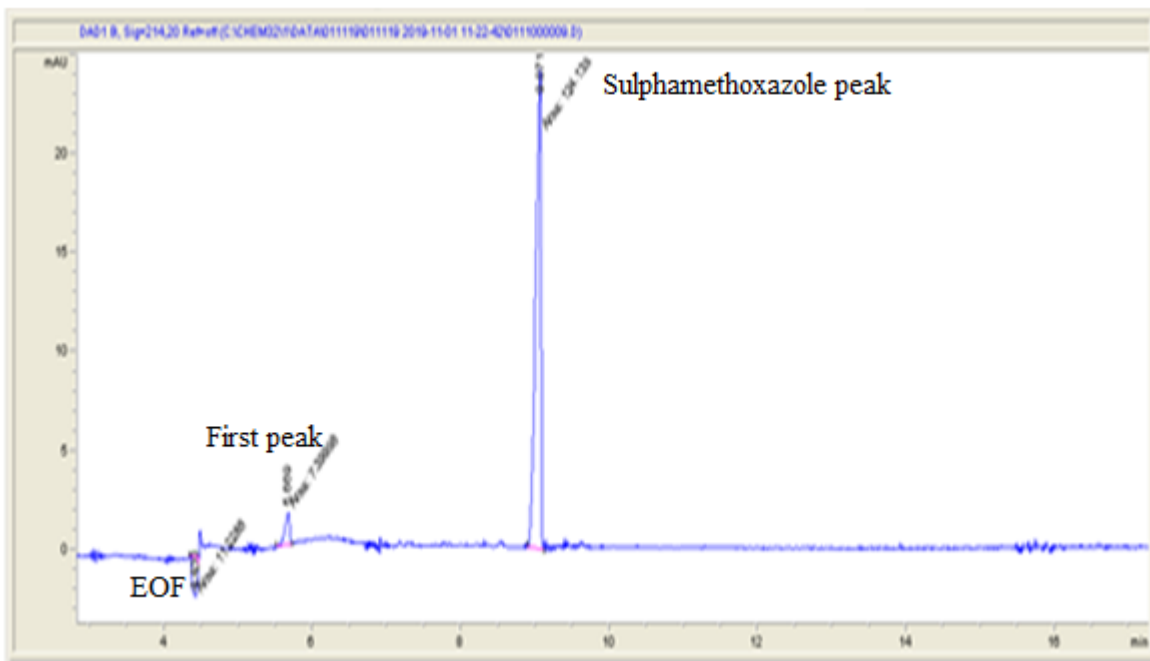
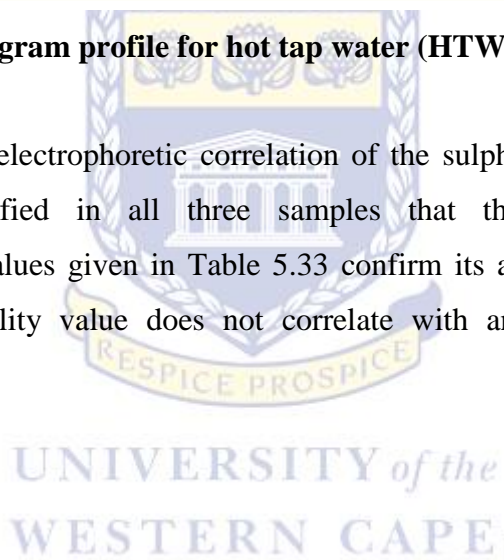


Figure 5.37: Electropherogram profile for hot tap water (HTW).

It is obvious by virtue of electrophoretic correlation of the sulphamethoxazole standard to that of the peak identified in all three samples that the peak correlated with sulphamethoxazole. The values given in Table 5.33 confirm its authenticity. The unknown peak electrophoretic mobility value does not correlate with any of the analytes under investigation.



5.6 Steroid content in waters of wastewater purification plants: determination with partial-filling micellar electrokinetic capillary chromatography (PF-MEKC) and UV detection

The analysis of steroid consists of the sex hormone compounds which include: androstenedione, testosterone, 17-beta-estradiol, and progesterone. These four steroid hormones were investigated using the partial-filling micellar electrokinetic capillary chromatography with UV detection (PF-MEKC-UV). The description of the experimental procedure for this analysis is given in sections 3.2.5, 3.2.6 and 3.2.7 of Chapter 3 respectively.

Presently, the determination of the presence of individual steroids compounds may be more necessary than the measuring their total quantity in water. Therefore, capillary electrophoresis (CE) with its high separation efficiency is a credible alternative to chromatographic techniques in the determination of steroids (Gorog, 2004; Liu *et al.*, 2011; Chang *et al.*, 2008; Chang *et al.*, 2011; Nelson & Lee, 1996). The analyses of CE are carried out in buffer solutions with the application of electricity. CE offers a very good separation for compounds which are structurally similar, for example, steroids and their metabolites. One of the advantages of CE is that it allows analyses of analytes even without enrichment of the analytes in multicomponent matrices because the concentration of these compounds is possible during the analysis.

The Micellar electrokinetic capillary chromatography (MEKC) is a method blend combining the principles of chromatographic and electrophoretic separations, and extends capillary electrophoretic methods application to neutral analytes, such as steroids. MEKC is based on the addition of surfactant (e.g. sodium dodecyl sulphate, SDS) into the buffer (electrolyte) solution (Siren & El Fellah, 2016). This surfactant works as a micellar pseudostationary phase that interacts with neutral analytes according to partitioning mechanisms. A special case of MEKC is partial-filling micellar electrokinetic chromatography (PF-MEKC) (Nelson & Lee, 1996), in which a small portion of the capillary is filled with a micellar solution for the separation of non-polar compounds; and the separation is as a result of the analyte interactions with the micelles.

5.6.1 Separation parameters optimisation

A PF-MEKC-UV method was developed and employed as the starting procedure for method optimisation for steroid hormones and metabolites in the water samples of water purification plant. The method instrumental parameters included 70 cm capillary length, 25 °C cassette temperature, and 25 kV voltage. The buffer concentration of 30 mM ammonium acetate, having its pH adjusted exactly to pH 9.68 with 25% ammonia, as ammonium acetate in water does not give the desired pH, 50 mbar pressure, 10 seconds injection time.

In partial-filling micellar electrokinetic injections capillary chromatography (PF-MEKC-UV), the electrolyte solution and the micelle solutions, form the mobile phase. A 100 mM sodium dodecyl sulphate (SDS) stock solution is one of the micelle solutions and the other micelle is 100 mM sodium taurocholate that was prepared with milli-Q water without any adjustment to its pH. The combination of the buffer electrolyte and the two micelle solutions forms the mobile phase responsible for the movement of the analytes through the capillary to the detector. However, the final electrolyte used in the PF-MEKC-UV was achieved by addition of 440 µL of 100 mM SDS into 1000 µL of 30 mM ammonium acetate solution (pH 9.68), and 50 µL of 100 mM sodium taurocholate solution. This order of addition is important, as there might be an intense formation of bubbles by SDS stock solution if the addition order was different.

In sequential order, the 30 mM ammonium acetate buffer electrolyte solution and the micelle were introduced into the capillary. A steroid concentration range of 0.5 – 6 µg/mL was used with method set-up including chemical changes (concentration and pH of the electrolyte, the micelle, and sample solvent) and instrumental modifications as described in section 3.2.5.1 of Chapter 3. The capillary length was fixed at 70 cm due to the possibility to couple the system with a mass spectrometer.

The result of this optimisation is shown in Figures 4.38 & 4.39 respectively, that present the electropherograms of the 5 ppm and 6 ppm steroid MIX analysis with the individual steroid analytes well separated and with good sensitivity from the capillary electrophoresis instrument. The separation of individual steroid analytes followed the order androstenedione, testosterone, 17-β-estradiol and progesterone respectively, as predicted by the peakmaster software.

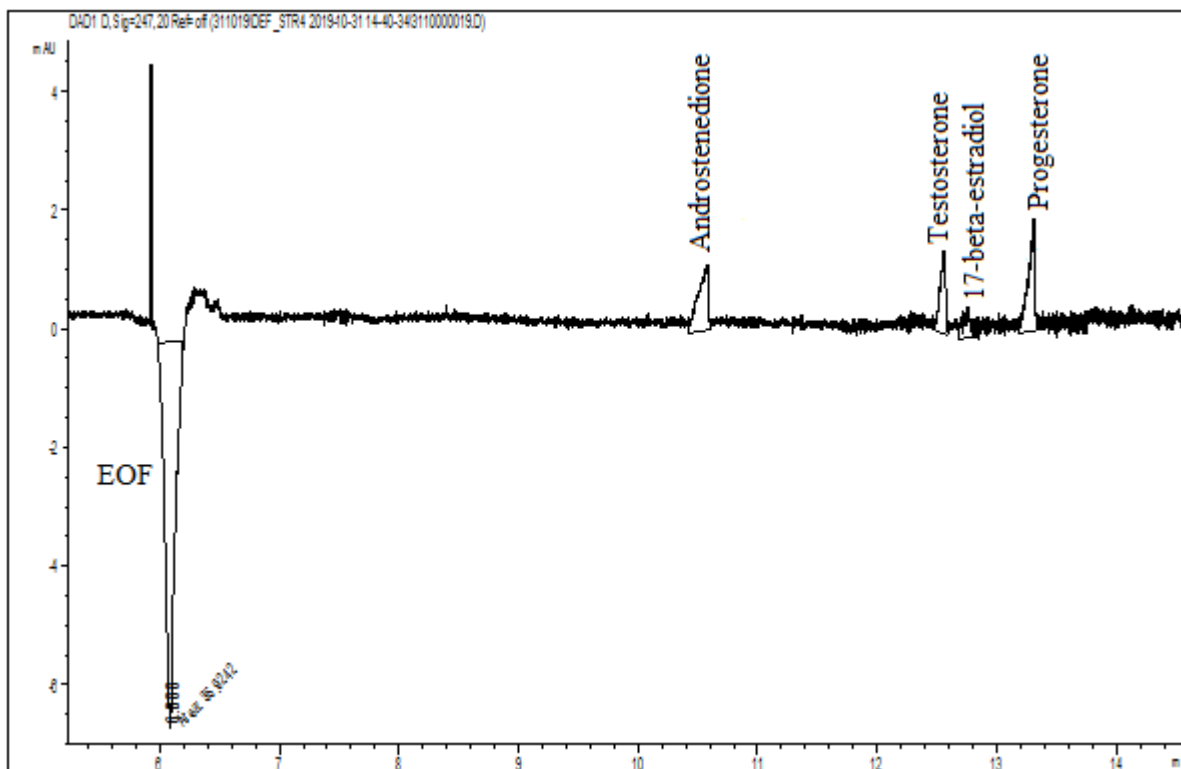
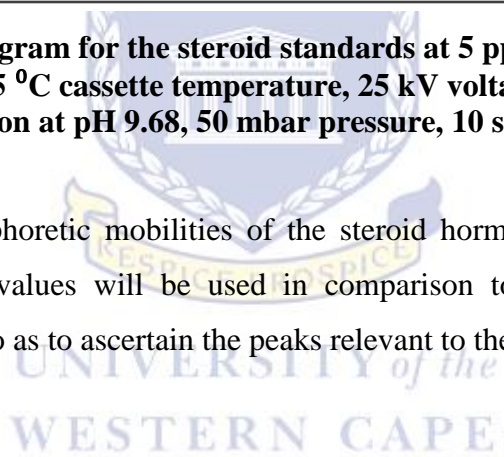


Figure 5.38: Electropherogram for the steroid standards at 5 ppm concentration. (70 cm capillary length, 25 °C cassette temperature, 25 kV voltage, 30 mM ammonium acetate buffer concentration at pH 9.68, 50 mbar pressure, 10 seconds injection time).

The results of the electrophoretic mobilities of the steroid hormone standard analytes are important, because these values will be used in comparison to the values that will be generated in the samples, so as to ascertain the peaks relevant to the respective analytes.



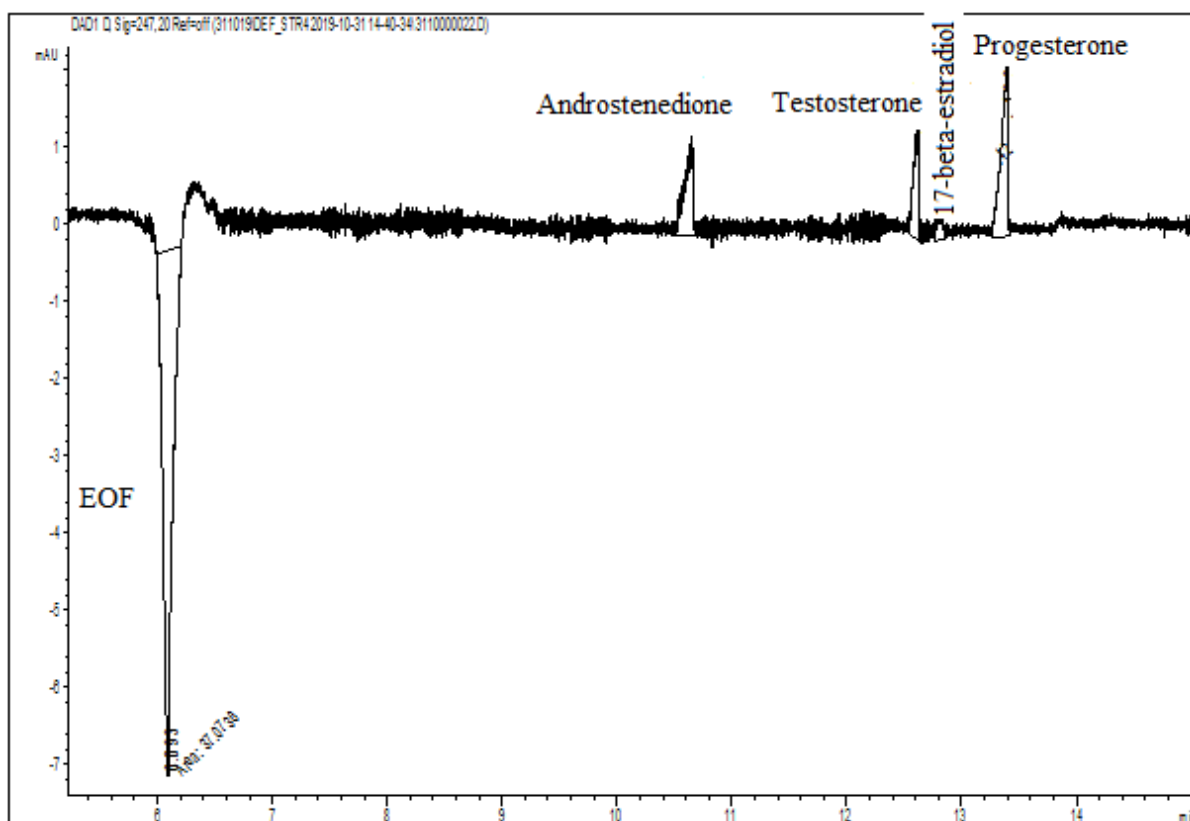


Figure 5.39: Electropherogram for the steroid standards at 6ppm concentration.

Table 5.34 shows the migration order and electrophoretic mobilities of individual steroid standard analytes. Certain factors are to be considered when capillary electrophoresis with UV detection is employed as the analysis method for steroids in water samples.

Table 5.34: Electrophoretic mobility of steroid analytes in PF-MEKC-UV

ANALYTE	(μ_{ep}) [m ² /Vs]
Androstendione	-2.630×10^{-8}
Testosterone	-3.100×10^{-8}
17-β-estradiol	-3.200×10^{-8}
Progesterone	-3.280×10^{-8}

At first, the method development requires an extensive optimisation as a result of the low detection sensitivity when dilute samples are investigated. Also, the quantities of the steroids in the multicomponent water need matrix construction. However, in this study, PF-MEKC

using selectively optimised UV absorption was used to enhance the sensitivity while steroid hormones were being investigated. Furthermore, in the determination of steroid hormones in water samples from the water treatment plants, steroid hormones must be isolated from the matrix by the sample preparation process. The analysis of androstenedione (precursor of testosterone and estrogens in the metabolic pathway), testosterone, and progesterone, are important contaminants from households since the wastewater contains a mixture of pollutants and urine with sex hormones.

In order to maximise the sensitivity of the analytes for the evaluation of the migration order of the steroids, total method optimisation was made. As a result, the steroid hormones migrated in the order: Androstenedione, testosterone, 17- β -estradiol, and progesterone respectively (Figure 5.40). The order for the migration of the individual steroid standard analytes is shown in Table 5.35.

Table 5.35: The migration order of the steroid standard analyte

Order	Compound
1	Androstendione
2	Testosterone
3	17- β -estradiol
4	Progesterone

The PF-MEKC-UV method enhanced movement of the non-polar and non-ionic steroid compounds in the capillary owing to the presence of the micelles which offered better interaction with the polar steroids compared to the conjugated ones.

5.6.2 Repeatability in PF-MEKC repetition series for individual steroid standard analytes

The electrophoretic data for the repeatability study was also carried out. Repeatability (RSD) of the method was very good, as it is noticed from the absolute migration times, electrophoretic mobilities, and electroosmosis values of 0.01–0.73%, 0.001–0.74%, and

0.58%, of the individual analytes respectively, as shown in the repeatability calculations in Tables 5.36, 5.37, 5.38, 5.39 and 5.40 respectively.

Table 5.36: Results of the repeatability calculations for electroosmosis using PF-MEKC. (70 cm capillary length, 25 °C cassette temperature, 25 kV voltage, 30 mM ammonium acetate buffer concentration at pH 9.68, 50 mbar pressure, 10 seconds injection time)

Electroosmosis (E=10 ⁴)			
Repetition Number	Migration [s]	Area	$\mu_{eo}[\frac{m^2}{Vs}]$
1	360.240	49.168	5.975E-08
2	364.380	42.916	5.907E-08
3	360.600	45.534	5.969E-08
4	359.820	46.734	5.982E-08
AVG	361.260	46.088	5.958E-08
STD DEV	0.035	2.599	0.035
RSD	0.583	5.640	0.580

Table 5.37: Results of the repeatability calculations for androstenedione using PF-MEKC. (70 cm capillary length, 25 °C cassette temperature, 25 kV voltage, 30 mM ammonium acetate buffer concentration at pH 9.68, 50 mbar pressure, 10 seconds injection time)

Androstenedione (E=10 ⁴)				
Repetition Number	Migration [s]	Area	$\mu [\frac{m^2}{Vs}]$	$\mu_{ep}[\frac{m^2}{Vs}]$
1	646.200	6.031	-2.626E-08	3.331E-08
2	645.600	6.512	-2.624E-08	3.334E-08
3	646.800	6.547	-2.630E-08	3.328E-08
4	646.200	6.525	-2.627E-08	3.331E-08
AVG	646.200	6.404	-2.627E-08	3.331E-08
STD DEV	0.008	0.249	0.028	0.003
RSD	0.076	3.887	2.621	0.074

Table 5.38: Results of the repeatability calculations for testosterone using PF-MEKC. (70 cm capillary length, 25 °C cassette temperature, 25 kV voltage, 30 mM ammonium acetate buffer concentration at pH 9.68, 50 mbar pressure, 10 seconds injection time)

Testosterone				
(E=10[^])				
Repetition Number	Migration [s]	Area	$\mu \left[\frac{m^2}{Vs} \right]$	$\mu_{ep} \left[\frac{m^2}{Vs} \right]$
1	759.000	2.427	-3.122E-08	2.836E-08
2	747.000	2.773	-3.077E-08	2.882E-08
3	750.000	2.171	-3.088E-08	2.870E-08
4	756.000	2.561	-3.111E-08	2.847E-08
AVG	753.000	2.483	-3.100E-08	2.859E-08
STD DEV	0.091	0.252	0.021	0.021
RSD	0.727	10.147	0.667	0.735

Table 5.39: Results of the repeatability calculations for 17-β-estradiol using PF-MEKC. (70 cm capillary length, 25 °C cassette temperature, 25 kV voltage, 30 mM ammonium acetate buffer concentration at pH 9.68, 50 mbar pressure, 10 seconds injection time)

17-β-estradiol				
(E=10[^])				
Repetition Number	Migration [s]	Area	$\mu \left[\frac{m^2}{Vs} \right]$	$\mu_{ep} \left[\frac{m^2}{Vs} \right]$
1	767.940	0.424	-3.155E-08	2.803E-08
2	767.820	0.634	-3.154E-08	2.803E-08
3	767.880	0.340	-3.155E-08	2.803E-08
4	768.000	0.547	-3.155E-08	2.803E-08
AVG	767.880	0.486	-3.155E-08	2.803E-08
STD DEV	0.001	0.130	0.001	0.0001
RSD	0.010	26.809	0.016	0.001

Table 5.40: Results of the repeatability calculations for progesterone using PF-MEKC. (70 cm capillary length, 25 °C cassette temperature, 25 kV voltage, 30 mM ammonium acetate buffer concentration at pH 9.68, 50 mbar pressure, 10 seconds injection time)

Progesterone					(E=10 ⁴)
Repetition Number	Migration [s]	Area	$\mu \left[\frac{m^2}{Vs}\right]$	$\mu_{ep}\left[\frac{m^2}{Vs}\right]$	
1	802.200	3.674	-3.275E-08	2.683E-08	
2	801.000	3.501	-3.271E-08	2.687E-08	
3	801.600	3.963	-3.273E-08	2.685E-08	
4	801.480	3.769	-3.272E-08	2.686E-08	
AVG	801.600	3.727	-3.273E-08	2.685E-08	
STD DEV	0.008	0.192	0.002	0.002	
RSD	0.0616	5.161	0.052	0.064	

Repeatability calculations were made from the four repetitions of the steroid standard MIX solution (10 seconds injection time, voltage 25 kV). It is noticed that the standard deviations and repeatability remain relatively low.

The various electrophoretic mobilities of the individual steroid standard analytes were calculated, and the total electrophoretic mobilities were calculated by subtracting the electroosmosis from the compounds that migrated after it. Here also, all the steroid standard analytes migrated after electroosmosis. Tables 5.36, 5.37, 5.38, 5.39 and 5.40 give the results for the repetition analysis and calculations for electrophoretic mobility and migration times for various individual steroid standard analytes including electroosmosis.

5.6.3 Concentration linearity and sensitivity

In this section, a six-set calibration standards of quadruple runs for each analyte, plots of calibration curves, determination of the equations for the linear regression lines from the calibration curves, LOD and LOQ determination for each steroid analyte and evaluation of the repeatability and reproducibility of method selectivity and sensitivity of each steroid analyte are determined.

The linearity of the method was measured at concentration range of 0.5–6 µg/mL using standard analyte mixtures. The result was a linear correlation between concentration and the peak area of the analyte, as is shown in Table 5.41.

Table 5.41: Linear regression calibration data of standard analytes

Steroid Standards	Calibration					
	range [µg/mL]	Linear equation	R ²	λ _{max} [nm]	LOD [µg/mL]	LOQ [µg/mL]
Androstenedione	0.5 - 6	y = 1.4687x - 0.8114	0.9965	247	0.105	0.315
Testosterone	0.5 - 6	y = 1.0256x - 0.3564	0.9977	247	0.065	0.195
17-β-estradiol	0.5 - 6	y = 1.9121x - 0.9934	0.9963	247	0.096	0.288
Progesterone	0.5 - 6	y = 1.9858x - 0.9241	0.9964	247	0.065	0.195

In Table 5.41, it can be seen that the equations correlate linearly with the detector response (area) obtained for the standard analyte mixtures. The partial-filling micellar electrokinetic injections capillary chromatography (PF-MEKC-UV) method permitting limits for detection (LOD) and quantification (LOQ) from 0.065 to 0.105 µg/mL (SPE concentrated 3.25 – 5.25) and from 0.195 to 0.315 (SPE concentrated 9.75 – 15.75), respectively. The instrument response to the detection of each of the standard analytes (steroids) showed linear sensitivity to increasing concentrations with R² values > 0.99 for all the four analytes (Table 5.41). The LOD value correlating to the signal-to-noise ratio of 3 was measured from the concentrations of the analytes as a mixture. The LOQ value for each analyte was then calculated with signal-to-noise ratio of 3 × LOD (9 × S/N). Figures 5.40, 5.41, 5.42, and 5.43 show the plots of calibration curves, determining the equations for the linear regression lines from the calibration curves for each of the four standard analytes, with their respective linear regression equations and R² values.

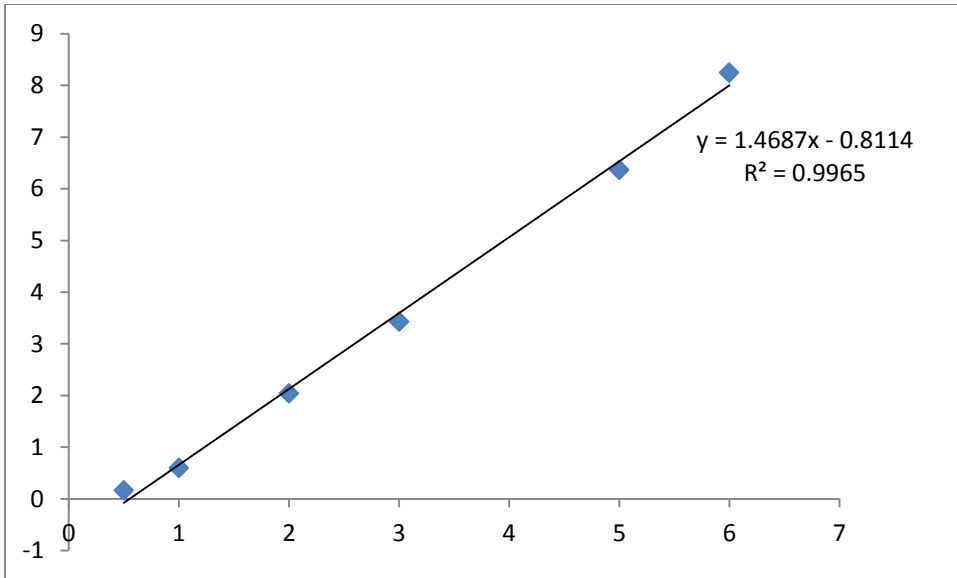


Figure 5.40: Calibration curve for Androstenedione standard

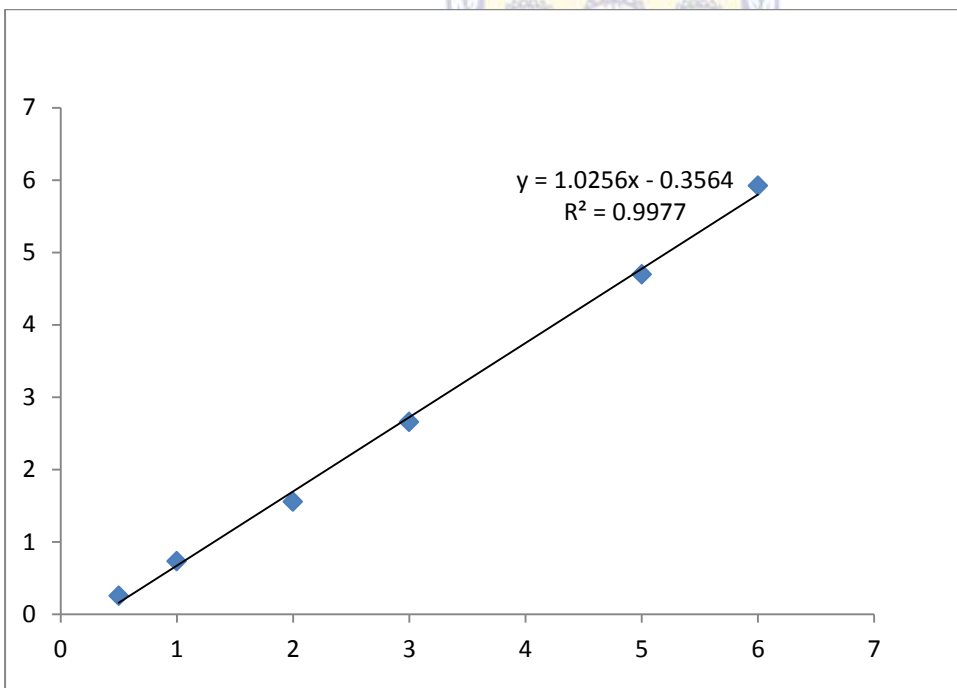


Figure 5.41: Calibration curve for Testosterone standard.

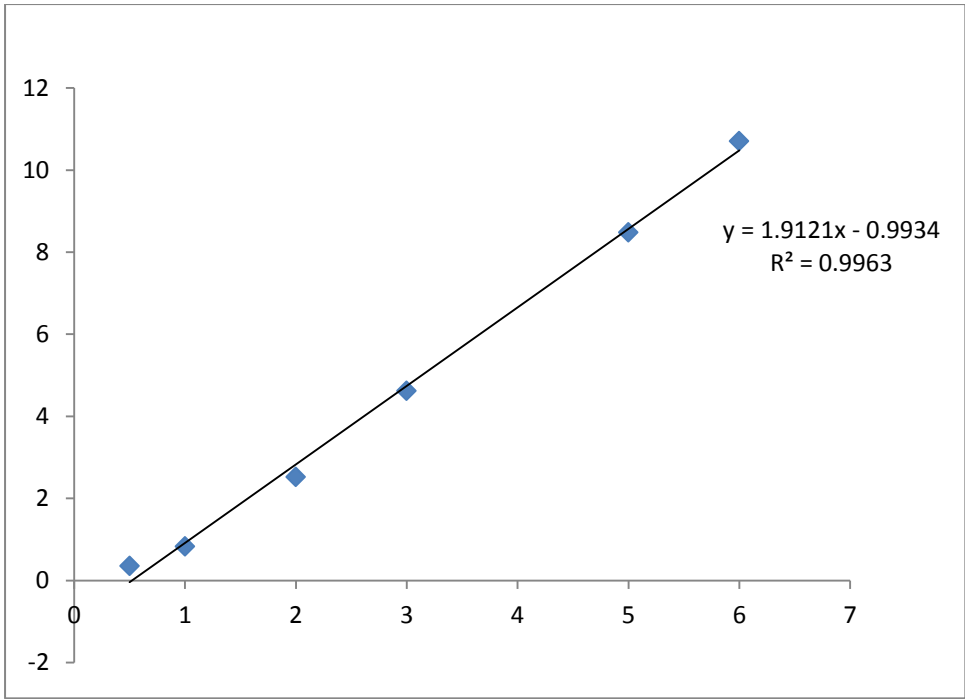


Figure 5.42: Calibration curve for 17-β-estradiol standard.

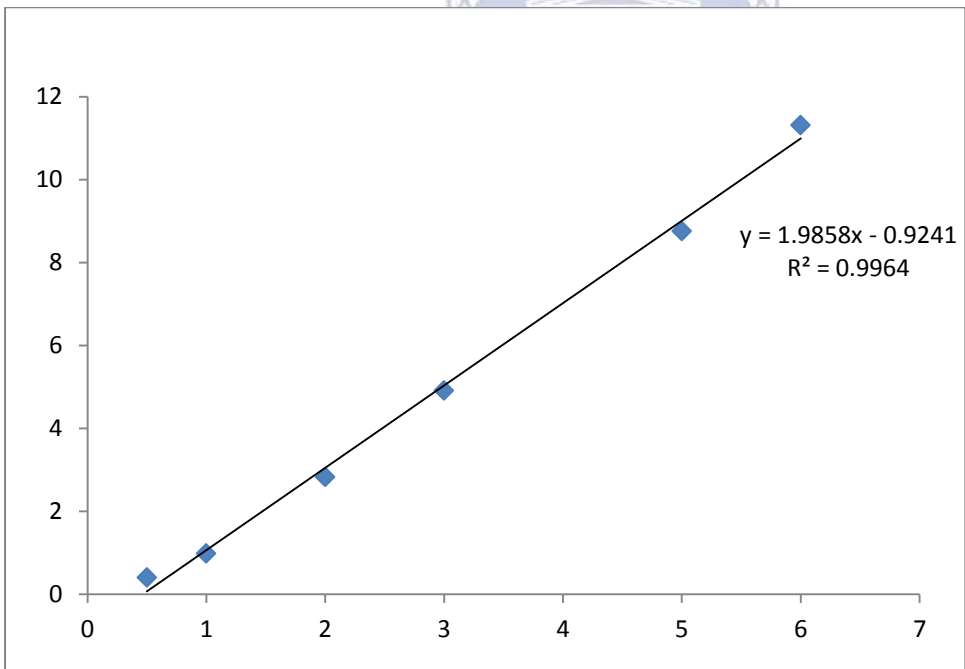


Figure 5.43: Calibration curve for Progesterone standard.

5.6.4 Recovery studies for steroid standard analytes using Solid Phase Extraction (SPE).

The efficiencies of the quantitative recovery of the standard analytes (Androstenedione, testosterone, 17- β -estradiol, and progesterone) using the SPE method were evaluated using the data from recovery experiments. The analytes were recovered from solution of 0.4 mg/L cocktail analyte standards in MeOH. The relative percentage recoveries of the analytes are given in Table 5.42.

Table 5.42: Mean recovery percentages for steroid standard analytes by SPE method

Steroid Standards	Expected concentration (mg/L)	Measured concentration (mg/L)	Average recovery (%)
Androstenedione	0.40	0.36	90.00
Testosterone	0.40	0.35	87.50
17- β -estradiol	0.40	0.35	87.50
Progesterone	0.40	0.37	92.50

The results revealed the measure of the affinity efficiency of the C₁₈ (Strata-X) non-polar sorbent cartridges to concentrate the tested steroids (standard analytes) was high. This shows that the use of C₁₈ (Strata-X) non-polar sorbent cartridges in solid phase extraction procedure is efficient and satisfactory for the concentration and recoveries of the selected steroid analytes from the aqueous matrices.

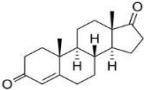
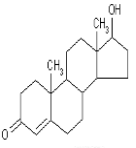
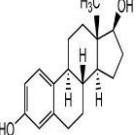
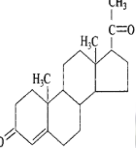
5.6.5 Determination of steroid hormones in water

This section focuses on measuring the steroid hormones (human-based androgens, estrogens, and synthetic progesterone) in environmental wastewater. Steroid hormones compounds such as androstenedione, testosterone, 17- β -estradiol, and progesterone, etc, are usually determined in environmental water (Jobling *et al.*, 2005; Liu *et al.*, 2011; Nelson & Lee, 1996; Thorpe *et al.*, 2003). The water samples studied for steroid hormones include: two different influent water samples and an effluent water sample from sewage water treatment plants, hot tap water, cold tap water, and Milli-Q water respectively. For both influent water samples influent A and B, the steroid hormones found in the highest concentration include

androstenedione and testosterone. In the influent A water sample, androstenedione was quantified to be 2.224 ng/L, testosterone was quantified to be 3.474 ng/L, 17- β -estradiol was quantified to be 0.96 ng/L and progesterone was 1.503 ng/L. Subsequently, the influent B water sample contained 2.224 ng/L of androstenedione, 3.142 ng/L of testosterone, 0.954 ng/L of 17- β -estradiol and 0.691 ng/L of progesterone respectively. In the purified effluent water samples of sewage water treatment plants however, the measurable steroid hormones quantities include 1.205 ng/L of androstenedione, 3.037 ng/L of testosterone, 0.550 ng/L of 17- β -estradiol and 0.440 ng/L of progesterone respectively. Based on the concentration levels of both influent and effluent water samples, it is not surprising, given the fact that almost 80% of effluent water samples from the plants have been reported to contain female hormones after clean-up of the water (Wen *et al.*, 2014). Owing to the very low concentration levels, the steroid hormones in the water samples have to be enriched and extracted from the major environmental matrix. As a result, in this analysis of steroids, the sampled water volume used was 2 L in order to enrich the steroid concentrations for maximal UV detection in the partial-filling micellar electrokinetic capillary chromatography (PF-MEKC) analyses, and to also embark on system validation to enhance its capability for long-term steroid monitoring.

The measured quantities of steroid hormones determined from the electropherograms of the influent and effluent water samples were ascertained by comparing the respective electrophoretic mobilities of the individual steroid analytes in the standards calibration to the electrophoretic mobilities of the individual steroid analytes in the influent and effluent water samples. Furthermore, the measured quantities in the effluents were lower than the quantities in the influent samples. When the analyte in a sample concentrate was clearly identified on the basis of absolute migration time, specific wavelengths, relative migration time and electrophoretic mobility, in the electropherogram, the sample was spiked with a 2 μ g/mL standard and quantification was done using the standard addition method. As a result, it was possible to ascertain the respective peaks belonging to the analytes under investigation. Table 5.43 shows the steroid analytes with their structures, theoretical and experimentally-measured exact molar masses with migration times and electrophoretic mobilities.

Table 5.43: Structures of androstenedione, testosterone, 17- β -estradiol and progesterone. Theoretical and experimentally-measured exact masses with migration times in CE

Compound	Structure	Molar mass [g/mol]	Experimental molar mass [M + H]	PF-MEKC-UV Migration time [min]	(μ_{ep}) [m^2/Vs]
Androstenedione C₁₉H₂₆O₂		286.410	287.200	10.770	-2.630 x 10 ⁻⁸
Testosterone C₁₉H₂₈O₂		288.420	289.216	12.550	-3.100 x 10 ⁻⁸
17-β-estradiol		272.380	273.185	12.798	-3.200 x 10 ⁻⁸
Progesterone C₂₁H₃₀O₂		314.462	315.232	13.360	-3.280 x 10 ⁻⁸

The electropherogram for influent A sample can be seen in Figure 5.44, and shows the retention time of the steroid analytes being investigated, which include androstenedione, testosterone, 17- β -estradiol and progesterone.

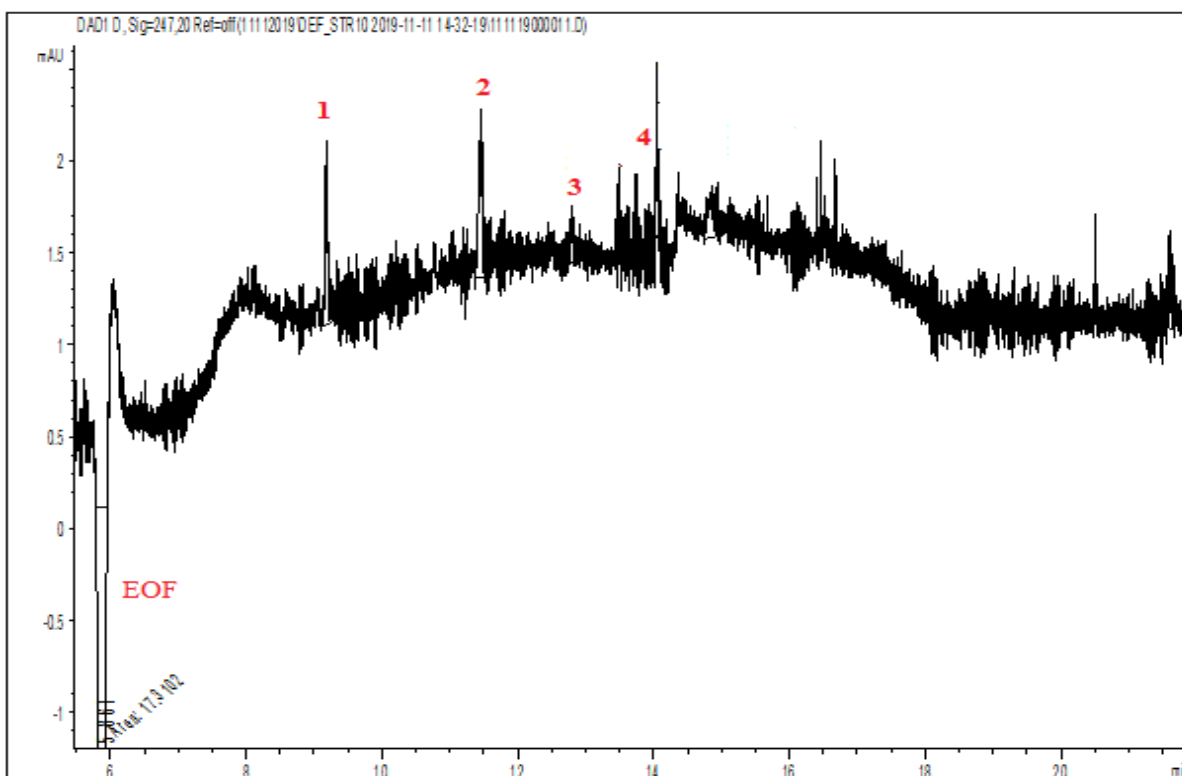


Figure 5.44: Electropherogram for influent A sample showing the peaks for the identified peaks including androstenedione (1), testosterone (2), 17-β-estradiol (3) and progesterone (4).

The respective analytes peaks were identified based on the calculation of their individual electrophoretic mobilities, in comparison or correlation to their respective mobilities in the standard analytes electrophoretic mobility calculations.

These individual analytes peaks are ascertained by the nearness in value to their respective peaks in the standard analytes electrophoretic mobility calculations by ± 0.2 . This is showcased in Table 5.44, where the electrophoretic mobilities calculations for the standard analytes, influent A, influent B and effluent water samples are displayed.

Table 5.44: Correlation between the electrophoretic mobilities of the steroid standards analytes with influent and effluents water samples

Compounds	Standards (μ_{ep}) [m ² /Vs]	Influent A (μ_{ep}) [m ² /Vs]	Influent B (μ_{ep}) [m ² /Vs]	Effluent (μ_{ep}) [m ² /Vs]
Androstendione	-2.630×10^{-8}	-2.200×10^{-8}	-2.640×10^{-8}	-2.200×10^{-8}
Testosterone	-3.100×10^{-8}	-2.980×10^{-8}	-2.874×10^{-8}	-2.750×10^{-8}
17-β-estradiol	-3.200×10^{-8}	-3.310×10^{-8}	-2.988×10^{-8}	-2.970×10^{-8}
Progesterone	-3.280×10^{-8}	-3.410×10^{-8}	-3.510×10^{-8}	-3.450×10^{-8}

There are other peaks present within the electropherogram belonging to other metabolites of the steroids being studied. However, their electrophoretic mobilities do not correlate with the electrophoretic mobility calculations of the steroids standard analytes, hence they are not taken into consideration. Figure 5.45 shows the electropherogram for the influent B water sample and it contains all the four steroid analytes under investigation, including androstenedione (1), testosterone (2), 17- β -estradiol (3) and progesterone (4) respectively.

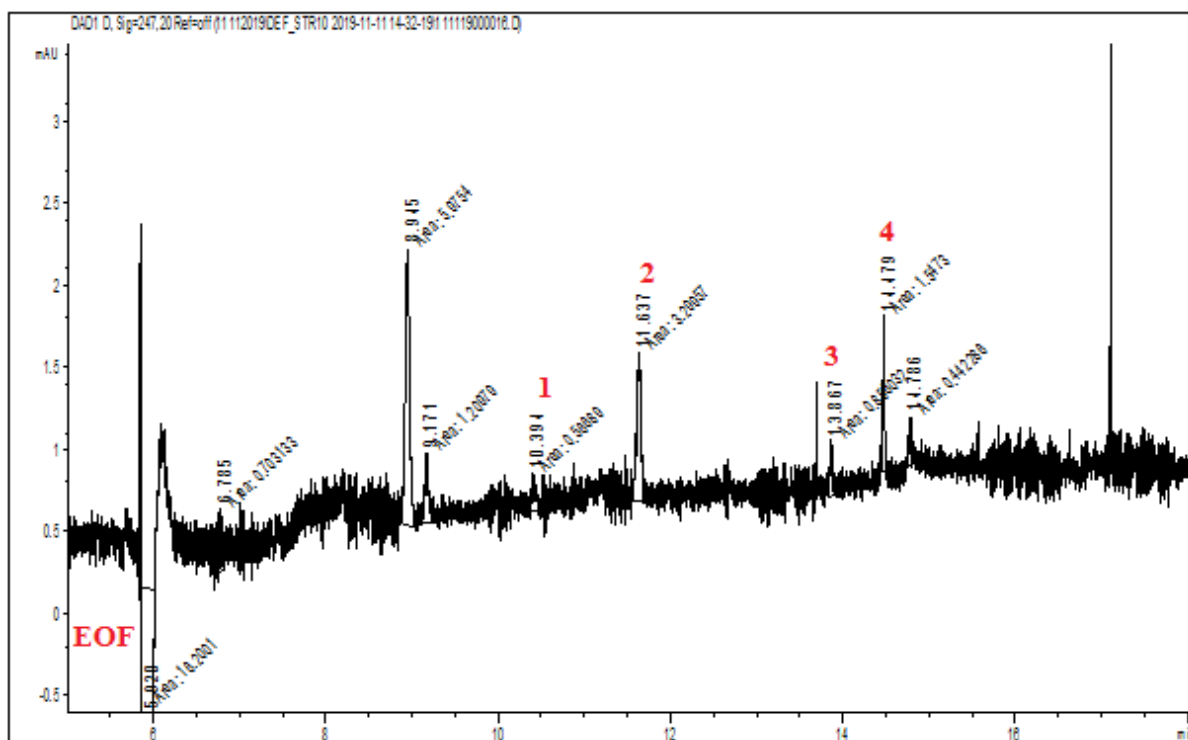


Figure 5.45: Electropherogram for influent B sample showing the peaks for the identified peaks including androstenedione (1), testosterone (2), 17- β -estradiol (3) and progesterone (4).

Tables 5.45, 5.46, and 5.47 give the detailed analysis account of the influent A, influent B and effluent water samples respectively, including the measured quantities of the steroid analytes, the mean, standard deviation and relative standard deviation of the parameters such as the migration time, peak area and peak height respectively.

Table 5.45: Identification of steroid hormones in the Influent A sample. Determination with PF-MEKC. Influent water sample purified with C18 (Strata-X) nonpolar sorbent

Compound	Migration time [min]	Peaks area [min × mAU]	Peak height [mAU]	Amount [ng/L]
Androstenedione				
Mean	9.161	2.455	0.938	2.224
SD	0.032	0.231	0.058	
RSD%	0.355	9.417	6.203	
Testosterone				
Mean	11.430	3.206	0.854	3.474
SD	0.056	0.310	0.066	
RSD%	0.487	9.676	7.721	
17-β-estradiol				
Mean	12.783	0.842	0.842	0.96
SD	0.036	0.015	0.015	
RSD%	0.280	1.810	1.810	
Progesterone				
Mean	13.797	2.060	0.926	1.503
SD	0.221	0.417	0.061	
RSD%	1.599	20.235	6.569	

Table 5.46: Identification of steroid hormones in the Influent B sample. Determination with PF-MEKC. Influent sample purified with C18 (Strata-X) nonpolar sorbent

Compound	Migration time [min]	Peaks area [min × mAU]	Peak height [mAU]	Amount [ng/L]
Androstenedione				
Mean	10.396	1.170	0.263	1.349
SD	0.079	0.108	0.024	
RSD%	0.769	9.200	9.281	
Testosterone				
Mean	11.448	2.866	0.939	3.142
SD	0.187	0.581	0.030	
RSD%	1.630	20.277	3.137	
17-β-estradiol				
Mean	11.515	0.830	0.429	0.954
SD	0.011	0.032	0.096	
RSD%	0.099	3.895	22.257	
Progesterone				
Mean	14.416	0.447	1.041	1.691
SD	0.124	0.024	0.070	
RSD%	0.859	5.394	6.743	

Table 5.47: Identification of steroid hormones in the Effluent water sample. Determination made with PF-MEKC. Effluent sample purified with C18 (Strata-X) nonpolar sorbent

Compound	Migration time [min]	Peaks area [min × mAU]	Peak height [mAU]	Amount [ng/L]
Androstenedione				
Mean	11.01	0.959	0.264	1.205
SD	0.045	0.063	0.051	
RSD%	0.405	6.529	19.177	
Testosterone				
Mean	11.777	2.758	0.728	3.037
SD	0.063	0.243	0.049	
RSD%	0.538	8.820	6.674	
17-β-estradiol				
Mean	14.005	1.206	0.407	0.550
SD	0.337	0.128	0.062	
RSD%	2.405	10.570	15.314	
Progesterone				
Mean	14.662	2.729	1.263	0.940
SD	0.357	0.099	0.063	
RSD%	2.436	3.641	5.025	

UNIVERSITY of the
WESTERN CAPE

Figure 5.46 shows the electropherogram for the effluent water sample and it contains the four steroid analytes under investigation, which includes androstenedione (1), testosterone (2), 17- β -estradiol (3) and progesterone (4) respectively.

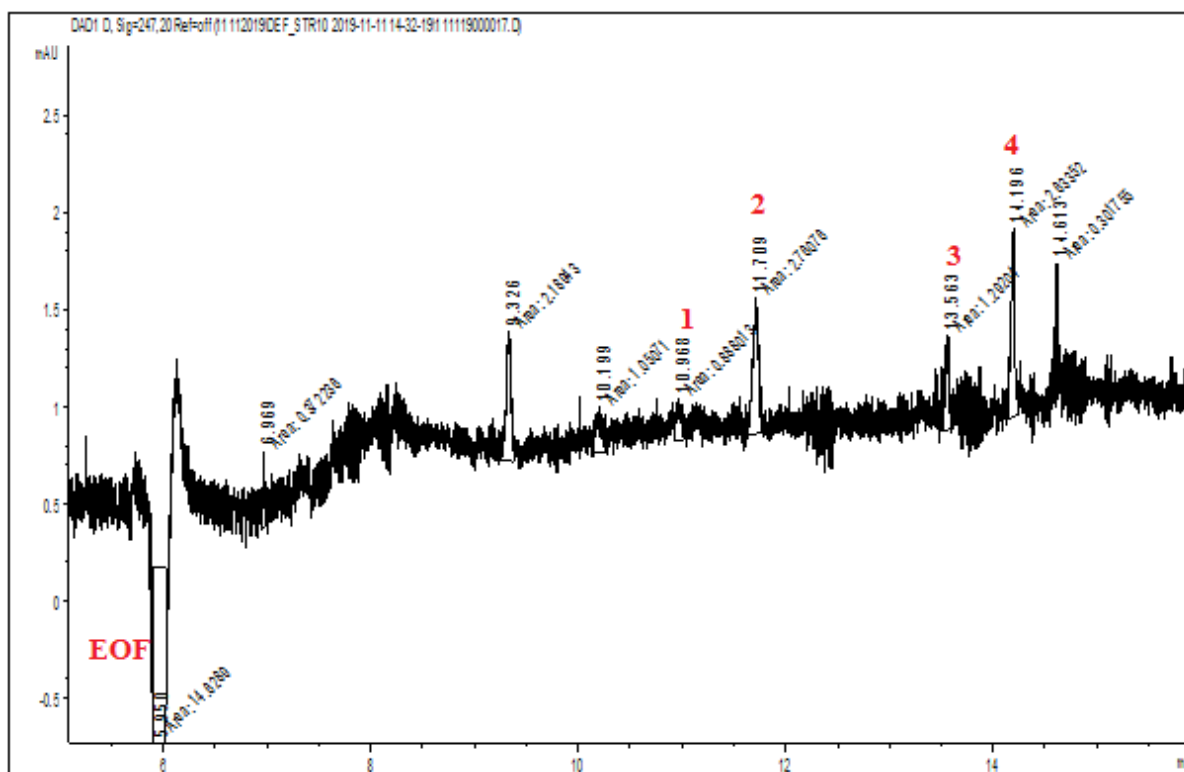


Figure 5.46: Electropherogram for effluent sample showing the peaks for the identified peaks including androstenedione (1), testosterone (2), 17- β -estradiol (3) and progesterone (4).

There are other peaks in the electropherogram for the effluent water sample also, which are not among the analytes being investigated in this study. But the electropherogram profile shows the water sample contains several other metabolites of steroid components, indicating the presence of other steroid hormonal compounds in the effluent water sample.

In Figures 5.47, 5.48 and 5.49, the electropherograms shows the overlay of the steroid standard mixture profiles with the influent A, influent B and effluent water sample profiles. It can be observed in the electropherograms that the influent and effluent water sample profiles contain other peaks aside from the analytes being investigated; at the same time, the matrix effect of the influent water samples also effected the non-alignment of the respective peaks. However, these individual peaks belonging to individual analytes were ascertained and confirmed from the calculations of their respective electrophoretic mobilities which correlate with those of the steroid analytes in the standard mixture. Standard addition was also done to verify the peaks of interest.

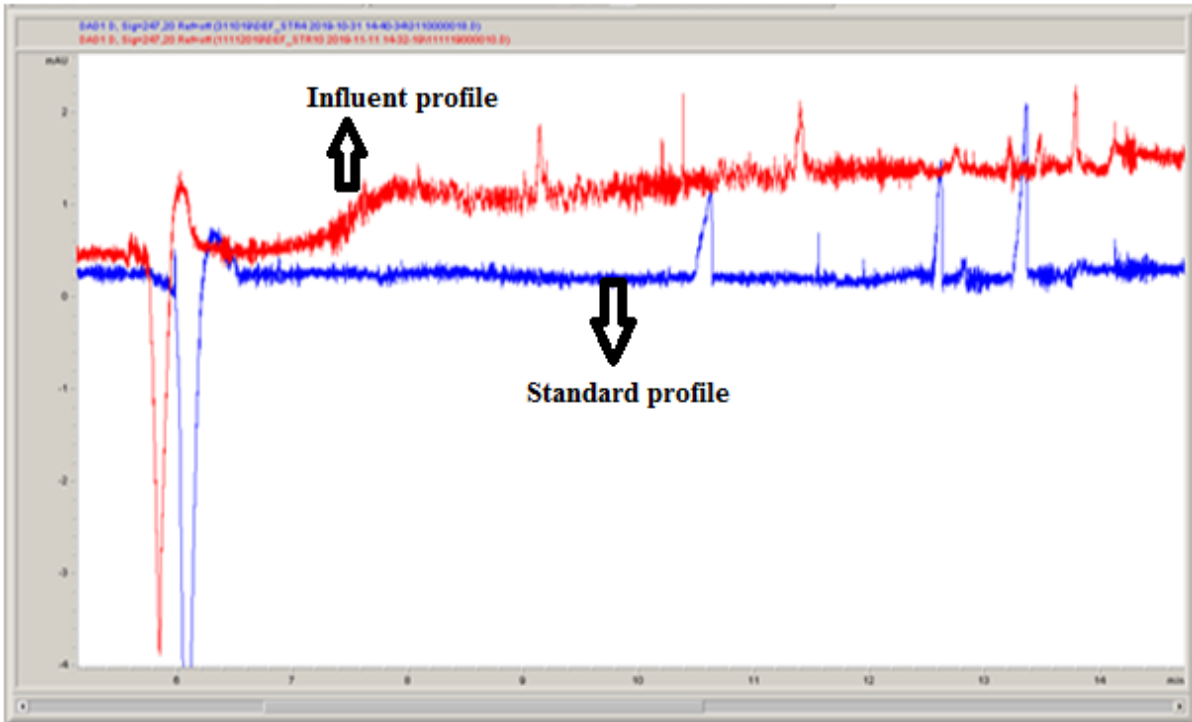


Figure 5.47: Electropherogram profile showing the steroids standards mixture profile overlay with the influent A sample profile.

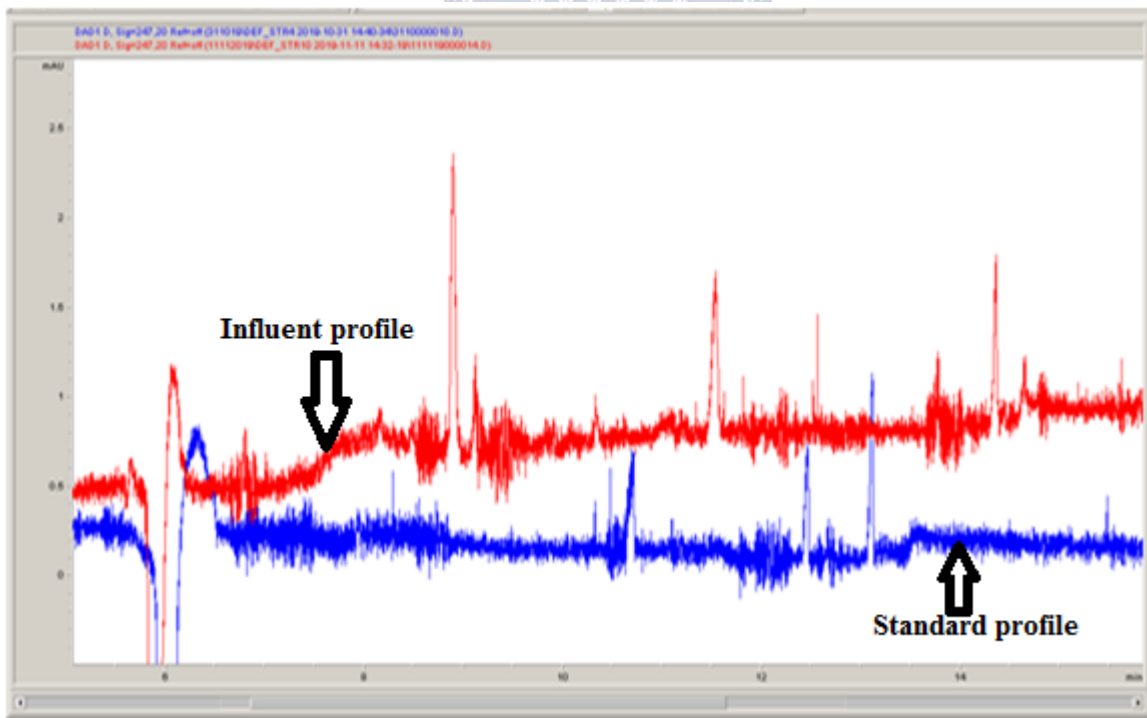


Figure 5.48: Electropherogram profile showing the steroids standards mixture profile overlay with the influent B sample profile.

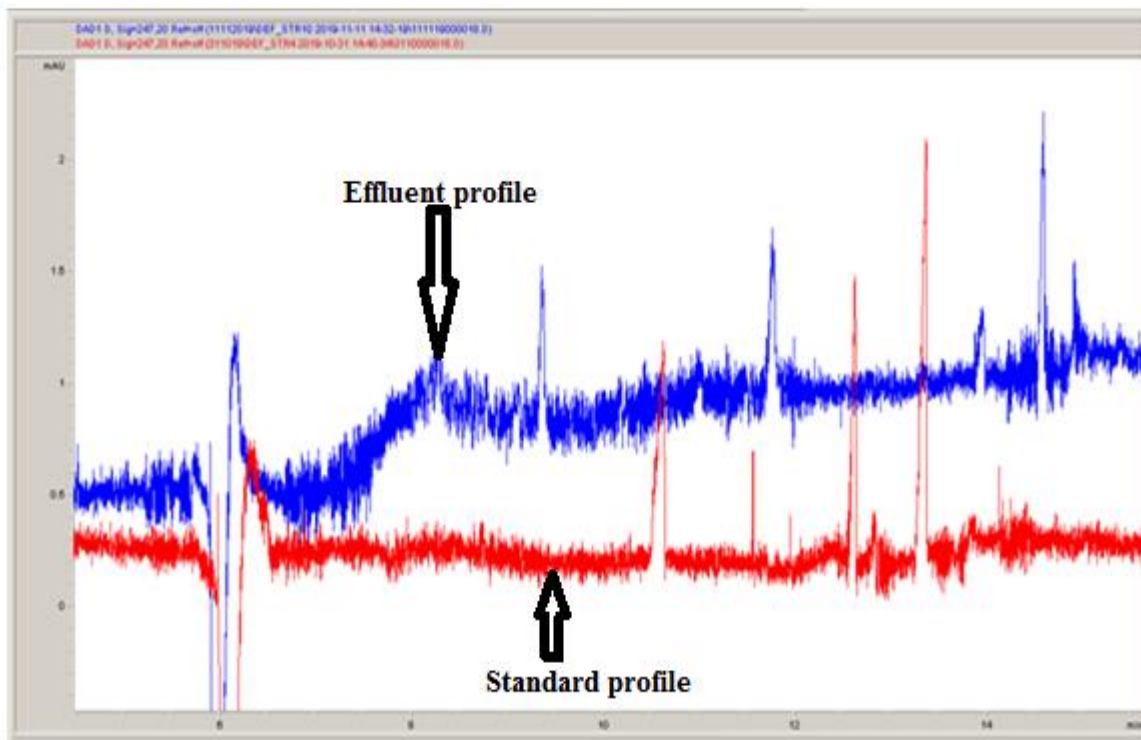
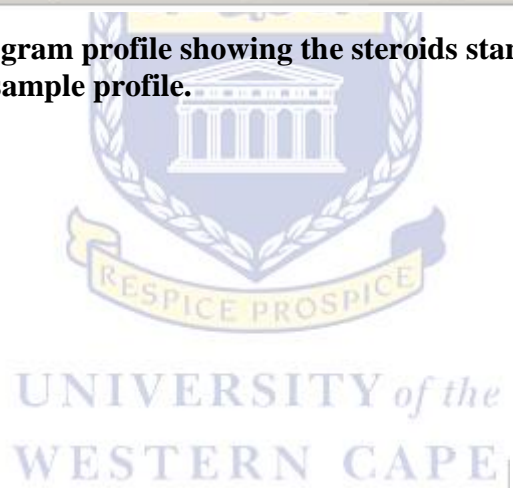


Figure 5.49: Electropherogram profile showing the steroids standards mixture profile overlay with the effluent sample profile.



However, to ascertain the authenticity of the analytes peaks, 2 µg/mL of the steroid standard of the specified analyte was spiked into the influent and the effluent water samples to double-check the authenticity of the particular peaks. Figure 5.50 describes the spiking of the effluent water sample with 2 µg/mL of androstenedione and testosterone in an overlay with both spiked and unspiked electropherograms.

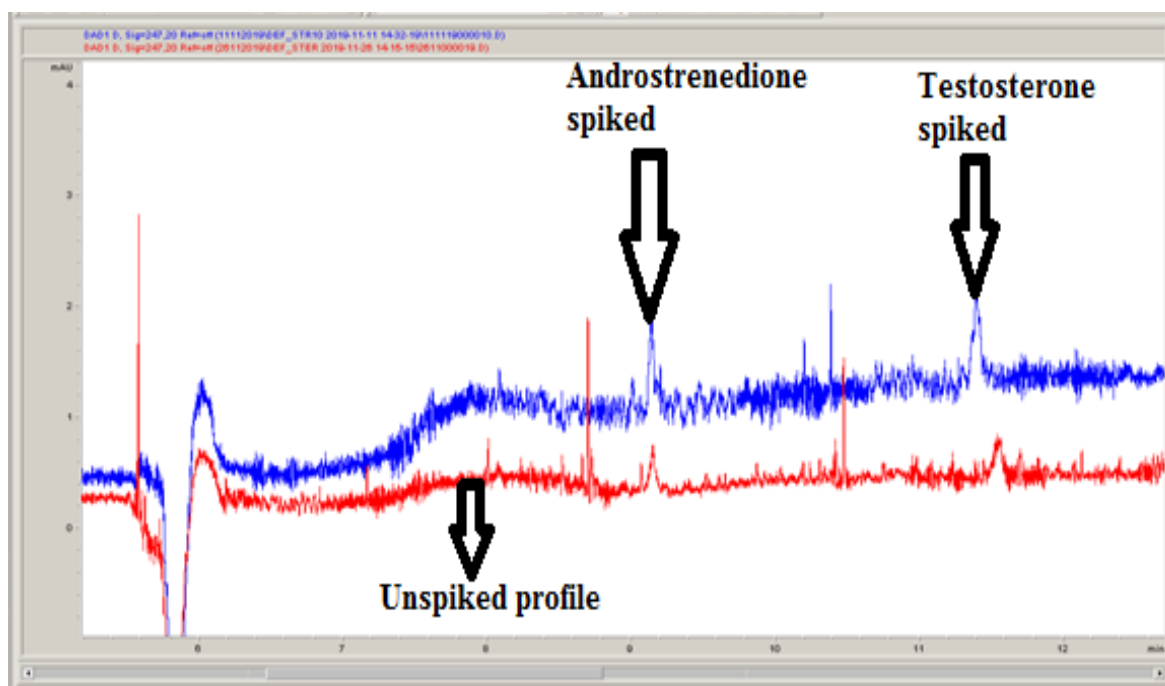


Figure 5.50: Electropherogram profile showing the androstenedione and testosterone-spiked and unspiked effluent profile

The possible reasons for the elevated steroid concentrations of the influent and effluent of the wastewater treatment plant can be evaluated by the study of the metals concentrations and other materials as the adsorbents for steroids, as these steroids are known to form complexes with metals; therefore, inorganic ions contamination of the influent and effluent wastewaters is known to be one of the reasons for steroid-load in wastewaters, and it is imperative to study its effects (Heli & El Fellah, 2016).

In Figure 5.51, the steroid hormones concentration amounts in the influent A, influent B and effluent water samples are given, also, Figure 5.52 gives the steroid hormones concentration amounts in the hot tap water and cold tap water samples.

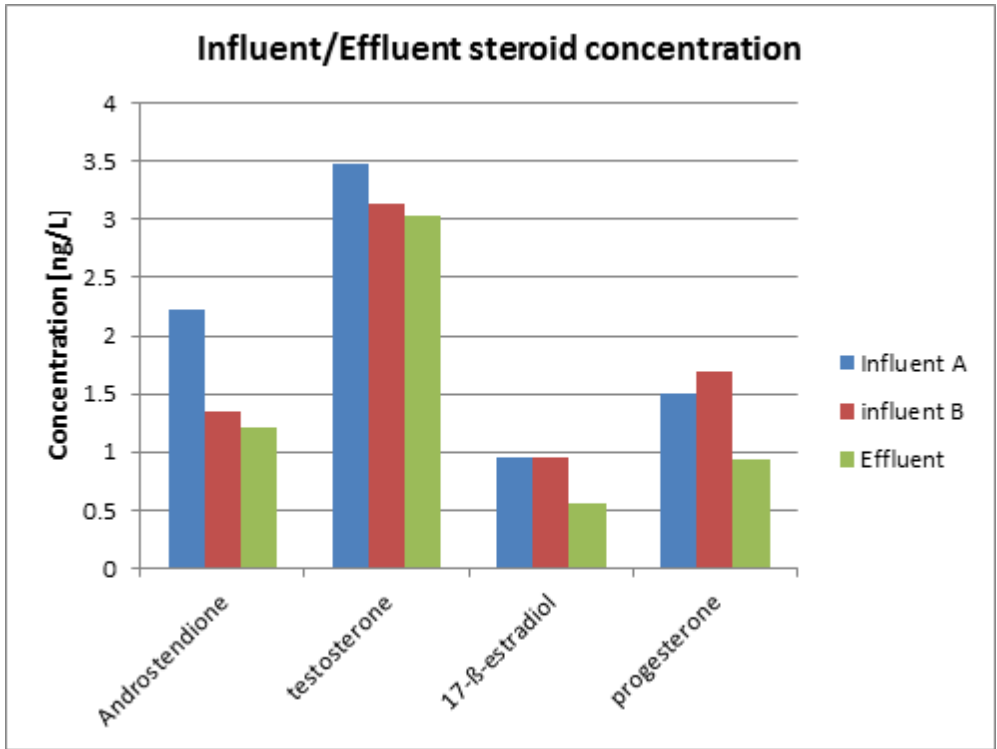


Figure 5.51: Steroid hormones concentration amounts in the influent A, influent B and effluent water samples.

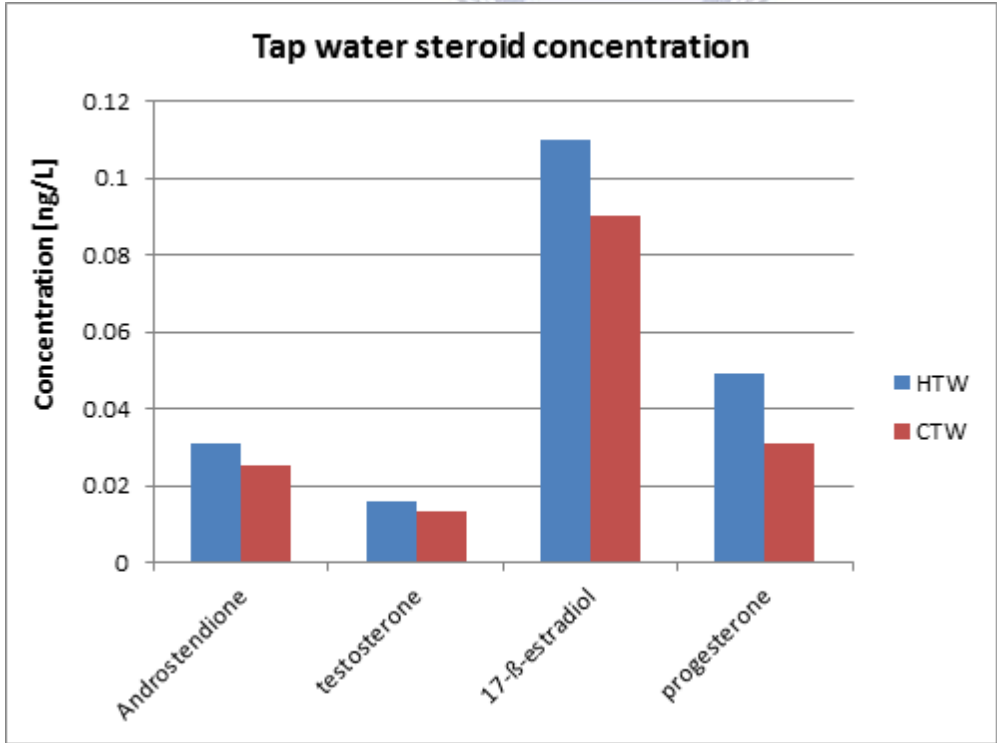


Figure 5.52: Steroid hormones concentration amounts in the hot tap water (HTW) and cold tap water (CTW) samples.

5.7 Inorganic anions and cations quantification in the household water and environmental water samples: Measurement with capillary electrophoresis and indirect-UV detection

Inorganic minerals in the drinking water supplied to homes, river water, drilled well water, etc; have an influence on the taste of such water. As a matter of fact, they may have a significant impact on human health (Zacs *et al.*, 2016). The experimental procedure for the investigation of inorganic ions in water samples is detailed in section 3.6 of Chapter 3.

The analytical samples were taken from the river systems, ground waters, and water supplied to homes for domestic consumptions and usage. It is presumed that high metal concentration, pH, and organic materials would be one of the reasons of steroid concentrations, since they support the adsorption and solubility of steroids. Therefore, the inorganic ions concentrations study was focussed upon alkali metals and alkaline earth metals, including calcium (Ca^{2+}), magnesium (Mg^{2+}), potassium (K^+) and sodium (Na^+). The anions investigated also include: chloride (Cl^-), nitrate (NO_3^-), and sulphate (SO_4^{2-}) respectively.

5.7.1 The background electrolyte solutions and optimization of the separation parameters

In the optimized capillary electrophoresis method for the inorganic ions investigation of the environmental water samples, the anions were separated in a buffer solution containing 2.25 mM pyromellitic acid, 6.50 mM NaOH, 0.75 mM hexamethonium hydroxide and 1.60 mM triethanolamine (pH 7.7 ± 0.2 , Fluka). On the contrary, the optimized capillary electrophoresis for the cations was performed in 9 mM pyridine-12 mM glycolic acid-5 mM 18-crown-6 ether at pH 3.6, adjusted with 0.1 M HCl. The parameters in capillary zone electrophoresis (CZE) analyses of inorganic anions and cations in this study, were chosen from the guidelines given in earlier studies carried out with the use of diverse capillary electrophoresis instruments (Hissa *et al.*, 1999; Harvanova & Boom, 2015).

In this study, the method for anions started with conditioning the capillary for 5 minutes with the electrolyte solution, which was followed by sample injection at 0.725 psi (50 mbar) for 5 seconds. Separation was achieved with the voltage of -20 kV (negative polarity) and finishing the analysis in 15 mins. The indirect UV detection was done at 220 nm and 254 nm with the reference wavelength of 420 nm. For cations, the capillary was preconditioned with the

electrolyte solution for 7 minutes, followed by sample injection at 50 mbar for 10 seconds, voltage for separation at positive polarity of +20 kV, and the analysis period of 15 minutes. The indirect UV detection wavelengths of the ions were fixed at 220 nm and 254 nm wavelengths, with the reference wavelength of 420 nm.

5.7.2 Determination of the inorganic ions with CZE-UV

In the determination of the anions, a concentration calibration range of 1 ppm, 2 ppm, 5 ppm, 10 ppm, and 15 ppm respectively was prepared and analysed, as described in section 3.6 of Chapter 3; alongside the 10 environmental water samples. For anions, the order of detection ranges from chloride, followed by sulphate, and then nitrate.

The calibration curves for the individual anions are given in Appendix A45 – A47. Figure 5.53 shows the electropherogram of the 2 ppm anions standard giving the correct order of the peak profile of the respective anions. Chloride comes first, followed by sulphate and nitrate respectively.

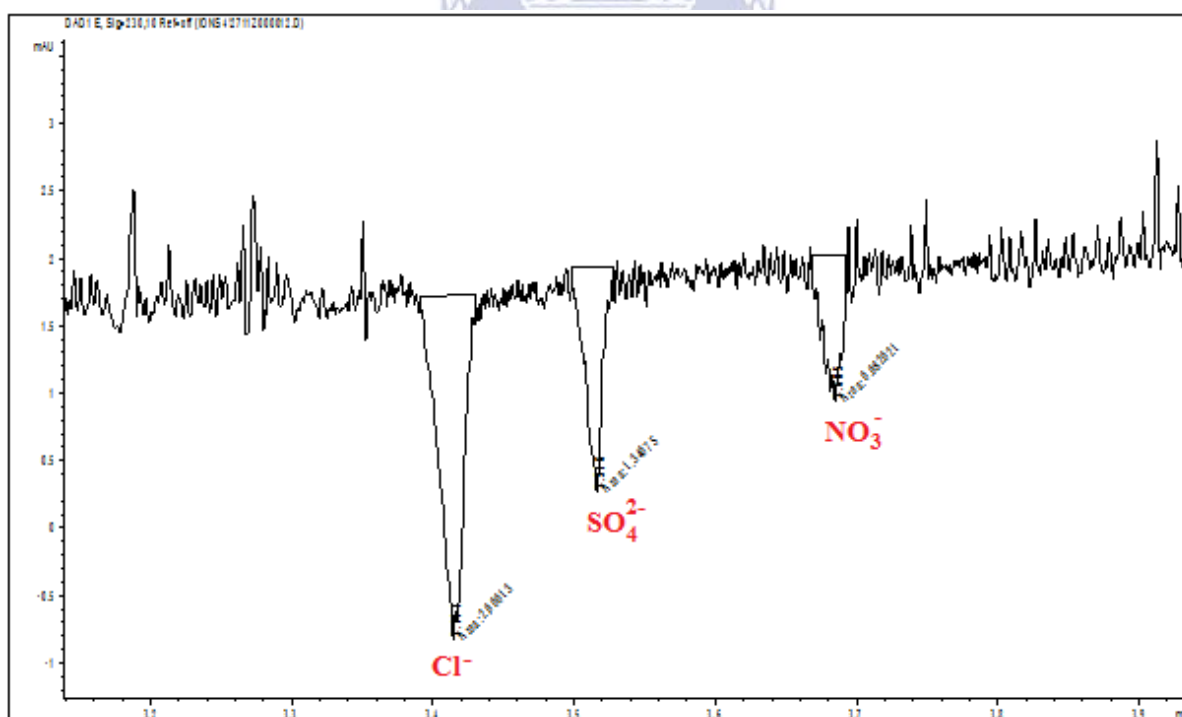


Figure 5.53: Electropherogram showing 2 ppm concentration of the anions' standard

Here in the indirect UV detection mode of the CZE, there is no electroosmosis profile, as a result of the indirect mode of operation of the instrument. Furthermore, in Figure 5.54, the electropherogram shows the profile of the 10 ppm of the anions calibration standard. It can be

observed that the peaks of the anions are more intense than in the 2 ppm standard as a result of the increased concentration due to ionic strength.

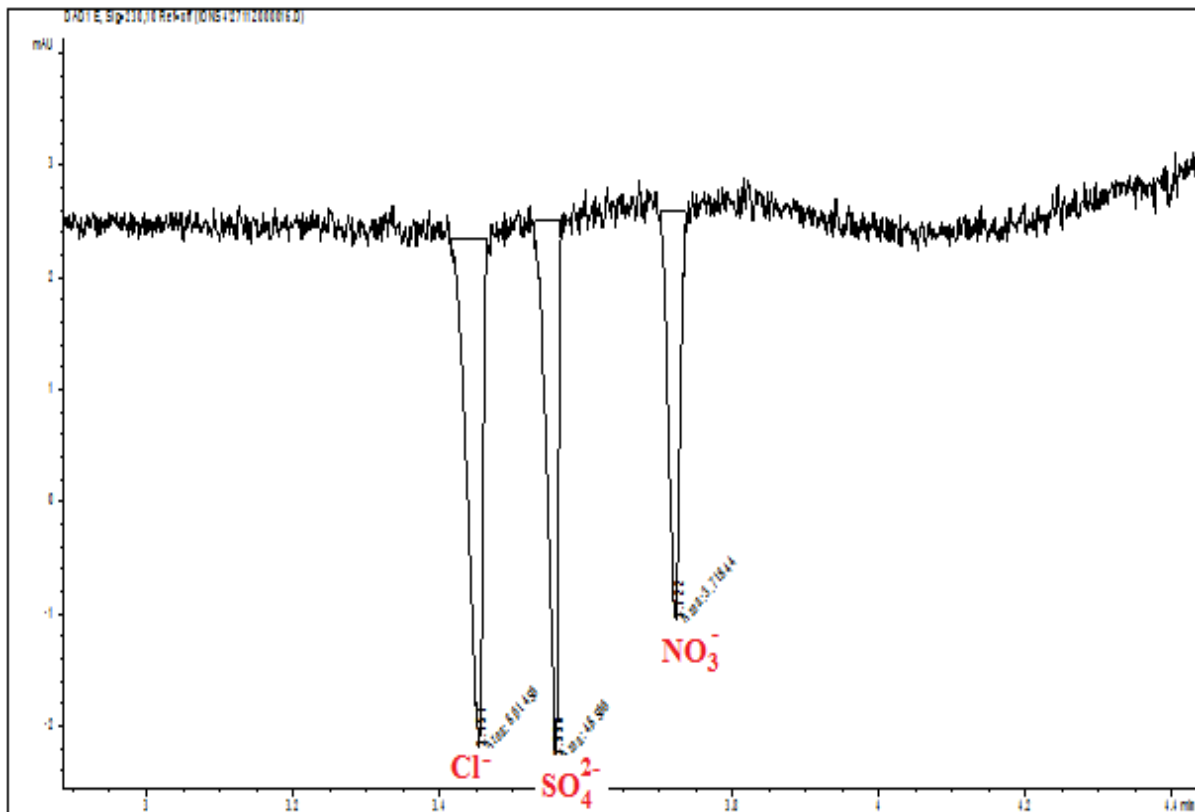


Figure 5.54: Electropherogram showing 10 ppm concentration of the anions standard.

The various amounts in concentration of the respective anions were determined from the standard calibration curves as given in Appendix A45 – A47. The electropherogram results of two of the water samples, river water 2 (RW 2) and hot tap water from the kitchen (KHTW) are presented in Figures 5.55 and 5.56.

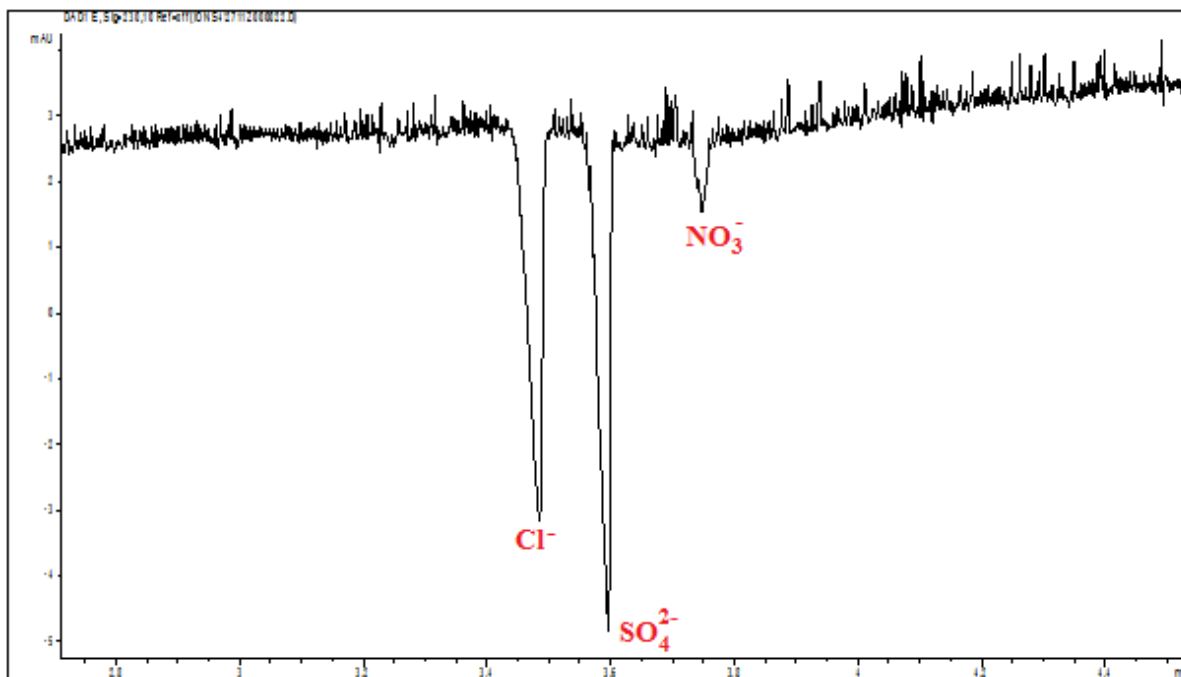


Figure 5.55: Electropherogram showing the anions profile for river water 2 (RW 2) sample.

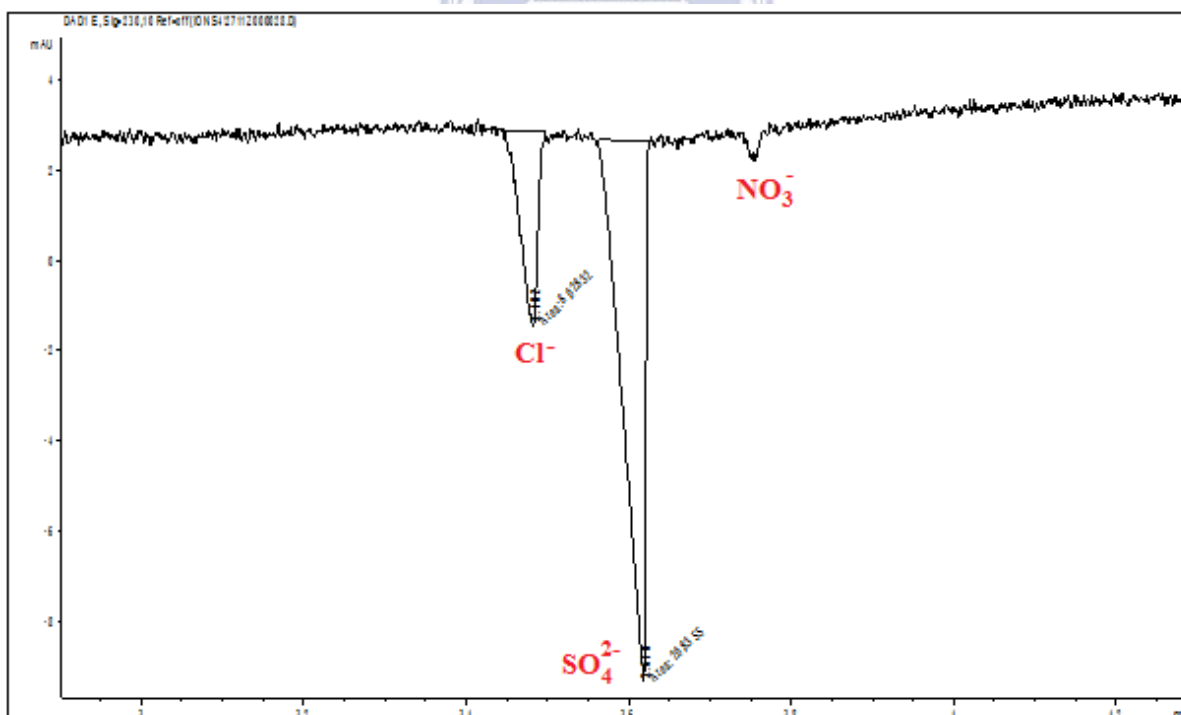


Figure 5.56: Electropherogram showing the profile for kitchen hot tap water (KHTW)

The electropherogram profile of the river water 2 sample shows the anionic profile with sulphate ion having the most intensity which translates to the most quantity in the profile. Nitrate ion had the least intensity which translates to least quantity in the profile. Also, the

high intensity peak translates to the strong ionic strength of the particular ion in solution, while low intensity peak translates to low ionic strength of that particular ion. Figure 5.56 shows the electropherogram profile for the hot tap water sample (KHTW) taken from the kitchen, it also shows sulphate having the most intensity which translates to the most ionic concentration, followed by chloride and then nitrate having the least ionic concentration respectively.

Furthermore, in the determination of the cations, a concentration calibration range of 2 ppm, 5 ppm, 10 ppm, 15 ppm, and 20 ppm respectively was prepared and analysed, as described in section 3.6 of Chapter 3; the cationic peaks appear in the positive mode. The calibration curves for the individual cations are given in Appendix A48 – A51. Figure 5.57 shows the 15 ppm cations standard calibration profile, followed by the electropherogram profiles of the environmental water samples depicting the ionic strength concentrations of the cations in the respective profiles.



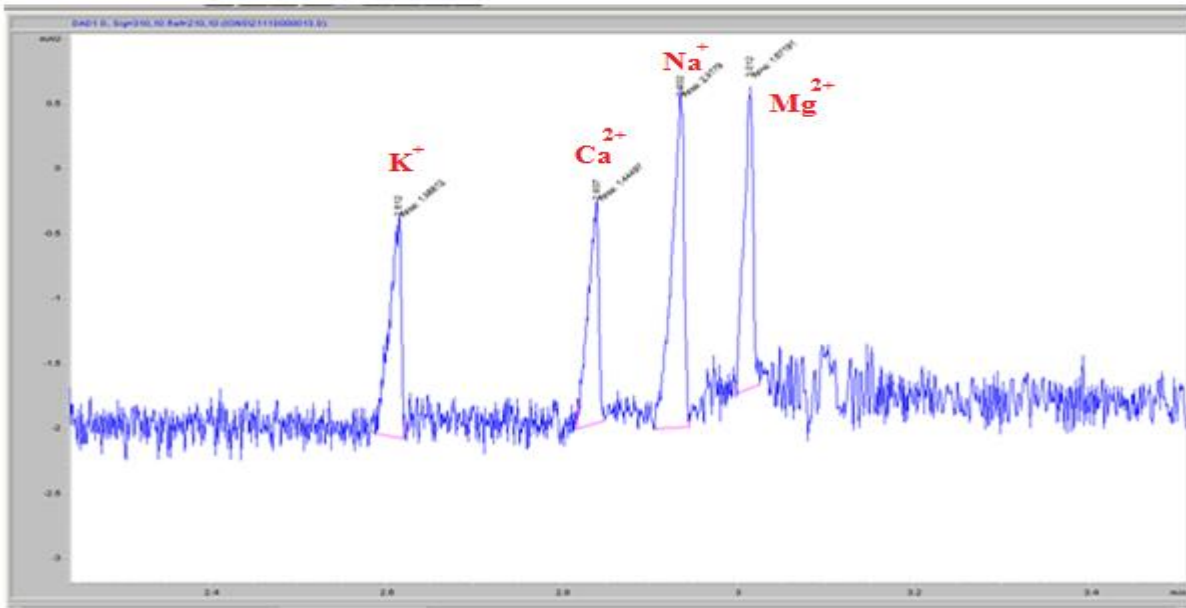


Figure 5.57: Electropherogram showing 15 ppm concentration of the cations standard.

In Figure 5.58, the profile shows the respective cations concentrations according to their ionic strengths in the river water 2 (RW 2) sample. It can be seen also that the cations concentrations in the environmental water sample are very high except for potassium ions found in least amount. Furthermore, the rest of the environmental water samples were analysed and their electropherogram profiles depicted their respective intensities similar to the anions and cations profiles already presented.

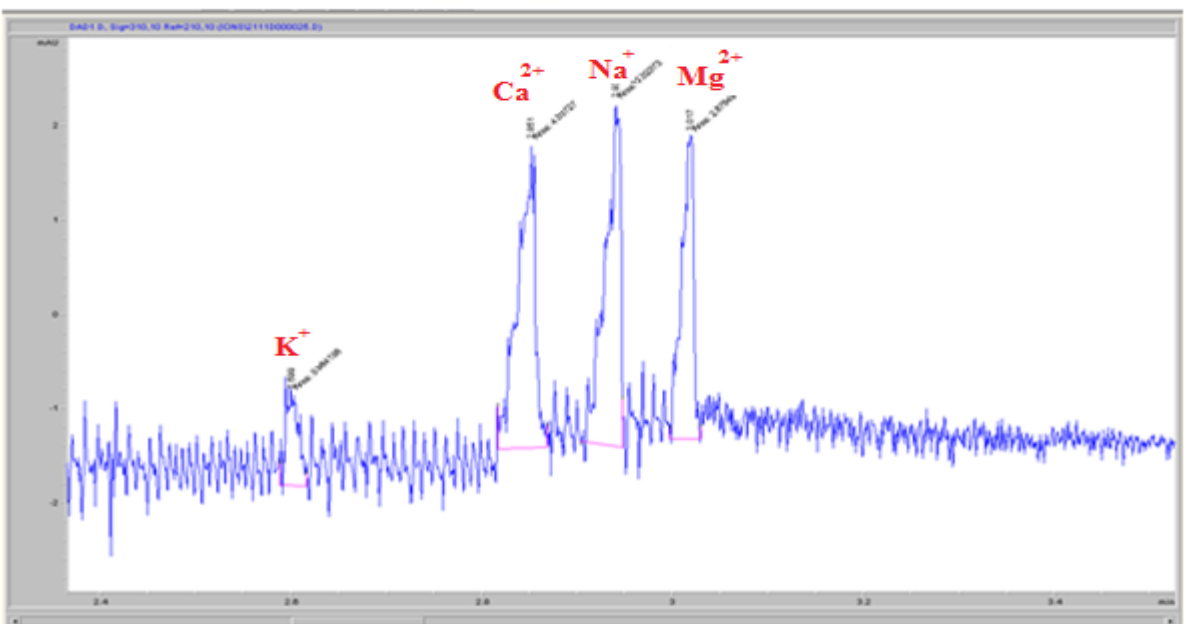


Figure 5.58: Electropherogram showing the cations profile for river water 2 (RW 2) sample.

Table 5.48 shows the concentration calibration range for both anions and cations, the CZE indirect-UV analysis for cations has the polarity from anode to cathode, and the analysis for anions has the polarity from cathode to anode.

Table 5.48: Calibration data of inorganic cations (metals) and anions measured with CZE-indirect-UV methods

Electrolyte	Analyte	Calibration		R ²	LOD [ppm]	LOQ [ppm]
		range [ppm]	Linear equation			
CZE	Potassium	2 - 20	$y = 0.0849x + 0.0542$	0.9897	1.13	3.39
Indirect-UV	Calcium	2 - 20	$y = 0.0658x + 0.2924$	0.9844	1.07	3.21
(Cations)	Sodium	2 - 20	$y = 0.0933x + 0.4681$	0.9872	0.98	2.94
	Magnesium	2 - 20	$y = 0.0761x + 0.2629$	0.9958	0.96	2.88
CZE	Chloride	1 - 15	$y = 0.5045x + 1.1971$	0.9898	0.14	0.42
Indirect-UV	Sulphate	1 - 15	$y = 0.4417x + 0.1709$	0.9947	0.15	0.45
(Anions)	Nitrate	1 - 15	$y = 0.3877x + 0.0481$	0.9967	0.21	0.63

The limits of detection of individual ions are given with their respective limits of quantifications. Also, their linear equations and the regression coefficients values are stated. As indicated earlier, there are 10 different environmental water samples investigated for the inorganic ions concentration evaluation, ranging from the drinking water supplied to homes for domestic consumption, river water, drilled well water, water from the taps in the laboratory, and milli-Q water.

The result of these evaluations is presented in Figures 5.59 and 5.60, giving the details of the respective concentrations of the different anions and cations.

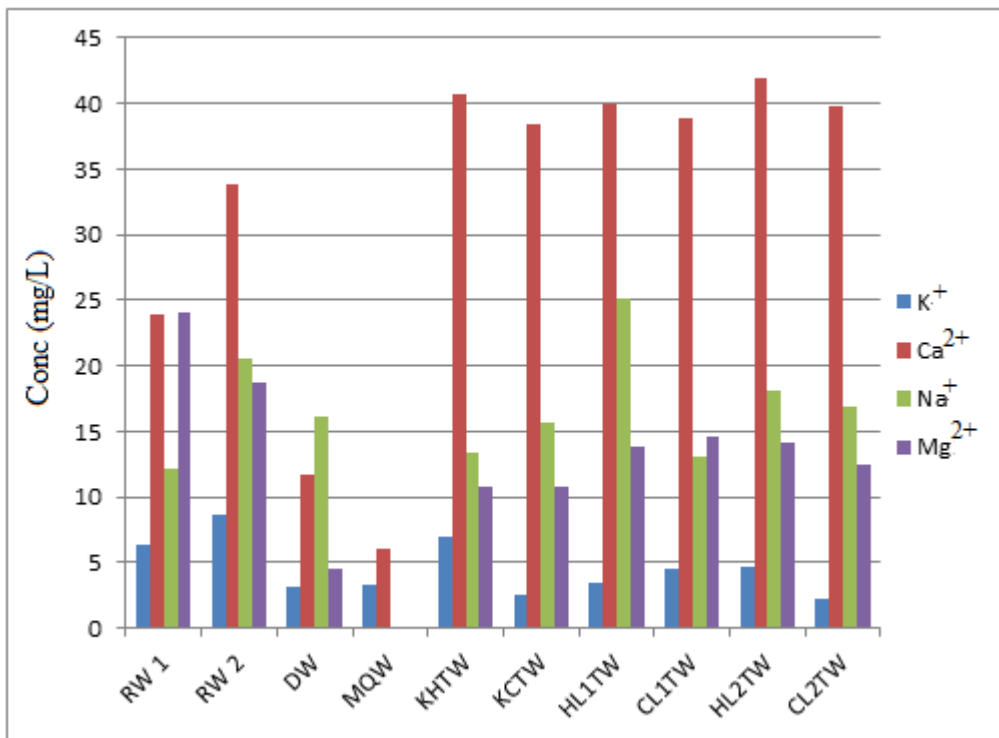


Figure 5.59: Cations in the drinking and environmental water samples

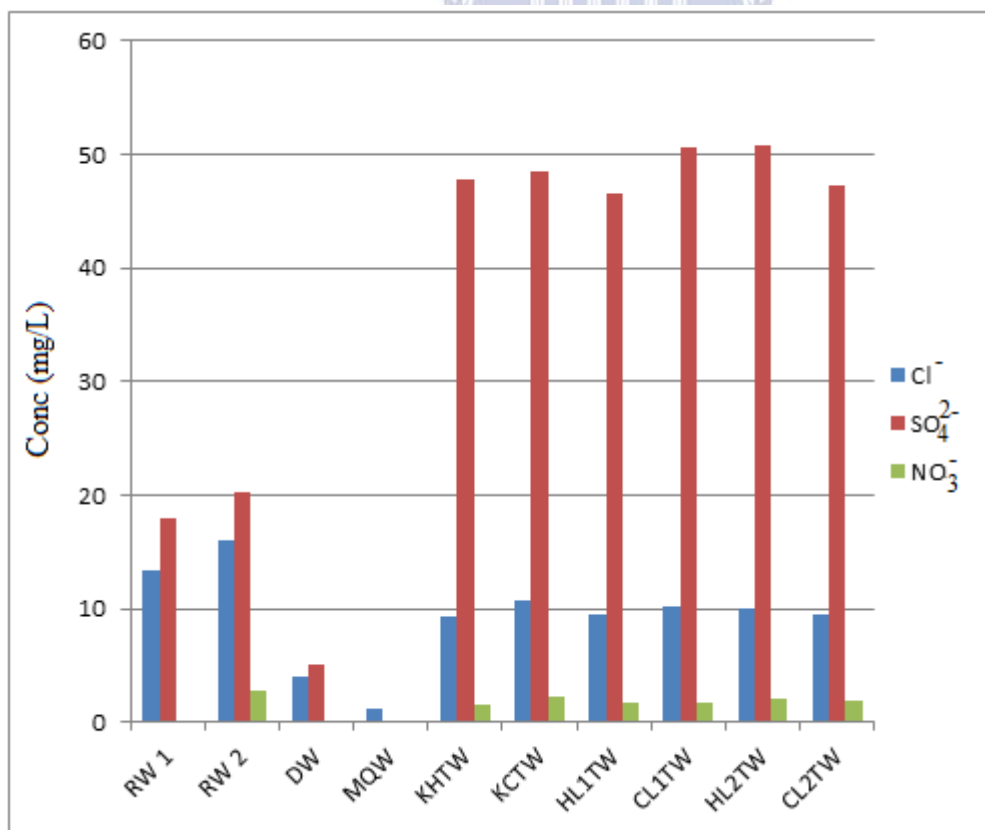


Figure 5.60: Anions in the drinking and environmental water samples.

In Figures 5.59 and 5.60, the water samples represented include RW 1 (river water 1), RW 2 (river water 2), DW (drilled well water), MQW (milli-Q water), KHTW (kitchen hot tap water), KCTW (kitchen cold tap water), HL1W (hot laboratory 1 tap water), CL1W (cold laboratory 1 tap water), HL2W (hot laboratory 2 tap water), and CL2W (cold laboratory 2 tap water) respectively. The results of the CZE-indirect-UV analyses in Figure 5:59 showed that in all the tap water samples, the main inorganic cationic compounds were Na (< 26 mg/L), K (< 8 mg/L), Ca (< 41 mg/L) and Mg (< 15 mg/L). The two river water samples also showed the amounts of inorganic cations to be Na⁺ (< 21 mg/L), K⁺ (< 9 mg/L), Ca²⁺ (< 34 mg/L) and Mg²⁺ (< 25 mg/L). The drilled well water sample also contained all the four inorganic cations in these respective amounts: Na (< 17 mg/L), K (< 4 mg/L), Ca (< 12 mg/L) and Mg (< 5 mg/L). The milli-Q water sample contained the least of all the inorganic cations, and was devoid of both sodium and magnesium ions respectively; this can be attributed to the purification process it was subjected to, since milli-Q water is being used for analytical purposes. In all the water samples, calcium ions have the highest concentrations of inorganic cations, except in drilled well water where the sodium ions were the highest. Furthermore, the average order of the inorganic cations concentration in all the 10 water samples is given as calcium > sodium > magnesium > potassium.

In the inorganic anions results of the CZE-indirect-UV analyses, it can be observed in Figure 5.60 that in all the tap water samples, the main inorganic anionic compounds were Cl⁻ (< 11 mg/L), SO₄²⁻ (< 51 mg/L), NO₃⁻ (< 3 mg/L). Subsequently, the two river water samples (RW 1 & 2) also showed the amount of amounts of the inorganic anions to be Cl⁻ (< 17 mg/L), SO₄²⁻ (< 21 mg/L), NO₃⁻ (< 3 mg/L). In fact, there was no nitrate detected in the RW 1 sample, but an amount of 2.767 mg/L was detected in the RW 2 sample. The drilled well water sample only contained Cl⁻ (< 4 mg/L), SO₄²⁻ (< 6 mg/L), and there was no nitrate detected in the drilled well water sample. The milli-Q water (MQW) only contained chloride in the smallest concentration amount, compared to the rest of the 10 water samples, with the amount Cl⁻ (< 2 mg/L).

Generally, it can be observed that sulphate ions have the highest anion concentrations across all the 10 water samples, followed by chloride, and then nitrates are found in the least amount across the respective water samples. The river water samples contained the highest concentrations of the chlorides, followed by the tap water samples, the drilled well water (DW), and the milli-Q water (MQW) samples respectively.

According to observations in this study, the clean-up techniques employed in the wastewater treatment plants did not entirely remove the steroid hormones in aqueous media. As mentioned earlier, the environmental waters are made up of organics and metals that may complex the steroids from other sources. These processes take place during the pre-treatment process, through deconjugation and reactivation in that process, or by the enzymes used in the wastewater treatment (Heli & El Fellah, 2016). Furthermore, this study has efficiently displayed sample preparation methods to selectively quantify a wide range of steroid components even at insignificantly low concentrations.

5.8 Chapter summary

In this chapter, the major objectives are to optimise the operating parameters (both chemical and instrumental) affecting the capillary electrophoresis; to identify and quantify the pharmaceutical compounds (including acetaminophen, diclofenac, aspirin, salicylic acid, ibuprofen and sulphamethoxazole) present in the influent and effluent environmental water samples, including drinking water supplied to homes, using the capillary zone electrophoresis (CZE) methods; to also identify the steroid hormone compounds (including androstenedione, testosterone, 17- β -estradiol and progesterone) present in the drinking water, influent and effluent environmental samples, using the partial-filling micellar electrokinetic capillary chromatography methods; and to determine the inorganic ions (anions and cations) present in the environmental water samples, using capillary electrophoresis with an indirect-UV detection.

In terms of the optimisation of the capillary electrophoresis (CE) instrument, this chapter has been able to elucidate the different parameters that affect the performance of the equipment. These parameters include: voltage which affects the field strength; the pH of the electrolyte solution that affects the separation and dissociation of the analytes according to their pKa values; and the injection type used which affects the detectability of the instrument. Furthermore, the capillary zone electrophoresis (CZE) with UV detection was employed in the identification and quantification of pharmaceuticals. For influent A sample, aspirin was quantified to be 13.52 ng/L, diclofenac as 14.15 ng/L, salicylic acid as 6.514 ng/L and sulphamethoxazole as 11.79 ng/L respectively. The influent B water sample contained 4.23 ng/L of aspirin, 8.235 ng/L of diclofenac, 1.199 ng/L of salicylic acid, 1.095 ng/L of

ibuprofen and 13.170 ng/L of sulphamethoxazole respectively. And in the effluent water samples of sewage water treatment plants the measurable pharmaceuticals quantities include 0.836 ng/L of aspirin, 0.802 ng/L of diclofenac, 1.343 ng/L of salicylic acid, 0.842 ng/L of ibuprofen and 10.241 ng/L of sulphamethoxazole.

The partial-filling micellar electrokinetic capillary chromatography (PF-MEKC) method was adopted for the identification and quantification of the steroid hormones. In the influent A water sample, androstenedione was quantified to be 2.224 ng/L, testosterone was quantified to be 3.474 ng/L, 17- β -estradiol was quantified to be 0.96 ng/L and progesterone was 1.503 ng/L. The influent B water sample contained 2.224 ng/L of androstenedione, 3.142 ng/L of testosterone, 0.954 ng/L of 17- β -estradiol and 0.691 ng/L of progesterone respectively. While in the purified effluent water samples of sewage water treatment plants however, the measurable steroid hormones quantities include 1.205 ng/L of androstenedione, 3.037 ng/L of testosterone, 0.550 ng/L of 17- β -estradiol and 0.440 ng/L of progesterone respectively. The steroid compounds content of the tap water (hot and cold) was also measured. For androstenedione, 0.031 ng/L and 0.025 ng/L were quantified for hot tap water and cold tap water respectively; testosterone accounted for 0.016 ng/L and 0.013 ng/L of hot tap water and cold tap water respectively; 17- β -estradiol accounted for 0.11 ng/L and 0.09 ng/L of hot tap water and cold tap water respectively; while progesterone gave 0.049 ng/L and 0.031 ng/L of hot tap water and cold tap water respectively.

Subsequently, the capillary zone electrophoresis (CZE) with an indirect UV detection was successfully employed in the quantification of the anions and cations in the environmental wastewaters. These analyses were able to show that the drinking water, including the environmental water samples contain anions and cations; the cations studied include sodium, potassium, calcium and magnesium ions respectively, and their quantities were given. Also, the anions studied include chloride, sulphate and nitrate, and their respective quantities were highlighted in this chapter.

The novelty of this research study is the development of the CZE-UV methods for the determination of selected pharmaceuticals including: acetaminophen, aspirin, diclofenac, ibuprofen, salicylic acid and sulphamethoxazole; and the use of PF-MEKC-UV method for the determination of steroids, including: androstenedione, testosterone, 17-beta-estradiol, and

progesterone in influent and effluent wastewaters, cold and hot tap waters; and two CZE-UV methods used for ion analyses.



UNIVERSITY *of the*
WESTERN CAPE

CHAPTER SIX

APPLICATION OF SILVER NANOPARTICLES-COATED POLYMER MEMBRANE IN THE DETECTION OF ORGANIC POLLUTANTS USING SURFACE-ENHANCED RAMAN SPECTROSCOPY

6 Introduction

In this chapter, the detailed results are presented of the modified and unmodified track-etched polyethylene terephthalate (PET) membrane, silver nanoparticles synthesis, and silver nanoparticles immobilisation on the surface of amine-modified track-etched PET membrane. The chapter also encompasses the discussion involving the procedures leading to a silver-coated track-etched PET membrane meant for the detection of an organic pollutant (acetaminophen as an example) in water with the use of surface-enhanced Raman spectroscopy (SERS).

The characterisation techniques employed in the fabrication of a silver-coated track-etched PET membrane include the following: Contact angle measurement, Fourier transform infrared (FTIR), Raman spectroscopy, Scanning electron microscopy (SEM), thermogravimetric analysis (TGA), UV-Vis spectroscopy, X-ray photoelectron spectroscopy (XPS), and zeta (ζ) potential.

The contact angle measurement was done to study the water attraction behaviour of the surface of the modified and unmodified track-etched PET membranes. Thermogravimetric analysis was used in the investigation of thermal effect arising from solid/liquid interface organic reaction of surface of track-etched PET membranes and diethylenetriamine solution and due to immobilisation of silver nanoparticles on the surface of amine-modified track-etched PET membrane. The ImageJ software was used in the calculation of size of the silver nanoparticles from the SEM images. While the Zeta potential technique was used for the determination of the stability of colloidal silver nanoparticles.

The chapter also details the results and discussion of the detection of acetaminophen and 4-aminothiophenol (4-ATP) on a modified surface of track-etched polyethylene terephthalate (PET) membrane. The results and the applicability of surface-enhanced Raman spectroscopy using silver-coated surface of track-etched PET membranes (10-AgPET, 20-AgPET and 30-

AgPET samples) for detection of acetaminophen and 4-aminothiophenol (4-ATP) were also discussed. The objective was to determine whether the silver-coated track-etched PET membranes would be able to enhance a weak Raman signal resulting from Raman scattering by acetaminophen and 4-aminothiophenol (4-ATP) molecules on the surface. The samples 10-AgPET, 20AgPET and 30-AgPET were prepared as described in Section 3.8.2.3. The samples were characterised by Raman spectroscopy as outlined in Section 3.9.3.

6.1 Track-etched polyethene terephthalate membrane chemical modification

Aminolysis of the surface of track-etched polyethene terephthalate (PET) membrane is one of the wet chemistry methods used to introduce amines on the surface of the polymer membrane via an amide bond. This wet chemistry method was employed in this study to modify the surface of the track-etched PET membrane. The organic reaction of the solid/liquid interface which involves polyethene terephthalate on the surface of track-etched PET membrane and diethylenetriamine solution results in scission of the ester bond and formation of amide bond. In a brief, the optimised experimental set up involved the immersion of a 3 x 3 cm track-etched PET membrane in aqueous solution of diethylenetriamine with the concentrations and for the time durations specified in Section 3.8.2.1. After this process, the track-etched PET membrane was washed with a suitable amount of water/ethanol mixture (1:1 v/v). The rinsed membranes were immersed in 1 mM of hydrochloric acid for 1 hour at ambient conditions. The track-etched PET membrane activated with 1 mM of hydrochloric acid was then immersed in a mixture of 1% trisodium citrate and 1 mM silver nitrate solution at a temperature and time specified in sections 6.2 and 6.3 respectively. In the solid/liquid interphase of the organic reaction, the variable parameters were the concentration of diethylenetriamine (100%, 80% or 60%) and the reaction times (20 hours, 15 hours or 10 hours). In the synthesis and immobilisation of silver nanoparticles on amine-modified track-etched PET membrane, the parameters that were varied include the temperature and time of reduction reaction of silver nitrate and the volume of 1% trisodium citrate. The reaction equation for this synthesis is shown in Figure 6. 1 (Irena *et al.*, 2009).



Figure 6.1: Aminolysis reaction equation.

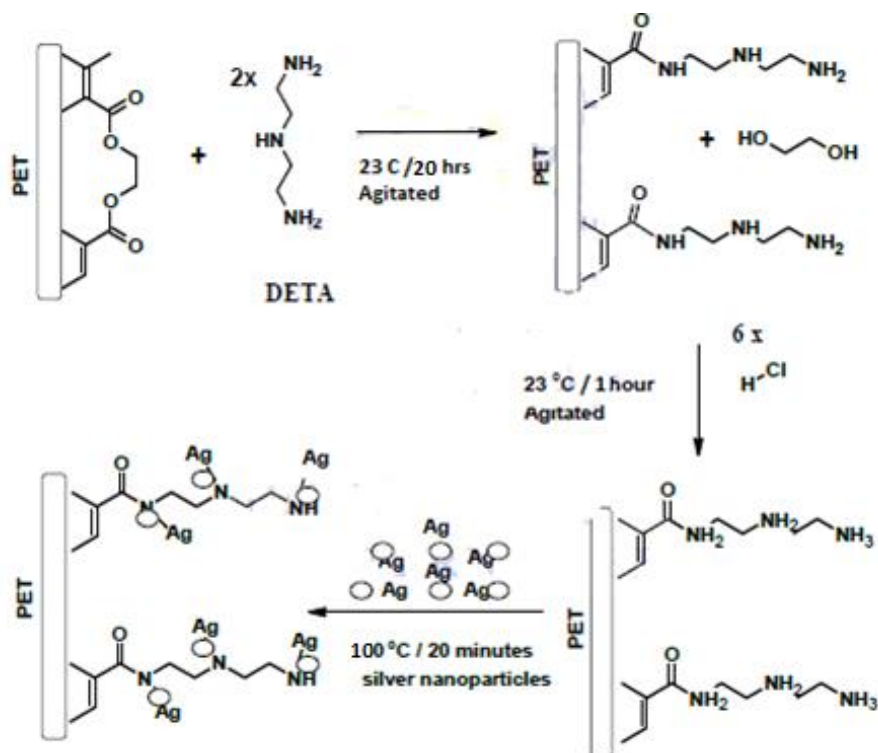


Figure 6.2: Modification mechanism of PET membrane with DETA and immobilisation of silver nanoparticles on the modified surface.

In Figure 6.2, the reaction pathway for the aminolysis reaction at the solid/liquid interface is displayed. A lone pair of electron on the nitrogen of diethylenetriamine attacks the partially positive carbon of carbonyl ester. The aminolysis results in the cleavage of the ester bond and formation of the amide bond losing the glycol moiety from the surface of the PET membrane. When the surface of the amine-modified track-etched PET membrane is activated with hydrochloric acid, it leads to the protonation of the nitrogen in the amine. Thereafter, silver nanoparticles were immobilised on the surface of amine-modified track-etched PET membrane through the protonated nitrogen.

6.2 Aminolysis of the track-etched polyethylene terephthalate (PET) membrane

The fixed and variable parameters presented in Table 6.1 were chosen in order to avoid serious degradation of the bulk of the track-etched PET membranes. All reactions were done at ambient conditions as described in 3.8.2.1.

Table 6.1: Sample codes for Fourier transform infrared and X-ray photoelectron spectroscopy with fixed and variable parameters (time of reaction and concentration of diethylenetriamine)

Sample code	Fixed condition	Variable condition
100A-PET	Time of reaction – 20 hours	Concentration of DETA (100%)
80A-PET	Time of reaction – 20 hours	Concentration of DETA (80%)
60A-PET	Time of reaction – 20 hours	Concentration of DETA (60%)
20-APET	Concentration 100%	Time of reaction (20 hours)
15-APET	Concentration 100%	Time of reaction (15 hours)
10-APET	Concentration 100%	Time of reaction (10 hours)
Con-PET	0 (% DETA)	0 (hours)

6.2.1 Analysis using the FTIR

The Fourier transform infrared (FTIR) was employed in the comparison of the different wet chemistry modifications of polyethylene terephthalate (PET) membrane using diethylenetriamine (DETA). The FTIR results are presented in two sets. The first results pertain to the reaction time studies, while the other set of results are based on the concentration of diethylenetriamine (DETA).

6.2.1.1 Study of the reaction times for surface modification

The reaction times study results are presented alongside the discussion for FTIR analysis. The study of the reaction times was carried out as described in Section 3.8.2.1. The diethylenetriamine (DETA) concentration was kept constant at 100%; while the reaction was carried out at ambient conditions for 10 hours, 15 hours or 20 hours. The modified track-etched PET membranes are coded 20-APET, 15-APET, 10-APET and the unmodified track-etched PET membrane coded Con-PET (Table 6.1). The sample named Con-PET refers to the control. Figure 6.3 shows the results of the reaction times study. The concentration of DETA was the fixed parameter, while the time of reaction was the variable parameter at ambient.

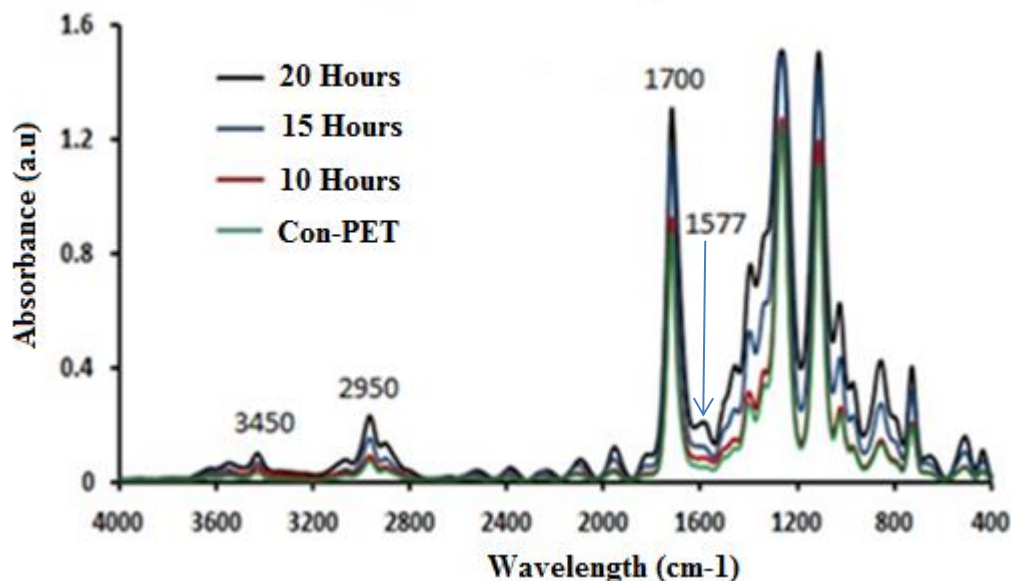


Figure 6.3: FTIR spectra for the unmodified track-etched PET membrane (Con-PET) and the modified track-etched PET membrane at 100% concentration of DETA and varied reaction times 10 hours (10-APET), 15 hours (15-APET), and 20 hours (20-APET).

The FTIR results show the change in absorbance in the region between 1500 cm^{-1} and 1600 cm^{-1} . The region shows the C-N bond stretching of PET membrane which has been exposed to diethylenetriamine for 15 hours and 20 hours. The absorbance peak for amide I bond occurs at 1648 cm^{-1} and the amide II occurs at 1577 cm^{-1} . However, when both exist in a molecule, the most prominent one overshadows the less prominent one (Drobota *et al.*, 2013). In Figure 6.3, the amide II is the most prominent as seen from its absorbance peak which appears at 1577 cm^{-1} . Therefore, the amide II absorbance peak overshadows that of amide I bond. Subsequently, the introduction of amine from DETA contributed to another notable change in absorbance peaks occurring between 3400 cm^{-1} and 3500 cm^{-1} . The absorbance peak change occurring at 3450 cm^{-1} emanates from N-H bond stretching. The peak of the absorbance spectra increases in size and depth with an increase in the time of reaction from zero for the unmodified track-etch PET membrane (Con-PET) to the PET membrane which was reacted with DETA for 20 hours (20-APET). An observed change occurred in the absorbance peak at 2950 cm^{-1} that is attributed to the ethylene C-H bond stretching from diethylenetriamine (the modifying agent). Nevertheless, there happens to be a loss of glycol with the ethylene moiety, but the introduction of DETA brings in two ethylene moieties. The absorbance peak change occurring between 3400 and 3500 cm^{-1} as a result of the introduced amine (N-H) is not really conspicuous, and this is in agreement with the observations by

Irena *et al.*, (2009), where that change is attributed to the aliphatic amine in the range between 3400 and 3500 cm^{-1} . The spectra of PET membranes which were exposed for 20 hours to diethylenetriamine solution show clearly the amide bonds' vibration band of 1500 to 1600 cm^{-1} , as observed by Drobota *et al.*, (2013). When the liquid/solid interface reaction occurs, the longer it is left to occur, the more prominent are the absorbance peaks for the amide. Findings from this study showed that the absorbance peaks at 3450 cm^{-1} and 2950 cm^{-1} of the track-etched PET spectra vary with the reaction time. As a result, an inference can be drawn that the longer the reaction time between the surface of the PET membrane and DETA, the more intense the notable changes in the absorbance peaks. This explains why 20-APET, treated for 20 hours gave a noticeable change in absorbance peak intensity, serving as an indication for the surface modification of the PET membrane.

The proposed reaction mechanism in Figure 6.2 is confirmed by the results in Figure 6.3. In Figure 6.2, an amide bond was attached to the surface of the PET membrane via a scission of the ester bond in polyethylene terephthalate, hence, the formation of an amide (C-N) bond (Drobota *et al.*, 2013). It can therefore be deduced that the results in Figure 6.3 are in agreement with the literature which states that track-etched PET membrane surface modification with amines results in the formation of the amide bond and the introduction of amines on the surface (Fatiyants *et al.*, 2013). Nissen *et al.*, (2008) observed that treating the membrane at high temperatures degrades its tensile strength. Therefore, in this research study, the concentration of the diethylenetriamine and the reaction time were optimised in order to determine the optimal surface modification conditions for the track-etched PET membrane at room temperature.

6.2.1.2 Modification concentration studies

The diethylenetriamine concentration studies were conducted as described in Section 3.8.2.1. Equal pieces of 3 x 3 cm track-etched polyethylene terephthalate (PET) membranes were immersed in aqueous solution of 100%, 80% or 60% diethylenetriamine (DETA) concentrations. The reaction was carried out at ambient conditions for a constant period of 24 hours. The FTIR spectra of the modified track-etched PET membranes are given the codes 100A-PET, 80A-PET, 60A-PET and unmodified track-etched PET membrane Con-PET. Con-PET served as a control. The concentration of DETA studies results are displayed in Figure 6.4. The DETA concentration was the varied parameter and the time of reaction was the fixed parameter at ambient conditions.

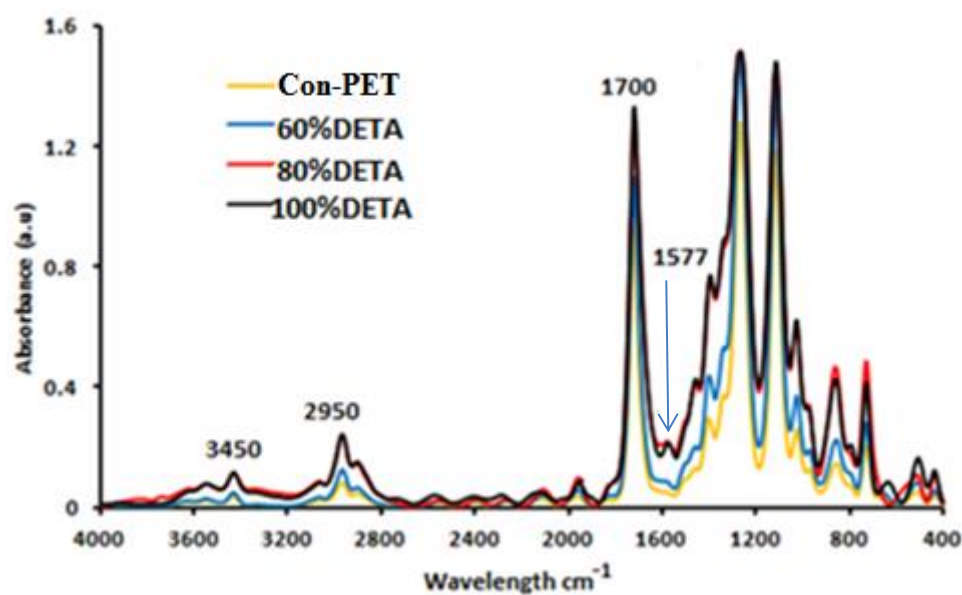


Figure 6.4: The FTIR spectra of unmodified track-etched PET membrane (Con-PET) and modified track-etched PET membranes at 24 hours reaction time and variable concentration of DETA of 100% (100A-PET), 80% (80A-PET), and 60% (60A-PET).

The FTIR results from the variation of concentrations of DETA follow a similar trend as the ones observed in the reaction time studies, where the time of reaction was the varied parameter and DETA concentration the fixed parameter as illustrated in Figure 6.3.

It can be seen in Figure 6.4 that the absorbance peak at 2950 cm⁻¹ becomes more prominent with the increase in DETA concentration. The absorbance peak at 2950 cm⁻¹ can be attributed to the C-H bond stretching from the ethylene moieties. The peak was attributed to the surface modification with DETA having two ethylene moieties in its molecular structure. Also,

another similar increase of the absorbance peak centred at 3450 cm^{-1} was observed too. This increase can be attributed to the N-H stretching. The N-H stretching vibrations are attributed to the amine moieties introduced on the surface from DETA. The absorbance band which appeared in the region between 1500 cm^{-1} and 1600 cm^{-1} is observed in the samples 100A-PET, 80A-PET and 60A-PET that were reacted with aqueous diethylenetriamine at concentrations of 100%, 80% and 60% respectively.

Similarly, the changes observed in Section 6.2.1.1 as regards the time studies can also be observed in Figure 6.4. The appearance of amide I being more pronounced in the spectral region of $1500\text{ -}1600\text{ cm}^{-1}$ when the track-etched PET membrane was reacted with 100% concentration of DETA. Also, it was reported in the literature that the bands of amide I and amide II were observed as a single absorbance peak, rather than separate absorbance peaks for a modified track-etched PET membrane which was subjected to aminolysis with the use of other amines such as ethylenediamine (Xue & Lu, 2013). Aqueous DETA solution (100%) resulted in the emergence of amide I and amide II bands assigned to stretching vibrations (N—C=O) which overlap each other between 1500 cm^{-1} and 1600 cm^{-1} . The presence of amide I and II bands on the FTIR spectra of the PET membrane which were subjected to DETA at different concentrations proves that the surface of the track-etched PET membrane was modified in each case. The peaks in the sample 100A-PET that was exposed to 100% concentration of DETA showed the greatest intensity.

6.2.2 X-ray photoelectron spectroscopy analysis

The analysis by the X-ray photoelectron spectroscopy (XPS) is to complement the Fourier transform infrared (FTIR) results. The purpose of the characterisation of the modified and unmodified track-etched polyethylene terephthalate membrane using X-ray photoelectron spectroscopy (XPS) is to actualise the elemental analysis of the track-etched PET membrane surfaces. The results of the XPS analysis presented in this section are for the unmodified track-etched polyethylene terephthalate (PET) membrane and a DETA-modified surface of PET membrane, with the codes Con-PET and 100A-PET respectively. The sample with the highest concentration of DETA (100A-PET) was the sample used for this analysis because it had the clearest FTIR results; the Con-PET sample serves as the control (unmodified track-etched PET membrane). The aminolysis of the sample 100A-PET was carried out by the immersion of $3 \times 3\text{ cm}$ PET membrane in 100% diethylenetriamine aqueous solution for 24 hours. Both samples (100A-PET and Con-PET) were characterised in the manner described

in Section 3.9.7. Both variable and fixed parameters used to prepare the samples are as given in Table 6.1. Table 6.2 shows the elemental percentages on the surfaces of 100A-PET and Con-PET samples.

Table 6.2: Elemental percentages from X-ray photoelectron spectroscopy for the surface of unmodified (CO-APET) and modified (75A-PET) track-etched PET membranes

Track-etched PET membrane	Atomic Percentage		
	Carbon (C1s)	Nitrogen (N1s)	Oxygen (O1s)
Con-PET	72.589	nil	27.407
100A-PET	72.538	4.958	22.498

The results showed the change in elemental percentages between the unmodified and modified samples. It can be seen in the XPS results that only the elemental carbon and oxygen were present on the surface of unmodified track-etched PET membrane named Con-PET, prior to the exposure of the membrane to DETA solution. The control sample Con-PET was devoid of nitrogen (N1s) atoms on its surface; while the amine-modified track-etched PET membrane sample (100A-PET) had a nitrogen atom (N1s) content percentage of 4.958% on its surface. As a consequence of the modification of the PET membrane by diethylenetriamine (DETA), XPS proved the presence of nitrogen (N1s) on the surface of the 100A-PET sample, indicating the replacement of some oxygen content already displaced via the process of aminolysis, involving the ester bond scission and formation of an amide bond (Noel et al., 2013). Amine and amide moieties are thus present on the surface of the amine-modified track-etched PET membrane, with the prominent presence of nitrogen as depicted in Table 6.2.

The general survey graphs of the X-ray photoelectron spectroscopy for both track-etched PET membrane samples (Con-PET and 100A-PET) which also includes the elemental compositions are given in Figure 6.5.

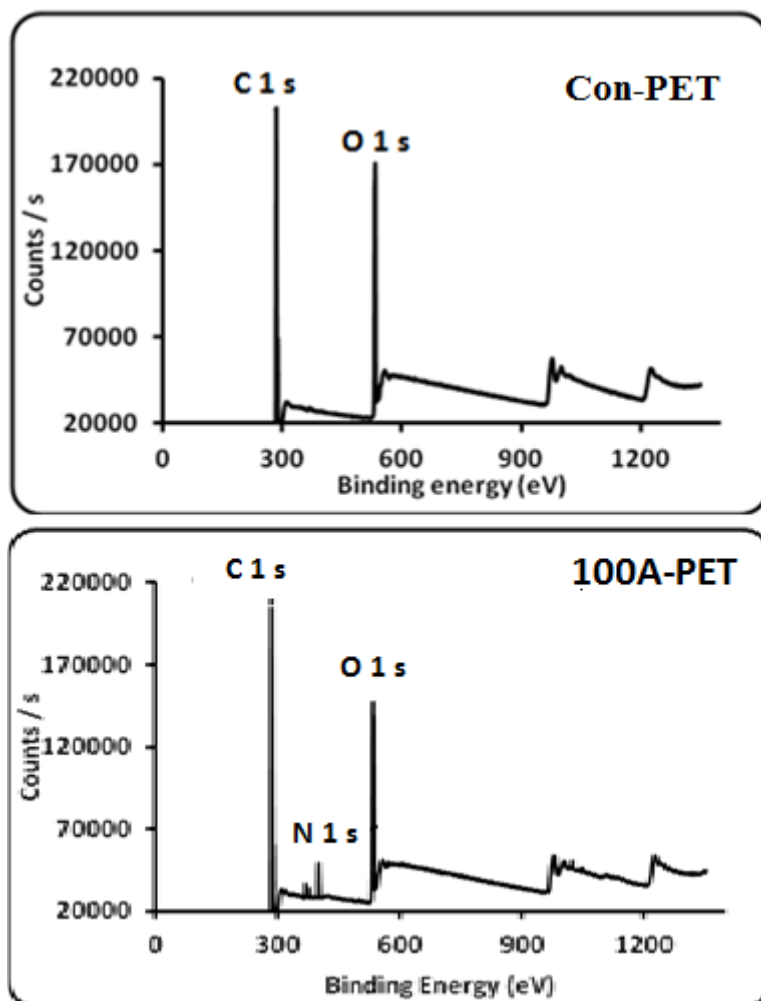


Figure 6.5: X-ray photoelectron spectroscopy general survey graphs of unmodified track-etched PET (Con-PET) and modified track-etched PET (100A-PET) showing elements within the detection limits.

Figure 6.5 presents the general survey graphs depicting the elemental peaks that make up the surface composition of PET membrane before and after modification with DETA. The X-ray photoelectron spectroscopy general surveys depict elements within the detection limits, and this is based on the chemical composition of the surface of the track-etched PET membrane. The peaks of carbon (C1s), oxygen (O1s) and nitrogen (N1s) are in the binding energy regions of 285.21 eV, 532.63 eV and 399.61 eV; as shown in the general survey graphs of samples Con-PET and 100A-PET respectively. In the general survey graph for Con-PET, there is no nitrogen peak, while that of 100A-PET displays a nitrogen peak. The general survey graph of 100A-PET shows that nitrogen is present on the surface of the modified track-etched PET membrane. These binding energies as shown in Figure 6.5 are in agreement with the observations reported in the literature (Awasthi *et al.*, 2014; Xue & Lu, 2013).

Figure 6.6 shows the chemical states of nitrogen (N1s) and carbon (C1s) on the surface of amine-modified track-etched PET membranes. The sample 100A-PET gives the chemical state graph for nitrogen (N1s). Also, the chemical state graph for carbon (C1s) shows the results for both samples Con-PET (0% DETA) and 100A-PET (100% DETA). The chemical state graph of carbon (C1s) depicts the chemical states of carbon when the PET membrane was not modified (sample Con-PET) and the subsequent changes that happened after the modification of the track-etched PET membrane (sample 100A-PET).

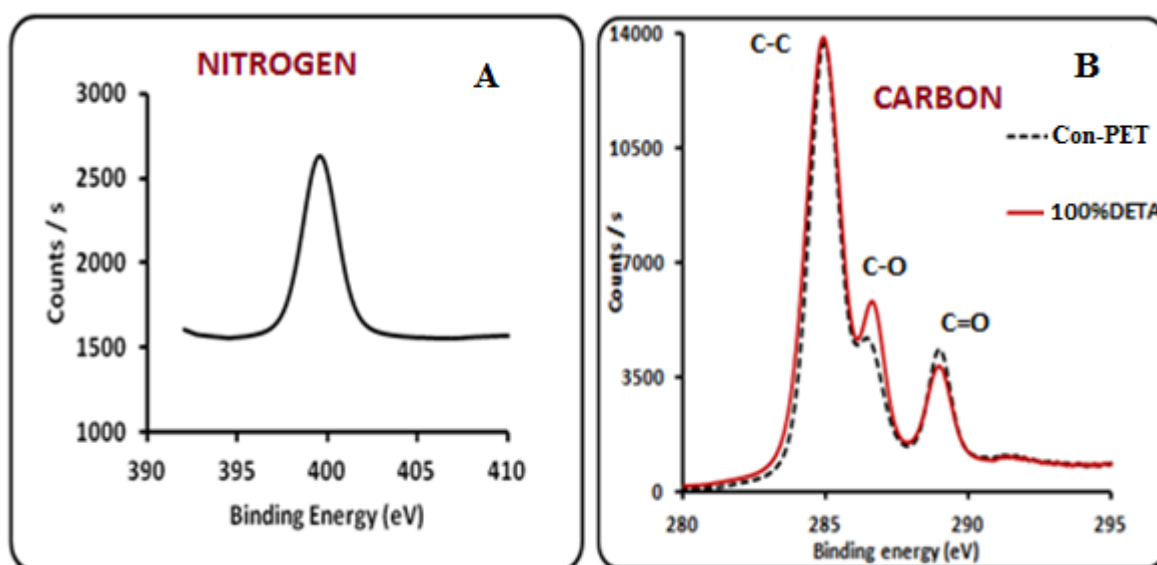


Figure 6.6: X-ray photoelectron spectroscopy spectra of N1s peaks of amine-modified track-etched PET (A) and C1s peaks for both unmodified (dotted black) and amine-modified (red) PET membrane (B).

Furthermore, the magnified N1s shell scan in Figure 6.6A shows the chemical state of nitrogen on the surface of the modified track-etched PET membrane sample with the code 100A-PET. In the graph in Figure 6.6A, it can be seen that the spectra peak for N1s is at a binding energy of 399.61 (≈ 400) eV which is known to be for nitrogen in the chemical state of C-NH₂ (Makiabadi *et al.*, 2010). However, in Figure 6.6B, the C1s scan reveals the chemical states of carbon from both samples (Con-PET and 100A-PET). The shell scan of C1s reveals three symmetrical peaks with binding energies at 284.9, 286.6 and 288.9 eV for the chemical states of C-C, C-O and O-C=O respectively (Vesel *et al.*, 2008). These peaks for the C1s spectra are characteristic peaks observed for polyethylene terephthalate polymer membranes.

The satellite peaks π - π^* observed, though not significantly pronounced between 291 and 292 eV is characteristic of polyethylene terephthalate polymer materials (Awasthi *et al.*, 2014; Basri *et al.*, 2011). In Figure 6.6B, it is shown that the changes in the peak heights of C-C and O-C=O, are as a result of the introduction of two ethylene (C-C) moieties from DETA, replacing one ethylene moiety in glycol and the formation of an amide bond (C-N) which replaces O-C=O with N-C=O. These changes in the peak heights occurring due to the changes in the chemical state of carbon are given in Table 6.3.

Table 6.3: The changes in peak heights of carbon chemical states

Elements chemical state	Peak height (count/second)	
	Con-PET	100A-PET
C-C	13.157	13.364
C-O	3.207	4.229
O-C=O	3.430	2.889

The formation of the amide bond results in the change in chemical state of carbon in O-C=O as can be observed in the reduction of the O-C=O peak height from 3430 to 2889 counts per second. The noticeable change in the C-O peak height is not the expected result, what is expected would be the reduction in height of the C-O spectrum peak as a result of the glycol loss during aminolysis. The reason could be that atmospheric carbon existing in C-O chemical state may have contributed during aminolysis reaction or storage.

6.3 Silver nanoparticles synthesis and immobilisation on polyethene terephthalate (PET) membrane

The results presented in this section and the subsections related to it are for the synthesis and immobilisation of silver nanoparticles on the surface of the modified track-etched polyethene terephthalate (PET) membrane. Section 3.8.2.2 gives the detailed experimental procedure for the synthesis of silver nanoparticles. Similarly, the laboratory experimental procedure for the immobilisation of silver nanoparticles on the modified surface of the polyethene terephthalate membrane (PET) is described in Section 3.8.2.3.

6.3.1 Silver nanoparticles synthesis and characterisation

In this section, the ultraviolet-visible spectroscopy (UV-Vis) results of the colloidal silver nanoparticles are presented. The results involve the optimisation studies for the synthesis of colloidal silver nanoparticles. The parameters studied in the optimisation include: volume of reducing agent, temperature of reduction, and time of reduction. For the study in which the reaction time was varied, temperature of reaction and volume of trisodium citrate were fixed parameters at ambient conditions. These samples were given codes 10-AgNP, 15-AgNP, 20-AgNP, 25-AgNP and 30-AgNP denoting the time series. Also, in the temperature variation series, the time of reaction and volume of trisodium citrate were fixed parameters, these samples were given codes 100C-AgNP, 90C-AgNP and 80C-AgNP denoting the temperature series. When the volume of trisodium citrate was the varied parameter, the temperature and time of reaction were fixed parameters. These samples were codes 1mL-TriNa, 2mL-TriNa, 3mL-TriNa and 4-TriNa respectively, denoting the volume series.

The synthesis of silver nanoparticles was achieved by adding varying volumes (1 mL, 2 mL, 3mL and 4 mL) of 1% of trisodium citrate to the already-heated 100 mL of 1 mM of silver nitrate solution for varying times (10 minutes, 15 minutes, 20 minutes, 25 minutes, and 30 minutes) at varying temperatures (100 °C, 90 °C and 80 °C). As one parameter was being varied, other parameters were kept constant.

6.3.1.1 Ultraviolet-visible spectroscopy of silver nanoparticles

The ultraviolet-visible (UV-Vis) spectroscopy technique is a widely used structural characterisation for silver nanoparticles. The silver nanoparticles that have surface plasmon excitation, show intense plasmonic peaks between the 380 nm and 450 nm absorption band of the ultraviolet-visible region (Aboul-el-Nour *et al.*, 2010).

6.3.1.2 Effect of temperature on silver nanoparticles synthesis

The effect of temperature studies on the synthesis of silver nanoparticles were carried as described in Section 3.8.2.2, and the respective sample codes are as given in Table 3.5 of Section 3.8.4. The temperature of the reaction was the variable parameter at 100 °C, 90 °C, or 80 °C. The fixed parameters were the time of reaction at 20 minutes and 2 mL volume of 1% trisodium citrate. The results for the temperature of reaction studies are shown in Figure 6.7.

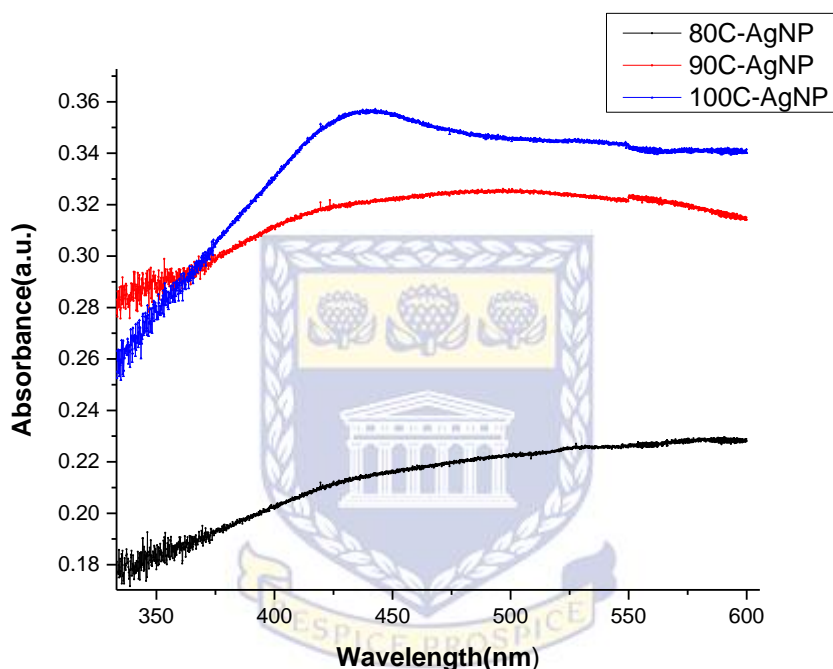


Figure 6.7: Ultraviolet-visible spectra of silver nanoparticles synthesised for 20 minutes using 2 mL of 1% trisodium citrate at varied temperatures of 100 °C (100C-AgNP), 90 °C (90C-AgNP) or 80 °C (80C-AgNP).

In Figure 6.7, the results depict changes in the plasmonic peaks which are relative to the temperature at which the reaction was done. The sample 100C-AgNP showed the higher plasmonic peak compared to samples 90C-AgNP and 80C-AgNP. As the temperature was increased from 80 °C to 100 °C, the peak height thus increased. The peaks also showed a wavelength shift towards longer wavelength (red shift) as the temperature was increased from 80 °C to 100 °C. This red shift could be attributed to a change in the silver nanoparticles morphology such that as the temperature was raised, so the size of nanoparticles also increased. The increment in peak height with an increase in temperature is a trend that is in agreement with the reviewed literature where it is shown that temperature has an effect on the

synthesis of silver nanoparticles (Khodashenas & Ghorbani , 2015; Abour-el-Nour *et al.*, 2010). The rise in the peak height shows a significant greater amount of silver nanoparticles synthesised at the highest temperature than at lower temperatures. These results indicate the complete reduction of silver ions to elemental silver that grows to form nanoparticles. In the following subsections, the optimisation studies are shown for time of reaction and volume of 1% trisodium citrate.

6.3.1.3 Effect of volume of trisodium citrate on silver nanoparticles synthesis

The effect of the volume of trisodium citrate in the synthesis of silver nanoparticles were carried out as described in Section 3.8.2.2, and the respective sample codes are as given in Table 3.5 of Section 3.8.4. The volume of 1% trisodium citrate was varied at 2 mL, 3 mL or 4 mL. The temperature of reaction at 100 °C and the reaction time of 20 minutes were the fixed parameters. The results of the effect of volume of 1% trisodium citrate on the synthesis of silver nanoparticles are shown in Figure 6.8.

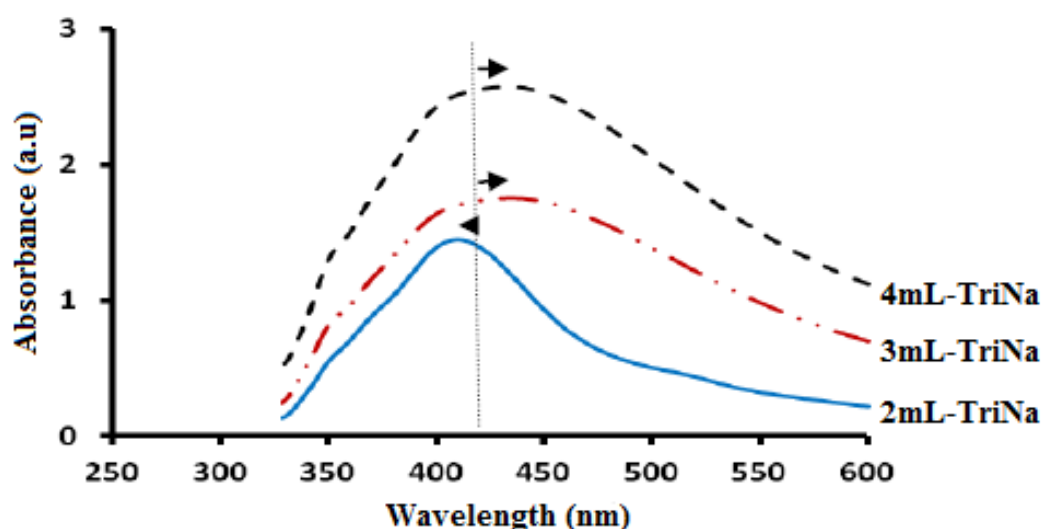


Figure 6.8: Ultraviolet-visible spectra of silver nanoparticles synthesised for 20 minutes at temperature of 100 °C at varied volumes of 1% trisodium citrate of 2 mL (2mL-TriNa), 3 mL (3mL-TriNa) and 4 mL (4mL-TriNa).

The results presented in Figure 6.8 show that as the volume of 1% trisodium citrate added to the silver nitrate solution increased, the plasmonic peak height increased. There is also a shift in wavelength towards longer wavelength (red shift) as the volume of 1% trisodium citrate added to silver nitrate solution (already heated at 100 °C) was increased. The red shift could be attributed to the increase in size of nanoparticles with an increase in volume of 1%

trisodium citrate. The plasmonic peaks became broader in shape, which is characteristic of plasmonic peaks of silver nanoparticles synthesised by the reduction of silver nitrate by trisodium citrate (Qin *et al.*, 2010). The 2 mL-TriNa plasmonic peak representing 2 mL of added 1% trisodium citrate was narrower compared to the 3 mL and 4 mL plasmonic peaks, which were observed in similar trend by Bastus *et al.*, (2014) and Qin *et al.*, (2010). It can therefore be concluded that the lower the volume of 1% trisodium citrate added the narrower the peak and the smaller the nanoparticles. When the 1% trisodium citrate was added in higher volumes, it resulted in rapid nucleation and growth of elemental silver to form nanoparticles of bigger sizes (Taurozzi & Tarabara, (2007).

6.3.1.4 Effect of reaction time on silver nanoparticles synthesis

The effect of reaction time on the silver nanoparticles synthesis was carried out as described in Section 3.8.2.2, and the respective sample codes are as given in Table 3.5 of Section 3.8.4. The time of reaction was the varied parameter, and the periods of reaction were 10 minutes, 20 minutes and 30 minutes respectively. The fixed parameters were the volume of 1% trisodium citrate of 2 mL and temperature of reaction at 100 °C. The results of time of reaction studies are shown in Figure 6.9.

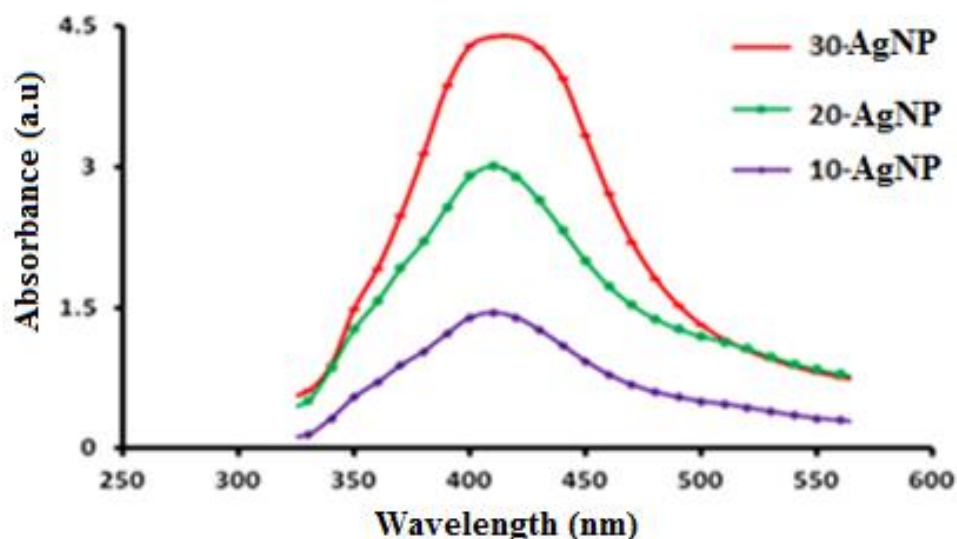


Figure 6.9: Ultraviolet-visible spectra of silver nanoparticles synthesised at temperature of 100 °C and 2 mL volume of 1% trisodium citrate at varied times of 10 minutes (10-AgNP), 20 minutes (20-AgNP) and 30 minutes (30-AgNP).

In Figure 6.9, it can be seen that there is an increase in peak height with an increase in reaction time from 10 minutes to 30 minutes. Similarly, the results also reveal that the plasmonic peak was doubled after 20 minutes, and subsequently tripled after 30 minutes. The increase in plasmonic peaks with the increase in reaction time of reduction could be attributed to the formation of silver nanoparticles within a narrow size range. The tiny shift in plasmonic peak can be as a result of the other parameters (temperature and volume of trisodium citrate) reaching their optimum. These results are in agreement with the observations in the reported literature (Khan *et al.*, 2011). Silver nanoparticles synthesis procedures are inferred to involve the reduction of silver ions by 1% trisodium citrate to elemental silver, which thereafter undergoes nucleation and growth to form silver nanoparticles (Kruszewski & Cyrankiewicz, 2011). The mechanism of ionic reaction which pertains to the reduction of the silver nitrate by citrate can be expressed in the following chemical equation (Kruszewski & Cyrankiewicz, 2011):



The stage of the synthesis nucleation depends on the reaction time, silver salt precursor relative concentration and the reducing agent (Khan *et al.*, 2011). The conditions most suitable for the synthesis of silver nanoparticles were a range of temperature between 90 °C to 100 °C and 30 minutes of reduction reaction; because the plasmonic peak was at the highest at this temperature. During the direct immobilisation of silver nanoparticles on the surface of amine-modified track-etched polyethylene terephthalate (PET) membrane, the optimum conditions of 100 °C, 30 minutes and 2 mL volume of 1% trisodium citrate were further used.

6.3.2 Zeta potential analysis of silver nanoparticles

The zeta potential of the synthesized silver nanoparticles was determined in order to investigate the stability of the colloidal silver nanoparticles relative to the duration of synthesis. Section 3.8.2.2 gives the detailed experimental procedure for the synthesis of silver nanoparticles. The results given are of the samples named as 10-AgNP, 20-AgNP and 30-AgNP, whose synthesis conditions are described in Table 3.5 of Section 3.8.4. These respective samples were chosen because the silver nanoparticles were synthesised using optimum temperature of 100 °C and 2 mL volume of 1% trisodium citrate. The time of

synthesis of silver nanoparticles (10 minutes, 20 minutes, and 30 minutes) was the variable parameter; while the fixed parameters were the temperature of 100 °C and 2 mL volume of 1% trisodium citrate added to the already-heated silver nitrate. The Zeta potential characterisation technique is described in Section 3.9.8. The Zeta potential measurement results are presented in Table 6.4.

Table 6.4: Zeta potential of the colloidal silver nanoparticles synthesised at 100 °C and with 2 mL volume of 1% trisodium citrate at 10 minutes (10-ANP), 20 minutes (20-AgNP) and 30 minutes (30-AgNP)

Silver Nanoparticle Sample	Zeta (ζ) Potential (mV)
10-AgNP	-23.6
20-AgNP	-24.9
30-AgNP	-25.3

In Table 6.4, the results show the increase in Zeta potential in the negative direction, as the time of synthesis increased. The potential values changed from -23.6 mV for 10-AgNP, synthesised in 10 minutes to -25.3 for sample 30-AgNP which was synthesised for 30 minutes under the applied fixed conditions. The relationship between time of synthesis of silver nanoparticles and the zeta potential of the silver nanoparticles can be seen in Figure 6.10.

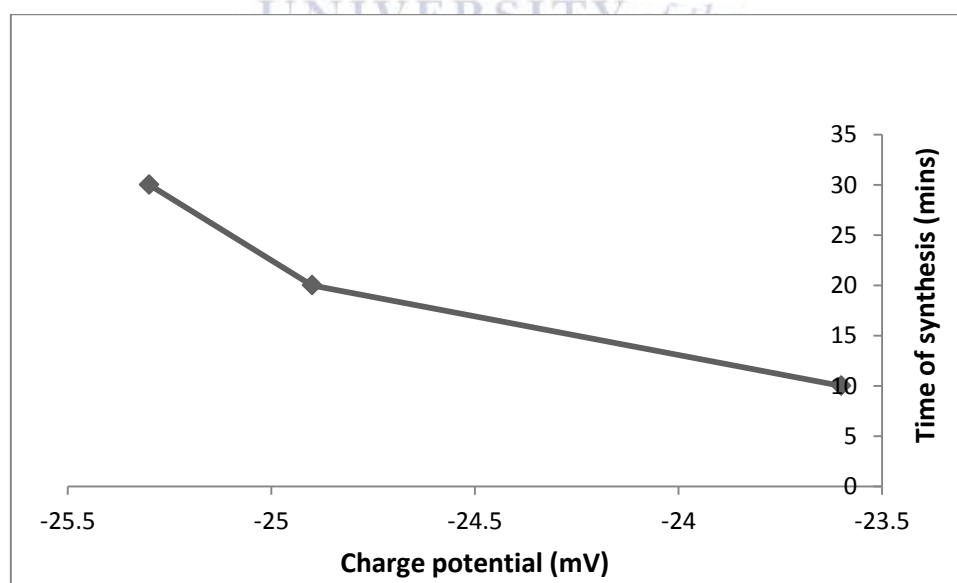


Figure 6.10: Graphical presentation showing the relationship between zeta potential (mV) of silver nanoparticles and time of synthesis.

In Figure 6.10, it can be seen from the trend of the graph that the Zeta potential increased in the negative direction with an increase in the time of reaction. This increase in the negative direction could be attributed to build up of negative charge as the nanoparticles increase in size. The colloidal silver nanoparticles stability is related to their zeta potential values such that any potential value within the range of +20 to -20 mV is considered as an unstable region (Makabiadi *et al*, 2010). In the region between the values -20 to +20 mV, the nanoparticles tend to form clusters as a result of the lack of strong forces of repulsion between the nanoparticles' nuclei (Makabiadi *et al*, 2010). The Zeta potential of silver nanoparticles for all samples falls outside the region -20 to +20 mV, which show that they were stable.

6.3.3 Silver nanoparticles immobilisation and characterisation of track-etched polyethylene terephthalate (PET) membrane

In this section, the results and discussion of the silver nanoparticles immobilisation on the modified surface of track-etched polyethylene terephthalate (PET) membrane are presented. The section also encompasses the results from the characterisation techniques including: scanning electron microscopy (SEM), ultraviolet-visible (UV-Vis) spectroscopy and X-ray photoelectron spectroscopy (XPS). The main objective of this was to investigate the immobilisation of silver nanoparticles with respect to the exposure time of the amine-modified track-etched PET membrane during reduction of silver nitrate by trisodium citrate. The procedures for the silver nanoparticles immobilisation on the modified surface of the track-etched PET membrane are described in Section 3.8.2.3.

In brief, the silver nanoparticles immobilisation was carried out by the immersion of acid-activated 3x3 cm pieces of amine-modified track-etched PET membranes during reduction of silver nitrate by 2 mL of 1% trisodium citrate at 100 °C for varying times of 10 minutes, 15 minutes, 20 minutes, 25 minutes and 30 minutes respectively. Acid activation of the amine-modified track-etched PET membrane was achieved by the immersing the PET membrane in 100 mL of 1 mM hydrochloric acid for 1 hour under agitation. The fixed and variable parameters for each sample with their sample codes are presented in Table 3.5.

6.3.3.1 Ultraviolet-visible spectroscopy (UV-Vis)

In this section, the ultraviolet-visible spectroscopy results and discussion of track-etched polyethene terephthalate (PET) membranes already coated with silver nanoparticles and the unmodified track-etched polyethene terephthalate (PET) membrane are presented. The procedure for the immobilisation of silver nanoparticles on the surface of amine-modified track-etched PET membranes is described in Section 3.8.2.3. The code names for the silver-coated track-etched PET membranes and unmodified track-etched PET membrane are described in Table 3.5. The characterisation technique is described in Section 3.9.6. The periods of 10 minutes, 15 minutes, 20 minutes, 25 minutes and 30 minutes of immobilising silver nanoparticles were a variable parameter while the temperature of 100 °C and 2 mL volume of 1% trisodium citrate were fixed parameters.

The results for sample codes 10-AgPET, 15AgPET, 20AgPET, 25AgPET and 30-AgPET are in Figure 6.11.

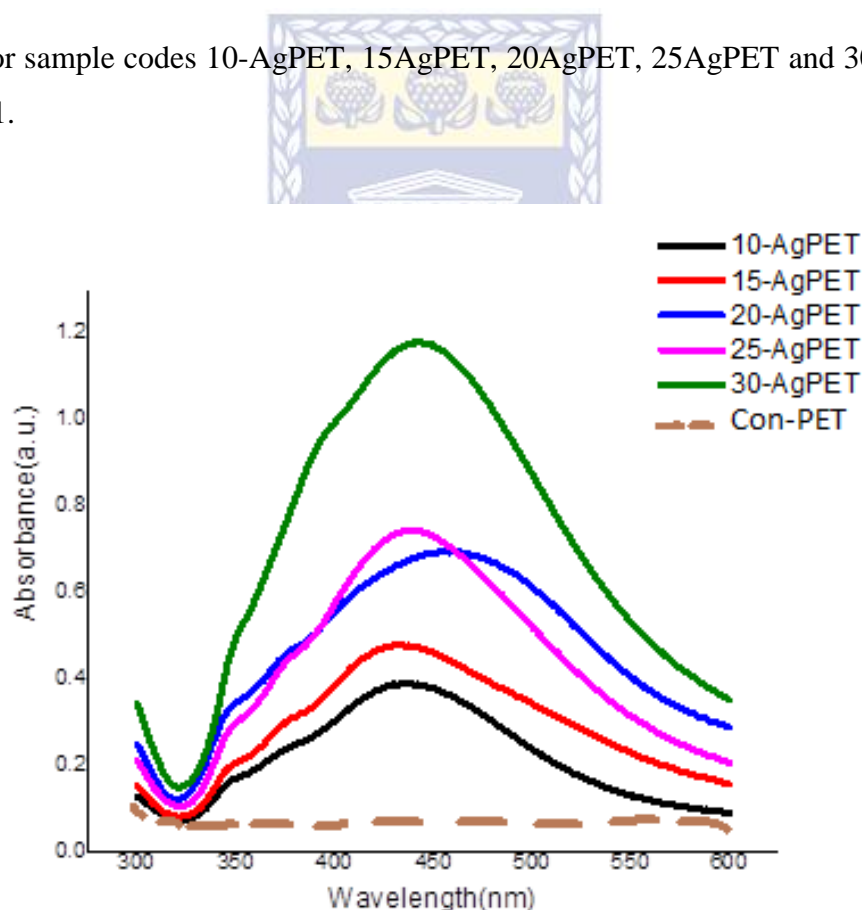


Figure 6.11: Ultraviolet-visible spectra of track-etched polyethene terephthalate (PET) membranes coated at 100 °C and with 2 mL volume of 1% trisodium citrate for different immobilisation times of 10 minutes (10-AgPET), 15 minutes (15-AgPET), 20 minutes (20-AgPET).

In Figure 6.11, the results show an increase in the plasmonic peak height of silver-coated modified track-etched polyethylene terephthalate (PET) membranes. The sample 10-AgPET had the lowest peak, while the sample 30-AgPET had the highest peak, with the rest in between. The plasmonic peak heights revealed an increasing trend from the sample that was immersed for 10 minutes (10-AgPET) to that immersed for 30 minutes (30-AgPET). The sample Con-PET, the control sample gave no plasmonic peak as a result of lack of silver nanoparticles on the surface of the track-etched polyethylene terephthalate (PET) membrane. The height of the peak crested at about 450 nm is presented in Figure 6.11.

Figure 6.12 shows the relationship between absorbance peak height and time of silver nanoparticles immobilisation on the surface of amine-modified track-etched PET membrane.

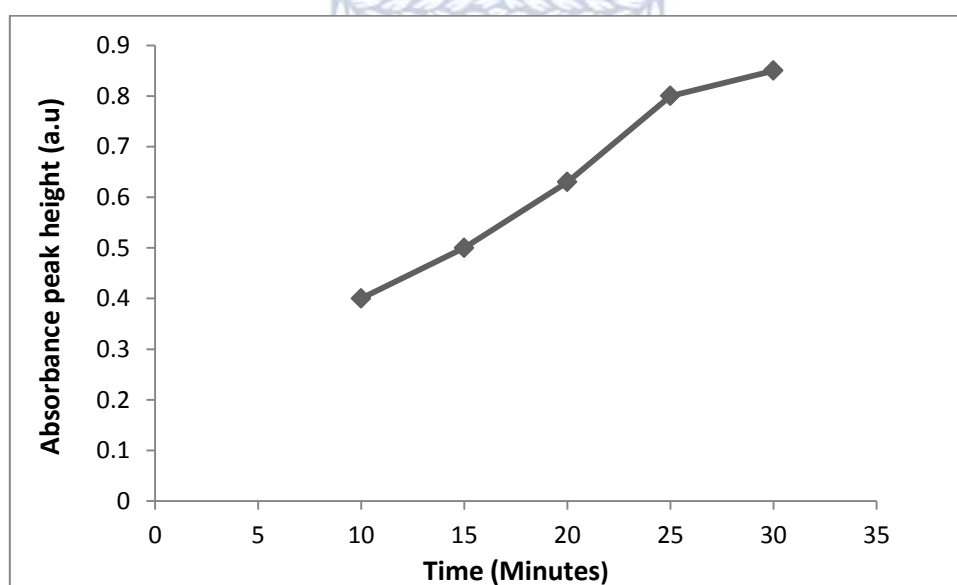


Figure 6.12: Graphical correlation of absorbance peak height to time of silver nanoparticle immobilisation.

Figure 6.12 reveals the correlation that as time of silver nanoparticles immobilisation was increased from 10 to 30 minutes the absorbance peak height also increased from 0.40 to 0.85 arbitrary units. The trend in the plasmonic peak height revealed that the quantity of the immobilised silver nanoparticles on the surface of track-etched polyethylene terephthalate (PET) membrane was directly proportional to the immobilisation time. The literature agrees with the trend in peak height where it states that as time of synthesis of silver nanoparticles increases so does the amount of nanoparticles (Solov'ev *et al.*, 2007). As the immobilisation time was increased from 10 minutes to 30 minutes, the plasmonic peaks showed a red shift.

This red shift happens to be the change in the plasmonic peak position from short wavelength towards longer wavelength which means that the size of silver nanoparticles changed with an increase in the immobilisation time.

6.3.3.2 X-ray photoelectron spectroscopy of silver-coated modified track-etched polyethylene terephthalate (PET) membrane

In this section, the results and discussion of X-ray photoelectron spectroscopy (XPS) for the silver-coated track-etched polyethylene terephthalate (PET) membranes are presented. The procedure for the immobilisation of silver nanoparticles on the surface of amine-modified track-etched PET membranes is described in Section 3.8.2.3. The immobilisation time of silver nanoparticle was the variable parameter while the temperature of 100 °C and 2 mL volume of 1% trisodium citrate were fixed parameters. The characterisation of the samples was carried out as described in Section 3.9.7. In Table 6.5, the results of samples 10-AgPET, 20-AgPET and 30-AgPET are presented.

Table 6.5: X-ray photoelectron spectroscopy results depicting the percentage of silver relative to immobilisation times on PET membrane surface at 10 minutes (10-AgPET), 20 minutes (20-AgPET), 30 minutes (30-AgPET)

Elements	Silver-coated track-etched PET membranes and their respective amount in percentage (%)		
	10-AgPET	20-AgPET	30-AgPET
Carbon (C)	70.63	69.50	67.75
Nitrogen (N)	5.04	4.65	4.80
Oxygen (O)	21.75	21.94	22.17
Silver (Ag)	2.52	3.65	5.22

In Table 6.5, the XPS results show the elemental percentages of carbon (C), nitrogen (N), oxygen (O) and silver (Ag) on the surface of silver-coated track-etched polyethylene terephthalate (PET) membranes at various times of 10 minutes, 20 minutes and 30 minutes of silver nanoparticles immobilisation. The results reveal that increasing the immobilisation time of silver nanoparticles results in the increase in the silver percentage on the surface of PET membrane from 2.52% to 5.22%.

In the results, the trends reveal that as the silver ions are reduced to elemental silver (Ag) during the reduction of silver nitrate by trisodium citrate, it resulted in an increase in the amount of silver immobilised on the surface of PET membrane over the period. The trends in Table 6.5 are in concord with the results depicted in Figure 6.11 that reveal an increase in the plasmonic peak heights as the time is increased for the the silver nanoparticles immobilisation on the surface of polyethylene terephthalate (PET) membrane. These observations are in conformation with the literature; where it is noted that the elemental atoms in a sample with higher concentration results in higher number of photoelectrons released by that element compared to the element of lower atomic concentration (Basri *et al.*, 2011).

6.3.3.3 Scanning electron microscopy (SEM)

This section presents the results and discussion of scanning electron microscopy (SEM) for the silver-coated track-etched polyethylene terephthalate (PET) membrane. The procedure for the immobilisation of silver nanoparticles on the surface of amine-modified track-etched PET membranes is described in Section 3.8.2.3. Various time periods of 10 minutes, 15 minutes, 20 minutes, 25 minutes and 30 minutes of silver nanoparticles immobilisation were the variable parameter, while the temperature of 100 °C and 2 mL volume of 1% trisodium citrate (2 mL) were fixed parameters. The sample characterisation was carried out as described in Section 3.9.4 and Table 3.5 outlines the experimental parameters.

The SEM microgram in 6.13A depicts silver nanoparticles immobilised on track-etched PET membrane which are spherical in shape and the corresponding histogram shows a nanoparticle size range of 10 to 45 nm. The histogram for sample 10-AgPET is asymmetric, and has a high frequency of silver nanoparticle sizes between 20 and 25 nm. The average size of the silver nanoparticles was 25 nm for sample 10-AgPET which was immobilised for 10 minutes.

The SEM microgram in 6.13B reveals silver nanoparticles immobilised on track-etched PET membrane which are also spherical in shape and the corresponding histogram shows a nanoparticle size range of 20 to 55 nm. The histogram for sample 15-AgPET is symmetric and has a high frequency of silver nanoparticle sizes between 30 and 35 nm. The average size of silver nanoparticles was 34 nm for the 15 minutes of immobilisation (15-AgPET). Also, the SEM microgram in 6.13C reveals silver nanoparticles immobilised on track-etched PET membrane and the corresponding histogram shows a nanoparticle size range of 20 to 80 nm.

The histogram for sample 20-AgPET is symmetric and has a high frequency of silver nanoparticle sizes between 40 and 50 nm. The average size of silver nanoparticles was 44 nm for the 20 minutes of immobilisation (20-AgPET).

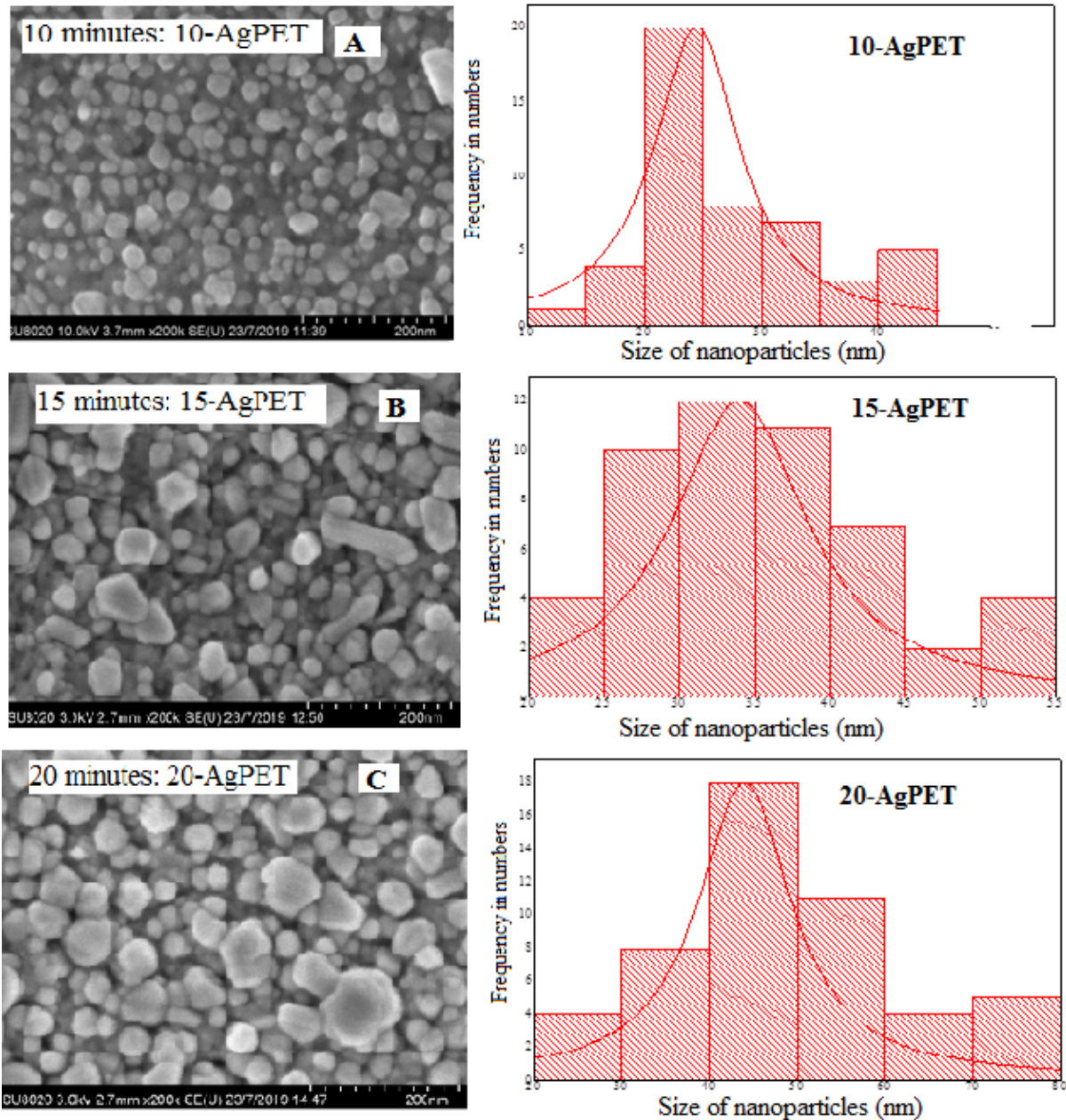


Figure 6.13: SEM images of silver-coated track-etched polyethene terephthalate (PET) membrane prepared at 100 °C and with 2 mL volume of 1% trisodium citrate for samples of A - 10-AgPET (10 minutes), B - 15-AgPET (15 minutes) and C - 20-AgPET (20 minutes).

In Figure 6.14D, the SEM microgram shows that the silver nanoparticles were immobilised on track-etched PET membrane and the corresponding histogram reveals a nanoparticle size range of 20 to 65 nm. The histogram for sample 25-AgPET is symmetric and also has a high frequency of silver nanoparticle sizes between 40 and 45 nm. The average size of silver nanoparticles was 44.5 nm for the 25 minutes of immobilisation (25-AgPET). Similarly, the SEM microgram in 6.14E reveals silver nanoparticles immobilised on track-etched PET membrane which are also mostly spherical in shape and the corresponding histogram shows a nanoparticle size range of 20 to 120 nm. The histogram for sample 30-AgPET has a high frequency of silver nanoparticle sizes between 60 and 80 nm. The average size of silver nanoparticles was 64 nm for the 30 minutes of immobilisation (30-AgPET).

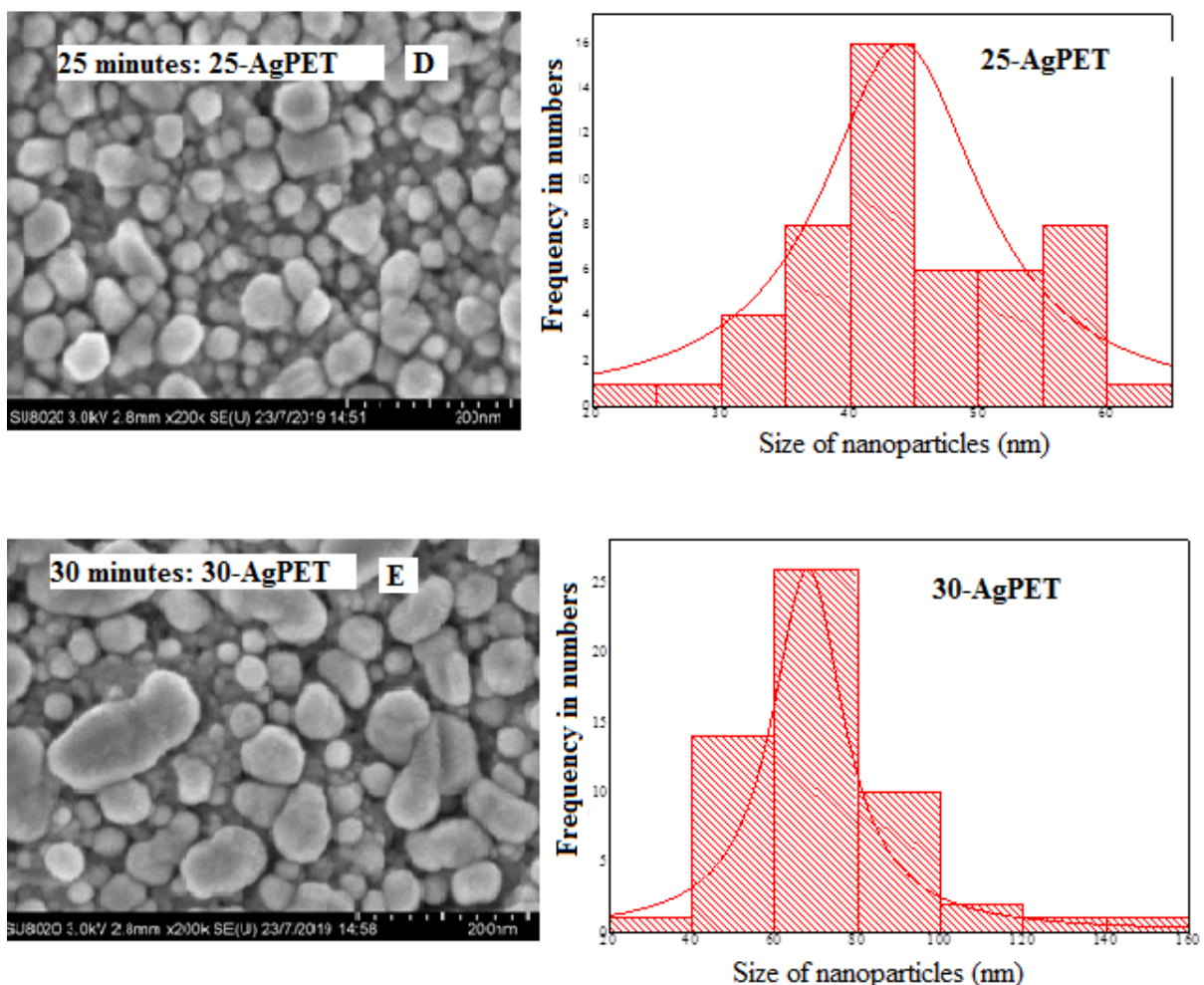


Figure 6.14: SEM images of silver-coated track-etched polyethene terephthalate (PET) membrane prepared at 100 °C and with 2 mL volume of 1% trisodium citrate for samples of D - 25-AgPET (25 minutes) and E - 30-AgPET (30 minutes).

The results in Figures 6.13 and 6.14 show that the morphology of silver nanoparticles was mostly spherical in shape. Silver nanoparticles size increased relative to the increase in the time of immobilisation of silver nanoparticles on the surface of track-etched PET membrane. These SEM results also conform to the ultraviolet-visible (UV-vis) spectroscopy results of the silver-coated membranes in Figure 6.11. In addition, the silver nanoparticle size was notably increased with the time of immobilisation during reduction of silver nitrate by trisodium citrate. The size increment and variation in the shape of silver nanoparticles on the surface of the modified track-etched PET membrane is in agreement with the broad plasmonic peaks and red shift of the plasmonic peaks in Figure 6.11, which was also reported by Reznikova *et al.*, (2014). It can also be noted that the SEM micrograms reveal that the silver nanoparticles on the PET membrane were not uniformly immobilised which complements UV-Vis spectroscopy at different points of the same sample. The histograms presented in Figures 6.13 and 6.14 depict the size distribution of the silver nanoparticles immobilised on the surface of amine-modified track-etched PET membrane. These results show that as immobilisation time was increased, the nanoparticle sizes also were increased, in agreement with literature reviewed (Solov'ev *et al.*, 2007).

6.3.3.4 Thermogravimetric analysis (TGA)

The thermogravimetric analysis (TGA) technique was carried out to investigate the thermal properties of the amine-modified track-etched PET membrane, silver-coated track-etched PET membrane and the unmodified track-etched PET membrane. The TGA technique was used to determine and compare changes in the thermal profile of the polyethene terephthalate (PET) membrane samples. In the analysis, weight loss was quantified relative to the applied temperature gradient, and the analysis was also used to quantify the silver nanoparticle loading. The comparison study includes the unmodified polyethene terephthalate (PET) membrane (Con-PET), amine-modified PET membrane (100A-PET) and silver-coated amine-modified PET membrane (30-AgPET) respectively. This experiment was carried out to monitor any thermal degradation as a result of the modification process.

The samples 100A-PET and 30-AgPET were used because they were prepared under optimised conditions, while Con-PET was used as the control sample. The thermogravimetric analysis (TGA) was carried out as described in Section 3.9.5. The characterised samples include 30-AgPET, 100A-PET and Con-PET which were prepared as described in Section 3.8.2.3. The conditions under which these samples were prepared are described in Table 3.5.

The thermal profile results of the samples 30-AgPET, 100A-PET and Con-PET are presented in Figure 6.15.

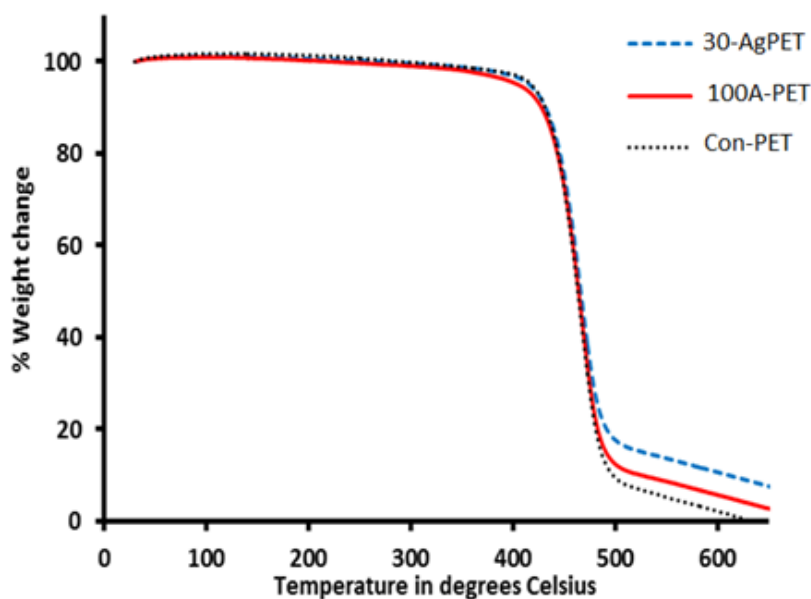


Figure 6.15: Thermogravimetric analysis (TGA) graph showing the thermal profile of unmodified track-etched PET (Con-PET), amine-modified track-etched PET (100A-PET) and silver-coated amine-modified track-etched PET (30-AgPET) membranes.

In Figure 6.15, the thermal profile reveals that all the membranes (30-AgPET, 100A-PET and Con-PET) are stable, without any weight loss, until a temperature of 300 °C where only a 2.5% weight loss is observed until a temperature of 390 °C reached. After the temperature of 390 °C, a high weight percent loss was observed until a temperature of 490 °C was reached. Between 390 °C and 490 °C temperature range, the weight loss was 87.5% for unmodified track-etched PET and 83.5% for amine-modified track-etched PET, and 77.5% for silver-coated track-etched PET membrane respectively. From the results, it can be indicated that after the temperature of 490 °C, the polymer membrane was mostly lost and the residue remaining was majorly elemental carbon for samples Con-PET and 100A-PET and elemental silver and carbon for sample 30-AgPET which is silver-coated amine-modified track-etched PET membrane.

After a temperature of 490 °C, the different profiles emanated from the different elemental compositions of residue which is made up of carbon and silver. At 500 °C the silver-coated amine-modified track-etched PET membrane sample named 30-AgPET had a 20% weight remaining, which is 10% more than Con-PET sample (unmodified track-etched PET

membrane) and 6% more than sample 100A-PET (amine-modified track-etched PET membrane). The 10% difference in weight between 30-AgPET and Con-PET is as a result of elemental silver and an additional carbon contributed by diethylenetriamine (DETA) which was present as a residue after the temperature of 490 °C. Furthermore, the difference of 4% between the samples 100A-PET and Con-PET could be attributed to the carbon in diethylenetriamine that has been functionalised on the PET membrane surface. On that basis, it can be inferred that the 6% of silver loading reveals the amount of immobilised silver on the surface of the amine-modified track-etched membrane. This supports the observation made in Figure 6.2, which shows a loss of ethylene glycol (two carbon atoms) which is replaced by four carbons from diethylenetriamine (DETA) functionalised on the surface of PET.

6.3.3.5 Contact angle measurements analysis

In order to investigate the changes made to the surface structures of the amine-modified and silver-coated track-etched polyethylene terephthalate (PET) membrane, contact angle measurements were performed. These measurements were carried out using distilled water at ambient conditions according to the description in Section 3.9.1. The contact angle measurements were performed on samples Con-PET (unmodified track-etched polyethylene terephthalate (PET) membrane), 100A-PET (amine-modified track-etched PET membrane) and 30-AgPET (silver-coated track-etched PET membrane). The results of contact angle measurements are presented in Table 6.6.

Table 6.6: Contact angles measurements of Con-PET, 100A-PET and 30-AgPET samples

Polyethylene terephthalate (PET) membranes	Average Contact angle (degrees)
Con-PET	87.9
100A-PET	48.4
30-AgPET	54.1

In Table 6.6, the results show a decrease in the contact angle after the modification of the PET membrane by diethylenetriamine (DETA). There was a decrease in the contact angle from 87.9 degrees of unmodified track-etched polyethylene terephthalate (PET) membrane

sample Con-PET, to 48.4 degrees for the amine-modified track-etched polyethene terephthalate (PET) membrane (sample 75A-PET).

Amines introduction on the surface of the amine-modified track-etched polyethene terephthalate (PET) membrane (sample 100A-PET) improved the wettability of the sample 100A-PET. The surface of the PET membrane became more hydrophilic as the track-etched PET membrane was modified with diethylenetriamine (DETA), which produced the ionisable groups known as the amines (NH_2). Thereafter, the amines were introduced onto the surface of the track-etched polyethene terephthalate (PET) membrane as depicted in the reaction mechanism in Figure 6.2. This observation is in agreement with the literature that ionisable functional groups on the surface of membranes contribute to the improvement of hydrogen bonding between water molecules and ionisable moieties on the surface of the membrane (Goddard & Hotchkiss, 2007). The contact angle increased after the immobilisation of silver nanoparticles on the surface, as a result of the loss of ionisable moieties (nitrogen) that have been obscured in part by the silver nanoparticles.

6.4 Applications of the silver nanoparticles-immobilised PET membrane for the detection of organic pollutants

This section presents the results and discussion of the detection of acetaminophen and 4-aminothiophenol (4-ATP) on the modified surface of track-etched polyethene terephthalate (PET) membrane. The results and the applicability of surface-enhanced Raman spectroscopy using silver-coated surface of track-etched PET membranes (10-AgPET, 20-AgPET and 30-AgPET samples) for detection of acetaminophen and 4-aminothiophenol (4-ATP) are also detailed.

Acetaminophen as well as other chemicals has functional groups that have peaks in their Raman spectra. The functional groups are phenyl, amide, carbonyl and hydroxyl groups. Although, acetaminophen has similar peaks to common functional groups, its overall Raman spectrum is specific to acetaminophen only, making the Raman spectrum, a fingerprint signature. The typical acetaminophen peaks identified in its spectrum are outlined in Table 6.7 (Kauffman *et al.*, 2008).

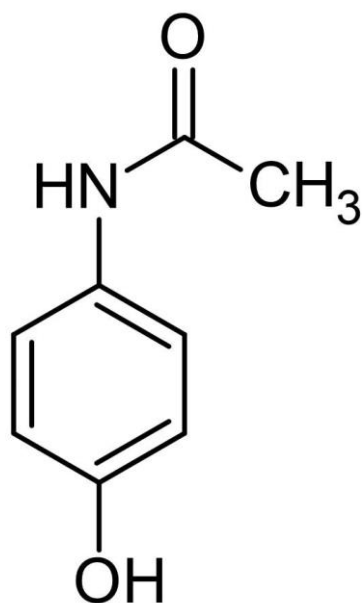


Figure 6.16: Chemical structure of acetaminophen.

Table 6.7: Peaks in Raman spectrum of acetaminophen

Proposed bond	Spectral peak cm^{-1}
C-N	1245, 1281, 1328
C-O	854, 861, 1170
C-C	1557, 1565, 1576
C=C	1608, 1615, 1623
C=O	1646, 1650

The respective peaks of the Raman spectrum in Table 6.7 were used to confirm the presence of acetaminophen on the prepared surfaces of unmodified track-etched PET membrane (Con-PET), silver-coated track-etched PET membrane (30-AgPET) and a control surface made of silver nanoparticles sputtered on a glass support (Quartz).

6.4.1 Platform preparation for Surface-enhanced Raman Spectroscopy

The development of the surface-enhanced Raman spectroscopy (SERS) platform for the detection of acetaminophen and 4-aminothiophenol (4-ATP) was carried out as described in section 3.8.2.3. Silver nanoparticles were immobilised on the surface of modified track-etched polyethylene terephthalate (PET) membranes as surface-enhanced Raman spectroscopy active materials to intensify the weak Raman scattering signal in an attempt to detect acetaminophen and 4-aminothiophenol (4-ATP) molecules on the surface. Silver

nanoparticles immobilisation was carried out at different times in order to find the best conditions that would suppress the polyethene terephthalate Raman signals. These conditions and the respective codes for samples are as outlined in Table 3.5. Meanwhile, in the first experiment with PET supports, the Raman signals from the PET supports were visualized before adding the analyte. In Figure 6.17, the Raman spectra are given of the silver-coated track-etched PET membranes (10-AgPET, 20-AgPET, 30-AgPET) and the unmodified track-etched PET membrane (Con-PET) as a baseline (control sample), prior to dosing the analyte.

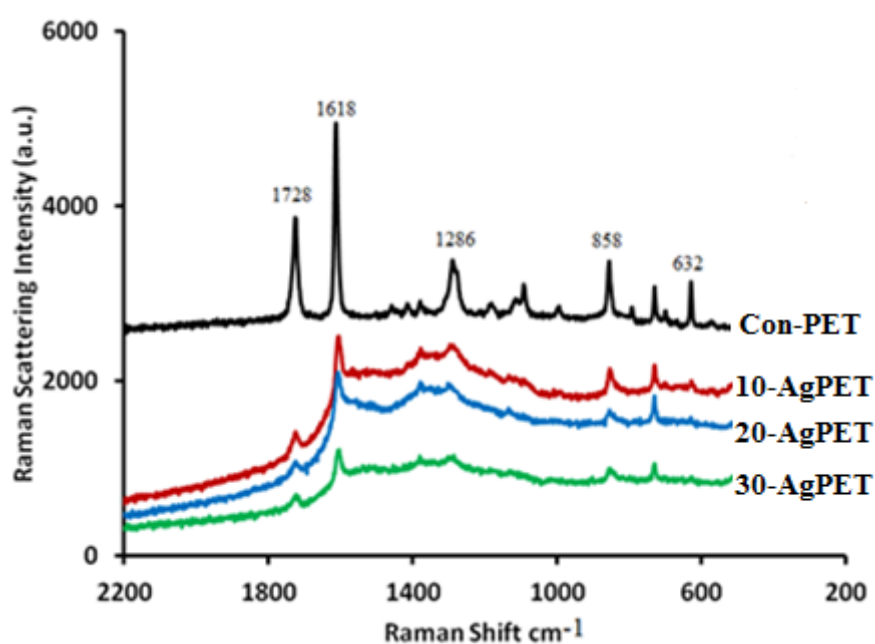


Figure 6.17: Raman spectra of silver-coated track-etched PET membranes at reaction times 10 minutes (10-AgPET), 20 minutes (20-AgPET), 30 minutes (30-AgPET) prepared at 100 °C using 2 mL of 1% trisodium citrate and unmodified PET membrane (Con-PET) as control.

It can be seen in Figure 6.17 that as the time of silver nanoparticle immobilisation increased, the intensity of the Raman peaks relating to the polyethene terephthalate (PET) membrane were reduced, having the lowest signal on the sample prepared at a reaction time of 30 minutes as shown by the spectrum of 30-AgPET. It is evident the Raman spectra of silver-coated track-etched polyethene terephthalate (PET) membranes (10-AgPET, 20-AgPET, 30-AgPET) without analyte show suppressed peaks relating to the polyethene terephthalate membrane and these peaks were not as prominent as for the unmodified track-etched PET membrane (Con-PET). It clearly shows that as the silver nanoparticle immobilisation time was increased from 10 minutes to 30 minutes, the PET membrane peaks' intensities were

suppressed due to the layer of silver nanoparticles. This suppression in PET peaks' intensities gives the indication of the size of silver nanoparticles immobilised on the surface of the polyethylene terephthalate (PET) membrane. Therefore, the silver-coated track-etched PET membrane of sample 30-AgPET was chosen as the most suitable platform for the detection of the analytes (acetaminophen and 4-aminothiophenol) using surface-enhanced Raman spectroscopy. This is because it showed the minimum peak intensities of the PET membrane, and the cut-off point of immobilising silver nanoparticles on modified track-etched PET membrane was set at 30 minutes because the size of silver nanoparticles of sample 30-AgPET, as observed in Section 6.3.3.3, fell within the average size range of 64 nm (Taurozzi and Tarabara, 2007).

6.4.2 Acetaminophen detection using silver-coated track-etched polyethylene terephthalate (PET) membrane.

The Raman spectrum is comprised of wavelength distribution of peaks equivalent in character to molecular vibrations specific to the analyte being characterised (Ferraro, 2003). The Surface-enhanced Raman spectroscopy (SERS) is an advanced Raman spectroscopy technique, and it was used in this study in the detection of the analytes (acetaminophen and 4-aminothiophenol) using silver nanoparticles as SERS active materials to enhance the Raman signal. The detection of analyte molecules on the silver-coated track-etched polyethylene terephthalate (PET) membrane was carried out at ambient conditions as described in Section 3.9.3. A solution of 20 μL of 0.1 mg/L aqueous acetaminophen was dropped and dried on the surfaces of the selected samples. The Raman spectra of acetaminophen detected on the surface of silver-coated track-etched polyethylene terephthalate (PET) membrane (30-AgPET), unmodified track-etched PET (Con-PET) and Quartz, a silver-coated glass surface (non-porous) as described in Section 3.8.1 are shown in Figure 6.18.

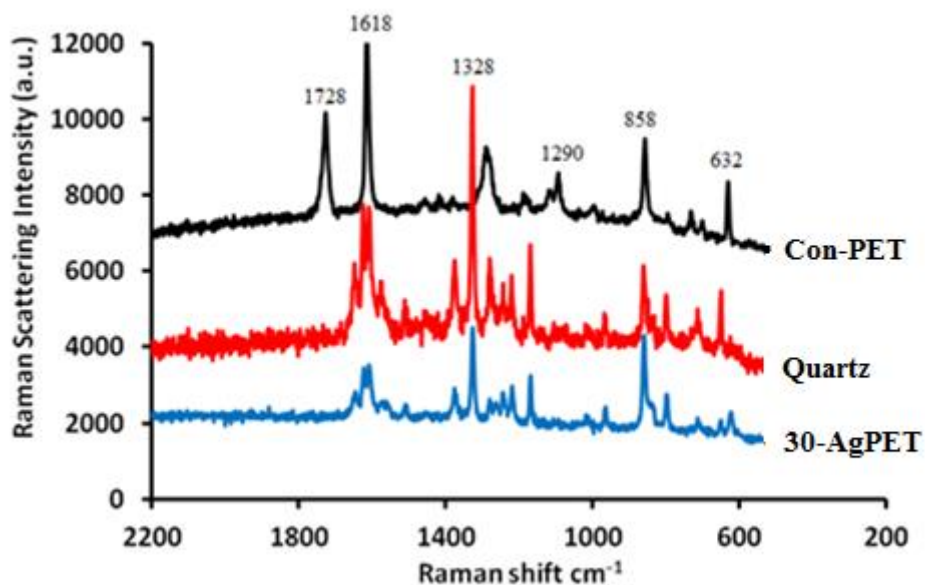


Figure 6.18: Raman spectra of 0.1 mg/L of acetaminophen on the surface of Con-PET (unmodified track-etched PET) membrane, Quartz (Non-porous) and 30-AgPET (silver-coated track-etched PET membrane).

Figure 6.18 shows the intensities of the acetaminophen peaks are higher for the sample Quartz (a non-porous silver-coated glass) than that of 30-AgPET, the track-etched silver-coated track-etched PET membrane. In the case of the control sample, Con-PET (the unmodified track-etched PET membrane), no characteristic peaks of acetaminophen could be observed among the overall prominent peaks of polyethylene terephthalate (PET) membrane. This could be attributed to lack of SERS signals on the surface of sample Con-PET membrane to enhance the Raman signal for acetaminophen. It can therefore be concluded that lack of silver nanoparticles is the main cause of the lack of acetaminophen peaks for the sample Con-PET. In the comparison of the Raman signal peak intensities of acetaminophen (as given in Table 6.7) on the Quartz sample, which is a non-porous SERS surface, against 30-AgPET (a track-etched silver-coated track-etched polyethylene terephthalate PET membrane), the majority of the acetaminophen vibrational bands on 30-AgPET were present but weak. The limited SERS intensity and the low spectral intensities could be due to the loss of some molecules of acetaminophen that may have leached through the pores.

6.4.3 Study of concentration for acetaminophen detection

Detection of acetaminophen concentration was performed using a silver-coated track-etched polyethylene terephthalate (PET) membrane sample 30-AgPET dosed with different concentrations of acetaminophen as described in Section 3.8.4. The solution of

acetaminophen was prepared using distilled water. The concentrations of 1 mg/L, 0.1 mg/L and 0.01 mg/L were prepared and subsequently assigned the sample codes Acet-001, Acet-002 and Acet-003 respectively. The volume of 20 μ L of acetaminophen solution for each concentration was dropped and dried on the surface of 30-AgPET. Figure 6.19 shows the Raman spectra for the concentrations of the acetaminophen at 1 mg/L, 0.1 mg/L and 0.01 mg/L detected on the surface of 30-AgPET membrane by Raman spectroscopy.

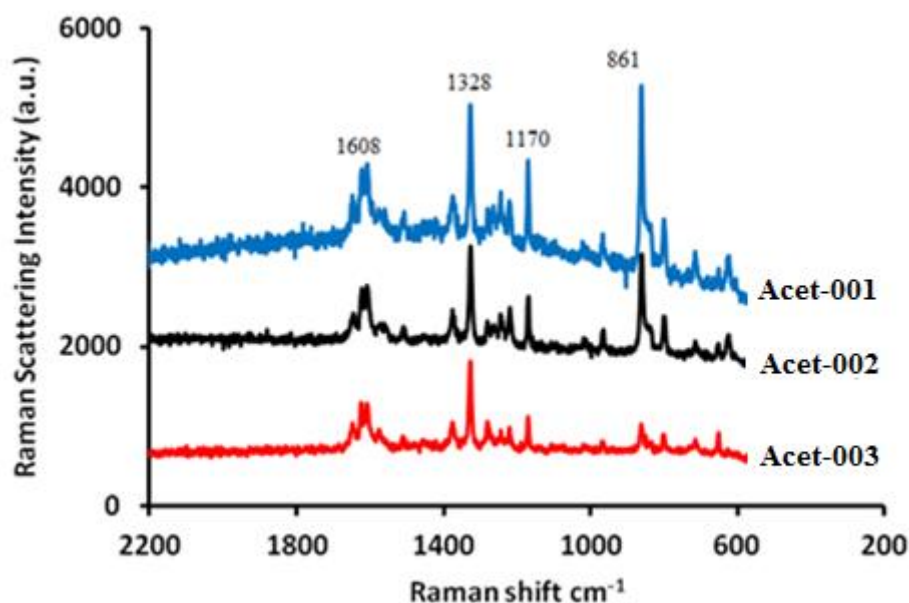


Figure 6.19: Raman spectra showing variations in peak intensity of different concentrations of acetaminophen in aqueous media 1 mg/L (Acet-001), (b) 0.1 mg/L (Acet-002) and 0.01 mg/L (Acet-003).

In Figure 6.19, it can be seen that the Raman peaks' intensity increased with an increase in acetaminophen concentration. This is in agreement with the reviewed literature that the Raman peak intensity is a function of the analyte concentration (Taurozzi and Tarabara, 2007). The Aceta-001 sample with the concentration 1 mg/L has its acetaminophen peak intensity greater than those of lower concentration (Aceta-002 and Aceta-003), which were 10 and 100 times more dilute respectively. The changes in the intensity of the peaks for acetaminophen spectrum are persistently changing with the change in concentration.

In theory, when there is a higher number of molecules on the hot sites of surface-enhanced Raman spectroscopy surface, there is a greater chance to observe from medium to strong Raman signals (Strachan *et al.*, 2007). This can also be seen in the spectra peaks in Figure 6.19. In the situation where more molecules of acetaminophen covered the surface of silver-

coated track-etched PET membrane, the possibility of observing a strong to medium Raman signal was higher. The effect of SERS is being provided by the localised surface plasmon resonance of silver nanoparticles. SERS contributions of electromagnetic and chemical effects (charge transfer) which arise from the adsorption of acetaminophen molecules on the silver nanoparticles could be responsible for the higher Raman scattering intensity. If acetaminophen exists in high concentration on the surface, there is a greater possibility for the acetaminophen to be adsorbed on the surface, enhancing the signal.

The noticeable trend in Figure 6.20 reveals that as the concentration increased, so the peak intensity height also increased. The difference in the trends is observed in the comparison of the rate of change among the specific bonds.

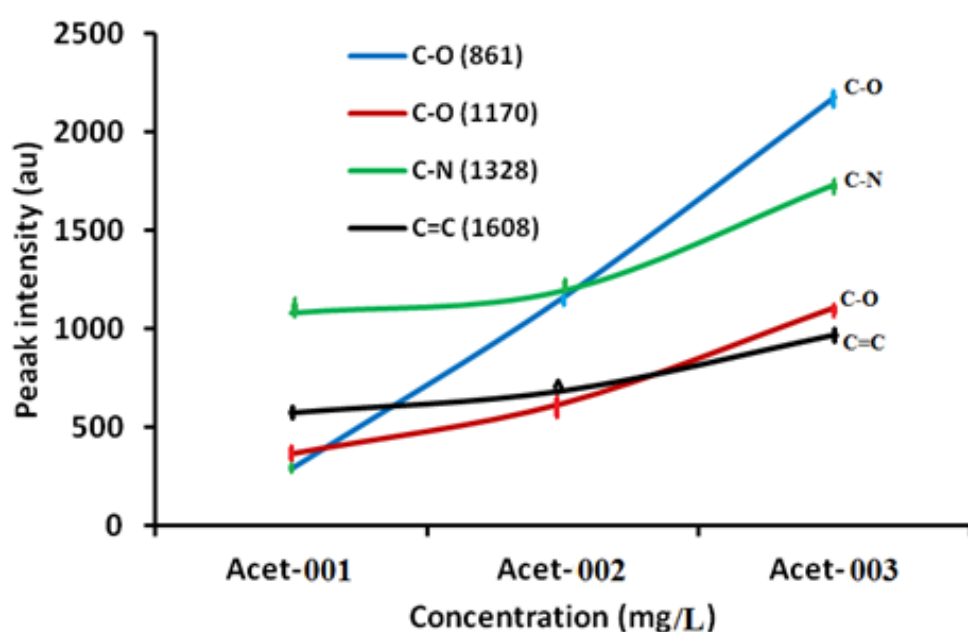


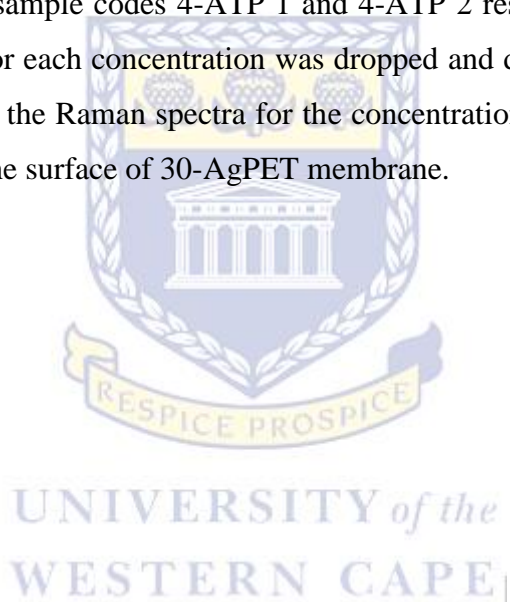
Figure 6.20: The graphical relationship between concentration of acetaminophen and trends in Raman peak height intensity at specific bond vibrations C-O (861), C-O (1170), C-N (1328) and C=C (1608).

In Figure 6.20, it can be seen that the rates of change for C-O (1170) and C-N (1328) have a similar trend, but the rates of change of C=C (1608) and C-O (1170) are not proportional. The intensity of peak trend for the C-O (861) vibration gives a linear response. The linearity of peak intensity of the C-O bond against the concentration gives the best correlation of the two factors. The vibrations of bonds involving C-O (1170), C-N (1328) and C=C (1608) show no linearity and if subjected to extrapolation towards zero concentration, they cross the peak intensity axis instead of the concentration axis. By extrapolating the linear correlation line of

C-O (861), it would give a limit of detection value of 0.0757 mg/L approximately. The only bottleneck with the intensity of peak heights is that the proportionality is not the same for all peak intensity heights. This means the increase in the peak intensity was not the same for all the spectrum peaks. This observation has not been made before in the literature, hence this study happens to be the first to report it.

6.4.4 Study of concentration for 4-ATP detection

The concentration study for the detection of 4-ATP was performed using a silver-coated track-etched polyethylene terephthalate (PET) membrane sample 30-AgPET with different concentrations as described in Section 3.8.4. The solution of 4-ATP was prepared using distilled water. Two different concentrations of 10^{-4} M and 10^{-6} M were prepared and subsequently assigned the sample codes 4-ATP 1 and 4-ATP 2 respectively. The volume of 20 μ L of 4-ATP solution for each concentration was dropped and dried on the surface of 30-AgPET. Figure 6.21 shows the Raman spectra for the concentrations of the 4-ATP at 10^{-4} M and 10^{-6} M detected from the surface of 30-AgPET membrane.



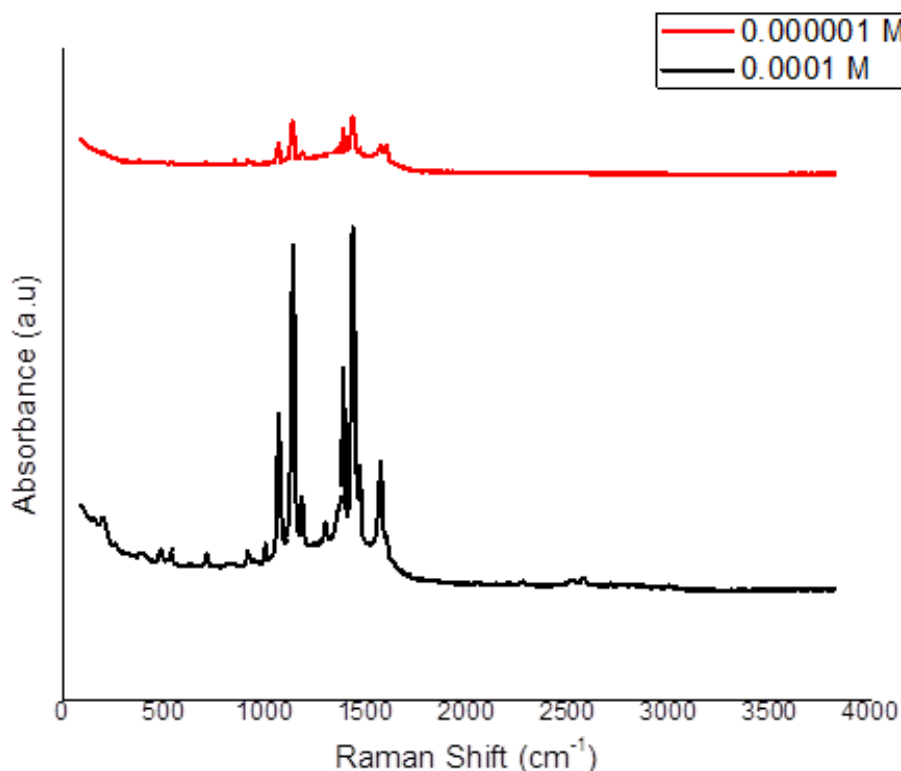


Figure 6.21: Raman spectra showing variations in intensity of different concentrations of 4-ATP in aqueous media 10^{-4} M or 0.0125 mg/L (4-ATP 1) and 10^{-6} M or 0.000125 mg/L (4-ATP 2).

Figure 6.21 shows that the Raman peaks intensity increased with an increase in 4-ATP concentration. This is also in agreement with the reviewed literature that the Raman peak intensity is a function of the analyte concentration (Taurozzi and Tarabara, 2007). The 4-ATP 1 sample with the concentration 10^{-4} M has its 4-ATP peak intensity greater than those of lower concentration (4-ATP 2), which was 100 times more dilute. This agrees with the explanations made already in Section 6.4.3.

6.4.5 Aminothiophenol (4-ATP) detection using silver-coated track-etched polyethylene terephthalate (PET) membrane

Among the isomers of aminothiophenol, 4-ATP is mostly studied owing to its simplicity of structure and profound interaction with silver nanoparticles (Bryant *et al.*, 2006; Aizpurua *et al.*, 2005; Valerio *et al.*, 2008).

Figure 6.22 shows the structure 4-aminothiophenol (4-ATP). 4-ATP is a bifunctional molecule which can adsorb to the silver-coated polyethene terephthalate (PET) membrane surface via the sulphur or nitrogen atom (Tiwari *et al.*, 2011).



Figure 6.22: Structure of 4-ATP.

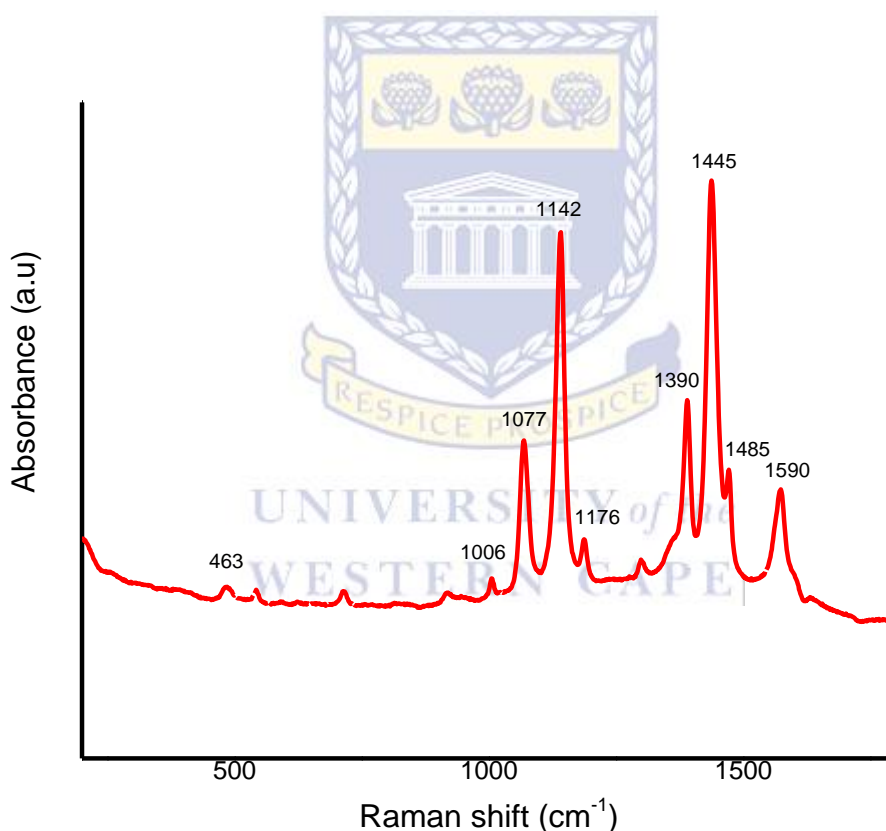


Figure 6.23: Raman spectrum of 10⁻⁴ M of 4-aminothiophenol (4-ATP) on the surface of 30-AgPET (silver nanoparticles-coated track-etched PET membrane).

Figure 6.23 shows the SERS spectrum of 4-aminothiophenol (4-ATP) obtained on the silver nanoparticles-coated polyethene terephthalate (PET) membrane (30-AgPET) at 785 nm excitation wavelength, which is close to the longitudinal absorption band of the nanoparticles (Tiwari *et al.*, 2011). The spectrum shows the peak intensities of the 4-ATP, with the bands at 1006 and 1176 cm^{-1} belonging to stretching/bonding vibration $\nu(\text{C}-\text{C})$, out-of-plane

deformation vibration γ (C–C), and deformation/bending vibration δ (C–H) respectively. These bands are associated with stretching vibrations of C–C and bending vibrations of C–H bonds.

The observed spectral bands in Raman spectroscopy of 4-aminothiophenols (4-ATP) have been classified into four different modes which are: a1, a2, b1, and b2 (Creighton, 1985). The modes a1 and b2 are assigned to in-plane vibrational modes and a2 and b1 species to the out-of-plane modes. The SERS spectrum of 4-aminothiophenol (4-ATP) on silver nanoparticles is dominated by the a1 and b2 modes. However, the bands at 463, 1006, 1077, 1490, and 1590 cm^{-1} belong to the a1 modes, whereas those at 1120, 1142, 1390, and 1445 cm^{-1} are attributed to the b2 modes. The b2 vibrational modes enhancement has been attributed to charge transfer from metal to adsorbate via Herzberg–Teller mechanism (Osawa et al., 1994). The b2 mode enhancement via charge-transfer mechanism also suggests the perpendicular orientation of the molecules on the gold surface (Tiwari *et al.*, 2011). The model proposed by Creighton, (1985), was used by Osawa et al., (1994), to interpret the orientation of 4-ATP on the silver surface. As stated by the models, the a2, b1, and b2 modes are enhanced in the order $b1 = b2 > a2$ for the standing-up orientation and $a2 = b1 > b2$ for the flat orientations of the molecules. The SERS spectrum of 4-ATP on silver nanoparticles displayed significant enhancement of the b2 modes compared to the a2 modes, which indicate perpendicular orientation. The slight enhancement of ring bending mode at 1006 cm^{-1} also supports the standing orientation of the molecule.

The next section presents the summary of the chapter.

6.5 Chapter summary

In this chapter, the accomplishments described include the successful chemical modification of the track-etched polyethylene terephthalate (PET) membrane through a wet chemistry method that involves a solid/liquid interface reaction, resulting in the immobilisation of silver nanoparticles on the track-etched PET membrane surface. The surface modification of the track-etched PET membrane using diethylenetriamine (DETA), followed by the immobilisation of silver nanoparticles on the surface has not been reported in literature. From the results presented in the chapter, it is shown that the ester bond scission and formation of amide bond occurred at the solid/liquid interface of diethylenetriamine solution and surface of the track-etched PET membrane. Fourier transform infrared (FTIR) and X-ray

photoelectron spectroscopy (XPS) confirmed the wet chemistry modification of the track-etched PET membrane surface. Silver nanoparticles immobilisation on the surface of the track-etched PET membrane during reduction of silver nitrate by trisodium citrate was confirmed by scanning electron microscopy (SEM), ultraviolet-visible (UV-vis) spectroscopy and XPS respectively. Scanning electron microscopy (SEM) was used to show the shape of silver nanoparticles that were immobilised on track-etched PET membrane surface, and to also confirm the size of the colloidal silver nanoparticles. The results of different characterisation techniques was combined in the chapter to confirm the surface modification of the surface of track-etched PET membrane, ascertaining the optimum conditions for synthesis of silver nanoparticles, then reports the immobilisation of silver nanoparticles. The FTIR characterisation of the modified track-etched PET membrane gave little noticeable changes in the absorbance spectra. The presence of silver was determined with XPS showing the amount in percentage of elemental silver immobilised on the surface. Subsequently, size distribution and concentration of silver nanoparticles on the amine-modified track-etched PET surface was confirmed by SEM and UV-vis spectroscopy respectively. A software known as ImageJ was employed in the calculation of the nanoparticles immobilised on the surface of amine-modified track-etched PET membrane from the SEM micrographs.

The chapter has also given in detail the results and characterisation of using the silver-coated track-etched polyethylene terephthalate (PET) membrane as a platform for the detection of acetaminophen and 4-aminothiophenol (4-ATP) by surface-enhanced Raman spectroscopy (SERS). The quartz platform was employed as control, to compare the detection using the surface-enhancement of silver nanoparticles of the silver-coated track-etched PET membrane against unmodified track-etched PET membrane. Silver nanoparticles were found to be responsible for the enhancement of the Raman signals of acetaminophen and 4-aminothiophenol (4-ATP) respectively. Extensive Raman characterisation of the PET membranes which were immobilised with silver nanoparticles at different times showed how effective the amount of silver nanoparticles and their size were for the suppression of the polyethylene terephthalate (PET) membrane signals. The chapter also made comparisons of analytes concentrations (acetaminophen and 4-aminothiophenol) showing increase in in peak height of spectra with an increase in concentration. In the next chapter, the conclusions and recommendations of the study's aims and objectives with findings are presented.

CHAPTER SEVEN

CONCLUSION AND RECOMMENDATIONS

7 Introduction

In this chapter, the summary of the major findings and achievements of this study are presented based on the aim and objectives highlighted in Chapter 1. It also details the extent to which the research objectives outlined in the introductory chapter were achieved and the research questions elucidated. This is subsequently followed by the significant findings from the study. In addition, the chapter outlines recommendations for future work.

7.1 Overview

In the introductory chapter, research hypothesis were formulated as follows:

- Capillary electrophoretic system is capable of carrying out quantification of diverse organic pollutants despite their complex aqueous matrices.
- Capillary electrophoretic system coupled to UV-detector or mass spectrometer is capable of quantifying low nanogram per litre levels of various selected pharmaceuticals and steroids.
- Capillary electrophoresis with an indirect UV detection can be used to determine and quantify the inorganic ions in environmental waters.
- Track-etched PET membrane can be used to pre-concentrate analytes (organic pollutants) of low concentration by retaining them on the modified PET surface.
- Modified track-etched membrane can be used as platform to detect and quantify selected organic pollutants adsorbed under SERS.

On the basis of the research hypothesis, the aim of the study was formed, and this was to separate, identify, and quantify selected persistent organic micropollutants in environment wastewater using the chromatographic techniques (CE & HPLC) and SERS. To achieve this, seven major objectives were detailed in the introductory chapter as follows:

- To develop a method in CE to identify selected pharmaceuticals and steroids in environmental.

- To develop suitable extraction procedures for recovery of analytes needed for the detection of a variety of emerging micropollutants.
- To optimise the separation, identification and quantification of emerging micropollutants using capillary electrophoresis with UV detection, with high pressure liquid chromatography (HPLC) and Surface Enhanced Raman Spectroscopy (SERS).
- To facilitate the separation of different pharmaceuticals and steroids from the aqueous matrix using the capillary electrophoresis system.
- To determine and quantify the inorganic ions (anions and cations) present in the environmental water samples
- To compare the benefits of the new analytical method with existing techniques so as to determine the advantage of the new method over the conventional methods.

In order to accomplish the set objectives, to prove or disprove the research hypothesis and to answer the research questions, various experimental procedures were employed; and based on the results obtained as detailed in the previous chapters, the answers to the research questions are summarized as follows:

Q1. Which extraction procedure is most suitable for the detection of a variety of emerging micropollutants in wastewater?

- Due to the usually low concentrations and complexity of the matrices in which the target compounds are present in the aquatic environments, it is a difficult task to analyse the POPs in the environment. These compounds are generally in complex water matrices and are present at trace levels making their analysis difficult.

In this study, the SPE method was used for the enrichment and clean-up of aqueous samples and extraction from aqueous matrices. The water samples were preconcentrated with Strata-X 33 μ m polymeric C₁₈ reverse phase columns (500 mg/6 mL), with very high percentage recovery for all analytes.

The efficiencies of the quantitative recovery of the standard analytes for pharmaceuticals including acetaminophen, diclofenac, acetylsalicylic acid, salicylic acid, ibuprofen and sulphamethoxazole using the SPE method were evaluated using the data from recovery experiments. The analytes were recovered from a solution of 5 mg/L cocktail of analyte standards in MeOH/H₂O (30:70) mixture. The relative percentage recoveries of the analytes

were 96.20 % for acetaminophen, 91.20 % for diclofenac, 99.20 % for aspirin, 95.20 % for salicylic acid, 92.40 % for ibuprofen, and 97.60 % for sulphamethoxazole respectively. Similarly, for the steroid analytes, the relative percentage recoveries of the analytes were 90.25 % for androstenedione, 88.00 % for testosterone, 86.25 % for 17-beta-estradiol, and 91.75 % for progesterone respectively.

From these results, it can be seen that the measure of the affinity efficiency of the C₁₈ (Strata-X) nonpolar sorbent cartridges to concentrate the tested pharmaceuticals and steroid hormones (standard analytes) was high. This suggests that the use of C₁₈ (Strata-X) nonpolar sorbent cartridges in solid phase extraction procedure is efficient and satisfactory for the concentration and recoveries of the selected pharmaceutical analytes and other POPs from aqueous matrices.

Q2. How effective is the capillary electrophoresis system in the separation of organic pollutants?

- The CE is among the various methods to analyse complex samples including the persistent organic pollutants. For the separation of the pharmaceutical analytes, a CZE-UV method involving a solvent dilution ratio of 30:70 (MeOH/H₂O) mixture was used to prepare the concentration calibration range of 0.5 ppm, 1 ppm, 2 ppm, 4 ppm, 6 ppm and 8 ppm respectively, for the six analyte mixture. A buffer concentration of 30 mM ammonium acetate, pH 9.68, 50 mbar pressure, 10 seconds injection time, 70 cm capillary length, 25 °C cassette temperature and 20 kV voltage gave effective separation of pharmaceutical analytes. The details are given in section 4.5.1.1 of chapter 4. In the separation of the steroid hormone analytes, a PF-MEKC-UV method was developed and used as the optimised method for steroid hormones and metabolites in the water samples of water purification plant. The method instrumental parameters include 70 cm capillary length, 25 °C cassette temperature, and 25 kV voltage. The buffer concentration of 30 mM ammonium acetate, having its pH adjusted exactly to pH 9.68 with 25% ammonia, (as ammonium acetate in water does not give the desired alkalinity), 50 mbar pressure, 10 seconds injection time. With these optimised parameters, an effective separation of the steroid hormones analytes was achieved. Therefore, with an optimised method in place, the CE system is very effective in the separation of a complex mixture of selected organic molecules.

Q3. What effect would pollutants concentration have on the capillary electrophoresis sensitivity?

- Various analytical techniques have been employed in the monitoring of environmental pollutants, but the majority of these techniques are incapable of detecting persistent organic pollutants at nanogram levels. Therefore, in such circumstances, an absence of pollutants is sometimes recorded; as was evident in the HPLC results presented in Chapter 4. Meanwhile, these pollutants are actually present at low but undetectable concentrations. Capillary electrophoresis however, allowed the detection at low levels, with robust separation efficiency and short analysis time. This study has been able to prove the presence of selected pharmaceuticals and steroid hormones concentration in the influent, effluent, and tap water samples in the low ng/L range.

Q4. What class of organic pollutants can be separated by capillary electrophoresis (with regards to functionality, hydrophilicity, hydrophobicity, polarity, etc.)?

- There are many persistent organic pollutants present in the environment and these pollutants are of organic, inorganic and biological origins; generally present at trace levels in the environment. In this study, the analytes ranged from pharmaceuticals to steroid hormones. The pharmaceutical analytes are polar; therefore, a capillary zone electrophoresis with UV detection method (CZE-UV) was adopted for their separation, with a suitable buffer solution as the background electrolyte. However, with the steroid hormones which are non-polar, a different method was adopted to enable the movement of the analytes in the capillary to the detector. This method is the partial-filling micellar electrokinetic injections capillary chromatography with the UV detection. (PF-MEKC-UV). In PF-MEKC-UV, the combination of the electrolyte solution and the micelle solutions forms the mobile phase for the movement of the analytes through the capillary to the detector. A 100 mM sodium dodecyl sulphate (SDS) stock solution is one of the micelle solutions and the other micelle is 100 mM sodium taurocholate that was prepared with milli-Q water without any adjustment to its pH. However, the final electrolyte used in the PF-MEKC-UV was achieved by addition of 440 μL of 100 mM SDS into 1000 μL of 30 mM ammonium acetate solution (pH 9.68), and 50 μL of 100 mM sodium taurocholate solution. This order of addition was important, as there might be an intense formation of bubbles by SDS

stock solution if the addition order was different. As a result of the diverse application range of CE system, it was able to separate a wide range of selected pollutants.

Q5. Is CE-UV detection mechanism suitable in the capillary electrophoretic system?

- Detection is a crucial factor in capillary electrophoresis, and according to the literature, the ultraviolet-visible detection is one of the most commonly used detectors for the detection at nano level. In this study, the UV detection was employed and it was capable of producing good sensitivity for the range of the analytes investigated in this work. This is evident in the electropherogram of the pharmaceuticals standard analytes in section 4.5.1.1 of chapter 4. Similarly, in the analyses of the influent, effluent and tap water samples, the CE instrument was sensitive to the detection of the analytes under investigation and sensitive to other samples that were not under investigation, but the focus was only based on the analytes of interest. Therefore, the capillary zone electrophoresis with UV detection (CZE-UV) method permitting limits for detection (LOD) and quantification (LOQ) were from 0.073 to 0.230 $\mu\text{g/mL}$ (SPE concentrated 3.65 – 11.5 pg/L) and from 0.219 to 0.690 $\mu\text{g/mL}$ (SPE concentrated 10.95 – 13.8 pg/L), respectively. The instrument response to the detection of each of the standard analytes (pharmaceuticals) showed linear sensitivity to increasing concentrations with R^2 values > 0.99 for all the six analytes.

Q6. How does the quantification done by HPLC compare to that of capillary electrophoretic system?

- Both CE and HPLC methods were efficient and sensitive enough to detect some organic pollutants, and this has been proven in the literature. However, the sampling points for the analytes quantified by the CE were different from the sampling points of the analytes quantified by the LC/MS. Nevertheless, both the CE and LC/MS methods were highly reproducible. From the samples analysed by the LC/MS, two compounds (diclofenac and sulphamethoxazole) were quantified in the effluent sample and the other samples under investigation were not, this could be either be due to the other analytes being below the limit of quantification of the instrument or that those analytes were not present in the effluent sample. Also, from the analysis of the tap water samples, there was nothing found as well, also pointing to inadequate detection limits. In the case of CE, all the pharmaceutical analytes under investigation

were detected and quantified except for acetaminophen and ibuprofen in influent A sample. For the influent B and effluent samples, all the analytes were detected and quantified by CE except for acetaminophen.

Q7. In the case of SERS, are the nanoparticles deposited on the modified track-etched polyethylene terephthalate (PET) membrane physically stable?

- The stability of the colloidal silver nanoparticles is related to their zeta potential values such that any potential value within the range of +20 to -20 mV is considered as an unstable region. In this study, the zeta potential of silver nanoparticles for all samples were outside the region -20 to +20 mV, which showed that they were stable.

Q8. Can the modified and nanoparticles-immobilised track-etched PET membrane be able to enhance the Raman signal in order to detect trace level analytes in water samples using SERS?

- The silver nanoparticles-coated track-etched PET membrane was able to successfully detect acetaminophen at levels as low as 0.01 mg/L and 4-aminothiophenol (4-ATP) as low as 0.0125 mg/L. The Raman signal was directly proportional to the analyte concentration. This detection was made possible by the immobilisation of silver nanoparticles on the surface of the PET membrane. Whereas, the unmodified track-etched PET membrane did not show any peaks belonging to the analyte (acetaminophen), but rather, the Raman spectrum solely belonged to the PET membrane. Hence, the silver nanoparticles immobilisation on the track-etched polyethylene terephthalate (PET) membrane was responsible for Raman signal enhancement in this study.

7.2 Significant findings of the study

7.2.1 Analysis with capillary electrophoresis (CE) and HPLC

In the analyses carried out to understand the different parameters that affect the performance of capillary electrophoresis, this study has been able to identify and optimize the different parameters that affect the performance of capillary electrophoresis, including: the pH of the electrolyte solution that affects the separation and dissociation of the analytes according to their pKa values; the voltage which affects the field strength; and the injection type used which affects the detectability of the instrument. The capillary zone electrophoresis

with UV detection (CZE-UV) was employed in the identification and quantification of selected pharmaceuticals. In the identification and quantification of pharmaceuticals in both influent and effluent samples, aspirin was quantified to be 13.52 ng/L, diclofenac as 14.15 ng/L, salicylic acid as 6.514 ng/L and sulphamethoxazole as 11.79 ng/L respectively in the influent A sample. Influent B sample contained 4.23 ng/L of aspirin, 8.235 ng/L of diclofenac, 1.199 ng/L of salicylic acid, 1.095 ng/L of ibuprofen and 13.170 ng/L of sulphamethoxazole respectively. The effluent water sample contained 0.836 ng/L of aspirin, 0.802 ng/L of diclofenac, 1.343 ng/L of salicylic acid, 0.842 ng/L of ibuprofen and 10.241 ng/L of sulphamethoxazole. In both influent and effluent water samples, acetaminophen was not found. The reason could be that acetaminophen might have degraded into other metabolites in the process of purification (Ojemaye & Petrik, 2018; Murkin, 2014) or might not be present in the sample at all; as CE gave a good sensitivity to both influent and effluent samples.

The partial-filling micellar electrokinetic capillary chromatography (PF-MEKC) method with UV detection was adopted for the identification and quantification of the steroid hormones. This method combines chromatographic and electrophoretic separation principles and extends the applicability of capillary electrophoretic methods to neutral analytes, such as steroids. The electrolyte solution and the micelle solution, combined to form the mobile phase. A 100 mM sodium dodecyl sulphate (SDS) stock solution was one of the micelle solutions and the other micelle is 100 mM sodium taurocholate that was prepared into milli-Q water without any adjustment to its pH. The combination of the buffer electrolyte and the two micelle solutions formed the mobile phase responsible for the movement of the analytes through the capillary to the detector. For the influent A water sample, androstenedione was quantified to be 2.224 ng/L, testosterone was quantified to be 3.474 ng/L, 17- β -estradiol was quantified to be 0.96 ng/L and progesterone was 1.503 ng/L. The influent B water sample contained 2.224 ng/L of androstenedione, 3.142 ng/L of testosterone, 0.954 ng/L of 17- β -estradiol and 0.691 ng/L of progesterone respectively. The effluent water sample contained 1.205 ng/L of androstenedione, 3.037 ng/L of testosterone, 0.550 ng/L of 17- β -estradiol and 0.440 ng/L of progesterone, respectively. In the tap water samples, androstenedione concentration was 0.031 ng/L and 0.025 ng/L for hot tap water and cold tap water respectively; testosterone concentration was 0.016 ng/L and 0.013 ng/L for hot tap water and cold tap water respectively; 17- β -estradiol concentration was 0.11 ng/L and 0.09 ng/L for hot

tap water and cold tap water, respectively; while progesterone levels were 0.049 ng/L and 0.031 ng/L in hot tap water and cold tap water, respectively.

In the case of the inorganic ions, the capillary zone electrophoresis (CZE) with an indirect UV detection was employed in the quantification of the anions and cations in the water samples. The optimized capillary electrophoresis method for the inorganic ions investigation of the environmental water samples, the anions were separated in a buffer solution containing 2.25 mM pyromellitic acid, 6.50 mM NaOH, 0.75 mM hexamethonium hydroxide and 1.60 mM triethanolamine (pH 7.7 ± 0.2 , Fluka). On the contrary, the optimized capillary electrophoresis for the cations was performed in 9 mM pyridine-12 mM glycolic acid-5 mM 18-crown-6 ether at pH 3.6, adjusted with 0.1 M HCl. This study was able to develop a method a CZE method with an indirect UV detection in the analysis of inorganic ions. The cations studied include sodium, potassium, calcium and magnesium ions respectively, and the results showed that in all the tap water samples, the main inorganic cationic compounds were Na^+ (< 26 mg/L), K^+ (< 8 mg/L), Ca^{2+} (< 41 mg/L) and Mg^{2+} (< 15 mg/L). The two river water samples also showed the amounts of inorganic cations to be Na^+ (< 21 mg/L), K^+ (< 9 mg/L), Ca^{2+} (< 34 mg/L) and Mg^{2+} (< 25 mg/L). The drilled well water sample also contained all the four inorganic cations in these respective amounts: Na^+ (< 17 mg/L), K^+ (< 4 mg/L), Ca^{2+} (< 12 mg/L) and Mg^{2+} (< 5 mg/L). The average order of the inorganic cations concentration in all the 10 water samples is given as calcium > sodium > magnesium > potassium. In the inorganic anions results of the CZE-indirect-UV analyses, in all the tap water samples, the main inorganic anionic compounds were Cl^- (< 11 mg/L), SO_4^{2-} (< 51 mg/L), NO_3^- (< 3 mg/L). Subsequently, the two river water samples (RW 1 & 2) also showed the amount of amounts of the inorganic anions to be Cl^- (< 17 mg/L), SO_4^{2-} (< 21 mg/L), NO_3^- (< 3 mg/L). There was no nitrate detected in the RW 1 sample, but an amount of 2.767 mg/L was detected in the RW 2 sample. The drilled well water sample only contained Cl^- (< 4 mg/L), SO_4^{2-} (< 6 mg/L), and there was no nitrate detected in the drilled well water sample. The milli-Q water (MQW) only contained chloride in the smallest concentration amount, compared to the rest of the 10 water samples, with the amount Cl^- (< 2 mg/L). The sulphate ions had the highest anion concentrations across all the 10 water samples, followed by chloride, and then nitrates are found in the lowest amount across the respective water samples. The highest concentrations of the chlorides was found in the river water samples (RW), followed by the tap water samples, the drilled well water (DW), and the milli-Q water (MQW) samples respectively.

In the study carried out by the HPLC-MS, various water samples including effluent wastewater from the wastewater treatment plant, cold tap water, hot tap water and milli-Q water samples were investigated for the pharmaceuticals under study, including 17-beta estradiol. Only diclofenac (3.306 ng/mL) and sulphamethoxazole (1.18 ng/mL) were detected from the effluent sample; while no compound was detectable in the other water samples. The other compounds were below the level of quantification.

The comparison of the limit of detection (LOD) and limit of quantification (LOQ) between the methods employed in capillary electrophoresis (CE) and liquid chromatography (LC) shows that the limit of detection (LOD) and the limit of quantification (LOQ) for the respective compounds in capillary electrophoresis (CE) are generally lower compared to LC method. The capillary electrophoresis LOD values of 0.230, 0.137, 0.186, 0.073, 0.085, and 0.096; as compared to HPLC LOD values of 0.286, 0.195, 0.224, 0.412, 0.291, and 0.331 for acetaminophen, aspirin, sulphamethoxazole, diclofenac, ibuprofen and 17-beta estradiol respectively. Furthermore, it is important to emphasize the inadequate level of sensitivity observed with HPLC analysis, which led to the reason most of the compounds analysed were not detectable or below the limit of quantification. However, the CE was able to generate quality data in less period of time, via flexible method optimization process. The diverse application range of CE has made it suitable for the analysis of wide range of compounds coupled with peak efficiency often in excess of 10^5 theoretical plates.

7.2.2 Analysis with SERS

In the study carried out using the Raman spectroscopy, it has been shown that the track-etched polyethylene terephthalate (PET) surface can be modified with the aid of diethylenetriamine (DETA) through aminolysis, which is a wet chemistry method. The spectra of the Fourier transform infrared spectroscopy (FTIR) and X-ray photoelectron spectroscopy (XPS) confirmed that the surface of the modified track-etched PET membrane was characterised by ester bond scission and an amide bond formation (C-N). The study using SERS has been able to show that the surface of track-etched PET membrane was successfully modified with diethylenetriamine (DETA). This modification resulted in changes as regards surface wettability as shown by the contact angle measurements. The introduction of amide bond and changes in chemical states of carbon (C1s) after the ester bond scission and amide bonds formation, leading to a percentage increase of C1s in the carbon-carbon chemical state and a subsequent decrease in the percentage of O-C=O

chemical state as evident in the XPS data. The XPS data was complementary to the observation of amide II absorbance in the FTIR spectrum of the amine-modified track-etched PET membrane at 1577 cm^{-1} . The synthesis of silver nanoparticles was also achieved by the reduction of silver nitrate (AgNO_3) with trisodium citrate, which served as both reducing and stabilising agent. The zeta (ζ) potential values of more than -20 mV confirmed the stability of colloidal silver nanoparticles.

The scanning electron microscopy (SEM) images of the silver-coated track-etched polyethylene terephthalate (PET) membranes revealed the successful immobilisation of silver nanoparticles on the modified PET surface. The results from the SEM images showed that the average sizes of the nanoparticles ranged between 25 nm and 64 nm for silver nanoparticles immobilised between 10 and 30 minutes. Also, the SEM results showed there was an increase in the size of silver nanoparticles with an increase in the time of immobilisation. In addition, the results from the XPS complemented the SEM results as regards the number of silver nanoparticles immobilised on the surface, where XPS data showed an increase in the percentage from 2.52 to 5.22% of silver nanoparticles relative to the increase in immobilisation time from 10 minutes to 30 minutes. It was also found out that the thermal nature of the track-etched PET membrane was not affected by the aminolysis process and the silver nanoparticles immobilisation at $100\text{ }^\circ\text{C}$. The TGA analysis revealed that at the temperature of $500\text{ }^\circ\text{C}$, silver-coated track-etched polyethylene terephthalate membrane still retained 20% of its original weight; this was estimated to be 6% more than the amine-modified track-etched PET membrane, and 10% than unmodified track-etched PET membrane. This 6% weight was ascribed to the residual silver nanoparticles immobilised on the surface. The immobilisation of a layer of silver nanoparticles leading to the suppression of Raman signal of PET membrane was confirmed by the Raman spectra of the silver-coated track-etched polyethylene terephthalate membrane. This means the more the silver nanoparticles immobilisation on the modified polyethylene terephthalate membrane, the more the suppression of the PET membrane Raman scattering signal. This is a pointer to the fact that an analyte on the surface of the PET membrane is detectable without any interference from the polyethylene terephthalate membrane spectrum.

Furthermore, the silver-coated track-etched polyethylene terephthalate (PET) membrane was employed to successfully detect acetaminophen and 4-aminothiophenol (4-ATP) with concentrations 0.01 mg/L and 0.0125 mg/L respectively. In the analysis comparing a quartz

platform which was non-porous, the spectra of acetaminophen detected from the surface of silver-coated track-etched polyethylene terephthalate (PET) membrane were of lower intensity. This was as a result of the loss of some of the acetaminophen molecules that leached through the pores of the track-etched PET membrane. The unmodified track-etched polyethylene terephthalate (PET) membrane did not reflect the peaks of the analytes (acetaminophen and 4-aminothiophenol), rather, the Raman spectrum for the PET membrane only reflected the polyethylene terephthalate monomer of the track-etched PET membrane itself. The concentration studies for the detection of the analytes (acetaminophen and 4-aminothiophenol), the Raman peak intensities for both analytes decreased with a decrease in concentration. Acetaminophen intensity of peak trend for the C-O (861) vibration gave a linear response to concentration; while the other bond vibrations C=C at 1608 cm^{-1} , C-N at 1328 cm^{-1} , and C-O at 1170 cm^{-1} gave no linearity. By the extrapolation of the linear correlation line of C-O (861), it gave a limit of detection value of 0.0757 mg/L for acetaminophen with the use of amine-modified track-etched polyethylene terephthalate membrane prepared using 100% DETA concentration, 24 hours period and duration of 30 minutes for silver nanoparticles immobilisation.

The SERS spectra of the analytes (acetaminophen and 4-aminothiophenol) were obtained at 785 nm excitation wavelength, close to the longitudinal absorption band of the nanoparticles (Tiwari *et al.*, 2011). For 4-aminothiophenol (4-ATP), the spectrum shows the peak intensities of the 4-ATP, with the bands at 1006 and 1176 cm^{-1} belonging to stretching/bonding vibration $\nu(\text{C-C})$, out-of-plane deformation vibration $\gamma(\text{C-C})$, and deformation/bending vibration $\delta(\text{C-H})$ respectively. These bands are associated with stretching vibrations of C-C and bending vibrations of C-H bonds.

The novelty of this research study is the development and application of the capillary zone electrophoresis method with UV detection (CZE-UV) in the detection, separation and quantification of selected pharmaceutical analytes including acetaminophen, aspirin, diclofenac, ibuprofen, salicylic acid, and sulphamethoxazole respectively. It also elucidates on the application of different methods in the detection of persistent organic pollutants. Also, the in-depth investigation of the factors affecting the performance of CE instrument, before the development of methods offered tremendous insight into an effective method for the separation of various organic pollutants. The study also showcased the versatility of CE instrument in the separation of neutral analytes, such as steroids, with the application of PF-

MEKC, and measurement of inorganic ions with a CZE with an indirect UV detection. SERS was also applied in the detection of pollutants.

In conclusion, too much emphasis on routine monitoring and perpetual upgrade is not sustainable, even as the emerging contaminants lists will continue to evolve.

7.3 Recommendations

Having achieved the research aims and objectives, more analyses can still be done in furtherance to the achievements made.

- Different water samples can be sampled around Cape Town and analysed with capillary electrophoresis and LCMS instruments for persistent organic pollutants, including the pharmaceuticals and steroid hormones. Then a comparison of the results should be made, in terms of the respective quantities of the analytes under investigation and the performance of both instruments.
- It is important to investigate the best nanoparticles size that will enhance the Raman signals most.
- There is a need to focus on the relationship between the concentration and Raman intensity of prominent peaks for the spectra of different compounds, as this can potentially give a calibration curve of Raman scattering against the analyte concentration, similar to conventional chromatography studies.

UNIVERSITY of the
WESTERN CAPE

REFERENCES

Abou-El-Nour, K. M. M., Eftaiha, A., Al-Warthan, A., & Ammar, R. A. A. 2010. Synthesis and applications of silver nanoparticles. *Arabian Journal of Chemistry*, 3(3), 135-140.

Agunbiade, F. O., & Moodley, B. 2016. Occurrence and distribution pattern of acidic pharmaceuticals in surface water, wastewater, and sediment of the Msunduzi River, KwaZulu-Natal, South Africa. *Environmental Toxicology and Chemistry*, 35(1), 36-46.

Ahmad, A., Abdulkarim, A., Ooi, B., & Ismail, S. 2013. Recent development in additives modifications of polyethersulfone membrane for flux enhancement. *Chemical Engineering Journal*, 223, 246-267.

Ahrens, L., Felizeter, S. & Ebinghaus, R. 2009. Spatial distribution of polyfluoroalkyl compounds in seawater of the German Bight. *Chemosphere*, 76, pp. 179–184.

Aizpurua, J., Bryant, G., Richter, L. & García de Abajo, F. 2005. “Optical properties of coupled metallic nanorods for field-enhanced spectroscopy,” *Phys. Rev. B* 71, 235420.

Altintas, Z., Chianella, I., Ponte, G. D., Paulussen, S., Gaeta, S., & Tothill, I. E. 2016. Development of functionalised nanostructured polymeric membranes for water purification. *Chemical Engineering Journal*, 300, 358-366.

Altria, K.D. 1999. Overview of capillary electrophoresis and capillary electrochromatography. *Journal of Chromatography A*, 856: 443–463

Alvarez -Puebla, R. A. 2012. Effects of the excitation wavelength on the SERS spectrum. *The Journal of Physical Chemistry Letters*, 3(7), 857-866.

Andrade, G. F., Fan, M., & Brolo, A. G. 2010. Multilayer silver nanoparticles-modified optical fiber tip for high performance SERS remote sensing. *Biosensors and Bioelectronics*, 25(10), 2270-2275.

Ankley, G. T., Brooks, B. W., Huggett, D. B. & Sumpter, J. P. 2007. Repeating history: pharmaceuticals in the environment. *Environ Sci Technol* 41:8211–8217.

Apel, P. 2001. Track etching technique in membrane technology. *Radiation Measurements*, 34(1), 559-566.

Apel, P. Y., Blonskaya, I., Dmitriev, S., Orelovich, O., & Sartowska, B. 2015. Ion track symmetric and asymmetric nanopores in polyethylene terephthalate foils for versatile applications. *Nuclear Instruments and Methods in Physics Research Section B: Beam Interactions with Materials and Atoms*, 365, 409-413.

Awasthi, K., Choudhury, S., Komber, H., Simon, F., Formanek, P., Sharma, A., et al. 2014. Functionalisation of track-etched poly (ethylene terephthalate) membranes as a selective filter for hydrogen purification. *International Journal of Hydrogen Energy*, 39(17), 9356-9365.

Badmus, K.O., Tijani, J.O., Massima, E. and Petrik, L. 2018. Treatment of persistent organic pollutants in wastewater using hydrodynamic cavitation in synergy with advanced oxidation process. *Environmental Science and Pollution Research*, 25, 7299–7314.

Banholzer, M. J., Millstone, J. E., Qin, L., & Mirkin, C. A. 2008. Rationally designed nanostructures for surface-enhanced Raman spectroscopy. *Chemical Society Reviews*, 37(5), 885-897.

Bantz, K. C., & Haynes, C. L. 2009. Surface-enhanced Raman scattering detection and discrimination of polychlorinated biphenyls. *Vibrational Spectroscopy*, 50(1), 29-35.

Bao, L.J., Wei, Y.L., Yao, Y., Ruan, Q.Q. & Zeng, E.Y. 2015. Global trends of research on emerging contaminants in the environment and humans: a literature assimilation, *Environmental Science and Pollution Research*, 22(3):1635–1643.

Barber, L. B., Brown, G. K., Nettesheim, T. G., Murphy, E. W., Bartell, S. E. & Schoenfuss, H. L. 2011. Effects of biologically-active chemical mixtures on fish in a wastewater-impacted urban stream, *Science of the Total Environment*, 409(22), pp. 4720–4728.

Barraclough, D., Kearney, T. & Croxford, A. 2005. Bound residues: environmental solution or future problem? *Environ Pollut* 133:85–90.

Basri, H., Ismail, A. F., & Aziz, M. 2011. Polyethersulfone (PES)–silver composite UF membrane: Effect of silver loading and PVP molecular weight on membrane morphology and antibacterial activity. *Desalination*, 273(1), 72-80.

Bastus, N. G., Merkoci, F., Piella, J., & Puntès, V. 2014. Synthesis of highly monodisperse citrate-stabilized silver nanoparticles of up to 200 nm: Kinetic control and catalytic properties. *Chemical Materials*, 26(9), 2836-2846.

Batt, A. L., Bruce, I. B. & Aga, D. S. 2006. Evaluating the vulnerability of surface waters to antibiotic contamination from varying wastewater treatment plant discharges. *Environmental Pollution*, 142 (2): 295 – 302

Battaglin, W., Jorg Drewes, B. B. & McHugh, M. 2007. Contaminants of emerging concern, *Water Resources Impact*, 9(3): article 36.

Belgiorno, V., Rizzo, L., Fatta, D., Rocca, C.D., Lofrano, G., Nikolaou, A., Naddeo, V. & Meric, S. 2007. Review on endocrine disrupting-emerging compounds in urban wastewater: Occurrence and removal by photocatalysis and ultrasonic irradiation for wastewater reuse. *Desalination*, 215:166–176.

Bell KY, Wells MJM, Traexler KA, Pellegrin M, Morse A, and Bandy J. 2011. Emerging Pollutants. *Water Environment Research*, 83: 1906-1984

Benotti, M. J., Trenholm, R. A., Vanderford, B. J., Holady, J. C., Stanford, B. D. & Snyder, S. A. 2009. Pharmaceuticals and endocrine disrupting compounds in US drinking water, *Environmental Science and Technology*, 43, pp. 597–603.

Berninger, J. P. & Brooks, B. W. 2010. Leveraging mammalian pharmaceutical toxicology and pharmacology data to predict chronic fish responses to pharmaceuticals. *Toxicol Lett* 193:69–78.

Biswas, A., Bayer, I. S., Biris, A. S., Wang, T., Dervishi, E., & Faupel, F. 2012. Advances in top-down and bottom-up surface nanofabrication: Techniques, applications & future prospects. *Advances in Colloid and Interface Science*, 170(1), 2-27.

Boithias, L., Acuña, V., Vergoñós, L., Ziv, G., Marcé, R. & Sabater, S. 2014. Assessment of the water supply: demand ratios in a Mediterranean basin under different global change scenarios and mitigation alternatives. *Science of the Total Environment*, 470-471: 567-577.

Borm, P.J., Robbins, D., Haubold, S., Kuhlbusch, T., Fissan, H., Donaldson, K., Schins, R., Stone, V., Kreyling, W., Lademann, J., Krutmann, J., Warheit, D. & Oberdorster, E. 2006. The potential risks of nanomaterials: a review carried out for ECETOC, *Particle and Fibre Toxicology*, 14(3):11-19.

Botti, S., Cantarini, L., Almaviva, S., Puiu, A., & Rufoloni, A. 2014. Assessment of SERS activity and enhancement factors for highly sensitive gold coated active materials probed with explosive molecules. *Chemical Physics Letters*, 592, 277-281.

Boujday, S., Chapelle, Marc Lamy de la, Srajer, J., & Knoll, W. 2015. Enhanced vibrational spectroscopies as tools for small molecule biosensing. *Sensors*, 15(9), 21239-21264.

Bound, J.P. & Voulvoulis, N. 2005. Household disposal of pharmaceuticals as a pathway for aquatic contamination in the United Kingdom. *Environmental Health Perspectives*, 113(12):1705-1711.

Boxall, A. B. A., Fogg, L. A., Kay, P., Blackwell, P. A., Pemberton, E. J. & Croxford, A. 2003. Prioritisation of veterinary medicines in the UK environment. *Toxicology Letters* 142 2003:207-218

Boxall ABA, Fogg LA, Blackwell PA, Kay P, Pemberton, E. J. & Croxford A 2004a Veterinary medicines in the environment. *Rev Environ Contam Toxicol* 180: 1-9.

Bradley, P.M. & Journey, C. A. 2014. Assessment of endocrine disrupting chemicals attenuation in a coastal plain stream prior to wastewater treatment plant closure. *Journal of the American Water Resources Association*, 50(2):388-400.

Braun, G. B., Lee, S. J., Laurence, T., Fera, N., Fabris, L., Bazan, G. C., et al. 2009. Generalized approach to SERS nanomaterials via controlled nanoparticle linking, polymer encapsulation, and small-molecule infusion. *The Journal of Physical Chemistry C*, 113(31), 13622-13629.

Brooks, B. W., Riley, T. M. & Taylor, R. D. 2006. Water quality of effluent-dominated stream ecosystems: ecotoxicological, hydrological, and management considerations. *Hydrobiologia* 556:365–379.

Brooks, B. W., Huggett, D. B., Boxall A. B. A. 2009. Pharmaceuticals and personal care products: research needs for the next decade. *Environ Toxicol Chem* 28:2469–2472.

Brown, R. J., de Banate, M.A. & Rother, K.I. 2010. “Artificial sweeteners: a systematic review of metabolic effects in youth,” *International Journal of Pediatric Obesity*, vol. 5, no. 4, pp. 305-312, 2010.

Bryant, G., Romero, I., Abejo, F. & Aizpurua, J. 2006. “Simulating electromagnetic response in coupled metallic nanoparticles for nanoscale optical microscopy and spectroscopy: Nanorod-end effects,” *Proc. SPIE* 6323, 632313.

Bu, Q., Shi, X., Yu, G., Huang, J., & Wang, B. 2016. Assessing the persistence of pharmaceuticals in the aquatic environment: Challenges and needs. *Emerging Contaminants*, 2 145-147.

Bull, R. J., Crook, J., Whittaker, M. & Cotruvo, J. A. 2011. Therapeutic dose as the point of departure in assessing potential health hazards from drugs in drinking water and recycled municipal wastewater, *Regulatory Toxicology and Pharmacology*, 60, pp. 1–19.

Byrne-Bailey, K. G., Gaze, W. H., Kay, P., Boxall, A. B. A., Hawkey, P. M. & Wellington, E. M. H. 2009. Prevalence of sulfonamide resistance genes in bacterial isolates from manured agricultural soils and pig slurry in the United Kingdom. *Antimicrob Agents Chemother* 53:696–702.

Calderbank, A. 1989. The occurrence and significance of bound pesticide residues in soil. *Rev Environ Contam Toxicol* 108:71–103.

Carol, C., López-Cartes, C., Zaderenko, P., & Mejias, J. A. 2008. Thiol-immobilized silver nanoparticle aggregate films for surface enhanced Raman scattering. *Journal of Raman Spectroscopy*, 39(9), 1162-1169.

Caragheorghopol, A., & Chechik, V. 2008. Mechanistic aspects of ligand exchange in gold nanoparticles. *Physical Chemistry Chemical Physics*, 10(33), 5029-5041.

CDER (Center for Drug Evaluation and Research). 1998. Guidance for Industry: Environmental Assessment of Human Drug and Biologics Applications. Washington, DC: CDER and Center for Biologics Evaluation and Research, Food and Drug Administration. Available:<http://www.fda.gov/downloads/Drugs/GuidanceComplianceRegulatoryInformation/Guidances/ucm070561.pdf> [accessed 17 July 2012].

Chang, H., Wu, S., Hu, J., Asami, M. & Kunikane, S. 2008. *J. Chrom. A* 1195, 44 (2008). doi:10.1016/j.chroma.2008.04.055.

Chang, H., Wan, Y., Wu, S., Fan, Z. & Hu, J. 2011. *Water Res.* 45, 732 (2011). doi:10.1016/j.watres.2010.08.046.

CHMP (Committee for Medicinal Products for Human Use). 2006. Guideline on the Environmental Risk Assessment of Medicinal Products for Human Use. EMEA/CHMP/SWP/4447/00 corr 1. London:European Medicines Agency. Available: http://www.ema.europa.eu/docs/en_GB/document_library/Scientific_guideline/2009/10/WC500003978.pdf [accessed 17 July 2012].

Chow, E., Hibbert, D. B., & Gooding, J. J. 2005. Electrochemical detection of lead ions via the covalent attachment of human angiotensin I to mercaptopropionic acid and thioctic acid self-assembled monolayers. *Analytica Chimica Acta*, 543(1), 167-176.

Cialla, D., März, A., Böhme, R., Theil, F., Weber, K., Schmitt, M., et al. 2012. Surface-enhanced Raman spectroscopy (SERS): Progress and trends. *Analytical and Bioanalytical Chemistry*, 403(1), 27-54.

Cifuentes, A. and Poppe, H. 1994 Rectangular capillary electrophoresis: some theoretical considerations. *Chromatographia* 39, 391–404.

Clark, J. H., Breeden, S. W. & Summerton, L. 2010 Green(er) pharmacy, in: K. Klaus & M. Hempel (Eds) *Green and Sustainable Pharmacy*, pp. 37–60 (Berlin: Springer).

Clarke, R.M. & Cummins, E. 2015. Evaluation of “Classic” and emerging contaminants resulting from the application of biosolids to agricultural lands: a review,” *Human and Ecological Risk Assessment*, 21(2):492–513.

Comerton, A. M., Andrews, R. C., & Bagley, D. M. 2009. Practical overview of analytical methods for endocrine-disrupting compounds, pharmaceuticals and personal care products in water and wastewater. *Philosophical Transactions of the Royal Society of London A: Mathematical, Physical and Engineering Sciences*, 367(1904), 3923-3939.

Cooney, C. M. 2009. Study detects trace levels of pharmaceuticals in US drinking water, *Environmental Science and Technology*, 43(3), pp. 551–551.

Corcoran E, Nellesmann C, Baker E, Bos R, Osborn D, Savelli H., 2010. Sick Water? The central role of wastewater management in sustainable development. A rapid response assessment, United Nations Environment Programme. UN-HABITAT, GRID; Arendal.

Costa, J., Sant’Ana, A., Corio, P., & Temperini, M. 2006. Chemical analysis of polycyclic aromatic hydrocarbons by surface-enhanced Raman spectroscopy. *Talanta*, 70(5), 1011-1016.

Craig, A. P., Franca, A. S., & Irudayaraj, J. 2013. Surface-enhanced Raman spectroscopy applied to food safety. *Annual Review of Food Science and Technology*, 4, 369-380.

Creighton, J. 1985. “The resonance Raman contribution to SERS: Pyridine on copper or silver in aqueous media,” *Surf. Sci.* 173, 665–672.

Culha, M., Cullum, B., Lavrik, N., & Klutse, C. K. 2012. Surface-enhanced Raman scattering as an emerging characterisation and detection technique. *Journal of Nanotechnology*, Vol. 2012. Article ID 971380. doi:10.1155/2012/971380

CVMP (Committee for Medicinal Products for Veterinary Use). 2000. VICH Topic GL6 (Ecotoxicity Phase I) Step 7: Guideline on Environmental Impact Assessment (EIAs) for Veterinary Medicinal Products–Phase I. CVMP/VICH/592/98. London:European Agency for the Evaluation of Medicinal Products. Available: http://www.ema.europa.eu/docs/en_GB/document_library/Scientific_guideline/2009/10/WC500004394.pdf [accessed 17 July 2012].

CVMP (Committee for Medicinal Products for Veterinary Use). 2004. Guideline on Environmental Impact Assessment for Veterinary Medicinal Products Phase II. CVMP/VICH/790/03-FINAL. London:European Agency for the Evaluation of Medicinal Products. Available: http://www.ema.europa.eu/docs/en_GB/document_library/Scientific_guideline/2009/10/WC500004393.pdf [accessed 17 July 2012].

Dams, R., Huestis, M., Lambert, W. and Murphy, C. 2003. Matrix Effect in Bio-Analysis of Illicit Drugs with LC-MS/MS: Influence of Ionization Type, Sample Preparation, and Biofluid. *Journal of the American Society for Mass Spectrometry*, 14, 1290-1294.

Daughton, C. G. & Ternes, T. A 1999. Pharmaceuticals and personal care products in the environment: agents of subtle change? *Environ Health Perspect* 107: 907–937.

Dauginet, L., Duwez, A., Legras, R., & Demoustier-Champagne, S. 2001. Surface modification of polycarbonate and poly (ethylene terephthalate) films and membranes by polyelectrolyte deposition. *Langmuir*, 17(13), 3952-3957.

de Jesus Gaffney, V., Almeida, C. M. M., Rodrigues, A., Ferreira, E., Benoliel, M. J., & Cardoso, V. V. 2015. Occurrence of pharmaceuticals in a water supply system and related human health risk assessment. *Water Research*, 72, 199-208.

Deldime, M., Dewez, J., Schneider, Y., & Marchand-Brynaert, J. 1995. Reactivity assay of surface carboxyl chain-ends of poly (ethylene terephthalate) (PET) film and track-etched microporous membranes using fluorine labelled-and/or ^3H -labelled derivatization reagents: Tandem analysis by X-ray photoelectron spectroscopy (XPS) and liquid scintillation counting (LSC). *Applied Surface Science*, 90(1), 1-14.

Department of Water Affairs (DWA) 2012. The Annual National State of water resources for the hydrological year 2012/2013. Published by Department of Water Affairs. Pretoria, South Africa.

Drobot, M., Persin, Z., Zemljic, L., Mohan, T., Stana-Kleinschek, K., Doliska, A., et al. 2013. Chemical modification and characterisation of poly (ethylene terephthalate) surfaces for collagen immobilization. *Open Chemistry*, 11(11), 1786-1798.

Drobot, M., Gradinaru, L. M., Ciobanu, C., & Vasilescu, D. S. 2015 Effect of chemical treatment of polyethylene terephthalate surfaces on mechanical and water-sorption properties. *Scientific Bulletin, Series B: Chemistry and Material Science*, Vol. 77 Issue 3, 2015, 131-140.

Du, J., & Jing, C. 2011. Preparation of thiol modified iron oxide (with silver) magnetic SERS probe for PAHs detection and identification. *The Journal of Physical Chemistry C*, 115(36), 17829-17835.

Duwez, A. 2004. Exploiting electron spectroscopies to probe the structure and organization of self-assembled monolayers: A review. *Journal of Electron Spectroscopy and Related Phenomena*, 134(2), 97-138.

ECETOC (European Centre for Ecotoxicology and Toxicology of Chemicals). 2008. *Intelligent Testing Strategies in Ecotoxicology: Mode of Action Approach for Specifically Acting Chemicals*. TR 102, Brussels: ECETOC.

ECETOC (European Centre for Ecotoxicology and Toxicology of Chemicals). 2010. *Significance of Bound Residues in Environmental Risk Assessment*. WR17. Brussels: ECETOC.

Environment Agency R&D Technical Report P2-T04/1, UK Environment Agency, Bristol, UK.

EPA, Technical fact sheet-perchlorate, Office, 2014.

Ericson, I., Domingo, J. L., Nadal, M., Bigas, E., Llebaria, X., van Bavel, B. & Lindström, G. 2009. Levels of perfluorinated chemicals in municipal drinking water from Catalonia, Spain: public health implications, *Archives of Environmental Contamination and Toxicology*, 57(4), pp. 631–638.

Everaerts, F. M., Beckers, J. L., Verheggen, T.P. 1976. *Isotachopheresis: Theory, Instrumentation and Applications*, Journal of Chromatography Library, Vol. 6, Elsevier, Amsterdam.

Fan, M., & Brolo, A. G. 2009. Silver nanoparticles self assembly as SERS active materials with near single molecule detection limit. *Physical Chemistry Chemical Physics*, 11(34), 7381-7389.

Fan, M., Andrade, G. F. S., & Brolo, A. G. 2011. A review on the fabrication of active materials for surface enhanced Raman spectroscopy and their applications in analytical chemistry. *Analytica Chimica Acta*, 693(1–2), 7-25.

Fanali, S. 1996. Identification of chiral drug isomers by capillary electrophoresis, *J. Chromatogr. A* 735: 77–121.

Fatiyants, E. K., Berezkin, V., & Kagramanov, G. 2013. Methods for modification of track-etched membranes designed for separation of biological objects. *Petroleum Chemistry*, 53(7), 471-481.

Fatta, D., Nikolaou, A., Achilleos, A. & Meric, S. 2007.. Analytical methods for tracing pharmaceutical residues in water and wastewater. *Trends in Analytical Chemistry*, Vol. 26, No. 6.

Fávaro, S. L., Rubira, A. F., Muniz, E. C., & Radovanovic, E. 2007. Surface modification of HDPE, PP, and PET films with KMnO₄/HCl solutions. *Polymer Degradation and Stability*, 92(7), 1219-1226.

Fawell, J. K. & Chipman, K. 2000. Endocrine disrupters, drinking water and public reassurance, *Water and Environmental Management*, 5(6), pp. 4–5.

Fawell, J. & Ong, C.N. 2012. Emerging contaminants and the implications for drinking water. *International Journal of Water Resources Development*, 28(2): 247–263

Ferguson, N. J., Braunschweiger, K. I., Braunschweiger, W. R., Smith, J. R., McCormick, J. J., Wasmann, C. C., et al. 1980. Hydrogen ion buffers for biological research. *Anal. Biochem.* 104, 300–310.

Ferraro, J. R. 2003. *Introductory Raman spectroscopy*. New York: Academic press.

Fick, J., Lindberg, R. H., Parkkonen, J., Arvidsson, B., Tysklind, M. & Larsson, D. G. 2010 Therapeutic levels of levonorgestrel detected in blood plasma of fish: results from screening rainbow trout exposed to treated sewage effluents, *Environmental Science and Technology*, 44(7), pp. 2661–2666.

Finklea, H., & Meyers, R. 2000. *Encyclopaedia of analytical chemistry: Applications, theory and instrumentations*. Vol. 11. Chichester: Wiley & Sons.

Floate, K. D., Wardhaugh, K. G., Boxall, A. B. A., Sherratt, T. N. 2005. Fecal residues of veterinary parasiticides: nontarget effects in the pasture environment. *Annu Rev Entomol* 50: 153–179.

Focazio, M. J., Kolpin, D. W., Barnes, K. K., Furlong, E. T., Meyer, M. T., Zaugg, S. D., Barber, L. B. & Thurman, M. E. 2008. A national reconnaissance for pharmaceuticals and other organic wastewater contaminants in the United States. II: Untreated drinking water sources, *Science of the Total Environment*, 402, pp. 201–216.

Fu, W., Franco, A., Trapp, S. 2009. Methods for estimating the bioconcentration factor of ionizable organic chemicals. *Environ Toxicol Chem* 28:1372–1379.

Garric, J., Vollat, B., Duis, K., Pery, A., Junker, T., Ramil, M, Fink, G. & Ternes, T.A. 2007. Effects of the parasiticide ivermectin on the cladoceran *Daphnia magna* and the green alga *Pseudokirchneriella subcapitata*. *Chemosphere* 69:903–910.

Gaw S, Thomas K V., Hutchinson T. H. 2014. Sources, impacts and trends of pharmaceuticals in the marine and coastal environment. *Philos Trans R Soc B Biol Sci* 369:20130572–20130572. doi: 10.1098/rstb.2013.0572

Gaze, W. H., Zhang, L., Abdousslam, N. A., Hawkey, P. M., Calvo-Bado, L. & Royle, J., et al. 2011. Impacts of anthropogenic activity on the ecology of class 1 integrons and integron-associated genes in the environment. *ISME J* 5:1253–1261.

Gevao, B. Semple, K. T. & Jones, K. C. 2000. Bound residues in soils: a review. *Environ Pollut* 108:3–14.

Goddard, J. M., & Hotchkiss, J. 2007. Polymer surface modification for the attachment of bioactive compounds. *Progress in Polymer Science*, 32(7), 698-725.

Görög, S. 2004. *Anal. Sci.* 20, 767. doi:10.2116/analsci.20.767.

Gühlke, M., Heiner, Z., & Kneipp, J. 2016. Surface-Enhanced Raman and Surface-Enhanced Hyper-Raman Scattering of Thiol-Functionalised Carotene. *The Journal of Physical Chemistry. C, Nanomaterials and Interfaces*, 120(37), 20702.

Halvorson, R. A., & Vikesland, P. J. 2010. Surface-enhanced Raman spectroscopy (SERS) for environmental analyses. *Environmental Science & Technology*, 44(20), 7749-7755.

Harvanová, J. & Boom, J. 2015. Capillary electrophoresis technique for metal species determination: a review. *J Liquid Chromatogr & Rel. Technol.*, 38 (2015), pp. 371-380.

Hayward, K. 2011. Emerging contaminants: the need for a sound-science solution, *Water*, 21, 13(3), pp. 17–18.

Headley, J. V. & McMartin, D. W. 2004. A review of the occurrence and fate of naphthenic acids in aquatic environments. *Journal of Environmental Science and Health, Part A: Toxic/Hazardous Substances and Environmental Engineering*, 39(8):1989–2010.

Heli Sirén & Samira El Fellah. 2016. Steroids contents in waters of wastewater purification plants: determination with partial-filling micellar electrokinetic capillary chromatography and UV detection. *International Journal of Environmental Analytical Chemistry*, 96:11, 1003-1021, DOI: 10.1080/03067319.2016.1232721.

Hering, K., Cialla, D., Ackermann, K., Dörfer, T., Möller, R., Schneidewind, H., et al. (2008). SERS: A versatile tool in chemical and biochemical diagnostics. *Analytical and Bioanalytical Chemistry*, 390(1), 113-124.

Heron, R. J. L. & Pickering, F. C. 2003. Health effects of exposure to active pharmaceutical ingredients (APIs). *Occup Med* 53:357–362.

Hiissa, T., Sirén, H., Kotiaho, T., Snellman, M. & Hautojärvi, A. 1999. Quantification of anions and cations in environmental water samples: measurements with capillary electrophoresis and indirect-UV detection *J. Chrom. A*, 853 (1999), pp. 403-411.

Homem, V. & Santos, L. 2011. Degradation and removal methods of antibiotics from aqueous matrices – A review. *Journal of Environmental Management*, 92 (10): 2304 – 2347

Houtman, C. J., van Oostveen, A. M., Brouwer, A., Lamoree, M. H. & Legler, J. 2004. Identification of estrogenic compounds in fish bile using bioassay-directed fractionation, *Environmental Science and Technology*, 38, pp. 6415–6423.

Houtman C. J. 2010. Emerging contaminants in surface waters and their relevance for the production of drinking water in Europe. *Journal of Integrative Environmental Sciences*, 7(4):271–295.

Howard, P. H. & Muir D.C.G. 2010. Identifying New Persistent and Bioaccumulative Organics Among Chemicals in Commerce. *Environmental science and Technology* 44 (7):2277-2285. doi: 10.1021/es903383a

Huerta-Fontela, M., Galceran, M. T., & Ventura, F. 2011. Occurrence and removal of pharmaceuticals and hormones through drinking water treatment. *Water Research*, 45(3), 1432-1442.

Huggett, D.B., Cook, J. C., Ericson, J. F. & Williams, R. T. 2003. A theoretical model for utilizing mammalian pharmacology and safety data to prioritize potential impacts of human pharmaceuticals to fish. *Hum Ecol Risk Assess* 9:1789–1799.

Huh, Y. S., Chung, A. J., & Erickson, D. 2009. Surface enhanced Raman spectroscopy and its application to molecular and cellular analysis. *Microfluidics and Nanofluidics*, 6(3), 285-297.

Hussaini, S., Shaikh, S. & Farooqui, M. 2013. COD reduction of waste water streams of active pharmaceutical ingredient – Atenolol manufacturing unit by advanced oxidation Fenton process. *Journal of Saudi Chemical Society*, 17: 199-202.

Illinois EPA, Blue-Green Algae and Algal Toxins, Illinois Environmental Protection Agency, Springfield, Ill, USA, 2012.

Irena, G., Jolanta, B., & Karolina, Z. 2009. Chemical modification of poly (ethylene terephthalate) and immobilization of the selected enzymes on the modified film. *Applied Surface Science*, 255(19), 8293-8298.

Jin X., Peldszus S. 2012. Selection of representative emerging micropollutants for drinking water treatment studies: A systematic approach. *Sci Total Environ* 414:653–663. doi: 10.1016/j.scitotenv.2011.11.035

Jobling, S., Williams, R., Johnson, A., Taylor, A., Gross-Sorokin, M., Nolan, M., Tyler, C. R., van Aerle, R., Santos, E. & Brighty, G. 2005. *Env. Health Persp.* 114, 32. doi:10.1289/ehp.8050.

Jones, D.M., Watson, J.S., Meredith, W., Chen, M. & Bennett, B. 2001. Determination of naphthenic acids in crude oils using nonaqueous ion exchange solid-phase, *Analytical Chemistry*, 73(3):703–707.

Jorgensen, J. W. and Lukacs, K. D. 1981. Zone electrophoresis in open-tubular glass capillaries. *Anal. Chem.* 53, 1298–1302.

Kauffman, J. F., Batykefer, L. M., & Tuschel, D. D. 2008. Raman detected differential scanning calorimetry of polymorphic transformations in acetaminophen. *Journal of pharmaceutical and biomedical analysis*, 48(5), 1310-1315.

Khan, Z., Al-Thabaiti, S. A., Obaid, A. Y., & Al-Youbi, A. 2011. Preparation and characterisation of silver nanoparticles by chemical reduction method. *Colloids and Surfaces B: Biointerfaces*, 82(2), 513-517.

Khodashenas, B., & Ghorbani, H. R. 2015. Synthesis of silver nanoparticles with different shapes. *Arabian Journal of Chemistry*. <https://doi.org/10.1016/j.arabjc.2014.12.014>

Klavarioti, M., Mantzavinos, D., & Kassinos, D. 2009. Removal of residual pharmaceuticals from aqueous systems by advanced oxidation processes. *Environment International*, 35(2), 402-417.

Kleinman, S. L., Frontiera, R. R., Henry, A., Dieringer, J. A., & Van Duyne, R. P. 2013. Creating, characterising, and controlling chemistry with SERS hot spots. *Physical Chemistry Chemical Physics*, 15(1), 21-36.

Knapp, C. W., Dolfing, J., Ehlert, P. A. I. & Graham, D. W. 2010. Evidence for increasing antibiotic resistance gene abundance in archived soils since 1940. *Environ Sci Technol* 44:580–587.

Kochkodan, V., & Hilal, N. 2015. A comprehensive review on surface modified polymer membranes for biofouling mitigation. *Desalination*, 356, 187-207.

Kolle, S.N., Ranmirez, T., Kamp, H.G., Buesen, R., Flick, B. & Strauss, V. 2013. A testing strategy for the identification of mammalian, systemic endocrine disruptors with particular focus on steroids. *Regulation and Toxicology Pharmacology*, 63:259–78.

Kolpin, D. W., Furlong, E. T., Meyer, M. T., Thurman, E. M., Zaugg, S. D., Barber, L. B. & Buxton, H. T. 2002. Pharmaceuticals, hormones, and other organic wastewater contaminants in U.S. streams, 1999–2000: a national reconnaissance, *Environmental Science and Technology*, 36(6), pp. 1202–1211.

Korolkov, I. V., Mashentseva, A. A., Güven, O., Zdorovets, M. V., & Taltenov, A. A. 2015. Enhancing hydrophilicity and water permeability of PET track-etched membranes by advanced oxidation process. *Nuclear Instruments and Methods in Physics Research Section B: Beam Interactions with Materials and Atoms*, 365, Part B, 651-655.

Kreuzig, R., Höltge, S. 2005. Investigations on the fate of sulfadiazine in manured soil: laboratory experiments and test plot studies. *Environ Toxicol Chem* 24:771–776.

Kristiansson, K., Fick, J., Janzon, A., Grabic, R., Rutgersson, C. & Weidegård, B., et al. 2011. Pyrosequencing of antibiotic-contaminated river sediments reveals high levels of resistance and gene transfer elements. *PLoS ONE* 6:e17038; doi:10.1371/journal.pone.0017038 [Online 6 February 2011].

Kruszewski, S., & Cyrankiewicz, M. 2011. Activation of silver colloids for enhancement of raman scattering. *Acta Physica Polonica A*, 119(6 A), 1018-1022.

Kshirsagar, P., Sangaru, S. S., Malvindi, M. A., Martiradonna, L., Cingolani, R., & Pompa, P. P. 2011. Synthesis of highly stable silver nanoparticles by photoreduction and their size fractionation by phase transfer method. *Colloids and Surfaces A: Physicochemical and Engineering Aspects*, 392(1), 264-270.

Kubackova, J., Fabriciova, G., Miskovsky, P., Jancura, D., & Sanchez-Cortes, S. 2014. Sensitive surface-enhanced Raman spectroscopy (SERS) detection of organochlorine pesticides by alkyl dithiol-functionalised metal nanoparticles-induced plasmonic hot spots. *Analytical Chemistry*, 87(1), 663-669.

Kunacheva, C., Tanaka, S., Fujii, S., Boontanon, S. K., Musirat, C. & Wongwattana, T. 2011. Determination of perfluorinated compounds (PFCs) in solid and liquid phase river water samples in Chao Phraya River, Thailand, *Water Science and Technology*, 64(3), pp. 684 – 692.

Kuster, M., de Alda, M. J., Hernando, M. D., Petrovic, M., Martin-Alonso, J. & Barcelo, D. 2008. Analysis and occurrence of pharmaceuticals, estrogens, progestogens and polar pesticides in sewage treatment plant effluents, river water and drinking water in the Llobregat river basin (Barcelona, Spain), *Journal of Hydrology*, 358, pp. 112–123.

Kwadijk, C.J., Korytar, P. & Koelmans, A.A. 2010. Distribution of perfluorinated compounds in aquatic systems in the Netherlands, *Environmental Science and Technology*, 44:3746–3751.

Lalia, B. S., Kochkodan, V., Hashaikeh, R., & Hilal, N. 2013. A review on membrane fabrication: Structure, properties and performance relationship. *Desalination*, 326, 77-95.

Lam, S. H., Mathavan, S., Tong, Y., Li, H., Karuturi, R. K., Wu, Y., Vega, V. B., Liu, E. T. & Gong, Z. 2008. Zebrafish whole-adult-organism chemogenomics for large-scale predictive and discovery chemical biology, *PLoS Genetics*, 4(7): e1000121.

Lam, S.H., Hlaing, M.M., Zhang, X., Yan, C., Duan, Z., Zhu, L., Ung, C.Y., Mathavan, S., Ong, C.N. & Gong, Z. 2011. Toxicogenomic and phenotypic analyses of bisphenol-a early-life exposure toxicity in zebrafish, *PLoS ONE*, 6(12): e28273.

Lamsal, R., Harroun, S. G., Brosseau, C. L., & Gagnon, G. A. 2012. Use of surface enhanced Raman spectroscopy for studying fouling on nanofiltration membrane. *Separation and Purification Technology*, 96, 7-11.

Lange, R., Hutchinson, T.H., Croudace, C.P., Siegmund, F., Schweinfurth, H., Hampe, P., Panter, G.H. & Sumpter, J.P. 2001. Effects of the synthetic estrogen 17 α -ethinylestradiol on the life-cycle of the fathead minnow (*pimephales promelas*). *Environmental Toxicology and Chemistry*, 20(6):1216–1227.

Lapworth, D., Baran, N., Stuart, M., & Ward, R. 2012. Emerging organic contaminants in groundwater: A review of sources, fate and occurrence. *Environmental Pollution*, 163, 287-303.

Laville, N., Ait-Aissa, S., Gomez, E., Casellas, C., Porcher, J. M. 2004. Effects of human pharmaceuticals on cytotoxicity, EROD activity and ROS production in fish hepatocytes. *Toxicology* 196: 41–55.

Le Ru, E., & Etchegoin, P. 2008. Principles of surface-enhanced Raman spectroscopy: And related plasmonic effects. Oxford: Elsevier.

Lee, P., & Meisel, D. 1982. Adsorption and surface-enhanced Raman of dyes on silver and gold sols. *Journal of Physical Chemistry*, 86(17), 3391-3395.

Lee, A., Elam, J. W., & Darling, S. B. 2016. Membrane materials for water purification: Design, development, and application. *Environmental Science: Water Research & Technology*, 2(1), 17-42.

Li, J.J., Hartono, D., Ong, C.N., Bay, B.H. & Yung, L.Y. 2010. Autophagy and oxidative stress associated with gold nanoparticles. *Biomaterials*, 31(23):5996–6003.

Li W, Shi Y, Gao L, Liu J, Cai Y. 2012. Occurrence of antibiotics in water, sediments, aquatic plants, and animals from Baiyangdian Lake in north China. *Chemosphere* 89:1307–1315.

Li, D., Li, D., Fossey, J. S., & Long, Y. 2010. Portable surface-enhanced Raman scattering sensor for rapid detection of aniline and phenol derivatives by on-site electrostatic preconcentration. *Analytical Chemistry*, 82(22), 9299-9305.

Li, D., Zhai, W., Li, Y., & Long, Y. 2014a. Recent progress in surface enhanced Raman spectroscopy for the detection of environmental pollutants. *Microchimica Acta*, 181(1-2), 23-43.

Li, Y., Qu, L., Li, D., Song, Q., Fathi, F., & Long, Y. 2013a. Rapid and sensitive in-situ detection of polar antibiotics in water using a disposable silver–graphene sensor based on electrophoretic preconcentration and surface-enhanced Raman spectroscopy. *Biosensors and Bioelectronics*, 43, 94-100.

Li, Q., Du, Y., Xu, Y., Wang, X., Ma, S., Geng, J., et al. 2013b. Rapid and sensitive detection of pesticides by surface-enhanced Raman spectroscopy technique based on glycidyl methacrylate–ethylene dimethacrylate (GMA–EDMA) porous material. *Chinese Chemical Letters*, 24(4), 332-334.

Li, W. C. 2014b. Occurrence, sources, and fate of pharmaceuticals in aquatic environment and soil. *Environmental Pollution*, 187, 193-201.

Lin, A. Y.-c., Yu, T.-h. & Lateef, S. K. 2009. Removal of Pharmaceuticals in secondary wastewater treatment processes in Taiwan. *Journal of Hazardous Materials*, 167: 1163 – 1169

Lin, J., Tang, C. Y., Huang, C., Tang, Y. P., Ye, W., Li, J., et al. 2016. A comprehensive physico-chemical characterisation of superhydrophilic loose nanofiltration membranes. *Journal of Membrane Science*, 501, 1-14.

Liu, S., Ying, G. G., Zhao, J. L., Chen, F., Yang, B., Zhou, L. J. & Lai, H. J. 2011. *J. Chrom. A* 1218, 1367. doi:10.1016/j.chroma.2011.01.014.

Liu, L., Deng, D., Xing, Y., Li, S., Yuan, B., Chen, J., et al. 2013. Activity analysis of the carbodiimide-mediated amine coupling reaction on self-assembled monolayers by cyclic voltammetry. *Electrochimica Acta*, 89, 616-622.

Lombardi, J. R., & Birke, R. L. 2009. A unified view of surface-enhanced Raman scattering. *Accounts of Chemical Research*, 42(6), 734-742.

Long, T. M., Prakash, S., Shannon, M. A., & Moore, J. S. 2006. Water-vapor plasma-based surface activation for trichlorosilane modification of PMMA. *Langmuir*, 22(9), 4104-4109.

Loos, R., Locoro, G., Comero, S., Contini, S., Schwesig, D., Werres, F., Balsaa, P., Gans, O., Weiss, S., Blaha, L., Bolchi, M. & Gawlik, B.M. 2010. Pan-European survey on the occurrence of selected polar organic persistent pollutants in ground water, *Water Research*, 44(14):4115–4126.

Lubick, N. 2009. India's drug problem. *Nature*, 457:640–641.

Lucotti, A., & Zerbi, G. 2007. Fiber-optic SERS sensor with optimized geometry. *Sensors and Actuators B: Chemical*, 121(2), 356-364.

Lukacs, K. D. and Jorgensen, J. W. 1985. Capillary zone electrophoresis: effect of physical parameters on separation efficiency and quantitation *J. High Resolut. Chromatogr. Chromatogr. Commun.* 8, 407.

Luo Y, Guo W, Ngo HH, et al .2014. A review on the occurrence of micropollutants in the aquatic environment and their fate and removal during wastewater treatment. *Sci Total Environ* 473–474:619–641. doi: 10.1016/j.scitotenv.2013.12.065

Lurie, I.S. 1992. Micellar electrokinetic capillary chromatography of the enantiomers of amphetamine, methamphetamine and their hydroxyphenethylamine precursors, *J. Chromatogr.* 605: 269–275.

Lurie, I.S., Klein, R.F.X., Dal Cason, T.A., LeBelle, M.J., Brenneisen, R. & Weinberger, R.E. 1994. Chiral resolution of cationic drugs of forensic interest by capillary electrophoresis with mixtures of neutral and anionic cyclodextrins, *Anal. Chem.* 66: 4019–4026.

Ma, P., Liang, F., Wang, D., Yang, Q., Cao, B., Song, D., et al. 2015. Selective determination of o-phenylenediamine by surface-enhanced Raman spectroscopy using silver nanoparticles decorated with α -cyclodextrin. *Microchimica Acta*, 182(1-2), 167-174.

Ma, Y., Ding, Q., Yang, L., Zhang, L., & Shen, Y. 2013. Silver nanoparticles as multifunctional SERS-active material for the adsorption, degradation and detection of dye molecules. *Applied Surface Science*, 265, 346-351.

Magureanu, M., Piroi, D., Gherendi, F., Mandache, N. & Parvulescu, V. 2008. Decomposition of Methylene Blue in Water by Corona Discharges. *Plasma Chemistry and Plasma Processing*, 28 (6): 677–688.

Makiabadi, T., Bouvrée, A., Le Nader, V., Terrisse, H., & Louarn, G. 2010. Preparation, optimization, and characterisation of SERS sensor active materials based on two-dimensional structures of gold colloid. *Plasmonics*, 5(1), 21-29.

Malik, A. K and Faubel, W. 2001. A Review of Analysis of Pesticides Using Capillary Electrophoresis. *Critical Reviews in Analytical Chemistry*, 31(3):223–279.

Marchand-Brynaert, J., Deldime, M., Dupont, I., Dewez, J., & Schneider, Y. 1995. Surface functionalisation of poly(ethylene terephthalate) film and membrane by controlled wet chemistry: Chemical characterisation of carboxylated surfaces. *Journal of Colloid and Interface Science*, 173(1), 236-244.

Markandya, A., Taylor, T., Longo, A., Murty, M. N., Murty, S. & Dhavala, K. 2008. Counting the cost of vulture decline—an appraisal of the human health and other benefits of vultures in India. *Ecol Econ* 67:194–204.

Matousek, P., & Parker, A. W. 2006. Bulk Raman analysis of pharmaceutical tablets. *Applied spectroscopy*, 60(12), 1353-1357.

Mauter, M. S., Wang, Y., Okemgbo, K. C., Osuji, C. O., Giannelis, E. P., & Elimelech, M. 2011. Antifouling ultrafiltration membranes via post-fabrication grafting of biocidal nanomaterials. *American Chemical Society Applied Materials & Interfaces*, 3(8), 2861-2868.

McCracken, D. I. 1993. The potential for avermectins to affect wildlife. *Vet Parasitol* 48:273–280.

McLachlan, M.S., Holmstrom, K.E., Reth, M. & Berger, U. 2007. Riverine discharge of perfluorinated carboxylates from the European continent, *Environmental Science and Technology*, 41:7260–7265.

McMahon, G. 2008. Analytical instrumentation: A guide to laboratory, portable and miniaturized instruments. Chichester: John Wiley & Sons.

McNay, G., Eustace, D., Smith, W. E., Faulds, K., & Graham, D. 2011. Surface-enhanced Raman scattering (SERS) and surface-enhanced resonance Raman scattering (SERRS): A review of applications. *Applied Spectroscopy*, 65(8), 825-837.

Megson, D., Reiner, E. J., Jobst, K. J., Dorman, F. L., Robson, M. & Jean-François Focant, J. 2016. A review of the determination of persistent organic pollutants for environmental forensics investigations. *Analytica Chimica Acta* 941: 10 - 25

Meheretu, G. M., Cialla, D., & Popp, J. 2014. Surface enhanced Raman spectroscopy on silver nanoparticles. *International Journal of Biochemistry and Biophysics*, 2(4), 63-67.

Meng, X., Tang, S., & Vongehr, S. 2010. A review on diverse silver nanostructures. *Journal of Materials Science & Technology*, 26(6), 487-522.

Meredith-Williams, M., Carter, L. J., Fussell, R., Raffaelli, D., Ashauer, R., Boxall, A. B. A. 2012. Uptake and depuration of pharmaceuticals in aquatic invertebrates. *Environ Pollut* 165:250–258.

Meyers, R. A. 2000. *Encyclopedia of analytical chemistry: Applications, theory and instrumentation*. [Raman spectroscopy, thermal analysis, X-ray photoelectron spectroscopy and auger electron spectroscopy, X-ray spectrometry, general articles, indexes]. London: Wiley & Sons.

Miraji, H., Othman, O.C., Ngassapa, F.N. & Mureithi, E.W. 2016. Research Trends in Emerging Contaminants on the Aquatic Environments of Tanzania. *Scientifica*, Volume 2016, Article ID 3769690, 6 pages

Mons, M. N., Hoogenboom, A. C. & Noij, T. H. M. 2003. Pharmaceuticals and Drinking Water Supply in the Netherlands, Kiwa Report BTO 2003.040 (Nieuwegein, the Netherlands: Kiwa Water Research).

Muehlethaler, C., Leona, M., & Lombardi, J. R. 2015. Review of surface enhanced Raman scattering applications in forensic science. *Analytical Chemistry*, 88(1), 152-169

Mulamattathil, S. G., Bezuidenhout, C., Mbewe, M., & Ateba, C. N. 2014. Isolation of environmental bacteria from surface and drinking water in Mafikeng, South Africa, and characterisation using their antibiotic resistance profiles. *Journal of Pathogens*, 2014, 371208.

Murkin, A. 2014. Metabolism of acetaminophen (paracetamol). Available from https://commons.wikimedia.org/wiki/File:Acetaminophen_metabolism.png [accessed 12 July 2017]

Muthuvijayan, V., Gu, J., & Lewis, R. S. 2009. Analysis of functionalised polyethylene terephthalate with immobilized NTPDase and cysteine. *Acta Biomaterialia*, 5(9), 3382-3393.

Nady, N., Franssen, M. C. R., Zuilhof, H., Eldin, M. S. M., Boom, R., & Schroën, K. 2011. Modification methods for poly(arylsulfone) membranes: A mini-review focusing on surface modification. *Desalination*, 275(1-3), 1-9.

Natsuki, J., Natsuki, T., & Hashimoto, Y. 2015. A review of silver nanoparticles: Synthesis methods, properties and applications. *International Journal Material Science Applied*, 4, 325-332.

Nebot, C., Gibb, S. W. & Boyd, K. G. 2007. Quantification of human pharmaceuticals in water samples by high performance liquid chromatography-tandem mass spectrometry. *Analytica Chimica Acta*, 598: 87 – 94

Nelson, W. M. & Lee, C. S. 1996. *Anal. Chem* 68, 3265 (1996). doi:10.1021/ac951137o.

Nentwig, G., Oetken, M., Oehlmann, J. 2004. Effects of pharmaceuticals on aquatic invertebrates—the example of carbamazepine and clofibrac acid. In *Pharmaceuticals in the Environment* Kummerer K (ed) , pp 195–208. Heidelberg, Germany: Springer.

Nghiem, L. D., Schäfer, A. I., & Elimelech, M. 2005. Pharmaceutical retention mechanisms by nanofiltration membranes. *Environmental Science & Technology*, 39(19), 7698-7705.

Nguyen, V. T., Reinhard, M. & Karina, G. Y. 2011. Occurrence and source characterization of perfluorochemicals in an urban watershed, *Chemosphere*, 82(9), pp. 1277–1285.

Nikolaou, A., Meric, S. & Fatta, D. 2007. Occurrence patterns of pharmaceuticals in water and wastewater environments. *Anal Bioanal Chem*, 387: 1225 – 1234.

Nissen, K., Stuart, B., Stevens, M., & Baker, A. 2008. Characterisation of aminated poly (ethylene terephthalate) surfaces for biomedical applications. *Journal of Applied Polymer Science*, 107(4), 2394-2403.

Niu, C., Zou, B., Wang, Y., Cheng, L., Zheng, H., & Zhou, S. 2016. Highly sensitive and reproducible SERS performance from uniform film assembled by magnetic noble metal composite microspheres. *Langmuir*, 32(3), 858-863.

Noel, S., Liberelle, B., Yogi, A., Moreno, M. J., Bureau, M. N., Robitaille, L., et al. 2013. A non-damaging chemical amination protocol for poly (ethylene terephthalate)–application to the design of functionalised compliant vascular grafts. *Journal of Materials Chemistry B*, 1(2), 230-238.

Novotny, M., Soini, H. & Stefansson, M. 1994. Chiral separation through capillary electromigration methods, *Anal. Chem.* 66: 646A–655A.

Oakes, K. D., Coors, A., Escher, B. I., Fenner, K., Garric, J. & Gust, T. M. 2010. Environmental risk assessment for the serotonin re-uptake inhibitor fluoxetine: case study utilizing the European risk assessment framework. *Integr Environ Assess Manag* 6(suppl 1):524–539.

Oaks, J.L., Gilbert, M., Virani, M.Z., Watson, R.T, Meteyer, C.U., Rideout, B.A., Shivaprasad, H.L., Ahmed, S., Chaudhry, M.J.I, Arshad, M., Mahmood, S., Ali, A. & Khan A.A. 2004. Diclofenac residues as the cause of vulture population decline in Pakistan. *Nature*, 427:630-633.

O'Connor, J., Sexton, B., & Smart, R. S. 2013. Surface analysis methods in materials science. Berlin: Springer Science & Business Media.

Ojemaye, C. Y., Petrik, L. F. 2018. Pharmaceuticals in the marine environment: A review. Environmental Reviews, (), er-2018-0054-. doi:10.1139/er-2018-0054

Ojemaye, C., Petrik, L. 2021. Pharmaceuticals and Personal Care Product in the Marine Environment Around False Bay, Cape Town, South Africa: Occurrence and Risk Assessment Study 30 March 2021, Environmental Toxicology and Chemistry—Volume 00, Number 00—pp. 1–21, 2021 <https://doi.org/10.1002/etc.5053>

Osawa, M., Matsuda, N., Yoshii, K & Uchida, I. 1994. “Charge transfer resonance Raman process in surface-enhanced Raman scattering from p-aminothiophenol adsorbed on silver: Herzberg-Teller contribution,” J. Phys. Chem. 98, 12702–12707 (1994).

Ozcam, A. E., Efimenko, K., Jaye, C., Spontak, R. J., Fischer, D. A., & Genzer, J. 2009. Modification of PET surfaces with self-assembled monolayers of organosilane precursors. Journal of Electron Spectroscopy and Related Phenomena, 172(1), 95-103.

Park, S. Y., Chung, J. W., Chae, Y. K., & Kwak, S. 2013. Amphiphilic thiol functional linker mediated sustainable anti-biofouling ultrafiltration nanocomposite comprising a silver nanoparticles and poly (vinylidene fluoride) membrane. American Chemical Society Applied Materials & Interfaces, 5(21), 10705-10714.

Parker, D.R. 2009. Perchlorates in the environment the key current issues. Environmental Chemistry, 6(1):1–2.

Pascoe D, Karntanut W, Muller C. T. 2003. Do pharmaceuticals affect freshwater invertebrates? A study with the cnidarian Hydra vulgaris. Chemosphere 51: 521–528.

Patil, R. S., Kokate, M. R., Jambhale, C. L., Pawar, S. M., Han, S. H., & Kolekar, S. S. 2012. One-pot synthesis of PVA-capped silver nanoparticles their characterisation and biomedical application. Advances in Natural Sciences: Nanoscience and Nanotechnology, 3(1), 015013.

Patterson, H. G. 2013. Scoping study and research strategy development on currently known and emerging contaminants influencing drinking water quality. WRC Report No. 2093/1/13

Pavlović, D. M., Ašperger, D., Tolić, D., & Babić, S. 2013. Development and optimization of the determination of pharmaceuticals in water samples by SPE and HPLC with diode-array detection. *Journal of Separation Science*, 36(18), 3042-3049.

Péron, O., Rinnert, E., Lehaitre, M., Crassous, P., & Compère, C. 2009. Detection of polycyclic aromatic hydrocarbon (PAH) compounds in artificial sea-water using surface-enhanced Raman scattering (SERS). *Talanta*, 79(2), 199-204.

Petrie, B., Barden, R. & Kasprzyk-Hordern, B. 2015. A review on emerging contaminants in wastewaters and the environment: Current knowledge, understudied areas and recommendations for future monitoring. *Water Research*, 72:3-27.

Petrovic, M., Sole, M., de Alda, M. J. L. & Barcelo, D. 2002 Endocrine disruptors in sewage treatment plants, receiving river waters, and sediments: integration of chemical analysis and biological effects on feral carp, *Environmental Toxicology and Chemistry*, 21, pp. 2146–2156.

Pieczonka, N. P., & Aroca, R. F. 2008. Single molecule analysis by surface-enhanced Raman scattering. *Chemical Society Reviews*, 37(5), 946-954.

Pillai, Z. S., & Kamat, P. V. 2004. What factors control the size and shape of silver nanoparticles in the citrate ion reduction method? *The Journal of Physical Chemistry B*, 108(3), 945-951.

Pinhancos, R., Maass, S., & Ramanathan, D. M. 2011. High-resolution mass spectrometry method for the detection, characterisation and quantitation of pharmaceuticals in water. *Journal of Mass Spectrometry*, 46(11), 1175-1181.

Pomati, F., Netting, A.G., Calamari, D., Neilan, B. A. 2004. Effects of erythromycin and ibuprofen on the growth of *Synechocystis* sp. and *Lemna minor*. *Aquat Toxicol* 67: 387–396.

Qin, Y., Ji, X., Jing, J., Liu, H., Wu, H., & Yang, W. 2010. Size control over spherical silver nanoparticles by ascorbic acid reduction. *Colloids and Surfaces A: Physicochemical and Engineering Aspects*, 372(1), 172-176.

Qu, L., Geng, Y., Bao, Z., Riaz, S., & Li, H. 2016. Silver nanoparticles on cotton swabs for improved surface-enhanced Raman scattering, and its application to the detection of carbaryl. *Microchimica Acta*, 183(4), 1307-1313.

Raghav, M., Eden, S., Mitchell, K. and Witte, B. 2013. *Contaminants of Emerging Concern in Water*, University of Arizona, Tucson, Ariz, USA.

Ramírez-Meneses, E., Montiel-Palma, V., Dominguez-Crespo, M. A., Izaguirre-López, M., Palacios-Gonzalez, E., & Dorantes-Rosales, H. 2015. Shape- and size-controlled silver nanoparticles stabilized by in situ generated secondary amines. *Journal of Alloys and Compounds*, 643, S51-S61.

Ratola, N., Cincinelli, A., Alves, A., & Katsoyiannis, A. 2012. Occurrence of organic microcontaminants in the wastewater treatment process. A mini review. *Journal of Hazardous Materials*, 239, 1-18.

Raveendran, P., Fu, J., & Wallen, S. L. 2003. Completely “green” synthesis and stabilization of metal nanoparticles. *Journal of the American Chemical Society*, 125(46), 13940-13941.

Reddersen, K., Heberer, T. & Dunnbier, U. 2002. Identification and significance of phenazone drugs and their metabolites in ground- and drinking water, *Chemosphere*, 49(6), pp. 539 –544.

Reddy, S. J. 2015. Silver nanoparticles-synthesis, applications and toxic effects on humans: A review. *International Journal of Bioassays*, 4(11), 4563-4573.

Reichenbacher, M., & Popp, J. 2012. *Challenges in molecular structure determination*. Berlin: Springer Science & Business Media.

Reznickova, A., Novotna, Z., Kolska, Z., & Svorcik, V. 2014. Immobilization of silver nanoparticles on polyethylene terephthalate. *Nanoscale Research Letters*, 9(1), 1.

Richardson, S.D. 2006. Environmental mass spectrometry: emerging contaminants and current issues. *Analytical Chemistry*, 78(12):4021–4046.

Richardson, S.D. & Ternes, T.A. 2011. Water analysis: emerging contaminants and current issues. *Analytical Chemistry*, 83 (12): 4614-4648.

Rivera-Utrilla, J., Sánchez-Polo, M., Ferro-García, M. Á., Prados-Joya, G., & Ocampo-Pérez, R. 2013. Pharmaceuticals as emerging contaminants and their removal from water. A review. *Chemosphere*, 93(7), 1268-1287.

Rodgers, J.H. 2008. *Algal Toxins in Pond Aquaculture*, Southern Regional Aquaculture Center.

Rodrigues, D. C., Andrade, G. F. S., & Temperini, M. L. A. 2013. SERS performance of gold nanotubes obtained by sputtering onto polycarbonate track-etched membranes. *Physical Chemistry Chemical Physics*, 15(4), 1169-1176.

Scarcella, D., Tagliaro, F., Turrina, S., Manetto, G., Nakahara, Y., Smith, F.P. & Marigo, M. 1997. Optimization of a simple method for the chiral separation of phenethylamines of forensic interest based on cyclodextrin complexation capillary electrophoresis and its preliminary application to the analysis of human urine and hair, *Forensic Sci. Int.* 89: 33–46.

Schlücker, S. 2014. Surface-Enhanced Raman spectroscopy: Concepts and chemical applications. *Angewandte Chemie International Edition*, 53(19), 4756-4795.

Schmidt, H., Bich Ha, N., Pfannkuche, J., Amann, H., Kronfeldt, H., & Kowalewska, G. 2004. Detection of polynuclear aromatic hydrocarbons (PAHs) in seawater using surface-enhanced Raman scattering (SERS). *Marine Pollution Bulletin*, 49(3), 229-234.

Schmitt, J., & Flemming, H. 1998. FTIR-spectroscopy in microbial and material analysis. *International Biodeterioration & Biodegradation*, 41(1), 1-11. doi:[http://dx.doi.org/10.1016/S0964-8305\(98\)80002-4](http://dx.doi.org/10.1016/S0964-8305(98)80002-4)

Schulte-Oehlmann, U., Oetken, M., Bachmann, J., Oehlmann, J. 2004. Effects of ethinylestradiol and methyltestosterone in prosobranch snails. In *Pharmaceuticals in the Environment* Kummerer K (ed), pp 233–246. Heidelberg, Germany: Springer.

Schriks, M., Heringa, M. B., van der Kooi, M. M., de Voogt, P. & van Wezel, A. P. 2009. Toxicological relevance of emerging contaminants for drinking water quality, *Water Research*, 44, pp. 461–476.

Seiler, J. P. 2002. Pharmacodynamic activity of drugs and ecotoxicology—can the two be connected? *Toxicol Lett* 131:105–115.

Sengelov, G., Agero, Y., Halling-Sorensen, B., Baloda, S. B., Andersen, J. S., Jensen, L. B. 2003. Bacterial antibiotic resistance levels in Danish farmland as a result of treatment with pig manure slurry. *Environ Int* 28: 587–595.

Sharma, V. K., Yngard, R. A., & Lin, Y. 2009. Silver nanoparticles: Green synthesis and their antimicrobial activities. *Advances in Colloid and Interface Science*, 145(1–2), 83-96.

Sharma, B., Cardinal, M. F., Kleinman, S. L., Greeneltch, N. G., Frontiera, R. R., Blaber, M. G., et al. 2013. High-performance SERS active materials: Advances and challenges. *Material Research Society Bulletin*, 38(08), 615-624.

Simon, D. C. & John, B. 2005. Ecosystem response to antibiotics entering the aquatic environment. *Marine Pollution Bulletin*, 51: 218 – 223

Singha, D., Barman, N., & Sahu, K. 2014. A facile synthesis of high optical quality silver nanoparticles by ascorbic acid reduction in reverse micelles at room temperature. *Journal of Colloid and Interface Science*, 413, 37-42.

Sirén, H. & El Fellah, S. 2016. Steroids contents in waters of wastewater purification plants: determination with partial-filling micellar electrokinetic capillary chromatography and UV detection. *International Journal of Environmental Analytical Chemistry* vol. 96, no. 11, 1003 – 1021.

Skutlarek, D., Exner, M. & Farber, H. 2006. Perfluorinated surfactants in surface and drinking waters, *Environmental Science and Pollution Research International*, 13:299–307.

Smith, W. 2008. Practical understanding and use of surface enhanced Raman scattering/surface enhanced resonance Raman scattering in chemical and biological analysis. *Chemical Society Reviews*, 37(5), 955-964.

Smith, R. D., Leo, J. A., Edmonds, C. G., Barinaga, C. J., and Usdeth, H. R. 1990. Sensitivity considerations for large molecule detection by capillary electrophoresis- electrospray ionization mass spectrometry. *J. Chromatogr.* 516, 157–165.

Smoluchowski, M. V. 1905. Elektrosche kataphorese. *Physik. Z.* 6, 529.

Smyth, C., Mirza, I., Lunney, J., & McCabe, E. 2013. Surface-enhanced Raman spectroscopy (SERS) using silver nanoparticle films produced by pulsed laser deposition. *Applied Surface Science*, 264, 31-35.

Snyder, S.A., Westerhoff, P., Yoon, Y. & Sedlak, D.L. 2004. Pharmaceuticals, personal care products, and endocrine disruptors in water: implications for the water industry. *Environmental Engineering Science*, 20(5):449–469.

Solov'ev, A. Y., Pote hina, T., Chernova, I., & Basin, B. Y. 2007. Trac membrane with immobilized colloid silver nanoparticles. *Russian Journal of Applied Chemistry*, 80(3), 438-442.

Sommer, C., Bibby, B. M. 2002. The influence of veterinary medicines on the decomposition of dung organic matter in soil. *Eur J Soil Biol* 38: 155–159.

Sperling, R. A., & Parak, W. J. 2010. Surface modification, functionalisation and bioconjugation of colloidal inorganic nanoparticles. *Philosophical Transactions. Series A, Mathematical, Physical, and Engineering Sciences*, 368(1915), 1333-1383.

Stackelberg, P. E., Furlong, E. T., Meyer, M. T., Zaugg, S. D., Henderson, A. K., & Reissman, D. B. 2004. Persistence of pharmaceutical compounds and other organic wastewater contaminants in a conventional drinking-water-treatment plant. *Science of the Total Environment*, 329(1-3), 99-113.

Stanford, B. D., Trenholm, R. A., Holady, J. C., Vanderford, B. J. & Snyder, S. A. 2010. Estrogenic activity of US drinking waters: a relative exposure comparison, *Journal of the American Water Works Association*, 110(11), pp. 55-65.

Steffen, W., Persson, A., Deutsch, L., Zalasiewicz, J., Williams, M., Richardson, K., Crumley, C., Crutzen, P., Folke, C., Molina, M., Ramanathan, V., Rockstrom, J., Scheffer, M., Schellnhuber, H.J., Svedin, U. 2011. The Anthropocene: From Global Change to Planetary Stewardship. *Ambio* 40:739-761.

Strachan, C. J., Rades, T., Gordon, K. C., & Rantanen, J. 2007. Raman spectroscopy for quantitative analysis of pharmaceutical solids. *Journal of pharmacy and pharmacology*, 59(2), 179-192.

Suez, J., Korem, T. & Zeevi, D. 2014. "Artificial sweeteners induce glucose intolerance by altering the gut microbiota," *Nature*, vol. 514, pp. 181-186.

Sukardi, H., Chng, H. T., Chan, E. C., Gong, Z. & Lam, S. H. 2011. Zebrafish for drug toxicity screening: bridging the in vitro cell-based models and in vivo mammalian models, *Expert Opinion on Drug Metabolism & Toxicology*, 7, pp. 579-589.

Sun, H., Li, F., Zhang, T., Zhang, X., He, N., Song, Q., Zhao, L., Sun, L. & Sun, T. 2011. Perfluorinated compounds in surface waters and WWTPs in Shenyang, China: mass flows and source analysis, *Water Research*, 45(15), pp. 4483-4490.

Švorčík , V., Ře níč ová, A., Sajdl, P., Kols á, Z., Ma ajová, Z., & Slepí č a, P. 2011. Gold nanoparticles grafted on plasma treated polymers. *Journal of Materials Science*, 46(24), 7917-7922.

Swartz, C., Genthe, B., Chamier, J., Petrik, L. F., Tijani, J. O., Adeleye, A., Coomans, C. J., Ohlin, A., Falk, D., Menge, J. G. 2018a. Emerging Contaminants in wastewater treated for direct potable re-use: The human health risk priorities in South Africa. Vol. 1—A Concise Research Report. [cited 2020 April 9]. Available from: <http://www.wrc.org.za/wp-content/uploads/mdocs/TT742Vol1web.pdf>

Swartz, C. D., Genthe, B., Chamier, J., Petrik, L. F., Tijani, J. O., Adeleye, A., Coomans, C. J., Ohlin, A., Falk, D., Menge, J. G. 2018b. Emerging contaminants in wastewater treated for direct potable re-use: The human health risk priorities in South Africa. Vol. 3—Occurrence, fate, removal and health risk assessment of chemicals of emerging concern in reclaimed water for potable reuse. [cited 2019 August 12]. Available from: <http://www.wrc.org.za/wp-content/uploads/mdocs/TT742Vol3web.pdf>

Tagliaro, F., Smythb, W.F., Turrinaa, S., Deyle, Z. and Marigoa, M. 1995. Capillary electrophoresis: a new tool in forensic toxicology. Applications and prospects in hair analysis for illicit drugs. *Forensic Science International*, 70 (1995) 93-104.

Tagliaroa, F., Manettoa, G., Crivellentea, F., Smith, F.P. 1998. A brief introduction to capillary electrophoresis. *Forensic Science International*, 92 (1998) 75–88.

Talbert, J. N., & Goddard, J. M. 2012. Enzymes on material surfaces. *Colloids and Surfaces B: Biointerfaces*, 93, 8-19.

Tan, K. S., & Cheong, K. Y. 2013. Advances of silver, copper, and silver–copper alloy nanoparticles synthesized via chemical reduction route. *Journal of Nanoparticle Research*, 15(4), 1-29.

Taurozzi, J. S., & Tarabara, V. V. 2007. Silver nanoparticle arrays on track etch membrane support as flow-through optical sensors for water quality control. *Environmental Engineering Science*, 24(1), 122-137.

Terabe, S., Otsuka, K. & Nishi, H. 1994. Separation of enantiomers by capillary electrokinetic techniques, *J. Chromatogr. A* 666: 295–319.

Ternes, T. 2001. Pharmaceuticals and metabolites as contaminants of the aquatic environment, in: C. G. Daughton & T. L. Jones-Lepp (Eds) *Pharmaceuticals and Care Products in the Environment*, pp. 39–55 (Washington, DC: American Chemical Society).

Thompson, J., Eaglesham, G. & Mueller, J. 2011. Concentrations of PFOS, PFOA and other perfluorinated alkyl acids in Australian drinking water, *Chemosphere*, 83(10), pp. 1320–1325.

Thormann, W., Molteni, S., Caslavská, J. and Schmutz, A. 1994. Clinical and forensic applications of capillary electrophoresis. *Electrophoresis*, 15: 3-12.

Thorpe, K. L., Cummings, R. I., Hutchinson, T. H., Scholze, M., Brighty, G., Sumpter, J. P. & Tyler, C. R. 2003. *Environ. Sci. Technol.* 37, 1142 (2003). doi:10.1021/es0201348.

Tijani, J. O., Fatoba, O. O. & Petrik, L. F. 2013. A review of pharmaceuticals and endocrine disrupting compounds: Sources, effects, removal and detections. *Water, Air and Soil Pollution*, 224:1770 DOI 10.1007/s11270-013-1770-3.

Tiwari, N.R, Liu, M.Y, Kulkarni, S. & Fang, Y. 2011. Study of adsorption behavior of aminothiophenols on gold nanorods using surface-enhanced Raman spectroscopy: *Journal of Nanophotonics*, 5(1) 053513.

Tolaymat, T. M., El Badawy, A. M., Genaidy, A., Scheckel, K. G., Luxton, T. P., & Suidan, M. 2010. An evidence-based environmental perspective of manufactured silver nanoparticle in syntheses and applications: A systematic review and critical appraisal of peer-reviewed scientific papers. *Science of the Total Environment*, 408(5), 999-1006.

Tran, Q. H., & Le, A. 2013. Silver nanoparticles: Synthesis, properties, toxicology, applications and perspectives. *Advances in Natural Sciences: Nanoscience and Nanotechnology*, 4(3), 033001.

Tran, N.H., Hu, J., Li, J. & Ong, S.L. 2014. "Suitability of artificial sweeteners as indicators of raw wastewater contamination in surface water and groundwater," *Water Research*, vol. 48, no. 1, pp. 443–456.

Trapido, M., Epold, I., Bolobajev, J. & Dulova, N. 2014. Emerging micropollutants in water/wastewater: growing demand on removal technologies. *Environmental Science and Pollution Research*, 21(21):12217-22

Urbansky, E.T. & Schock, M.R. 1999. Issues in managing the risks associated with perchlorate in drinking water. *Journal of Environmental Management*, 56(2):79–95.

USEPA. 2013. Basic Information about Disinfection Byproducts in Drinking Water: Total Trihalomethanes, Haloacetic Acids, Bromate, and Chlorite, U.S. Environmental Protection Agency.

USGS (US Geological Survey). 2014. Emerging Contaminants In the Environment: Accessed October 2014. <http://toxics.usgs.gov/regional/emc/>

Val'erio, E., Abrantes, L. & Viana, A. 2008. "4-Aminothiophenol self-assembled monolayer for the development of a DNA biosensor aiming the detection of cylindrospermopsin producing cyanobacteria," *Electroanalysis* 20, 2467–2474.

VanOrman, B. B., Liversidge, G. G., and McIntire, G. L. 1991. Effects of buffer composition on electroosmotic flow in capillary electrophoresis. *J. Microcol. Septo.* 2, 176.

Vashist, S. K. 2012. Comparison of 1-ethyl-3-(3-dimethylaminopropyl) carbodiimide based strategies to crosslink antibodies on amine-functionalised platforms for immunodiagnostic applications. *Diagnostics*, 2(3), 23-33.

Velleman, L., Losic, D., & Shapter, J. G. 2012. The effects of surface functionality positioning on the transport properties of membranes. *Journal of Membrane Science*, 411, 211-218.

Vesel, A., Junkar, I., Cvelbar, U., Kovac, J., & Mozetic, M. 2008. Surface modification of polyester by oxygen-and nitrogen-plasma treatment. *Surface and interface analysis*, 40(11), 1444-1453.

Vieno, N. M., Harkki, H., Tuhkanen, T. & Kronberg, L. 2007. Occurrence of Pharmaceuticals in River Water and Their Elimination in a Pilot-Scale Drinking Water Treatment Plant. *Environmental Science & Technology*, 41 (14): 5077 – 5084

Vinther, A. and Soeberg, H. 1991. Temperature elevation of the sample zone in free solution capillary electrophoresis under stacking conditions. *J. Chromatogr.* 559, 3–26.

Vinther, A. and Soeberg, H. 1991. Mathematical model describing dispersion in free solution capillary electrophoresis under stacking conditions. *J. Chromatogr.* 559, 27–47.

Virtanen, R. and Kivalo, P. 1969. Quantitative high-voltage zone electrophoresis method. *Suomen Kemistilehti B* 42, 182.

Voeten, R. L. C., Ventouri, I. K., Haselberg, R. & Somsen, G. W. 2018. Capillary Electrophoresis: Trends and recent advances. *Anal Chem.* 90: 1464 – 1481.

Wang, A. X., & Kong, X. 2015. Review of recent progress of plasmonic materials and nano-structures for surface-enhanced Raman scattering. *Materials*, 8(6), 3024-3052.

Ward, T.J. 1994. Chiral media for capillary electrophoresis, *Anal. Chem.* 66: 633A–640A.

Watts, M.M., Pascoe, D. & Carroll, K. 2002. Population responses of the freshwater amphipod *Gammarus pulex* (L.) to an environmental estrogen, 17 α -ethinylestradiol. *Environmental Toxicology and Chemistry*, 21:445–450.

Watts and Crane Associates. 2007. Desk Based Review of Current Knowledge on Pharmaceuticals in Drinking Water and Estimation of Potential Levels: Final Report to DWI (Defra Project Code: CSA 7184/WT02046/ DWI70/2/213) (Faringdon, UK: Watts and Crane Associates).

Weihrauch, M.R. & Diehl, V. 2004. "Artificial sweeteners—do they bear a carcinogenic risk?" *Annals of Oncology*, vol. 15, no. 10, pp.1460–1465.

Wen, Y., Chen, L., Li, J., Liu, D. & Chen, L. 2014. *Trends Anal. Chem.* 59, 26. doi:10.1016/j.trac.2014.03.011.

Wenzel, A., Müller, J. & Ternes, T. 2003. Study on endocrine disrupters in drinking water: Final Report ENV.D.1/ETU/2000/0083 (Smallenberg: European Commission).

Westergaard, K., Müller, A. K., Christensen, S., Bloem, J., Sørensen, S. J. 2001. Effects of tylosin on the soil microbial community. *J Soil Biol Biochem* 33: 2061–2071.

Whatley, H., 2001. Basic principles and modes of capillary electrophoresis. In *Clinical and Forensic Applications of Capillary Electrophoresis* (pp. 21-58). Humana Press.

WHO (World Health Organization). 1998. Antimicrobial Resistance. Fact Sheet no. 194. Geneva:WHO. Available: <http://www.who.int/mediacentre/factsheets/fs194/en/> [accessed 18 July 2012].

WHO. 2002. Global Assessment of the State-of-the-Science of Endocrine Disruptors, WHO/PCS/EDC/02.2 (Geneva: World Health Organization).

WHO. 2011a. Pharmaceuticals in Drinking Water (Geneva: World Health Organization).

WHO. 2011b. Guidelines for Drinking-Water Quality, 4th ed. (Geneva: World Health Organization).

WHO/UNEP. 2013. State of the science of endocrine disrupting chemicals – 2012. An assessment of the state of the science of endocrine disruptors prepared by a group of experts for the United Nations Environment Programme (UNEP) and WHO. Accessed at <http://www.who.int/ceh/publications/endocrine/en/>.

Wood, T. P., Duvenage, C. S., & Rohwer, E. 2015. The occurrence of anti-retroviral compounds used for HIV treatment in South African surface water. *Environmental Pollution*, 199, 235-243.

Xu, G., Qiao, X., Qiu, X., & Chen, J. 2008. Preparation and characterisation of stable monodisperse silver nanoparticles via photoreduction. *Colloids and Surfaces A: Physicochemical and Engineering Aspects*, 320(1), 222-226.

Xue, L., & Lu, Y. 2013. Electroless copper plating on 1, 2-ethylenediamine grafted poly (ethyleneterephthalate) for the fabrication of flexible copper clad laminate. *Journal of Materials Science: Materials in Electronics*, 24(7), 2211-2217.

Yan Xu. 1996. Tutorial of Capillary Electrophoresis. *The Chemical Educator*, 2, 1430-4171.

Yang Y, Ok YS, Kim K-H, et al. 2017. Occurrences and removal of pharmaceuticals and personal care products (PPCPs) in drinking water and water/sewage treatment plants: A review. *Sci Total Environ* 596–597:303–320. doi: 10.1016/j.scitotenv.2017.04.102

Yin, J., Yang, Y., Hu, Z., & Deng, B. 2013. Attachment of silver nanoparticles (AgNPs) onto thin-film composite (TFC) membranes through covalent bonding to reduce membrane biofouling. *Journal of Membrane Science*, 441, 73-82.

Young, W. F., Whitehouse, P., Johnson, I., Soroki, N. 2002. Proposed predicted no-effect concentrations (PNECs) for natural and synthetic steroid oestrogens in surface waters.

Yuan, S., Jiang, X., Xia, X., Zhang, H., & Zheng, S. 2013. Detection, occurrence and fate of 22 psychiatric pharmaceuticals in psychiatric hospital and municipal wastewater treatment plants in Beijing, China. *Chemosphere*, 90(10), 2520-2525.

Zacs, D., Perkons, I. & Bartkevics, V. 2016. Determination of steroidal oestrogens in tap water samples using solid-phase extraction on a molecularly imprinted polymer sorbent and quantification with gas chromatography-mass spectrometry (GC-MS). *Environmental Monitoring and Assessment* volume 188, Article number: 433 - 445.

Zhang, Z., Yu, Q., Li, H., Mustapha, A., & Lin, M. 2015. Standing gold nanorod arrays as reproducible SERS active materials for measurement of pesticides in apple juice and vegetables. *Journal of Food Science*, 80(2), N450-N458.

Zhang, T., Sun, H., Lin, Y., Wang, L., Zhang, X., Liu, Y., Geng, X., Zhao, L., Li, F. & Kannan, K. 2011. Perfluorinated compounds in human blood, water, edible freshwater fish, and seafood in China: daily intake and regional differences in human exposures, *Journal of Agriculture and Food Chemistry*, 59(20), pp. 11168–11176.

Zhao, C., Xue, J., Ran, F., & Sun, S. 2013. Modification of polyethersulfone membranes – A review of methods. *Progress in Materials Science*, 58(1), 76-150.



UNIVERSITY *of the*
WESTERN CAPE

APPENDIX

Appendix A1: Peakmaster software.

CE Expert Lite

CE Expert Lite can be used to estimate fluid deliveries. The answers presented should be taken as approximations, not as absolutes.

Quick Start Enter System Type, Capillary Dimensions, and Conditions. Click on Calculate to display results.

System Type:

OPA 800 and P/ACE System MDQ

Generic CE

Capillary Dimensions:

48.5	Total Length (cm)
40	Length to Window
50	Inside Diameter

Conditions:

25	Temperature (°C)
0.5	Pressure (psi)
10	Time (sec)

Hydrodynamic Injection (nl)	12.24
Capillary Volume (nl)	952
Capillary Volume to Window (nl)	785
Injection Plug Length (mm)	6.22
Plug % Length to Window	1.55
Capillary Volumes Replaced	0.012866
Seconds to replace 1 volume	778
Injection Pressure-seconds	5
Relative Viscosity (cp)	891

This program provides results based on theoretical principles. The answers presented here should be taken as approximations, not absolutes.

Appendix A2: The migration order of standard compounds in pH 8.5.

Run parameters

Total capillary length (cm)	48.5
Capillary length to detector (cm)	40
Polarity (at injection site)	Positive
Driving voltage (V)	25000
EOF	Marker time
EOF marker time (min)	3

Run settings

Ionic strength correction

[Amplitudes and Shapes]

Signal

Direct

System parameters

pH	8.547
Ionic strength (mM)	10.000
Conductivity (S/m)	7.91e-02
Resistivity (Ohmcm)	12.645
Buffer capacity (mM)	6.531
EOF marker time (min)	3.000
EOF mobility (1e-9 m ² /V/s)	43.111
1. system eigenmobility	0.000
2. system eigenmobility	-0.180

BGE constituents

Name	c (mM)	u_eff	c(-) (mM)	c(0) (mM)	c(+1) (mM)
TRICINE-ANI	14.000	-21.421	9.996	4.004	
SODIUM	10.000	51.900		7.04e-05	10.000

Analytes

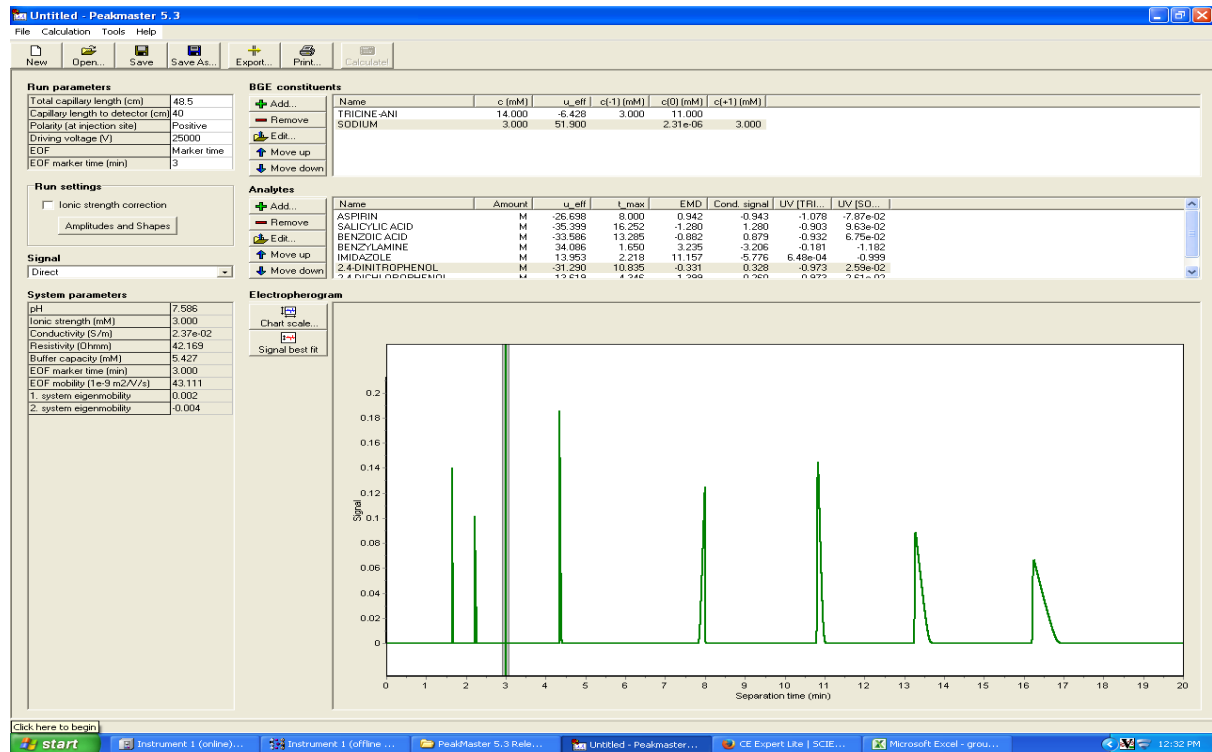
Name	Amount	u_eff	L_max	EMD	Cond. signal	UV [TRIL...]	UV [SD...]
BENZOIC ACID	M	-33.539	13.469	-0.869	0.869	-0.931	6.67e-02
BENZYLAMINE	M	29.786	1.758	4.736	-3.980	-0.182	-1.181
ASPIRIN	M	-26.700	7.833	0.955	-0.955	-1.077	-7.97e-02
IMIDAZOLE	M	2.002	2.849	30.976	-7.271	-3.57e-02	-0.956
2,4-DICHLOROPHENOL	M	-27.413	8.130	-0.842	0.308	-0.973	2.55e-02
2,4-DINITROPHENOL	M	-31.299	10.913	-0.318	0.318	-0.973	2.50e-02
CALCIUM ACID	M	26.400	12.623	1.376	1.376	0.967	9.82e-03

Electropherogram

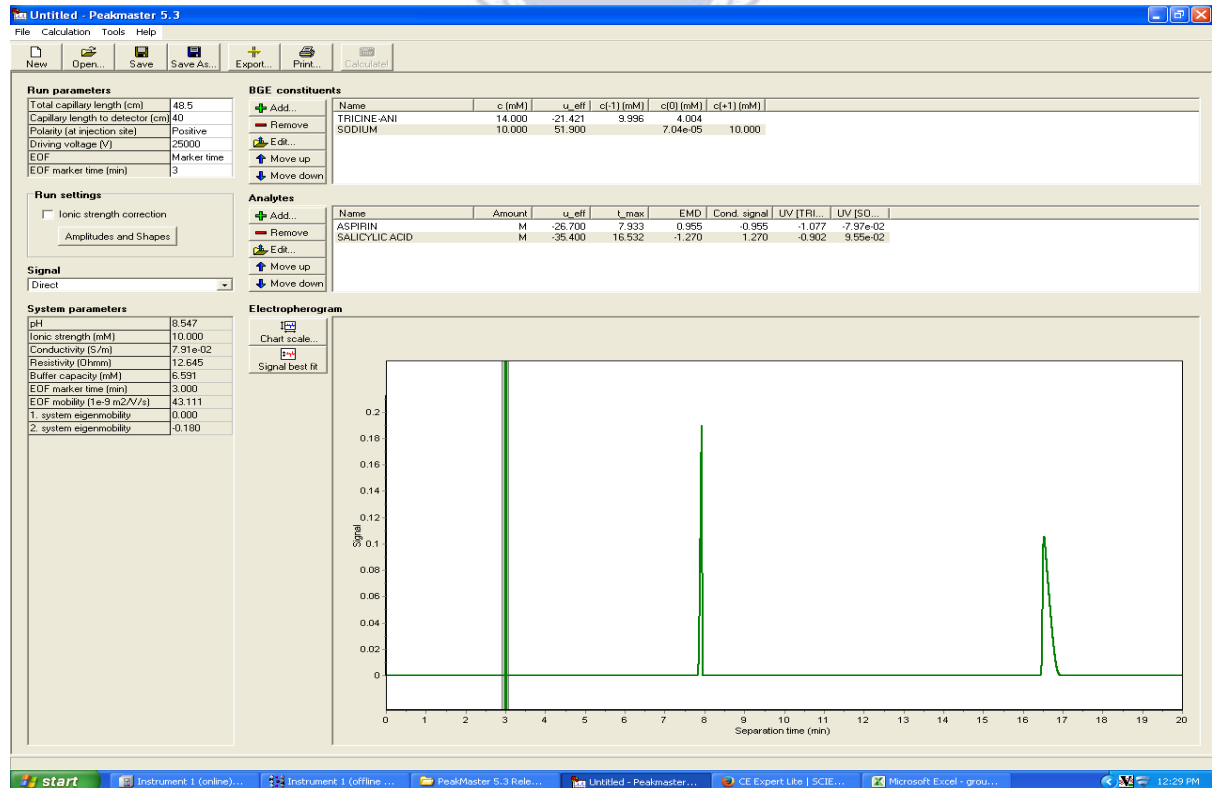
Chart scale...
Signal best fit

The chromatogram shows seven distinct peaks labeled 1 through 7, corresponding to the analytes listed in the table above. The x-axis represents Separation time (min) from 0 to 20, and the y-axis represents Signal from 0 to 0.2.

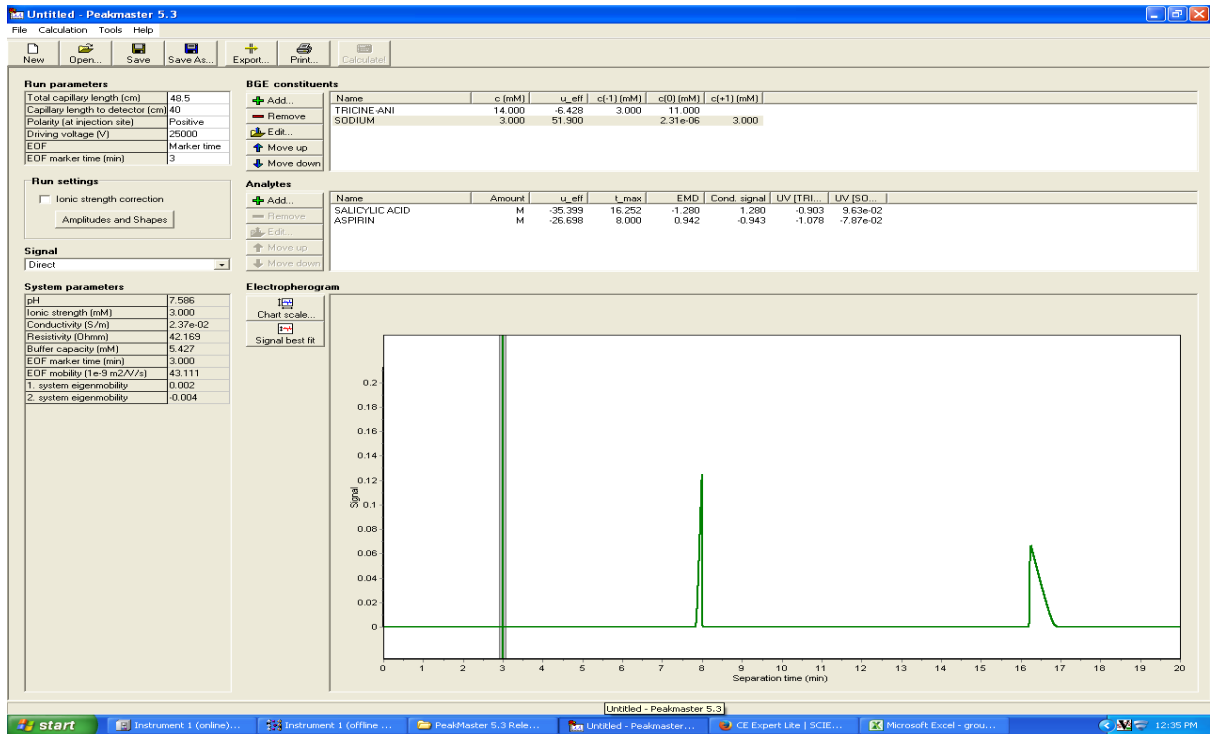
Appendix A3: The migration order of standard compounds in pH 7.5.



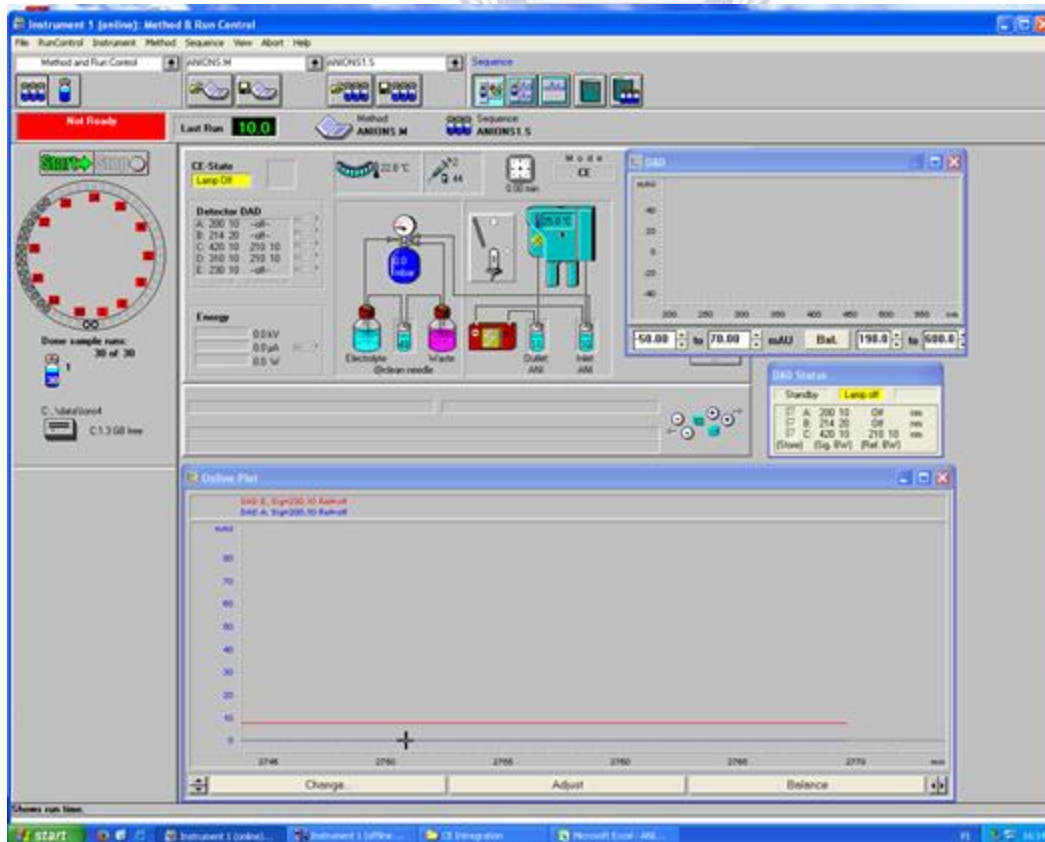
Appendix A4: The migration order of acetylsalicylic acid (1) and salicylic acid (2) in pH 8.5.



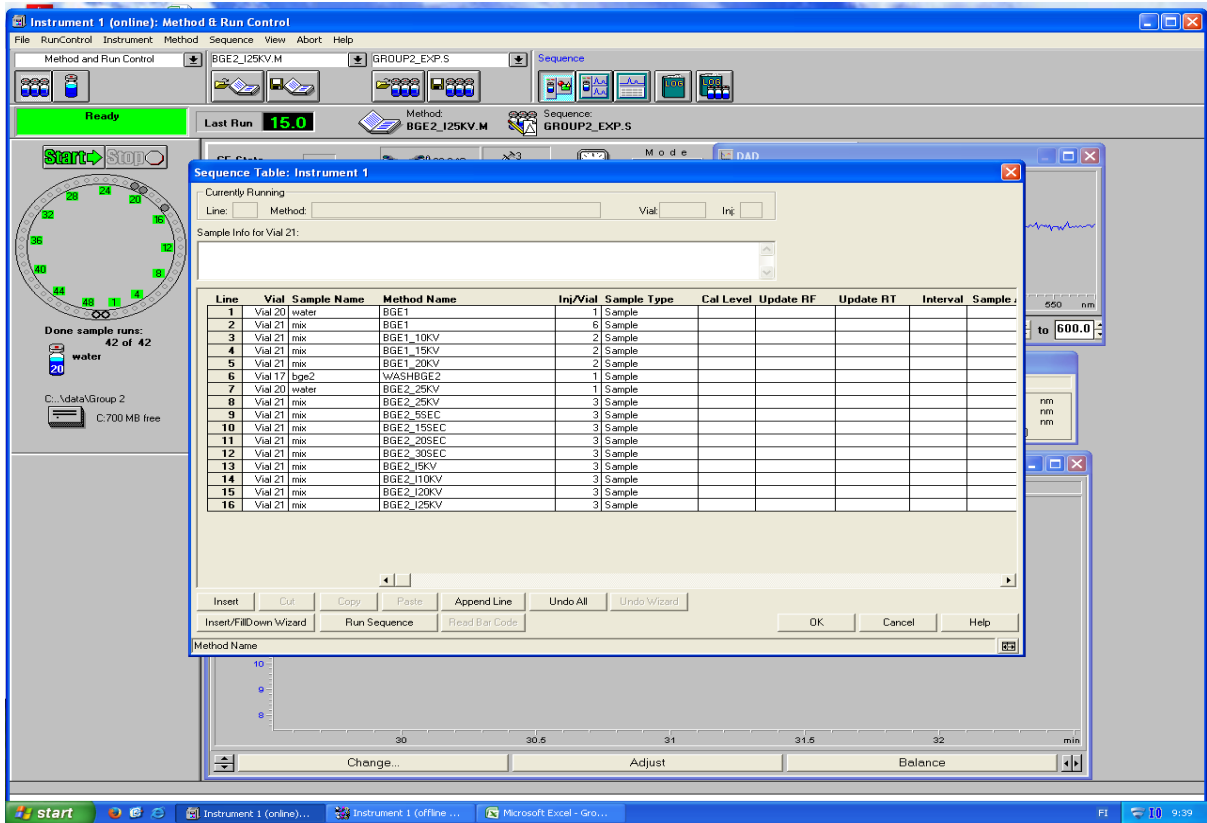
Appendix A5: The migration order of acetylsalicylic acid (1) and salicylic acid (2) in pH 7.5.



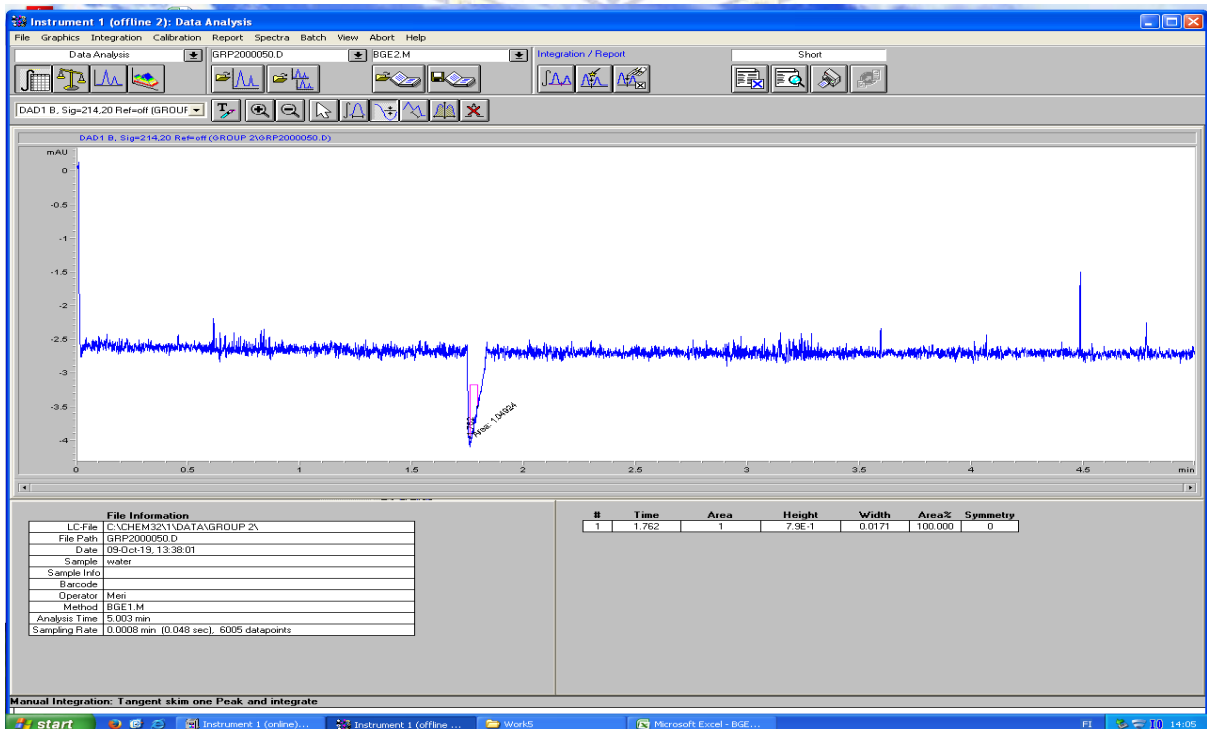
Appendix A6: Working screen of capillary electrophoresis.



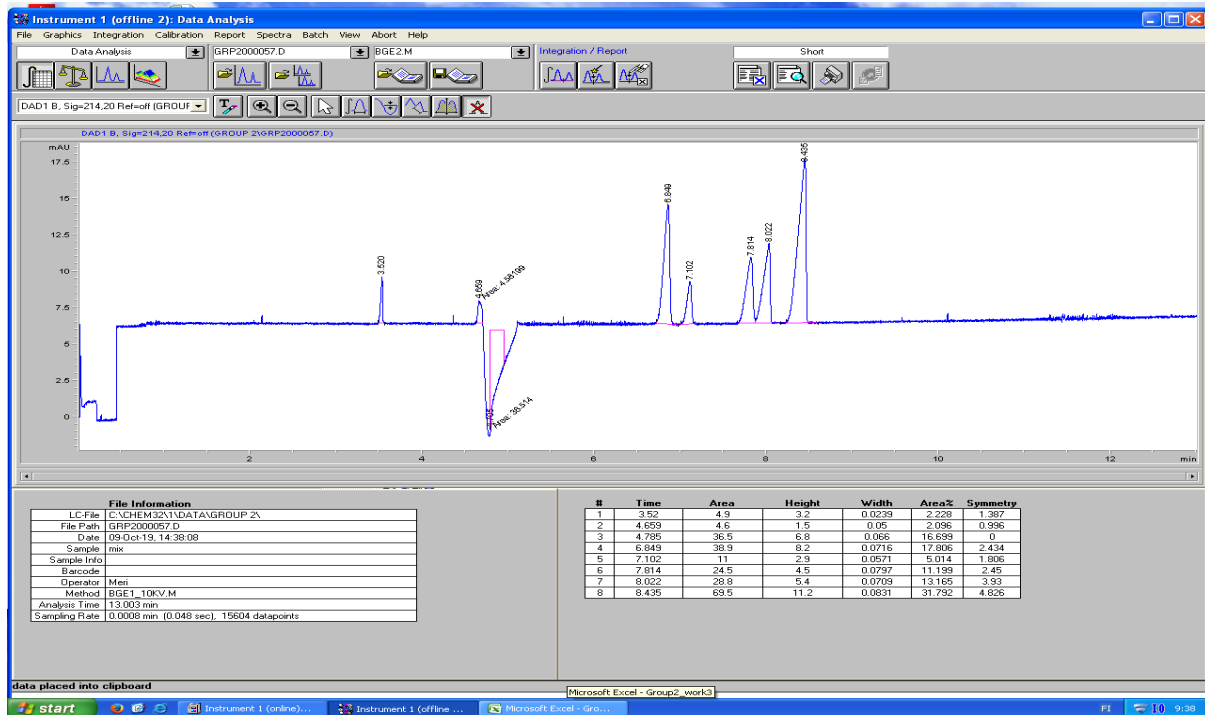
Appendix A7: The sequence table of the analysis.



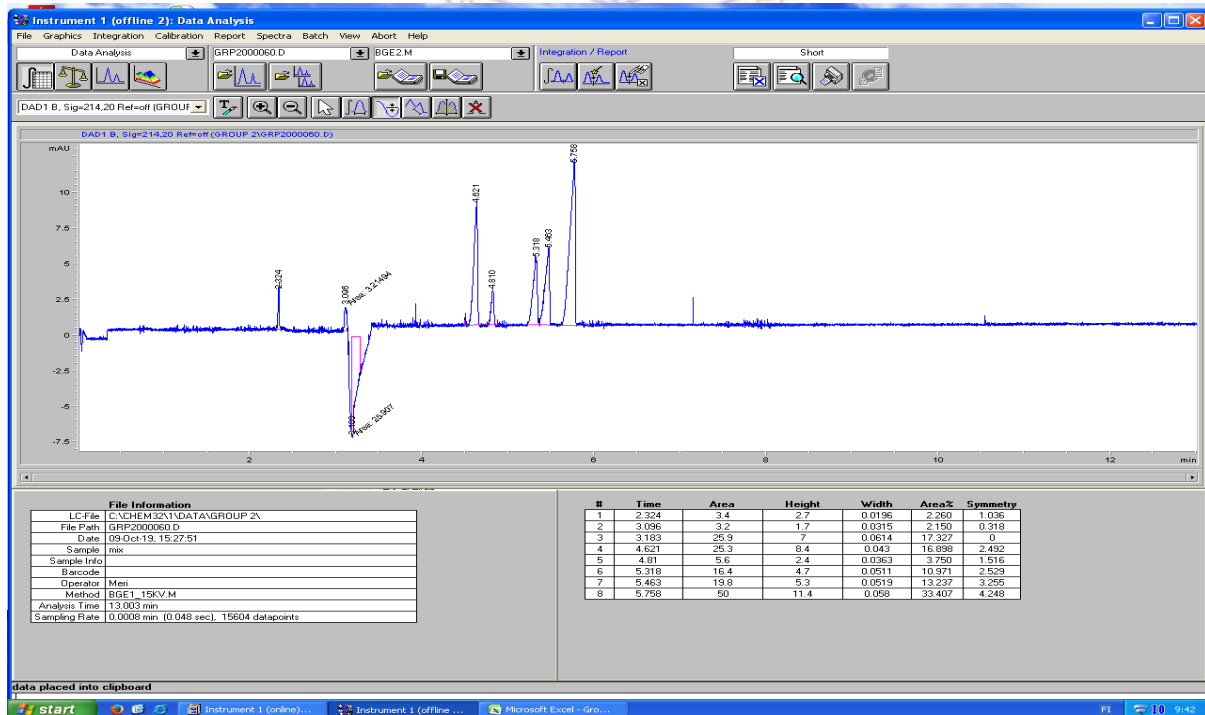
Appendix A8: BGE1 Blank, methanol:MilliQ-water (50:50), 25 kV, 5 minutes analysis time, showing only the EOF.



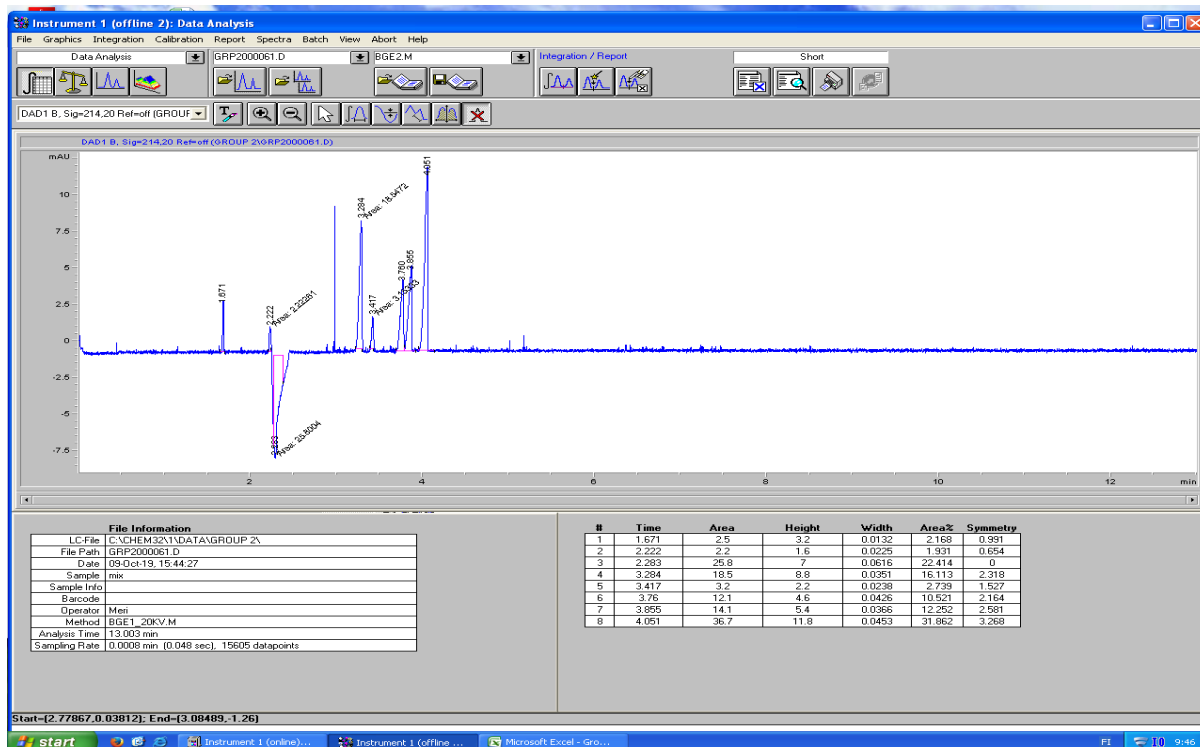
Appendix A9: BGE1 10 kV, standard sample, 13 minutes analysis time, showing the respective analytes peaks as predicted.



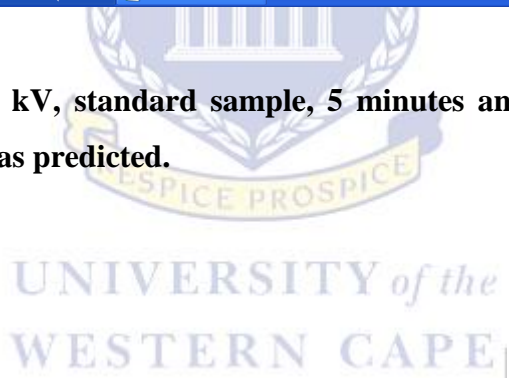
Appendix A10: BGE1 15 kV, standard sample, 13 minutes analysis time, showing the respective analytes peaks as predicted.

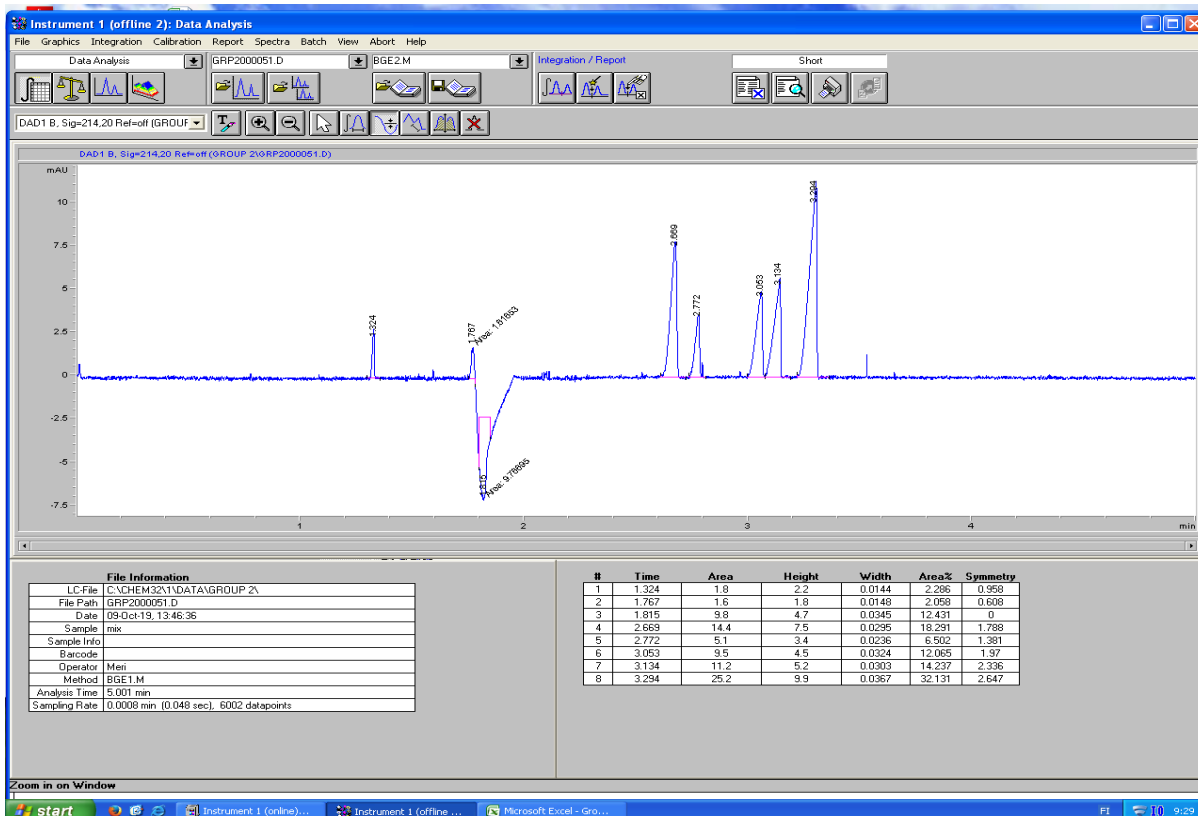


Appendix A11: BGE1 20 kV, standard sample, 13 minutes analysis time, showing the respective analytes peaks as predicted.

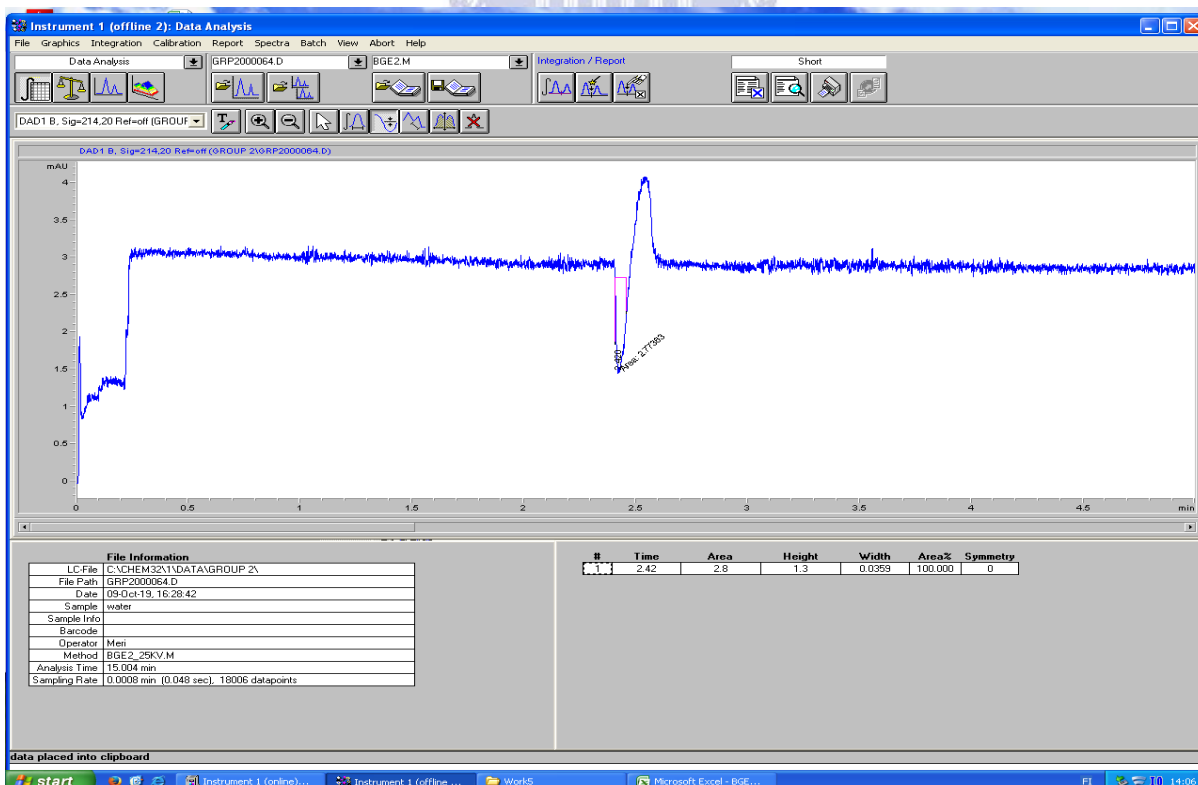


Appendix A12: BGE1 25 kV, standard sample, 5 minutes analysis time, showing the respective analytes peaks as predicted.

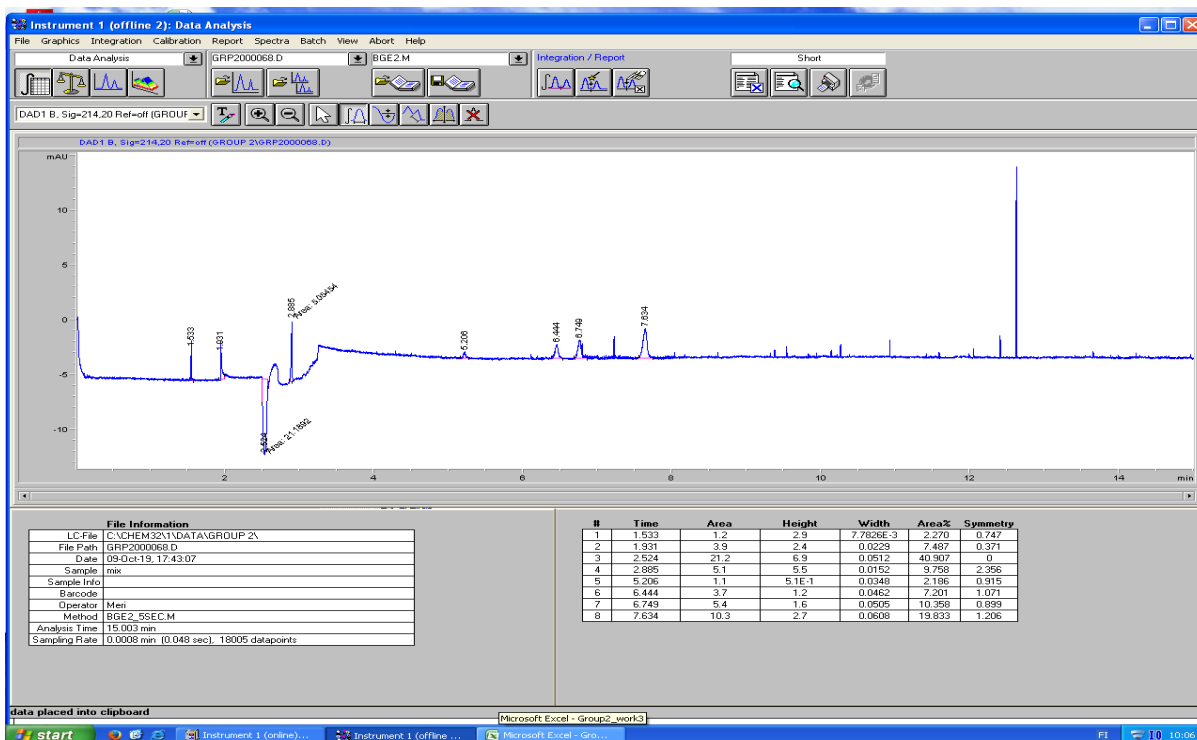




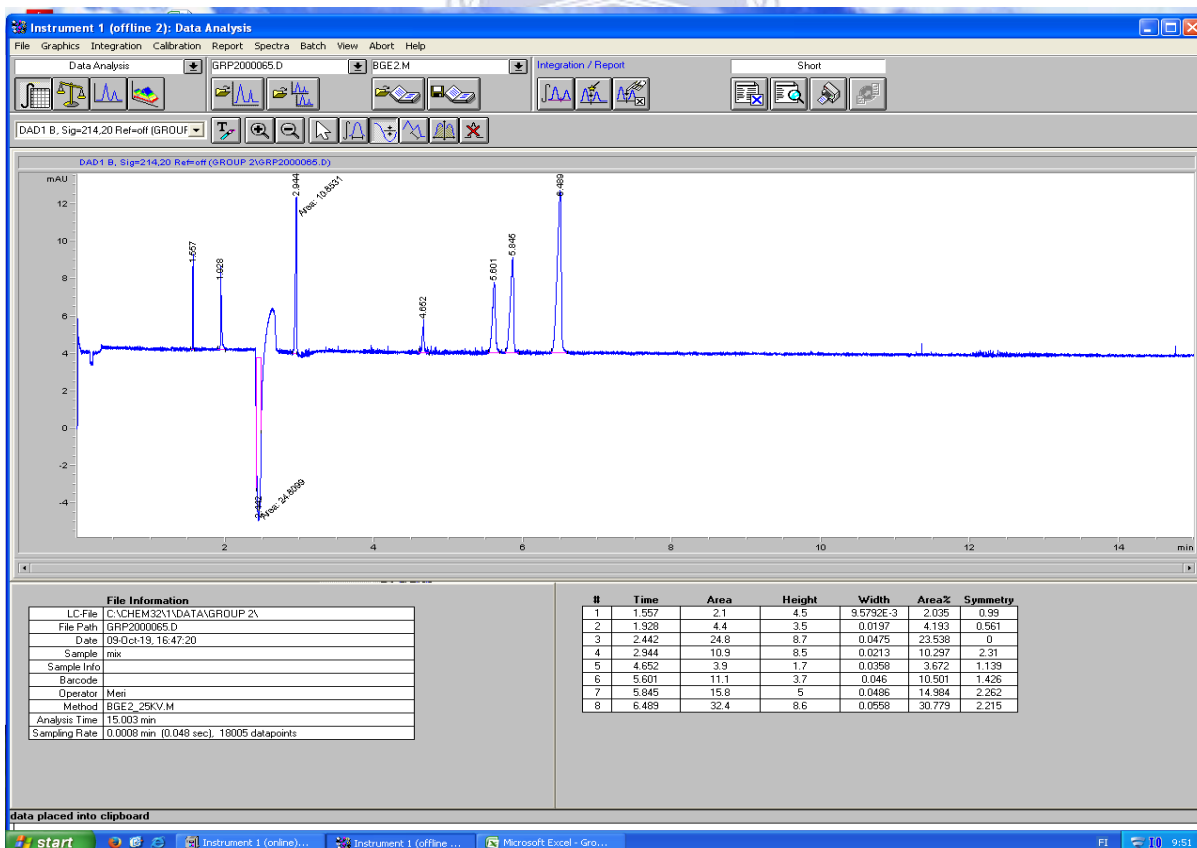
Appendix A13: BGE2 MilliQ-water blank, 25 kV, 15 minutes



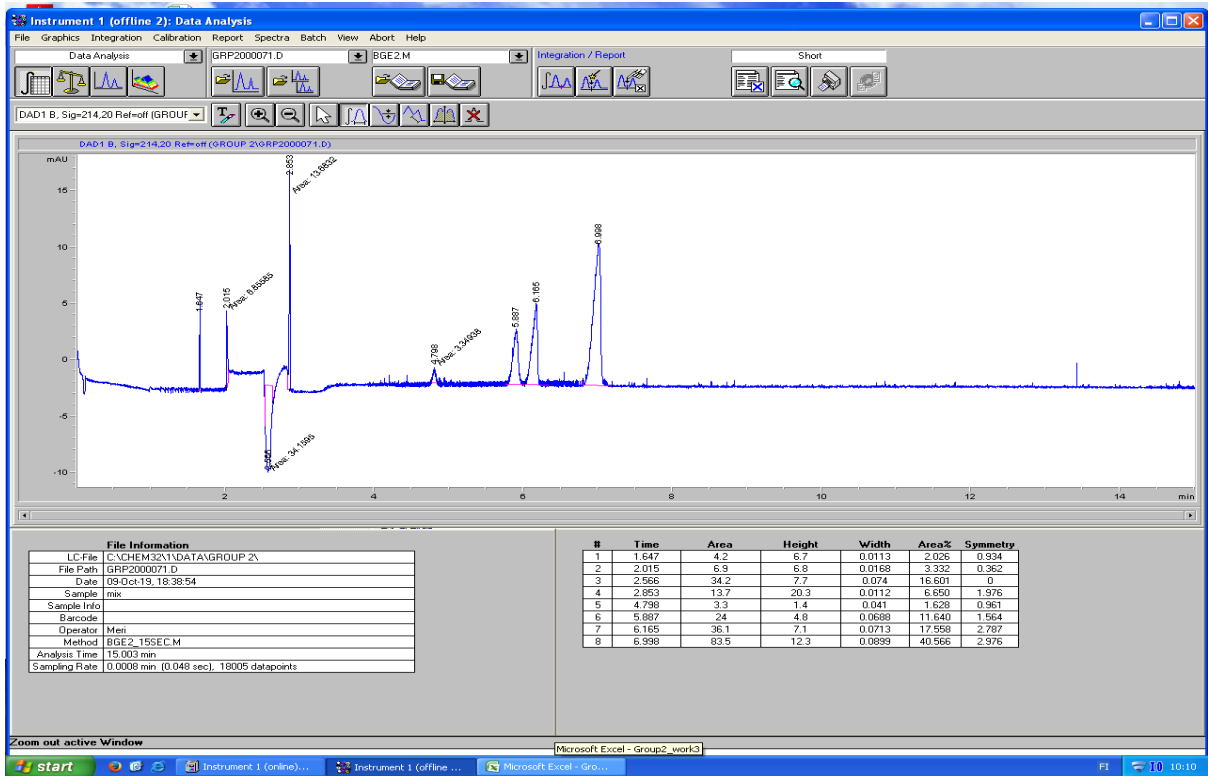
Appendix A14: BGE2, 5 seconds injection, 25 kV, standard.



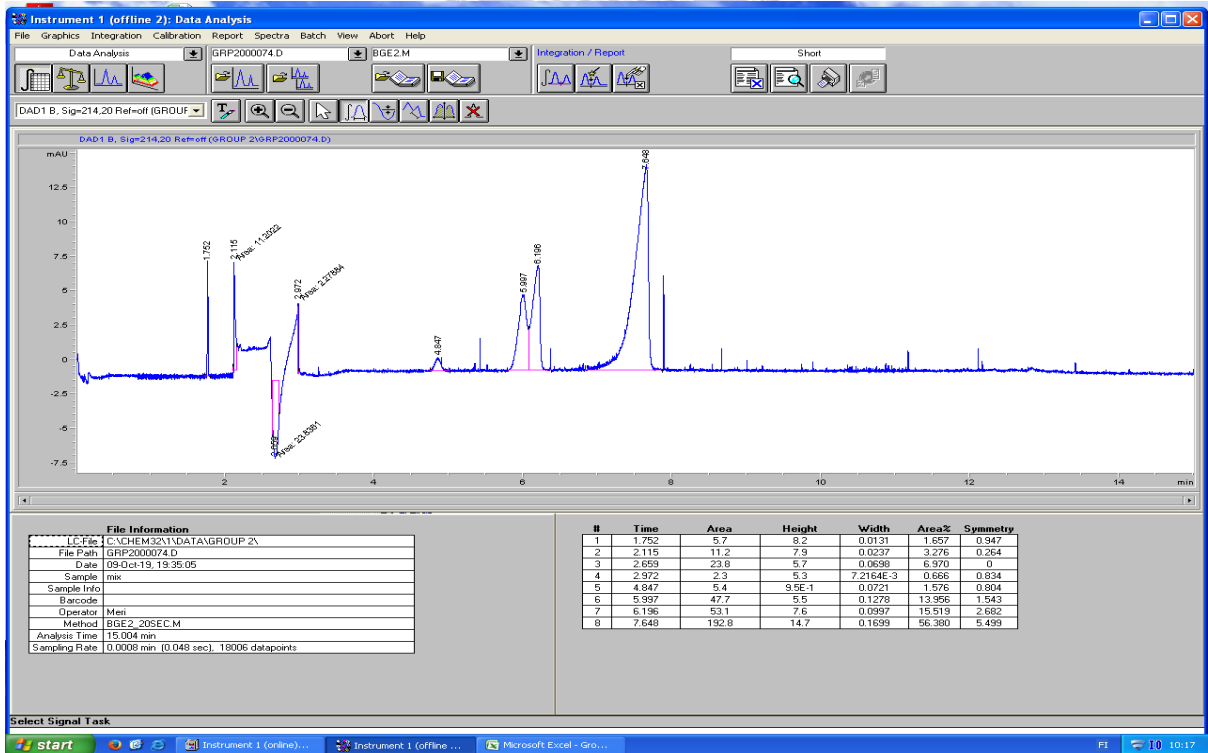
Appendix A15: BGE2, 10 seconds injection, 25 kV, standard.



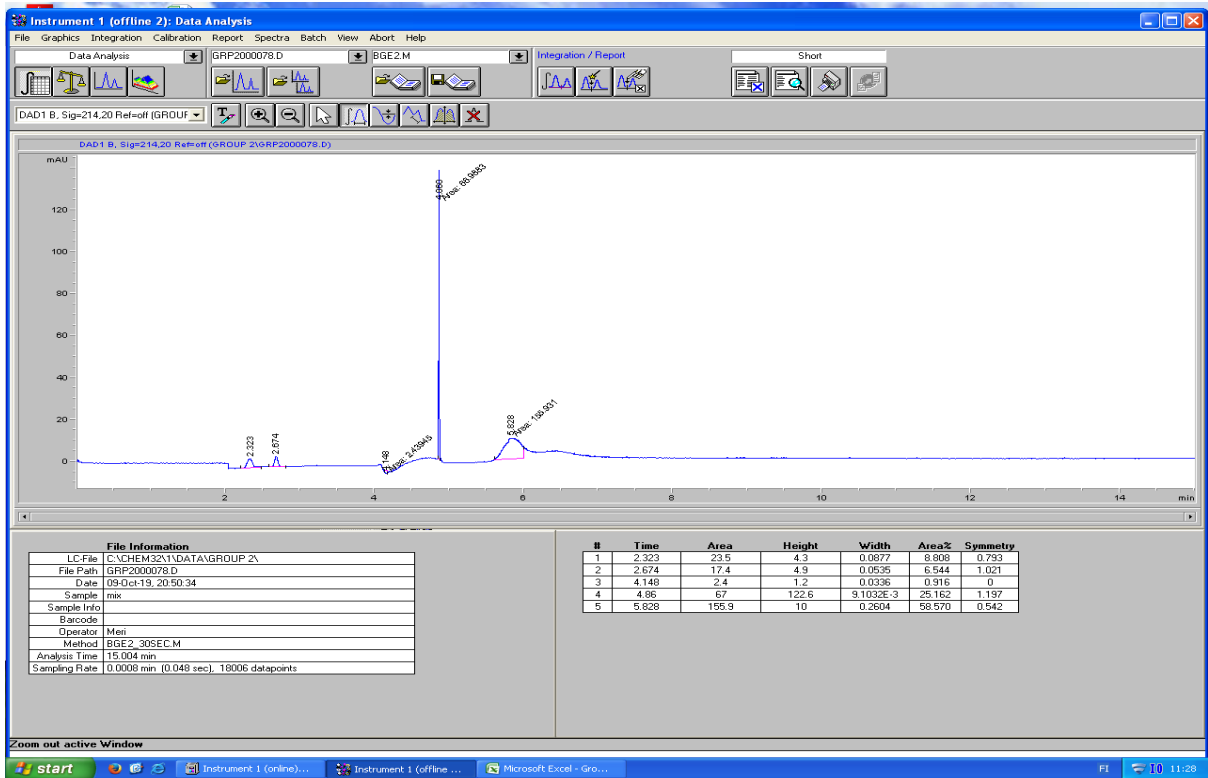
Appendix A16: BGE2, 15 seconds injection, 25 kV, standard.



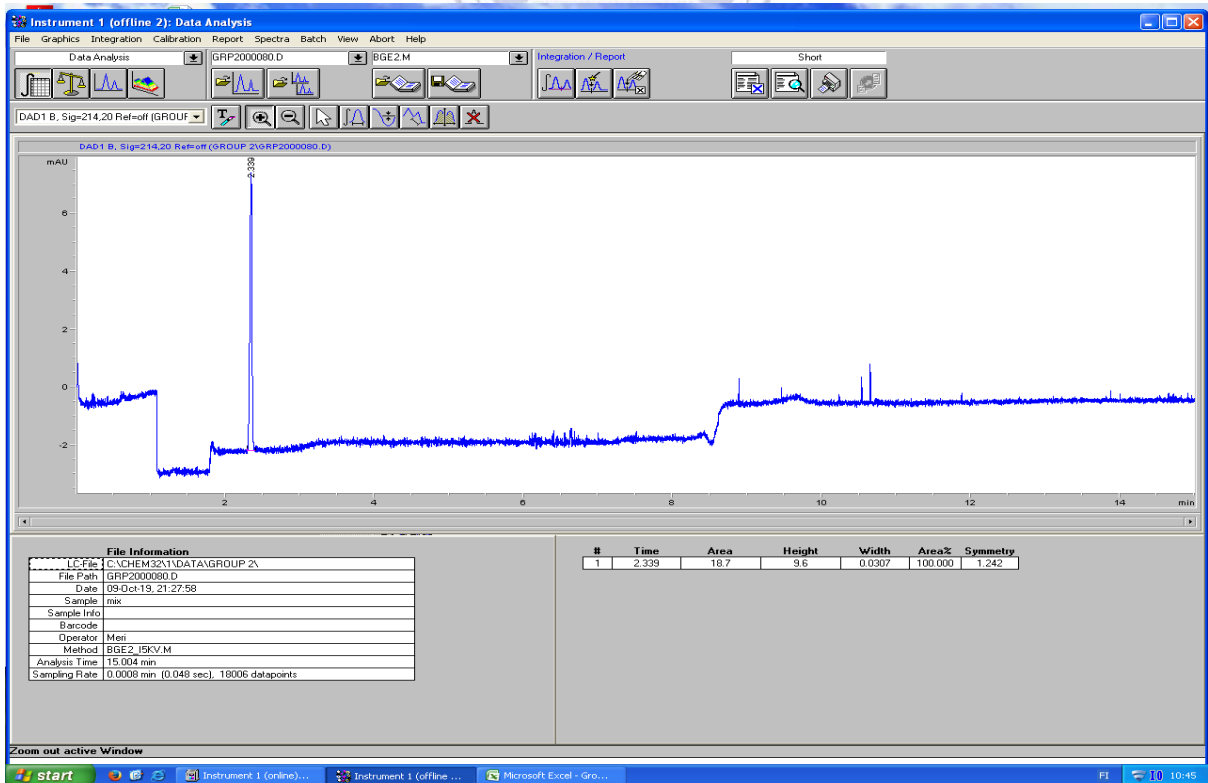
Appendix A17: BGE2, 20 seconds injection, 25 kV, standard.



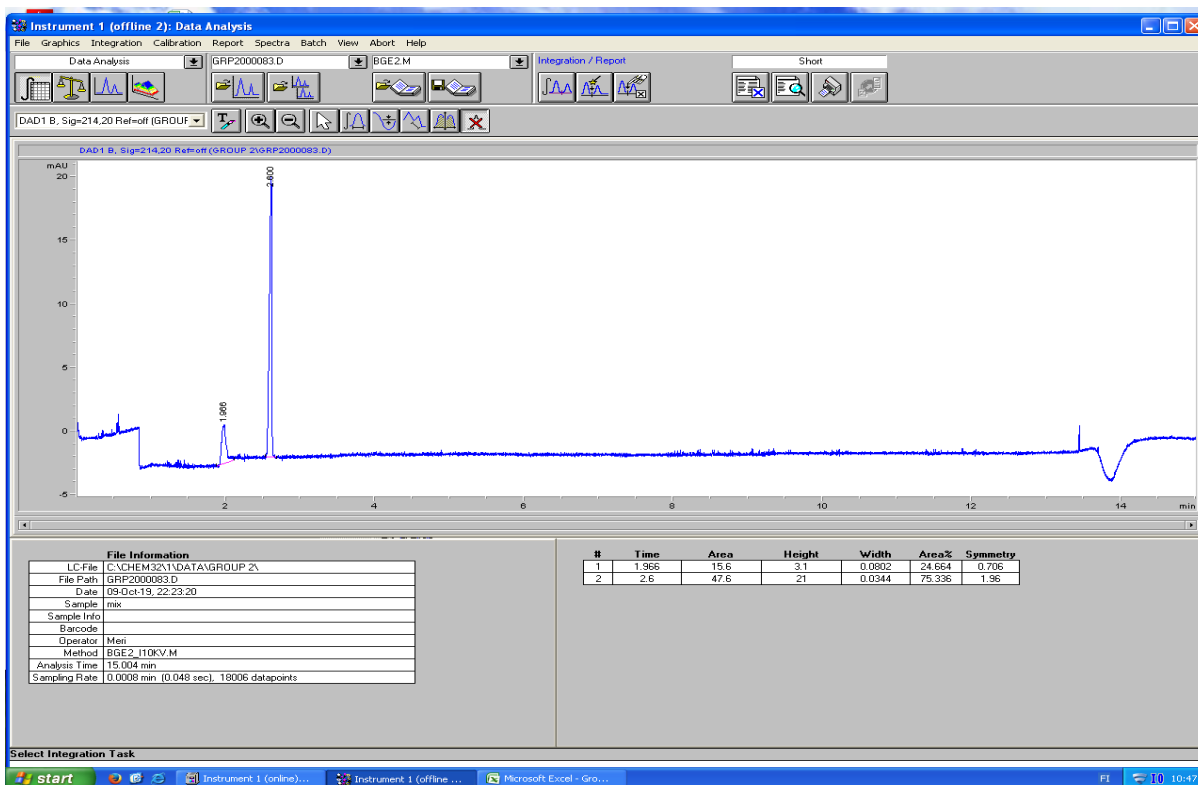
Appendix A18: BGE2, 30 seconds injection, 25 kV, standard.



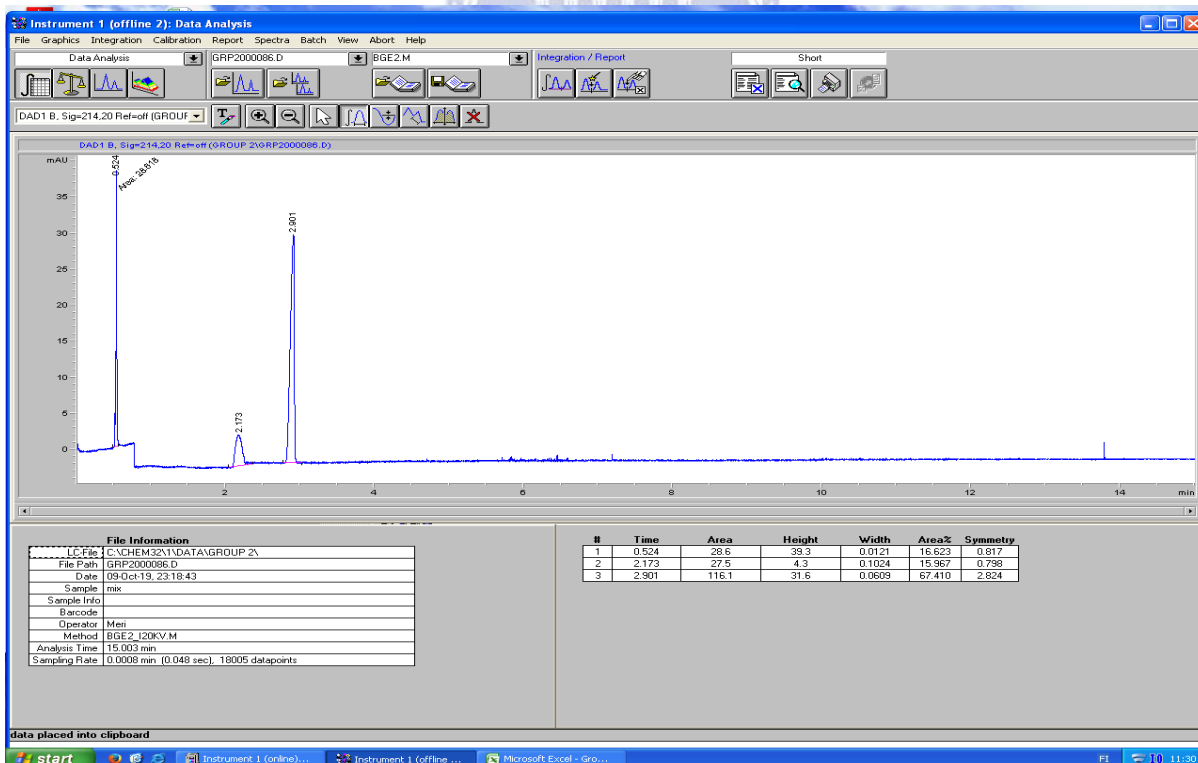
Appendix A19: BGE2 electrokinetic injection, 5 kV, 5 seconds injection, standard.



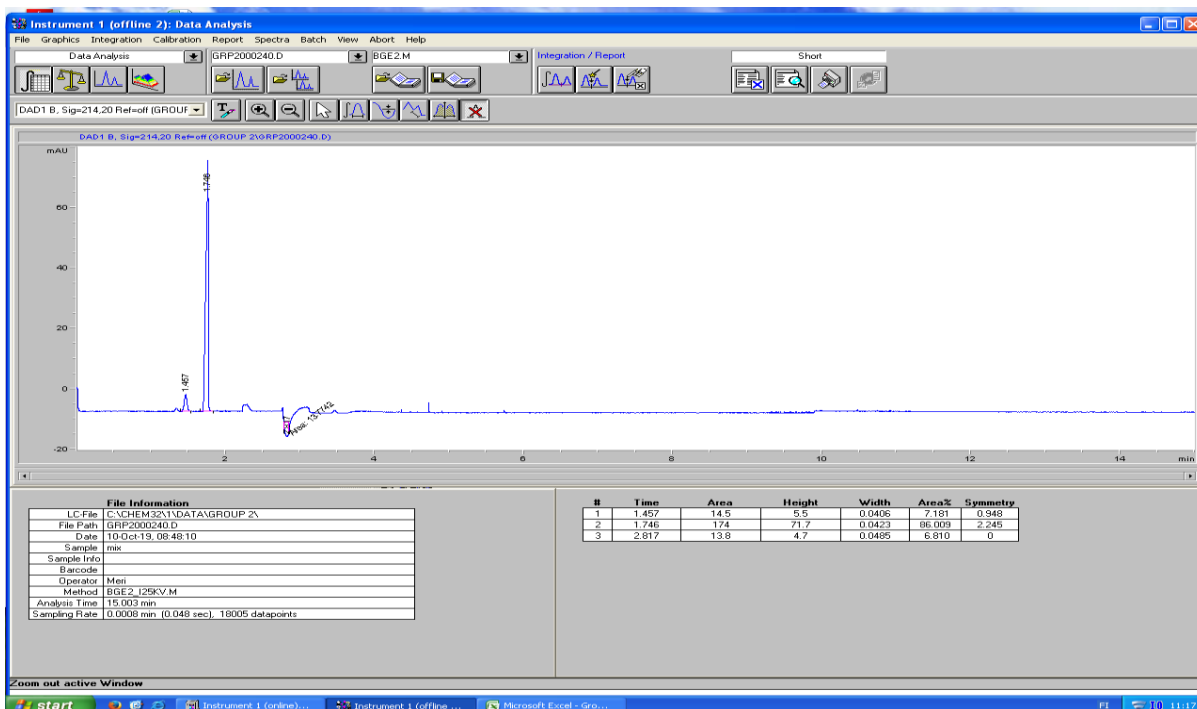
Appendix A20: BGE2 electrokinetic injection, 10 kV, 5 seconds injection, standard.



Appendix A21: BGE2 electrokinetic injection, 20 kV, 5 seconds injection, standard.



Appendix A22: BGE2 electrokinetic injection, 25 kV, 5 seconds injection, standard.



Appendix A23: Results of the repeatability calculations for Benzylamine (pKa=9.4) using BGE 1

Benzylamine		(E=10 ⁸)			
Repetition Number	Migration [s]	Area	$\mu \left[\frac{m^2}{Vs} \right]$	$\mu_{ep} \left[\frac{m^2}{Vs} \right]$	
1	79.44	1.796	1.690E-07	9.772E-08	
2	79.26	1.806	1.692E-07	9.789E-08	
3	79.14	2.189	1.695E-07	9.810E-08	
4	78.72	1.501	1.701E-07	9.861E-08	
5	79.74	1.681	1.681E-07	9.730E-08	
6	79.68	1.708	1.680E-07	9.737E-08	
AVG	79.33	1.780	1.690E-07	9.783E-08	
STD DEV	0.378	0.229	8.302E-10	4.869E-10	
RSD	0.477	12.835	0.498	0.463	

Appendix A24: Results of the repeatability calculations for Imidazole (pKa = 7.0) using BGE1.

Imidazole					(E=10[^])
Repetition Number	Migration [s]	Area	$\mu \left[\frac{m^2}{Vs} \right]$	$\mu_{ep} \left[\frac{m^2}{Vs} \right]$	
1	106.004	1.617	1.445E-07	7.320E-08	
2	105.918	1.384	1.446E-07	7.326E-08	
3	105.583	1.513	1.449E-07	7.350E-08	
4	105.585	1.508	1.450E-07	7.350E-08	
5	106.598	1.614	1.436E-07	7.280E-08	
6	106.746	1.788	1.433E-07	7.270E-08	
AVG	106.073	1.571	1.443E-07	7.316E-08	
STD DEV	0.497	0.137	7.038E-10	3.423E-10	
RSD	0.471	8.699	0.498	0.544	

Appendix A25: Results of the repeatability calculations for Electroosmosis using BGE1

Electroosmosis					(E=10[^])
Repetition number	Migration (min)	Migration (s)	Area	$\mu_{eo} (m^2/V*s)$	
1	1.815	108.904	9.767	7.126E-08	
2	1.813	108.790	8.735	7.133E-08	
3	1.811	108.658	16.708	7.142E-08	
4	1.808	108.487	14.766	7.153E-08	
5	1.827	109.632	18.416	7.078E-08	
6	1.831	109.865	15.195	7.063E-08	
AVG	1.818	109.056	13.931	7.116E-08	
STD	0.009	0.559	3.859	3.639E-10	

Appendix 26: Results of the repeatability calculations for Aspirin (Acetyl salicylic acid) (pKa = 3.5) using BGE 1.

Acetylsalicylic acid (E=10 [^])				
Repetition Number	Migration [s]	Area	$\mu \left[\frac{m^2}{Vs} \right]$	$\mu_{ep} \left[\frac{m^2}{Vs} \right]$
1	160.140	14.370	-2.280E-08	4.846E-08
2	159.562	13.145	-2.270E-08	4.863E-08
3	159.259	12.836	-2.269E-08	4.873E-08
4	159.783	12.639	-2.296E-08	4.857E-08
5	160.553	15.571	-2.245E-08	4.833E-08
6	160.713	14.229	-2.235E-08	4.829E-08
AVG	160.002	13.798	-2.266E-08	4.850E-08
STD DEV	0.569	1.127	2.263E-10	1.726E-10
RSD	0.471	8.699	0.498	0.544

Appendix A27: Results of the repeatability calculations for 2,3-dichlorophenol (pKa = 7.5) using BGE 1.

2,3-Dichlorophenol (E=10 [^])				
Repetition Number	Migration [s]	Area	$\mu \left[\frac{m^2}{Vs} \right]$	$\mu_{ep} \left[\frac{m^2}{Vs} \right]$
1	166.309	5.109	-2.460E-08	4.666E-08
2	166.010	4.122	-2.459E-08	4.674E-08
3	165.758	4.439	-2.460E-08	4.682E-08
4	166.057	3.476	-2.480E-08	4.673E-08
5	167.084	3.980	-2.434E-08	4.644E-08
6	167.850	4.050	-2.440E-08	4.623E-08
AVG	166.511	4.196	-2.455E-08	4.660E-08
STD DEV	0.798	0.545	1.643E-10	2.226E-10
RSD	0.471	8.699	0.498	0.544

Appendix A28: Table 4.7: Results of the repeatability calculations for 2,4-dinitrophenol (pKa = 4.0) using BGE 1.

2,4-Dinitrophenol (E=10 [^])				
Repetition Number	Migration [s]	Area	μ [$\frac{m^2}{Vs}$]	μ_{ep} [$\frac{m^2}{Vs}$]
1	183.162	9.479	-2.889E-08	4.237E-08
2	182.572	9.263	-2.883E-08	4.250E-08
3	182.582	8.967	-2.892E-08	4.250E-08
4	182.726	8.017	-2.906E-08	4.247E-08
5	183.912	9.406	-2.859E-08	4.219E-08
6	185.066	9.056	-2.870E-08	4.193E-08
AVG	183.337	9.031	-2.883E-08	4.233E-08
STD DEV	0.988	0.534	1.670E-10	2.270E-10
RSD	0.534	5.918	0.498	0.524

Appendix A29: Results of the repeatability calculations for Benzoic acid (pKa = 4.2) using BGE 1.

Benzoic acid (E=10 [^])				
Repetition Number	Migration [s]	Area	μ [$\frac{m^2}{Vs}$]	μ_{ep} [$\frac{m^2}{Vs}$]
1	188.043	11.185	-2.999E-08	4.127E-08
2	187.342	10.748	-2.991E-08	4.142E-08
3	187.441	10.571	-3.002E-08	4.140E-08
4	187.537	9.408	-3.015E-08	4.138E-08
5	188.750	10.934	-2.967E-08	4.111E-08
6	189.935	10.718	-2.978E-08	4.086E-08
AVG	188.175	10.594	-2.992E-08	4.124E-08
STD DEV	1.008	0.618	1.738E-10	2.200E-10
RSD	0.542	5.836	0.498	0.515

Appendix A30: Results of the repeatability calculations for Salicylic acid (pKa = 2.97) using BGE 1.

Salicylic acid				
(E=10 [^])				
Repetition Number	Migration [s]	Area	$\mu \left[\frac{m^2}{Vs} \right]$	$\mu_{ep} \left[\frac{m^2}{Vs} \right]$
1	197.619	25.244	-3.199E-08	3.927E-08
2	196.884	25.261	-3.192E-08	3.941E-08
3	196.980	25.071	-3.202E-08	3.939E-08
4	197.093	21.502	-3.216E-08	3.937E-08
5	198.441	25.741	-3.168E-08	3.910E-08
6	199.779	26.040	-3.179E-08	3.884E-08
AVG	197.799	24.810	-3.193E-08	3.923E-08
STD DEV	1.129	1.660	1.715E-10	2.228E-10
RSD	0.570	6.692	0.498	0.476

Appendix A31: Electrophoretic mobilities in the BGE1 voltage series for Benzylamine.

Benzylamine				
(E=10 [^])				
(AVG in 25 kV)	10 kV	15 kV	20 kV	25 kV
Migration time (min)	3.476	2.262	1.671	1.322
Migration time (s)	208.579	135.708	100.262	79.324
Area	5.079	2.994	2.495	1.780
Velocity, v (m/s)	0.002	0.003	0.004	0.005
μ (m ² /V*s)	1.617E-07	1.653E-07	1.676E-07	1.690E-07
(= $\mu_{ep} + \mu_{eo}$)				
μ_{ep} (m ² /V*s)	9.301E-08	9.530E-08	9.675E-08	9.783E-08
Electric field, E (V/m)	20618.560	30927.840	41237.110	51546.390

Appendix A32: Electrophoretic mobilities in the BGE1 voltage series for Imidazole.

Imidazole				
(E=10 [^])				

(AVG in 25 kV)	10 kV	15 kV	20 kV	25 kV
Migration time (min)	4.589	3.001	2.222	1.768
Migration time (s)	275.366	180.043	133.343	106.073
Area	4.535	3.060	2.223	1.571
Velocity, v (m/s)	0.001	0.002	0.003	0.004
μ ($\text{m}^2/\text{V}\cdot\text{s}$) (= $\mu_{ep} + \mu_{eo}$)	1.391E-07	1.418E-07	1.436E-07	1.443E-07
μ_{ep} ($\text{m}^2/\text{V}\cdot\text{s}$)	7.045E-08	7.183E-08	7.274E-08	7.316E-08
Electric field, E (V/m)	20618.560	30927.840	41237.110	51546.390

Appendix A33: Electrophoretic mobilities in the BGE1 voltage series for Electroosmosis.

Electroosmosis	(E=10 ⁴)			
(AVG in 25 kV)	10 kV	15 kV	20 kV	25 kV
Migration time (min)	4.709	3.081	2.283	1.818
Migration time (s)	282.569	184.871	136.989	109.056
Area	36.890	29.745	25.800	13.931
Velocity (m/s)	0.001	0.002	0.003	0.004
μ_{eo} ($\text{m}^2/\text{V}\cdot\text{s}$)	6.866E-08	6.996E-08	7.081E-08	7.116E-08
E (V/m)	20618.560	30927.840	41237.110	51546.390

Appendix A34: Electrophoretic mobilities in the BGE1 voltage series for Acetylsalicylic acid.

Acetylsalicylic acid	(E=10 ⁴)
----------------------	----------------------

(AVG in 25 kV)	10 kV	15 kV	20 kV	25 kV
Migration time (min)	6.700	4.424	3.284	2.667
Migration time (s)	402.013	265.460	197.020	160.002
Area	35.049	23.258	18.547	13.798
Velocity, v (m/s)	0.001	0.002	0.002	0.002
μ (m ² /V*s) (= μ_{ep} - μ_{eo})	-2.040E-08	-2.124E-08	-2.158E-08	-2.266E-08
μ_{ep} (m ² /V*s)	4.826E-08	4.872E-08	4.923E-08	4.850E-08
Electric field, E (V/m)	20618.560	30927.840	41237.110	51546.390

Appendix A35: Electrophoretic mobilities in the BGE1 voltage series for 2,3-Dichlorophenol.

2,3-Dichlorophenol (E=10 ⁴)				
(AVG in 25 kV)	10 kV	15 kV	20 kV	25 kV
Migration time (min)	6.700	4.424	3.284	2.667
Migration time (s)	402.013	265.460	197.020	160.002
Area	35.049	23.258	18.547	13.798
Velocity, v (m/s)	0.001	0.002	0.002	0.002
μ (m ² /V*s) (= μ_{ep} - μ_{eo})	-2.040E-08	-2.124E-08	-2.158E-08	-2.266E-08
μ_{ep} (m ² /V*s)	4.826E-08	4.872E-08	4.923E-08	4.850E-08
Electric field, E (V/m)	20618.560	30927.840	41237.110	51546.390

Appendix A36: Electrophoretic mobilities in the BGE1 voltage series for 2,4-Dinitrophenol.

2,4-Dinitrophenol (E=10 ⁴)				
--	--	--	--	--

(AVG in 25 kV)	10 kV	15 kV	20 kV	25 kV
Migration time (min)	7.643	5.056	3.760	3.056
Migration time (s)	458.604	303.331	225.583	183.337
Area	23.625	14.906	12.111	9.031
Velocity, v (m/s)	0.001	0.001	0.002	0.002
μ (m ² /V*s) (= μ_{ep} - μ_{eo})	-2.635E-08	-2.732E-08	-2.781E-08	-2.883E-08
μ_{ep} (m ² /V*s)	4.230E-08	4.264E-08	4.300E-08	4.233E-08
Electric field, E (V/m)	20618.560	30927.840	41237.110	51546.390

Appendix A37: Electrophoretic mobilities in the BGE1 voltage series for Benzoic acid.

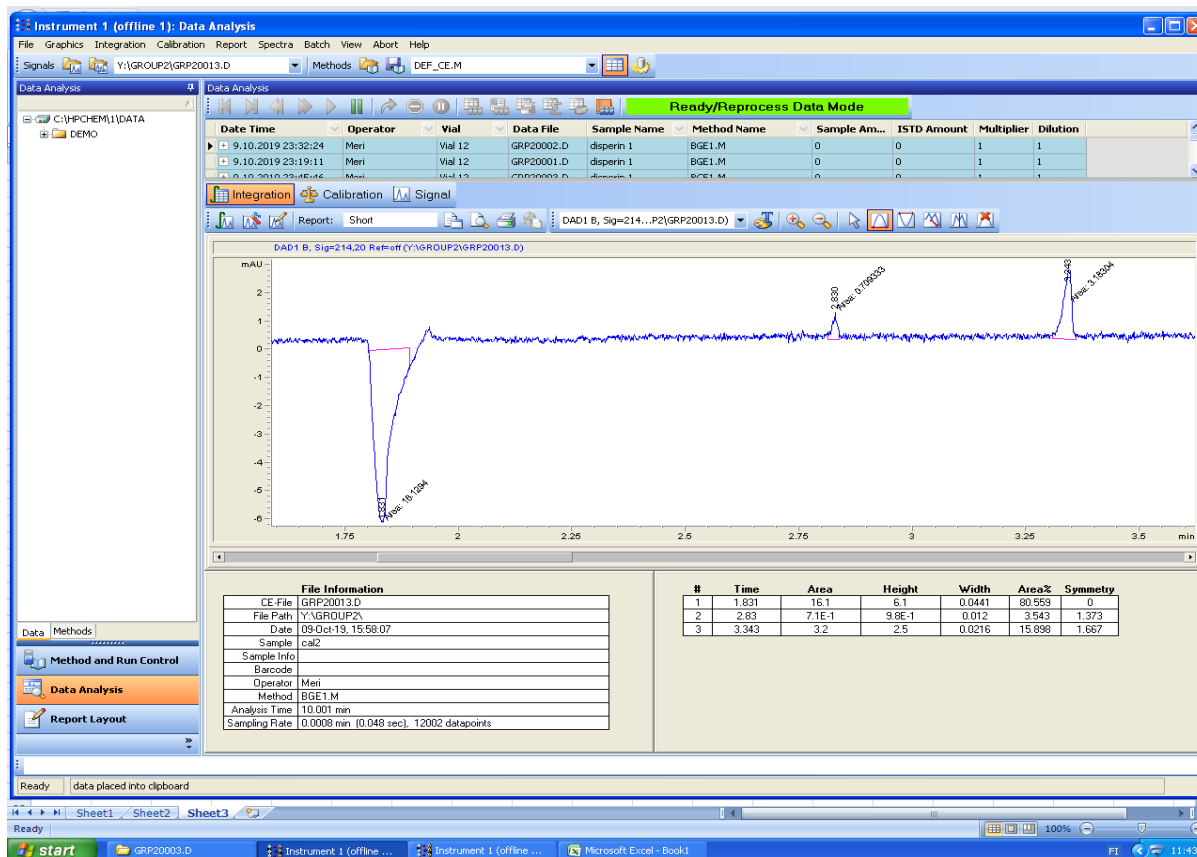
Benzoic acid (E=10 ⁴)				
(AVG in 25 kV)	10 kV	15 kV	20 kV	25 kV
Migration time (min)	7.843	5.185	3.855	3.136
Migration time (s)	470.575	311.101	231.294	188.175
Area	28.308	17.979	14.103	10.594
Velocity, v (m/s)	0.001	0.001	0.002	0.002
μ (m ² /V*s) (= μ_{ep} - μ_{eo})	-2.743E-08	-2.839E-08	-2.887E-08	-2.992E-08
μ_{ep} (m ² /V*s)	4.123E-08	4.157E-08	4.194E-08	4.124E-08
Electric field, E (V/m)	20618.560	30927.840	41237.110	51546.390

Appendix A38: Electrophoretic mobilities in the BGE1 voltage series for salicylic acid.

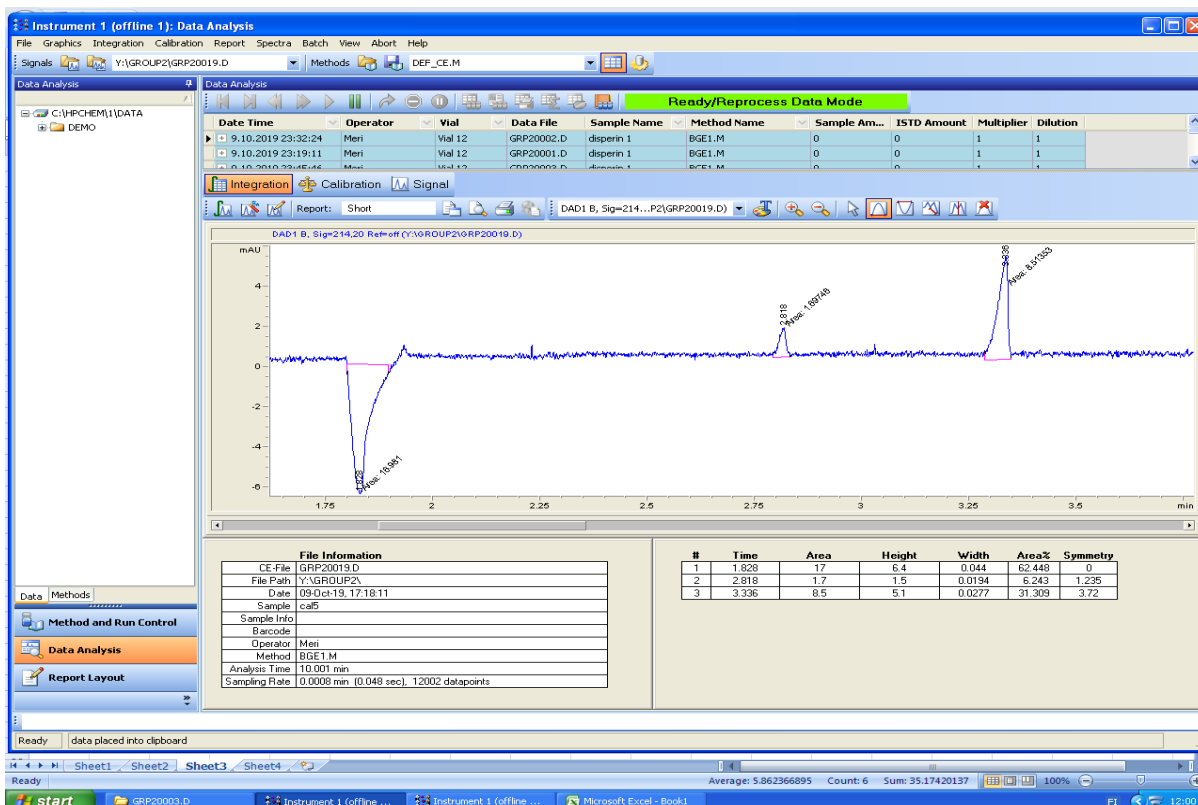
Salicylic acid (E=10 ⁴)				
(AVG in 25 kV)	10 kV	15 kV	20 kV	25 kV
Migration time (min)	8.240	5.448	4.051	3.297
Migration time (s)	494.397	326.871	243.068	197.799

Area	68.588	44.589	36.675	24.810
Velocity, v (m/s)	0.001	0.001	0.002	0.002
\square ($m^2/V*s$) ($=\square ep - \square eo$)	-2.942E-08	-3.039E-08	-3.090E-08	-3.192E-08
$\square ep$ ($m^2/V*s$)	3.924E-08	3.957E-08	3.991E-08	3.923E-08
Electric field, E (V/m)	20618.560	30927.840	41237.110	51546.390

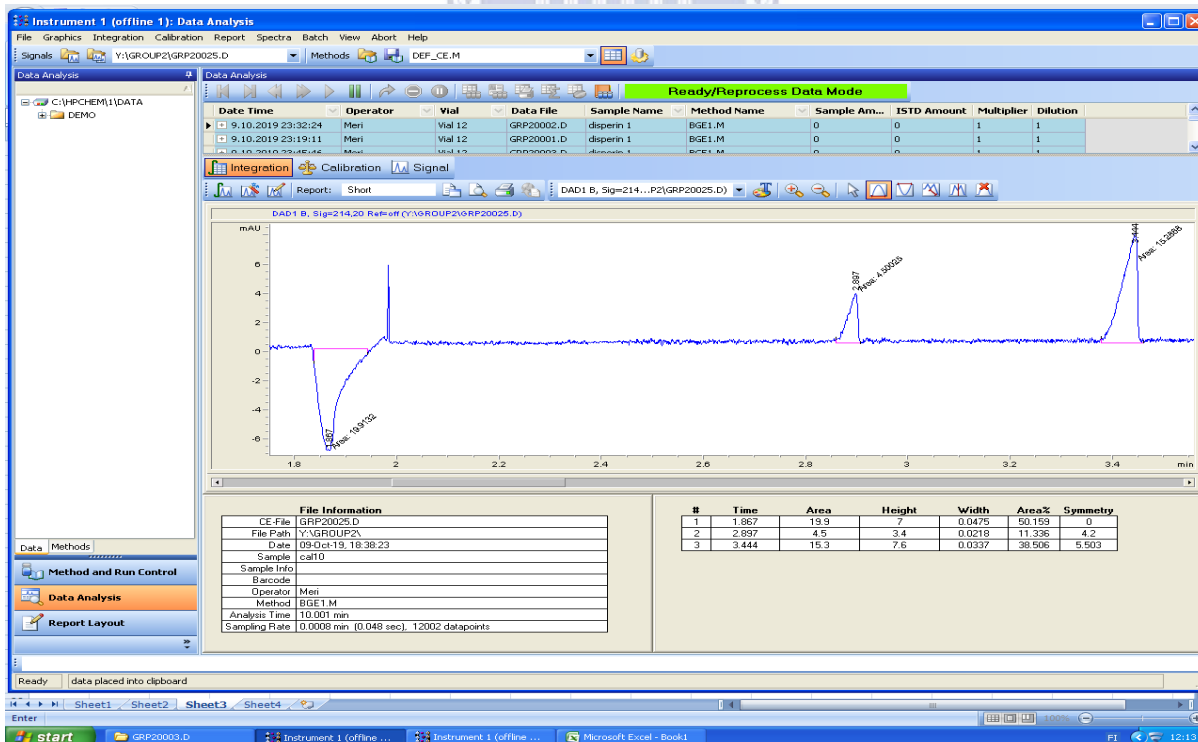
Appendix A39: Calibration standard 2 ppm, 25 kV, BGE 1.



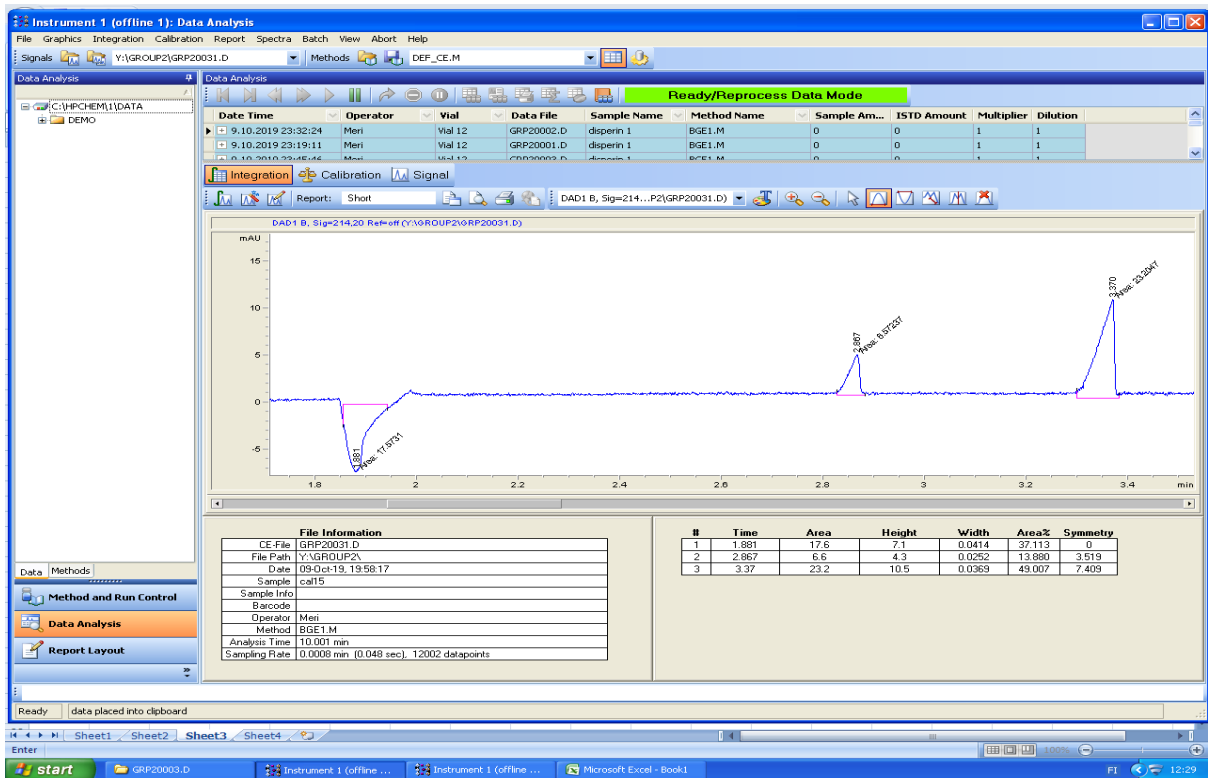
Appendix A40: Calibration standard 5 ppm, 25 kV, BGE 1.



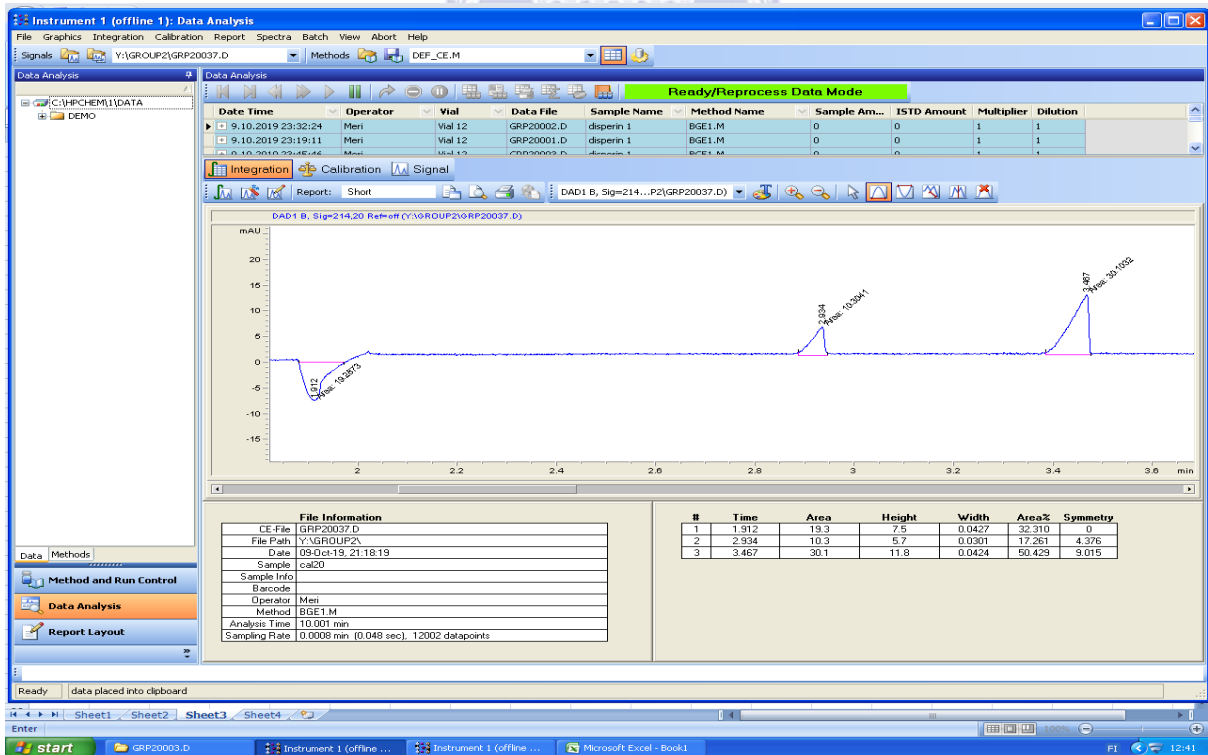
Appendix A41: Calibration standard 10 ppm, 25 kV, BGE 1.



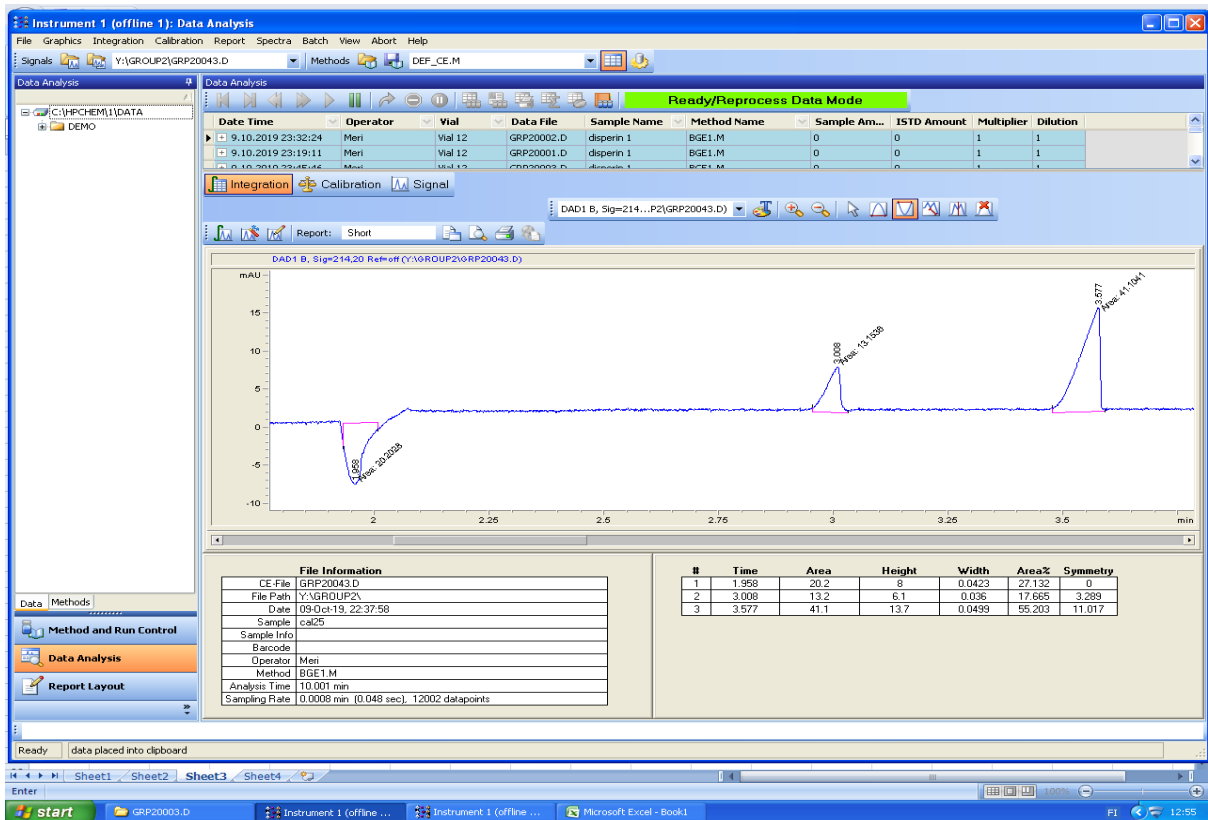
Appendix A42: Calibration standard 15 ppm, 25 kV, BGE 1.



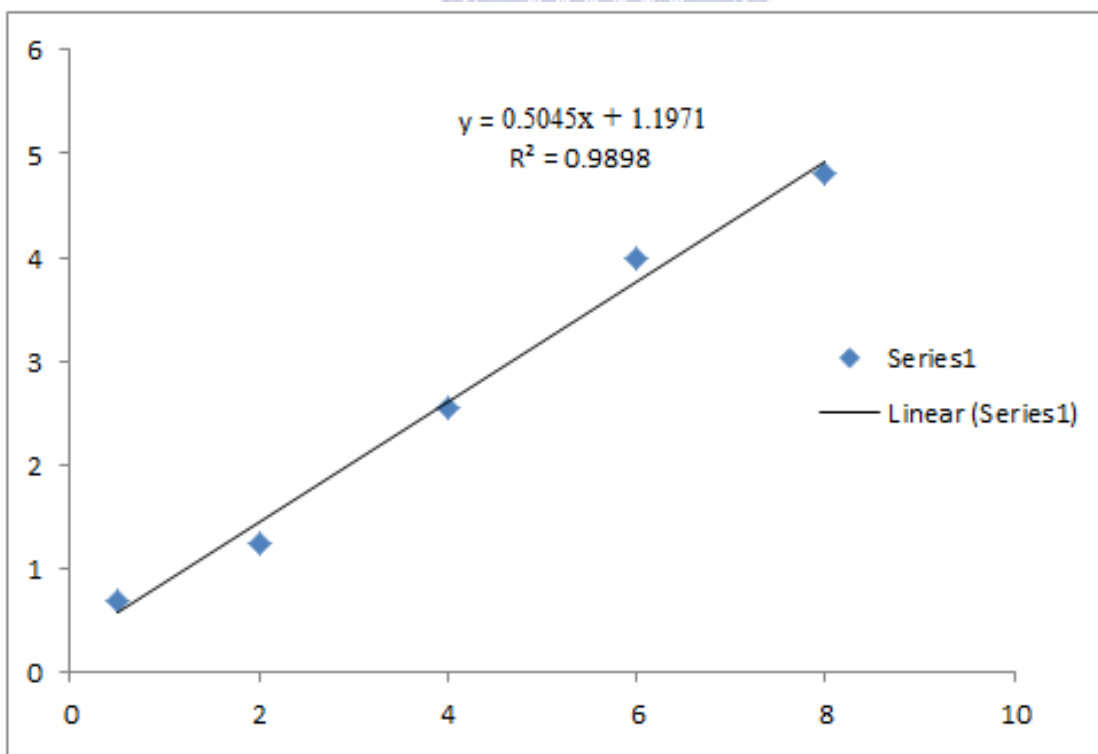
Appendix A43: Calibration standard 20 ppm, 25 kV, BGE 1.



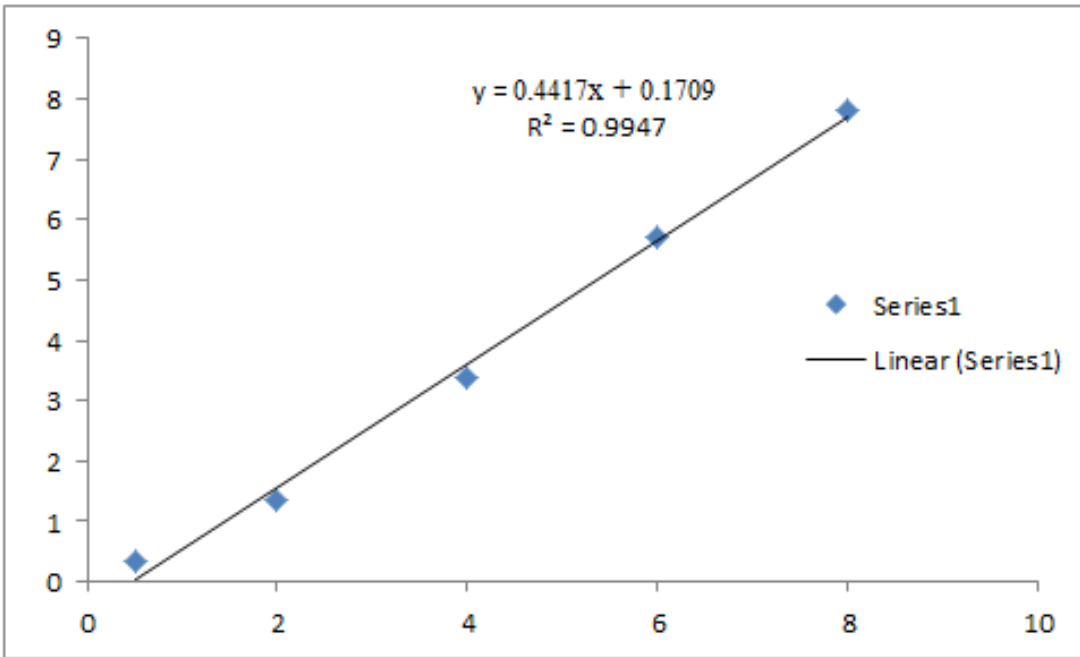
Appendix A44: Calibration standard 25 ppm, 25 kV, BGE 1



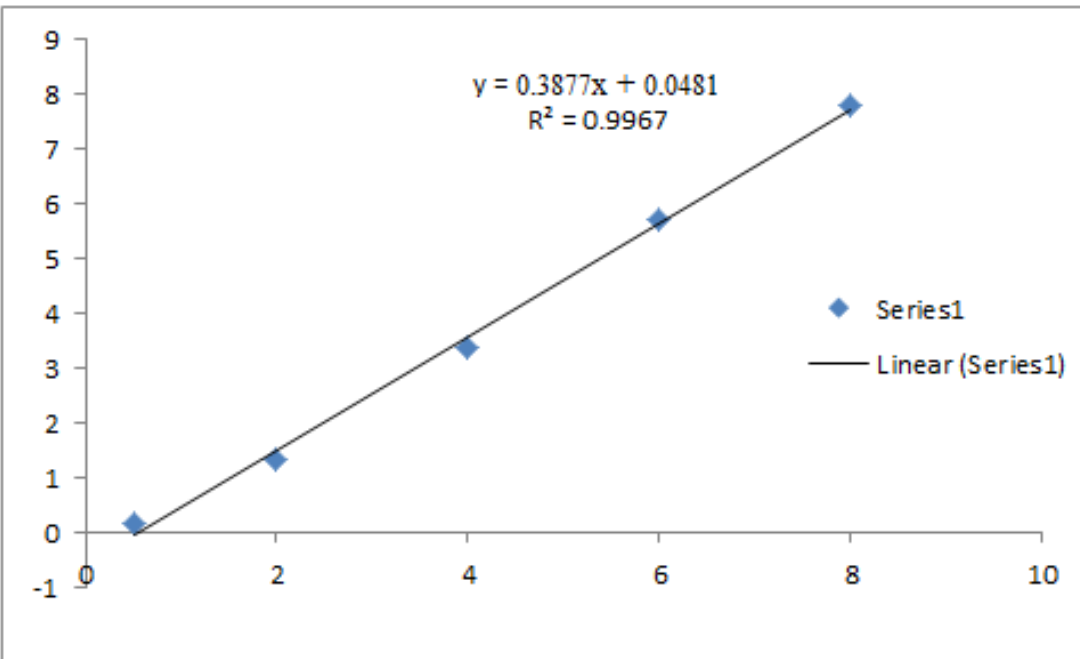
Appendix A45: Calibration curve for chloride ion



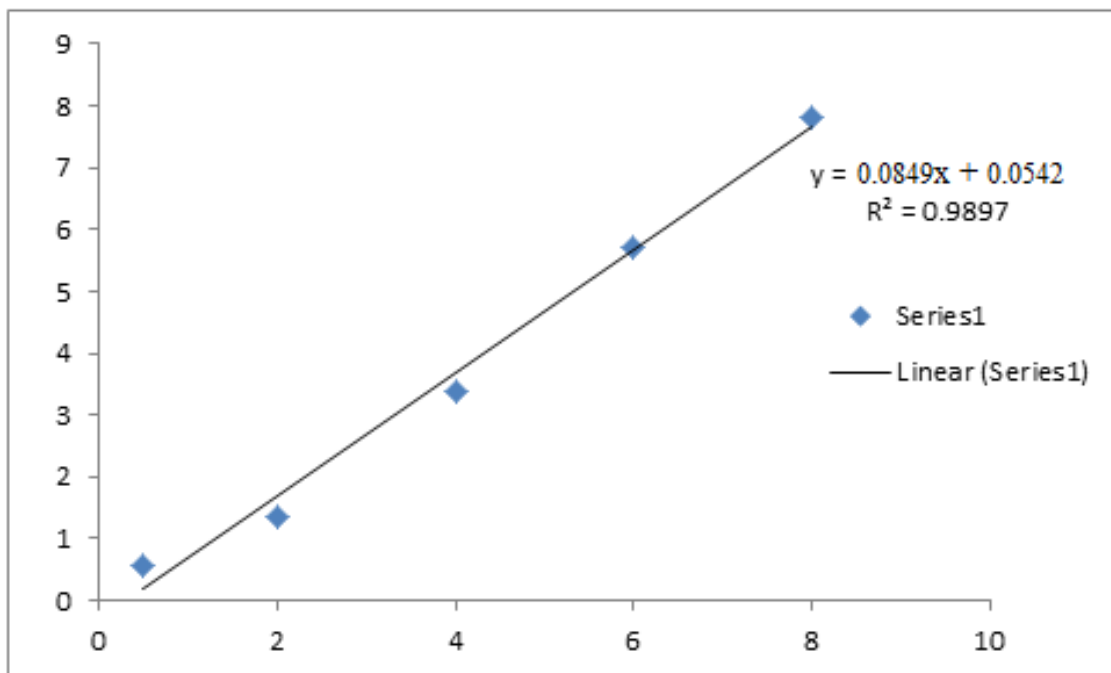
Appendix A46: Calibration curve for sulphate ion



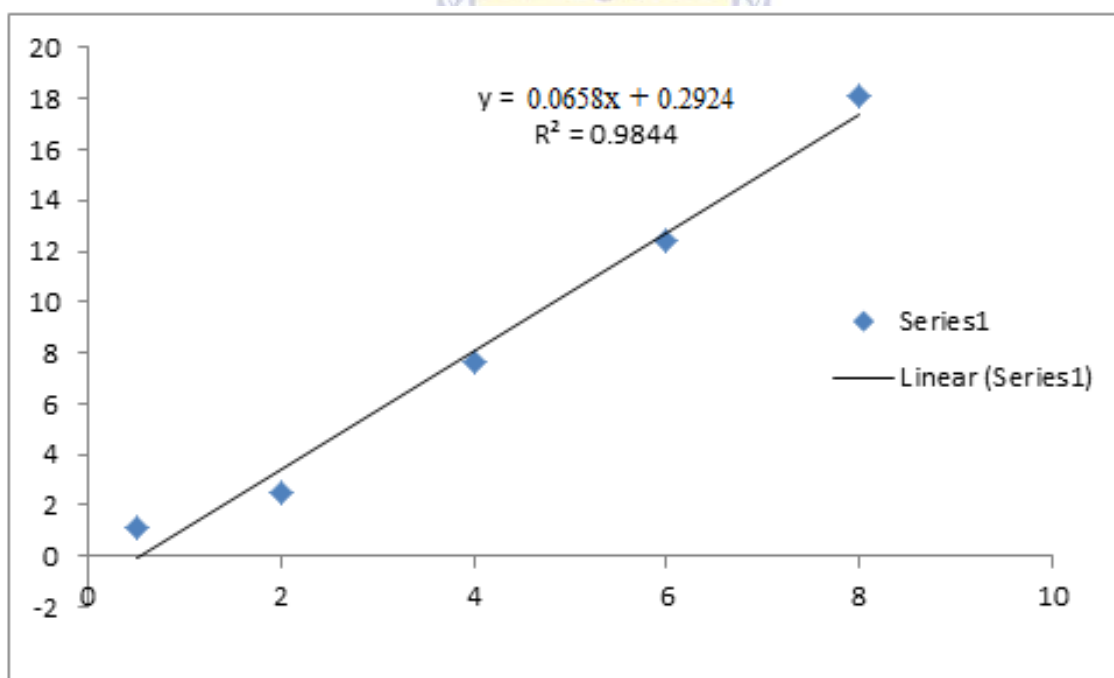
Appendix A47: Calibration curve for nitrate ion



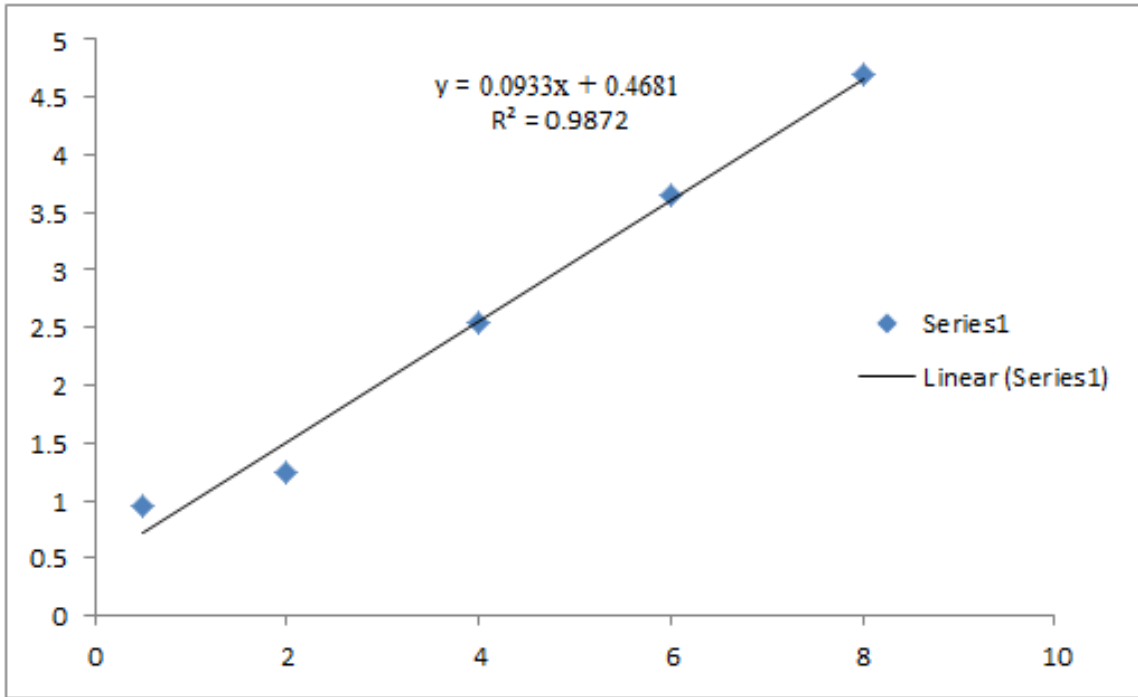
Appendix A48: Calibration curve for potassium ion



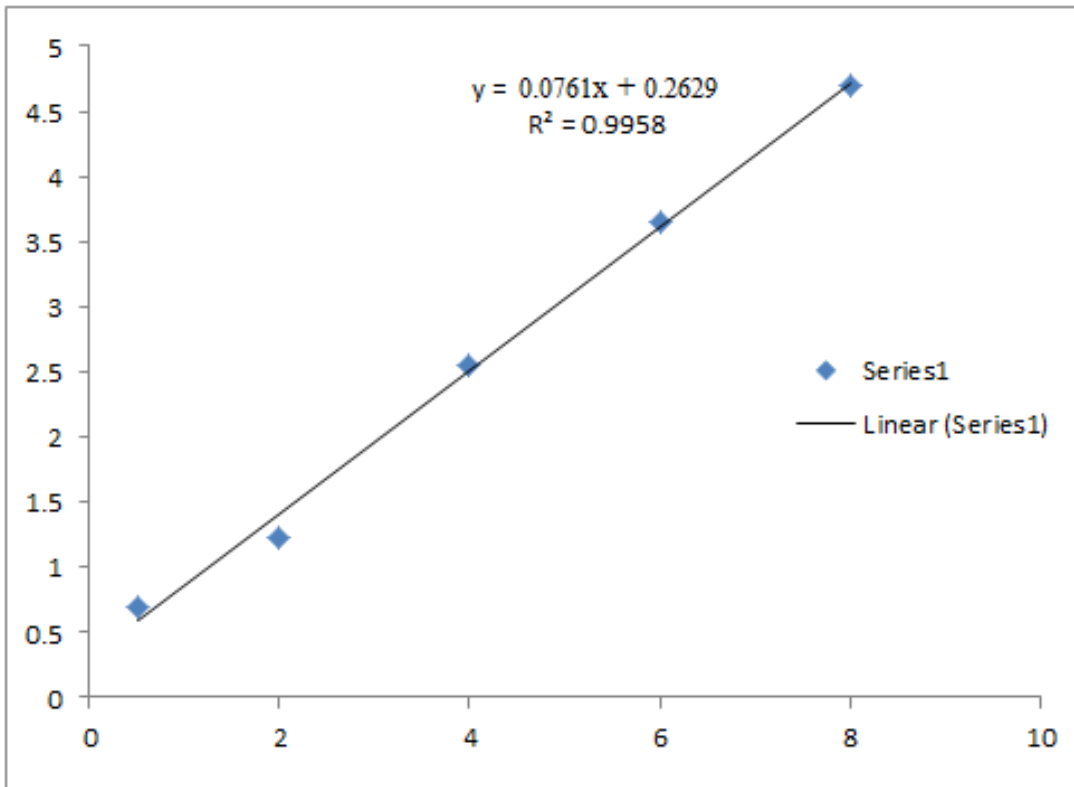
Appendix A49: Calibration curve for calcium ion



Appendix A50: Calibration curve for sodium ion

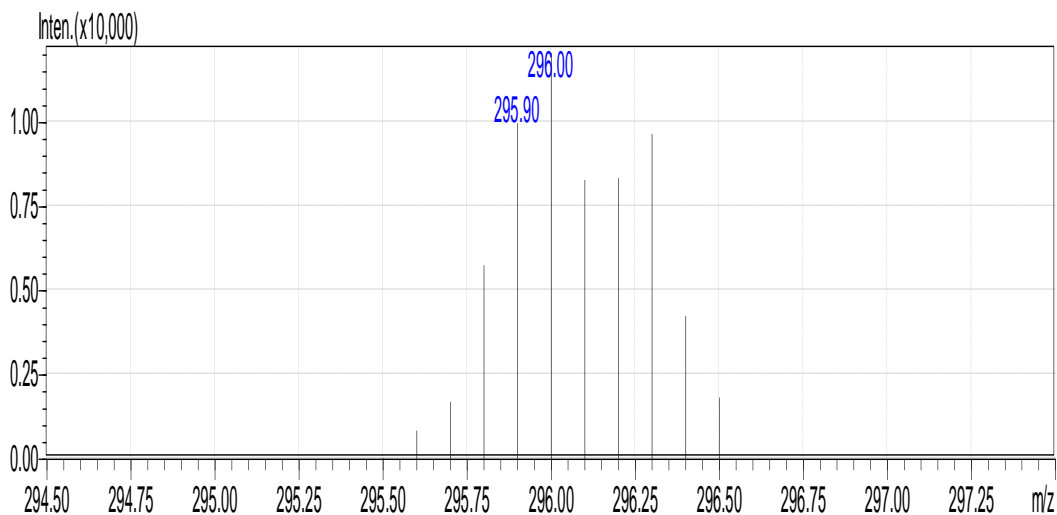


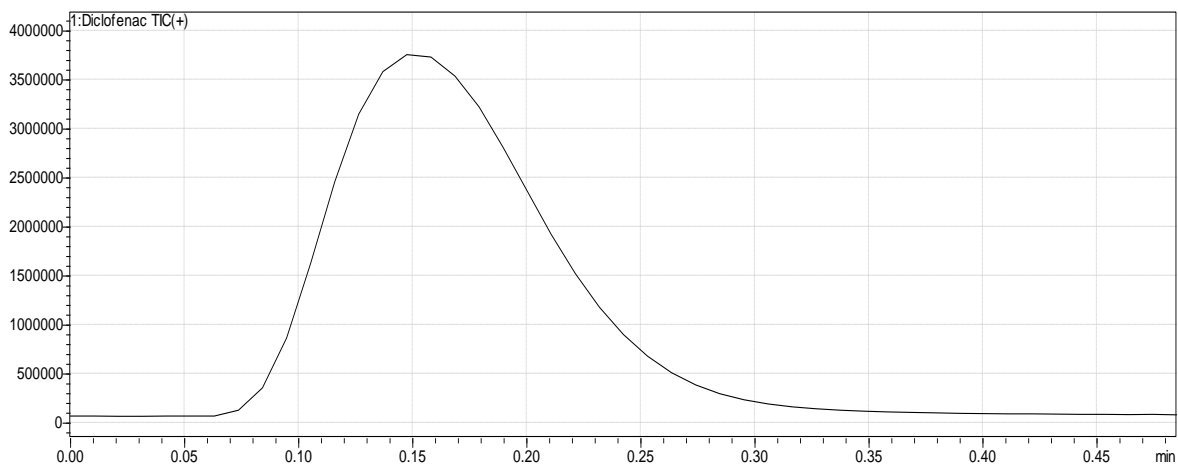
Appendix A51: Calibration curve for magnesium ion



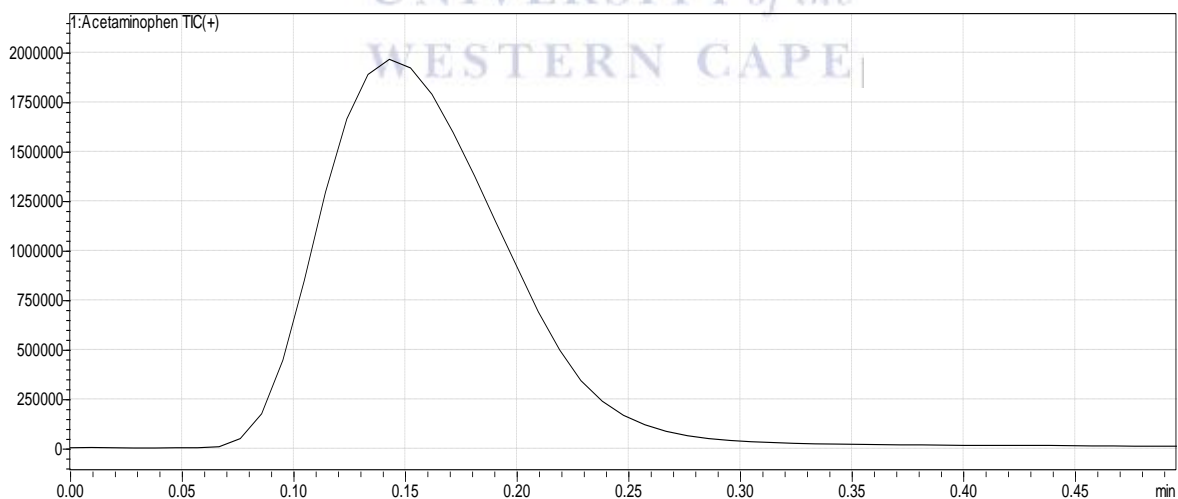
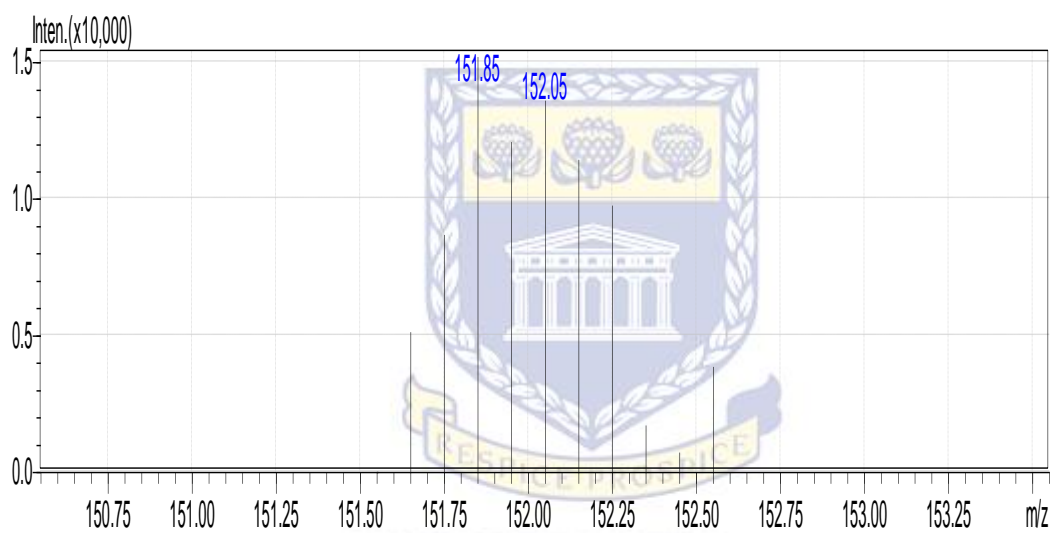
Appendix A52: Table of concentration data set for individual analytes in HPLC

ID#	Name	Type	ISTD Group	m/z	Ret. Time	Conc.(1)	Conc.(2)	Conc.(3)	Conc.(4)	Conc.(5)	Conc.(6)	Conc.(7)	Conc.(8)	Conc.(9)	Conc.(10)	Event	
1	Diclofenac	Target	1	297.6500	>252.1000	5.819	100	50	25	12.5	6.25	3.125	1.5625	0.7818	0.3906	0.195	1:MRM(+)
2	Sulfamethaxazole	Target	1	253.9000	>92.0500	3.167	100	50	25	12.5	6.25	3.125	1.5625	0.7818	0.3906	0.195	4:MRM(+)
3	Acetaminophen	Target	1	151.8500	>110.0000	1.868	100	50	25	12.5	6.25	3.125	1.5625	0.7818	0.3906	0.195	5:MRM(+)
4	Acetaminophen	Target	1	151.8500	>110.1500	1.870	100	50	25	12.5	6.25	3.125	1.5625	0.7818	0.3906	0.195	6:MRM(+)
5	Diclofenac	Target	1	295.8000	>213.9500	5.835	100	50	25	12.5	6.25	3.125	1.5625	0.7818	0.3906	0.195	7:MRM(+)
6	Sulphamethoxazole	Target	1	253.8500	>92.0000	3.178	100	50	25	12.5	6.25	3.125	1.5625	0.7818	0.3906	0.195	8:MRM(+)
7	Aspirin	Target	1	180.8500	>85.0000	0.001	100	50	25	12.5	6.25	3.125	1.5625	0.7818	0.3906	0.195	9:MRM(+)
8	Ibuprofen	Target	1	223.9500	>91.0000	0.001	100	50	25	12.5	6.25	3.125	1.5625	0.7818	0.3906	0.195	10:MRM(+)
9	17-BetaEstradiol	Target	1	290.0000	>169.3000	0.001	100	50	25	12.5	6.25	3.125	1.5625	0.7818	0.3906	0.195	11:MRM(+)
11	Sulfamethaxazole	Target	1	252.0500	>156.1500	3.178	100	50	25	12.5	6.25	3.125	1.5625	0.7818	0.3906	0.195	15:MRM(-)

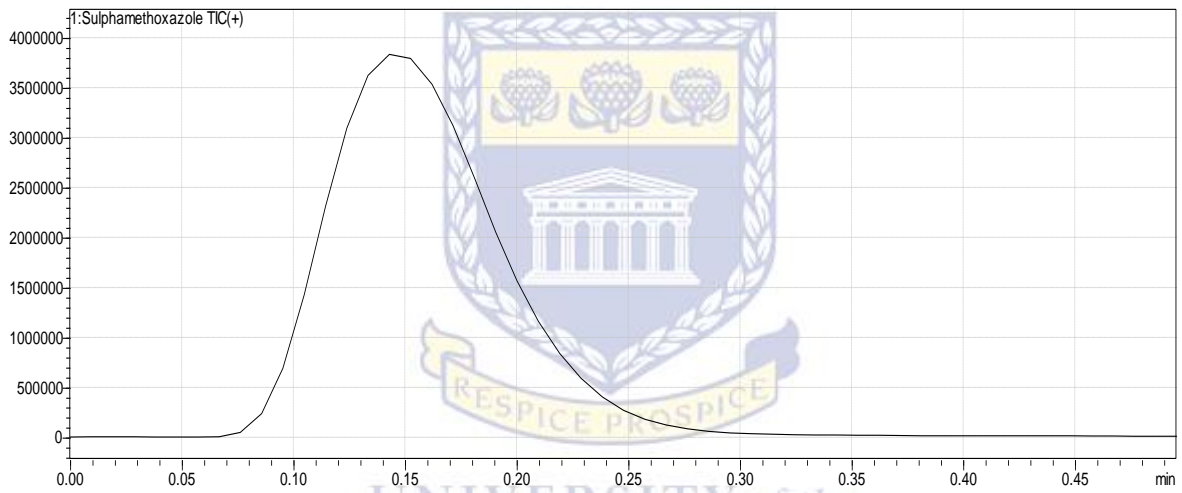
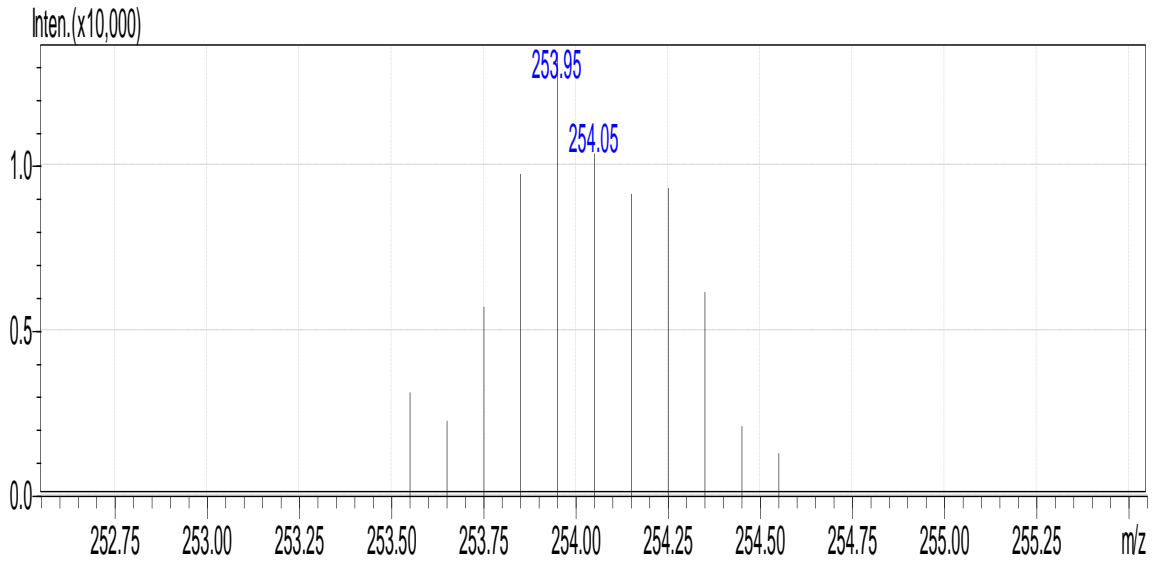




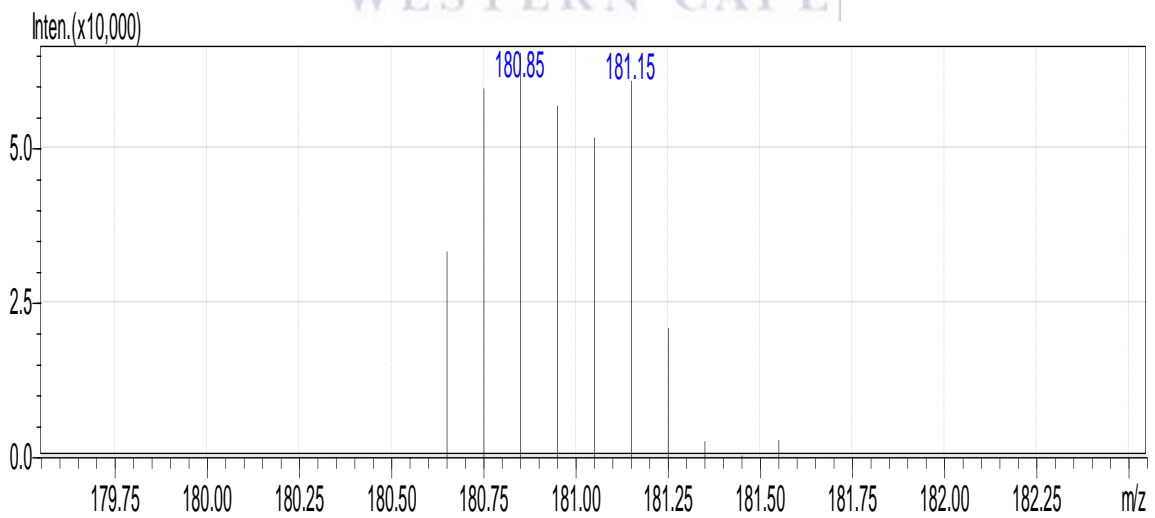
Appendix A53:MS result for Diclofenac

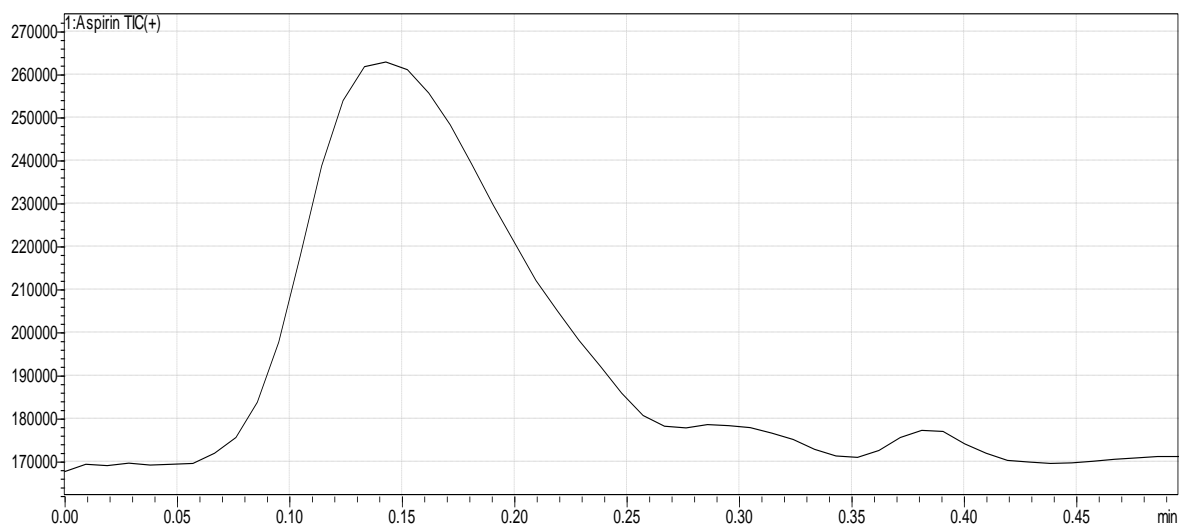


Appendix A54: MS result for Acetaminophen

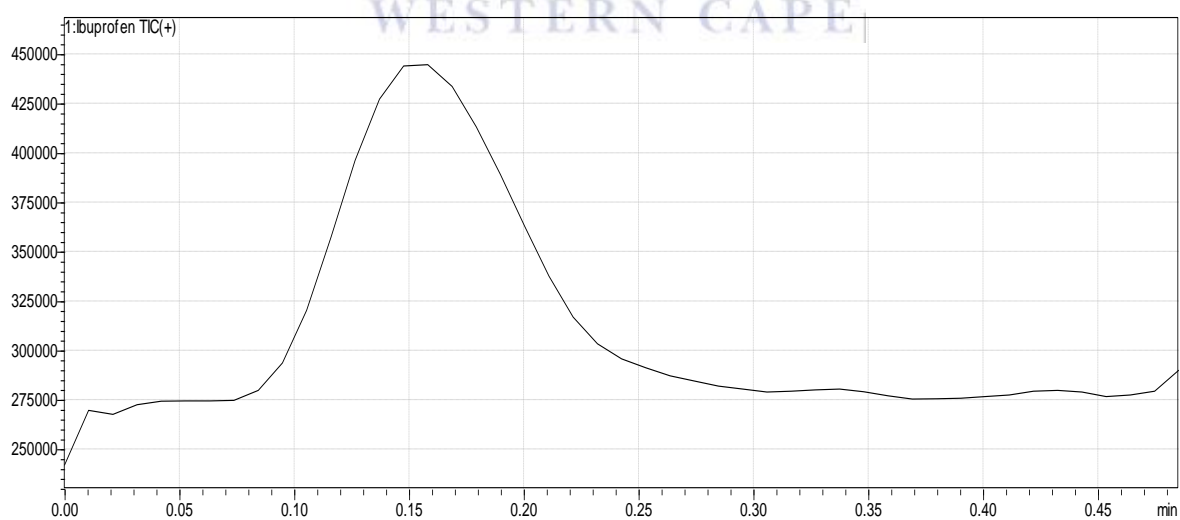


Appendix A55: MS result for Sulphamethoxazole

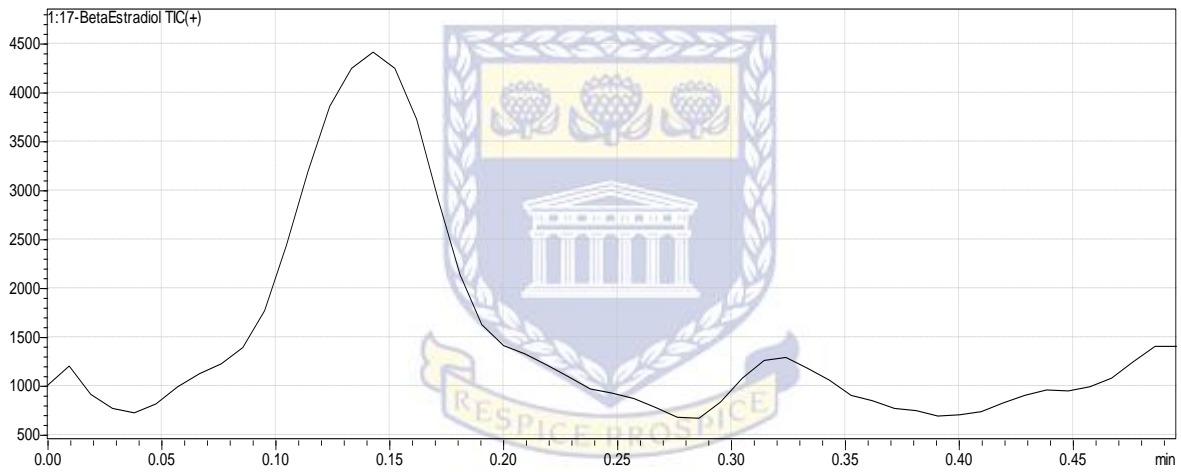
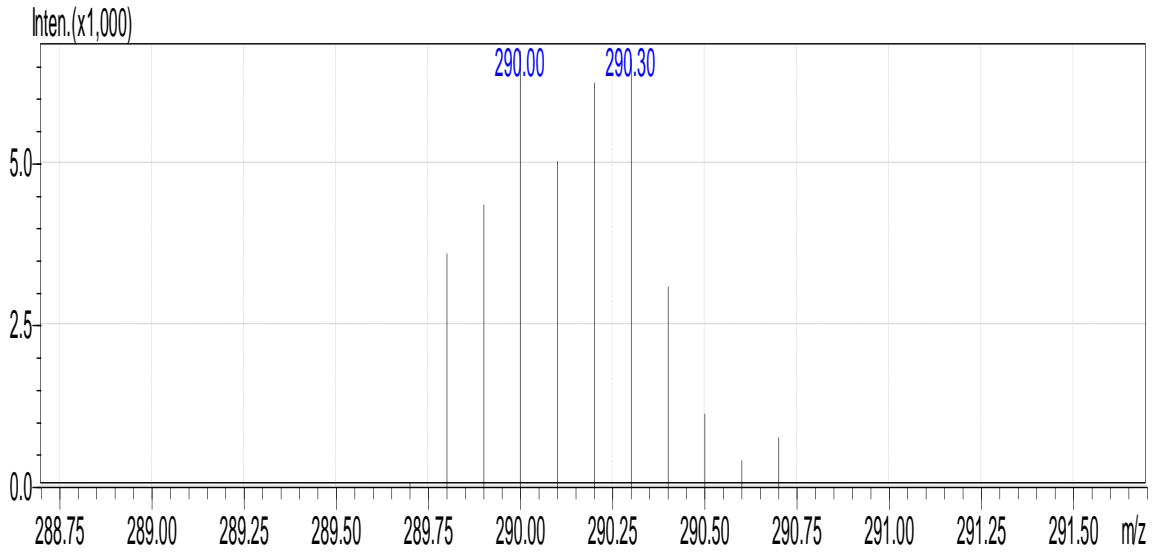




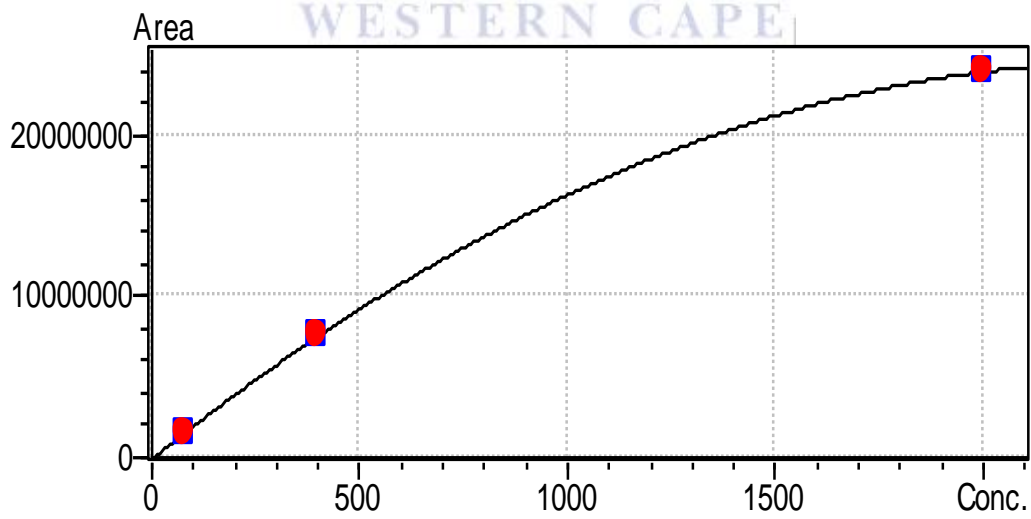
Appendix A56: MS result for Aspirin



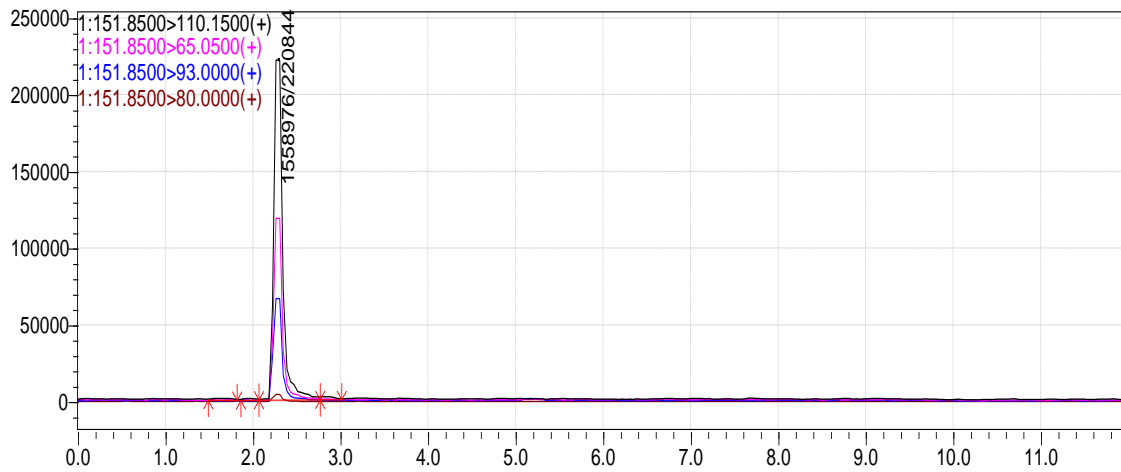
Appendix A57: MS result for Ibuprofen



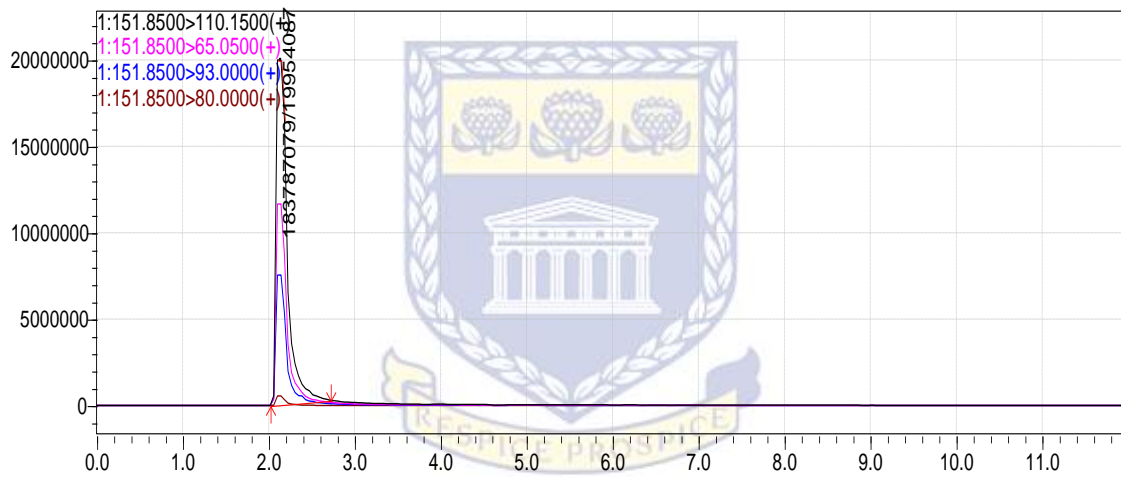
Appendix A58: MS result for 17-betaEstradiol



Appendix A59: Acetaminophen calibration curve

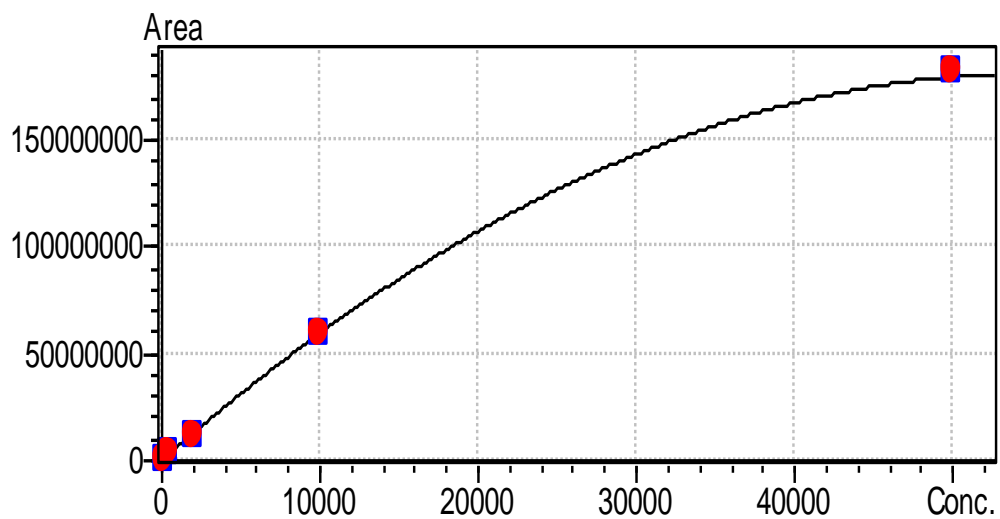


Appendix A60: Acetaminophen lower limit of quantification (LLOQ)

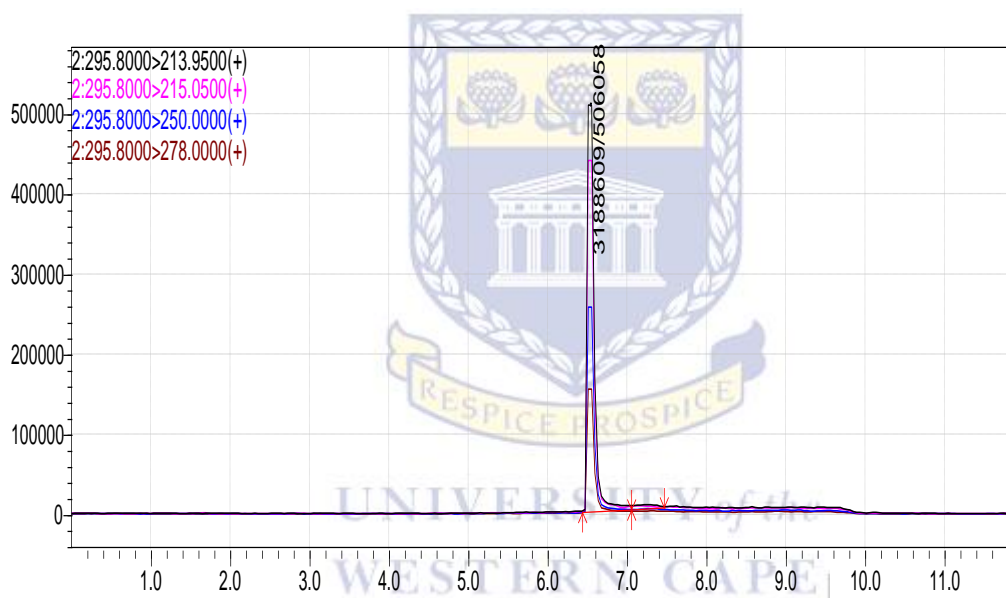


Appendix A61: Acetaminophen upper limit of quantification (ULOQ)

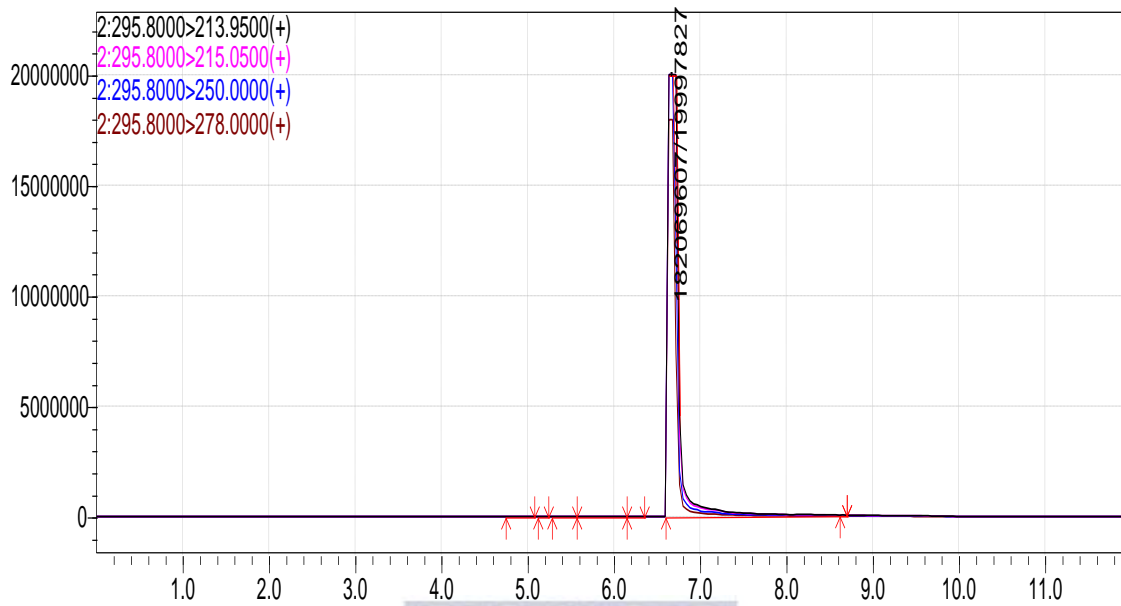
$Y = aX^2 + bX + c$
 $a = -0.0592414$
 $b = 6\,558.28$
 $c = 195\,451$
 $r^2 = 0.9869571$ $r = 0.9934572$



Appendix A62: Diclofenac calibration curve

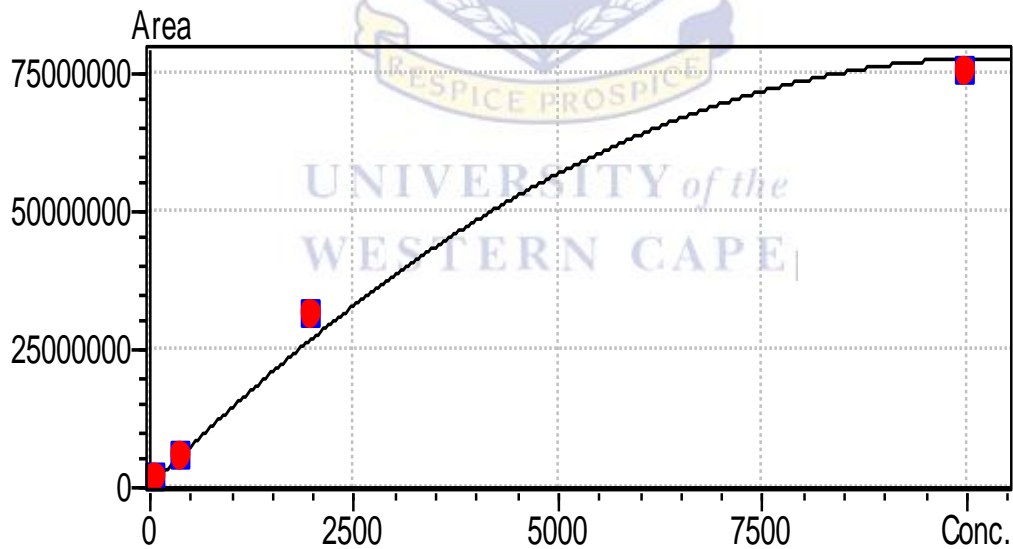


Appendix A63: Diclofenac lower limit of quantification (LLOQ)

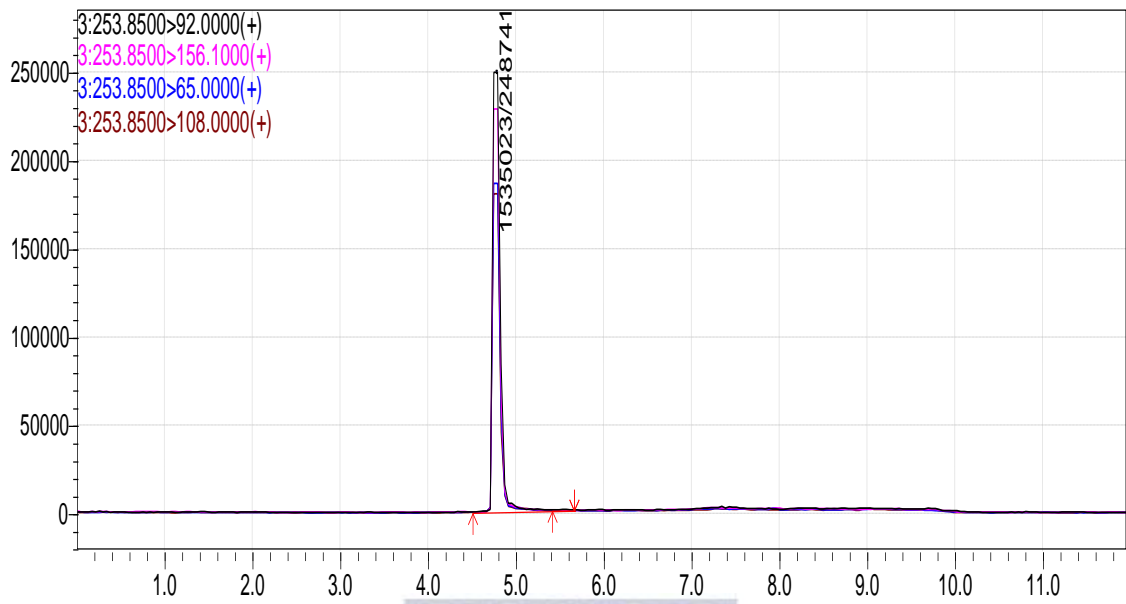


Appendix A64: Diclofenac upper limit of quantification (ULOQ)

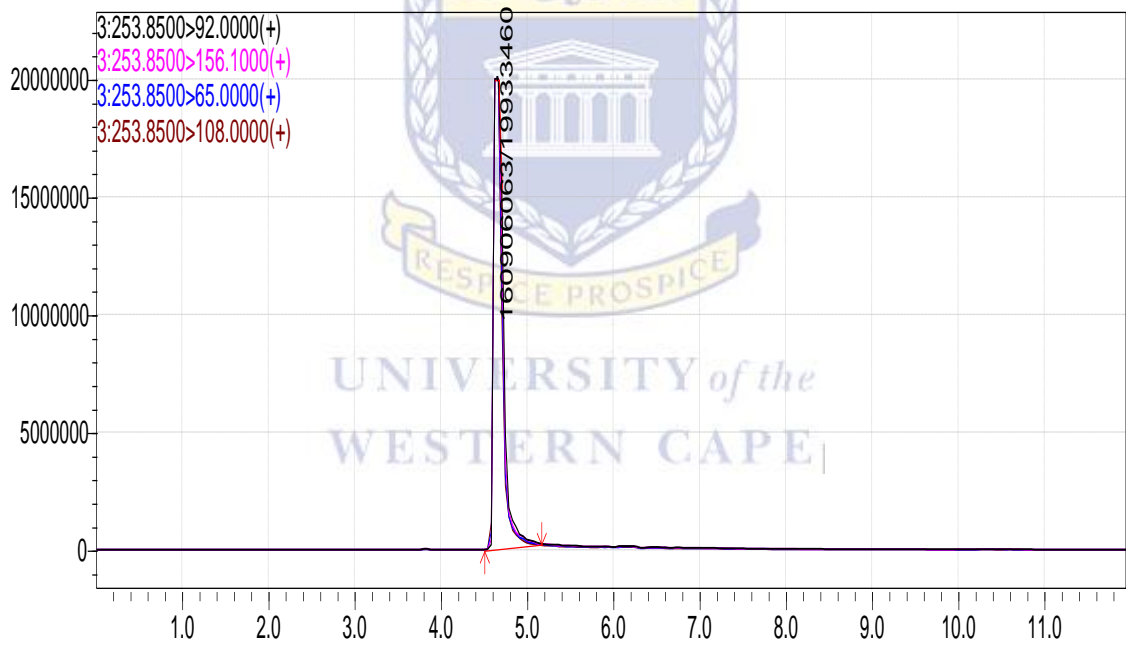
$Y = aX^2 + bX + c$
 $a = -0.714126$
 $b = 14\ 876.6$
 $c = 326\ 958$
 $r^2 = 0.9824979$ $r = 0.9912103$



Appendix A65: Sulphamethoxazole calibration curve



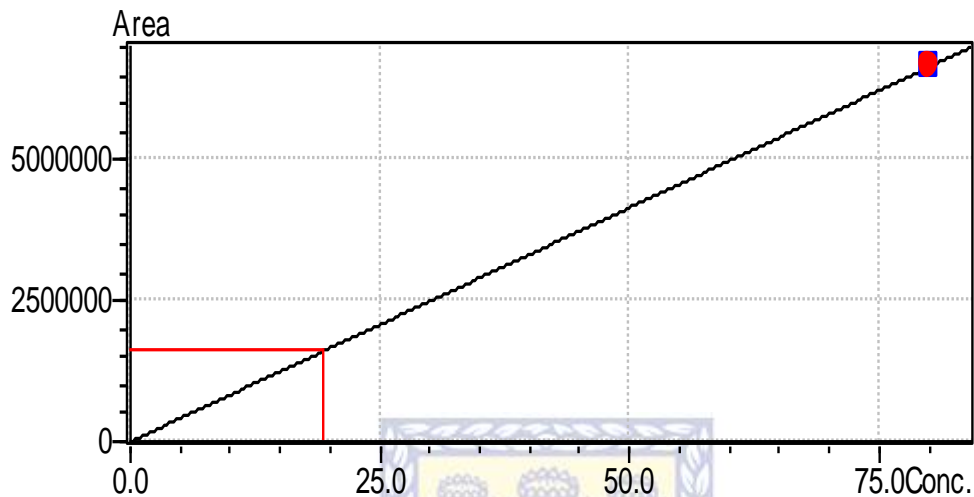
Appendix A66: Sulphamethoxazole lower limit of quantification (LLOQ)



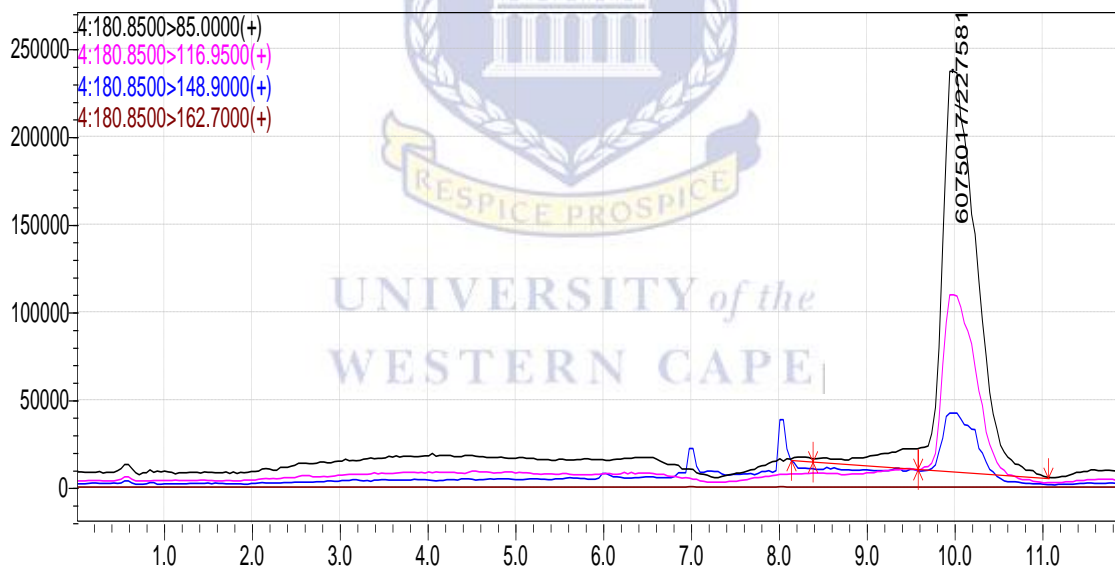
Appendix A67: Sulphamethoxazole upper limit of quantification (ULOQ)

Aspirin

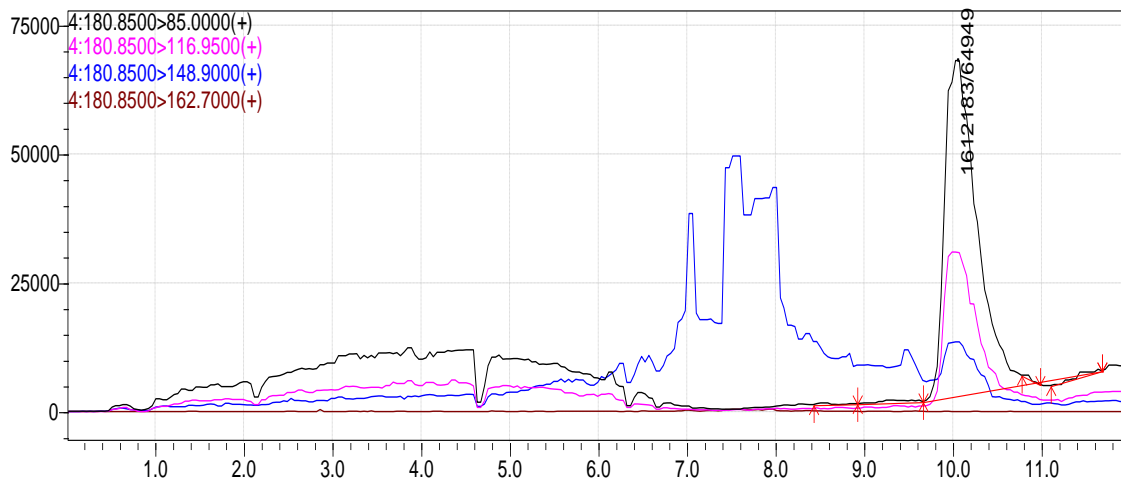
$Y = aX^2 + bX + c$
 $a = 0$
 $b = 83\,195.4$
 $c = 0$
 $r^2 = 1.000000$ $r = 1.000000$



Appendix A68: Aspirin calibration curve



Appendix A69: Aspirin lower limit of quantification (LLOQ)

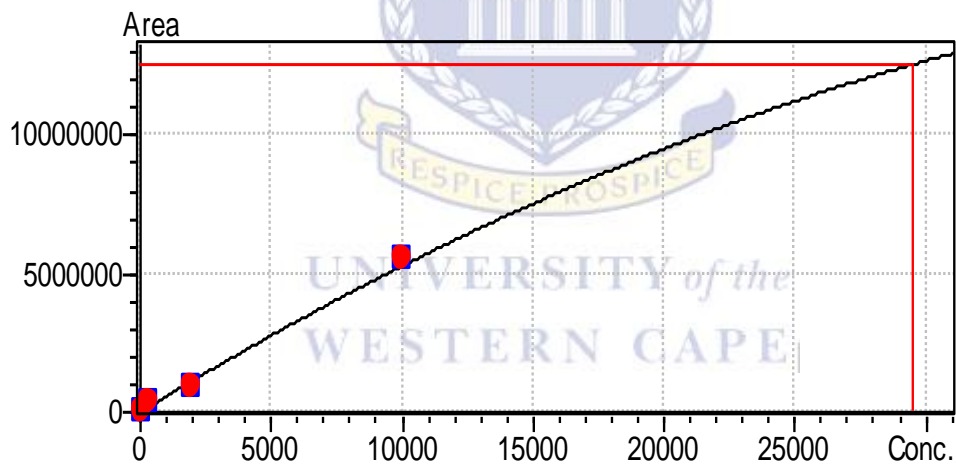


Appendix A70: Aspirin upper limit of quantification (ULOQ)

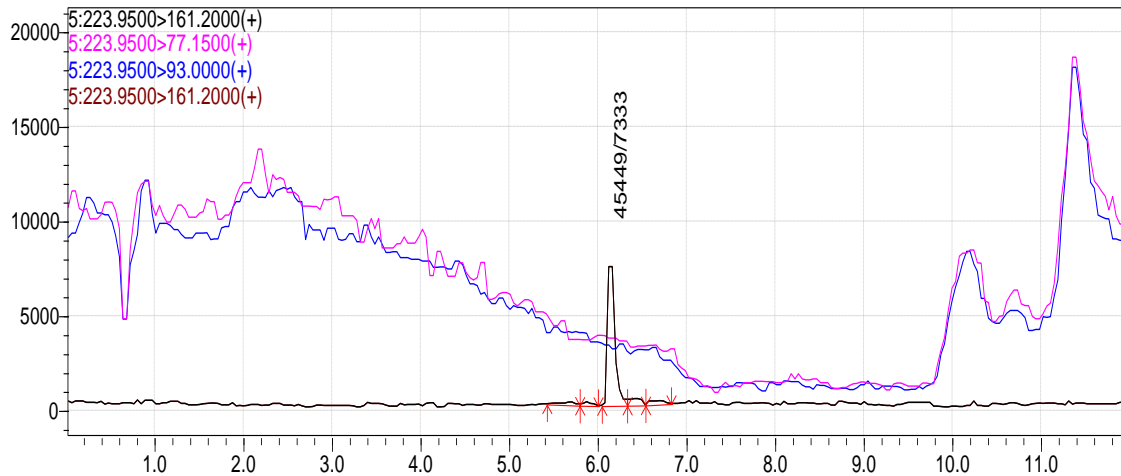
Ibuprofen

$$Y = aX^2 + bX + c$$

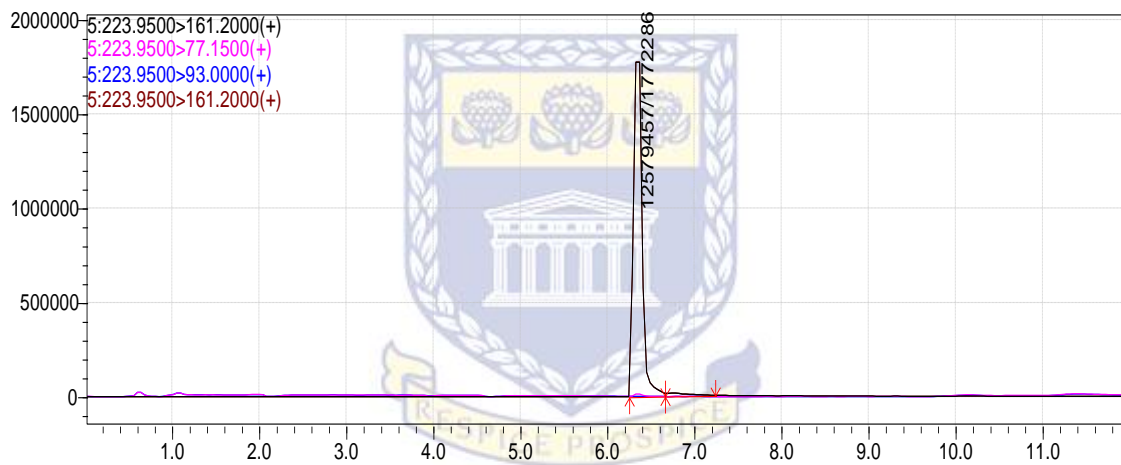
$a = -0.00527142$
 $b = 582.063$
 $c = 884.183$
 $r^2 = 0.9421980$ $r = 0.9706688$



Appendix A71: Ibuprofen calibration curve

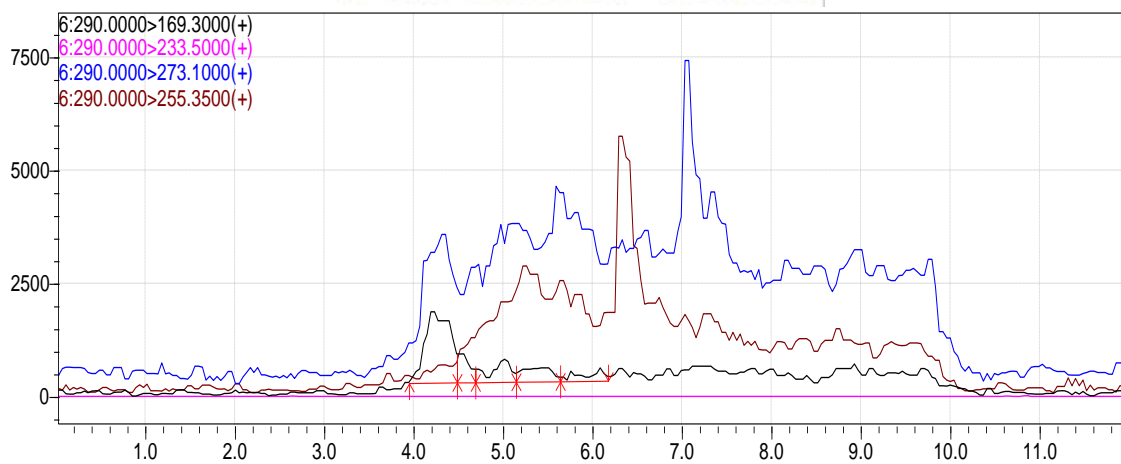


Appendix A72: Ibuprofen lower limit of quantification (LLOQ)

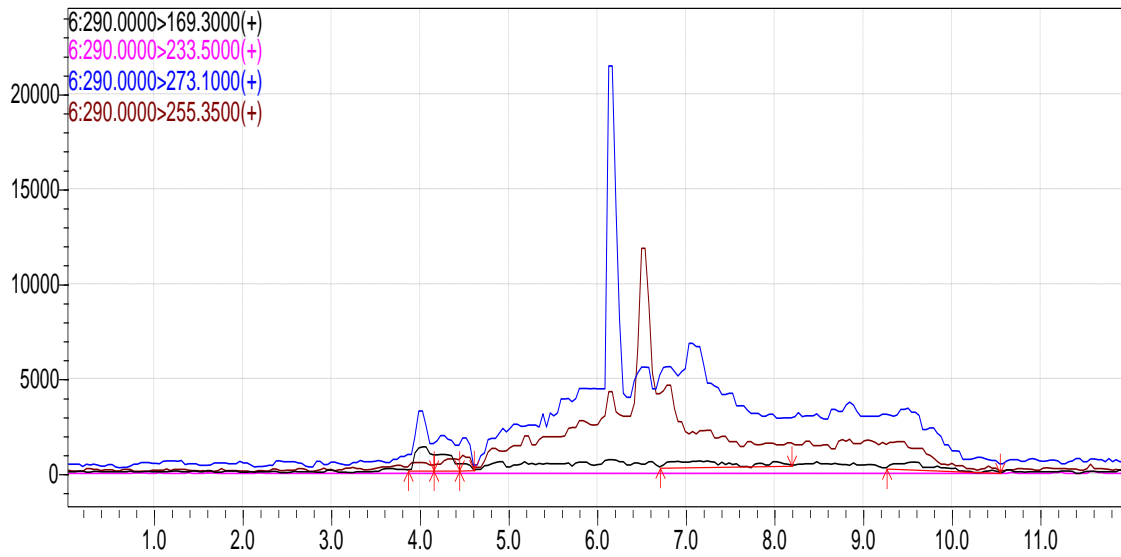


Appendix A73: Ibuprofen upper limit of quantification (ULOQ)

17-BetaEstradiol



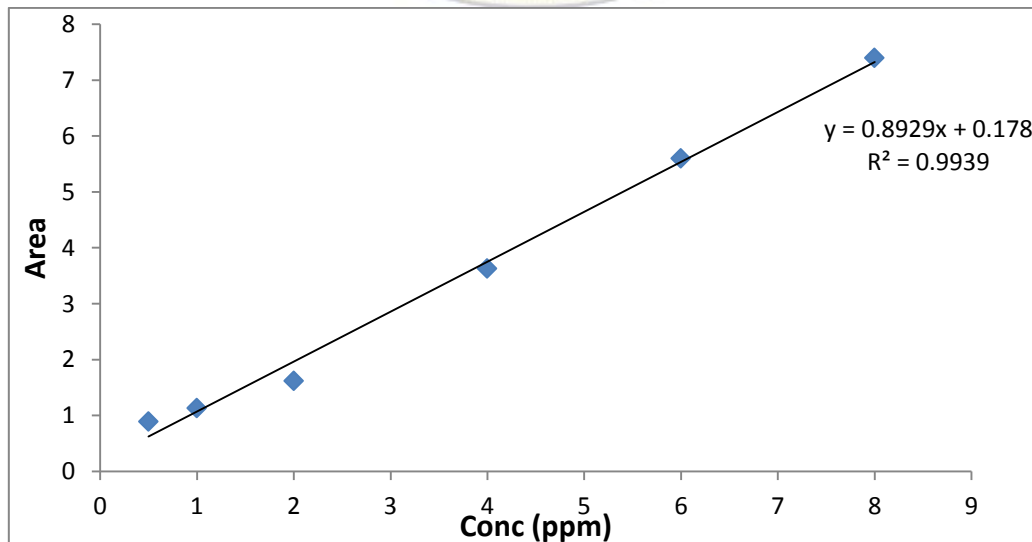
Appendix A74: 17-BetaEstradiol lower limit of quantification (LLOQ)



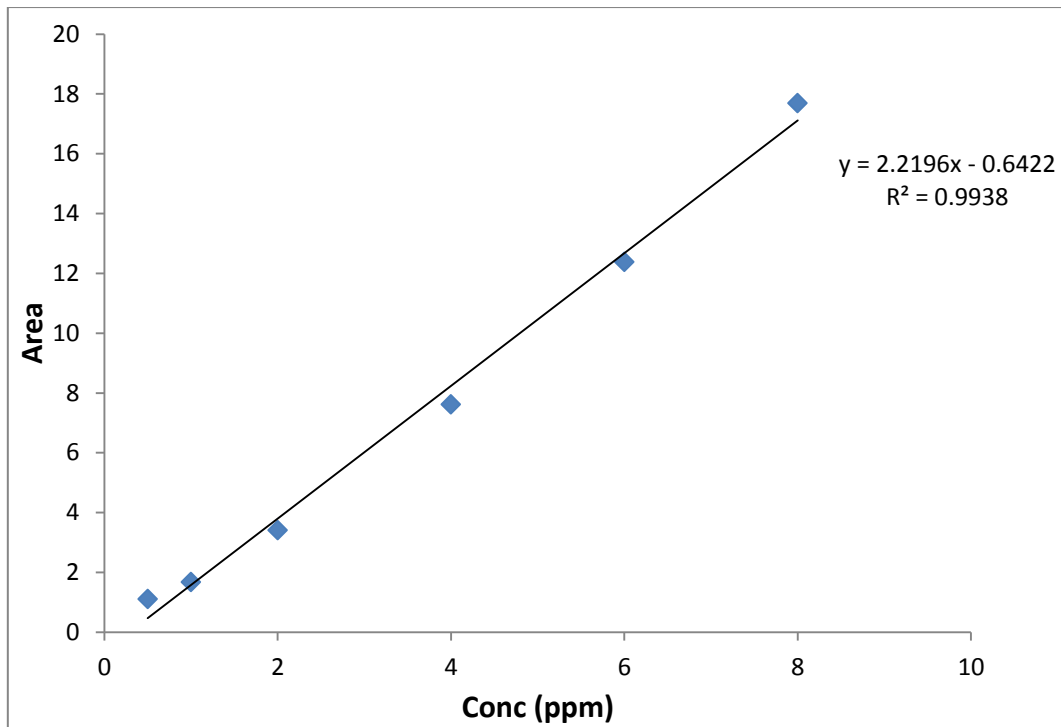
Appendix A75: 17-BetaEstradiol upper limit of quantification (ULOQ)

The concentration for the first ASA was calculated according to the following from the curve formula ($y = 0.5136x - 0.4449$, where y =peak area, x =concentration): From Figure 5.12,Page 141.

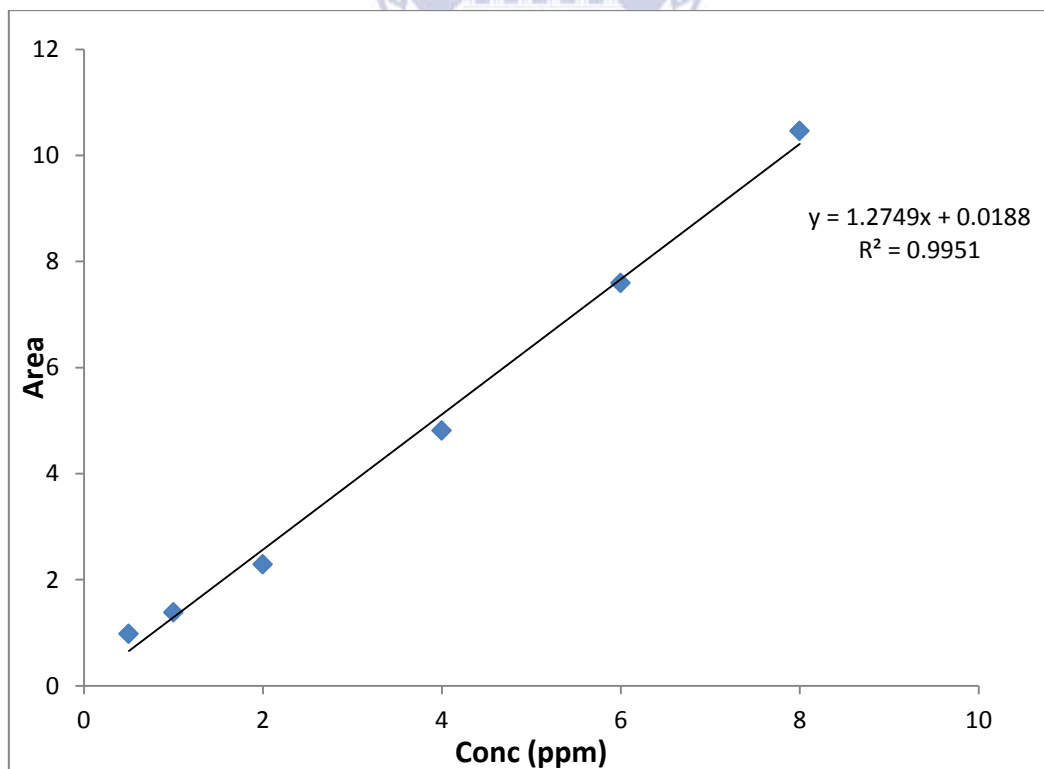
$$c = \frac{\text{peak area} + 0.4449}{0.5136} = \frac{5.36 + 0.4449}{0.5136} = 11.302.$$



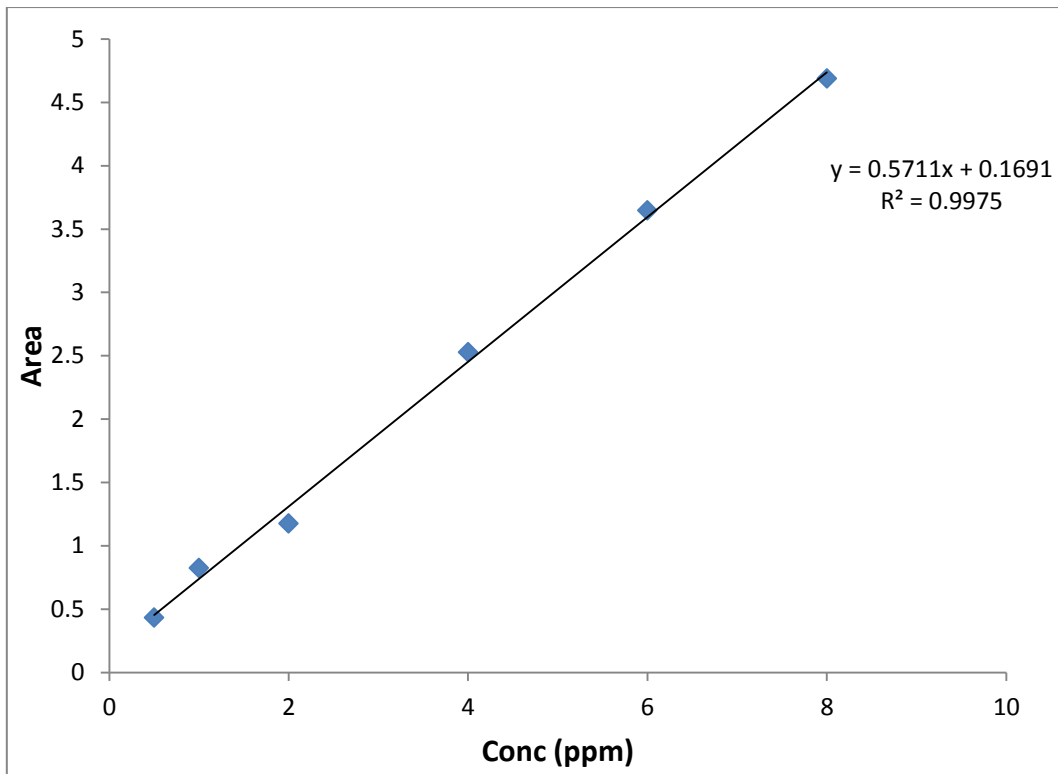
Appendix A76: Calibration curve for Acetaminophen standard.



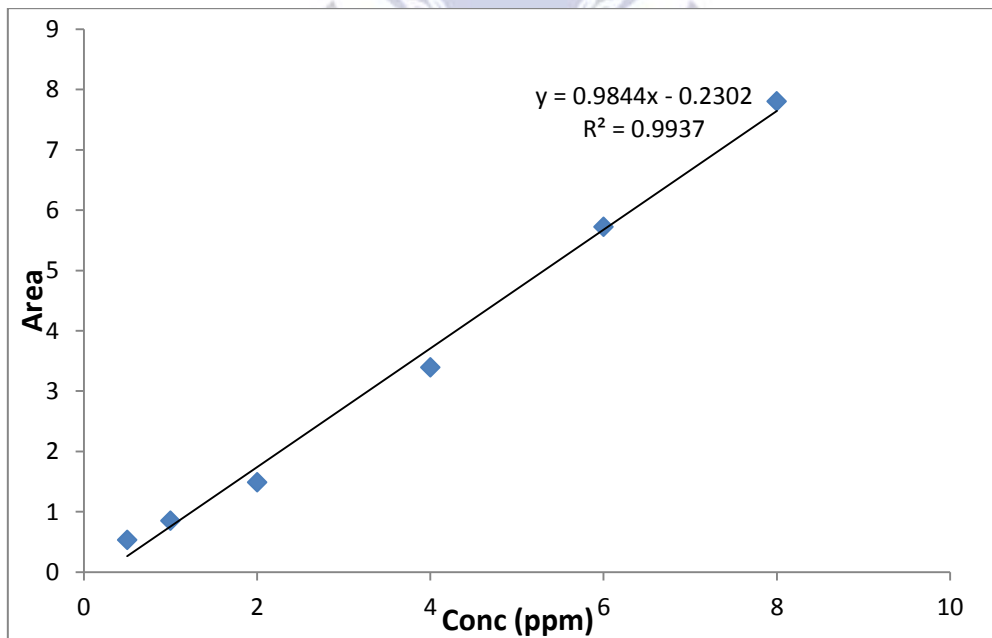
Appendix A77: Calibration curve for Diclofenac standard.



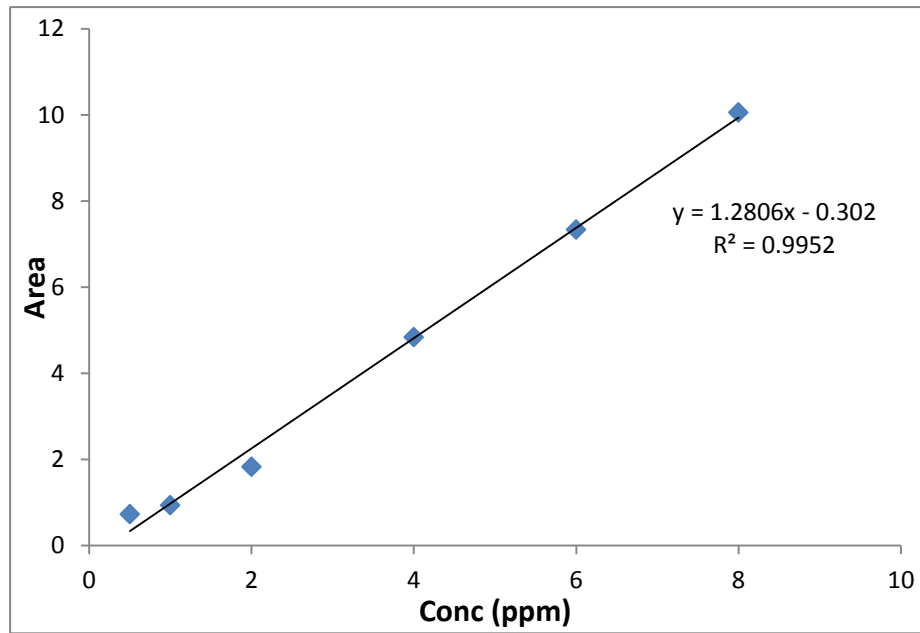
Appendix A78: Calibration curve for Aspirin (Acetylsalicylic acid) standard.



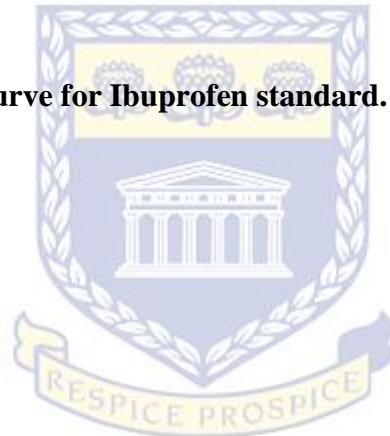
Appendix A79: Calibration curve for Salicylic acid standard.



Appendix A80: Calibration curve for Ibuprofen standard.



Appendix A81: Calibration curve for Ibuprofen standard.



UNIVERSITY of the
WESTERN CAPE